e-ISSN : 2320-0847
p-ISSN : 2320-0936

American Journal of Engineering Research (AJER)

Volume 2 Issue 9 - September 2013

www.ajer.org ajer.research@gmail.com

Editorial Board

American Journal of Engineering Research (AJER)

Volume-2 Issue-9

S.No.	Title Name	Page No.
01.	**A Finite Element Analysis of Fiber Optic Acoustic Sensing Mandrel for Acoustic pressure with Increased Sensitivity** Prashil M. Junghare, Dr. Cyril Prasanna Raj P, Dr. T. Srinivas, Dr. Preeta Sharan	01-07
02.	**Effect of controlling parameters on heat transfer during spray impingement cooling of steel plate** Purna C. Mishra, Santosh K. Nayak, Rajeswari Chaini, Durga P. Ghosh, Bibhuti B. Samantaray	08-16
03.	**Corrosion Inhibition Of Mild Steel In 0.5 M H2so4 By 1-(2- Methyl-4-(2-Methylphenyldiazenyl) Phenyl) Azonapthalen-2-Ol** S.Ananth Kumar, Dr.A.Sankar, ,S.Rameshkumar	17-22
04.	**Enhancing the Bandwidth of a Microstrip Patch Antenna using Slots Shaped Patch** Atser A. Roy, Joseph M. Môm, Gabriel A. Igwue	23-30
05.	**The Effects of Propagation Environment on Cellular Network Performance** Joseph M. Môm, Nathaniel S. Tarkaa, And Cosmas I. Ani	31-36
06.	**Studies on Compressive Strength Of Ternary Blended Concretes At Different Water Binder Ratios** D.Audinarayana, P.sarika, Dr.Seshadri Sekhar.T, Dr.Srinivasa Rao, Dr P Sravana G.Apparao	37-45
07.	**An Inflationary Inventory Model for Weibull Deteriorating Items with Constant Demand and Partial Backlogging Under Permissible Delay in Payments** Sushil Kumar, U. S .Rajput	46-54
08.	**Computation of Modulus of Elasticity of Concrete** Onwuka, D.O, Egbulonu, R.B.A, and Onwuka, S.U	55-61
09	**Smart input based user authentication and challenges towards multi-tiered cyber security** Ziaur Rahman, Md. Baharul Islam, A. H. M. Saiful Islam	62-70
10.	**Free Convective Heat Transfer From A Vertical Surface For The Case Of Linearly Varying Thermal Potential** Parvataneni	71-75
11.	**Client-Side Validation and Verification of PHP Dynamic Websites** K.Sowjanya, N. Deepika, P.V.S.Srinivas	76-80
12.	**Poincare Plot Used as a Confirmative Tool in Diagnosis of LV Diastolic Dysfunction for Diabetic and Hypertensive Patients** Manjusha Joshi, Dr.K.D.Desai, Dr.M.S.Menon	81-86

13.	**Analysis of Order of Singularity at a Vertex in 3D Transversely Isotropic Piezoelectric Single-Step Bonded Joints** Md. Shahidul Islam, Md. Golam Kader, Md. Kamal Uddin, and Mohiuddin Ahmed	87-99
14.	**Efficient Power Allocation Strategy Based Co-Operative Networks** Srinivas MRSP, U Mahender, P.V.S. Srinivas	100-102
15.	**Effect of NGBFS and CBA as fine aggregate on the chloride permeability of concrete** İsa Yüksel, Ozan Demirtaş	103-109
16.	**Technical Properties of Pond Ash - Clay Fired Bricks – An Experimental Study** Prashant G. Sonawane, Dr. Arun Kumar Dwivedi	110-117
17.	**A Novel Approach for Image Steganography Using Dynamic Substitution and Secret Key** Saeed Ahmed Sohag, Dr. Md. Kabirul Islam, Md. Baharul Islam	118-126
18..	**Brain Image Segmentation Technique Using Gabor filter parameter** Dr. Debmalya Bhattacharya, Mrs. Jibanpriya Devi, Ms. Payal Bhattacherjee	127-132
19.	**Stabilization of Dune Sand with Ceramic Tile Waste as Admixture** Dr. N. K. Ameta, Dr. Wayal A. S., Puneet Hiranandani	133-139
20.	**MHD Natural convection in the localized heat sources of an inclined trapezoidal Nanofluid-filled enclosure** M. A. Mansour, A.Y. Bakier, M. A. Y. Bakeir	140-146
21.	**Experimental Study of Turbidity Control by Coagulation for Salt Gradient Solar Pond** S P Shekhawat, Dr N V Halegowda, and Dr M Husain	147-153
22.	**IBC Secured Key Partition for A Peer-To-Peer Network** Suneeta peddireddy, Lokesh A, Prapulla C	154-162
23.	**Design the High Gain and Low Power Amplifier for Radio over Fiber Technology at 2.4 GHz** A. Salleh, N. R. Mohamad, M. Z. A Abd Aziz, M. N. Z Hashim, M. H. Misran, M. A. Othman	163-170 □
24.	**The Use of Alternate Ligno-cellulosic Raw Materials Banana (Musa sapientum) Ankara (Calotropis procera) and Pineapple (Ananas comosus) in Handmade Paper & their Blending with Waste Paper.** Atul Kumar, Brij Pal Singh, Rakesh Kumar Jain, and Ashwini Kr. Sharma	171-189

25.	**Mathematical Modelling Of Cyanide Inhibition on Cassava Wastewater Treatment** E. Onukwugha, and A.O. Ibeje	190-197
26.	**Estimation Of The Electric Power Potential Of Human Waste Using Students Hostel Soak-Away Pits** Onojo, O.J, Chukwudebe, G.A, Okafor, E.N.C, Ononiwu, G.C., Chukwuchekwa, N., Opara, R. O., Dike, D. O.	198-203
27.	**Estimation of the Current Occasion Parameters Using SuccessiveSampling Approach** A.E. Anieting, and V. O. Ezugwu	204-207
28.	**Evaluating of Mashhad urban development plans from compact city viewpoint** Mohammad rahim Rahnama, Ali Homaeefar, Toktam Piruz	208-213
29.	**Evaluating sustaiable development factors on stress residential (case study: Mashhad Sarshur neighborhood)** Mohammad Rahim Rahnama, Ali Homaeefar	214-223
30.	**Measurement of Natural Radioactivity in Soil Along the Bank of River Kaduna – Nigeria.** Abdullahi, M. A., Mohammed, S.S. and Iheakanwa, I. A.	224-227
31.	**On the choice of importance of Resampling schemes in Particle Filter** Mr. J.Joseph Ignatious, Dr.S.Abraham Lincon	228-233
32.	**Analysis Of Convective Plane Stagnation Point Chemically Reactive Mhd Flow Past A Vertical Porous Plate With A Convective Boundary Condition In The Presence Of A Uniform Magnetic Field** Adeniyan, A., Adigun, J. A	234-243
33.	**Assessing the Impact of Heavy Metal Exposure in Green Leafy Vegetables in Singrauli District of Madhya Pradesh, India** Dr. Vinod Kumar Dubey, Shalini Singh ☐	244-246
34.	**The Certified Written Press As An Element of The Information Society: Case of Algeria** Dr. Khaled Rouaski, Dr. Rachid Toumache, and Mss.Sabah Fadel	247-250
35.	**Water and Soil Pollution in Punjab with Special Reference to Mandi Gobindgarh & Surrounding Areas** Dr. Shalini Gupta, Dr. D S Grewal, Ajay Gupta	251-257
36.	**Drivers for Energy Efficiency in Indian Railway Workshops** Suresh D. Mane, N. Nagesha	258-264

37.	**Analyzing Public Emotion and Predicting Stock Market Using Social Media** Jahidul Arafat, Mohammad Ahsan Habib, and Rajib Hossain	265-275
38.	**Analysis and Evaluation of Government-Websites' Accessibility: Bangladesh Perspective** Subhra Prosun Paul, Afzal Hossain, Sharmin Rashid	276-281
39.	**A Study of Labour Productivity and Work-Hour Loss -Case Study for Brick Masonry** Sunil V. Desale, Dr. Sharad V. Deodhar	282-289
40.	**Generalised Gaussian Quadrature over a triangle** K. T. Shivaram	290-293

American Journal of Engineering Research (AJER)
e-ISSN : 2320-0847 p-ISSN : 2320-0936
Volume-02, Issue-09, pp-01-07
www.ajer.org

Research Paper Open Access

A Finite Element Analysis of Fiber Optic Acoustic Sensing Mandrel for Acoustic pressure with Increased Sensitivity

Prashil M. Junghare, Dr. Cyril Prasanna Raj P, Dr. T. Srinivas, Dr. Preeta Sharan

[1] *Associate Professor, Dept. of ECE, M. S. Engineering College, Bangalore*
[2] *Professor and Head (R & D), M. S. Engineering College, Bangalore*
[3] *Associate Professor, Head of Photonics Lab, IIS'c Bangalore*
[4] *Professors, Dept. of ECE, The Oxford College of Engineering, Bangalore*

Abstract: - This paper investigates the influence of material properties on the performance of an optical fiber wound mandrel composite fiber optic interferometer mandrel by using the ANSYS Cad tool, The acoustic sensitivity of an optical fiber considered analytically, High sensitivity obtained with low young modulus, very thick polymer coatings. The thick coating realized by embedding optical fiber in polyurethane. A flexible composite fiber-optic interferometric acoustic sensor has been developed by wrapping single mode fiber in a winding manner and then embedding a fiber in a thin polyurethane layer. The acoustic sensitivity has to be found more in a frequency range of (2.5-5.0 KHz). In this paper we studied the structural and material properties of a mandrel sensor with foaming layer in such way to get the optimal performance. The sensor was found to be compatible with water. Also the performance of optical fiber is analytically verified using the MATLAB software. In this paper the design was simulated in ANSYS Cad Tool, to verify the sensitivity of the Optical Mach-Zehnder Interferometric Sensor for increased sensitivity. The main objective and focus of the above work is concentrated on choosing the optimal foaming layer material by varying the Young Modulus E to choose the perfect foaming material for implementing in the design of mandrel.

Keywords: *Young modulus (E), Interferometer, Mandrel, ANSYS, Sensitivity.*

I. INTRODUCTION

Mach–Zehnder interferometer is a device used to determine the relative phase shift between two collimated beams (sensor arm & reference arm) from a coherent light source by using light modulation technique, to measure small phase shift in one of the two arm caused by a small sample or the change in length of one of the paths. Interferometric fiber optic sensor exploits the changes in an optical path length induced by transverse load in the optical fibers [1]. MZI sensors modulate the phase of the electromagnetic waves propagating within the optical waveguide. One of the major areas of application for MZI is in defense. There are numerous reasons for this interest which range from cost and performance to the geometric versatility of the sensing head. In coated fiber sensors the optical fiber is wound in a coil as a sensing element and the size is comparatively large. Since the optic coupling of the fiber waveguide is weak, a long fiber is generally used to increase the induced phase change. Pressure sensitivity is a complex function of a Young's modulus, Poisson's ratio, and the cross-sectional area of an outer coating. In the case of a mandrel sensor, a thin jacket fiber is typically wrapped around a compliant mandrel. The optical fiber then measures the pressure-induced strain in the mandrel. It is important to maximize the scale of the sensor in order to maintain a high sensitivity and a flat pressure response. So composite concentric mandrel has some improvements over the fiber wound mandrel even though bounded by some structural limitations [9].

The basic design of a hydrophone consists of two single-mode optical fibers. One fiber carries the signal light beam and the other carries the reference beam. Transduction in such a device depends directly on the acoustically induced phase modulation of the signal beam. After modulation both beams are combined and sent to a photomultiplier tube

for detection. When the two beams are adjusted so that they are 120 degrees out of phase of each other and at the output of the 3x3 coupler we get the three different output waveforms, these outputs are feed as inputs to the photo Multiplier Tube which processes the signal to detect the impact of the differential pressure caused by the acoustic events.

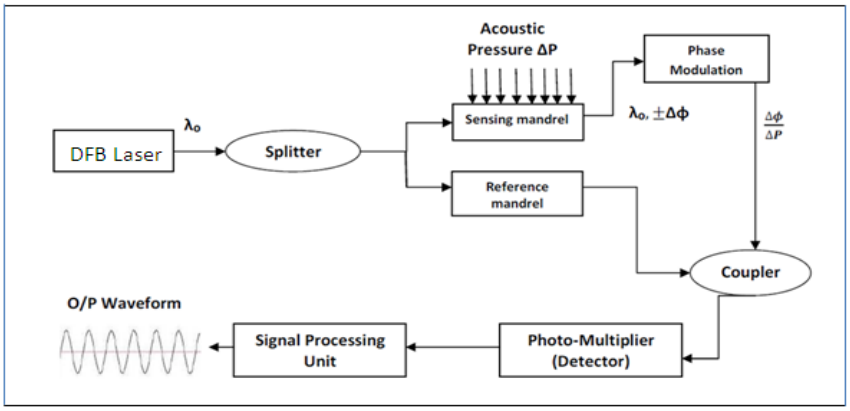

Fig 1 – Basic block diagram of Fiber Optic Hydrophone based on MZI.

In a composite fiber wounded mandrel of MZI Sensor, a thin jacket fiber is typically wrapped around a compliant mandrel and thin elastic polyurethane of 1cm thick, is coated over the fiber as protection during operation. The optical fiber measures the pressure-induced strain in the mandrel and protecting layer. Mandrel sensors are important because they are easy to produce and they exhibit a high sensitivity and amenability to spatial shading. Consider the cross section view of the mandrel sensor shown in Fig 2. A hollow cylindrical composite mandrel of length L_{eff} and radius Rm is radially wrapped with a single-mode fiber of length 150 meter over a length Lm[9].

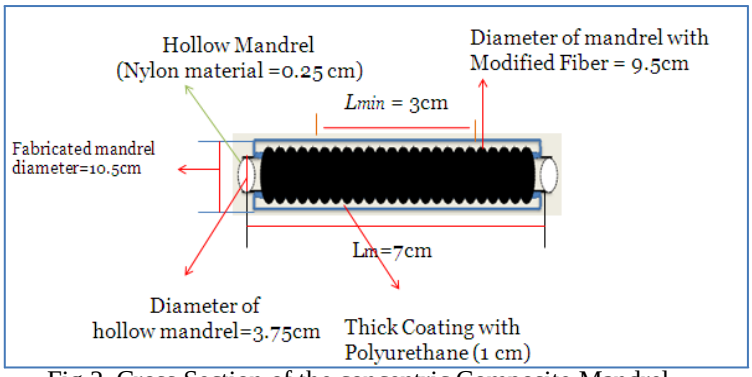

Fig 2. Cross Section of the concentric Composite Mandrel.

II. NOVEL DESIGN CONSIDERATIONS

The Novel MZI Optical fiber wounded concentric composite mandrel as shown below in Fig 3 consists of mainly five layers made up of different materials, the basic layer is Nylon which is coated in the inner diameter of the mandrel with a thickness of 0.25Cm, then the core of the mandrel is made of Aluminum (Al) metal which acts as a supporting structure for the entire mandrel the thickness of Al layer is 2Cm, above the aluminum layer consist of one of the important constituent material i.e., the foaming layer, this acts as flexible material supporting the Optical fiber, here the optical fiber is actually sandwiched between foaming layer with a thickness of 1Cm and the elastic Polyurethane coating of 1 Cm thickness [4],[7]. So when an acoustic event strikes or impacts on the effective length $L_{eff}$of sensor, the pressure exerted by the acoustic wave on the sensor is experienced by the elastic polyurethane coating and this makes an efficient impact of stress & strain on the optical fiber which causes some slight deformation on the fiber, Consequently makes a considerable change in length and diameter of the optical fiber this in turn causes change in optical path length and changes the phase of the light emitted from the Laser source. Hence this is the technique of finding the change in phase shift for the Mach-Zehnder Interferometric based sensors.

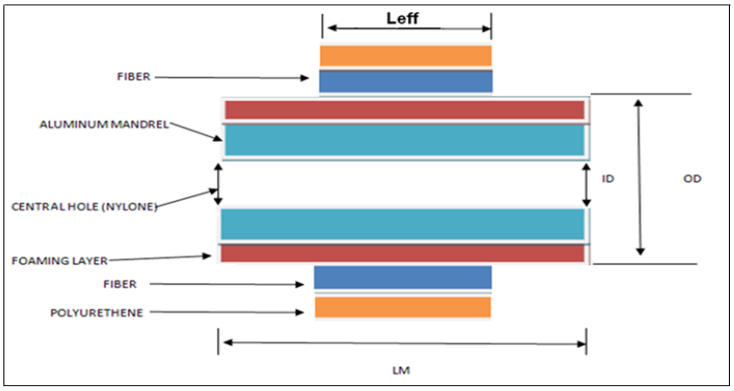

Fig 3: Schematic Structure of Novel MZI optical fiber wounded concentric composite mandrel.

In the above the layout and design of above mandrel has significant changes, i.e. as we know from the basic concepts of the physics that as area increases pressure exerted decreases and as area decreases pressure exerted increases, in the above mandrel the polyurethane and optical fiber layers have been specifically placed at the center of the overall length of the mandrel and its design is restricted for the effective length L_{eff} so that whenever an acoustic even has occurred the acoustic pressure exerted by the wave will strike the L_{eff} effective length of the mandrel and we get a good sensitivity of detecting the sound underwater as compared to the other designs where in the polyurethane and optical fiber are spread across the overall length of the mandrel.
A pressure P interacting with the fiber induces a change in phase $\Delta\phi/P$ and is given by

$$\frac{\Delta\Phi}{P} = k_0 n\Delta L + Lk_0\Delta n_0 \quad \text{..... (1)}$$

Where the first term corresponds to the change in the length of the fiber and the second term corresponds to the photo elastic effect. This photo elastic effect describes the relation between the mechanical strain in the fiber and the resulting change in the refractive index.
Therefore, the pressure sensitivity of the mandrel sensor per unit of air pressure becomes.

$$\frac{\Delta\Phi}{\Phi} = \varepsilon_z - \frac{n^2}{2}[(P_{11} + P_{12})\varepsilon_r + P_{12}\varepsilon_z] \text{..... ..(2)}$$

Equation (2) means that the phase change of the mandrel sensor can be found once we determine the appropriate strain distribution in relation to the unit of applied pressure, which then leads to the analysis of the transducer performance. In this paper, the strain distribution is calculated by using the MATLAB. Eq. (2) is written in the form of a summation of the strains distributed over all the discrete elements in the MATLAB. The values for Pockel's coefficients of the unclad fiber are assumed in the calculations of the pressure sensitivity with the MATLAB; we came at a reference that the wavelength (typically 850 - 1550nm) has the level of highest sensitivity [5].Therefore, MATLAB Simulink gives a mathematical analysis of interferometer-which keeps a promise to give accuracy in the measurement of all the parameter and higher possibility of sensitivity. Here parameters like phase, Wavelength for MZI and optical fiber length shown in the following graph as seen in Fig 4are simulated by MATLAB, gives the pressure sensitivity. Interferometric arms differ by virtue of the perturbation in one of the fiber legs, and the phase shift between the two light signals provides the measurement.

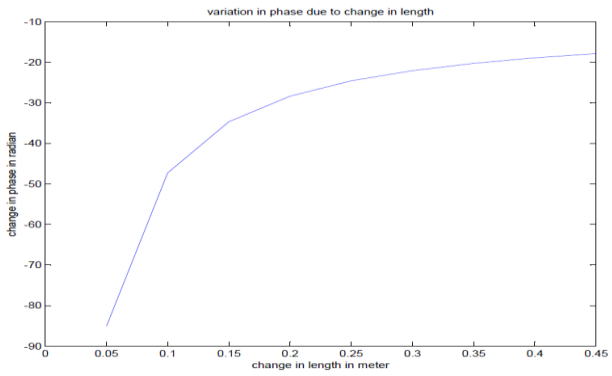

Because the measurements are made with the interference of two light signals with a small

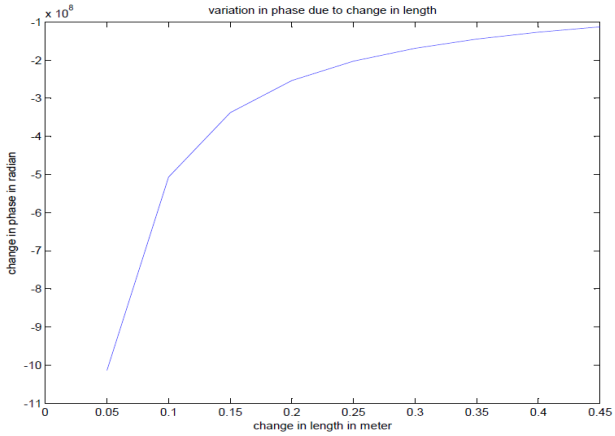

Fig 4: MATLAB graph of Variation in phase due to change in length.

As shown in Fig 4. Changing the length causes variation in phase and from another Fig. beside, another parameter also keeping the promises of more sensitive like pressure (transverse load) occurs with the change in phase w.r.t the different optical source wavelength (890 nm – 1550 nm) [3], [6].

III. PRESSURE SENSITIVITY CALCULATION

To prove the novel design consideration of the Concentric Composite mandrel as designed & simulated in ANSYS Cad tool the following calculations are shown as a proof for the new design. From Equation (2) we have, from [2]

$$\frac{\Delta\Phi}{\Phi} = \varepsilon_z - \frac{n^2}{2}[(P_{11}+P_{12})\varepsilon_r + P_{12}\varepsilon_z] \text{..... ..(2)}$$

Where ϵ_r=0.575*10^{-4}, ϵ_z=0.001975
and P_{11} =0.121, P_{12}=0.27

$$\frac{\Delta\phi}{\phi} = 0.001975 - \frac{(1.46)2}{2}[(0.121+0.27)*0.575*10^{-4} + (027*0.001975)]$$

$$\frac{\Delta\phi}{\phi} = 1.382700302*10^{-3}* \pi/180$$

We know that ϕ = 1.54*10^7 radians

$$\Delta\phi = 371.643 \text{ radians}$$

As we know that,

$$Sm = \frac{\Delta\phi}{P} \text{ ..... (3)}$$

Assume P= Pressure (2Mpa)

$$Sm = 371.643/2$$
$$Sm = 185.8215$$
$$\text{Sensitivity} = 20 \log (Sm/Sr) \text{..... (4)}$$
$$Sr = 1 rad/\mu Pa$$
$$S (dB) = 20 \log (185.8215/1\ \mu Pa)$$

So, Pressure Sensitivity = -74.61 dB

IV. FINITE ELEMENT ANALYSIS IN ANSYS

The analysis & performance evaluation of the MZI interferometric composite concentric optical fiber based mandrel is analyzed in the commercial available software ANSYS 11.0; this is based on FEM nodal analysis. A static analysis of the MZI based mandrel for hydrophone was performed by applying a pressure of 2 Mega Pascal to depict the real underwater environmental conditions. By the above analysis made we achieved,an improved sensitivity nearabout 9dB. The foaming layer is more soft and flexible than the base layer that is Al, by sandwiching the optical fiber in between the foaming layer and the outer polyurethane elastic layer improved the sensitivity of the designed mandrel radial pressure sensitivity due to its superior compliance.

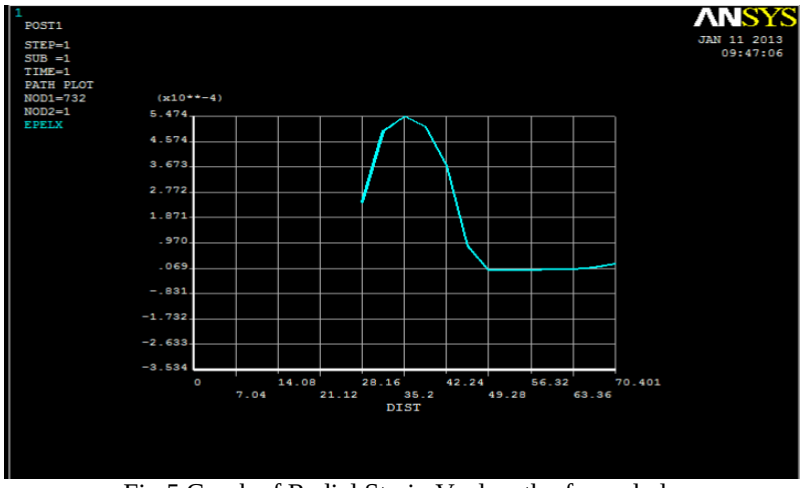

Fig 5.Graph of Radial Strain Vs. length of mandrel.

In the above graph of Strain Vs. length of mandrel graph of ANSYS we have shown that at the X axis we have the overall length of the mandrel and Y axis we have taken the Strain, the graph clearly indicates that exactly at the effective length L_{eff} the strain is maximum at the center of the overall length of mandrel. This graph response strongly supports the proposed design.

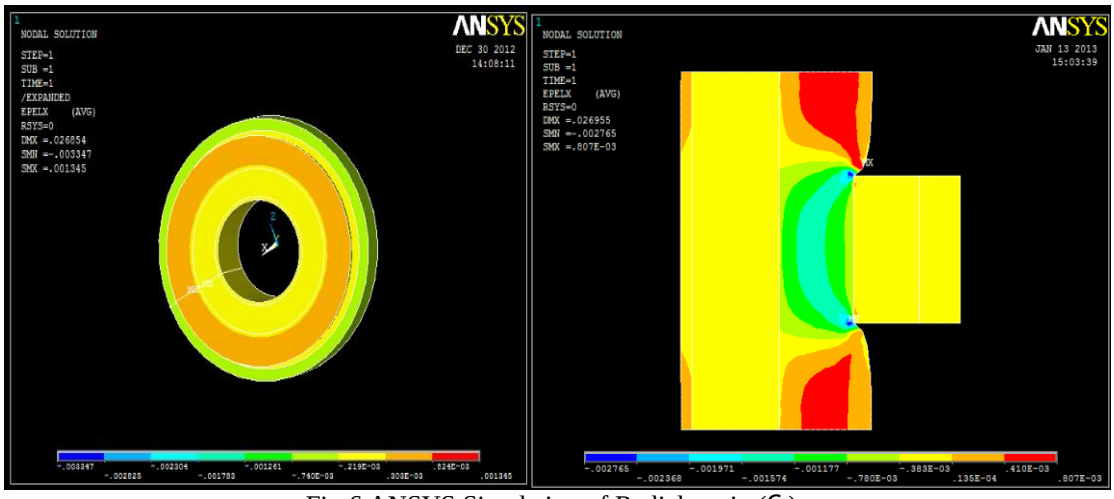

Fig 6.ANSYS Simulation of Radial strain (€r).

The figure's 6 & 7 are the snap shots of the designed mandrel in the ANSYS Cad tool, the simulation results of both axial strain and radial strain were obtained in ANSYS by using the material properties as shown in Table 1.

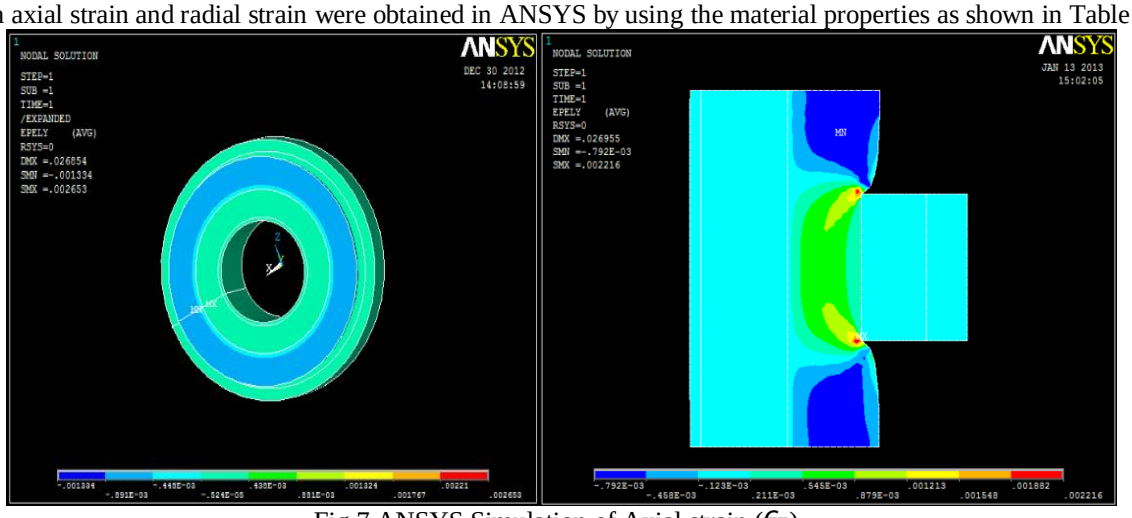

Fig 7.ANSYS Simulation of Axial strain (€z).

V. RESULTS AND DISCUSSION

In this paper, various performance evaluation parameters with respect to pressure sensitivity are studied and simulated the performance parameters include such as length of Mandrel, Wavelength, Young Modulus (E) of foaming layer for radial pressure.This analysis reportgives the proof for highest possible value of sensitivity of optical fiber based on interferometer principle which shows the optimized performance of the mandrel w.r.t Young modulus of the foaming layer. As Pressure increases, changes in light path i.e., phase modulation will occurs depending on the radial load in the sensor arm which in comparisons with reference arm will be more so, the effective changes in the fiber length (Δl) will be more and *vice-versa*. In this paper, we concluded, pressure increases which changes in Δl *w.r.t*length of the fiber wrapped around the mandrel 'L' will be more and consequently the phase related to optical signal will be more depending on the wavelength of the optical signal.

Structure	Central Hole	First layer	Second layer	Third layer	Elastic layer
Composition	Nylon	Aluminum	Foaming Layer	Si - glass	Polyurethane
Diameter (mm)	2.5	20	20	15	10
Young modulus	2.14e3	73e3	0.45e3	19.6e3	1.3e3
Poisson's ratio	0.48	0.33	0.45	0.34	0.45
P_{11}				0.126	
P_{12}				0.27	
Refractive Index				1.458	

Table1: Specifications of Material Properties.

The above Table 1 provides the information of the designed mandrel material properties and its composition ration which help to enhance the pressure sensitivity [2]. The foaming layer works as a real compliance material layer that supports & actuates more deformations on the optical fiber when it is exposed to an external acoustic pressure, the base material Al of the mandrel supports the overall structure of sensor. For the foaming layer, the material properties that have efficient effect on the acoustic sensitivity of the mandrel are mainly the Young's modulus & the Poisson's ratio. In a composite concentric mandrel the foaming layer should be more soft and flexible than the Al base material to get more enhanced sensitivity. [2] The Young's modulus of the foaming layer is found to be lying in the range of 0.1 to 10Gpa, and its Poisson's ratio 0.35 to 0.45 and is as shown in the Table 1. The Higher sensitivity for this novel design was obtained and verified by considering the optimized design parameters as shown in Table 3.

Table 2 lists the material properties of the constituent parts of the proposed mandrel design. Other design features were selected to increase sensitivity and were associated with the mandrel properties and thickness of the foaming layer.

Layers	Material	Young's modulus(Gpa)	Density (kg/m^3)	Poisson's ratio
Base layer	Aluminum Al	73	2700	0.33
Foaming layer	Polystyrene	0.45	1208	0.85
Fiber	Si-glass	19.6	1404	0.34
Molding	Polyurethane	1.3	960	0.45

Table 2: Material properties of the constituent parts of optical fiber Mandrel for MZI Sensor.

PRESSURE (Mpa)	POISSON' S Ratio	ID (cm)	OD (cm)	LM (cm)	THICKNES S (cm)	YOUNG'S MODULUS (Gpa)	SENSITIVITY (dB)
2	**0.45**	**3.75**	**8**	**7**	**2**	**0.45**	**-74.61**
2	0.45	3.75	8	7	2	0.50	-76.32
2	0.45	3.75	8	7	2	0.55	-77.92
2	0.45	3.75	8	7	2	0.60	-78.87
2	0.45	3.75	8	7	2	0.65	-80.02
2	0.45	3.75	8	7	2	0.70	-81.13
2	0.45	3.75	8	7	2	0.75	-82.21
2	0.45	3.75	8	7	2	0.80	-83.05

Table 3: Tabulation of Young's Modulus Vs. Sensitivity.

The values tabulated in table 3shows the results of the sensitivity Vs. Young's Modulus here as we can infer from the table that only the Young's modulus is varied by keeping constant Pressure, Poisson's ratio, ID & OD and length of the mandrel etc., this clearly gives us the result that as the Young's modulus (E) increases the sensitivity decreases & henceforth good sensitivity is obtained and from this it is easy to find the detection of the sound underwater.

VI. CONCLUSION

From the design and analysis of structural properties of material required for mandrel, As the Young modulus (E) increases the sensitivity decreases & henceforth we got the good optimized sensitivity for the young modulus value 0.45 for the foaming layer material and from this we can detect the sound as well as where it is coming from in underwater medium. In above designed mandrel as we change the material properties and the design for different layers we obtained a significant change of 10dB higher sensitivity as previously designed mandrels.

VII. ACKNOWLEDGEMENTS

We immensely thank full to Cdr. Vijay Singh, Deputy of the Director Navel Research Board (NRB), New Delhi for their constant source of support and encouragement for carrying out the project.

REFERENCES

[1] Simulation of High-Sensitivity Hydrophone Based on ANSYS, international conference, MEMS 2012 Published by Yingying Wang and Chang Wang, Atlantis Press, page no. 797-699.
[2] A fiber-optic hydrophone with an acoustic filter, Advanced Sensor Systems and Applications III, edited by Yun-Jiang Rao, Yanbiao Liao, Gang-Ding Peng, Proc. of SPIE Vol. 6830, 683011, (2007)
[3] Sensitivity Improvements in Fiber Optic Hydrophone, supported by NIH, R. Gopinath, K.Srinivasan, S.Umchid*, L. Bansal+, A.S. Daryoush, P.A. Lewin* M. El-Sherif+ IEEE-2008
[4] N. Lagakos, J. A. Bucaro, and R. Hughes, Appl. Opt., vol. 19, p-3668, 1980
[5] A Finite Element Analysis of an Interferometric optical fiber hydrophone with a concentric composite mandrel including a foaming layer, Jong-in Im and Yongrae Roh. June 1999.
[6] Comparison of the Simulated Phase Sensitivity of Coated and Uncoated Optical Fibers From Plane-Strain Vibration and Static Pressure Models Marilyn J. Berliner - Submarine Sonar Department, 7 June 1996.
[7] Peter Shajenko, James P. Flatley, and Mark B. Moffett, "On fiber hydrophone sensitivity" Naval Underwater system Center, New London Laboratory, New London, Connecticut 06320.
[8] S. Africk, T. Burton, P. Jameson, and A. Ordubadi, "Design studies for fiber optic hydrophones," Report No. 4658, Bolt, Beranek & Newman, Inc., Cambridge, Mass (1981).
[9] R. Hughes and J. Jarzynski, "Static pressure sensitivity amplification in interferometric fiber optic hydrophones, "Applied Optics, 19(1), 1 (1980)
[10] J. A. Bucaro, N. Lagakos, J. H. Cole, and T. G. Giallorenzi, "Fiber optic acoustic transduction," Physical Acousticsedited by R. H. Thurston, 16, 385 (1982)
[11] G. B. Hocker, "Fiber Optic sensing of pressure and temperature" Applied Optics, 18(9), 1445 (1979).
[12] Mach-ZehnderInterferometer sensor for acoustic detection with optimal performance, *IOSR* Journal of Electronics and Communication Engineering *(IOSRJECE) ISSN: 2278-2834 Volume 2, Issue 5 (Sep-Oct 2012), PP 29-33.*

American Journal of Engineering Research (AJER)
e-ISSN : 2320-0847 p-ISSN : 2320-0936
Volume-02, Issue-09, pp-08-16
www.ajer.org

Research Paper Open Access

Effect of controlling parameters on heat transfer during spray impingement cooling of steel plate

Purna C. Mishra, Santosh K. Nayak, Rajeswari Chaini, Durga P. Ghosh, Bibhuti B. Samantaray
[1] *School of Mechanical Engineering, KIIT University, Bhubaneswar – 751024, Odisha, India*

Abstract: - The heat transfer characteristics of air-water spray impingement cooling of stationary steel plate was experimentally investigated. Experiments were conducted on an electrically heated flat stationary steel plate of dimension 120 mm x 120 mm x 4 mm. The controlling parameters taken during the experiments were air-water pressures, water flow rate, nozzle tip to target distance and mass impingement density. The effects of the controlling parameters on the cooling rates were critically examined during spray impingement cooling. Air assisted DM water was used as the quenchant media in the work. The cooling rates were calculated from the time dependent temperature profiles were recorded by NI-cRIO DAS at the desired locations of the bottom surface of the plate embedded with K-type thermocouples. By using MS-EXCEL the effects of these cooling rate parameters were analysed The results obtained in the study confirmed the higher efficiency of the spray cooling system and the cooling strategy was found advantageous over the conventional cooling methods in the present steel industries.

Keywords: *- Heat transfer coefficient, Heat transfer enhancement, spray Impingement Cooling, Optimal cooling, Patternator.*

Nomenclature:

ΔT	Measured temperature difference
ΔT^*	Non-dimensional temperature difference
Tc	Temperature of cooling water
T	Time
t^*	Non-dimensional time
l	Length of the steel plate
α	Coefficient of thermal expansion
CR	Cooling rate
CR*	Non-dimensional cooling rate
d	Hole diameter
D	Shower exit to surface distance
K	Thermal conductivity
lt	Liter
min	Minute
m	Meter
s	Second
Pw	Water Pressure

I. INTRODUCTION

Spray Impingement cooling (SIC) is a very promising thermal management technique for high heat flux applications like Runout Table Cooling in Hot Strip Mill. Heat fluxes as high as 10 MW/m^2 with SIC has been reported by Selvam and Ponnappan, [1].

Several technologies [2–5] to increase the cooling rate in the ROT have been recently developed. Ultrafast cooling technology [2, 3] increases the conventional cooling rate of 30 ^{0}C/s to 80 ^{0}C/s, depending on the final thickness, to 300 ^{0}C/s on 4-mm-thick hot strip. An accelerated cooling technology [4, 5] having more than 200 ^{0}C/s on 3-mm thickness makes it possible to increase the strength of steel or to achieve the same level of strength with a low carbon equivalent design. These technologies use larger flow rates than conventional cooling methods (such as spray or water column cooling), basically. In the ultrafast cooling, total water flow is well known as 17,000 L/min m^2 [3] of cooling length. This corresponds to 9200 L/min m^2 assuming a 1.8-m width, [4] which is more than double the maximum flow rate for the conventional ROT cooling [3]. Bhattacharya et al., [6] reported that Ultra Fast Cooling (UFC) in Hot Strip Mill entails cooling rate of about 300 ^{0}C/s, which corresponds to heat transfer rate of 4.37MW for a 4 mm thick carbon steel strip. The cooling rate obtained was an order of magnitude higher than conventional laminar jet cooling.

As such, there is very less information about the method to achieve high strip cooling rate with SIC in open literature. Using air/ water spray impingement cooling instead of conventional laminar water jet impingement cooling might help to achieve the ultra-high strip cooling rate of SIC.

Investigations involving air and water flow rates and impact-water fluxes within ranges of practical interest to continuous casting (i.e., 5 to 10 g/s (i.e., 3.9 to 7.8 NL/s), 0.3 to 0.6 L/s, and 2 to 90 L/m^2 s, respectively) have shown that the droplet dynamics persist in having an important influence on impaction heat transfer [7-9].

In recent times, Ravikumar et al [10] tested the atomized spray cooling on a plate maintained at the initial surface temperature of 900^{0}C. They concluded that air atomized cooling provides very high cooling rates which lead to produce high strength steels on ROT. Yu Hou et al.[11] experimentally studied on phase change spray cooling. A R22 pressure spray cooling system was designed and built. The system cooling performance was experimentally investigated with the nozzle inlet pressure in the range of 0.6 MPa to 1.0 MPa. Enhancement of cooling rate of an AISI 304 steel plate by air atomized spray cooling with different types of surfactant additives has been studied in the present work. The heat transfer during spray cooling was studied experimentally by Zhen Zhang et al.[12] on one flat and three enhanced surfaces using deionized water for flow rates from 22.2 L/h to 60.8 L/h, orifice-to-surface distances from 0.5 cm to 3.0 cm and spray inclination angles from 0^0 to 45^0. J. Wendelstorf [13]was studied about the heat transfer for spray water cooling of clean surfaces using full cone nozzles (v_d=14 m/s, d_d =350 lm) in the parameter range V_S = 3–30 kg/(m2 s) and surface temperatures between 200 and 1100 ^{0}C were investigated. An additional temperature dependency in the high temperature(Leidenfrost effect) was found. The stable film boiling regime shows an HTC decreasing with temperature difference for VS > 10 kg/(m2 s) and DT above =800 K .The absolute accuracy of the HTC measurement was better than 11% in the film boiling regime.

II. EXPERIMENTAL SET UP

Figure 1 shows the schematic of the experimental setup with details of its components used in the present work. The experimental setup was used to investigate quenching heat transfer with air/water sprays. The test piece consisted of an electrically heated steel sheet of dimension 120 x 120 x 4 mm. A square base electrical coil-heater of 2.5 KW capacity was used to heat the plate to the desired temperature, upper side of which was cooled by the air/water spray being investigated. Three full cone air atomizing nozzles were used to generate the spray. The delivery water pressure from the pump was controlled by pressure regulator. The spray cooling test stand got regulated water and air from the pumping system. The nozzle water output was changed to various combinations of water pressure and air pressure to attain required flow rate of air-water mixture. A simple mechanical patternator was used to measure the local and average water impingement density. The local time-dependent surface temperature distribution was measured on the bottom side embedded with K-type thermocouples at desired locations. For each test four thermocouple data were obtained through the data acquisition system (cRIO) supplied by NI Systems Ltd. The obtained data were processed using LabVIEW software.

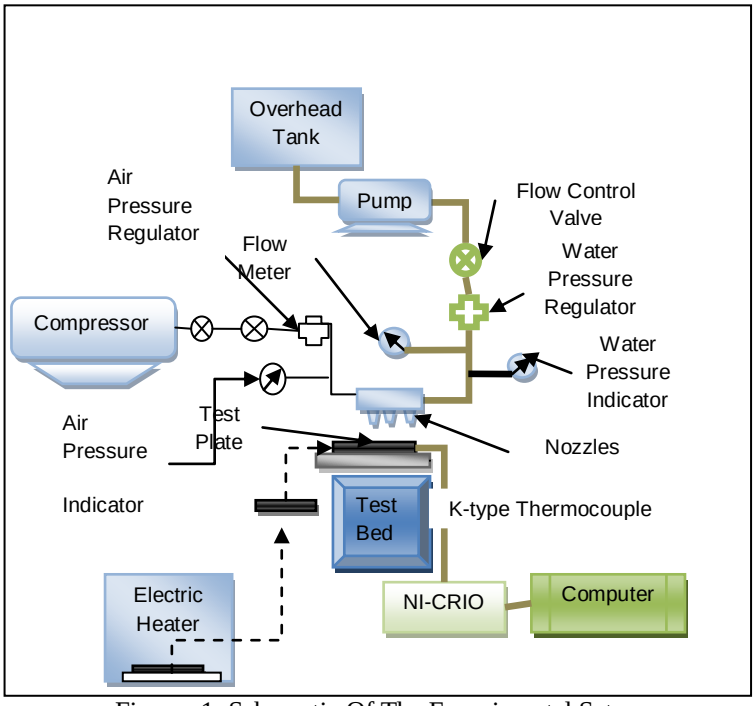

Figure- 1: Schematic Of The Experimental Setup

A sample of thermocouple arrangement on the plate is shown in the following.

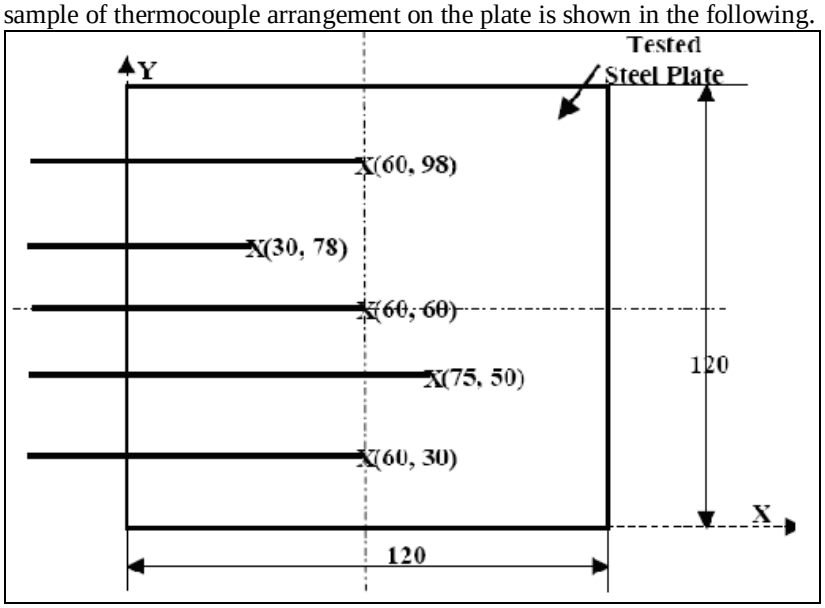

Figure 2. Sketch Of Thermocouple Installation Location

III. EXPERIMENTAL PROCEDURE

The steel plate had to be heated to a temperature slightly higher than the test temperature because some amount of heat would be lost from the heated test plate during the transfer from heater to the test bed. Then this hot steel plate was taken out of the heater and positioned on the test bed (underneath the air atomizing nozzles). While the temperature of the steel plate dropped the required temperature, the spray was turned on and impinged on the hot plate surface. The spray was set at different combinations of air and water pressures. The air pressure ranged from 0.0 bar to 4.0 bar and water pressure varied from 2.0 bar to 4.0 bar. At each combinations of air and water pressure, the water flow rate was recorded directly by using the flow meter during spray impingement cooling. The real time data of temperature history of plate heating and cooling was recorded continuously by

using the NI cRIO DAQ system and supported LabVIEW software. The dimensionless initial temperature differences (ΔT^*) of test plate in these experiments were varied from 16.67 to 30. The nozzle to surface spacing was considered as fixed at 42 mm. In addition to the heat transfer measurement, the local impingement density at various air-water pressure combinations was measured by using the simple mechanical patternator. From the transient time-temperature data obtained in the experiments, the maximum dimensionless cooling rate was computed and recorded for further parametric analysis.

IV. RESULT AND DISCUSSION

Cooling rate is one of the important factors used to determine the rate of heat transfer during a cooling on a hot steel plate by water/air mixture spray cooling. The experimental data obtained concerning the rate of heat transfer has been presented to summarize the behavior of spray impingement cooling processes.

4.1. Effect of the Injection Point and Cooling Curves:

The injection point has great influence on the cooling profile during spray impingement cooling of a flat steel plate. The non-dimensional temperature difference is computed as the ratio of measured temperature difference (ΔT) and cooling water temperature (T_C), while the non-dimensional cooling time is obtained from Equation 1.

$$\Delta T^* = \frac{\Delta T}{T_C} \text{ and } t^* = \frac{l^2}{\alpha} \cdot t \qquad 1$$

The possible influence of the injection point are shown in Figure 3 and figure 4, where the dimensionless plate surface temperature difference (ΔT^*) is plotted with respect to dimensionless cooling time (t^*) for different air pressure and at water pressure of 3bar and 2.5 bar respectively. It is observed from Figure 4 that the central thermocouple shows an interesting cooling trend between dimensionless temperature difference (ΔT^*) and cooling time (t^*) during air-water spray cooling. From the point of injection there is a rapid drop of temperature as the cooling time passing. At different values of air pressure the temperature difference profiles show different trends from which the contribution of air in the spray cooling can easily be identified. It is clear that at combined air and water pressures at 2.0 bar and 3.0 bar, the temperature distribution is sharp while at 3.5 bar air pressure and 3.0 bar water pressure, it is relatively flattened. This is due to the fact that with increase of air pressure to a higher value the atomisation also increases, but the water flow rate decreases, decreasing the heat transfer and the tiny water droplets evaporate before falling on the plate. Thus, the air-water pressure combination is to be optimized to achieve the optimal heat transfer rate, which is also evident from Figure 4. From Figure 4, the cooling effect is clearly understood for air-water mixed spray impingement cooling. In the absence of air (i.e., P_A = 0.0 bar), the convection process is only possible due to water and the dimensionless temperature difference profile greatly changes. It is due to the atomization.

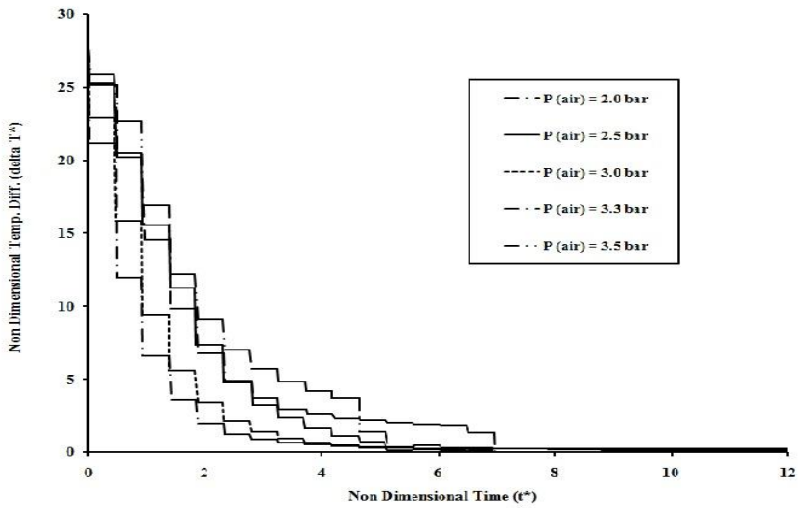

Figure3.Non Dimensional Temperature Difference (Δt^*) Vs. Time (T^*) At Different Air Pressures And 3.0 Bar Water Pressure.

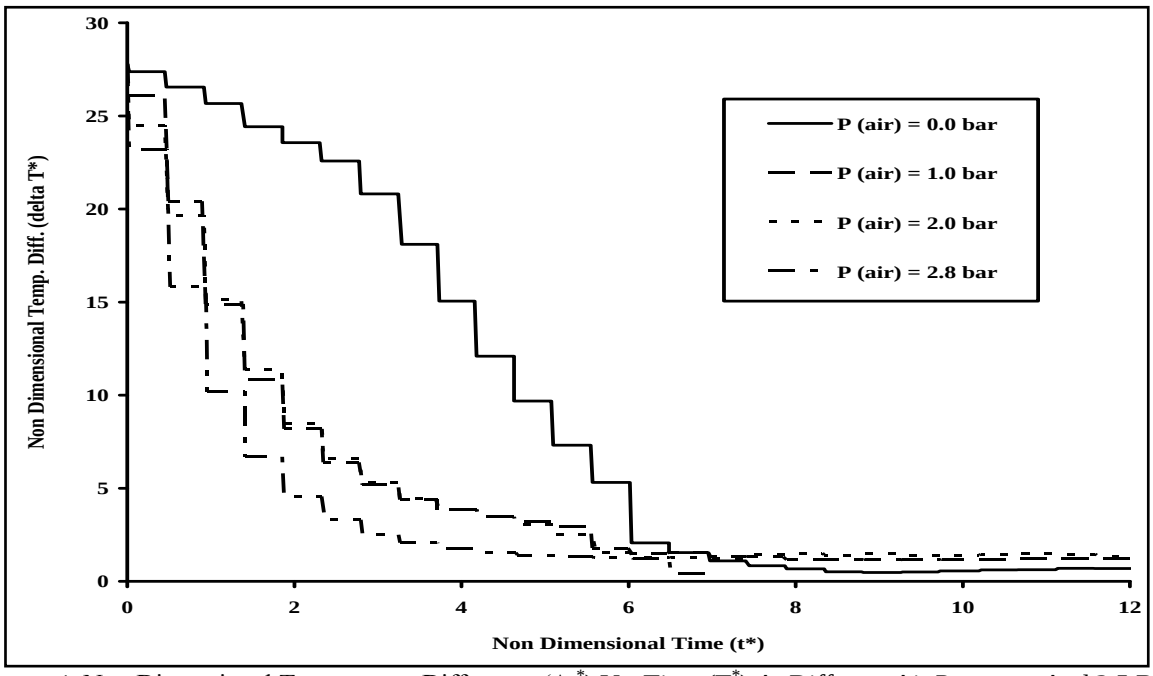

Figure 4: Non Dimensional Temperature Difference (Δt^*) Vs. Time (T^*) At Different Air Pressures And 2.5 Bar Water Pressure.

4.2. Cooling Rate (CR):

From the measured dimensionless time dependent temperature distribution curves at each thermocouple location, the corresponding maximum value of cooling rates were computed by taking the peak values of temperature and time and using Equation 2.

$$CR = \frac{T_2 - T_1}{t_2 - t_1}, {}^0C/Sec \qquad 2$$

Further, the cooling rate in Equation 2 is non-dimensionalized by using Equation 3.

$$CR^* = \left[\frac{\Delta T^*}{t^*}\right] = \frac{l^2}{\alpha \cdot T_C}\left[\frac{\Delta T}{t}\right] \qquad 3$$

The highest and lowest values of dimensionless cooling rate (CR^*) obtained in the experiments were 13.65 and 5.89, respectively.

4.3. Effect of Air/Water Pressure:

Figure 5 shows the effect of air pressure on the dimensionless cooling rates achieved for different fixed water pressures. From Figure 5, it could be observed that the highest value of non dimensional cooling rate (CR^*) obtained for the central thermocouple at the 1.0 bar air and 2.5 bar water pressure combination is 9.104, whereas the highest value of non dimensional cooling rate of central thermocouple at air and water pressure combination of 2.5 bar and 3.0 bar is 14.67. Experimental results reveal that the more is the air pressure, there is a significant change in the cooling rate at a fixed water pressure. Hence, mixing of air with water has a predominant role in enhancing the heat transfer rate from the steel plate surface during spray quenching.

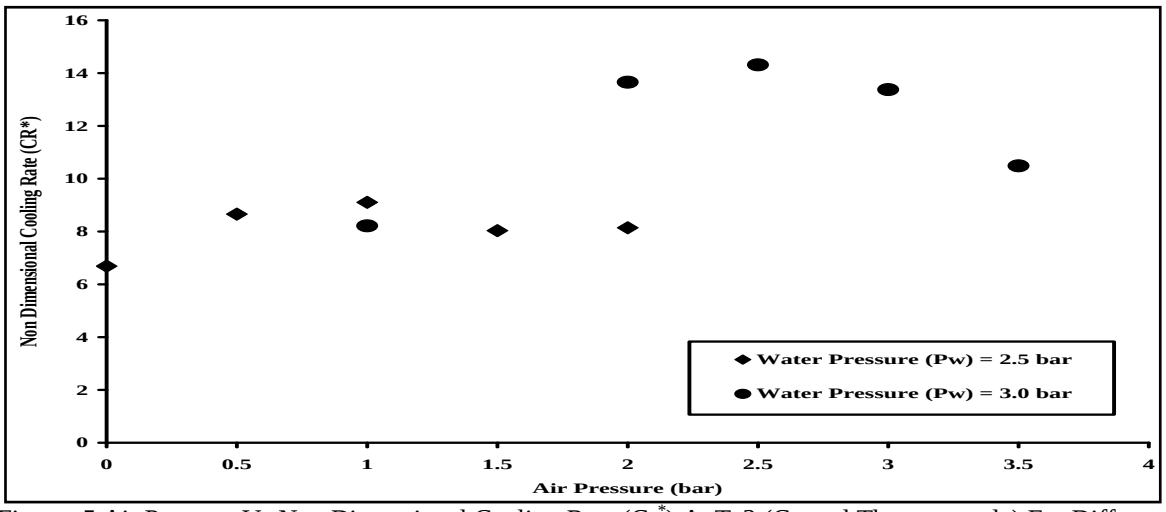

Figure- 5.Air Pressure Vs.Non Dimensional Cooling Rate (Cr^*) At Tc3 (Central Thermocouple) For Different Fixed Water Pressures

As the pressure of the cooling water increased at a constant air pressure, the flow rate of the water increased. The mass flow ratio increased with increasing water pressure or decreasing air pressure.

4.4. Effect of Water Flow Rate:

Figures 6 represent the effect of water flow rates to the dimensionless cooling rates at the location of central thermocouple on the steel plate surface for different water pressure values. From Figure 6, it could be observed that, there was no definite trend between cooling rate and water flow rate. This was because of the fact that in this case cooling was caused both by air flow and water spray. The contribution of both air and water were significant and responsible for cooling effect. Hence water flow rate alone cannot be used to improve the cooling rate. High flow rate in a spray quench accelerates cooling but there still exists the "limit" of the cooling rate in each specific operating condition. The nature of the distribution shows that an optimal value of the dimensionless cooling rate exists. The optimal value of cooling rate can be obtained through optimisation of water flow rate, i.e., optimising the air-water pressure values. The low was the air pressure, the higher water flow rate achieved and less atomization appeared. Whereas, for the very high values of air pressure, the water flow rate values were low and atomization was high. From Figure 6, it is clear that for higher value of water pressure (P_w), the cooling rate was enhanced. In one set of experiments, for a fixed water pressure of 2.5 bar and variation of water flow rate from 300 LPH to 500 LPH, the highest non dimensional cooling rate (CR^*) achieved at the centrally place thermocouple was ranged from 6.68 to 9.1.

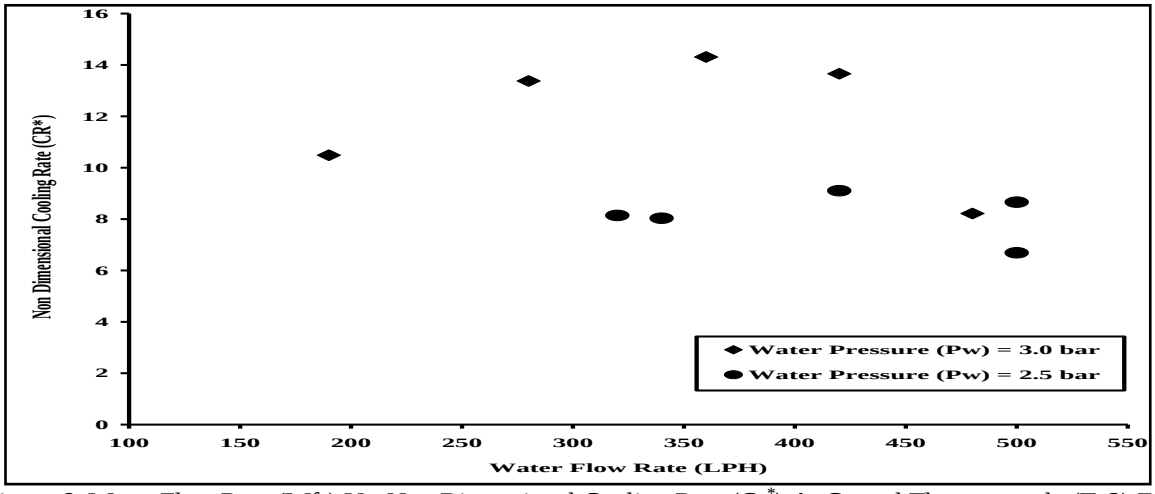

Figure 6: Water Flow Rate (Wfr) Vs. Non Dimensional Cooling Rate (Cr^*) At Central Thermocouple (Tc3) For Different Water Pressures (P_w).

While, in the other set of experiments, with 3.0 water pressure and water flow rate in the range of 190 LPH to 420 LPH, the non dimensional cooling rate (CR^*) obtained was in the range of 10.4 to 13.6. Hence, it can be predicted that the optimal value of cooling rate could be achieved by optimizing the water flow rate during spray cooling through appropriate combination of air and water pressure values.

4.5. Mass Impingement Density :

The liquid mass flux plays major role in metal quenching applications, especially in the heat transfer characteristics investigations during spray cooling. A simple mechanical patternator, the liquid mass flux (or liquid impingement density) was measured at various combinations of the air and water pressures. The local impingement density values were plotted against the tube distances in Figures 7. The measurements were at a constant water pressure and varying air pressure for all the three air atomizing nozzles.

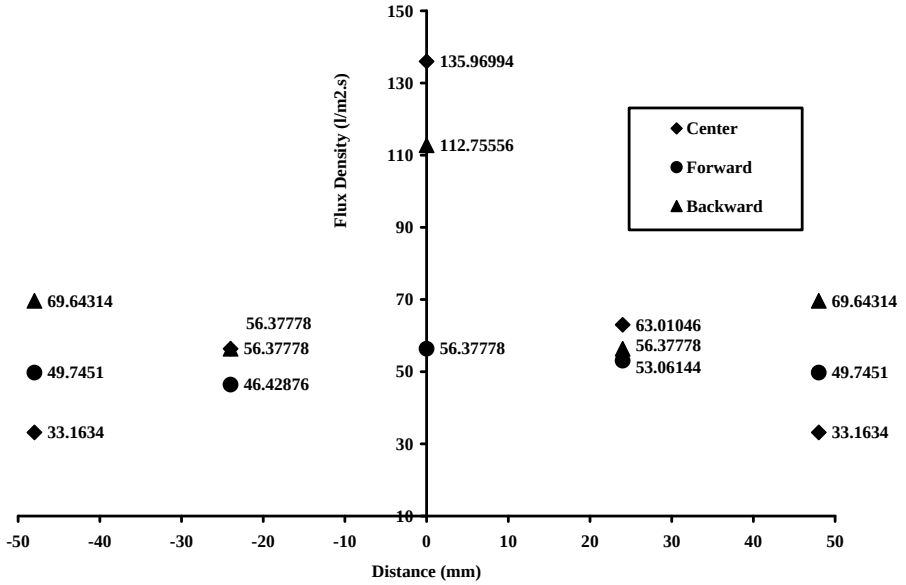

Figure- 7: Local Impingement Density vs. Tube Distance.

It can be seen from above Figures 7 that a bell-shaped profile results with a maximum impingement density at the center of the spray. For constant water flow and increasing air pressure the maximum impingement density decreases. This is because of the fact that at higher air pressure, smaller drops were formed, which followed the airflow better and were thus more dispersed. This led to reduction in impingement density at the plate center. All the results were obtained at three locations, i.e., at the center of the nozzle bank, 15 mm forward and 15 mm backward positions.

1.6. Effect of Spray Impingement Density on Heat Transfer:

Figure 8 presents the data of non-dimensional cooling rate with respect to mean spray density and standard deviation spray density, which show a very clear trend of increasing with mass flux. At low values of mean spray density, this non-dimensional cooling rate is higher for the vertical down spray. Also, at low mean spray density values, the non-dimensional cooling rate at the center location are higher than that at the side location of a downward spray. These observations of orientation and angle of attack effects do not appear in high spray density tests, since the spray impingement is the dominant factor. The cooling characteristics can be well understood by statistical analysis of cooling data.

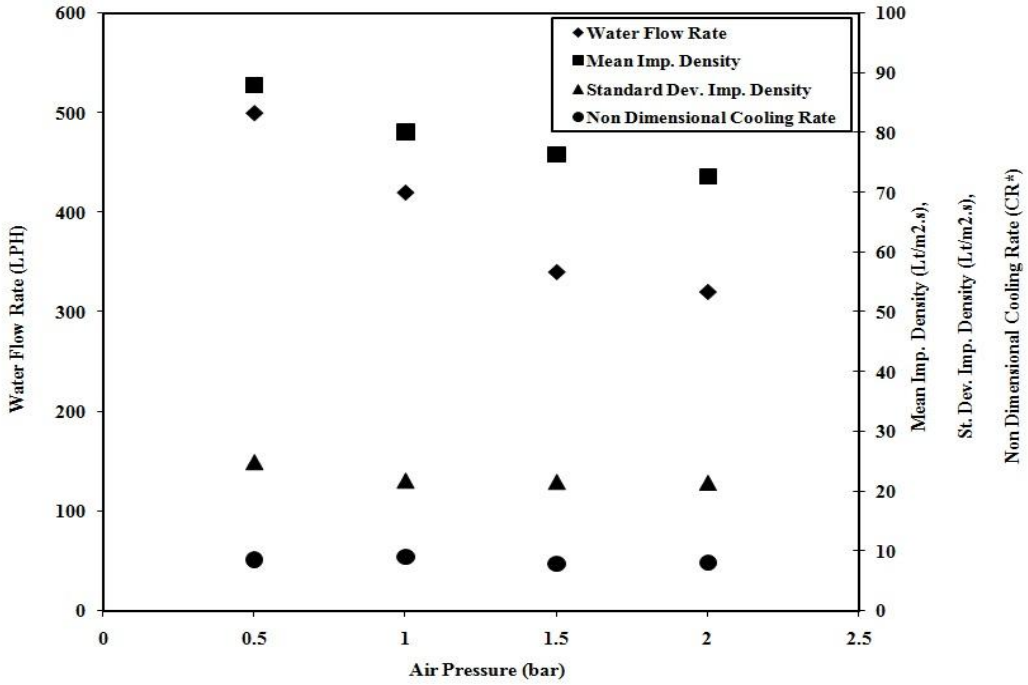

Figure8. Cooling Rate Versus Spray Impingement Density At Fixed Water Pressure = 2.5 Bar.

V. CONCLUSION

A transient method was used for investigating the heat transfer characteristics of atomized air-water spray impingement cooling of flat steel plate with application to the design of impingement cooling facility. Air–water spray impingement cooling was found as an efficient alternative cooling technique over the conventional laminar water jet impingement cooling to achieve the optimal and very high cooling rate. Air assisted double distilled water was chosen as the quenchant. The heat transfer distribution was measured from a multi-droplet array of liquid at varied range of spray flux density.

The heat transfer phenomena of this atomized air-water spray impingement cooling systems, which have been demonstrated, are as follows:

1. The surface temperature profiles provided a better understanding of impingement heat transfer during quenching of high hot steel plate. They also provided more insight for parametric analysis.
2. It is possible to obtain the very high strip cooling rate in a 4 mm thick steel strip by spray impingement cooling provided very small droplet size. These results have a good agreement with the results obtained analytically by Bhattacharya et al. [6].
3. With the variation of air-to-water mass flow ratio, the value of dimensionless cooling rate (CR^*_{max}) accordingly changed but the consistent variation tendencies against either the increase of airflow rate or water flow rate are not found. The optimal selection of water flow ratio of a spray impinging jet for obtaining the maximum heat transfer value thus depends on the airflow rate.
4. For a fixed water pressure and varying air pressure, the cooling rate increases with increase in air pressure at the fixed water pressure.
5. At different combinations of air and water pressures, the higher cooling rate was achieved at the centrally located thermocouple where the local impingement density was maximum.
6. The present cooling technique was found greatly advantageous because, due to contributory effect of air present in the mixture the water consumption was very less and effectively high cooling rate was achievable for Spray cooling.
7. It is believed that at higher spray density, the effect of droplet size or orientation on heat transfer is minimal. The droplet velocity, on the other hand, may have important effect.

REFERENCES

[1] Selvam, R.P., Lin, L., Ponnappan, R. "Direct simulation of spray cooling: Effect of vapor bubble growth and liquid droplet impact on heat transfer".Int. J. Heat Mass Transfer (49) , 2006 , pp- 4265-4278.

[2] Lucas, A., Simon, P., Bourdon, G., Herman, J.C., Riche, P., Neutjens, J.,Harlet, P. "Metallurgical aspects of ultra fast cooling in front of the down-coiler", Steel Research 75 (2), 2004,pp- 139-146.

[3] Herman, J.C. "Impact of new rolling and cooling technologies on thermo-mechanically processed steels", Ironmaking& Steelmaking 28 (2),2001, pp- 159-163.

[4] Akio, F. and Kazuo, O. JFE Technical Report(5), 2005, pp. 10–15 .

[5] Akio, F., Sadanori, I., Yoshimich, H. Toru, M., Yoichi, M., and Shozo, I . EP Patent Application, 2002, EP1210 993 A (1).

[6] Bhattacharya, P., Samanta, A. N., Chakraborty, S . "Spray evaporative cooling to achieve ultra fastcooling in runout table", Int. Journal of Thermal Sciences, 2009,pp- 1–7.

[7] Buyevich, Y.A., and Mankevich, V.N. Int. J. Heat Mass Transfer, vol. 38,1995, pp. 731–44.

[8] Yao, S.C., and Cai, K.Y. Exp. Therm. Fluid Sci., vol. 1, 1988, pp. 363–71.

[9] Jenkins, M.S., Story, S.R., and David, R.H . Proc. 19th Australasian Chem. Eng. Conf., CHEMECA 91, Newcastle, New South Wales, Australia, Sept. 12–20, Institute of Chemical Engineers, North Melbourne, 1991.

[10] Satya V. Ravikumar , Jay M. Jha , IshitaSarkar , Soumya S. Mohapatra , Surjya K. Pal , SudiptoChakraborty . "Achievement of ultrafast cooling rate in a hot steel plate by air-atomized spray with different surfactant additives". Experimental Thermal and Fluid Science (50), 2013, pp-79–89.

[11] Yu Houa, Xiufang Liu , Jionghui Liu , MengjingLi , Liang Pu . "Experimental study on phase change spray cooling". Experimental Thermal and Fluid Science (46), 2013, pp-84–88.

[12] Zhen Zhang , Jia Li , Pei-Xue Jiang ."Experimental investigation of spray cooling on flat and enhanced surfaces". Applied Thermal Engineering (51) ,2013, 102e111 .

[13] 1.J. Wendelstorf *, K.-H. Spitzer, R. Wendelstorf , Spray water cooling heat transfer at high temperatures and liquid mass fluxes, International Journal of Heat and Mass Transfer 51 , 2008, 4902–4910 .

American Journal of Engineering Research (AJER)
e-ISSN : 2320-0847 p-ISSN : 2320-0936
Volume-02, Issue-09, pp-17-22
www.ajer.org

Research Paper Open Access

Corrosion Inhibition Of Mild Steel In 0.5 M H_2so_4 By 1-(2-Methyl-4-(2-Methylphenyldiazenyl) Phenyl) Azonapthalen-2-Ol

S.ANANTH KUMAR[a] Dr.A.SANKAR*[a],S.RAMESHKUMAR[b],
[a]*Kandaswami Kandar's College, P. velur, Namakkal-638 182, India*
[b]*PSG College of Technology Peelamedu, Coimbatore 641 004, India*

Abstract: - The effect of addition of1-(2-methyl-4-(2-methylphenyldiazenyl) phenyl) azonapthalen-2-ol on the corrosion of steel in 0.5M H_2SO_4 acid has been studied by weight loss measurements, potentiodynamic polarization and Electrochemical Impedance Spectroscopy (EIS) measurements. The inhibition efficiency was found to increase with inhibitors content to attain 61.00% and 79.66% 1-(2-methyl-4-(2-methylphenyldiazenyl) phenyl) azonapthalen-2-ol and 25ppm(Tetra butyl ammonium bromide)TBAB respectively. Data obtained from EIS studies were analyzed to determinate the model inhibition process through appropriate equivalent circuit models. Inhibition efficiency E (%) obtained from the various methods is in good agreement.

Key words: - *Inhibitor, 1-(2-methyl-4-(2-methylphenyldiazenyl) phenyl) azonapthalen-2-ol*

I. INTRODUCTION

Acid solutions are often used in industry for cleaning, decaling and pickling of steel structures, processes which are normally accompanied by considerable dissolution of the metal. A useful method to protect metals deployed in service in such aggressive environments against corrosion is the addition of species to the solution in contact with the surface in order to inhibit the corrosion reaction and reduce the corrosion rate. A number of organic compounds [1-8] are known to be applicable as corrosion inhibitors for steel in acidic environments. Such compounds typically contain nitrogen, oxygen or sulphur in a conjugated system and function via adsorption of the molecules on the metal surface, creating a barrier to corrodent attack. To further upgrade the performance of such organic inhibitors, extensive studies have been undertaken to identify synergistic effects of other additives. Interestingly, addition of halide ions to sulphuric acid solutions containing some organic compounds has been reported to yield the required enhancement [1-13]. The inhibitive effects for the halides have been Observed to increase in the order Cl- < Br- < I-, with the iodide ion being the most Effective. It is thought that the initial specific adsorption of the halide ions on the metal surface facilitates the adsorption of organic cations by forming Intermediate bridges between the positively charged metal surface and the positive end of the inhibitor. A few reports from our laboratory highlighted the synergistic effect of halide ions on the corrosion of mild steel in acidic solution [15-17], while the synergistic inhibition between organic compounds and iodide ions has been reported by some research groups [18-22]. However, reports on synergistic influence of halide ions and polymers are very scanty [23, 24]. As part of our contribution to the growing interest of exploring polymeric materials as corrosion inhibitors, the present study investigates the inhibitive effect of 1-(2-methyl-4-(2-methylphenyldiazenyl) phenyl) azonapthalen-2-ol (Sudan-IV) on mild steel corrosion in sulphuric acid, including the synergistic effect of iodide ions using weight loss and potentiodynamic polarization methods.

II. MATERIAL AND METHODS

2.1 Preparation of Stock solution :

1-(2-methyl-4-(2-methylphenyldiazenyl) phenyl) azonapthalen-2-ol (Sudan-IV) was purchased from NICE chemicals.0.1g of sample was dissolved in ethanol, and made up to 100 ml. This solution was used as corrosion inhibitor in the present study.

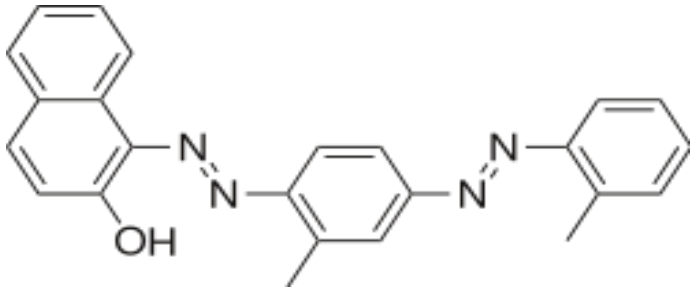

1-(2-methyl-4-(2-methylphenyldiazenyl) phenyl) azonapthalen-2-ol (Sudan-IV)

2.2 Preparation of specimens

Carbon steel specimens (0.022% S, 0.038% Mn, 0.027%P, 0.086 C) of dimension 1.0 cm *4.0cm*0.2cm were polished to a mirror finished with the emery sheets of various grades and degreased with trichloroethylene.

2.3 Weight loss method.

Carbon steel specimens in triplicate were immersed in 100 mL of the inhibited and uninhibited 0.5 M H_2SO_4 solutions two hours. The weight of each specimen before and after immersion was determined using shimadzu balance, model Ay 62.The inhibition efficiency (IE) was then calculated using the expression;

$$IE\% = \left(\frac{W_1 - W_2}{W_1}\right) \times 100 \quad \text{I}$$

Where $W_1$and W_2 are the corrosion rates in the absence and presence of the inhibitor, respectively.

2.4 Electrochemical impedance measurements

The impedance measurements were performed using a computer –controlled potentiostat (model Solartron SI-1260) and the data were analysed using gain phase analyser electrochemical interface (Solartron SI-1287). A three electrode set up was employed with Pt foil as the auxiliary electrode and a saturated calomel electrode as the reference electrode. The Teflon coated mild steel rod, with the surface prepared as described in the weight loss experimental method, served as the working electrode. The measurements were carried out in the frequency range 10^6–10^{-2} Hz at the open circuit potential by superimposing sinusoidal AC signal of small amplitude, 10 mV, after an immersion period of 30 min in the corrosive media. The double layer capacitance (C_{dl}) and charge transfer resistance (R_{ct}) were obtained from the impedance plots as described elsewhere [25]. Because R_{ct} is inversely proportional to corrosion current density, it was used to determine the inhibition efficiency (IE%) using the relationship;

$$IE\% = \frac{Rct - R^{\circ}ct}{Rct} \times 100$$

Where R_{ct} and R^0_{ct} are the charge transfer resistance values in the inhibited and uninhibited solutions respectively.

2.5. Polarization measurements

The potentiodynamic polarization curves were recorded using the same cell setup employed for the impedance measurements. The potentials were swept at the rate of 1.66mV/s, primarily from a more negative potential than E_{ocp} to a more positive potential than E_{ocp} through E_{corr}. The inhibition efficiencies were calculated using the relationship [26];

$$IE\% = \frac{I^{\circ}corr - Icorr}{I^{\circ}corr} \times 100$$

Where I^0_{corr} and I_{corr} are the corrosion current densities in the absence and in the presence of inhibitor, respectively

III. RESULTS AND DISCUSSION

3.1 Analysis of results of mass loss method

The corrosion rates and inhibition efficiency values, calculated using weight loss data, for various concentrations of Sudan-IV solution in 0.5M H_2SO_4 solutions are presented in Table.1. It is apparent that the

inhibition efficiency increased with the increase in inhibitor concentration. This behavior can be explained based on the strong interaction of the inhibitor molecule with the metal surface resulting in adsorption. The extent of adsorption increases with the increase in concentration of the inhibitor leading to increased inhibition efficiency. The maximum inhibition efficiency was observed at an inhibitor concentration of 100 ppm. Generally, inhibitor molecules suppress the metal dissolution by forming a protective film adsorbed to the metal surface and separating it from the corrosion medium. The corrosion suppressing ability of the inhibitor molecule originates from the tendency to form either strong or weak chemical bonds with the lone pair of electrons present on the O and π electrons in benzene ring. It is also seen from table.1 that the Sudan-III at 10 ppm and 100ppm concentrations shows 64.02 % and 81.31 % inhibition efficiencies respectively.

Table1.Corrosion rate (CR) of mild steel in 0.5M H_2SO_4 solutions the absence and presence of inhibitor and the inhibition efficiency (IE) obtained by weight loss method.

Inhibitor concentration (ppm)	**CR (mg cm^{-2} h^{-1})**	**IE %**
0	128.54	-
10	46.24	64.02
25	43.70	66.00
50	27.90	78.29
75	25.42	80.22
100	24.02	81.31

3.2 Electrochemical impedance spectroscopic measurements (EIS)

Impedance spectra obtained for corrosion of mild steel in 0.5 M H_2SO_4 contains a semicircle, representing the interaction of metal surface with the corrosive environment.. The -R(CR) model best describes this situation. The semicircle in the impedance plots contain depressed semicircles with the centre below the real axis. The size of the semicircle increases with the inhibitor concentration, indicating the charge transfer process as the main controlling factor of the corrosion of mild steel. It is apparent from the plots that the impedance of the inhibited solution has increased with the increase in the concentration of the inhibitor. The experimental results of EIS measurements for the corrosion of mild steel in 0.5 M H_2SO_4 in the absence and presence of inhibitor are given in Table 3. Said that sum of charge transfer resistance (R_{ct}) and adsorption resistance (Rad) is equivalent to polarization resistance (Rp).

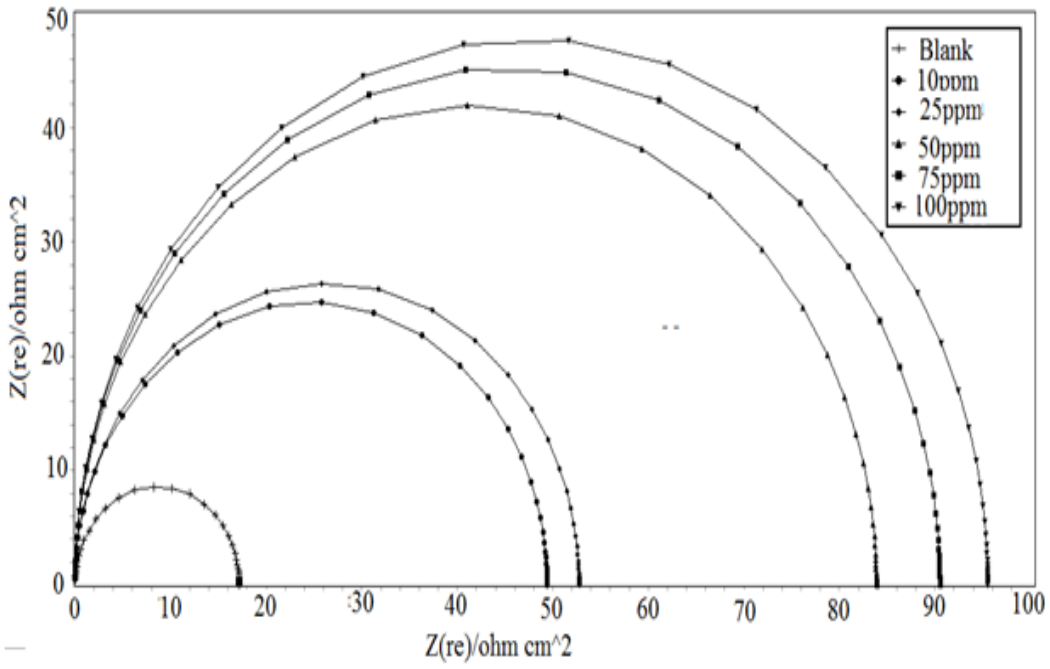

Table 2. Impedance parameters obtained from electrochemical impedance studies.

Inhibitor concentration ppm	Rct Ohm cm^2	C_{dl} µF	IE%
0	17.2	9.2578×10^{-3}	-
10	65.2	2.442×10^{-6}	49.42
25	67.4	2.362×10^{-6}	52.76
50	79.5	2.002×10^{-6}	83.90
75	81.0	1.965×10^{-6}	90.53
100	82.0	1.941×10^{-6}	95.55

3.3. polarization measurements

Fig 2. Potentiodynamic polarization curves of mild steel immersed in 0.5M H_2SO_4 solution in the absence and presence of inhibitors

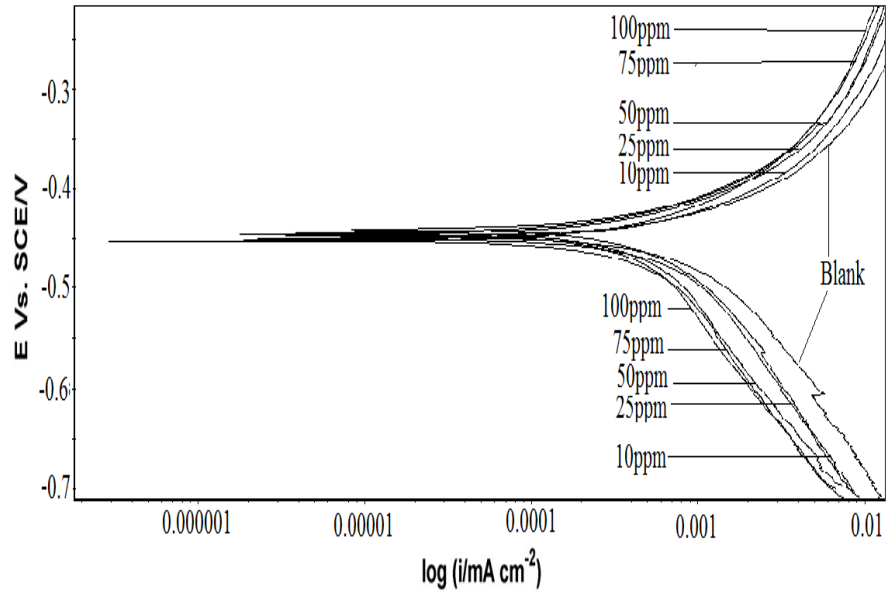

Table. 3 . Corrosion parameters in the presence and absence of inhibitor obtained from polarization measurements.

Inhibitor concentration ppm	$-E_{corr}$ (mV)	β_c (mV/)	β_a (mV)	$I_{corr}\times10*6$ µA	IE%
0	457	127	68	1.35	-
10	450	160	70	0.473	65.0
25	451	163	72	0.446	67.0
50	452	167	75	0.284	79.0
75	453	170	76	0.257	81.0
100	455	172	78	0.246	81.8

The polarization curves obtained for the corrosion of mild steel in the inhibited (100 ppm) and uninhibited 0.5 M H_2SO_4 solutions in Fig.2. Electrochemical parameters such as corrosion potential (E_{corr}), corrosion current density (I_{corr}), cathodic and anodic tafel slopes (β_c and β_a) and percentage inhibition efficiency according to polarization studies are listed in table 3. Here I_{corr} decreased with increasing inhibitor concentration. From the figures, it can be interpreted that the addition of this inhibitor to corrosive media changes the anodic and cathodic tafel slopes. The changes in slopes showed the influence of the inhibitor both in the cathodic and anodic reactions. However, the influence is more pronounced in the cathodic polarization plots compared to that in the anodic polarization plots. Even though β_c and β_a values (table.3) change with an increase in inhibitor concentrations, a high β_c value indicates that the cathodic reaction is retarded to a higher extent than the anodic reaction[27].

From Fig.2 it is also clear that the addition of the inhibitor shifts the cathodic curves to a greater extent toward the lower current density when compared to the anodic curves. The E_{corr} value is also shifted to the more negative side with an increase in the inhibitor concentration. These shifts can be attributed to the decrease in the

rate of the hydrogen evolution reaction on the mild steel surface caused by the adsorption of the inhibitor molecule to the metal surface[28]. It has been reported that a compound can be classified as an anodic and cathodic type inhibitor on the basis of shift of E_{corr} value. If displacement of E_{corr} value is greater than 85 mv, towards anode or cathode with reference to the blank, then an inhibitor is categorized as either anodic or cathodic type inhibitor otherwise inhibitor is treated as mixed type[29,30]. In our study, maximum displacement in E_{corr} value was around 6 mV, indicating the inhibitor is a mixed type and more anodic nature and does not alter the reaction mechanism. The inhibition effect has occurred due to simple blocking of the active sites, thereby reducing available surface area of the corroding metal [31-34].

IV. CONCLUSION

The effect of acid concentration and the effect of addition the 1-(2-methyl-4-(2-methylphenyldiazenyl) phenyl) azonapthalen-2-ol on the corrosion of Mild steel has been studied. The following conclusions may be drawn:

1) The chemical results showed that the corrosion rate of mild steel sample is increase with increasing acid concentrations 10 ppm to 100 ppm

2) The polarization measurements also showed that, the increase of 0.5 M H_2SO_4 concentration leads to displacement of the anodic and cathodic curves to high current densities (I_{corr}.), also increase the corrosion rate will be found.

3) The electrochemical impedance measurements showed that the corrosion of mild steel sample is mainly controlled by charge transfer process.

4) The ethanolic solution of 1-(2-methyl-4-(2-methylphenyldiazenyl) phenyl) azonapthalen-2-ol acts as good inhibitor for the corrosion of mild steel in 0.5 M H_2SO_4 solution.

5) Electrochemical polarization results indicates that the 1-(2-methyl-4-(2-methylphenyldiazenyl) phenyl) azonapthalen-2-ol act as mixed type inhibitor and impedance results showed that the corrosion of mild steel is mainly controlled by a charge transfer process and the presence of 1-(2-methyl-4-(2-methylphenyldiazenyl) phenyl) azonapthalen-2-ol in acid solution does not alter the mechanism of mild dissolution.

V. AKNOWELEDGEMENTS

The authors generously acknowledge the support by Dr.R.Somasundaram M.D., Dr.R.Arul M.Sc.,Ph.D.,Dr.S.Vedanayaki M.Sc.,Ph.D.,President ,Principal and head of the department chemistry respectively of Kandaswami Kandar's college,P.Velur for providing necessary chemical and lab facilities to carry out chemical studies..

REFERENCES

[1] J. Mathiyamsu, I.C. Nebru, P. Subramania, N. Palaniswamy, N.S.Rengaswamy, *Anticorros. Methods & Mater.* 48 (5) ,2001, 342.
[2] N. Ochao, F. Moran, N. Pebre, *J. Appl. Electrochem.* 34 ,2004, 487.
[3] E.E. Oguzie, C. Unaegbu, C.N. Ogukwe, B.N. Okolue, A.I. Onuchukwu,*Mater. Chem. Phys.* 84 ,2004, 363.
[4] E.E. Oguzie, *Mater. Chem. Phys.* 87 ,2004, 212.
[5] S. Rajendran, R. Maria Joany, B.V. Apparao, N. Palaniswamy, *Trans.SAEST* 35 (3/4) ,2000, 113.
[6] S. Rajendran, B.V. Apparoa, N. Palaniswamy, *Anticorros. Methods &Mater*. 44(5) ,1998, 338.
[7] M.N. Shalaby, M.M. Osman, *Anti-corros. Methods Mater*. 48(5) ,2001,309.
[8] E.E. Ebenso, *Mater. Chem. Phys.* 79 ,2003, 58.
[9] E.E. Ebenso, *Bull. Electrochem.* 19 (5) ,2003, 209.
[10] E.E. Ebenso, *Bull Electrochem.* 20 (12) ,2004, 551.
[11] G.K. Gomma, *Asian J. Chem*. 5 (3) ,1993, 761.
[12] G.K. Gomma, *Mater. Chem. Phys*. 54 ,1998, 241.
[13] D. Gopi, N. Bhauvanerwaran, S. Rajewari, *Bull. Electrochem.* 18 (1) ,2002,120.
[14] E. Kalman, I. Lukovits, G. Palinkas, *ACH Models Chem.* 132 (4) ,1995,527.
[15] E.E. Ebenso, U.J. Ekpe, S.A. Umoren, E. Jackson, O.K. Abiola, N.C.Oforka, *J. Appl. Polym . Sci.* 100(4) ,2006, 2889.
[16] S.A. Umoren, O. Ogbobe, E.E. Ebenso, U.J. Ekpe, *Pigment & Resin Tech.*35(5) ,2006, 284.
[17] S.A. Umoren, O. Ogbobe, E.E. Ebenso , *Bull. Electrochem.* 22(4) ,2006,155.
[18] M. Bouklah, B. Hammouti, A. Aounti, M. Benkaddour, A. Bouyanzer,*Appl. Surf. Sci.* 252 ,2006, 6236.
[19] Y. Feng, K.S. Siow, W.K. Teo, A.K. Hsieh, *Corros. Sci.* 41 ,1999, 829.
[20] M. Abdallah, E.A. Helal, A.S. Fouda, *Corros. Sci.* 48 ,2006, 1639.
[21] M.A. Quraishi, J. Rawat, *Mater. Chem. Phys.* 70 ,2001, 95.
[22] D.Q. Zhang, L.X. Gao, G.D. Zhou, J. *Appl. Electrochem.* 33 ,2003, 361.

[23] L. Larabi, Y. Harek, *Portugaliae Electrochim. Acta* 22 ,2004, 227.
[24] L. Larabi, Y. Harek, M. Traisnel, A. Mansri, *J. Appl. Electrochem.* 34,2004, 833
[25] Ashassi-Sorkhabi.H,.Shaabani.B,Seifzadeh.D, Electrochim.Acta,50, 2005,3446.Shahin.M, Bilgie.S, Yilmaz.H, *Appl. Surf. Sci*. 195, 2003,1.
[26] Silverman D. C., "*Practical Corrosion Prediction Using Electrochemical Techniques*", ch. 68 *in Uhlig's Corrosion Handbook, 2nd edition* (Revie,.R.W, ed.), *The Electrochemical Society*, 2000.
[27] Prabhu., T.V. Venkatesha, A.V. Shanbhag. Praveen. B.M, Kulkarni. G.M,.Kalkhambkar R.G, *Mater. Chem. Phys.* 108 , 2008,283
[28] Sanghvi. R.A, M.J., et al., *Bull. Electrochem.* 13, 1999, 358.
[29] Felicia Rajammal Selvarani, S.Santhanalakshmi, J. Wilson sahayaraja, A. John Amalraj,and Susai Rajendran , *Bull. Electrochemistry*. 20 , 2004, 561-565.
[30] Susai RajendranS. Mary Reenkala, Noreen Anthony and Ramaraj,R. *Corros Sci*, 44, 2002, 2243-2252.
[31] Scully. J. R., "*Polarization Resistance Method for Determination of Instantaneous Corrosion Rates*", *Corrosion, Vol.*,56, *2000* p. 199.
[32] Kumaravel Mallaiyaa, Rameshkumar Subramaniama, Subramanian Sathyamangalam Srikandana,S. Gowria, N. Rajasekaranb, A. Selvaraj,*Electrochimica Acta* 56 , 2011,3857–3863
[33] Ananth Kumar.S, Sankar.A, and Ramesh Kumar.S.,. *International Journal of Chemistry and Chemical Engineering*. Volume 3, Number 1(2013), pp. 7-14

American Journal of Engineering Research (AJER)
e-ISSN : 2320-0847 p-ISSN : 2320-0936
Volume-02, Issue-09, pp-23-30
www.ajer.org

Research Paper Open Access

Enhancing the Bandwidth of a Microstrip Patch Antenna using Slots Shaped Patch

Atser A. Roy, Joseph M. Môm, Gabriel A. Igwue
Department of Electrical and Electronics Engineering, University of Agriculture, Makurdi, Nigeria

Abstract: - In this work, three different geometry shapes, the U, E and H are developed from a rectangular patch of the width (W) = 32mm and length (L) = 24mm. The proposed antennas are simulated using Sonnet software and the results compared with the conventional rectangular patch antenna. The results obtained clearly show that, bandwidth of conventional rectangular microstrip antenna can be enhanced from 4.81% (100MHz) to 28.71% (610 MHz), 28.89% (630MHz) and 9.13% (110MHz) respectively using U, E and H-patch over the substrate. The E-shaped patch antenna has the highest bandwidth followed by U-shaped patch antenna and H-shaped patch antenna. The substrate material used for the proposed antennas is Alumina 96%, with the dielectric constant of 9.4 and loss tangent of 4.0e-4. The proposed antennas may find applications in Wireless Local Area Network (WLAN).

Keywords: - *bandwidth, dielectric constant, microstrip antenna, slot patch, substrate*

I. INTRODUCTION

Communication can be broadly defined as the transfer of information from one point to another [1]. Communication between human beings was first done through voice. With the desire to increase the distance of communication, devices such as Drums, signal flags and smoke were used. These optical communication devices of course utilized the light part of the electromagnetic spectrum. It has been of recent in human history that the electromagnetic spectrum, outside the visible region has been employed for communication, through the use of Radio. One of the greatest human scientific evolutions is the emergence of electromagnetic spectrum and antenna has been instrumental in harnessing the resource. Through the years, microstrip antenna structures are most common option used to realize millimeter wave monolithic integrated circuits for microwave, radar and communication purposes. The shape and operating mode of the patch are selected, designs become very versatile in terms of operating frequency, polarization, pattern and impedance [2].

Microstrip patch antenna consists of a radiating patch which is generally made of conducting material such as gold or copper and can take any possible shape. The radiating patch and the feed lines are usually photo etched on the dielectric substrate which have a ground plate as shown in Fig. 1.

In order to simplify analysis and performance prediction, the patch is generally square, rectangular, circular, triangular, and elliptical in shape.

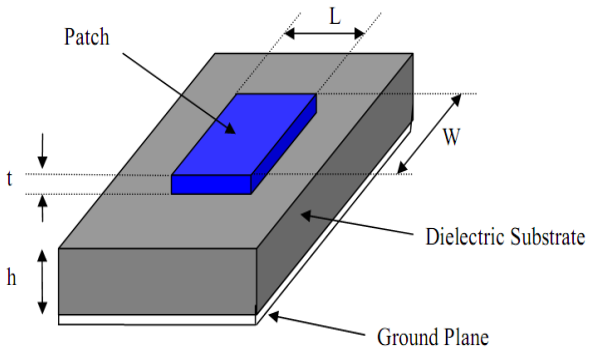

Figure 1. Structure of a microstrip patch antenna

For a rectangular patch, the length L of the patch is usually $0.333\lambda o < L < 0.5\lambda o$, where λo is the free space wavelength. The patch is selected to be very thin such that the patch thickness $t << \lambda o$. The height h of the dielectric constant of the substrate (ε_r) is typically in the range $2.2 \leq \varepsilon r \leq 12$. The microstrip patch antennas radiate primarily because of the fringing fields between the patch edge and the ground plane. For good antenna performance, the choice of substrate used is an important factor. There are numerous substrates that can be used for the design of microstrip antennas within the dielectric constants range of $2.2 \leq \varepsilon r \leq 12$. The low dielectric constant εr is about 2.2 to 3, the medium around 6.15 and the high approximately above 10.5[1].

A thick dielectric substrate having a low dielectric constant is desirable since this provides better efficiency, larger bandwidth and better radiation. However, such a configuration leads to a larger antenna size. In order to design a compact microstrip patch antenna, substrate with higher dielectric constants must be used which are less efficient and result in narrower bandwidth. Hence a trade-off must be realized between the antenna dimensions and antenna performance [3].

II. DESIGN METHODOLOGY

2.1 Design Equations

The effective dielectric constant ε_{eff} is given as

$$\varepsilon_{eff} = \frac{\varepsilon r + 1}{2} + \frac{\varepsilon r - 1}{2}\left(1 + \frac{12h}{w}\right)^{-1/2} \quad (1)$$

Where, εr = Dielectric constant, h = height of dielectric substrate, w = width of the patch.
The Hammerstad formula for the fringing extension is [4]

$$\frac{\Delta L}{h} = 0.412\left[\frac{(\varepsilon eff + 0.3)\left(\frac{W}{h} + 0.264\right)}{\varepsilon eff - 0.258)(\frac{W}{h} + 0.8)}\right] \quad (2)$$

The effective length of the patch L_e now becomes

$$L_e = L + 2\Delta L \quad (3)$$

The resonance frequency f_o for the (1, 0) mode is given by

$$f_0 = \frac{c}{2L_e\sqrt{\varepsilon_r}} \quad (4)$$

Where C is the speed of light.

2.2 Feeding Techniques

Microstrip patch antennas can be fed by a variety of methods. These methods can be classified into two categories-contacting and non-contacting methods. The RF power is fed directly to the radiating patch using a connecting element such as a microstrip line. In the non-contacting scheme, electromagnetic field coupling is done to transfer power between the microstrip line and the radiating patch [2]. The four most popular feed techniques used are the microstrip line, coaxial probe (both contacting schemes), aperture coupling and proximity coupling (both non-contacting schemes).

2.3 Method of Analysis

There are many methods of analysis for microstrip antenna. The most popular models are the transmission-line, cavity and full-wave. The transmission-line model is the easiest of all, it gives good insight and it is adequate for most engineering purposes and requires less computation. However, it is less accurate. The cavity model is more accurate and gives good physical insight but is complex [5]. The full-wave models are very accurate, very versatile, and can treat single elements, finite and infinite arrays, stacked elements, arbitrary shaped elements and coupling. However, they are the most complex models and usually give less physical insight.

2.4 Bandwidth

The most serious limitation of the microstrip antenna is its narrow *BW*. The bandwidth could be defined in terms of its *VSWR* or input impedance variation with frequency or in terms of radiation parameters. For the circularly polarized antenna, bandwidth is defined in terms of the Axial Ratio. *VSWR* is a very popular parameter for determining the bandwidth of a particular antenna configuration ($1 \leq VSWR \leq 2$) as an acceptable

interval for determining the bandwidth of the antenna. Bandwidth is presented more concisely as a percent where

$$\%BW = \frac{\Delta f}{f_o} \times 100 \quad (5)$$

Where Δf is the width of the range of acceptable frequencies, and f_o is the resonant frequency of the antenna [6]. The expressions for approximately calculating the percentage BW of the (RMSA) antenna in terms of patch dimensions and substrate parameters is given by [7].

$$\%BW = \frac{A \times h}{\lambda o\sqrt{\varepsilon r}}\sqrt{\frac{W}{L}} \quad (6)$$

Where A is constant, and can take the values 180, 200 and 220.
for A = 180

$$\frac{h}{\lambda o\sqrt{\varepsilon r}} \leq 0.045$$

for A = 200

$$0.045 \leq \frac{h}{\lambda o\sqrt{\varepsilon r}} \leq 0.075$$

for A = 220

$$\frac{h}{\lambda o\sqrt{\varepsilon r}} \leq 0.07$$

With an increase in *W*, bandwidth increases. However, *W* should be taken less than λ to avoid excitation of higher order modes. The *BW* of the *MSA* can also inversely proportional to its quality factor Q and is given by [3].

$$BW = \frac{VSWR - 1}{Q\sqrt{VSWR}} \quad (7)$$

The *BW* is usually specified as frequency range over which *VSWR* ≤ 2. However, in recent years considerable effort has been spent to improve the bandwidth of the microstrip antenna, in part by using alternative feeding schemes [8].

2.5 Return Loss

The return loss is another way of expressing mismatch. It is a logarithmic ratio measured in *dB* that compares the power reflected by the antenna to the power that is fed into the antenna from the transmission line. The relationship between *VSWR* and return loss is as follows [9].

$$Return\ loss\ (in\ dB) = 20log_{10}\left(\frac{VSWR}{VSWR - 1}\right) \quad (8)$$

III. ANTENNA DESIGN AND ANALYSIS

The designed parameters for the proposed patch antenna were calculated using (1) – (4) and presented Table 1.

TABLE 1: Antenna Parameters

Frequency of operation f_o	2GHz
Height of Substrate (h)	2mm
Dielectric constant (ε_r)	9.4
Width of the Patch (W)	32mm
Length of the Patch (L)	24mm
Loss Tangent	4.0e-4

The proposed antenna is to be used for the wireless local area network (WLAN). The antenna is to operate in the frequency range from 1GHz to 3GHz. The dielectric material selected is Alumina 96% which has a dielectric constant of 9.4. The dielectric constant is kept high in order to get a reduced antenna size. The objective is to get an improve bandwidth from the conventional rectangular patch since the higher dielectric substrate results in size reduction at the expense of bandwidth reduction.

In this design, we have proposed three different geometry shapes the U, H and E from a patch of width (W) = 32mm and length (L) =24mm. The three proposed antennas are simulated using Sonnet software, under the same conditions and results compared with the conventional rectangular patch antenna, and the shape with improve bandwidth is adopted, and implemented. The bandwidth was obtained where return loss is less than -10dB which is an acceptable level to describe the loss of the power which reflects back from the antenna without being radiated.

Fig. 2, shows the geometry of conventional rectangular microstrip antenna (RMSA). The antenna is designed for the resonance frequency of 2GHz. It consists of radiating patch of length *L* and width *W*.

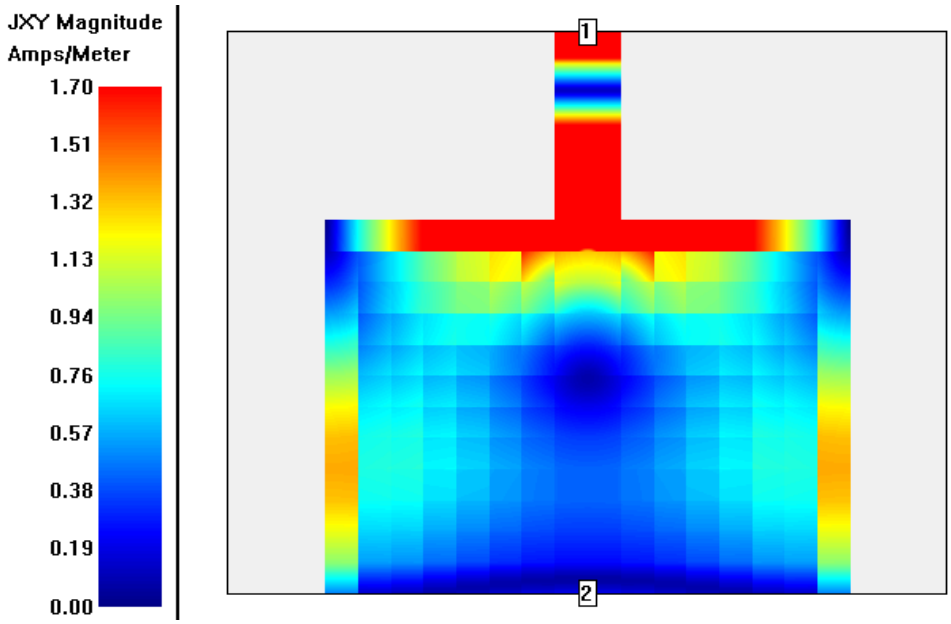

Figure 2. Rectangular Patch shape with Current distribution and feed points

Fig. 3, shows the geometry of E-shaped radiating patch fabricated from the rectangular patch.

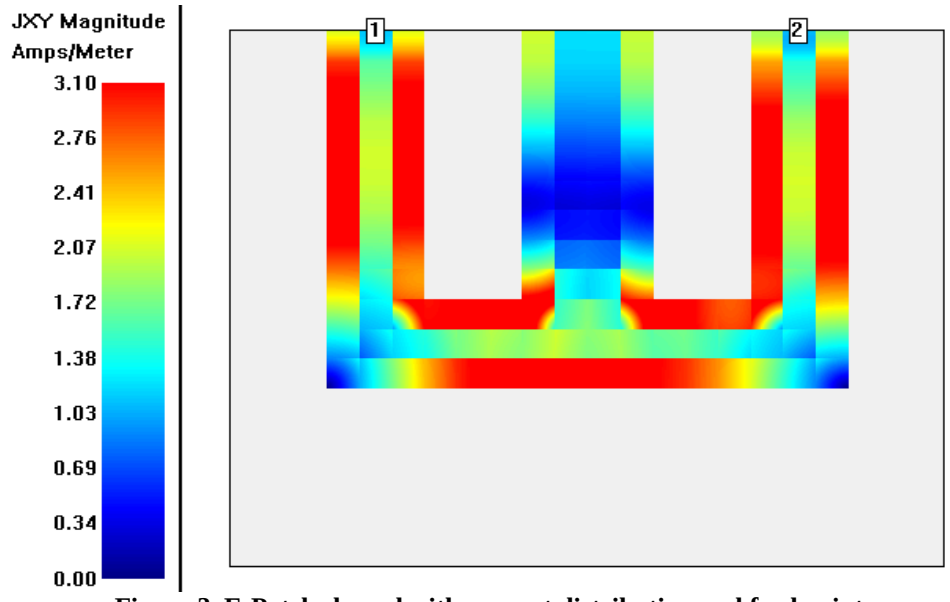

Figure 3. E-Patch shaped with current distribution and feed points

U and H are also fabricated from the same patch size as shown in Fig. 4 and Fig. 5 respectively.

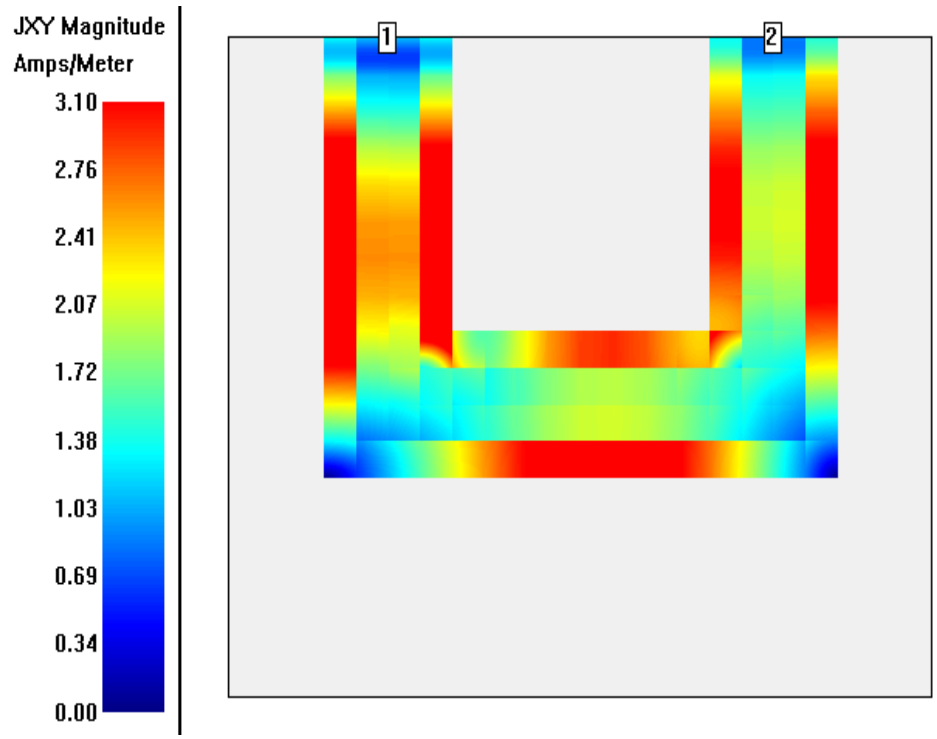

Figure 4. U- Patch shape Antenna with Current distribution and feed points

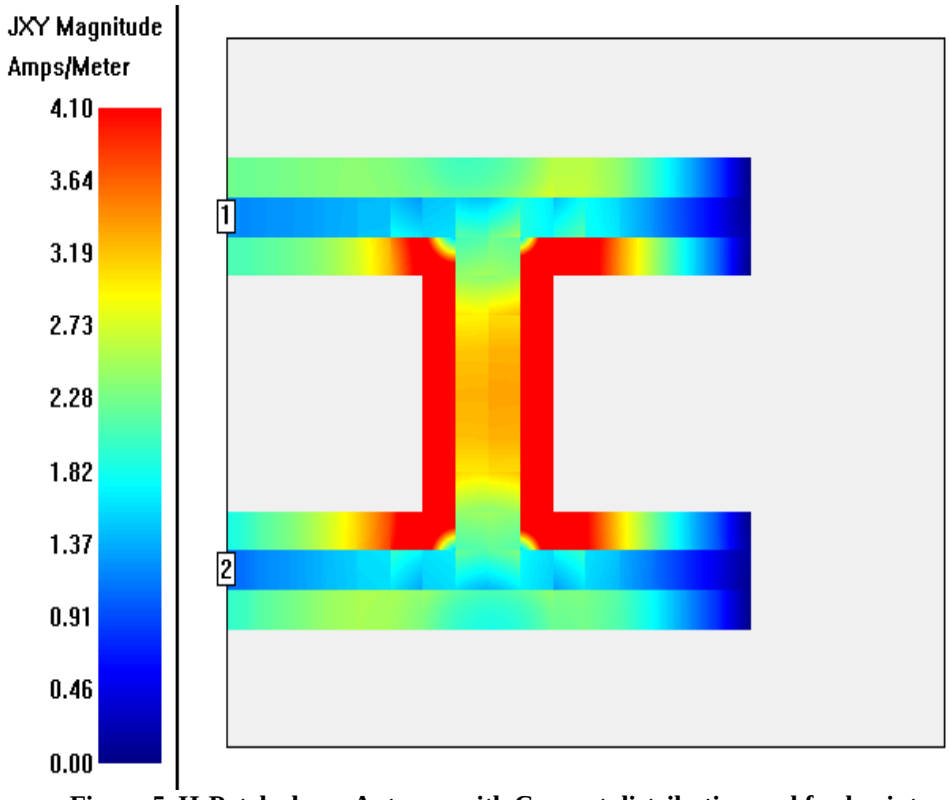

Figure 5. H-Patch shape Antenna with Current distribution and feed points

Fig. 6, shows the variation of return loss versus frequency plot of RMSA resonate at 2.1 GHz of frequency which is close to the designed frequency of 2GHz.

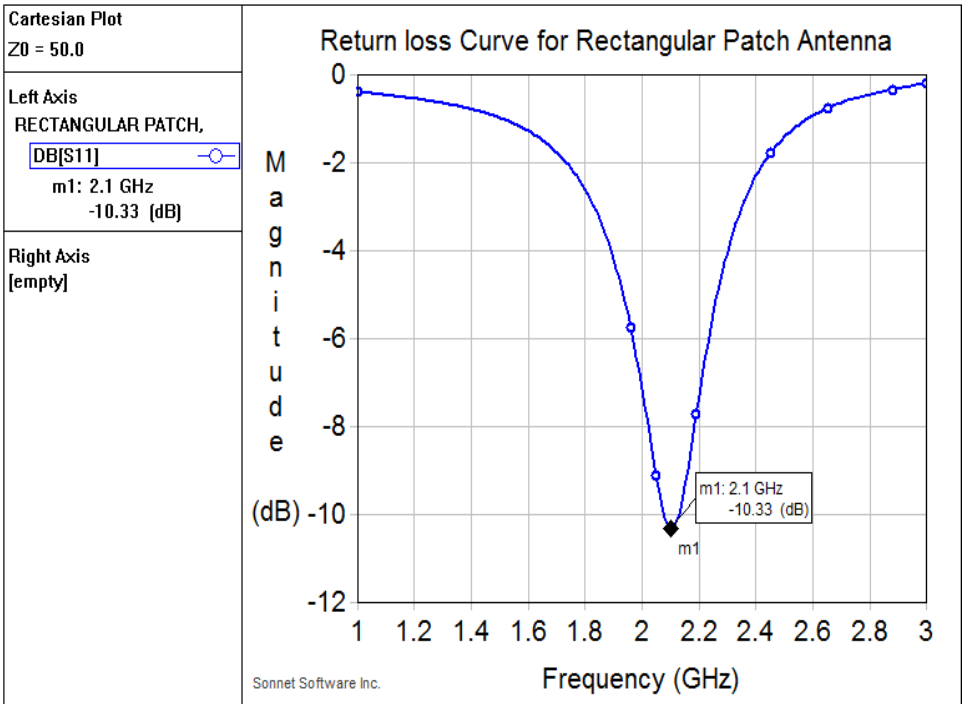

Figure 6. Simulated Return loss of Rectangular patch Antenna

From the graph, the experimental bandwidth is calculated using the formula

$$\%BW = \frac{U_f - L_f}{C_f} \times 100 \qquad (9)$$

Where, U_f and L_f are upper and lower cut-off frequencies of the bandwidth respectively when its return loss reaches -10dB and C_f is the center frequency between U_f and L_f.

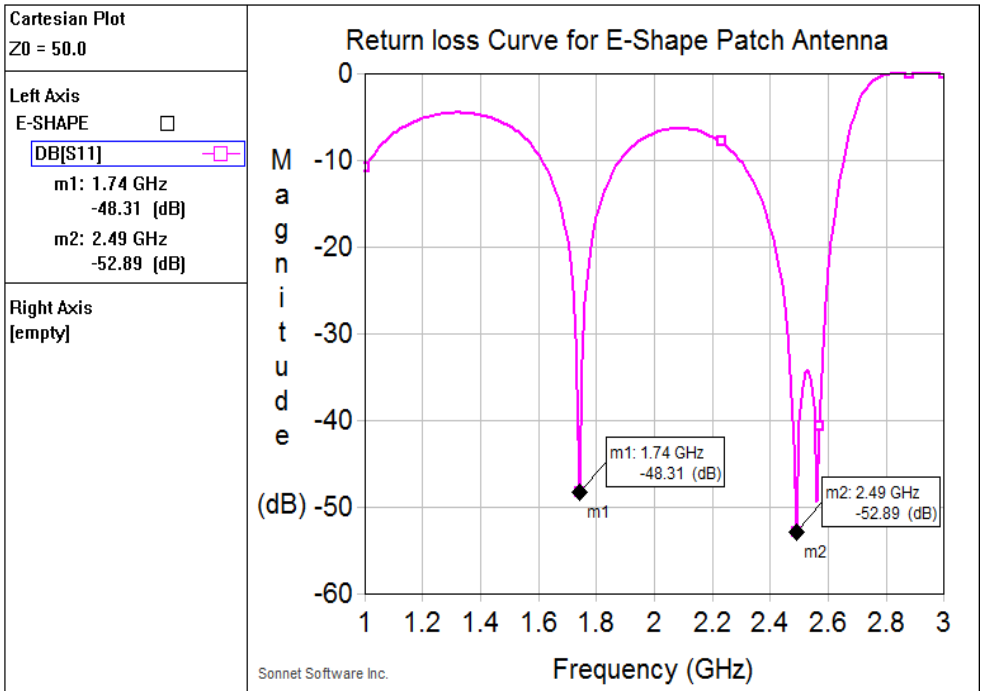

Figure 7. Simulated Return loss of E-patch Antenna

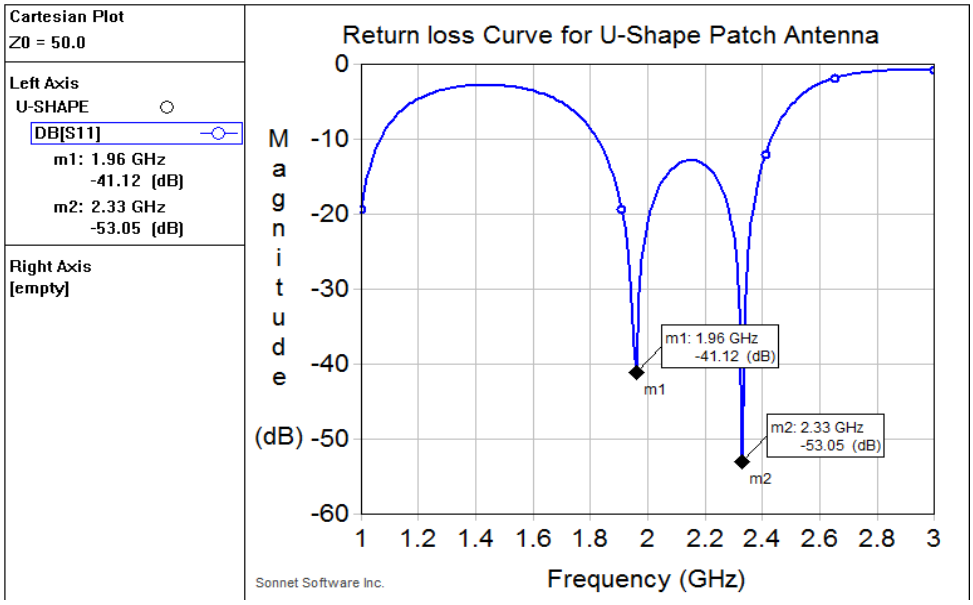

Figure 8. Simulated Return loss of U- shape Antenna

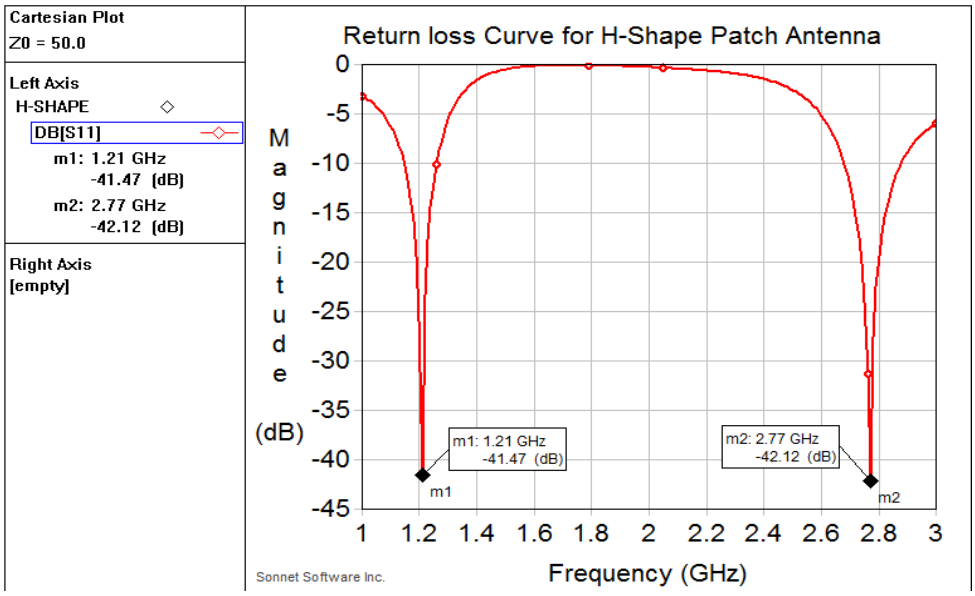

Figure 9. Simulated Return loss of H-shaped patch Antenna

The percentage bandwidth of the conventional RMSA is found to be 4.81% with bandwidth of 100MHz.The expressions for approximately calculating the percentage bandwidth of the RMSA in terms of patch dimensions and substrate parameters is given by [7].

$$\%BW = \frac{A \times h}{\lambda o \sqrt{\varepsilon r}} \sqrt{\frac{W}{L}} \qquad (7)$$

Where, A is constant, which is found to be 180 [7]. The BW calculated using equation (6) is 4.52% which is not too far from experimental result.

Figure 6, shows the variation of return loss versus frequency of E- shape patch antenna. The antenna resonates at two bands of frequencies 1.74GHz and 2.49GHz. This development is as a result of the slots. The overall bandwidth at (1.74GHz and 2.49GHz) is found to be 28.89% (that is 630MHz).

Figure 7, shows the variation of return loss versus frequency of U-shaped patch antenna. The antenna resonates at two bands of frequencies at 1.96GHz and 2.33GHz, due to the U-slots. The overall bandwidth is 28.71 (that 610MHz).

Figure 8, shows the variation of return loss versus frequency of H- shape patch antenna. The antenna resonates at two bands of frequencies at 1.21GHz and 2.77GHz. The overall bandwidth is 9.13% (that is 110MHz).

This clearly shows that slot can be either resonant or non-resonant. If it is resonant, the current along the edges of the slot introduces additional resonances near the patch resonance, adding them together causes enhancement in the bandwidth.

Figure 6 and figure 7 give the highest bandwidth of 28.89% (630MHz) and 28.71% (610MHz) which is more than bandwidth of conventional RMSA. This further enhancement in bandwidth when compare to RMSA is as a result of insertion of slots used for the construction of E and U-shaped patches. The current along the edges of the slot induces an additional resonance, which adds to the fundamental resonance of the radiating element that helps to increase bandwidth [10].

IV. CONCLUSION

In this work, the aim was targeted at improving the bandwidth of microstrip antennas constructed with dielectric material with higher dielectric constant. We have selected three different patch antennas and the simulated results compare with the conventional microstrip patch antenna. The results obtained clearly show that bandwidth of conventional RMSA made with dielectric substrates having higher dielectric constants can be improved using U and E-shaped patch antenna. We have observed that E-shaped patch antenna has the highest bandwidth follow by U-shaped patch antenna and H-shaped antenna.

REFERENCES

[1] K.T Ahmed, M. B Hossain and M.J Hossain, "Designing a high bandwidth patch Antenna comparison with the former patch Antenna" Canadian journal on multimedia and wireless network Vol.2, No. 2 April,2011.

[2] S.K Behera, "Novel Tuned Rectangular Patch Antenna as a load for phase power combining" Ph.D Thesis, Jadavpur University, Kolkata, India.

[3] C. A Balanis, "Antenna Theory Analysis and Design" Wiley, 2nd edition, chapter 14. 1997

[4] J. R James and P. S Hall, "Handbook of microstrip Antennas" Volume 2. Peter Peregrinus Ltd, London, 1989.

[5] H. Pues and A. V Capelle, "Accurate transmission-line model for the rectangular microstrip antenna, "Proc. IEEE, vol. 131, no.6, pp. 334-340, December 1984.

[6] I. J. Bahl and P. Bhartia, "Microstrip Antenna" Artech House, 1980.

[7] K. P Ray, "Broadband, dual-frequency and compact microstrip Antennas" Ph.D Thesis, Indian Institute of Technology, Bombay, India, 1999.

[8] D. R Jackson and J .T Williams, "A comparison of CAD models for radiation from rectangular microstrip patch," Intl. Journal of microwave and millimeter-wave computer Aided Design, vol 1, no.2 pp.236-248, April 1991.

[9] http://wireless.ictp.it/handbook/C4.pdf

[10] G. Z Rafi and L. Shafai, "wider band V-slotted diamond-Shaped microstrip patch antenna, "Electronics letters, vol. 40, no. 19, 1166-1167, 2004.

[11] H. Zewdu, "comparative study on bandwidth enhancement techniques of microstrip patch antenna," Research publications report, Addis Ababa University, January 2008.

American Journal of Engineering Research (AJER)
e-ISSN : 2320-0847 p-ISSN : 2320-0936
Volume-02, Issue-09, pp-31-36
www.ajer.org

Research Paper Open Access

The Effects of Propagation Environment on Cellular Network Performance

Joseph M. Môm[1], Nathaniel S. Tarkaa[1] And Cosmas I. Ani[2]
[1]*Department of Electrical and Electronics Engineering, University of Agriculture, Makurdi, Nigeria*
[2]*Department of Electronic Engineering, University of Nigeria, Nsukka*

Abstract: - In this paper, the effects of the propagation environment are analyzed for an operative GSM network in terms of the following traffic-related parameters: call arrivals (number of call attempts), traffic intensity; call duration; drop-call probability; channel availability; and utilization factor. Four diverse geographical areas were selected for the study with each assumed as representing a separate propagation environment. Starting from performance data obtained from the said network, the stated parameters were either used directly or statistically evaluated for MSC centers from the four geographical areas. The results showed significant variations in these parameters, from one region to another.

Keywords: - *Call Arrivals, Traffic Intensity, Call Duration, Drop-call Probability, Channel Availability, Utilization Factor, MSC, Propagation.*

I. INTRODUCTION

Cellular networks involve radio and wire line links as well as switching hardware, software, and database operations. However, in the most part, it is the performance of the radio network that determines service quality [5]. The radio network is the part of the network that includes the base station otherwise known as Base Transceiver Station (BTS) and the Mobile Station (MS) and the interface between them. As this is the part of the network that is directly connected to the mobile user, it assumes considerable importance. The BTS should be capable of communicating with the mobile station within a certain coverage area and maintaining call quality standards [4]. There are three critical factors that impact the performance of both voice and data networks: radio frequency (RF) signal level (in both uplink and downlink; level of radio interference (also in both uplink and downlink); and available radio channel capacity [4], [9].

To provide any sort of service, the Received Signal Strength Indicator (RSSI) of both uplink and downlink transmissions must be sufficiently above the level of thermal RF noise to allow for successful recovery of the modulated information stream. The ratio of the desired RF carrier signal power to the linear sum of interference power is called C/I [5], [15].

As in the case of marginal RSSI, the required C/I to support voice service in GSM networks is fairly defined while the adaptive coding in GPRS causes data throughput rates to vary over a substantial range of C/I [5].

Traditionally, wireless operators have used a number of metrics that collectively provide a measurement of network service quality from the user's perspective, but overall service quality will generally be determined by a combination of four key performance indicators (KPIs), namely system coverage; call blockage; voice quality; and dropped call rate [5]. Within the cell, coverage and the other KPIs are dependent upon the area covered by the signal. The distance travelled by the signal is dependent upon the radio propagation characteristics in the given area. Radio propagation varies from region to region and should be studied carefully, before predictions for both coverage and capacity are made [4].

The signal that is transmitted from the transmitting antenna (BTS/MS) and received by the receiving antenna (MS/BTS) travels a small and complex path [4], [7]. This signal is exposed to a variety of man-made structures, passes through different types of terrain, and is affected by the combination of propagation environments. All these factors contribute to variation in the signal level, so varying the signal coverage and quality in the network [4], [7], and [14]. Moreover, any signal that is transmitted by antenna will suffer

attenuation during its journey in free space. The received signal strength by an MS at any given point in space will be inversely proportional to the distance covered by the signal [4]. Unlike fixed point-to-point systems, there are no simple formulas that can be used to determine anticipated path loss [14]. By the nature of the continuously varying environment of the mobile subscriber, there is a very complicated relationship between the mobile telephone received signal strength and time. As in the typical call placed form a moving car, the signal variation is a formidable problem that can be approached only on a statistical level [14].

The received signal by an MS could be considered as consisting of three components, namely a free space path loss component, a slow fading component due to shadowing, and a fast fading component due to vehicle velocity [4], [14]. However, when determining handover necessities, the received signal is averaged, and over the normal averaging periods, the fast fading component of the signal is averaged out [10,14]. The shadowing component of the signal is a function of the cell propagation environment, and is a random variable that conforms to lognormal distribution. Therefore, the propagation characteristics of the cell environment could be represented by the statistics of the lognormal distribution [4], [10], [14]. The free space path loss component that gives rise to the mean value of the received signal can appropriately be described by the empirical formula given by Hata [4], [10], and [14].

Some major effects of the propagation environment on signal behavior are caused by reflections and multipath, diffraction and shadowing, building and vehicle penetration, propagation of signal over water, propagation of signal over vegetation (foliage loss), fading of the signal, interference [3], [4], [6], [9], [14]. The mobile station may experience a slow or rapid fluctuation in the signal level in a radio network. This may be due to one or more of the factors mentioned above. These factors form the basis of cell coverage criteria. Many previous studies on this subject area were based on the prediction either of the signal power or C/I using various path loss models. Such propagation evaluations are at best an approximation with a relatively high degree of uncertainty [14].

Other models dealing with the subject of cellular network performance evaluation mostly considered handover as the sole contributor to service quality degradation. For instance, the common denominator of drop-call probability modeling due to handover is the assumptions about network characteristics. They implicitly consider that an appropriate radio planning has been carried out; therefore, propagating conditions are neglected [1], such assumptions lead to consider that calls are dropped only due to the failure of the handover procedure. That is, the connection of an active user changing cell several times is terminated only due to lack of communication resources in the new cell [2]. For this reason, researchers have focused their attention on developing analytical models which relate handovers with traffic characteristics [1], [2].

Although such models were very useful in the early phase of mobile network deployment, they are not very effective in a well-established cellular network [1], [2]. In such a system, network-performance optimization is carried out continuously by mobile phone operators so that, the call dropping due to lack of communication resources is usually a rare event (i.e., blocking probability of new calls and handovers is negligible) [1], [2]. One of the latest drop-call probability model was based on the call dropping phenomenon caused by a heterogeneous mixture of drop-call causes. The main conclusion of drop cause analysis was that, in a well-established cellular network, call termination is mainly due to propagation conditions [1].

As a typical example, slightly more than 50% of the causes of drop calls for a single cell was reported to be caused mainly by electromagnetic causes like poor attenuation, deep fading, and so on [1], [2]. A lot of calls are dropped due to irregular user behavior (e.g. mobile equipment failure, phones switched off after ringing, subscriber charging capacity exceeded during the call). Other causes are due to abnormal network response (e.g. radio and signaling protocol error). It is highlighted that only few calls are blocked due to handover failure [1], [2].

II. TRAFFIC CHARACTERISTICS

The aggregate calls including call attempts offered or carried by some defined parts of a network, such as a group of circuits or switches with account being taken of both the number of calls and their duration is referred to as traffic [8,12,13]. In traffic engineering, any occupancy of a circuit or device caused directly or indirectly by a subscriber making or attempting to make use of the system is regarded as a call [8, 12, and 13]. The amount of traffic carried by a group of circuits will always exhibit daily and seasonal variations. Of more significance, however, are the changes that occur with the time of the day, leading to the concept of the busy hour when the traffic carried is at its peak. During such a period, the number of call arrivals and departures are essentially equal and the system is said to be in a state of statistical equilibrium [1, 2, 13, and 15]. In this state, the average number of calls existing simultaneously gives a measure of the density of the traffic.

1.1 Traffic Offered, Traffic Carried and Traffic Lost

The concept of traffic offered, traffic carried, and traffic lost is illustrated in Figure 1 [13], [15], [16].

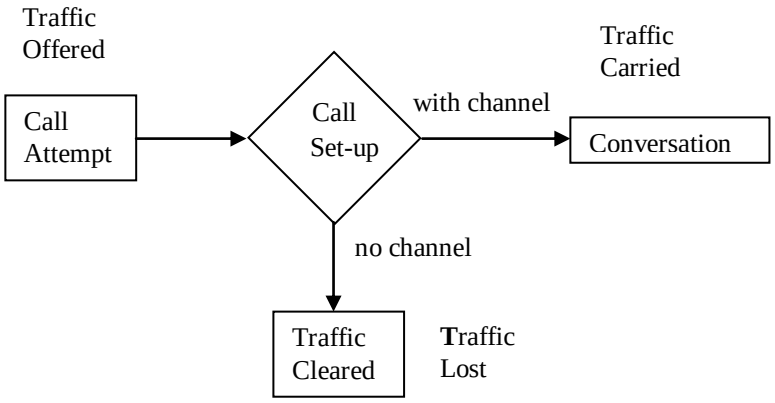

Figure 1: Traffic Offered, Traffic Carried, and Lost Traffic

Traffic carried = Traffic Offered – Traffic Lost (1)

1.2 Traffic Intensity

The traffic carried is the traffic that actually occupies a group of trunks or switches. The average number of simultaneously occupied trunks or switches gives its average intensity in Erlangs [11], [12]. Traffic intensity is the load presented to a system, that is, the amount or volume of traffic carried by the group of trunks or switches and is given by [11] -[13], [15], [16]:

$$A = \lambda h \quad (2)$$

λ= mean rate of calls attempted per unit time, h = mean holding time per successful call, A = average number of calls arriving during average holding period, for normalized λ and is expressed in Erlang-hours.

2.3 Call Arrival Rate

Call arrival rate, λ_t refers to the traffic offered expressed as the number of call attempts per unit time which is given as [11], [12]:

$$\lambda_t = \frac{Number\ of\ Call\ Attempts}{Unit\ Time} \quad (3)$$

2.4 Busy Hour

It is a given period within a day that bears the highest traffic intensity. The "busy hour" traffic is used to work out the equipment quantities of the network. The reason to use busy hour traffic is that this period usually has the highest amount of blocked or lost calls. If the dimensioning of the equipment at this period is correct and the blocked calls can be minimized, all other non-busy hour traffic should then be handled satisfactorily [1], [2], [8], and [12].

2.5 Erlang-B Formula

The Erlang B formula [10], [13], [15] is expressed as GoS or probability of finding N channels busy. The assumptions in the Erlang B formula are:

- Traffic originates from an infinite number of traffic sources independently.
- Lost calls are cleared assuming a zero holding time.
- Number of trunks or service channels is limited.
- Full availability exists.
- Inter-arrival times of call requests are independent of each other.
- The probability of a user occupying a channel (called service time) is based on an exponential distribution.
- Traffic requests are represented by a Poisson distribution implying exponentially distributed call inter-arrival times.

$$B = \frac{\frac{A^N}{N!}}{\sum_{k=0}^{N} \frac{A^k}{k!}} \quad (4)$$

Where B = blocking probability, A = offered traffic intensity in Erlangs, N = available number of channels

2.6 Prediction of Call Dropping

Dropping events constitute a Poisson process; let v_d be its intensity. Hence, if Y is the random variable which counts the number of drops, the probability that there are n drops in the interval $T = t$ is [1], [2]:

$$P(Y = n) = \frac{(v_d t)^n}{n!} e^{-v_d t}, \qquad n \geq 0 \qquad (5)$$

2.7 Channel Utilization

The channel utilization is a measure of trunking efficiency and is defined as [15]:

$$\rho = \frac{Traffic\ Intensity}{Number\ of\ channels} \qquad (6)$$

III. DATA COLLECTION

In this paper, several data have been collected from a GSM network in Nigeria. The data sets collected were from four MSCs carefully chosen as representative of four different propagation environments. The data collection is shown in Table 1.

Table 1. Network Performance Data

MSC	Number of Active Base Stations	Period	Traffic Intensity	Drop Call Rate in busy hour (%)	Drop-call rate with handover (%)	Number of Call Attempts in Busy Hour
Abuja	65	March	5211	2.10	0.05	250014
		April	5190	2.38	0.06	251185
		May	4933	3.17	0.06	248991
		June	5098	2.80	0.08	249492
Kaduna	89	March	3988	1.35	0.07	228825
		April	4315	2.35	0.056	220306
		May	4591	1.92	0.05	231222
		June	3977	1.99	0.04	201650
Port Harcourt	54	March	1836	3.17	0.04	116561
		April	2071	2.69	0.06	129988
		May	1920	2.85	0.06	113818
		June	1848	2.34	0.09	134853
Lagos	51	March	1718	1.99	0.09	117876
		April	1801	2.20	0.065	115928
		May	1698	2.32	0.08	112131
		June	1607	1.98	0.08	113339

IV. EXPERIMENTAL RESULTS AND ANALYSIS

The collected data were first analyzed to determine values, per base station, of the traffic intensity; number of call attempts; number of dropped calls; call duration and drop-call probability for each of the four MSCs. Similarly, using Erlang B calculator, the number of channels and channel utilization factor were estimated. The data analysis is shown in Table 2.

TABLE II: Evaluation of Network Parameters Per Base Station (Cell)

MSC A	Number of Active Base Stations B	Period C	Traffic No. of 24 Hrs D	No. of Call Attempts in Busy Hour E	Drop Call Rate (%) F	No. of dropped Calls G	Traffic No. of 24 Hrs/ cell (D/B) H	No. of dropped calls/ cell (G/B) J	No. of Call Attempts in Busy Hour /cell (E/B) K	Call Arrival Rate(λ_t) (Calls/s) K/(60x60x4) L	Call Duration sec. (H/ L) M	Drop-Call Probability (%) N
Abuja	65	March	5211	25001	2.10	5250	80	81	3846	0.27	296	0.5
		April	5190	25118	2.38	5978	80	92	3864	0.27	296	2.8
		May	4933	24899	3.17	7893	76	121	3831	0.27	282	0.6
		June	5098	24949	2.80	6985	78	108	3838	0.27	289	3.0
Kaduna	89	March	3988	22882	1.35	3089	45	35	2571	0.18	250	0.7
		April	4315	22030	2.35	5177	49	58	2475	0.17	288	2.4
		May	4591	23122	1.92	4440	52	50	2598	0.18	289	5.6
		June	3977	23165	1.99	4610	45	52	2603	0.18	250	5.1
Port Harcourt	54	March	1836	11656	3.17	3695	34	68	2159	0.15	227	4.0
		April	2071	12998	2.69	3497	38	65	2407	0.17	224	4.8
		May	1920	11381	2.85	3244	36	60	2108	0.15	240	4.8
		June	1848	13485	2.34	3156	34	58	2497	0.17	200	4.3
Lagos	51	March	1718	11787	1.99	2346	34	46	2311	0.16	213	5.6
		April	1801	11592	2.20	2550	35	50	2273	0.16	219	5.4
		May	1698	11213	2.32	2601	33	51	2199	0.15	220	5.1
		June	1607	11333	1.98	2244	32	44	2222	0.15	213	5.1

Table 3 shows the mean values of these parameters. The results indicate that all the parameters vary from one region to another. There is no better reason that can be used to explain this behavior than the differing propagation conditions in the four MSCs, since each of these parameters is channel related and therefore vary unpredictably, as earlier stated, throughout the propagation environment, and especially as we are dealing with a well-established network.

TABLE III: Mean Values of Computed Traffic Channel Parameters

MSC	Traffic Intensity (Erlangs)	No. of Call Attempts	Call Duration (s)	Drop-call Probability (%)	Number of Channels	Utilization Factor
Abuja	79	3845	291	1.7	82	0.96
Kaduna	48	2562	269	3.5	53	0.90
Port Harcourt	35	2293	223	4.5	41	0.85
Lagos	29	2251	216	5.3	37	0.78

Notice that Abuja stands out uniquely from the rest of the regions with a drop call probability of 1.7%. Lagos at 5.3% and Port Harcourt at 4.5% appears to be going together and Kaduna at 3.5% is oriented either towards Abuja or Lagos in some cases. It can be readily seen how Lagos and Port Harcourt are very close and Kaduna swings between Abuja and the two. This is indeed a very striking outcome since the Lagos and Port Harcourt environments, apart from coming from the same geographical zone of the country, have many common climatic conditions as shown in Table 4. The same thing applies to Abuja and Kaduna, and in many respects, Abuja has a unique terrain and clutter.

TABLE IV: Climatic Conditions of Propagation Environment of the Selected Areas

Propagation Environment	Lat (^{O}N)	Long (^{O}E)	Elevation (m)	Air temp (^{O}C)	Rel humidity (%)	Atmospheric pressure (kPa)	Wind speed (m/s)
Abuja	9.2	7.2	573	24.7	64.9	95.7	2.4
Kaduna	10.5	7.4	615	24.6	59.4	94.7	2.5
Port Harcourt	4.9	7.0	18	26.7	83.0	101.1	2.0
Lagos	6.5	3.5	32	25.7	81.4	100.3	2.8

Source: NASA

The foregoing leads us to conclude that Abuja MSC has the best propagation characteristics, followed by Kaduna, Port Harcourt and Lagos, if drop-call probability is considered, since it has the lowest value for Abuja (see Figure 5). If the number of call arrivals (call attempts), traffic intensity, call duration, number of channels, and utilization factor are considered, again Abuja stands out as the best since these are highest in that region and is followed by the other regions as earlier stated. Therefore, evidently, this study has once again demonstrated the influence of the propagation environment on cellular network performance. Thus, it might be concluded that, the study has given rise to a fairly good approach to network evaluation and optimization.

V. CONCLUSIONS

In this paper, the effects of the propagation environment on cellular network performance have been studied and confirmed. We started with the collection of operations data from four MSCs of a well-established GSM network. The MSCs were carefully chosen as representative of four different propagation environments in Nigeria. Using these data, several network performance indicators, namely number of call attempts (all arrivals); traffic intensity; call duration; drop-call probability; number of channels, and channel utilization factor, were estimated per base station for each of the four MSCs. An analysis of the results showed that these KPIs varied instructively from one region to another. Even the analysis indicated the relative performances of the four MSCs. We conclude that there is no better reason that can be used to explain this outcome than the effects of the differing propagation conditions in the four MSCs, since each of the affected parameters is traffic/channel related and therefore vary unpredictably, as earlier stated, throughout the propagation environment. Therefore, this study has once again demonstrated the influence of the propagation environment on cellular network performance. Thus, it might be concluded that, the study has given rise to a fairly good approach to network evaluation and optimization. The method is particularly most suited for well-established networks in which network performance optimization is carried out continuously so that, call dropping and blocking due to lack of communication resources is usually a rare event.

REFERENCES

[1] Gennaro Boggia, Pietro Camarda, and Alessandro D'Alconzo, "Modeling of Call Dropping in Well-Established Cellular Networks", EURASIP Journal on Wireless Communications and Networking, Vol. 2007, Article ID 17826, October, 2007.

[2]] G. Boggia, P. Camarda, A. D'Alconzo, A. De Biasi and M. Siviero, "Drop Call Probability in Established Cellular Networks: from Data Analysis to Modeling", DEE – Politecnico di Bari, Via E. Orabona, 4 – 70125 Bari (Italy), Proc. IEEE VTC Spring 2005.,Vol. 5, pp2775-2779, 2005.

[3]] Bruce L Cragin, "Prediction of Seasonal Trends in Cellular Dropped Call Probability", IEEE, Capital City Applied Research, Researh Paper, 2375 Club Mredian Dr. #B7, Okemos, MI 48864, USA, 2006.

[4] A. R. Mishra, "Fundamentals of Cellular Network Planning & Optimization", 2004 John Willey & Sons, Ltd. ISBN: 0-470-86267-X, PP 21-29.

[5] Roni Abiri, "Optimizing Service Quality in GSM/GPRS Networks", e-Newsletter, 2001 http://telephonyonline.com/news/telecom_optimizing_service_quality/

[6] Hussein M. Aziz Basi, M.B.R. Murthy, "Improved Performance of Traffic Dependent Outage Rate Cellular System", Journal of Computer Science, Jan, 2005.

[7] Maciej J. Nawrocki, Mischa Dohler and A. Hamid Aghvami, "Modern Approaches to Radio Network Modeling and Planning" – "Understanding UMTS Radio Network, Modeling, Planning and Automated Optimisation", 2006 John Willey & Sons Ltd.

[8] Abdullahi Salisu Umar, "GSM Network Performance Improvement: A case study of M-TEL Network Area VI, Kaduna", MSc Thesis, Department of Electrical Engineering, Ahmadu Bello University, Zaria, Nigeria, 2007.

[9] Hongxia Sun and Carey Williamson, "Simulation Evaluation of Call Dropping Policies for Stochastic Capacity Networks", Department of Computer Science University of Calgary, Calgary, AB, Canada T2N 1N4, 2005.

[10] Pasi Lehtimaki, "Data Analysis Methods for Cellular Network Performance Optimization", DSc Dissertation, Faculty of Information and Natural Sciences, Helsinki University of Technology, Espoo, Finland, April, 2008.

[11] Dajab D.D., Tarka S.N., Bajoga B.G., "Simulation and Analysis of Drop-call Probability Model: A case Study of MTEL", Nigerian Journal of Engineering, Vol. 16, No.1, 2009.

[12] Tarka S. Nathaniel, "Effects of Network characteristics on Conditional Drop Probability: A case Study of MTEL", MSc Thesis, Department of Electrical Engineering, Ahmadu Bello University, Zaria, 2009.

[13] Vijay Garg, "Wireless Communications and Networking", Morgan Kaufmann, 2007

[14] Robert G. Winch, "Telecommunication Transmission Systems", McGraw-Hill, 1998.

[15] C.Y. Lee, Mobile Cellular Telecommunications Systems, McGraw-Hill, 2nd Edition, 1995.

[16] J.F. Flood, "Telecommunication Switching, Traffic and Networks", Prentice Hall, 1995.

American Journal of Engineering Research (AJER)
e-ISSN : 2320-0847 p-ISSN : 2320-0936
Volume-02, Issue-09, pp-37-45
www.ajer.org

Research Paper Open Access

Studies on Compressive Strength Of Ternary Blended Concretes At Different Water Binder Ratios

D.Audinarayana, P.sarika, Dr.Seshadri Sekhar.T, Dr.Srinivasa Rao, Dr P Sravana G.Apparao

[1] *Research Scholar ,JNTUK, Kakinada*
2 Student, Dept of Civil Engineering, VNR&VJIET , Bachupally, Hyderabad
[3 6] *Professor Department of Civil Engineering , Gitam University*
[4,5] *Professor Jawaharlal Nehru Technological University, College of Engineering, Hyderabad, Andhra Pradesh, India*

Abstract: - The Present experimental investigation is carried out in the optimisation of a Ternary Blended Cementitious system based on Ordinary Portland Cement (OPC)/ Fly Ash / Micro Silica for the development of high- performance concrete. Compressive Strength of Ternary Blended Concrete at the ages of 28, 90, 180 days for various combinations of Fly Ash and Micro Silica mixes were investigated. Fly Ash was replaced by 0%, 15% and 20% along with Micro Silica of 0%, 5%, and 10%. All the mixes were studied at three water binder ratios of 0.55, 0.45 and 0.35.

I. INTRODUCTION

Now a day the world is witnessing the construction of very challenging and difficult structures, concrete being the most important and widely used structural material is called upon to possess very high strength. The main ingredient in the conventional concrete is Portland cement. The amount of cement production emits approximately equal amount of carbon dioxide into the atmosphere. Cement production is consuming significant amount of natural resources. To overcome the above ill effects, the advent of newer material and construction techniques and in this drive, admixture has taken newer things with various ingredients has become a necessity. The addition of pozzolanic materials with OPC a century old practice is an alternative in the construction industry. Fly ash one of the byproducts of thermal power plants is one of the most common mineral admixture used in concrete world wide. Fly ash largely improves the durability of concrete. One of the greatest drawbacks while using fly ash as pozzolanic material in concrete is the early age performance of concrete. The early age strength development of fly ash blended binary concretes shows poor performance than the ordinary concrete. Researchers all over the world are developing Ternary Blended Concretes by adding a superfine mineral admixture like Micro Silica to the binary blended concretes of fly ash. Micro Silica in the ternary blend improves the early age performance of concrete and fly ash improves the properties at the later age.

II. LITERATURE REVIEW

Shweta Goyal [1] et.al investigated on the role of Fly Ash addition on the superplasticiser dosage, slump, and 28 day and 90 day Compressive Strength of Micro Silica concrete .It was concluded that in the binary mixes Micro Silica increased the superplasticiser demand while Fly Ash decreased the optimum dosage of superplasticiser for constant workability. Three component systems can be designed for high workability with low superplasticiser dosage without impairing much in strength. **Murthi [2] et.al** in their experimental study intended to identify the relationship ofCompressive Strength and splitting tensile strength of Ternary Blended Concrete. For this purpose, the applicability of 0.5 power relationship as per IS 456-2000 and then a similar kind of relationship developed for Ternary Blended Concrete. Two kinds of binary blended concrete systems were considered in this study using the optimum replacement of cement by ASTM class Fly Ash (FA) and rice husk

ash (RHA). The Ternary Blended Concrete was developed by replacing the cement content in the binary system using Micro Silica (MS). The replacement of cement in the binary system by MS was suggested as 4%, 8% and 12% of total powder content by weight. **Khan [3] et.al** investigated on the optimization of a ternary blended cementitious system based on ordinary Portland cement (OPC)/ pulverized Fly Ash (PFA)/ Micro Silica (MS) for the development of high performance concrete. Cement pastes covering a wide range of PFA/MS blending proportions were investigated. Compressive Strength at ages of 7,28 and 90 days for cement paste containing 0%, 15%, 20%, 25%, 30%, 35%, 40% and 45% PFA along with 0%, 5%, 10% and 15% MS as partial replacement at a water binder ratio of 0.30 were investigated. **Tahir kemal erdem [4] et.al** investigated on the combinations of cement additions to provide more benefits for concrete than a single one. In this study, 80 high strength concretes containing several types and amounts of additions were produced. In the first stage Micro Silica contents in the binary blends that gave the highest strength were determined for different binder contents. The amount of Micro Silica that was used as replacement was 5%, 10% and 15% by mass of cement. In the second stage a third binder(class F or class C Fly Ash or ground granulated blast furnace slag) was introduced to concretes already containing Portland cement and Micro Silica in the amounts found in the first stage. Results indicated that ternary blends almost made it possible to obtain higher strengths than binary blends provided that the replacement by additions were chosen properly. The performance of slag in the ternary blends was better than class F Fly Ash but worse than class C Fly Ash. **Murthi [5] et.al** investigated on an essential assumption that porosity variation plays a role in influencing Compressive Strength of hardened concrete. The normal strength concrete with W/C ratio of 0.55 was used for this experimental investigation. The partial replacement of cement by Fly Ash was done to reduce the porosity and make concrete with a dense microstructure. The initial strength development of Fly Ash based blended concrete was less compared to the normal concrete. An attempt has been made to overcome the delay in strength development of concrete during the early ages by making the Ternary Blended Concrete. Fly Ash (FA) and Rice Husk Ash (RHA) were used for preparing the binary blended concrete and Micro Silica (MS) was used for developing the Ternary Blended Concrete. The results of the porosity of the concrete obtained from absorption tests showed that the porosity of blended concrete was less than that of the normal concrete. The Compressive Strength of the blended concrete was determined and it was observed that the early strength of Ternary Blended Concrete improved more than that of binary blended concrete. **Anwar [6]** presented the results from laboratory studies on properties of concrete that contain ternary blends of Portland cement, Micro Silica and Fly Ash. Selected four concrete mixes were prepared with water to cementitious material ratio of 0.4. The different combinations that were studied were 5%MS + 15% FA, 5%MS + 25% FA, 10% MS + 15% FA and 10% MS + 15% FA. The concrete mixes were designed to have the same degree of workability and percentage of air content. The results indicated that the concrete made with these systems generally showed good fresh and hardened properties since the combination of Micro Silica and Fly Ash is somewhat synergistic. Fly Ash appears to compensate for some of the workability problems associated with the Micro Silica where as the Micro Silica appears to compensate for the low early age strength of Fly Ash concrete.

III. EXPERIMENTAL INVESTIGATION

The present investigation is aimed to study the combination of Micro Silica and Fly Ash that is required that produces the maximum Compressive Strength. The cement was replaced from a minimum of 0% to a maximum of 30% in the Ternary blends. A total of five combinations were studied. 5% Micro Silica + 15% Fly Ash, 5% Micro Silica + 20% Fly Ash, 10% Micro Silica + 15% Fly Ash , 10% Micro Silica + 20% Fly Ash and 0% Micro Silica + 0% Fly Ash by weight of cement with different W/B ratios of 0.55,0.45 and 0.35 were studied. The Compressive Strength was calculated at the age of 28, 90 and 180 days.

IV. MATERIALS

Cement

Ordinary Portland cement of 53 grade having specific gravity of 3.02 and fineness of 3200cm^2/gm was used . The Cement used has been tested for various proportions as per IS 4031-1988 and found to be confirming to various specifications of 12269-1987.

Coarse Aggregate

Crushed angular granite metal of 10 mm size having the specific gravity of 2.65 and fineness modulus 6.05 was used .

Fine Aggregate

River sand having the specific gravity of 2.55 and fineness modulus 2.77 was used .

Fly Ash
Type-II fly ash confirming to I.S. 3812 – 1981of Indian Standard Specification was used .

Micro Silica
The Micro silica having the specific gravity 2.2 was used .
Superplasticizer:
Superplasticizer CONPLAST 430 was used as water reducing admixture. It increases workability.

V. DISCCUSSION OF RESULTS

Workability of Ternary Blended Concrete

When Fly Ash and Micro Silica are used in combination the beneficial effect of Fly Ash on fluidity can be used to compensate for the loss of workability with Micro Silica addition. Further for the same Micro Silica content (5% Micro Silica) increasing the Fly Ash content from 15% to 20% resulted in decrease in dosage of superplasticizer dosage indicating the positive influence of Fly Ash on the optimum superplasticizer dosage in the ternary mixes. The trend was reversed when the Micro Silica content increased from 5% to 10% for the same Fly Ash percentage (15%). For water to binder ratios the combination of 5% Micro Silica + 20% Fly Ash exhibited the least superplasticizer dosage while the mix 10% Micro Silica + 15% Fly Ash exhibited the highest optimum superplasticizer dosage. It was observed that as the water to binder ratio decreases the optimum dosage of superplasticiser increases. With the decrease in water to binder ratio, more superplasticiser molecules are required for adsorption on the surface of cement and mineral admixture particles to increase the fluidity of the mix. The optimum dosage increased sharply as the water to binder ratio decreased from 0.45 to 0.35. For control mixes superplasticiser was not required for water to binder ratios of 0.55 and 0.45 but for water to binder ratio of 0.35, 7% of cementitious material was required to get medium workability. For the combination of 10% Micro Silica + 15% Fly Ash the cementitious material increased from 5% to 8.5% as the water to binder ratio decreased from 0.45 to 0.35 to attain medium workability. This is because at very low water to binder ratio, cement particles are very closely placed and to overcome inter particle friction and inter particle forces of attraction, additional quantum of superplasticiser is required to arrive at the optimum dosage.

Compressive Strength Studies on Ordinary and Ternary Blended Concrete

The combination of Micro Silica and Fly Ash leads to increase in Compressive Strength as compared to control mix proportions given in tables 1.0 to 5.0 irrespective of water to binder ratios at the age of 90 and 180 days . The combination of 5% Micro Silica, 15% Fly Ash and 80% cement represents the optimum among the four combinations studied for all the water to binder ratios. It was noticed that replacing the cement by more than 20% tended to lower the efficiency of mineral admixtures. The other combination i.e. 5% Micro Silica + 20% Fly Ash and 10% Micro Silica + 15% Fly Ash that used 25% of mineral admixtures as replacement of cement did not show significant increase in strength. The combination of 10% Micro Silica + 20% Fly Ash showed a decrease in strength compared to control concrete at the age of 28 days for W/B ratios of 0.55 and 0.45.
From Table 6.0, 7.0 and 8.0 we observe the variation in Compressive Strength from 35.20 to 73.24 MPa for Ordinary Concrete , 40.64 to 96.70MPa for Ternary Blended Concrete(TBC) (5% Micro Silica + 15% Fly Ash) , 38.47 to 90.00 MPa for Ternary Blended Concrete(TBC) (5% Micro Silica + 20% Fly Ash) , 39.11 to 94.82 MPa for Ternary Blended Concrete(TBC) (10% Micro Silica + 20% Fly Ash) , 34.10 to 80.12 MPa for Ternary Blended Concrete(TBC) (10% Micro Silica + 20% Fly Ash) with W/B ratios of 0.55, 0.45, 0.35 respectively

The addition of Micro Silica to Fly Ash based binary blended concrete resulted in increase in compressive strength. The improved performance of Micro Silica concrete could be attributed to the improvement in bond between the hydrated cement matrix and aggregate. This in turn is due to the combined effect of secondary pozzolanic reaction and the fineness of Micro Silica particles.

Increase of Compressive Strength of Ternary Blended Concrete (5% Micro Silica + 15% Fly Ash) compared with Ordinary Concrete
From graph 1.0 the increase in Compressive Strength of Ternary Blended Concrete compared to Ordinary Concrete from 28 days to 180 days is observed to be 15% to 32 % for all W/B ratio
Increase of Compressive Strength of Ternary Blended Concrete (5% Micro Silica + 20% Fly Ash) compared with Ordinary Concrete
From graph 2.0 the increase in Compressive Strength of Ternary Blended Concrete compared to Ordinary Concrete from 28 days to 180 days is observed to be 9% to 23 % for all W/B ratio

Increase of Compressive Strength of Ternary Blended Concrete (10% Micro Silica + 15% Fly Ash) compared with Ordinary Concrete

From graph 3.0 the increase in Compressive Strength of Ternary Blended Concrete compared to Ordinary Concrete from 28 days to 180 days is observed to be 11% to 29 % for all W/B ratio

Increase of Compressive Strength of Ternary Blended Concrete (10% Micro Silica + 20% Fly Ash) compared with Ordinary Concrete

From graph 4.0 the increase in Compressive Strength of Ternary Blended Concrete compared to Ordinary Concrete from 28 days to 180 days is observed to be 3.0% to9.0 % for all W/B ratio

Increase of Compressive Strength of Ternary Blended Concrete(5% Micro Silica + 15% Fly Ash) at the age of 90 and 180 days with its 28 day strength.

From graph 5.0 the increase in Compressive Strength of Ternary Blended Concrete with its 28 day strength is observed from 10% to 30% for all W/B ratios.

Increase of Compressive Strength of Ternary Blended Concrete(5% Micro Silica + 20% Fly Ash) at the age of 90 and 180 days with its 28 day strength.

From graph 6.0 the increase in Compressive Strength of Ternary Blended Concrete with its 28 day strength is observed from 10% to 29% for all W/B ratios.

Increase of Compressive Strength of Ternary Blended Concrete(10% Micro Silica + 15% Fly Ash) at the age of 90 and 180 days with its 28 day strength.

From graph 7.0 the increase in Compressive Strength of Ternary Blended Concrete with its 28 day strength is observed from 11% to 30% for all W/B ratios.

Increase of Compressive Strength of Ternary Blended Concrete(10% Micro Silica + 20% Fly Ash) at the age of 90 and 180 days with its 28 day strength.

From graph 8.0 the increase in Compressive Strength of Ternary Blended Concrete with its 28 day strength is observed from 13% to 31% for all W/B ratios.

VI. CONCLUSIONS

1 The combination of 5% Micro Silica + 20% Fly Ash required the least dosage of superplasticiser for all the three W/B ratios studied.

2 The combination of 5% Micro Silica + 15% Fly Ash performed the best at all ages and at all the W/B ratios studied in terms of Compressive Strength among the four combinations studied.

3 The combination of 10% Micro Silica + 20% Fly Ash gave the least Compressive Strength among the ternary mixes at all ages and at all W/B ratios.

4 The percentage increase in Compressive Strength of Ternary Blended Concrete (5% Micro Silica + 15% Fly Ash) for various W/B ratios compared with Ordinary Concrete is observed to be 15% to 32%.

5 The percentage increase in Compressive Strength of Ternary Blended Concrete (5% Micro Silica + 15% Fly Ash) at the age of 90 and 180 days with its 28 day strength is observed to be 10% to 30%.

6 The percentage increase in Compressive Strength of Ternary Blended Concrete is found to be higher at higher ages for all water to binder ratios.

7 Results show that Ternary Blended Concrete offer significant advantages over control concrete. Such Concretes show generally good properties and offset the problems associated with using Fly Ash and Micro Silica when these materials are used individually. More attention must be given to the development of a new types of cements incorporating combination of the cementitious material in the Ternary cementitious systems.

8 The combination of Micro Silica and Fly Ash is complimentary. The Micro Silica improves the early age performance of concrete with the Fly Ash continuously refining the peoperties of hardened concrete as it matures.

REFERENCES

[1] **Shweta Goyal, Maneek Kumar and B. Bhattacharjee** " Potential Benefits of incorporating Fly Ash in Micro Silica concrete" THE INDIAN CONCRETE JOURNAL August 2008 pg 38 – 46

[2] **P Murthi and V Siva Kumar** " Studies on the relationship between Compressive Strength and splitting tensile strength of Ternary Blended Concrete" Vol. 89 February 2009 IE(I) Journal CV

[3] **M.I. Khan, C.J. Lynsdale, P. Waldron** " Porosity and strength of PFA/MS/OPC ternary blended paste" Cement and Concrete Research 30 (2000) pg 1225 – 1229

[4] **Tahir Kemal Erdem, Onder Kirca** " Use of binary and ternary blends in high strength concrete" Construction and Building Materials 22 (2008) pg 1477 – 1483.

[5] **P Murthi and V Siva Kumar** " Strength porosity relationship for Ternary Blended Concrerte" THE INDIAN CONCRETE JOURNAL July 2008 pg 35 – 41

[6] **M Anwar** " Concrete properties of ternary cementitious systems containing Fly Ash and Micro Silica" HBRC Journal Vol. 2 No. 1 January 2006

Table 1.0 Quantities of Materials required per 1 m^3 of Ordinary Concrete

S.No	W/C	Cement	Fine Aggregate.	Coarse Aggregate	Water	Super Plasticizer
1	0.55	324	736	1084	178	0
2	0.45	391	697	1070	176	0
3	0.35	497	629	1050	174	3480

Table 2.0 Quantities of Material required per 1 m^3 of Ternary Blended Concrete (5% Micro Silica – 15% Fly Ash)

S.No	W/B	Cement	Micro Silica.	Fly Ash	Fine Aggregate.	Coarse Aggregate	Water.	Super Plasticizer
1	0.55	259	16.20	48.6	736.0	1084.0	178	0
2	0.45	312	`19.55	58.65	697.0	1070.0	176	0
3	0.35	397	24.85	74.55	629.0	1050.0	174	2980

Table 3.0 Quantities of Material required per 1 m^3 of Ternary Blended Concrete (5% Micro Silica – 20% Fly Ash)

S.No	W/B	Cement	Micro Silica	Fly Ash.	Fine Aggregate.	Coarse Aggregate	Water	Super Plasticizer
1	0.55	243	16.20	64.8	736.0	1084.0	178	0
2	0.45	293	19.55	78.2	697.0	1070.0	176	0
3	0.35	373	24.85	99.4	629.0	1050.0	174	2798

Table 4.0 Quantities of Material required per 1 m^3 of Ternary Blended Concrete (10% Micro Silica – 15% Fly Ash) **Table 4.0 Quantities of Material required per 1 m^3 of Ternary Blended Concrete (10% Micro Silica – 15% Fly Ash)**

S. No	W/B	Cement	Micro Silica	Fly Ash	Fine Aggregate.	Coarse Aggregate	Water	Super Plasticizer
1	0.55	243	32.4	48.6	736.0	1084.0	178	0
2	0.45	293	39.1	58.65	697.0	1070.0	176	1465
3	0.35	373	49.7	74.55	629.0	1050.0	174	3170

Table 5.0 Quantities of Material required per 1 m^3 of Ternary Blended Concrete (10% Micro Silica – 20% Fly Ash)

S.No	W/B	Cement	Micro Silica	Fly Ash	F.A.	C.A.	Water	Super Plasticizer
1	0.55	227	32.4	64.8	736.0	1084.0	178	0
2	0.45	274	39.1	78.2	697.0	1070.0	176	1370
3	0.35	348	49.7	99.4	629.0	1050.0	174	3132

Table 6.0 Compressive Strength of Ordinary and Ternary Blended Concrete at 28, 90, 180 days at W/B ratio of 0.55

Sl. No	W/B	Mineral Admixture ,% replacement of cement		Compressive Strength (MPa)		
		Micro Silica	Fly Ash	28 Days	90 Days	180 Days
1	0.55	0%	0%	35.20	37.42	40.44
2		5%	15%	40.64	44.87	48.81
3		5%	20%	38.47	42.35	46.80
4		10%	15%	39.11	43.56	47.64
5		10%	20%	34.10	38.60	42.00

Table 7.0 Compressive Strength of Ordinary and Ternary Blended Concrete at 28, 90, 180 days at W/B ratio of 0.45

Sl. No	W/B	MA, % replacement of cement		Compressive Strength (MPa)		
		Micro Silica	Fly Ash	28 Days	90 Days	180 Days
1	0.45	0%	0%	42.32	45.61	49.42
2		5%	15%	50.22	57.00	63.73
3		5%	20%	47.00	52.90	59.84
4		10%	15%	48.75	55.51	61.63
5		10%	20%	41.12	47.78	51.98

Table 8.0 Compressive Strength of Ordinary and Ternary Blended Concrete at 28, 90, 180 days at W/B ratio of 0.35

Sl. No	W/B	MA, % replacement of cement		Compressive Strength (MPa)		
		Micro Silica	Fly Ash	28 Days	90 Days	180 Days
1	0.35	0%	0%	60.04	66.72	73.24
2		5%	15%	74.78	85.00	96.70
3		5%	20%	69.88	80.04	90.00
4		10%	15%	73.08	83.14	94.82
5		10%	20%	61.30	72.20	80.12

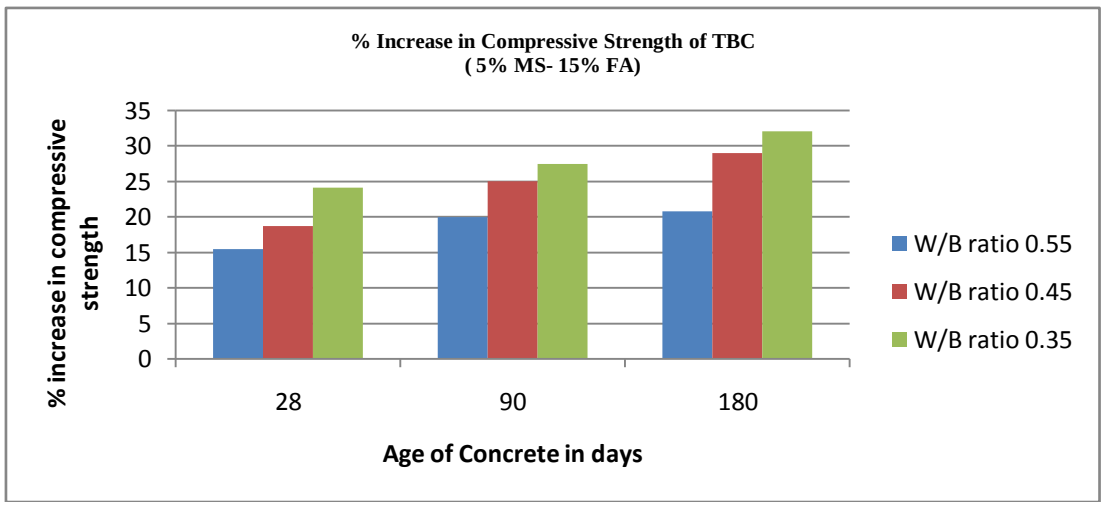

Graph 1.0 Percentage increase in Compressive Strength of Ternary Blended Concrete (5% MS + 15% FA) with respect to Ordinary Concrete at the age of 28,90,180 days

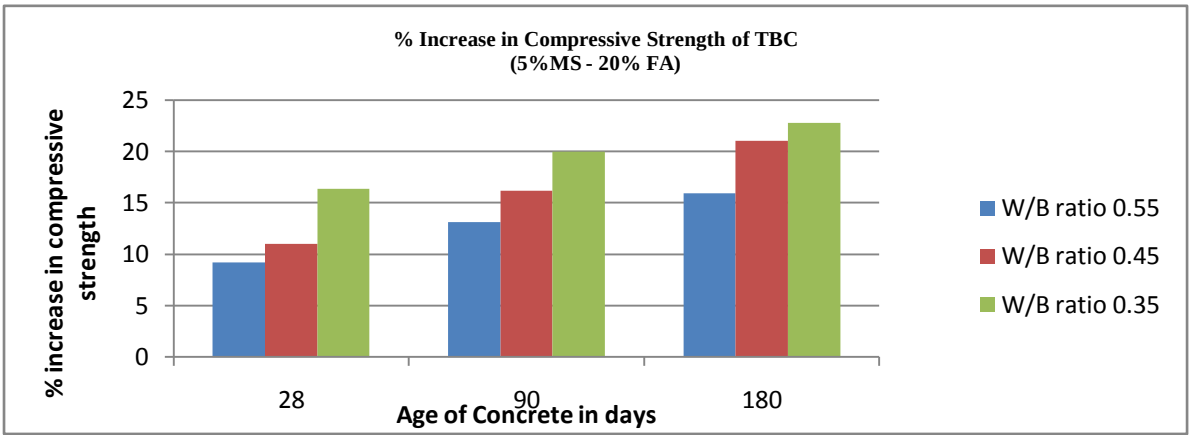

Graph 2.0 Percentage increase in Compressive Strength of Ternary Blended Concrete (5% MS + 20% FA) with respect to Ordinary Concrete at the age of 28,90,180 days.

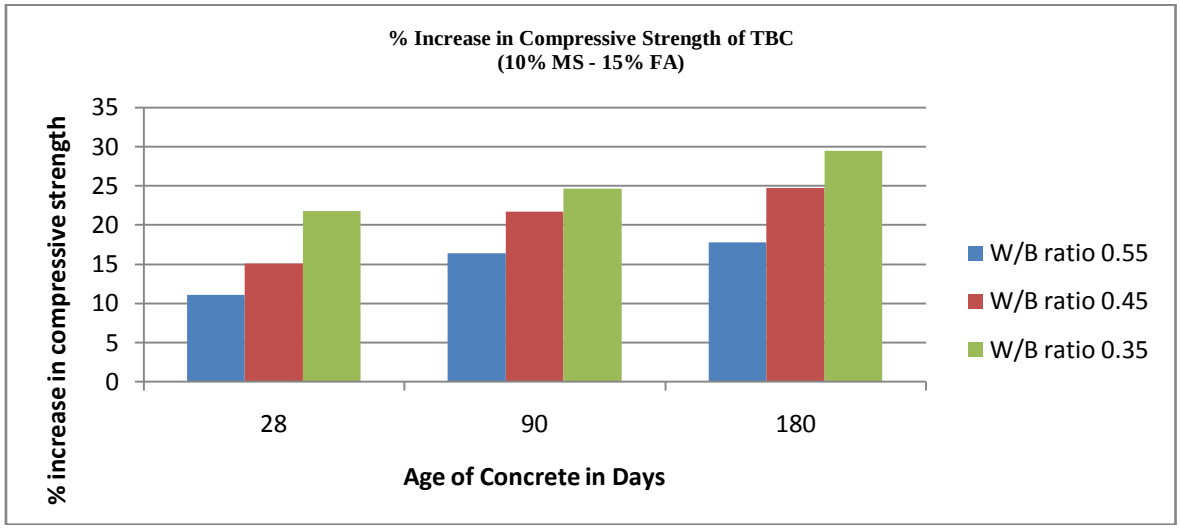

Graph 3.0 Percentage increase in Compressive Strength of Ternary Blended Concrete (10% MS + 15% FA) with respect to Ordinary Concrete at the age of 28,90,180 days.

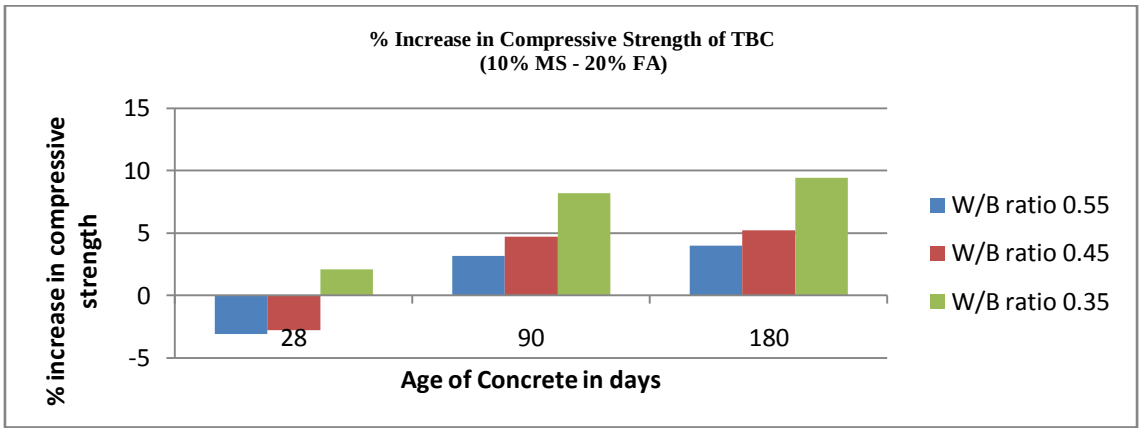

Graph 4.0 Percentage increase in Compressive Strength of Ternary Blended Concrete (10% MS + 20% FA) with respect to Ordinary Concrete at the age of 28,90,180 days

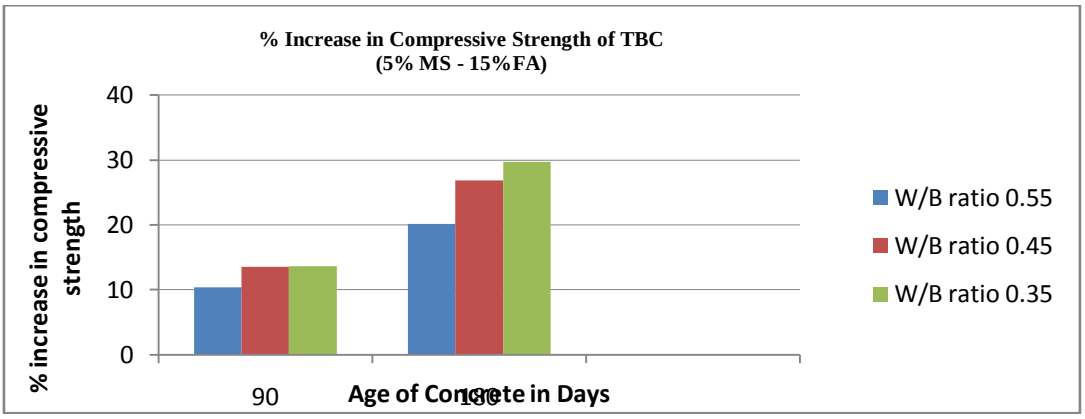

Graph 5.0 Percentage increase in Compressive Strength of Ternary Blended Concrete (5% MS + 15%FA) at the age of 90 and 180 days with its 28 day strength.

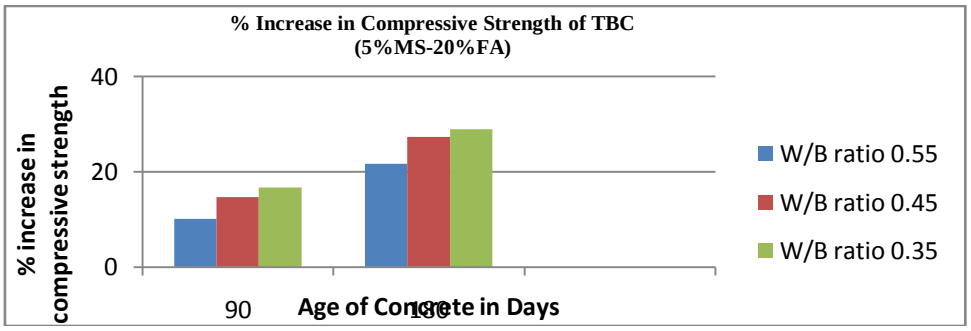

Graph 6.0 Percentage increase in Compressive Strength of Ternary Blended Concrete (5% MS + 20% FA) at the age of 90 and 180 days with its 28 day strength.

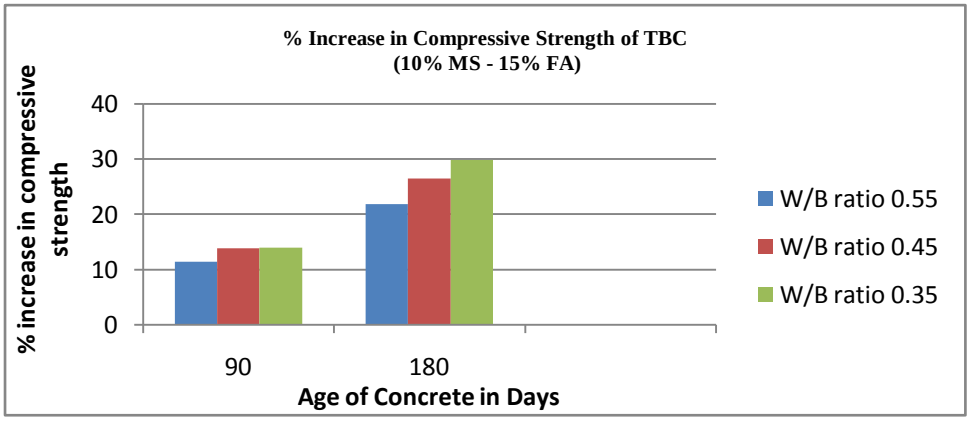

Graph 7.0 Percentage increase in Compressive Strength of Ternary Blended Concrete (10% MS + 15% FA) at the age of 90 and 180 days with its 28 day strength.

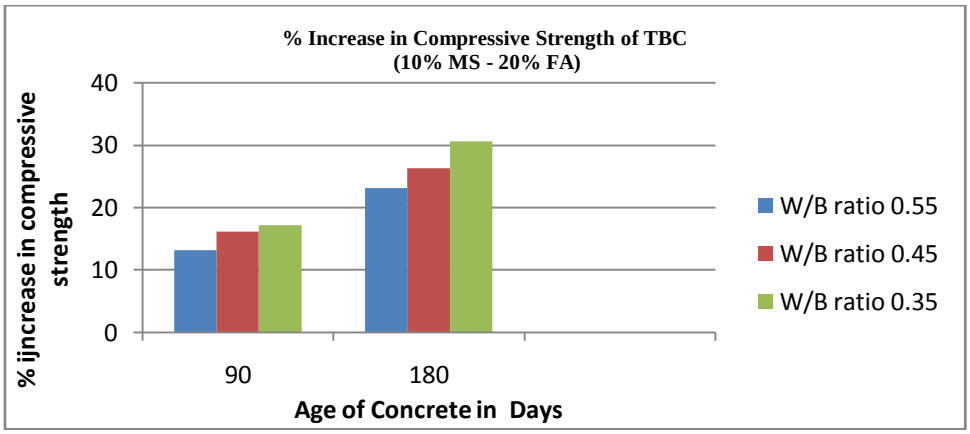

Graph 8.0 Percentage increase in Compressive Strength of Ternary Blended Concrete (10% MS + 20% FA) at the age of 90 and 180 days with its 28 day strength.

D. Audinarayana, Research Scholar, JNTUK, Kakinadana.
Specialized in structural engineering. Having 30 years of industrial experience. Working as Executive Engineer (Civil) in Quality control cell., Ramagundam and Bellampalli regions., "The Singareni Collieries Company Limited (A Government company)" in A.P. Delivered lectures on Building Construction and concrete technology. Member of Indian Association of Structural Engineers.

P.Sarika , Student
Pursuing B.Tech Civil Engineering from VNRVJIT , Bachupally, Nizampet , Hyderabad. Her interest area is on pecial Concretes. She got Eight papers to her credit.

Dr .P.Srinivasa Rao ,Professor ,JNTU college of Engineering, JNTUH.
Specialized in structural engineering. Research interests are Concrete Technology, Structural Design, High Performance Concrete, Prefabricating Structures, Special Concretes and use of Micro Silica, Fly Ash in Building Materials. He has been associated with a number of Design projects, for number of organizations and involved as a key person in Quality control and Mix Designs. Has 24 years of academic, research and industrial experience published over 100 research papers. He guided four Ph.Ds and 100 M.Tech projects. Guiding 15 Ph.D students delivered invited lecturers in other organizations and institutions. Member of ISTE, Member of ICI and Member of Institute of Engineers.

Dr. P.Sravana Professor,JNTU college of Engineering, JNTUH. Specialized in transportation engineering. Research interests are Concrete Technology, High Performance Concrete, Special Concretes, use of Micro Silica, Fly Ash in Building Materials and Pavement Design. She has been associated with a number of Design projects, for number of organizations and involved as a key person in Quality control , Mix Designs and Bitumen Emulsion Tests . Has 18 years of academic, research and industrial experience published over 70 papers.

Dr. Seshadri Sekhar.T , Professor and Head Department of Civil Engineering, Gitam University, Specialized in structural engineering. Research interests are Concrete Technology, High Performance Concrete, Special Concretes and use of Micro Silica, Fly Ash in Building Materials. Has 23 years of academic, research and industrial experience published over 100 research papers. He is associated with three Ph.Ds and presently guiding one Ph.D candidate and 25 M.Tech projects. Life Member of ISTE, Fellow Member of Institution of Engineers , Member institution of Civil Engineers India , Fellow of IETE and Member of IEEE.

Mr.Apparao Gandi, Assistant Professor
Specialized in Transportation Systems Engineering. Research interests are Pavement Materials, Highway Design, and Concrete Technology. He has 3 years of academic experience and published 8 research papers. He was guided 3 M.Tech projects and currently associated with numerous M.Tech and B.Tech Projects. He involved various consultancy works with private and state government projects. Associate member of ASCE, Member of IRC. .

American Journal of Engineering Research (AJER)
e- ISSN: 2320-0847 p-ISSN : 2320-0936
Volume-02, Issue-09, pp-46-54
www.ajer.org

Research Paper Open Access

An Inflationary Inventory Model for Weibull Deteriorating Items with Constant Demand and Partial Backlogging Under Permissible Delay in Payments

Sushil Kumar, U. S .Rajput
Department of Mathematics & Astronomy, University of Lucknow Lucknow- 226007. U.P. India.

Abstract: - In this paper we developed a general inventory model for Weibull deteriorating items with constant demand under the consideration of time dependent partial backlogging and deterioration. Further it is illustrated with the help of numerical examples by minimizing the total variable inventory cost.

Keywords: - *Weibull-distribution, partial backlogging, inflation and permissible delay in payments.*

I. INTRODUCTION

Many mathematical models have been developed for controlling inventory and in the earlier models many researchers consider the constant demand rate which is a feature of static environment while the dynamic environment nothing is fixed or constant. So in most of the cases the demand for items increases with time and the items that are stored for future use always loose part of their value with passage of time. In inventory this phenomenon is known as deterioration of items. The rate of deterioration is very small in some items like hardware, glassware, toys and steel. The items such as medicine, vegetables, gasoline alcohol, radioactive chemicals and food grains deteriorate rapidly over time so the effect of deterioration of physical goods cannot be ignored in many inventory systems. The deterioration of goods is a realistic phenomenon in many inventory systems and controlling of deteriorating items becomes a measure problem in any inventory system. Due to deterioration the problem of shortages occurs in any inventory system and shortage is a fraction that is not available to satisfy the demand of the customers in a given period of time. The researchers have continuously modified the deteriorating inventory models so as to become more practicable and realistic. Dye [2002] developed an inventory model with partial backlogging and stock dependent demand. Chakrabarty et al. [1998] extended the Philip's model [1974]. Skouri and Papachristors [2003] determine an optimal time of an EOQ model for deteriorating items with time dependent partial backlogging. Manjusri Basu and Sudipta Sinha [2007] extended the Yan and Cheng model [1998] by considering time dependent backlogging rate. Rau et al. [2004] considered an inventory model for determining an economic ordering policy of deteriorating items in a supply chain management system. Teng and Chang [2005] determined an economic production quantity in an inventory model for deteriorating items. Dave and Patel [1983] considered an instantaneous replenishment policy for deteriorating items with time proportional demand and no shortage. Roychowdhury and Chaudhury [1983] considered an order level inventory model with finite rate of replenishment and allowing shortages. Mishra [1975], Dev and Chaudhuri [1986] assumed time dependent deterioration rate in their models. In this regard an extended summary was given by Raafat[1991]. Berrotoni [1962] discussed the difficulties of fitting empirical data to mathematical distributions. Covert and Philip [1973] developed an inventory model for deteriorating items by considering two parameters weibull distribution. Mandal and Phaujdar [1989] developed a production inventory model for deteriorating items with stock dependent demand and uniform rate of production. In this direction some valuable work was also done by Padmanabhan and Vrat [1995]. Ray and Chaudhuri [1997], Mondal and Moiti [1999], Biermans and Thomas [1997], Buzacoh [1975], Chandra and Bahner [1988], Jesse et al. [1983], Mishra [1979] developed their models and show the effect of inflation in inventory models by assuming a constant rate of inflation. Liao et al [2000] developed an inventory model for deteriorating items under inflation and discuss the effect of permissible delay in payment. Bhahmbhatt [1982] developed an EOQ model with price dependent inflation rate. Ray and Chaudhuri [1997] considered an EOQ

model with shortages under the effect of inflation and time discount. Goyal [1985] developed an EOQ model under the conditions of permissible delay in payment. Chung et al [2002] and Hung [2003] considered an optimal replenishment policy for EOQ model under permissible delay in payments. Aggarwal and Jaggi [1995] extended the EOQ model with constant rate of deterioration. Hwang and Shinn [1997] determined the lot size policy for the items with exponential demand and permissible delay in payment. Chung and Hung [**2005**] developed an EOQ model in the presence of trade credit policy. Vinod kumar Mishra and Lal sahab singh [2010] developed an inventory model for deteriorating items with time dependent demand and partial backlogging. Mandal [2013] developed an inventory model for random deteriorating items with time dependent demand and partial backlogging. In the present paper we developed an inventory model for weibull deteriorating items with constant demand and time dependent partial backlogging.

II. ASSUMPTIONS AND NOTATIONS

we consider the following assumptions and notations

1. The demand rate D is constant.
2. The replenishment rate is instantaneous.
3. The inventory system involves only one item.
4. The deterioration rate is $\theta(t) = \alpha\beta\, t^{\beta-1}, where\ \ 0 < \alpha << 1 and\ \beta \geq 1.$
5. Shortages are allowed and backlogging rate is defined by $R(t) = \dfrac{D}{1+\delta(T-t)}$ where backlogging parameter δ is a positive constant.
6. I(t) is the inventory level at any time t.
7. I(0) is the stock level at the beginning of each cycle after fulfilling back orders.
8. H is the length of planning horizon.
9. r is the inflation rate.
10. $C(t) = C_0 e^{rT}$ is the unit purchase cost of an item at any time t.
11. C_2 is the shortage cost \$ per unit per time.
12. C_3 is the ordering cost per cycle.
13. i_e is the interest earned \$ per time.
14. i_p is the interest charged \$ per time.
15. T is the cycle length.
16. M is the permissible delay in setting the account.
17. T_1 is the time at which shortages start.
18. $TC(T, T_1)$ is the average total inventory cost per unit time.

III. MATHEMATICAL FORMULATION

The instantaneous inventory level at any time t in $[0, T_1]$ is given by the differential equations

$$\frac{dI}{dt} + \alpha\beta t^{\beta-1} = -D, \quad 0 \leq t \leq T_1. \qquad \ldots\ldots\ldots (1)$$

Where $0 < \alpha << 1 \ and \ \ \beta \geq 1$

With the Boundary Condition $I(T_1) = 0$, …….. (2)

Again the instantaneous inventory level at any time t in $[T_1, T]$ is given by the differential equation

$$\frac{dI}{dt} = -\frac{D}{1+\delta(T-t)}, \quad T_1 \leq t \leq T. \qquad \ldots\ldots\ldots (3)$$

With the Boundary Condition $I(T_1) = 0$, …… (4)

The solution of equation (1) is

$$I(t) = D[1 - t - \alpha t^{\beta} + \frac{\alpha\beta t^{\beta+1}}{(\beta+1)} + \frac{\alpha T_1^{\beta+1}}{(\beta+1)}] \qquad \ldots\ldots\ldots (5)$$

Neglecting the powers of α higher than one
And the solution of equation (3) is

$$I(t) = \frac{D}{\delta}[\log\{1+\delta(T-t)\} - \log\{1+\delta(T-T_1)\}], \quad \ldots\ldots\ldots (6)$$

The ordering cost is per unit time is

$$O_C = \frac{C_3}{T}[\sum_{n=0}^{m-1} C(nT)]$$

$$= \frac{C_3}{T}[C(0) + C(T) + C(2T) + \ldots\ldots\ldots + C(n-1)T]$$

$$= \frac{C_0 C_3}{T}\left(\frac{e^{rH}-1}{e^{rT}-1}\right), \quad \text{where H= nT}$$

$\ldots\ldots\ldots\ldots\ldots (7)$

The holding cost per unit time

$$H_C = \frac{h}{T}\sum_{n=0}^{m-1} C(nT)\int_0^{T_1} I(t)dt$$

$$= \frac{hDC_0}{T}\left(\frac{e^{rH}-1}{e^{rT}-1}\right)[T_1 - \frac{T_1^2}{2} - \frac{\alpha T_1^{\beta+1}}{(\beta+1)} + \frac{2\alpha T_1^{\beta+2}}{(\beta+2)}], \ldots\ldots\ldots (8)$$

The number of deteriorated units in $[0, T_1]$ are

$$= \text{I(0)} - \int_0^{T_1} Ddt$$

$$= D[1 - T_1 + \frac{\alpha T_1^{\beta+1}}{(\beta+1)}]$$

The deterioration cost per unit time is

$$D_C = DC_0\left(\frac{e^{rH}-1}{e^{rT}-1}\right)[1 - T_1 - \frac{\alpha T_1^{\beta+1}}{(\beta+1)}], \ldots\ldots\ldots\ldots (9)$$

The shortage cost per unit time

$$S_C = C_0 C_2\left(\frac{e^{rH}-1}{e^{rT}-1}\right)\int_{T_1}^{T} I(t)dt$$

$$= C_0 C_2\left(\frac{e^{rH}-1}{e^{rT}-1}\right)\int_{T_1}^{T} \frac{D}{\delta}[\log\{1+\delta(T-t)\} - \log\{1+\delta(T-T_1)\}]$$

$$= \frac{C_0 C_2 D}{\delta}\left(\frac{e^{rH}-1}{e^{rT}-1}\right)[T_1 - T + (1 - T + \delta T)\log\{1+\delta(T-T_1)\}] \quad \ldots\ldots\ldots (10)$$

Now we consider the following two cases
Case I The permissible delay in payment say M is less than the period of inventory stock in hand say T_1
Case II The permissible delay in payment say M is greater than the period of inventory stock in hand say T_1
Case I Since the permissible delay in payment say M is less than the period of on hand inventory stock say T_1 i.e $M < T_1$ (payment before depletion), Then the interest earned per unit time in $[0, T_1]$ is

$$IE_1 = \frac{i_e}{T}\sum_{n=0}^{m-1} C(nT)\int_0^{T_1} (T_1 - t)Ddt$$

$$= \frac{Di_e C_0}{T}\left(\frac{e^{rH}-1}{e^{rT}-1}\right)\frac{T_1^2}{2}, \ldots\ldots\ldots (11)$$

The interest payable per cycle per unit time for the inventory not being sold after due date say M is

$$IP_1 = \frac{i_p}{T}\sum_{n=0}^{m-1} C(nT)\int_M^{T_1} I(t)dt$$

$$= \frac{Di_pC_0}{T}\left(\frac{e^{rH}-1}{e^{rT}-1}\right)\left[T_1 - M - \frac{(T_1^2 - M^2)}{2} - \frac{\alpha(1+M)T_1^{\beta+1}}{(\beta+1)} + \frac{\alpha M^{\beta+1}}{(\beta+1)}\right.$$

$$\left. + \frac{2\alpha T_1^{\beta+2}}{(\beta+2)} - \frac{\alpha\beta M^{\beta+2}}{(\beta+1)(\beta+2)}\right], \quad \text{..... (12)}$$

Therefore the average total variable cost per unit time is

$$TC(T,T_1) = \frac{1}{T}[O_C + H_C + D_C + S_C + IP_1 - IE_1]$$

$$= \frac{C_0}{T}\left(\frac{e^{rH}-1}{e^{rT}-1}\right)\left[C_3 + hD\left\{T_1 - \frac{T_1^2}{2} - \frac{\alpha T_1^{\beta+1}}{(\beta+1)} + \frac{2\alpha T_1^{\beta+2}}{(\beta+2)}\right\} + D\left\{1 - T_1 + \frac{\alpha T_1^{\beta+1}}{(\beta+1)}\right\}\right.$$

$$\left. + \frac{C_2 D}{\delta}\{T_1 - T + (1 - T + \delta T)\log\{1 + \delta(T - T_1)\}\} + Di_p\left\{T_1 - M - \frac{(T_1^2 - M^2)}{2}\right.\right.$$

$$\left.\left. - \frac{\alpha(1+M)T_1^{\beta+1}}{(\beta+1)} + \frac{\alpha M^{\beta+1}}{(\beta+1)} + \frac{2\alpha T_1^{\beta+2}}{(\beta+2)} - \frac{\alpha\beta M^{\beta+2}}{(\beta+1)(\beta+2)}\right\} - \frac{Di_e T_1^2}{2}\right], \quad \text{..... (13)}$$

For the minimization of $TC(T,T_1)$, $\frac{\partial TC(T,T_1)}{\partial T} = 0$ *and* $\frac{\partial TC(T,T_1)}{\partial T_1} = 0$ Give the values of T=T*for which

$$\left(\frac{\partial^2 TC(T,T_1)}{\partial T^2}\right)\left(\frac{\partial^2 TC(T,T_1)}{\partial T_1^2}\right) - \frac{\partial^2 TC(T,T_1)}{\partial T \partial T_1} > 0, and \quad \frac{\partial^2 TC(T,T_1)}{\partial T^2} > 0, \forall T = T^*$$

Case II Since the permissible delay in payment say M is greater than the period of on hand inventory stock say T_1 i.e $M > T_1$ (payment after depletion),then the interest payable per unit time per cycle is zero for $T < M < T_1$, because the supplier paid in full at M so the interest earned per unit time per cycle is

$$IE_2 = \frac{i_e C_0}{T}\left(\frac{e^{rH}-1}{e^{rT}-1}\right)\left[\int_0^{T_1}(T_1 - t)Ddt + (M - T_1)\int_0^{T_1} Ddt\right]$$

$$= \frac{C_0 Di_e}{T}\left(\frac{e^{rH}-1}{e^{rT}-1}\right)\left[MT_1 - \frac{T_1^2}{2}\right], \quad \text{..... (14)}$$

Therefore the average total variable cost per unit time is

$$TC(T,T_1) = \frac{C_0}{T}\left(\frac{e^{rH}-1}{e^{rT}-1}\right)\left[C_3 + hD\left\{T_1 - \frac{T_1^2}{2} - \frac{\alpha T_1^{\beta+1}}{(\beta+1)} + \frac{2\alpha T_1^{\beta+2}}{(\beta+2)}\right\} + D\left\{1 - T_1 + \frac{\alpha T_1^{\beta+1}}{(\beta+1)}\right\}\right.$$

$$\left. + \frac{C_2 D}{\delta}\{T_1 - T + (1 - T + \delta T)\log\{1 + \delta(T - T_1)\}\} - Di_e\left(MT_1 - \frac{T_1^2}{2}\right)\right] \quad \text{..... (15)}$$

For the minimization of the $TC(T,T_1)$, $\frac{\partial TC(T,T_1)}{\partial T} = 0$ *and* $\frac{\partial TC(T,T_1)}{\partial T_1} = 0$ give the values of T = T*

for which $\left(\frac{\partial^2 TC(T,T_1)}{\partial T^2}\right)\left(\frac{\partial^2 TC(T,T_1)}{\partial T_1^2}\right) - \frac{\partial^2 TC(T,T_1)}{\partial T \partial T_1} > 0, and \quad \frac{\partial^2 TC(T,T_1)}{\partial T^2} > 0, \forall T = T^*$

IV. THEORETICAL RESULTS

For a I st order approximation of $e^{rT} = 1 + rT$ and $e^{rH} = 1 + rH$

Then from equation (13)

$$TC(T,T_1) = \frac{C_0 H}{T^2}[C_3 + hD\{T_1 - \frac{T_1^2}{2} - \frac{\alpha T_1^{\beta+1}}{(\beta+1)} + \frac{2\alpha T_1^{\beta+2}}{(\beta+2)}\} + D\{1 - T_1 + \frac{\alpha T_1^{\beta+1}}{(\beta+1)}\}$$

$$+ \frac{C_2 D}{\delta}\{T_1 - T + (1 - T + \delta T)\log\{1 + \delta(T - T_1)\}\} + Di_p\{T_1 - M - \frac{(T_1^2 - M^2)}{2} - \frac{\alpha(1+M)T_1^{\beta+1}}{(\beta+1)}$$

$$+ \frac{\alpha M^{\beta+1}}{(\beta+1)} + \frac{2\alpha T_1^{\beta+2}}{(\beta+2)} - \frac{\alpha\beta M^{\beta+2}}{(\beta+1)(\beta+2)}\} - Di_e\frac{T_1^2}{2}], \quad \ldots\ldots\ldots\ldots (16)$$

$$\frac{\partial TC(T,T_1)}{\partial T} = -\frac{2C_0 H}{T^3}[C_3 + hD\{T_1 - \frac{T_1^2}{2} - \frac{\alpha T_1^{\beta+1}}{(\beta+1)} + \frac{2\alpha T_1^{\beta+2}}{(\beta+2)}\} + D\{1 - T_1 + \frac{\alpha T_1^{\beta+1}}{(\beta+1)}\}$$

$$+ \frac{C_2 D}{\delta}\{T_1 - T + (1 - T + \delta T)\log\{1 + \delta(T - T_1)\}\} + Di_p\{T_1 - M - \frac{(T_1^2 - M^2)}{2} - \frac{\alpha(1+M)T_1^{\beta+1}}{(\beta+1)}$$

$$+ \frac{\alpha M^{\beta+1}}{(\beta+1)} + \frac{2\alpha T_1^{\beta+2}}{(\beta+2)} - \frac{\alpha\beta M^{\beta+2}}{(\beta+1)(\beta+2)}\} - \frac{Di_e T_1^2}{2}] + \frac{C_0 H}{T^2}[\frac{C_2 D}{\delta}\{-1 + (\delta - 1)\log\{1 + \delta(T - T_1)\}$$

$$+ \frac{(1 - T + \delta T)\delta}{(1 + \delta(T - T_1)}\}]$$

$\ldots\ldots\ldots\ldots (17)$

$$\frac{\partial TC(T,T_1)}{\partial T_1} = \frac{C_0 HD}{T^2}[\{1 + \delta(T - T_1)\}\{(h - 1 + \frac{C_2}{\delta} + i_p) - (h + i_p + i_e)T_1 + \{1 - h - i_p(1+M)\}\alpha T_1^{\beta}$$

$$+ 2\alpha(h + i_p)T_1^{\beta+1}\} - C_2(1 - T + \delta T)], \quad \ldots\ldots\ldots\ldots (18)$$

$$\frac{\partial^2 TC(T,T_1)}{\partial T^2} = \frac{6C_0 H}{T^4}[C_3 + hD\{T_1 - \frac{T_1^2}{2} - \frac{\alpha T_1^{\beta+1}}{(\beta+1)} + \frac{2\alpha T_1^{\beta+2}}{(\beta+2)}\} + D\{1 - T_1 + \frac{\alpha T_1^{\beta+1}}{(\beta+1)}\}$$

$$+ \frac{C_2 D}{\delta}\{T_1 - T + (1 - T + \delta T)\log\{1 + \delta(T - T_1)\} + Di_p\{T_1 - M - \frac{(T_1^2 - M^2)}{2}$$

$$- \frac{\alpha(1+M)T_1^{\beta+1}}{(\beta+1)} + \frac{\alpha M^{\beta+1}}{(\beta+1)} + \frac{2\alpha T_1^{\beta+2}}{(\beta+2)} - \frac{\alpha\beta M^{\beta+2}}{(\beta+1)(\beta+2)}\} - \frac{Di_e T_1^2}{2}]$$

$$- \frac{2C_0 H}{T^3}[\frac{C_2 D}{\delta}\{-1 + (\delta - 1)\log\{1 + \delta(T - T_1)\} + \frac{(1 - T + \delta T)\delta}{1 + \delta(T - T_1)}]$$

$$+ \frac{C_0 H}{T^2}[\frac{C_2 D}{\delta}\{\frac{\delta(\delta - 1)}{1 + \delta(T - T_1)} - \frac{\delta(1 - \delta T_1 + \delta^2 T_1)}{\{1 + \delta(T - T_1)\}^2}\}], \quad \ldots\ldots\ldots\ldots (19)$$

From the equation (15)

$$TC(T,T_1) = \frac{C_0 H}{T^2}[C_3 + hD\{T_1 - \frac{T_1^2}{2} - \frac{\alpha T_1^{\beta+1}}{(\beta+1)} + \frac{2\alpha T_1^{\beta+2}}{(\beta+2)}\} + D\{1 - T_1 + \frac{\alpha T_1^{\beta+1}}{(\beta+1)}\}$$

$$+\frac{C_2D}{\delta}\{T_1-T+(1-T+\delta T)\log\{1+\delta(T-T_1)\}\}-Di_e(MT_1-\frac{T_1^2}{2})]$$

…….. (20)

$$\frac{\partial TC(T,T_1)}{\partial T}=\frac{-2C_0H}{T^3}[C_3+hD\{T_1-\frac{T_1^2}{2}-\frac{\alpha T_1^{\beta+1}}{(\beta+1)}+\frac{2\alpha T_1^{\beta+2}}{(\beta+2)}\}+D\{1-T_1+\frac{\alpha T_1^{\beta+1}}{(\beta+1)}\}+\frac{C_2D}{\delta}\{T_1-T$$

$$+(1-T+\delta T)\log\{1+\delta(T-T_1)\}\}-Di_e(MT_1-\frac{T_1^2}{2})]$$

$$+\frac{C_0H}{T^2}[\frac{C_2D}{\delta}\{-1+(\delta-1)\log\{1+\delta(T-T_1)\}+\frac{(1-T+\delta T)\delta}{1+\delta(T-T_1)}\}],\quad \text{…… (21)}$$

$$\frac{\partial TC(T,T_1)}{\partial T_1}=\frac{C_0H}{T^2}[hD\{1-T_1-\alpha T_1^{\beta}+2\alpha T_1^{\beta+1}\}+D\{-1+\alpha T_1^{\beta}\}+\frac{C_2D}{\delta}\{1-\frac{(1-T+\delta T)\delta}{1+\delta(T-T_1)}\}$$

$$-Di_e(M-T_1)]$$

…….. (22)

$$\frac{\partial^2 TC(T,T_1)}{\partial T^2}=\frac{6C_0H}{T^4}[C_3+hD\{T_1-\frac{T_1^2}{2}-\frac{\alpha T_1^{\beta+1}}{(\beta+1)}+\frac{2\alpha T_1^{\beta+2}}{(\beta+2)}\}+D\{1-T_1+\frac{\alpha T_1^{\beta+1}}{(\beta+1)}\}+\frac{C_2D}{\delta}\{T_1-T$$

$$+(1-T+\delta T)\log\{1+\delta(T-T_1)\}\}-Di_e(MT_1-\frac{T_1^2}{2})]$$

$$-\frac{2C_0H}{T^3}[\frac{C_2D}{\delta}\{-1+(\delta-1)\log\{1+\delta(T-T_1)\}+\frac{(1-T+\delta T)\delta}{1+\delta(T-T_1)}\}]$$

$$-\frac{2C_0H}{T^3}[\frac{C_2D}{\delta}\{-1+(\delta-1)\log\{1+\delta(T-T_1)\}+\frac{(1-T+\delta T)\delta}{1+\delta(T-T_1)}\}]$$

$$+\frac{C_0H}{T^2}[\frac{C_2D}{\delta}\{\frac{\delta(\delta-1)}{1+\delta(T-T_1)}-\frac{\delta(1-\delta T_1+\delta^2T_1)}{\{1+\delta(T-T_1)\}^2}],\quad \text{…….. (23)}$$

Numerical example: Let us consider the following parameters in the appropriate unit as

$[\alpha,\beta,\delta,C_0,C_2,C_3,i_e,i_p,h,D,M]$= [0.005, 1, 5.0, 0.5, 0.8, 50, 0.10, 0.20, 2.0, 500, 0.2]

And H= 0.08219(1 year)

Case I Payment before depletion

Table 1

	Change in Parameters	T	T_1	TC
α	0.005	0.24283 0.88262 66.4718	0.139305 1.45469 103.7260	472.3465 -41.9297 -56.0082
	0.010	0.24282 0.89116 32.9398	0.13923 1.46777 51.4409	472.38169 -42.2403 -56.2829
	0.020	0.242804 0.909455 16.1603	0.13907 1.49582 25.2773	472.46852 -42.8623 -56.2592

β	1.00	0.24283 0.88262 66.4718	0.139305 1.45469 103.7260	472.3465 -41.9297 -56.0082
	2.00	0.242836 0.88582 6.15291	0.139372 1.45999 9.76629	472.3078 -42.2045 -66.6267
	3.00	0.24294 0.953874 8.7476 66.3587	0.139987 1.57309 11.9131 68.4851	471.86770 -48.49855 211.062950 28974.3164
M	0.2	0.24283 0.88262 66.4718	0.13931 1.45469 103.7260	472.3465 -41.9297 -56.0082
	0.4	0.23822 0.87729 66.5374	0.13824 1.4497 103.7340	477.9967 -42.6808 -55.8870
δ	5.00	0.24283 0.88262 66.4718	0.139305 1.45469 103.7260	472.3465 -41.9297 -56.0082
	8.00	0.15471 0.79988 58.25610	0.06497 1.50021 103.6180	1096.8469 -107.0528 -113.56188

Increase in the parametric values of α, M and δ also increases the value of TC.

Increase in the parametric values of β also decreases the value of TC.

Case II Payment after depletion

Table II

	Change in Parameters	T	T_1	TC
α	0.005	0.06883 135.940	0.35403 95.4690	4695.0255 16.5064
	0.010	0.06895 68.2756	0.35405 47.9690	4679.9299 16.62630
	0.020	0.06918 34.44205	0.35408 24.2191	4667.21736 16.8667
β	1.00	0.06883 135.940	0.35403 95.4690	4695.0255 16.5064
	2.00	0.06876 14.3009	0.35402 9.98745	4705.4034 16.43740
	3.00	0.06873 6.76414	0.35402 4.72757	4708.8323 17.38170
M	0.2	0.06883 135.940	0.35403 95.4690	4695.0255 16.5064
	0.4	0.06289 135.9350	0.35196 95.4646	5596.9645 16.5045
δ	5.00	0.06883 135.940	0.35403 95.4690	4695.0255 16.5064
	8.00	0.08539 129.0880	0.29330 95.4319	2989.09957 2.65941

Increase in the parametric values of β and M also increases the valves of TC.

Increase in the parametric values of α and δ also decreases the value of TC.

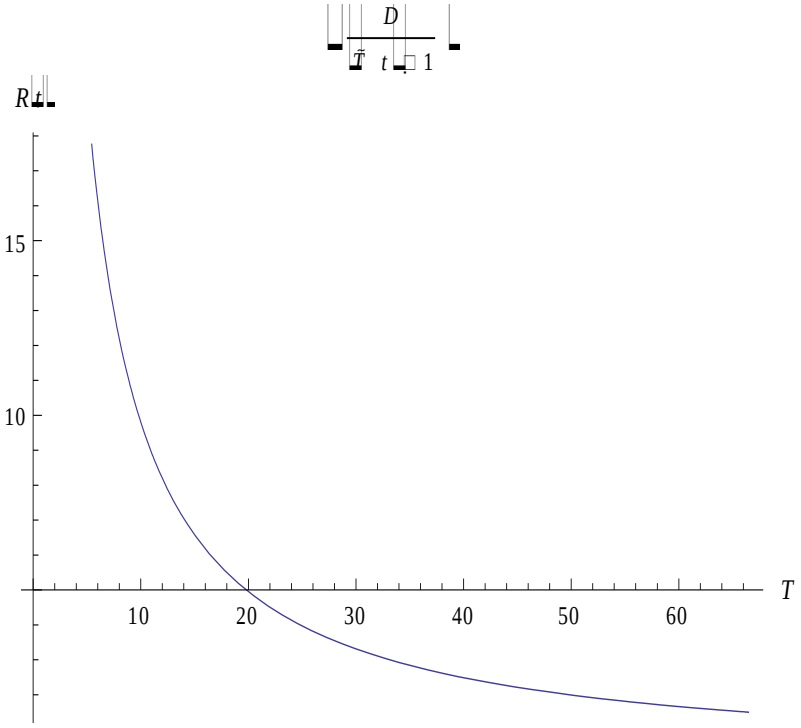

Figure I Backlogging rate at t=0, with respect to α

V. CONCLUSION

In the present paper we developed an inflationary inventory model for Weibull deteriorating items with constant demand and time dependent partial back-logging. We discussed the model by considering two cases namely case I payment before depletion and case II payment after depletion. We make a decision to determine the optimum cycle time for minimizing the total average inventory cost. From the table I it is obvious that the increases in the deterioration parameters α, M and δ also increase the total variable inventory cost and increases in the deterioration parameter β also decrease the total variable cost. From the table II it is obvious that the increases in the deterioration parameters β and M also increase the total variable cost and increases in the deterioration parameters α and δ also decrease the total variable inventory cost. From these results it is obvious as we increase the time of permissible delay in payment then the total variable inventory cost increases and the purchaser earn more by investing the resources.

REFERENCES

[1] Aggarwal, S.P. and Jaggi, C.K. (1995), Ordering policies of deteriorating items under permissible delay in payments. Journal of Operational Research Society 46, 658-662.

[2] Berrotoni, J.N. (1962) Practical Applications of Weibull distribution. ASQC. Tech. Conf. Trans. 303-323.

[3] Biermans, H. and Thomas, J. (1977) Inventory decisions under inflationary conditions. Decision Sciences 8, 151-155.

[4] Buzacott, J.A. (1975) Economic order quantities with inflation. Operational Research Quarterly 26, 1188-1191.

[5] Bhahmbhatt, A.C. (1982) Economic order quantity under variable rate inflation and mark-up prices. Productivity 23, 127-130.

[6] Chakrabarty, T., Giri, B.C. and Chaudhuri, K.S. (1998) An EOQ model for items with weibull distribution deterioration, shortages and trended demand. An extension of Philip's model Computers and Operations Research 25, (7/8), 649-657.
[7] Chandra, J.M. and Bahner, M.L. (1988) The effects of inflation and the value of money or some inventory systems. International Journal of Production Economics 23, (4) 723-730.
[8] Chung, K.J., Huang, Y.F. and Huang, C.K. (2002) The replenishment decision for EOQ inventory model under permissible delay in payments. Opsearch 39, 5 & 6, 327-340.
[9] Chung, K.J. and Huang, T-S. (2005) The algorithm to the EOQ model for Inventory control and trade credit. Journal of Operational Research Society 42, 16-27.
[10] Chung, K.J. and Hwang, Y.F. (2003) The optimal cycle time for EOQ inventory model under permissible delay in payments. International Journal of Production Economics 84, 307-318.
[11] Covert, R.P. and Philip, G.C. (1973) An EOQ model for deteriorating items with weibull distributions deterioration. AIIE Trans 5, 323-332.
[12] Dave, U. and Patel, L.K. (1983) (T.So.) policy inventory model for deteriorating items with time proportional demand. J. Opl. Res. Soc. 20, 99-106.
[13] Deb, M. and Chaudhuri K.S. (1986) An EOQ model for items with finite of production and variable rate of deterioration. Opsearch 23, 175-181.
[14] Dye, C.Y. (2002) a deteriorating inventory model with stock dependent demand and partial backlogging under condition of permissible delay in payments. Opsearch 39, (3 & 4).
[15] Goyal, S.K. (1985) Economic order quantity under conditions of permissible delay in payments. Journal of Operational Research Society 36, 335-338.
[16] Hwang, H. Shinn, S.W. (1997) Retailer's pricing and lot sizing policy for exponentially deteriorating products under condition of permissible delay in payments. Computers and Operations research 24, 539-547.
[17] Jamal, A.M. , Sarkar, B.R. and Wang, S. (1997) An ordering policy for deteriorating items with allowable shortage and permissible delay in payment. Journal of Operational Research Society 48, 826-833.
[18] Jesse, R.R., Mitra, A. and Cox, J.F. (1983) EOQ formula : Is it valid under inflationary conditions? Decision Sciences 14(3), 370-374.
[19] Liao, H.C., Tsai, C.H. and SU, C.T.(2000) An inventory model with deteriorating items under inflation when a delay in payment is permissible. International Journal of Production Economics 63, 207-214.
[20] Mandal, B.N. and Phaujdar, S. (1989) An inventory model for deteriorating items and stock dependent consumption rate. Journal of Operational Research Society 40, 483-488.
[21] Mishra, R.B. (1975) Optimum production lot- size model for a system with deteriorating inventory. Int. J. Prod. Res. 13, 161-165.
[22] Mondal, M. and Motti, M. (1999) Inventory of damageable items with variable replenishment rate, stock dependent demand and some units in hand. Applied Mathematical Modeling 23, 799-807.
[23] Mishra, V.K. and Singh, L.S. (2010) Deterministic inventory model for deteriorating items with shortage and partial backlogging Applied Mathematical Sciences 4, no-72, 3611-3619.
[24] Mandal, Biswarajan (2013) Inventory model for random deteriorating items with a linear trended in demand and partial backlogging. 2(3), 48-52.

American Journal of Engineering Research (AJER)
e-ISSN : 2320-0847 p-ISSN : 2320-0936
Volume-02, Issue-09, pp-55-61
www.ajer.org

Research Paper Open Access

Computation of Modulus of Elasticity of Concrete

Onwuka, D.O, Egbulonu, R.B.A, and Onwuka, S.U
a,b Civil Enineering, Federal University of Technology, Owerri, Nigeria.
c, Project management Department, Federal University of Technology, Owerri, Nigeria.

Abstract: - In this presentation, a computer based method which uses a set of algebraic equations and statistical data, were used to compute concrete mixes for prescribeable elastic concrete modulus, and vice versa. The computer programs based on Simplex and Regression theories can be used to predict several mix proportions for obtaining a desired modulus of elasticity of concrete made from crushed granite rock and other materials. The modulus of elasticity of concrete predicted by these programs agreed with experimentally obtained values. The programs are easy and inexpensive to use, and give instant and accurate results. For example, if the modulus of elasticity is specified as input, the computer instantly prints out all possible concrete mix ratios that can yield concrete having the specified elastic modulus. When the concrete mix ratio is specified as input, the computer quickly prints out the elastic modulus of the concrete obtainable from a given concrete mix ratio.

Keywords: - *Modulus of elasticity, Concrete, Computer programs, Simplex theory, Regression theory.*

I. INTRODUCTION

The predictions of the values of modulus of elasticity of concrete for the design of concrete structures have always required extensive sampling and testing. This has always limited design to only specific concrete mixtures whose values are known. The existing empirical methods of obtaining specific values of elastic modulus of concrete are cumbersome, labor intensive and time consuming with high degree of errors (Simon,2003).

In this work, simplex design method (1958) and a modified regression design method (2003) that use the theory of statistics and experimental results to obtain response functions, were employed in the development of computer programs for the computation of elastic modulus of concrete obtainable from a specified mix proportion and vice versa. The advantages of the developed programs, are that the programs eliminate the need for trial mixes, save time and cost, and give more accurate results.

II. NUMERICAL ANALYSIS

The computer programs are developed from response functions based on two statistical theories, namely, simplex theory and regression theory for determining properties of concrete mixes. The main advantage of this statistical approach, is that computer programming can be applied to the response functions derived from theories.

2.1 Simplex Response Function

The first response function for the computation of the elastic modulus of a normal concrete, is derived from simplex theory (1958), which uses practical data from laboratory tests, to formulate expression for determining the modulus of elasticity. The response function, Y_i, gives the relationship between the response (i.e. the property sought) and the proportions of concrete constituents.

In simplex theory, the general response function applicable to a mixture with 'q' constituents is as follows:

$$Y_i = b_0 + \sum_{i=1}^{q} b_i x_1 + \sum_{i=1}^{q} \sum_{j}^{q} b_{ij} x_i x_j \quad \ldots\ldots (1)$$

where b_i and b_{ij} are constants
X_i and X_j are pseudo constituents

Two conditions must be satisfied for Eqn(1) to hold, namely,

(i) The first condition is that the i^{th} component, X_i , must be greater than zero and or less than or equal to one. .i.e.

$$0 < X_i \leq 1 \quad \text{.....(2)}$$

where $i = 1,2,....q$

(ii) And the second condition is that the sum of the components must be equal to one, i.e.

$$X_1 + X_2 + X_3 + ...X_q = 1 \quad \text{..... (3)}$$

For a four- component mixture,

X_1 = proportion of water-cement (w/c) ratio
X_2 = proportion of cement
X_3 = proportion of sand
X_4 = proportion of crushed rock

The response function, Y_i , developed for a mixture with four pseudo components and two degree reaction, is given by Eqn(4).

$$Y_i = b_1X_1 + b_2X_2 + b_3X_3 + b_4X_4 + b_{12}X_1X_2 + b_{13}X_1X_3 + b_{14}X_1X_4 + b_{23}X_2X_3 + b_{24}X_2X_4 + b_{34}X_3X_4 \quad \text{..... (4)}$$

And the final response function formulated for the determination of elastic modulus of concrete, using simplex theory and experimental results, is as follows:

$$Y = 41.31X_1 + 50.04X_2 + 25.21X_3 + 19.24X_4 - 95.58X_1X_2 - 28.64X_1X_3 + 22.10X_1X_4 - 55.76X_2X_3 - 25.96X_2X_4 + 14.26X_3X_4 \quad \text{..... (5)}$$

The details of the derivation of the function is given by Egbulonu (2011).

The actual components, Z_i, used in the mixture experiment are transformed from the Eqn (6)

$$[Z] = [A][X] \quad \text{.....(6)}$$

Conversely,

$$[X] = [B][Z] \quad \text{.....(7)}$$

where,

[Z] = matrix of real component proportions
[X] = matrix of pseudo component proportions
[A] = matrix of arbitrary mix proportions based on past experience.
[B] = inverse of matrix A

The values of the real components, Z_i, are used for conducting the laboratory tests for the determination of experimental values of the elastic modulus Y_i and Y_{ij}

2.2 REGRESSION RESPONSE FUNCTION

The second computer program is based on a continuous regression function which can be differentiated with respect to its variables, Z_i. For a mixture such as concrete whose responses (desired properties), are dependent on the proportions of its constituents, its response function is as follows:

$$Y = \sum_{i=1}^{4} a_i Z_i + \sum_{i=1}^{4} \sum_{j=1}^{4} a_{ij} Z_i Z_j \quad \text{..... (8)}$$

where

Z_i and Z_j = Predictors or fractional portion of the ith and jth components respectively.

a_i and a_j = coefficients of the regression function

Since the property of interest in this work, is the the modulus of elasticity, E, of concrete, the response function developed for it using Eqn(8) is as follows:

$$Y = a_1Z_1 + a_2Z_2 + a_3Z_3 + a_4Z_4 + a_{12}Z_1Z_2 + a_{13}Z_1Z_3 + a_{14}Z_1Z_4 + a_{23}Z_2Z_3 + a_{24}Z_2Z_4 + a_{34}Z_3Z_4 \quad \text{.....(9)}$$

At the 'nth' observation point, the response function, $Y^{(n)}$ corresponding with the predictor, Z_i, is given by Eqn(10)

$$[Y^{(n)}] = [Z^{(n)}]\{a\} \quad \text{.....(10)}$$

where

$[Y^{(n)}]$ = matrix of the response functions
$[Z^{(n)}]$ = matrix of Predictors
$[a]$ = matrix of constant coefficients

The elements of the response matrix $[Y^{(n)}]$, are obtained from the laboratory tests while the elements of the matrix of predictors, $[Z^{(n)}]$ are obtained from the matrix of actual proportions $[S^{(n)}]$. And the values of the coefficient matrix, $[\alpha]$ are determined from Eqn(10) and substituted into Eqn(9) to obtain the final regression response function i.e Eqn(11)) on which the second program is based.

$$\mathbf{Y} = 5351667.6400\mathbf{Z_1} + 888151.9143\mathbf{Z_2} + 1835.219102\mathbf{Z_3} + 2392.479301\mathbf{Z_4} - 10609392.05\mathbf{Z_1Z_2} - 5791804.077\mathbf{Z_1Z_3} - 5620199.635\mathbf{Z_1Z_4} - 699734.4294\mathbf{Z_2Z_3} - 786415.528\,\mathbf{Z_2Z_4} + 12085.08274\,\mathbf{Z_3Z_4} \quad \ldots\ldots (11)$$

Thus, the modulus of elasticity of a four- component concrete mixture, can be determined from Eqn(11). Full details of its derivation are contained in the works of Egbulonu(2011).

III. COMPUTER PROGRAMS

Computer programs based on these models, were developed for easy, quick, cheap and precise computation of mix proportions of concrete given its elastic modulus, E. The computer programs can also determine modulus of elasticity, E, from a given concrete mix proportion. The programs based on simplex theory and regression theory are as presented in Appendix A and Appendix B respectively. And Tables 1 and 2 contain the outputs of the computer programs.

IV. RESULTS AND ANALYSIS

The inputs required to run the programs are either modulus of elasticity or mix proportions. If the desired modulus of elasticity is fed into the computer, the computer either:

(a) Prints out all possible combinations of actual mix proportions (Z_i) and the corresponding pseudo proportions (X_i) that match the elastic modulus, Y.
(b) Prints out the maximum elastic modulus that can be predicted from program.
(c) Notify the user if there is no matching combination.

On the other hand, if the mix proportion is the input, the computer prints out the elastic modulus obtainable from the given mix proportion.
These outputs are summarized in Tables 1 and 2.
The result of computer programs for specified modulus of elasticity of 36N/mm^2, is presented in Tables 1 and 2.

Table 1: Output of simplex mix ratios corresponding to an input of elastic modulus, Y, of 36N/mm^2

S/N	X_1	X_2	X_3	X_4	Y	Z_1	Z_2	Z_3	Z_4
1	0.08	0.82	0.09	0.01	36.00	0.55	1.00	1.93	2.99
2	0.10	0.79	0.01	0.10	36.00	0.50	1.00	2.00	3.06

where

X_1 = pseudo values of water — Z_1 = actual values of water
X_2 = pseudo values of cement — Z_2 = actual values of cement
X_3 = pseudo values of sand — Z_3 = actual values of sand
X_4 = pseudo values of coarse aggregate — Z_4 = actual values of coarse aggregate

Table 2: Output of Regression- based mix ratios corresponding to an input of elastic modulus, Y, of 36N/mm^2

S/N	Z_1	Z_2	Z_3	Z_4	Y	S_1	S_2	S_3	S_4
1	0.06	0.10	0.25	0.59	36.00	0.64	1.00	2.58	5.98
2	0.08	0.15	0.30	0.46	36.00	0.56	1.00	2.00	3.07
3	0.10	0.20	0.32	0.37	36.00	0.51	1.00	1.62	1.85
4	0.11	0.23	0.34	0.32	36.00	0.50	1.00	1.52	1.42
5	0.13	0,26	0.34	0.34	36.00	0.49	1.00	1.30	1.07
6	0.13	0.27	0.26	0.34	36.00	0.47	1.00	0.95	1.24

where

S_1 =Actual portion of water
S_2 = Actual portion of cement
S_3 = Actual portion of sand
$\mathbf{S_4}$ = Actual portion of coarse aggregate

Table 3: Computer output of modulus of Elasticity, Y, corresponding to input of Various mix proportions

S/N	Simplex function					Regression functionl				
	Given mix ratios				MOE,Y N/mm^2	Given mix ratios				MOE
	Z_1	Z_2	Z_3	Z_4		S_1	S_2	S_3	S_4	
1	0.5600	1.0	1.7	3.05	**19.40**	0.5600	1.0	1.7	3.05	**20.35**
2	0.5650	1.0	2.0	3.30	**30.88**	0.5650	1.0	2.0	3.30	**30.17**
3	0.5825	1.0	2.1	3.65	**23.64**	0.5825	1.0	2.1	3.65	**24.80**
4	0.5850	1.0	2.1	3.60	**23.77**	0.5850	1.0	2.1	3.60	**24.54**
5	0.5900	1.0	2.2	3.70	**24.64**	0.5900	1.0	2.2	3.70	**24.53**
6	0.6400	1.0	2.8	4.80	**22.72**	0.6400	1.0	2.8	4.80	**22.07**

4.1 COMPARISON OF RESULTS

The sets of results (i.e elastic modulus) obtained from Simplex and regression functions, are comparable. Table 4 indicates that the maximum percentage difference between the modulus of elasticity obtained from Simplex function and those obtained from the Regression function, is 4.15%. Thus, the percentage differences is negligible. And so, the results are in agreement.

Table 4: Comparison of Simplex-based and Regression-based elastic moduli

S/N	Modulus of Elasticity (N/mm^2)		Difference	Percentage Difference
	Simplex Values	Regression Values		
1	19.40	20.35	0,95	4.91
2	30.88	30.17	0.71	2.30
3	23.64	24.80	1.16	4.91
4	23.77	24.50	0.79	3.24
5	24.64	24.53	0.11	0.45
6	22.72	22.07	0.65	2.95

V. CONCLUSIONS

Based on the analysis of the results, the following conclusions were reached:

- Either of the programs based on Simplex theory or Regression theory, can be used in determining elastic modulus of normal concrete if the mix ratios are given as input.
- In addition, it can be used to determine the mix proportions that can produce concrete of desired elastic modulus.
- The maximum elasticity modulus that can be determined from the program , is 50.04 N/mm^2.
- The programs are easy and inexpensive to use, and give instant and accurate results.

REFERENCES

[1] Aggarwal, M.I., (2002). "Mixture Experiments". Design Workshop lecture notes. University of Delhi, Delhi. India. Pp.77-89

[2] BS 1881, Part 110(1983), "Method of making test cylinders from fresh concrete". BSI-London.

[3] BS 1881, Part 111(1983), "Method of normal curing of test specimens (20C method)". BSI-London.

[4] BS 1881, Part 118(1983), "Method of determination of Static modulus of elasticity in compression". BSI-London.

[5] Civil Engineering Department, University of New Mexico (2006)". C469 Standard Test method of Static modulus of Elasticity and Poisson ratio of concrete in compression. Available from <http//www.google.com./search>

[6] Clark, D.(1980), Computer Aided Structural Design, John Wiley and Sons.

[7] Egbulonu, R.B. A.(2011) "Optimization models for predicting the modulus of elasticity and Flexural strength of

[8] concrete". Unpublished Master Degree Thesis, Department of Civil Engineering, Federal University of

[9] Technology, Owerri, Nigeria.

[10] Gagula M., (1993). ''Design and Analysis of Sensory Optimization ''. Wiley Blackwell, Connecticut, USA.

[11] Grubl,P., Ruhl,M. and Buhrer, M.."Evaluation of Modulus of Elasticity of Concrete with recycled aggregate Available from <http//www.g>

[12] Henry Scheffe, (1963). "Simplex-Centroid Design for Experiments with mixtures". Journal of Royal statistics society, series B, vol.25, No 2, pp.235-263.

[13] Malaikah, A., (2004). ‘‘Predicting Modulus of Elasticity Report’’. pp.1-8. Available from <http//www.google.com./search>
[14] Osadebe, N.N., 2003, “ Generalized Mathematical Modeling of Compressive Strength of Normal Concrete as a Multi-Variant function of the properties of its Constituent Components”. A paper delivered at the Faculty of Engineering. University of Nigeria, Nsukka.
[15] Sanders, P., (2007) “Basic Approaches to Optimization Problems”. College of Information Sciences and Technology, Pennsylvanian state University. Available from <http//www.google.com./search>
[16] Simon, M. J.,(2003). “Concrete mixture optimization using statistical methods”. TTHRC, FHWA publication on FHWA-RD 03-060. Mc lean pub. VA, USA.

APPENDIX A:PROGRAM FOR COMPUTATION MODULUS OF ELASTICITY OF CONCRETE USING SIMPLEX MODEL

```
CLS
 REM A Q-BASIC PROGRAMM THAT OPTIMISES CONCRETE MIX PROPORTIONS
 REM THIS WAS WRITTEN BY BEN EGBULONU
 REM X1,X2,X3,X4,Z1,Z2,Z3,Z4,Ymax,Yout,Yin
 REM MODEL USED ELASTIC MODULUS: BY SCHEFFE'S MODEL
 REM MAIN PROGRAMM BEGINS
    REM TO DEFINE WHAT IS GIVEN AND WHAT REQUIRED TO DETERMINE.
    REM WHEN MIX IS GIVEN G=1 0R G=2 IF E IS GIVEN
    PRINT "DEFINE WHAT IS GIVEN AS G="; G;
    INPUT G
    IF G = 1 THEN  ELSE GOTO 5
    REM MIX GIVEN AS Z1,Z2,Z3,Z4.
    PRINT "ENTER VALUE OF W/C=Z1"; Z1
    INPUT Z1
    PRINT "ENTER VALUE OF CEMENT=Z2"; Z2
    INPUT Z2
    PRINT "ENTER VALUE OF SAND=Z3"; Z3
    INPUT Z3
    PRINT "ENTER VALUE OF AGG=Z4"; Z4
    INPUT Z4
    LET X1 = 40 * Z1 - 16 * Z2 + 0 * Z3 - 2 * Z4
    LET X2 = -60 * Z1 + 26 * Z2 + 1 * Z3 + 2 * Z4
    LET X3 = -20 * Z1 + 9 * Z2 - 2 * Z3 + 2 * Z4
    LET X4 = 40 * Z1 - 18 * Z2 + 1 * Z3 - 2 * Z4
    LET E = 41.31 * X1 + 50.04 * X2 + 25.21 * X3 + 19.24 * X4 - 95.58 * X1 * X2 - 28.64 * X1 * X3 + 22.1 *
X1 * X4 + -55.76 * X2 * X3 - 25.96 * X2 * X4 + 14.26 * X3 * X4
    REM PRINT VALUE E
    PRINT "VALUE OF E="; E; "X1"; X1, "X2"; X2; "X3"; X3; "X4"; X4;
    GOTO 7
5 LET COUNT = 0
 CLS
 GOSUB 10
7 END
 REM END OF MAIN PROGRAMM
10 REM PROCEDURE BEGINS
 LET Ymax = 0
 PRINT
 PRINT
 REM A COMPUTER MODEL FOR COMPUTING CONCRETE MIX PROPORTIONS
 PRINT "CORRESPONDING TO A REQUIRED ELASTIC MODULUS"
 PRINT
 INPUT "ENTER DESIRED ELASTIC MODULUS"; Yin
 GOSUB 70
  FOR X1 = O TO 1 STEP .01
   FOR X2 = O TO 1 - X1 STEP .01
    FOR X3 = O TO 1 - X1 - X2 STEP .01
```

```
    LET X4 = 1 - X1 - X2 - X3
LET Yout = 41.31 * X1 + 50.04 * X2 + 25.21 * X3 + 19.24 * X4 - 95.58 * X1 * X2 - 28.64 * X1 * X3 + 22.1 *
X1 * X4 - 56.1 * X2 * X3 - 25.96 * X2 * X4 + 14.26 * X3 * X4
    GOSUB 80
IF (ABS(Yin - Yout) <= .001) THEN 20 ELSE 30
20   LET COUNT = COUNT + 1
    GOSUB 90
30   NEXT X3
   NEXT X2
  NEXT X1
  PRINT
  IF (COUNT > 0) THEN GOTO 40 ELSE GOTO 50
40 PRINT "THE MAXIMUM ELASTIC MODULUS PREDICTABLE"
  PRINT "BY THIS MODEL IS"; Ymax; "N/sq.mm"
  SLEEP (2)
  GOTO 60
50 PRINT "SORRY! DESIRED ELASTIC MODULUS OUT OF RANGE OF MODEL"
  SLEEP 2
60 RETURN
70 REM PROCEDURE PRINT HEADING
  REM
  PRINT "COUNT X1 X2 X3 X4 Y Z1 Z2 Z3 Z4"
  REM
  RETURN
80 REM PROCEDURE CHECK MAX
  IF Ymax < Yout THEN Ymax = Yout ELSE Ymax = Ymax
  RETURN
90 REM PROCEDURE OUT RESULTS
  LET Z1 = .5 * X1 + .55 * X2 + .6 * X3 + .65 * X4
  LET Z2 = X1 + X2 + X3 + X4
  LET Z3 = X1 + 2 * X2 + 2 * X3 + 3 * X4
  LET Z4 = 1.5 * X1 + 3 * X2 + 4 * X3 + 5 * X4
  PRINT TAB(1); COUNT; USING "###.##"; X1; X2; X3; X4; Yout; Z1; Z2; Z3; Z4
  RETURN
```

APPENDIX B:PROGRAM FOR COMPUTATION OF MODULUS OF ELASTICITY OF CONCRETE USING REGRESSION MODELCLS

```
REM ** 100% CORRECT** OK ** NO MAXIMUM** RUN TIME =60sec TO 5mins ***
REM A Q-BASIC PROGRAMM THAT OPTIMISES CONCRETE MIX PROPORTIONS
REM THIS WAS WRITTEN BY BEN EGBULONU
REM VARIABLES USED ARE : Z1,Z2,Z3,Z4,S1,S2,S3,S4,Ssum,Ymax,Yout,Yin
REM MODEL USED ELASTIC MODULUS
REM PROGRAM PRINTING SPLIT IN 1ST-17, THEN 20s TO ENTER PRINTING WINDOW.
REM MAIN PROGRAMM BEGINS
    REM WHEN MIX IS GIVEN G=1 0R G=2 IF E IS GIVEN
    PRINT "DEFINE WHAT IS GIVEN AS G="; G;
    INPUT G
    IF G = 1 THEN  ELSE GOTO 5
    REM MIX GIVEN AS ACTUAL MIX RATIOS, S1.S2.S3.S4.
    PRINT "ENTER VALUE OF W/C=S1"; S1
    INPUT S1
    PRINT "ENTER VALUE OF CEMENT=S2"; S2
    INPUT S2
    PRINT "ENTER VALUE OF SAND=S3"; S3
    INPUT S3
    PRINT "ENTER VALUE OF AGG=S4"; S4
    INPUT S4
    LET Ssum = S1 + S2 + S3 + S4
    REM CALCULATING FRACTIONAL PARTS
```

```
    LET Z1 = S1 / Ssum: Z2 = S2 / Ssum: Z3 = S3 / Ssum: Z4 = S4 / Ssum
REM         ****** CEFFICIENTS OS REGRESSION *******
    A1 = 5351667.64#: A2 = 888151.9142999999#: A3 = 1835.219102#
    A4 = 2392.479301#: A5 = -10609392.05#: A6 = -5791804.077#
    A7 = -5620199.635#: A8 = -699734.4294#: A9 = -786415.528#
    A10 = 12085.08274#
REM CALCULATING ACTUAL MODULUS OF ELASTICITY
    LET MOE = A1 * Z1 + A2 * Z2 + A3 * Z3 + A4 * Z4 + A5 * Z1 * Z2 + A6 *
    Z1 * Z3 + A7 * Z1 * Z4 + A8 * Z2 * Z3 + A9 * Z2 * Z4 + A10 * Z3 * Z4
    REM PRINT VALUE OF MOE
    PRINT "VALUE OF MOE="; MOE; "S1"; S1; "S2"; S2; "S3"; S3; "S4"; S4;
    "Z1"; Z1; "Z2"; Z2; "Z3"; Z3; "Z4"; Z4
    GOTO 7
5 LET COUNT = 0
 CLS
 GOSUB 10
7 END
 REM END OF MAIN PROGRAMM
10 REM PROCEDURE BEGINS
 LET Ymax = 0
 PRINT
 PRINT
 REM A COMPUTER MODEL FOR COMPUTING CONCRETE MIX PROPORTIONS
 PRINT "CORRESPONDING TO A REQUIRED MODULUS OF ELASTICITY"
PRINT
 INPUT "ENTER DESIRED MODULUS OF ELASTICITY"; Yin
 GOSUB 70
 FOR Z1 = O.035 TO .25 STEP .001
 FOR Z2 = .07 TO .28 STEP .001
 FOR Z3 = .22 TO .35 STEP .001
 LET Z4 = 1 - Z1 - Z2 - Z3
REM         ****** CEFFICIENTS OS REGRESSION *******
    A1 = 5351667.64#: A2 = 888151.9142999999#: A3 = 1835.219102#
    A4 = 2392.479301#: A5 = -10609392.05#: A6 = -5791804.077#
    A7 = -5620199.635#: A8 = -699734.4294#: A9 = -786415.528#
    A10 = 12085.08274#
LET Yout = A1 * Z1 + A2 * Z2 + A3 * Z3 + A4 * Z4 + A5 * Z1 * Z2 + A6 * Z1 * Z3 + A7 * Z1 * Z4 + A8 *
Z2 * Z3 + A9 * Z2 * Z4 + A10 * Z3 * Z4
 IF ABS(Yin - Yout) <= .001 THEN 20 ELSE GOTO 30
20 LET COUNT = COUNT + 1
 GOSUB 90
30 NEXT Z3
 NEXT Z2
 NEXT Z1
 PRINT
 IF (COUNT > 0) THEN GOTO 60 ELSE GOTO 50
50 PRINT "SORRY! DESIRED MOE OUT OF RANGE OF MODEL"
  SLEEP 1
60 RETURN
70 REM PROCEDURE PRINT HEADING
 REM
 PRINT "COUNT Z1 Z2 Z3 Z4 Y S1 S2 S3 S4"
 REM
 RETURN
90 REM PROCEDURE OUT RESULTS
 LET S1 = Z1 / Z2: S2 = Z2 / Z2: S3 = Z3 / Z2: S4 = Z4 / Z2
 REM ************** 1ST PRINTING 0-18,NEXT 17-37,ETC.**********
 PRINT TAB(1); COUNT; USING "###.##"; Z1; Z2; Z3; Z4; Yout; S1; S2; S3; S4
100 RETURN
```

American Journal of Engineering Research (AJER)
e-ISSN: 2320-0847 p-ISSN : 2320-0936
Volume-02, Issue-09, pp-62-70
www.ajer.org

Research Paper Open Access

Smart input based user authentication and challenges towards multi-tiered cyber security

Ziaur Rahman, Md. Baharul Islam, A. H. M. Saiful Islam
[1](*Department of ICT, Mawlana Bhashani Science & Technology University, Tangail-1902, Bangladesh*)
[2](*Department of Multimedia Technology and Creative Arts, Daffodil International University, Bangladesh*)
[3](*Department of Computer Science and Engineering, Daffodil International University, Bangladesh*)

Abstract: - Ever been a situation where a cyber crime investigation authority is searching for a convicted user who has allegedly done something illegal and the authority only can identify the system where from the crime is committed instead of having any information about the acquitted user exactly they are looking for. If we compare this scenario with our real world offenses that means the police has found the site where the crime is held but they have no idea or clue about the criminal. It should deserve a great concern that this type of thing is happening in our today's modern cyber world in each every day. We can easily find any system or network that is doing something offensive and fraud but it is not clear to us how we can find the acquitted user who has used that system to commit that fraud. We've tried to find a solution towards a sound solution of the problem we've been ever facing in our cyber world. In this paper we have proposed a smart input based user authentication method that can reduce online fraud in the cyber world.

Keywords: *- activity history, biometric devices, finger print pattern, feature noise, online security, smart button*

I. INTRODUCTION

Sensitive mouse or keyboard is not an unknown term. We're going to tell here a similar concept might not be much unknown. We do many activities in our daily life by using our computer system where basically we use Input / Output (IO) devices. For example if we want to surf internet we usually need to open a browser to write an address on address bar. For this we need an event generated by mouse or keyboard or by any device we ever have. Monitoring input can play a vital role especially when we're talking about monitoring our cyber world. In this paper we've proposed a new type of keyboard and mouse layout where ENTER key of the keyboard and RIGHT BUTTON of the mouse are sensitive or there is an extra input button on the input systems that is biometrically sensitive. That means when a user will enter an account using this key or button a special interruption will be sent to the client or server containing identifiable user information. Identifying information may vary from user's finger print, Retinal Scan Code, Iris Recognizer, Vein Pattern, Face Recognition Code, Iris Scan code, Hand or Leg Print Readable Code or geometry, Voice prints, Keystroke timing, Signature, Smart Passport Voice Analyzer to DNA mapping code analysis. Here we've used an input system what can only read the finger print of the user. To be more explicit is that in our research we've tested this type of smart input just using finger print scanning. When a user will press ENTER key or sensitive BUTTON to login into his account the smart input key or button will send that user's special information to the system through interruption.

II. BACKGROUND RESEARCH

One may ask why we're going to choose finger print technology inside the smart input device to identify the user. Fingerprint based authentication although sometimes not as high-profile as other high-tech crime-solving methods like DNA typing, is still very much used in criminal investigations and other fraud detection cases. Though the principle that no two persons could have the same fingerprints cannot be scientifically authenticated, fingerprint evidence is generally considered to be highly secure, reliable and is particularly accessible to juries. It doesn't need much talk to conceive that your fingers contain a map of ridges and whorls that is completely unique without any confusion. There are different types of classification as available at present all over the world. In the Henry system of classification, there are three basic fingerprint

patterns. These are loop, whorl and arch. Loop constitutes 60–65%, whorl constitutes 30–35% and arch constitutes 5% of all fingerprints. Another complex systems used by most experts are similar to the Henry system of classification. In general, it consists of five fractions R, L, I, m, and t where R stands for right, L for left, i for index finger, m for middle finger, t for thumb, r for ring finger and p (pinky) for little finger. The fractions are as follows:

$$R_i/R_t + R_r/R_m + L_t/R_p + L_m/L_i + L_p/L_r$$

Because of its availability and development fingerprints are more useful because than DNA according to forensic experts say. In the last decade several papers published aimed at illustrating the intersection among biometrics devices, cryptographic system and so forth. David, et al. (1998) was among the first to suggest offline biometric authentication what was actually a PKI (Public Key Infrastructure) like environment with local fingerprint matching. The flaw was that it required local authentication. Then Fuzzy Commitment Scheme Juels et al. (1999) is encoded with the association of standard error correcting code such Hamming or Reed- Solomon and then XORed. Major problem of this system was that biometric data was often subject to reordering and erasures which cannot be handled using this scheme. Another strategy Nichols et al. (1999) was provided using the phase information of a Fourier transformation of the scanned image. The fingerprint information and a randomly chosen key are mixed to make it impossible to recover one without other. This was not address how much these steps reduce the entropy of the original images thus it was not clear that there exists a set of parameters which will allow the system to determine the legitimate users while providing a reasonable amount of security. In his paper Monrose et al. (1999) is item to add entropy to user's passwords on a computer system through data from the way in which they type their passwords. As biometric is being used so that radically different from fingerprints, their results are not applicable to the solution. Juels and Sudan (2002) proposed fuzzy commitment scheme, which is more compatible with partial and reordered data.

2.1. Fuzzy Vault

Let's see the original fuzzy vault, with some slight notational differences. As with any cryptosystem, there is some message m to be decrypted for that symmetric fuzzy key that could be used. Suppose the message *m* is first encoded as the coefficient of some degree *k* polynomial in *x* over a finite field F_q.. Here the polynomial f*(x)* needs to protect. Locking set L is a set of values $l_i \in F_q$ making up the fuzzy encryption key, where $t > k$. The lock vault contains all the pairs $(l_i, f(l_i))$ and some large number of chaff points (α_j, β_j), where $f(\alpha) \neq \beta_j$. After adding the chaff points, the total number of items in the vault is *r*. In order to crack the system, an attacker must separate the chaff points from the legitimate points in the vault. The difficulty of this operation is a function of the number of chaff points, among other things. To successfully interpolate the polynomial an unlocking set U of t elements such that $L \cap U$ contains at least $k + 1$ element. Here $f(x)$ is a degree k polynomial in $F_q[x]$, $t \geq k$ points in L interpolate through $f(x)$ and $r \geq t$ is total number of points in the vault. This vault shall be referred to as $V(F_q, r, t, k)$.

2.2. Polynomial Interpolation

To reconstruct the secret locked within the fuzzy vault, the points in the unlocking set must be used to interpolate a polynomial. Usually using brute-force search polynomial could be recovered where $k + 1$ element subsets of the unlocking set are used to interpolate a degree k polynomial, using Newtonian Interpolation Hilderband (1956). Another method is to use Reed-Solomon decoder Massey (2003) as suggested Juels and Sudan. RS decoding algorithm could be categorized into two: the Berlekamp-Massey (1969) algorithm and the Guruswami-Sudan (1998) algorithm. Another field called noisy polynomial interpolation has some recent advances, notably by Arora and Khot (2002) and Bleichenbacher and Nguyen (2000).

2.3. Feature Extraction

The Feature extraction process Verifinger (2009) is visually represented in the following figure 1.

(a) (b) (c)

Figure 1: Feature Extraction Process: (a) Original Image (b) After Edge Detection, (c) Including Feature Points

In (a), image scan of a fingerprint is available which is received from the Fingerprint device. After applying different edge detection algorithms the information inside is converted into (b). And in the (c) the fingerprint *minutiae* the location where fingerprint ridge either splits or ends are shown. Here the black box is considered as feature extraction and alignment. This yields to normalized *(x,y)* pixel coordinates of minutiae.

2.4. Feature Noise

A typical print consists of a certain set of minutie locations $m_i = (x_i,y_i) \in M$. Because of errors in capturing, processing and aligning noise is added. In that case it seems like this equation. $m_i' = (x_i + n_{xi}, y_{i,+} n_{yi})$. If N sample images are taken from a person the result is a set of expected values $(\overline{x_i}, \overline{y_i})$ for every achieved minutiae. The number $n \leq N$ of samples of having a minutiae in that neighboring region. The variance and covariance of those n minutiae of those n minutiae $(\sigma^2_{x,i}, \sigma^2_{y,i}, \rho_i)$. To get the geometrical spatial transformation (RST), let us consider an image function *f* defined in (w, z) coordinate system to get an image *g* over (x, y) Mehfuza Holia (2010).

(a) (b) (c) (d) (e)

Figure 2: (a) Original Image (b) Gray Scale Image (c) Binarized Image (d) Thinned Image (e) Final Minutiae

In the algorithm this RST transformation is applied on the each input fingerprint image to see how much it is rotated or scaled or translated with respect to the database image or the original image. In figure 12 (a) shows the original image, (b) shows the gray scale image, (c) shows the binary image, (d) shows thinned image and lastly (e) shows the final minutiae image. Two common features of the fingerprint image are ridge termination and ridge bifurcations Mandi (2012). Minutiae detection is a trivial task when an ideal thinned ridge map is available. After this result we will take any arbitrary point as reference point and align this to the origin. Then consider the shortest distances and find the relations as per considered two images. The Table 1 here shows FAR and FRR at different values. The summary is that FRR increases as threshold value increases, FAR decreases as threshold increases and at 0.023, they match each other. This is also known as Equal Error rate. In the table above GA stands for Genuine Accept.

Table I: False acceptance rate and False Rejection Rate

	TH-1	TH-2	TH-3	TH-4	TH-5
TH	0.01	0.017	0.023	0.03	0.04
FA	15	12	4	1	0
FA (%)	21.7	17.4	5.8	1.4	0.0
FR	0	0	4	22	29
FR (%)	0.0	0.0	5.8	31.9	42.0
GA	54	54	52	36	30
Accuracy	91.5	91.5	88.1	61.0	50.8

III. PROPOSED RESEARCH

User authentication consists of a computer verifying that you are who you claim to be. There are three main techniques:

- what you know
- what you have
- what you are

Biometric devices like our proposed smart input (fingerprint analyzers or biometric devices or even DNA code analyzer) almost fit into the last category. Actually our opinion is that if we confidentially can authenticate “who you are?” then anything else is almost optional. If these categories are combined together then the security will be multi-tiered security .This is done by adding smart input with the existing systems.

3.1. Research Environment

In our research plan we have done an experiment with a system consisting of sensitive mouse and keyboard. For this we have used SecuGenOptiMouse Plus Fingerprint Reader (Model MSDU03M2) and Keyboard (Microsoft Optical Desktop - MS BZ5-00002) as in Figure 3. Both Devices are USB portable and easy to use immediate after installing the respective software associated with it. SccuGenOptimouse is an optical mouse with an integrated ultra-fast, high performance fingerprint reader that holds three programmable buttons and let fingerprints act like a digital password.

Figure 3: SecuGenOptiMousePlus Fingerprint Reader (Model MSDU03M2) and Microsoft Optical Desktop - MS BZ5-00002

We fetch the devices with the system and prepared the desired environment to work as a smart input system. After installing the necessary software for both devices we've connected the system the system with the internet. To test how the Smart Input works we will use a simple email system that we've titled as "Smart Input Email System" which we've already developed using some common API and PHP. This site is able to communicate with the sensitive devices connected with the system.

3.2. Hypothesis

Just like other typical biometric system our proposed smart input system has four basic units (as shown in the Figure 4) are Sensing, Storage, Signal Processing and Interface Unit. Sensing unit varies as the type of sensor device changes. We've applied optical sensor but Charged Coupled device (CCD), Complementary Metal Oxide Semiconductor (CMOS) or even Thermal or Pressure also could be applied. However, CMOS imager or CCD could be used for face, iris, retinal or leg or handprint recognition. Storage could be SDRAM or Flash which are connected to Digital Signal Processing (DSP) device. Here, the processing element is generally a microprocessor. But in another case digital signal processor, computer or any other similar device may be used. A programmable DSP from Texas Instrument® is suggested to use here for the better output. The purpose of the Storage Element is to store the enrolled template that is recalled to execute the matching operation at the time of authentication. Random Access Memory (RAM) or flash EPROM or some any other form of Integrated Circuit(IC) or even data server may be used. Finally, there is an output interface that will communicate the decision of the system to user. This could be general communication protocol like RS232 or the higher bandwidth USB portable protocol. Or even TCP/IP protocol using wired medium e.g 10/100 Ethernet or wireless medium or Bluetooth or any other cellular protocol could be used. In our experiment we suggest to use USB storage for smooth outcome.

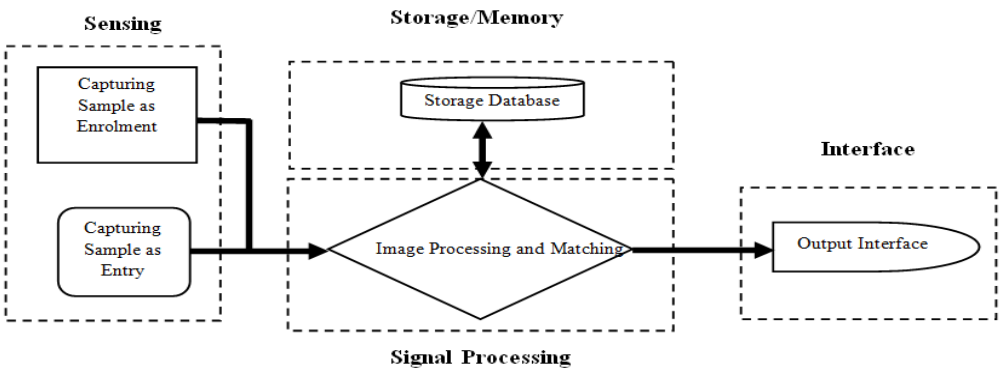

Figure 4: Working elements of fingerprint as smart input

IV. RESEARCH STUDY

First of all we need redirect the registration page which is known as Signup Wizard to create a new account. For registration we have to enter Name, Username, Password and others. Then we need to press the "Press Sensor Key to Proceed" button which we called smart button as a sample snapshot is shown in the Figure 5. While the user presses the Smart button (Fingerprint sensor key) the software will store his fingerprint code with other information

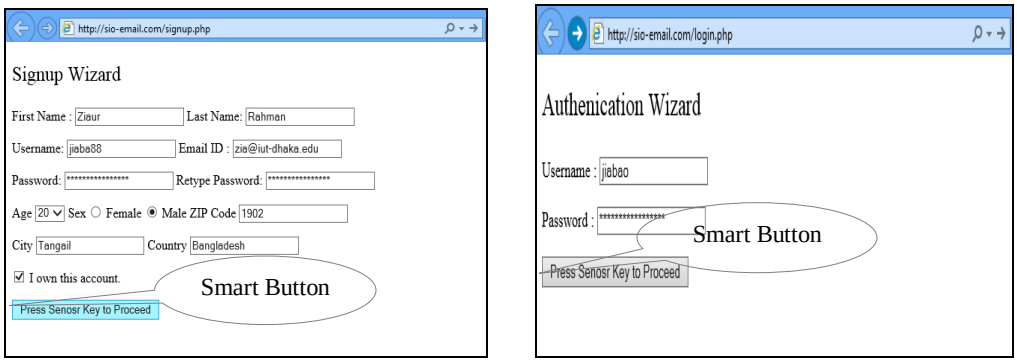

Figure 5: Sample signup wizards to register into the site able to work and authentication wizard to login into the site using smart input

Then to login into the Email system we as usually need to authenticate our identity. For that, if we click on login tab available in the home page of the Email Page we'll be shown the window as shown in Figure 5. Here after entering the username and password we'll have to again press the Smart Key. This time it will validate user's entered information with the information which is stored in the Databases. If the information does match then we'll be given access to the email system otherwise access will be denied. If someone tried to login into the Smart Email Input System by entering the arbitrary username or password it could be caught easily by monitoring the Activity History generated by the host server. The host server where the Email system is hosted is able to generate this history automatically. To show this more precisely a snapshot of the Activity History Window is attached here in the Figure 6.

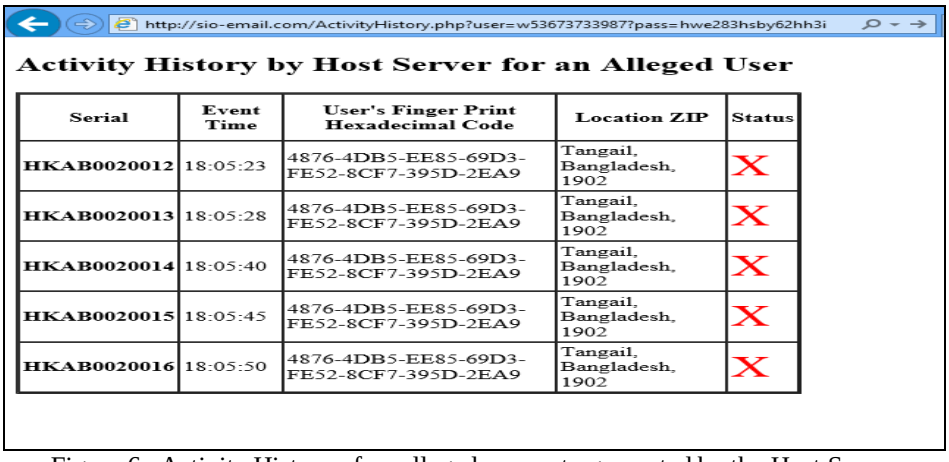

Serial	Event Time	User's Finger Print Hexadecimal Code	Location ZIP	Status
HKAB0020012	18:05:23	4876-4DB5-EE85-69D3-FE52-8CF7-395D-2EA9	Tangail, Bangladesh, 1902	X
HKAB0020013	18:05:28	4876-4DB5-EE85-69D3-FE52-8CF7-395D-2EA9	Tangail, Bangladesh, 1902	X
HKAB0020014	18:05:40	4876-4DB5-EE85-69D3-FE52-8CF7-395D-2EA9	Tangail, Bangladesh, 1902	X
HKAB0020015	18:05:45	4876-4DB5-EE85-69D3-FE52-8CF7-395D-2EA9	Tangail, Bangladesh, 1902	X
HKAB0020016	18:05:50	4876-4DB5-EE85-69D3-FE52-8CF7-395D-2EA9	Tangail, Bangladesh, 1902	X

Figure 6: Activity History of an alleged user auto generated by the Host Server

V. CHALLENGES

Fingerprinting critics level three main arguments. First, fingerprint examiners have not established objective and proven standards for evaluating whether two prints "match." Second, the error rate for fingerprinting as a technique has been inadequately studied. Third, there is no statistical foundation for assessing the likelihood that two people might have prints with any given number of corresponding characteristics. This lack of statistical foundation is especially troubling in cases involving distorted and smudged fingerprints. We will examine each argument in more detail. The first claim is that fingerprint examiners in the United States have not developed uniform standards for determining what counts as a sufficient basis for an identification. In some countries, fingerprint examiners require a certain number of "points of identification" before declaring a match; England, for example, requires sixteen such points, while France requires twelve.

2.5. Finger Print Accuracy Rate

One of the important Challenges is the accuracy. Calculations of accuracy of finger print extraction with the system are

- False Acceptance Rate (FAR): The fault where someone of user which don't enlist will be held true by System. An Equation to express FAR is given below.

$$FAR = \sum_{n=1}^{N} \frac{FAR(n)}{N} \quad (1)$$

- False Rejection Rate (FRR). The fault when someone which registered in the system was refused by system.

$$FPR = \sum_{n=1}^{N} \frac{FPR(n)}{N} \quad (2)$$

- Failure to Enroll (FTE). A fault when system fail to enlist a new user ID:

$$FTE = \sum_{n=1}^{N} \frac{FTE(n)}{N} \quad (3)$$

- Equal Error Rate (EER) and Failure to Acquire (FTA) also could be calculated following the same way.

It is a challenge to understand the relationship between False Rejection Rate (FRR) and False Acceptance Rate (FAR) errors Frost and Sulliva (2000). For a system if the match score threshold is set lower, the FRR goes down and FAR goes up. There is a always a way out to represent this relationship using a plot FRR versus FAR on a Receiver Operating Characteristic (ROC) curve as shown in the figure below. Here in the figure above FRR affects usability and convenience, while FAR represents a security risk.

2.6. Finger Print Unlocking Complexity

In case of complexity of Valid User the objective is to minimize the complexity. But as per considered the complexity of an Attacker we always wish to increase the complexity as if an attacker cannot crack the vault. Two general ways could be applied for unlocking the vault. Brute-force method, or *bf(r,t,k)*, where r denotes total number of points, t for number of real points and k is the degree of the polynomial. For an attacker r, t are the same but for the valid user, r is the size of their unlocking set and t is the number of non chaff points. The respective theorem is that the complexity of the *bf(r,t,k)* problem using a suitable δ to ensure a unique result is-

$$C_{bf} = \binom{r}{\delta}\binom{t}{\delta}^{-1} \quad (4)$$

This illustrates that a brute-force decoding algorithm is less than ideal a valid user.

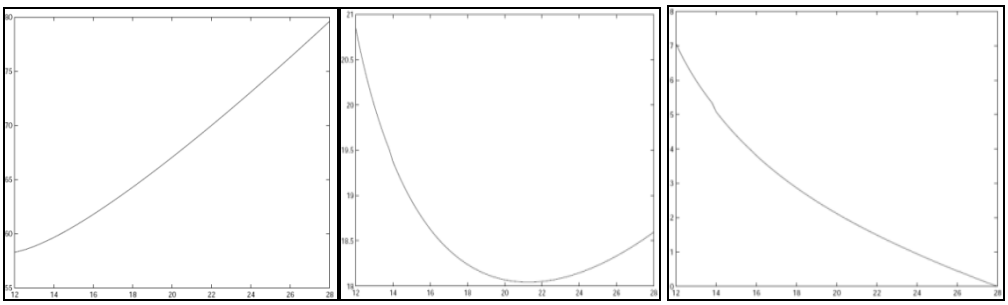

Figure 7: Log of Complexity for Reed Solomon decoding as a function of codeword size;(a)Complexity of full attack, rs (995, 40, n, 11); (b) Complexity of Partial information attack, rs(120, 40, n, 11);(c) Complexity of legitimate unlocking rs(31, 22, n, 12)

Another approach to unlock the vault is the use of Reed-Solomon decoder. In *rs(r, t, n,δ)* problem, r,t and δ have the same meaning as it had before whereas n is the size of the Reed-Solomon codewords involved. In that case the theorem is got the fashion below. The complexity of the *rs(r, t, n,δ)* problem over F_p^2 is

$$C_{rs} = \binom{r}{n}\left(\sum_{i=\max\left(\frac{n+\delta}{2},n-r+t\right)}^{\min(n,t)} \binom{r-t}{n-i}\binom{t}{i}\right) \text{ such that}$$

$$n \text{ satisfies } \delta \leq n \leq \min(r, 2t-\delta) \text{ and } (n|p^2-1) \quad (v)$$

The MATLAB simulation of Reed Solomon Complexity of different scans is shown below.

2.7. Two Fingerprints Logistic Integration Challenges

Let $I_i(x_i)$ and $G_i(x_i)$ be the imposter and genuine distributions of the i[th] matcher, $i = 1, 2$. x_1 and x_2 are considered as the output scores. If we use logistic transform of two fingerprints matching and the logistic regression to $\hat{\pi}(x)$, the estimate will be

$$\pi(x): \log it\{(\hat{\pi})\} = (\alpha + \beta x_1 + \gamma x_2) \quad (6)$$

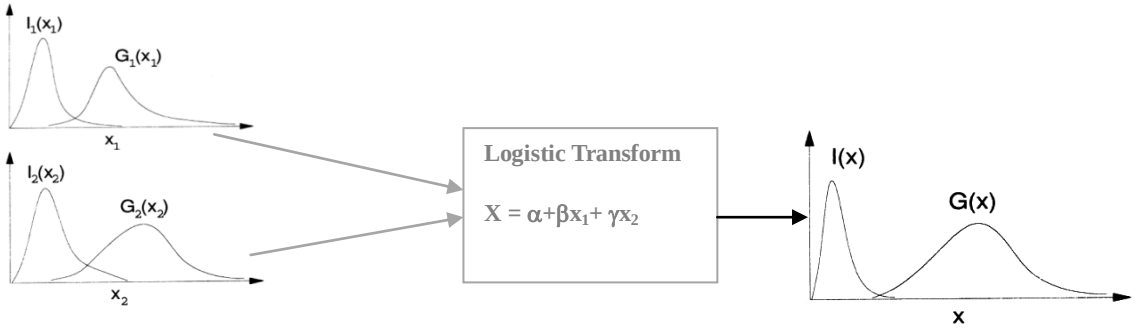

Figure: 8. Integration of two fingerprint matching algorithms using a logistic transform with tunable parameters α, β and γ

Here,

$$x = l(\alpha + \beta x_1 + \gamma x_2 \quad (7)$$

$$= \frac{\exp(\alpha+\beta x_1+\gamma x_2)}{1+(\alpha+\beta x1+\gamma x2)} \quad (8)$$

Here α, β and γ three parameters The objective of the integration is to estimate the parameters such that the FRR is minimized for specified level of FAR. Let x_1 and x_2 are independent, the joint imposter and genuine distributions $I_i(x_i)$ and $G_i(x_i)$, respectively could be expressed as

$$I_i(x_i) = \iint I_1(x_1) I_2(x_2)\, dx_1\, dx_2 \quad (9)$$

and

$$G_i(x_i) = \iint G_1(x_1) G_2(x_2)\, dx_1\, dx_2 \quad (10)$$

Therefore, the new probability distribution functions I(x) and G(x) of imposter and genuine individuals, respectively, after logistic transform, can be written as

$$G(x) = \iint I_1(x_1) I_2(x_2)\, \delta(\alpha+\beta x_1+\gamma x_2 - l^{-1}(x))\, dx_1\, dx_2 \quad (11)$$

and

$$G(x) = \iint G_1(x_1) G_2(x_2)\, \delta(\alpha+\beta x_1+\gamma x_2 - l^{-1}(x))\, dx_1\, dx_2 \quad (12)$$

Here δ(.) is the delta function. In other words I(x) and G(x) are line integrals of $I(x_1,x_2)$ and $G(x_1,x_2)$,respectively along the line $\alpha+\beta x_1+\gamma x_2 = l^{-1}(x)$ on the (x_1,x_2) plane. The FRR, p_{frr} for a given α , β and γ and FAR, t_{far}, is

$$p_{frr}(\alpha, \beta, \gamma, t_{far}) = p_{frr}(t) = \int_{-\infty}^{t} G(x)dx \quad (13)$$

Where

$$t = \arg_x \inf_x \{p_{frr}(x) \geq t_{far}\} \quad (14)$$

$$= \arg_x \inf_x \{\int_x^{+\infty} I(x)dx \geq p_{frr}\} \quad (15)$$

And

$p_{frr}(t)$ and $t_{far}(t)$ are the FRR and FAR levels at the threshold t.

The integration of two fingerprints matching algorithms can be formulated as follows. For specified FAR levels$t_{far}^{(i)}$, i= 1, 2…, L compute the set of parameters (α_i , β_i, γ_i, t_i) which satisfy the following optimization criterion:

$$(\alpha_i, \beta_i, \gamma_i, t_i) = arg \ \min_{\alpha,\beta,\gamma}\left\{p_{frr}\left(\alpha, \beta, \gamma, t_{far}^{(i)}\right)\right\} \quad (16)$$

And,

$$t_i = \arg_x \ \inf_x \left\{p_{far}(x) \geq t_{far}^{(i)}\right\} \quad (17)$$

$$t_i = \arg_x \inf_x\left\{\int_x^{+\infty} I(x)dx \geq t_{far}^{(i)}\right\} \quad (18)$$

The minimization criterion estimates parameters (α_i , β_i, γ_i, t_i) such that the FRR is minimized at each given FAR level. Here the challenge is that as we do not know the analytical form of *I(x)* and *G(x)*, it is not possible to solve the minimization problem analytically. But in this Equation $(\alpha_i, \beta_i, \gamma_i, t_i) = arg \ \min_{\alpha,\beta,\gamma}\left\{p_{frr}\left(\alpha, \beta, \gamma, t_{far}^{(i)}\right)\right\}$ minimization may be solved using efficient algorithms.

VI. CONCLUSION

Using Fingerprint as a mean of smart input could bring better outcome comparing with other biometric ways existing today. But the fingerprint technique we are using nowadays has some security challenges. Some of the important drawbacks are discussed here in this paper, many of those are not. However, towards a secure and sustainable cyber world we certainly should use a security technique that is easy to use and available to all considering costs, complexities and other factors. Answering the security question in user authentication is basis of user privacy. But the username, password and so called capthca have some threats that we've already realized while we use theses. Beside this existing authentication technique if we add smart input technique then the security check will be multi-tiered and more trustworthy. Here in our continuous research work we suggest using this type of smart and sensitive key will be a very good solution towards multi-tiered online and cyber security.

REFERENCES

[1] M Ozaki, Y. Adachi, Y. Iwahori, and N. Ishii, Application of fuzzy theory to writer recognition of Chinese characters, *International Journal of Modelling and Simulation, 18(2),* 1998, 112-116.

[2] Arora, S., and Khot, S. 2002, Fitting algebraic curve to noisy data, ACM Symposium on Theory of Computing, STOC 2002

[3] Bellare, M., Canettiy, R., Krawczyk, H., (1996), Keying Hash Functions for Message Authentication, Advances in Cryptology, Vol. 1109, Springer-Verlag

[4] Bergman, P., Berman, S., *The Criminal Law Handbook: Know Your Rights, Survive the System.*

[5] Blahut, R. 2003 *Algebraic Codes for data Transmission* Cambridge University Press

[6] Bleichenbacher, D., and Nguyen, P. Q. 2000, Noisy polynomial interpolation and noisy Chinese remaindering. Advances in Cryptography, EUROCRYPT 2000

[7] Clancy, T.C., Kiyavash, N. and D. J. Lin, D. J. 2013 Secure Smartcard-Based Finger Print Authentication

[8] Coklin, Gardner, B. and Shortelle, D. 2002, Encyclopedia of Forensic Science: a Compendium of Detective Fact and Fiction. Westport, Conn. : Oryx, 2002, Print.

[9] Davida, Frankel, Y., and Matt, B., (1998), On enabling secure applications through off-line biometric identification. IEEE Symposium on Privacy and Security

[10] Frost and Sullivan, A Best Practices Guide to Fingerprint Biometrics http://www.frost.com

[11] Guruswami, V., and Sudan, M. 1998, Improved decoding of reed-solomon and algebraic geometric codes. Symposium on Foundations of Computer Science, FOCS1998

[12] Hildebrand, F. B. 1956, Introduction *to Numerical Analysis.* McGraw-Hill

[13] Kaufman, C., Perlman, R., Speciner, M. *Network Security: Private Communication in a Public World*, Second Edition.

[14] Jain, A. K. Prabhakar, S., Chen, S. Combing multiple matches for a high security fingerprint verification system

[15] Juels, A., and Sudan, M 2002, A fuzzy vault scheme. ACM Conference on Computer and Communication Security, CCS.

[16] Juels, A., and Watenberg, M., (1999), A fuzzy commitment scheme, ACM Conference on Computer and Communications Security

[17] Kekre, H. B. Sudeep D. 2012, Thepade, Dimple Parekh, Comparison of Fingerprint Classification using KFCG Algorithm with Various Window Sizes and Codebook, International Journal of Computer Applications, pp 0975-8887, Volume 46-No.17.
[18] Massey, J. L. 1969, Shift register synthesis and bch decoding. *IEEE Transactions on Information Theory vol. 15*, no. 1, pp. 122-127.
[19] Mandi, R. M., Lokhande, S. S. 2012 Rotation-Invariant Fingerprint Identification System, International Journal of Electronics Communication and Computer Technology (IJECCT), Volume 2 Issue 4
[20] Miao, D., Tang, Q and Fu, W. 2007, Fingerprint Minutiae Extraction Based on Principal Cures, the Journal of the Pattern Recognition Letters, vol. 28, pp. 2184-2189
[21] Mehfuza, H., Thakar, V. K., 2010, Image registration for recovering affine transformation using Nelder Mead Simplex method for optimization.
[22] Morrose, F., Reiter, M., and Wetzel, S (1999), Password hardening based on keystroke dynamics. ACM Conference on Computer and Communication Security
[23] National, R. C., (2002), Cyber security Today and Tomorrow: Pay Now or Pay Later, National Academy Press, Washington, D.C.
[24] Nichols, R. K., (1999) Ed. *ICSA Guide to Cryptography*. McGraw-Hill, Chapter, Biometric Encryption
[25] Oliveira, L. B., Kansal, A., Priyantha, B., Goraczko, M., Zhao F., (2009), Secure-TWS: Authenticating Node to Multi-user Communication in Shared Sensor Networks, 8th International Conference on Information Processing in Sensor Networks, (IPSN'09), April 13–16, 2009, San Francisco, California, USA.
[26] Ritter, M. 2001, Fingerprint Evidence Faces Hurdles, FDIAI News
[27] Singhai, N 2010, '*A Survey on: Content Based Image Retrieval Systems*', International Journal of Computer Applications (0975-8887) Vol 4, No. 2, pp. 22-26.
[28] Smeulders, AWM 2000, '*Content based image retrieval at the end of the early years',* IEEE Transactions on pattern analysis and machine intelligence, pp. 1349-1380.
[29] Veringer 2013, Neurotechnologija Ltd. http://www.nurotechnologija.com

American Journal of Engineering Research (AJER)
e-ISSN : 2320-0847 p-ISSN : 2320-0936
Volume-02, Issue-09, pp-71-75
www.ajer.org

Research Paper Open Access

Free Convective Heat Transfer From A Vertical Surface For The Case Of Linearly Varying Thermal Potential

Parvataneni
Andhra University

Abstract: - The present theoretical investigation deals with the problem of free convective heat transfer from a vertical plate having linear temperature gradient along its surface to the surrounding thermally stratified fluid. Integral method of analysis is adopted to investigate the effect of four parameters viz., the gradients of temperature in the fluid and the wall, Grashof number and Prandtl number on heat transfer coefficients. It is observed from the numerical results that an increase in the surface temperature gradient would result in higher heat transfer coefficients than those observed in isothermal wall case.

I. INTRODUCTION

In the atmosphere around us we continually encounter transport processes in fluids wherein the motion is driven by the buoyancy effect due to temperature differences. The problem of natural convection from a vertical surface is solved [1] for the case of either constant temperature of the surface or constant heat flux at the surface. Also, the problem of natural convection heat transfer from bodies submerged is stratified fluids arises in many important applications. A few studies on the effect of stratification are available [2,3,4]. However, in certain practical instances, the temperature of the wall may vary arbitrarily, thus not conforming to either of the two cases mentioned above, namely the case of constant wall temperature and the case of constant wall heat flux. In view of this fact, for the sake of completeness in the literature, presently a different situation is considered in which a linear variation in temperature along the vertical surface is imposed together with linear thermal stratification in the bulk fluid. The problem for this case solved theoritically to study the effect of heat transfer rate of various parameters such as Grashof number and Prandtl number of the fluid and thermal gradients of the surface and the fluid.

II. FORMULATION AND ANALYSIS

In the physical model under consideration, as shown in Fig.1 Heat transfer by free convection takes place from a vertical surface into a thermally stratified fluid. The heating conditions on the surface are maintained such that there is a linear variation in the temperature along the surface. Further, the thermal stratification in the fluid is assumed to be linear. Thus, the temperature variations along the surface and in the fluid medium are characterised by the following equations.

$$y = 0, \frac{dT_W}{dx} = m_1 = \text{constant} \quad .. \quad (1)$$

$$y = \delta, \frac{dT_\infty}{dx} = m_2 = \text{constant} \quad .. \quad (2)$$

The rate of heat transfer from the vertical surface to the fluid medium under the conditions stated above is governed by the conservation equations in integral form as shown below

$$\frac{d}{dx}\int_0^\delta u^2 dy = -\nu \frac{\partial u}{\partial y}|y = 0 + g\,\beta \int_0^\delta (T - T_\infty) dy \quad ..(3)$$

$$\frac{d}{dx}\int_0^\delta (T - T_\infty) dy + m_2 \int_0^\delta u\, dy = -a \frac{\partial T}{\partial y}|y = 0 \quad ..(4)$$

The following velocity and temperature profiles are chosen in the boundary layer, i.e. for $0 \le y \le \delta$

$$\frac{u}{u_0} = y^+(1-y^+)^2 \quad ..(5)$$

$$\frac{T-T_\infty}{T_W-T_\infty} = (1-y^+)^2 \quad ..(6)$$

where $y^+ = y/\delta$

Eqs. (5) and (6) obey the boundary conditions.

y = 0, u = 0 .. (7)

y = 0, $T = T_W$ where $T_W = T_\infty(x)$ ..(8)

y = $\delta, u = 0 \; and \; \frac{\partial u}{\partial y} = 0$ ..(9)

y = $\delta, \frac{\partial T}{\partial y} = 0 \; and \; T = T_\infty$

where $T_\infty = T_\infty(x)$ ..(10)

Eqs. (3) and (4) are evaluated with the aid of equations (5) and (6) to yield the system of constitutive differential equations in dimensionless form as given below:

$$\frac{d\delta^+}{dx^+} = \frac{15(7\,\mathrm{Pr}+8)}{\mathrm{Pr}\,Gr^{1/2}\delta^+ U_0^+} - \frac{35\delta^+}{U_0^{+2}}$$

$$\frac{\delta^+}{\theta}(2\,M_1 + 3\,M_2) \quad ..(11)$$

$$\frac{dU_0^+}{dx^+} = \frac{35\theta}{U_0^+} - \frac{15(7\,Pr+4)}{Pr\,Gr^+\delta^{+2}} + \frac{U_0^+}{2\theta}(2M_1 + 3M_2) \quad ..(12)$$

Eqs. (11) and (12) are numerically solved by Fourth-order Runge-Kutta method with the initial condition that at x = 0, $\delta^+ = 0 \; and \; U_0^+ = 0$. The heat transfer coefficient is defined by the equations

$$-\lambda \frac{\partial T}{\partial Y}|y=0 \; = \alpha\,(T_W - T_\infty) \quad ..(13)$$

Results are presented to study the efforts of various system parameters on local as well as average heat transfer coefficients.

III. DISCUSSION OF RESULTS

In the present theoretical investigation effects of parameters M_1, M_2, Grashof number and Prandtl number on heat transfer rates are studied, where $M_1 \; and \; M_2$ signify the gradient in surface temperature and the degree of thermal stratification in the fluid respectively. In Fig.2 effect of M_2 on local Nusselt number is shown where M_1 is maintained constant at zero.

Fig.2 indicates that an increase in the degree of thermal stratification in the fluid is associated with an increase in the local Nusselt number, thus reaffirming the previous analyses [5,6]. It is found that a gradient in the surface temperature namely M_1 would cause a greater effect on local heat transfer coefficients, as evident from Fig.3. A positive gradient feature favours the local heat transfer rates, while a negative gradient cause a decrease in local heat transfer coefficient. However there is a limitation together on the values of $M_1 \; and \; M_2 \; such \; that \; at \; x = 1, \; (1 + M_1 - M_2)$ should always be greater than zero. A general observation of Fig.4, Fig.5, reveals the fact that the effect of M_1 on the average Nusselt number is more pronounced than that of M_2. In conclusion a combined effect of a gradient in the surface temperature and a thermal stratification in the fluid on the heat transfer rates is studied. The effect of these parameters is to greatly enhance the heat transfer rates in relation to the isothermal case of wall and ambient medium.

IV. NOMENCLATURE

$\bar{h}$ average heat transfer coefficient

m_1 gradient in the temperature of the surface, dT_W/dx

m_2 degree of thermal stratification in the fluid dT_x/dx

M_1 $1m_1/(T_{W_0} - T_{\infty_0})$

M_2 $1m_2/(T_{W_0} - T_{\infty_0})$

$\bar{N}u$ average nusselt number, $\bar{h}1/K$

U_0 convection velocity
U_0^+ $u_0/[g\ 1\ \beta\ (T_{W_0} - T_{\infty_0})]$
x^+ $x/1$
y^+ y/δ
δ thickness of boundary layer
δ^+ $\delta/1$
θ $(T_W - T_\infty)/(T_{W_0} - T_{\infty_0})$

Subscripts
o $at\ x = o$
w wall
∞ $bulk\ fluid$

V. ACKNOWLEDGEMENT

Thanks are due to the University Grants Commission, Government of India, New Delhi, for the financial assistance.

REFERENCES

[1] 'Natural convection Flows and Stability' by B.Gebhart, Advance in Heat Transfer, Vol9,Ch.IV pp. 282-302, 1973.
[2] Eichhorn R, 'Natural Convection in a Thermally Stratified Fluid', Progress is Heat and Mass Transfer Vol.2, Pergamon Press 1969,pp.41-53.
[3] Fujii, T., Takenchi M., and Morioka, I., 'Laminar Boundary Layer of Free Convection in a Temperature stratified Environment', Proceedings, Fifth International Heat Transfer Conf.Tokyo,NC 2.2,1974.
[4] Chem C.C.and R.Eichhorn 'Natural Convection from a vertical surface to a thermally stratified fluid', J.of Heat Transfer Trans. of the ASME, Vol. 198, Series C No.3,pp. 446, Aug.76.
[5] Holman J.P Heat Transfer, International student Edition, Fifth Ed. Ch 7, pp. 266 to 272, 1981.
[6] Sparrow E.M. and Acharya S, 'A Natural Convection with Solution - Determined Non-monotonically Varying Heat Transfer Coefficient', J.of Heat Transfer, Trans. of ASME Vol.103, 2, May 1981.

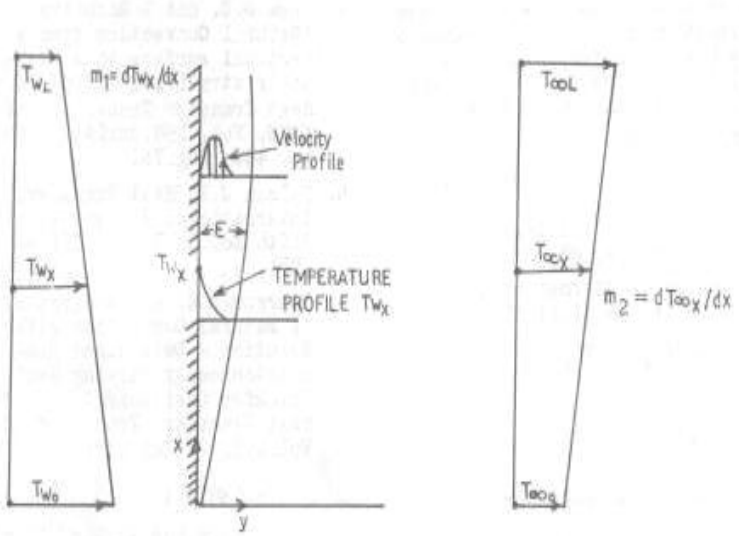

Fig.1 PHYSICAL MODEL

Figures

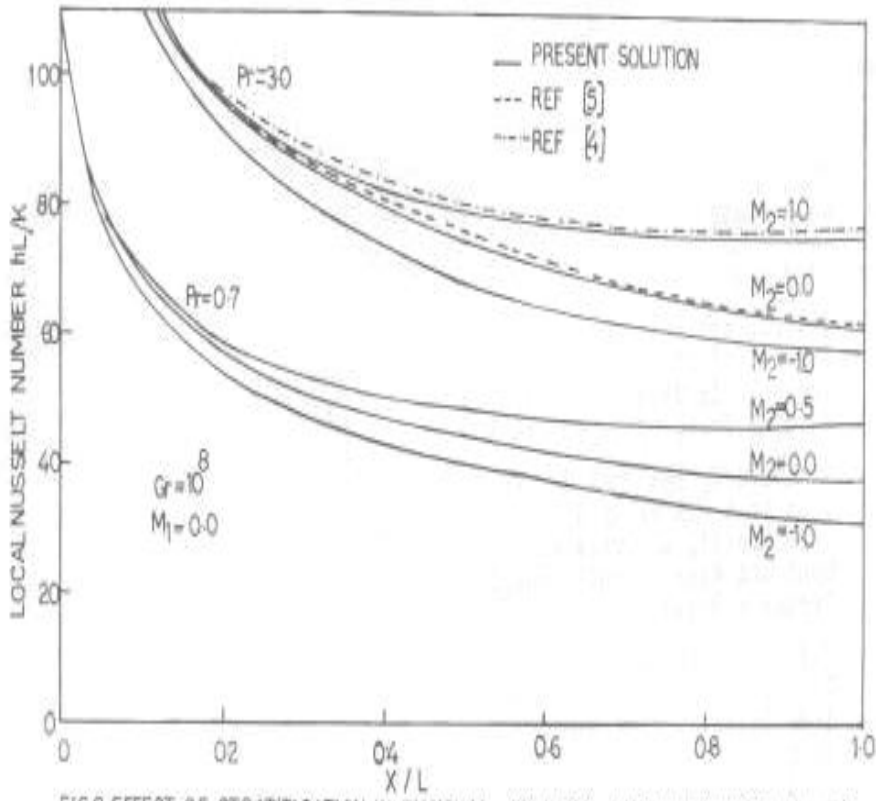

FIG.2 EFFECT OF STRATIFICATION IN FLUID M_2 ON LOCAL NUSSELT NUMBER, $M_1=0.0$

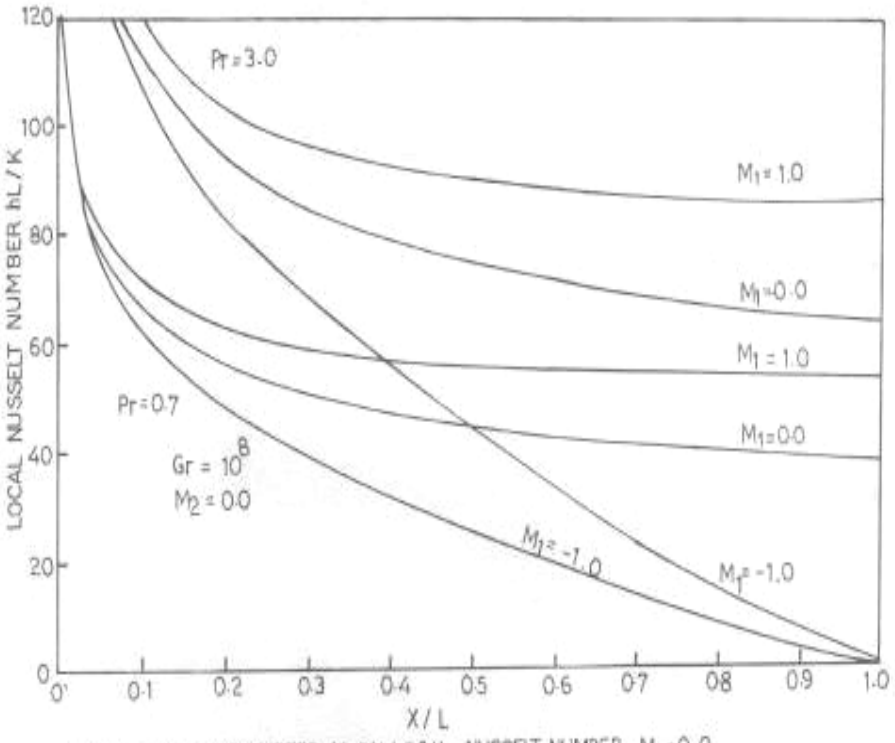

FIG.3 EFFECT OF PARAMETER M_1 ON LOCAL NUSSELT NUMBER, $M_2=0.0$

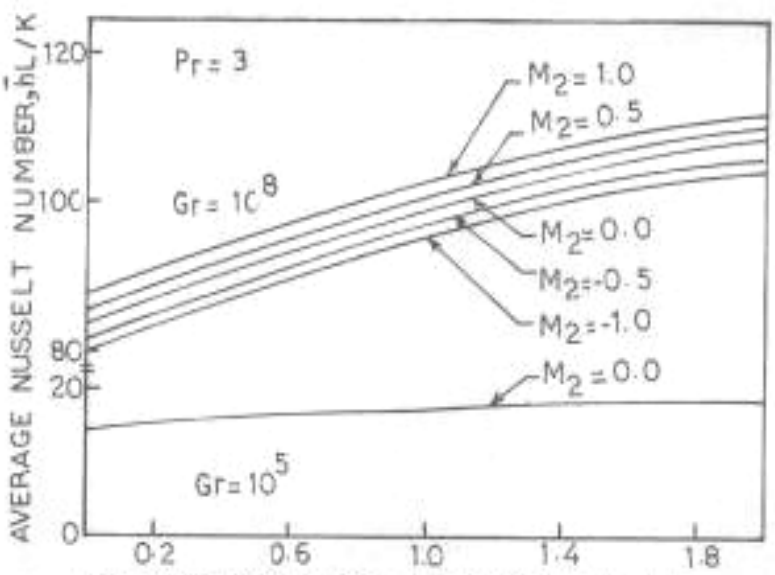

FIG.4 EFFECT OF M_1 ON $\bar{N}u$ WITH M_2 AS PARAMETER

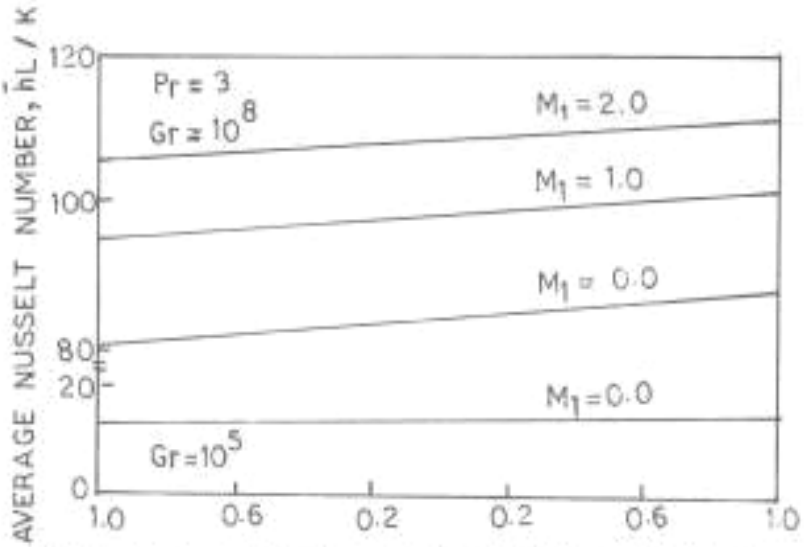

FIG.5 EFFECT OF M_2 ON $\bar{N}u$ WITH M_1 AS PARAMETER.

American Journal of Engineering Research (AJER)
e-ISSN : 2320-0847 p-ISSN : 2320-0936
Volume-02, Issue-09, pp-76-80
www.ajer.org

Research Paper Open Access

Client-Side Validation and Verification of PHP Dynamic Websites

K.Sowjanya, N. Deepika, P.V.S.Srinivas
[1]*PG Scholar, Department of Computer Science and Engineering, TKR College of Engineering and Technology Hyderabad, A.P-500 097, India*
[2]*Assistant Professor, Department of Computer Science and Engineering, TKR College of Engineering and Technology Hyderabad, A.P-500 097, India*
[3]*Professor& Head, Department of Computer Science and Engineering TKR College of Engineering and Technology Hyderabad, A.P-500 097, India*

***Abstract*:** In contemporary, populace are interested in fault-localization techniques which are based on statistical analysis of program statements executed by going through and unexpected executions. Here we explore three fault localization algorithms which are referred as Tarantula, Ochiai and Jaccard can be evaluated to localize faults perfectly in web applications which are developed in PHP. These algorithms uses source mapping for conditional and function-call statements. We developed different fault localization techniques and test-generation cases in Apollo, and explored them on many open-source PHP apps. Then the ultimate output of tests are that Ochiai algorithm contains all our enhancements which localizes more than 80% of all faults in executed statements, compared to unenhanced Ochiai algorithm where it gives only quarter percent amount. And also we checked that , the strategies which are used for test generation taken under part are efficient to know the algorithm perfectness. And also these algorithms are cost efficient. Moreover, normally, a straight forward concept which depends upon similarities of path-constraint gets high range perfectness in less than 10 test generation, when compared to other strategies where we have to do more like almost half century.

Keywords: - *Fault localization, statistical debugging, program analysis, web applications, PHP.*

I. INTRODUCTION

Web application provides a user friendly interface to the users. Proper functionality and security testing should be done on the web application, prior to the web application release. The scope of the paper is to identify bugs in the usage of web apps in the network with the help of dynamic test generation. Web applications can be developed using server side programming languages (JSP, PHP, ASP etc,) or client side programming languages or with static web pages (HTML) and with combination of the languages. In the dynamic web sites, developed with server side programming languages accepts inputs from the remote users [9]. The remote user can pass web application expected inputs or can pass malicious inputs. If malicious inputs are passed to the web application, the behavior of the web application may change. The web application may crash at some instance. The web application response may be an unexpected that causes the browser to crash. The web application should be thoroughly tested for the functionality and in the security aspect. The draw backs in existing system are that it approaches are for testing the webpage validation. The existing approaches cannot identify the dynamic pages. The approaches cannot test the web application with the dynamic inputs. These cannot identify the dynamic pages and cannot generate test cases dynamically [3].

It identifies the expected response using state model maintenance. The state model is the request verves response combinations in the normal scenario. Should identify the security flaws of the web application. The proposed system is only for the web application developed with the server side scripting language PHP. Bug report contains a failure, a set of path constraints exposing the generates a report of a set of bugs. Each failure and a set of inputs exposing the failure. The path constraint minimization algorithm. The

method intersects returns the set of conjuncts that are present in all given path constraints and the method shortest returns the path constraint with fewest conjuncts.

In detail EB apps are developed based upon various languages of programming, such as Java- Script which was on interface of user, and PHP on mostly server side in embedded Structured Query Language (SQL) commands on the server side[7]. Such applications evaluate output in structured format with dynamic HTML pages those were helped in the execution of additional scripts. As with any program, programmers make mistakes and introduce faults. In the domain of web applications, some faults manifest themselves as web-application crashes and as malformed HTML pages that are not displayed properly in a web browser. While malformed HTML failures may seem trivial, and indeed many of them are at worst minor annoyances, they have on occasion been known to create serious vulnerabilities, e.g., via denial-of-service attacks.

Furthermore, such failures in the HTML code may be difficult to localize because HTML code is often dynamically generated by server side code written, for example, in PHP or Java and so, when a failure is detected, there really is no HTML file or line number to point the developer to. In this paper, we present Apollo, the first fully automatic tool that efficiently finds and localizes malformed HTML and execution failures in web applications that execute PHP code on the server side [6].

II. ARCHITECTURE

In particular, 1) it integrates an HTML validator to check for failures that manifest themselves by the generation of malformed HTML, 2) it automatically simulates interactive user input, and 3) it keeps track of the interactive session state that is shared between multiple PHP scripts[3]. However, our previous work focused exclusively on finding failures by identifying inputs that cause an application to crash or produce malformed HTML. We did not address the problem of pinpointing the specific web application instructions that cause these failures, and fixing the underlying faults can be very difficult and time consuming if no information is available about where they are located.

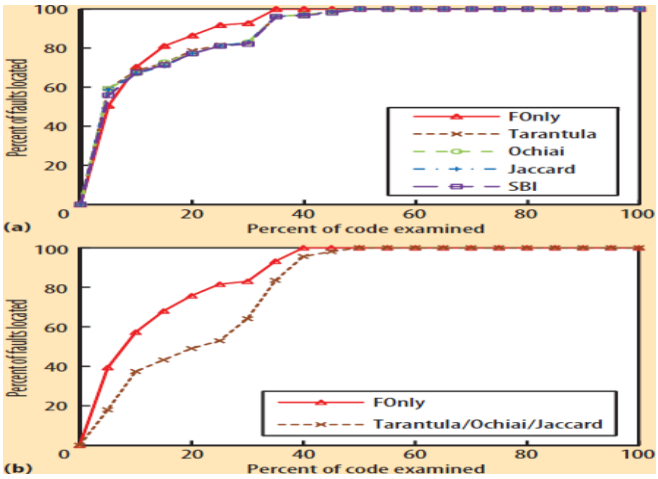

Fig.1 Fault localization technique

This paper addresses the problem of determining where in the source code changes need to be made in order to fix the detected failures. This task is commonly referred to as fault localization, and has been studied extensively in the literature [8]. The fault- localization algorithms explored in this paper attempt to predict the location of a fault based on a statistical analysis of the correlation between passing and failing tests and the program constructs executed by these tests. In particular, we investigate variations on three popular statistical fault-localization algorithms, known as Tarantula Ochiai and Jaccard. These algorithms predict the location of a fault by computing, for each statement, the percentages of passing and failing tests that execute that statement [7]. From this, a suspiciousness rating is computed for each executed statement. Programmers are encouraged to examine the executed statements in order of decreasing suspiciousness.

The effectiveness of a fault localization technique can be measured by determining how many statements need to be inspected, on average, until the fault is found. Our work differs from most previous research on fault localization in that it does not assume the existence of a test suite with passing and failing test cases. Instead, we rely on combined concrete and symbolic execution to generate passing and failing runs. This paper advances the state of the art in fault localization in two ways. First, we present enhancements to previous

statistical fault- localization techniques that make them significantly more effective at localizing the faults responsible for execution failures, and for the generation of malformed HTML pages in PHP web applications [10]. These enhancements include: The use of an extended domain. We apply existing statistical fault-localization techniques on an extended domain of pairs, in which the runtime value serves to differentiate occurrences of the statement at runtime. Applying this technique to conditional statements helps fault localization with the identification of errors of omission such as missing branches, and applying the technique to function calls enables us to differentiate normal return values from values such as null that are often correlated with erroneous [4]. The use of a source mapping [9]. We modified the PHP interpreter to maintain a source mapping that records the statement in the PHP application that produced each fragment of output at runtime; thus, it is a map from print statements to regions of the HTML file. This mapping when combined with the report of the HTML validator, which indicates the parts of the HTML output that are incorrect provides an additional source of information about possible fault locations, and is used to fine-tune the suspiciousness ratings of existing fault- localization techniques[5]. A second main research topic explored in this paper has to do with the fact that existing fault-localization approaches assume the existence of a test suite.

To summarize, the contributions of this paper are as follows:

1. We present two mechanisms, the use of an extended domain and the use of a source mapping, that significantly enhance the effectiveness of existing fault-localization techniques such as Tarantula, Ochiai, and Jaccard.
2. To evaluate these fault-localization techniques in Apollo, we implemented each of the fault localization techniques; localized 115 randomly selected faults in five PHP applications, and compared the technique‘s effectiveness. Our findings show that, using our best technique, an enhanced version of Ochiai, 87.8 percent of the faults are localized to within 1 percent of all executed statements, compared to only 37.4 percent for the unenhanced Ochiai algorithm [1]. Similar improvements were obtained for enhanced versions of the Jaccard and Tarantula algorithms.
3. We present a family of directed test-generation techniques, based on combined concrete and symbolic execution that are capable of generating small test suites with high fault- localization effectiveness. These techniques overcome the important limitation of many previous fault-localization methods that a test suite be available upfront [10].
4. To evaluate directed test generation, we implemented these directed test-generation techniques in Apollo. Our evaluation shows that a directed technique based on path-constraint similarity reduces test suite size by 86.1 percent and generation time by 88.6 percent when compared to an existing undirected test-generation technique, without compromising fault-localization effectiveness [1].
   These findings show that automated techniques for fault localization, which were previously primarily evaluated on programs with artificially seeded faults, are effective at localizing real faults in open-source PHP web applications.

The remainder of this paper is organized as follows:

Section 2 reviews the PHP language and the kinds of failures that may arise in PHP programs. Section 3 reviews the Tarantula, Ochiai, and Jaccard fault-localization algorithms and presents our extensions to these algorithms [6]. In Section 4, we present algorithms for test generation that are directed by similarity criteria toward the generation of test suites with high fault-localization effectiveness. Section 5 presents an implementation of our work in the context of the Apollo tool. Section 6 presents an evaluation of our fault localization and test-generation algorithms on a set of open source PHP programs.

Fault localization

In this section, we first review the basic fault-localization algorithms we implemented and extended: Tarantula, Jaccard, and Ochiai [4]. We then present an alternative technique that is based on source mapping and positional information obtained from an oracle. Next, a technique is presented that combines the former with the latter. Finally, we discuss how the use of an extended domain for conditional and return-value expressions can help improve the basic algorithm‘s effectiveness [2].

III. IMPLEMENTATION

Step 1: state manager
The module keeps track of all the pages to be visited.
If finds the absolute urls that are possible on the site under test.
It maintains the state of the url.

Step 2: Shadow Interpreter
It executes the server side program for testing
It interprets each url that are to be processed.
It executes programs with, without, negative values, and large values as input arguments
It gathers the web pages produced for each interpretation.

Step 3: UI Option analyser
It gathers all the input variables that are used in each server side program.
It finds the arguments names such as "name","id"etc,.
It works based on syntactic analysis on the program.

Step 4: symbolic driver
It consists of all the syntactic symbols and their states for identifying the input arguments.

For example:
- GET_[' -> symbol
- '] -> symbol

Step 5: constraint solver
It arranges the absolute urls with all possible combinations.
Eg: login.php has id, pwd as input args.
URL 1: http://www.xyz.com?id=
URL 2: http://www.xyz.com?id=asdf&pwd=123

Step 6: input value generator
Based on the input argument type, an integer can have negative, positive values.
It produces and assigns null values for the input arguments.
It produces large values for integer, float, char etc,

Step 7: bug finder

The outputs of shadow interpreter are a web page.
The page is validated against W3C validator.
If W3C validator confirms with any bug, the URL and the page is considered as reproducible scenario.

Step8: path constraint minimization
It tries to eliminate the unnecessary urls that are causing same bug.
The minimized urls set and its value causes the reduced and optimal bug report.

IV. RELATED WORK

This section reviews the literature on fault localization, focusing primarily on fault localization techniques that predict the location of faults based on the analysis of data from multiple tests or executions. In addition, we discuss research that explores the impact of test-suite composition on fault-localization effectiveness.

Fault Localization
In previous works these fault localization was used for slicing purpose in programming. As inverse here are the two people who used these fault localization for the sake of dicing which was used for combining those slices of programming [2]. Those scientists are Lyle and Weiser. The way of these fault localization works in order to find these faults in information. For example if we take A and B values if we get perfect result for a and some wrong for B then we have to check with respect B variation.[5] These variations are later invented by Pan and Spafford and Agrawal et al.

Trace comparisons
Renieris and Reiss use set-union, set-intersection, and nearest neighbor methods for fault localization; these all work by comparing execution traces of passing and failing program runs. Set-union. It computes the bunch of each and every statement that which are executed by sending test cases and cutoffs when it was executed by failing test case these from bunch of statements. The set which was the outcome of

failing test includes statements which are suspicious. This is the where programmer interacts first.

Here faulty statement was not included an report, based upon System Dependence Graph (SDG) scientists Renieris and Reiss proposed a ranking technique. Here the ranking technique involves additional statements [8]. These statements are set of things based upon distance and Set-intersection where the previous reports are edge touched them. It discovers the statements which are went successfully through all test cases, not only by single case failing test, and address errors of omission testing attempts don‘t under take or won‘t consider failing test case in the execution of statement. It chooses the passing test case that contains feature of execution spectrum that has common similarities with the failing test case distance criteria. In the event the faulty statement does not contain in the report, based upon System Dependence Graph scientists Reiner‘s and Reiss proposed a ranking technique. Here the ranking technique involves additional statements [11]. These statements are set of things based upon distance. Nearest Neighbor was evaluated on the Siemens suite, and was found to be superior to the set-union and set intersection techniques.

V. CONCLUSION

Until now, statistical fault-localization techniques that analyze execution data from multiple tests have been applied primarily in the context of traditional imperative programming languages such as C and Java. In this paper, we have shown how such fault localization techniques can be made effective in the domain of PHP web applications. We have presented two enhancements to the existing Tarantula, Jaccard, and Ochiai fault-localization techniques that greatly increase their effectiveness:

The use of an extended domain of pairs for conditional statements and function calls. The use of source mapping that correlates statements in the PHP application with the fragments of output that they produce at runtime. The former helps with the localization of certain common kinds of failures such as missing branches in conditional statements and the return of unexpected values by functions due to corner cases that are not handled properly[11]. The latter increases the precision of fault localization by leveraging the fact that PHP applications are expected to produce syntactically valid HTML output, and that the location of errors in these generated pages can often be determined quite precisely.

Briefly the existing systems cannot analyze the dynamic pages, and cannot generate dynamic test cases. The proposed approach can generate dynamic test case for the dynamic web pages. The proposed approach can generate test cases for finding the security bugs.

REFERENCES

[1] R. Abreu, P. Zoeteweij, and A.J.C. van Gemund, “An Evaluation of Similarity Coefficients for Software Fault Localization,”Proc. 12th Pacific Rim Int‘l Symp. Dependable Computing, pp. 39-46, 2006.

[2] R. Abreu, P. Zoeteweij, and A.J. van Gemund, “On the Accuracy of Spectrum-Based Fault Localization,’’ Proc. Testing: Academic and Industry Conf. Practice and Research Techniques, pp. 89-98, Sept. 2007.

[3] R. Abreu, P. Zoeteweij, and A.J.C. van Gemund, “An Evaluation of Similarity Coefficients for Software Fault Localization,’’ Proc. 12th Pacific Rim Int‘l Symp. Dependable Computing, pp. 39-46, 2006.

[4] H. Agrawal, J.R. Horgan, S. London, and W.E. Wong,”Fault Localization Using Execution Slices and Dataflow Tests,’’Proc. Int‘l Symp. Software Reliability Eng., pp. 143-151, 1995.

[5] S. Artzi, J. Dolby, S. Jensen, A. Møller, and F. Tip, “A Framework for Automated Testing of JavaScript Web Applications,’’ Proc. Int‘l Conf. Software Eng., 2011.

[6] S. Artzi, J. Dolby, F. Tip, and M. Pistoia, “Directed Test Generation for Effective Fault Localization,’’ Proc. 19th Int‘l Symp. Software Testing and Analysis, pp. 49-60, 2010.

[7] S. Artzi, J. Dolby, F. Tip, and M. Pistoia, “Practical Fault Localization for Dynamic Web Applications,’’ Proc. 32nd ACM/ IEEE Int‘l Conf. Software Eng., vol. 1, pp. 265-274, 2010.

[8] S. Artzi, A. Kie_zun, J. Dolby, F. Tip, D. Dig, A. Paradkar, and M.D. Ernst, “Finding Bugs in Dynamic Web Applications,’’ Proc. Int‘l Symp. Software Testing and Analysis, pp. 261-272, 2008.

[9] S. Artzi, A. Kie_zun, J. Dolby, F. Tip, D. Dig, A. Paradkar, and M.D. Ernst,”Finding Bugs in Web Applications Using Dynamic Test Generation and Explicit State Model Checking,”IEEE Trans. Software Eng., vol. 36, no. 4 pp. 474-494, July/Aug. 2010.

[10] P. Arumuga Nainar, T. Chen, J. Rosin and B. Liblit, “Statistical Debugging Using Compound Boolean Predicates,’’Proc. Int‘l Symp. Software Testing and Analysis, S. Elbaum, ed., July 2007.

[11] P. Arumuga Nainar and B. Liblit, ―Adaptive Bug Isolation,‖ Proc. 32nd ACM/IEEE Int‘l Conf. Software Eng., pp. 255-264, 2010.

American Journal of Engineering Research (AJER)
e-ISSN : 2320-0847 p-ISSN : 2320-0936
Volume-02, Issue-09, pp-81-86
www.ajer.org

Research Paper Open Access

Poincare Plot Used as a Confirmative Tool in Diagnosis of LV Diastolic Dysfunction for Diabetic and Hypertensive Patients.

Manjusha Joshi, Dr.K.D.Desai, Dr.M.S.Menon
[1](*Electronics and Telecommunication Department, MPSTME /NMIMS Deemed to be University, India)*
[2](*Maharshi Parashuram College of engineering, Mumbai University,India)*
[3](*Cardiology department,Fortis-S.L.Raheja Hospital,Mahim –W,Mumbai, India)*

Abstract: - The clinical symptoms of myocardial ischemia and infarction are not observable at an earlier stage. Early diagnosis of the same is very crucial to avoid sudden cardiac deaths. Left ventricular dysfunction is a common pathway to various cardiac disorders. Left ventricular dysfunction resulting into inefficient pumping of the oxygenated blood further causes structural and functional changes in the heart. The paper proposes an early, safe, easily deployable, cost effective and non-invasive technique that can be used as confirmative diagnostic tool obtained from 2-lead ECG sample collected for 3-5 minutes duration that diagnoses left ventricular dysfunction. The proposed index derived from Poincare plot of RR interval provides a guideline to the echo-cardiologist and saves his time and also controls inter operator diagnostic variation. Also the test can be performed by paramedical personnel saving the echo-cardiologist's time. The proposed paper lists the results of index of control group, hypertensive subjects and diabetic subjects. The index value is found to match the left ventricular dysfunction diagnosed from echocardiogram findings.

Keywords: - *Myocardial ischemia, myocardial Infarction, left ventricular diastolic dysfunction (LVDD), heart rate variability, nonlinear HRV tool, Poincare plot and standard descriptor*.

a. INTRODUCTION

Cardiovascular disease is the world's leading killer, accounting for 16.7 million or 29.2 per cent of total global deaths in 2003. The World Health Organization (WHO) estimates that 60 per cent of the world's cardiac patients will be Indian by 2010 [1]. Also it has been found out that India has more number of cardiovascular deaths claiming younger population than in America [1]. The major reasons contributing to sudden deaths are due to myocardial infarction (commonly known as heart attack). Myocardial infarction is the most commonly found episode in sudden casualty. The paper addresses a novel and simple method to diagnose the myocardial ischemia/infarction at an early stage and also diagnoses the left ventricular dysfunction without performing the echo cardiology test. This also establishes analogy between ECG signal analysis and echo cardiogram results.

The paper is organized as follows-
Section I provides an overview of symptoms physiology and prognosis of myocardial ischemia/infarction.
Section II emphasizes on the etiology of left ventricular diastolic dysfunction and the need of early diagnosis of the same.
Section III describes the concept of HRV, it's significance and methods of HRV analysis used in the proposed paper.
Section IV describes further details of Poincare plot and it's significance.
Section V describes about the proposed method, modification of Poincare plot technique and it's significance.
Section VI specifies the algorithm for the modified Poincare plot analysis used in diagnosis of LVDD.
Section VII describes about the results and findings of the proposed method.
Section VIII states about the further scope and future work.
Section IX states the details of the references used for the proposed method.

II. OVERVIEW OF MYOCARDIAL INFARCTION

Myocardial infarction is the necrosis of heart wall muscle due to reduced blood supply to the heart. This is a slow process and does not show any symptoms till the permanent damage has occurred. Therefore it is very essential that early diagnosis of the symptoms leading to onset on of myocardial infarction should be as quick as possible [2]. The beginning of myocardial infarction results in to the changes in ECG of the patient. But since ECG signals are highly subjective, the changes in ECG cannot be the confirmative diagnostic outcome. [3] Normally the patient is further referred to other more specific tests. Myocardial Infarction refers to damage or death (infarction) of heart muscle (myocardium). The damage results from the interruption of blood supply to part of the heart causing heart cells to die. This is most commonly due to occlusion of a coronary artery following the rupture of a vulnerable atherosclerotic plaque, which is an unstable collection of lipids (cholesterol and fatty acids) and white blood cells in the wall of an artery. If left untreated for a long period, this leads to permanent death of heart wall muscle. Since heart wall expansion and contraction is essential for proper functioning of heart, the damage of the wall affects the functioning of the heart resulting in heart failure.[2] The type of infarction depends upon which part of the heart wall is damaged. The heart wall is mainly divided in three zones as shown in figure-1.The prominent types of infarction are –Anterior infarction, Lateral infarction and Inferior infarction .

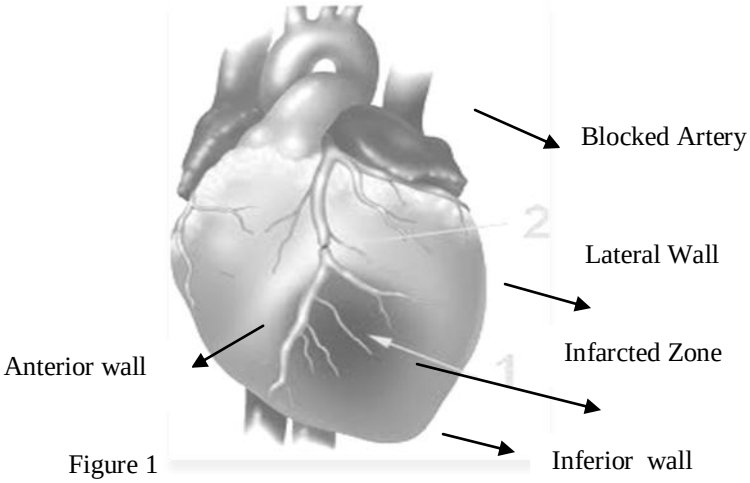

Figure 1

Acquiring ECG is non invasive, safe tool that gives instantaneous results. The ECG of an infracted heart is different than that of a normal heart. The change in ECG is the dependent upon the location of infarct.[2] The anterior wall infarction can be properly represented by V1 to V4 and extending to V5-V6 leads. (Refer figure 2a).

The Lateral infarction is identified by typical changes in Leads I, aVL and V5-6. Over all changes in ST segment can be the confirmative indication. These changes in the ECG can be compared to that with the normal ECG. (Refer figure 2c).

The Lateral infarction is identified by typical changes in Leads I, aVL and V5-6. Over all changes in ST segment can be the confirmative indication. These changes in the ECG can be compared to that with the normal ECG. (Refer figure 2c).

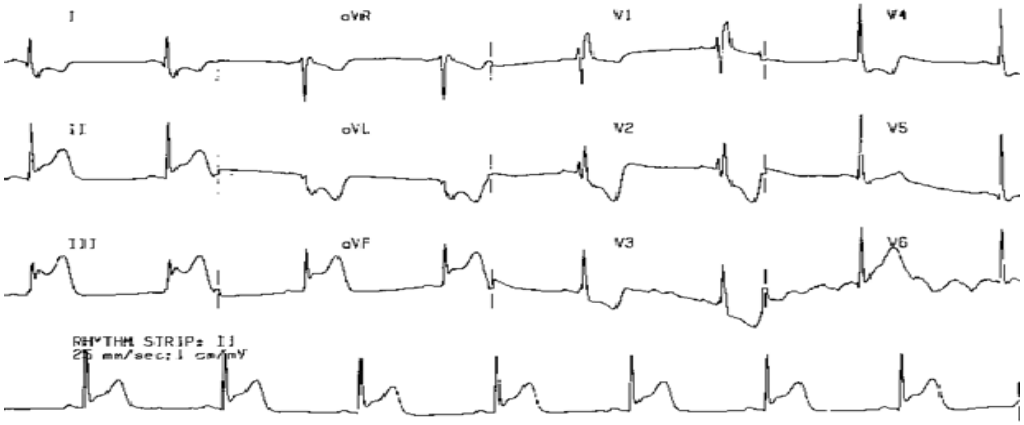

Figure 2a ECG of Inferior Infarction

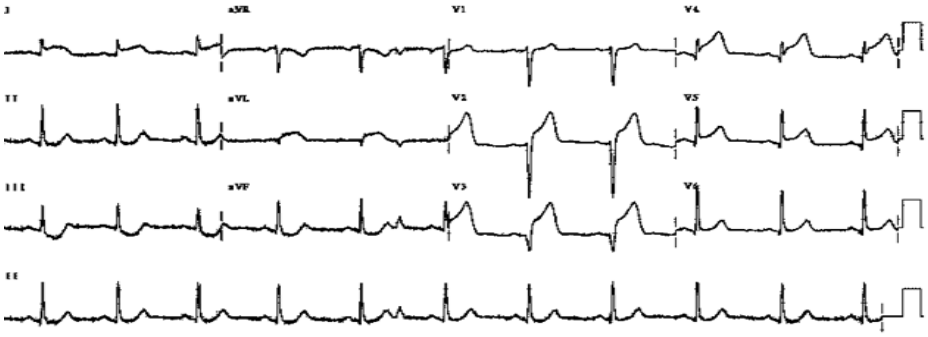

Figure 2b Required ECG leads representing Inferior Infarction

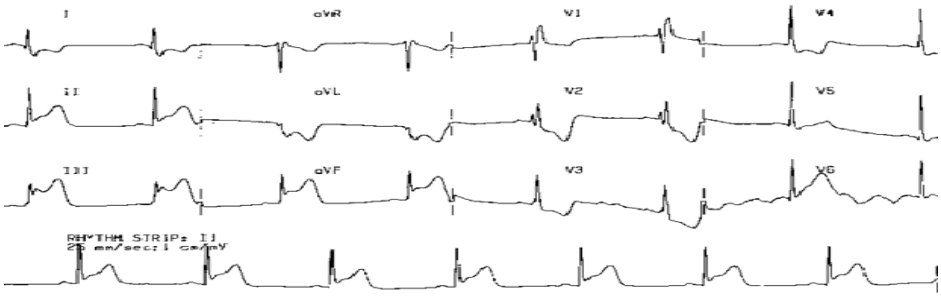

Figure 2c Required ECG leads representing Anterior Infarction

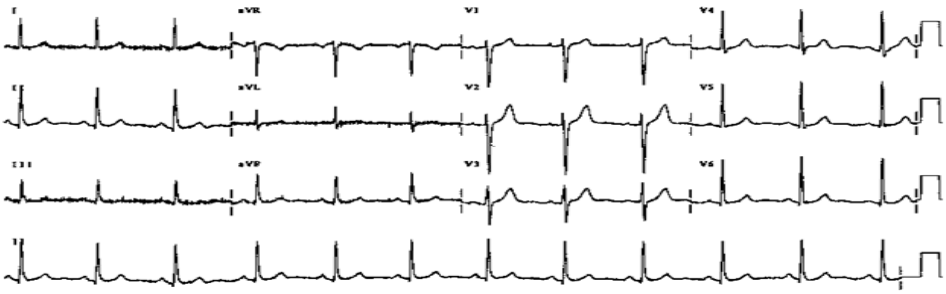

Figure 2d Normal ECG

III. LEFT VENTRICULAR DYSFUNCTION

The left ventricular dysfunction is often the root cause of many sub clinical and clinical cardiac symptom complexes. It causes to develop compensatory mechanisms that cause structural and functional changes in the heart. In the presence of persisting ischemia, the myocardium undergoes changes resulting in thinning of the wall, alterations in wall stress and contractility and spherical remodeling from an original elliptical contour. Changes in contractility may affect concentric, longitudinal and also in the oblique/ rotational axis, constituting left ventricular systolic dysfunction. Anatomic changes in chamber volumes due to aging, degeneration and disease may alter mitral valve flexibility and change the rates of LV filling in early and late diastole and may reflexely increase atrial pressures thereby affecting LV filling pressure. Such changes contribute to LV diastolic dysfunction and may be associated with apparently normal systolic function. This causes further complications as reduced mechanical efficiency and worsens the congestive heart failure.[3] Also left ventricular dysfunction causes reflex activations of neuro harmonal axis further affecting the autonomous nervous system. The specific, safe, quick and non invasive diagnostic technique is the echocardiogram. The algorithm of diagnosing left ventricular diastolic dysfunction by echocardiogram is as follows-

Step1-If subject suffers from progressive dyspnea and / nocturnal or decubitus dyspnea,

Step2-Check for evidence of effective left ventricular systolic function (Ejection fraction greater than 50%),

Step3-Check for evidence of LV diastolic dysfunction by evaluating Mitral diastolic early/ late pressures and for evidence of raised LV filling pressure by Tissue Doppler at the Mitral annulus. (E/E' is the ratio of maximal values of passive mitral inflow velocity to medial / lateral early mitral diastolic velocity indicating various grades of diastolic dysfunction).

Step4- Check if PA pressure is raised (by PA systolic pressure greater than 10 mmHg or RVSP > 40 mmHg by

TR jet method. The figure 2 shows the variation of A/E and E/E' in different stages of left ventricular diastolic dysfunction.

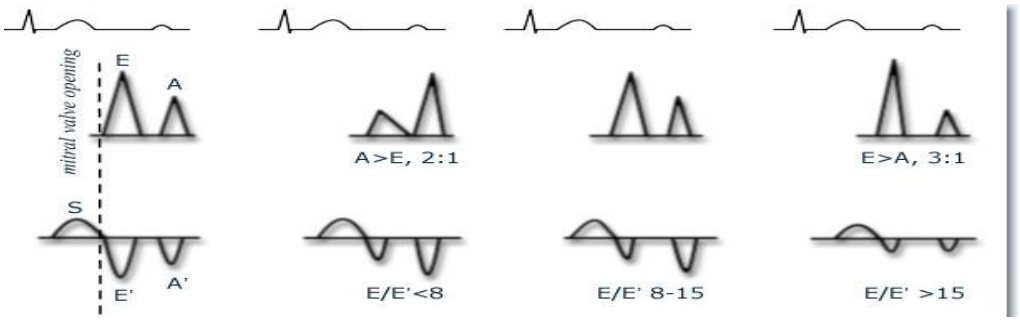

Figure 3 variation in A/E and E/E' in LVDD

IV. OVERVIEW OF HRV ANALYSIS

The HRV is an old technique stated by Hales in 1956.The RR intervals of a healthy heart shows variation of greater extent compared to the impaired heart. A healthy heart is sensitive to physiological, physical and psychological changes in the body and it modifies the heart rate accordingly. It has been observed that the impaired heart has reduced the variation in the heart rate as the demanded by different activities of body. The normal person's ECG that shows more changes in the heart rate during different activities is compared to that of the patient with reduced heart rate variability (HRV). Figure 4 shows the HRV and the power spectral density distribution in case of sympathetic and parasympathetic intervention of a normal subject and a diabetic subject.[4]

The HRV analysis produces certain diagnostic indices that are obtained from spectral analysis of RR interval acquired for 3-5 minutes. The AR analysis represents three prominent frequency bands VLF band -0.0-0.04Hz, LF band- 0.04-0.15Hz and HF band- 0.15 to 0.4Hz. The ratio of the peak power of the HF to LF band represents the sympathetic to parasympathetic balance that provides an index stating the close loop response of heart. The ratio is increased if the normal subject is made to change the position from resting position. Whereas,in case of subject suffering from impaired or reduced HRV the ratio does not show a significant increase in the value as shown in the figure 4. This method diagnoses the orthostatic imbalance diagnosed by modulated HF/LF ratio in case of subjects suffering from impaired or reduced HRV. This test is a popularly used in literature of research though not used clinically.

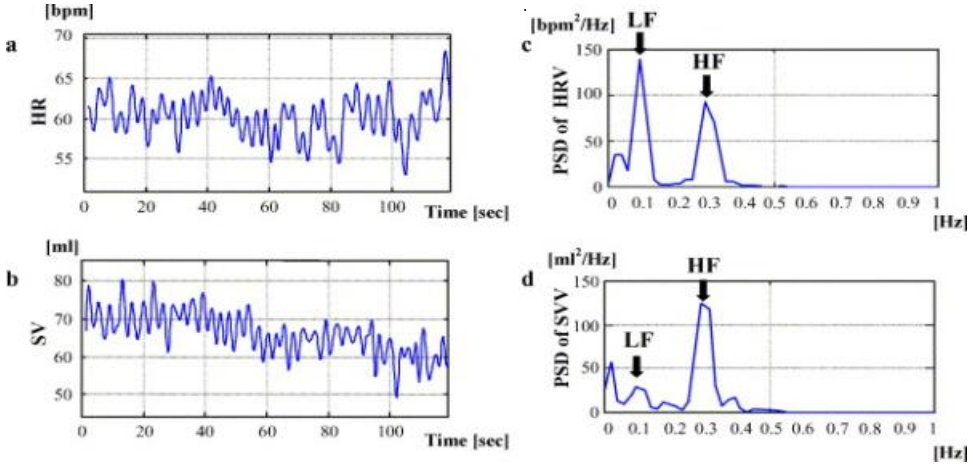

Figure 4 RR interval and frequency analysis of RR interval

But it suffers from severe limitations. There is a difference of opinions between researchers regarding the contributions of HF and LF band as to represent sympathetic or parasympathetic modulations.[3] Some researchers state that LF band represents the modulation of sympathetic activity and HF band represents the parasympathetic activity. Whereas some researchers state that HF band represents both sympathetic and parasympathetic modulation. Also the analysis assumes that ECG is a linear signal and it has been discussed and accepted that ECG is a nonlinear signal.

V. POINCARE PLOT ANALYSIS.

The paper hence uses modified nonlinear HRV analysis using Poincare technique. This method of computing heart rate variability proposed in the above paper also takes into consideration the non linearity of ECG signal and hence is more accurate then the prevailing methods used in time and frequency domain techniques. [5] The Poincare plot is a plot of RR_i versus RR_{i+1} for all i€N-1 where data set of N RR intervals is considered. The Poincare plot is a visual tool and uses the ratio between standard descriptors for short term correlation (SD1) and long term correlation (SD2) between RR intervals to assess the health of the heart. It has been found that the peculiar shape of RR interval is not an artifact or mere placement of point but a specific temporal correlation between the successive RR intervals and hence prelates closely to the natural rhythm of heart as a response to many different complex closed loop systems controlling the heart.[5]The shape of the RR interval distribution shows an elliptical pattern and the ratio of SD1/SD2 should be higher for a healthy person. The shape of RR interval distribution is non- eeliiptical pattern and ratio is much lower for a subject with impaired heart or reduced HRV. The typical cases of normal and impaired subject are as shown in the right panels of the figure (4). Their corresponding HR variations are also shown in the left panel of the figure 5.

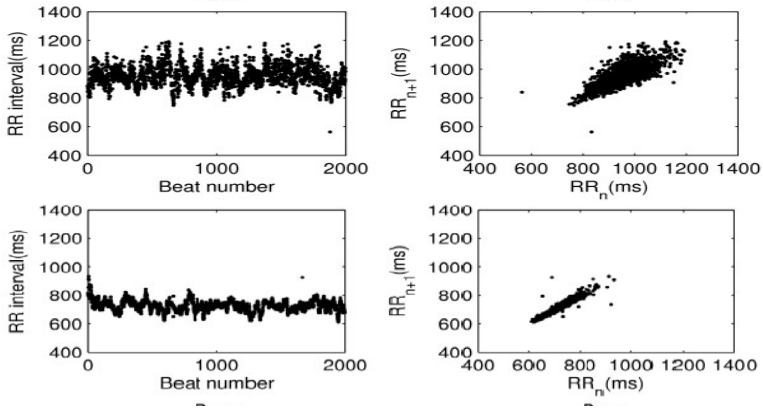

Figure 5 RR plot Vs .time and Poincare plot

VI. MODIFIED POINCARE PLOT ANALYSIS USED IN PROPOSED METHOD.

The paper proposes further division of SD1 into two new descriptors $SD1_{up}$ and $SD1_{down}$ that represent decelerations and accelerations of RR interval respectively. The line of $\pi/4$ slope i.e. y=x line in the Poincare plot represents the equal consecutive RR intervals. The RR interval points with increased heart rate are represented below the line and The RR interval points with decreased heart rate are represented above the line. There is a typical asymmetry found in all Poincare plots. This asymmetry finds correlation that can be explained physiologically that the parasympathetic power spectral densities are higher than the sympathetic power spectral densities [5].

VII. ALGORITHM OF MODIFIED POINCARE PLOT ANALYSIS

1. Compute RR interval from the ECG sample acquired from the data acquisition equipment.
2. Compute the average RR interval.
3. Compute the deviation from the average value for all the RR interval values.
4. If the corresponding RR interval is greater than average the resulting value is negative.Store it in array1.
5. Else if the value is positive, store it in array2.
6. Compute the average of the two arrays. The average of first array is the $SD1_{up}$ and the average of the second array is $SD1_{down}$
7. Compute the ratio of the two for all the datasets of the ECG acquired.

It has been observed that for all the datasets the ratio gives the values that matches with the physiological analogy. Further it can be stated that in case of modulated autonomous nervous system the ratio is found to be much higher. This statement of observation also finds suitable reinforcement from the physiological fact that in case of reduced heart rate variability it has been found that parasympathetic activity is predominant. Hence the $SD1_{down}$ index has higher values and the ratio is decreased. The results are correlating with the above stated fact. Also the increase in this ratio correlates with the evidence of LV dysfunction. LV dysfunction is an abnormality that results due to myocardial ischemia/infarction. So the paper also provides information to the cardiologist about the left ventricular performance without performing echo cardiology test.

VIII. RESULTS AND DISCUSSION

Study was carried out 30 control group varying in age.sex and economic class and 30 subjects suffering from hypertension and 30 from diabetes. All the cases were recorded at Fortis-S.L.Raheja hospital Mahim (W). Care was taken that the duration of diabetes and hypertension was at least 5 year old. As it is clearly seen in figure 5, all the subjects examined are observed to have lower ratio values compared to that of control group were also observed to suffer from LVDD from their echocardiogram reports. The results are tabulated in the form of bar chart shows that the ratio values are higher for control group (0.6268 $\pm$ 0.4933) and significantly low for diabetic group (0.3262$\pm$ 0.1158) for patients suffering from diabetes and hypertension and (0.4262 $\pm$ 0.5820) for patients suffering from hypertension. From figure 5, it can be observed that ratio values are lower for diabetic and hypertensive patients compared to hypertensive patients. This observation can be explained as the presence of diabetic neuropathy in the patients suffering from diabetes and hypertension which leads to compromised neuro harmonal balance. It can be seen that deviation is more for hypertensive patients. The reason patients suffering from LVH are also found to have LVDD are also included. Such patients had a very low value of the ratio than the patients suffering from LVDD alone. This may be due to the fact that age group scatter was more for the hypertensive patients.

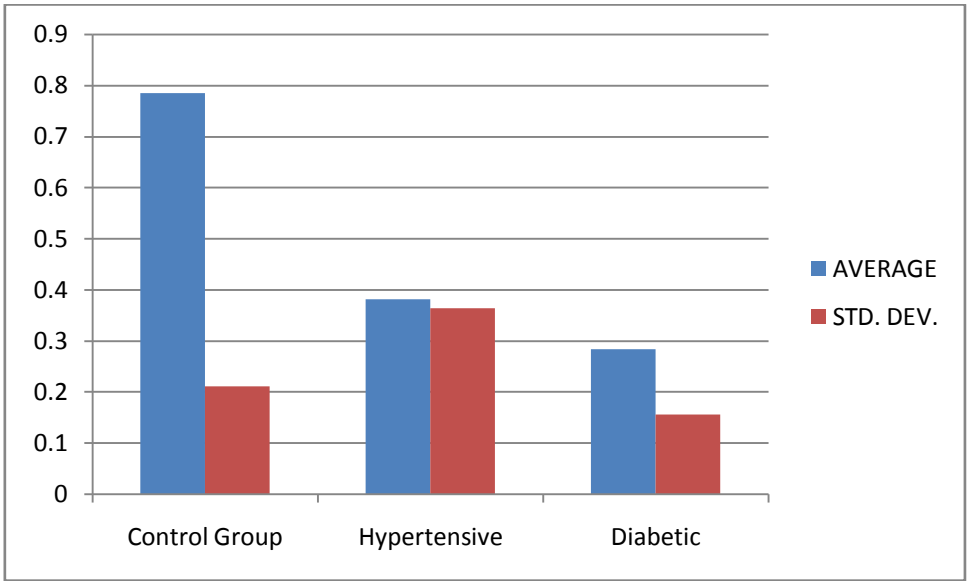

Figure 5 Data samples from S.L.Raheja Hospital

IX. FURTHER SCOPE

More work can be done by taking more samples and results and discussion can be further more confirmative. Also it is possible to explore more by taking different time interval windows of myocardial infarction. More analysis is also possible if one takes ECGs specific to one disease and actual patient data.

REFERENCES

[1] cardiovascular disease trends in India, www.expresshealthcaremgmt.com/20041215/criticare06.shtml.
[2] Manjusha Joshi, Dr. K.D.Desai, ECG Signal analysis used as confirmative tool in quick diagnosis of Myocardial Infarction., International Journal Scientific engineering and research Vol.3 March-2012.
[3] Paul W.Armstrong,Heart 2000, Left Ventricular dysfunction: causes, natural history and hoped for natural reversal, 84(suppl I):i15-i17,
[4] Benhur Aysin,member IEEE,Joe Colombo, member IEEE, and Elif Aysin, Comparison of HRV analysis methods during orthostatic challenge:HRV with respiration or without? EMBS Cite' Internatioale' Lyon France,August 23-26 ,2007.
[5] J Piskorski and P.guzic, Geometry in Poincare' plot of RR intervals and it's asymmetry in healthy adults Physiol. Meas.28 (2007) 287-300
[6] Standard of measurement, physiological interpretation and clinical use American The North Guidelines,European heart journal(1996) 17,354-381.

American Journal of Engineering Research (AJER)
e-ISSN : 2320-0847 p-ISSN : 2320-0936
Volume-02, Issue-09, pp-87-99
www.ajer.org

Research Paper Open Access

Analysis of Order of Singularity at a Vertex in 3D Transversely Isotropic Piezoelectric Single-Step Bonded Joints

Md. Shahidul Islam, Md. Golam Kader, Md. Kamal Uddin, and Mohiuddin Ahmed
Dept. of Mechanical Engineering, Khulna University of Engineering & Technology, Khulna, Bangladesh

Abstract: - The stress singularity field occurs at a vertex on an interface due to a discontinuity of materials. The distribution of stress singularity field near the vertex of bonded joints is very important to maintain the reliability of intelligent materials. Piezoelectric materials are being widely used in the electronics industry, due to their high piezoelectric performance. Piezoelectric material, due to its characteristic direct-converse piezoelectric effect, has naturally received considerable attentions. In this paper, order of singularity at vertex in 3D transversely isotropic piezoelectric single-step bonded joints is analyzed. Eigen analysis based on FEM is used for stress singularity field analysis of piezoelectric bonded joints. The Eigen equation is used for calculating the order of stress singularity, and the angular function of elastic displacement, electric potential, stress and electric displacement. The numerical result shows that the angular functions have large value near the interface edge than the inner portion of the joint. From the numerical result, it was observed that the possibility of debonding at the interface edge of the piezoelectric bonded joints, due to the higher stress concentration at the free edge.

Keywords: - *Order of Singularity, Piezoelectric Single-step Joints, Transversely Isotropic material, Smart Structure, Finite Element Method.*

I. INTRODUCTION

In recent years, intelligent or smart structures and systems have become an emerging new research area. Piezoelectric material, due to its characteristic direct-converse piezoelectric effect, has naturally received considerable attentions [1,2]. Piezoelectric materials have been extensively used as transducers and sensors due to their intrinsic direct and converse piezoelectric effects that take place between electric fields and mechanical deformation, and they are playing a key role as active components in many fields of engineering and technology such as electronics, laser, microwave infrared, navigation and biology [3]. For example, piezoelectric materials are acting as very important functional components in sonar projectors, fluid monitors, pulse generators and surface acoustic wave devices.

Mechanical stress occurs in piezoelectric material for any electric input. The stress concentrations caused by mechanical or electric loads may lead to crack initiation and extension, and sometimes the stress concentrations may be high enough to fracture the material parts. In the case of multilayer piezoelectric stacks, the electrodes that terminate inside the material body are a source of electric field, which can result in high stress concentrations. Reliable service lifetime predictions of piezoelectric components demand a complete understanding of the debonding processes of these materials. Industrial products such as electronic devices and heat endurance parts are composed of dissimilar materials. A mismatch of material properties causes a failure at the free edge of joint, because a stress concentration occurs along the free edge of interface especially at the vertex of bonded joint [4].

Sosa has suggested a general method of solving plane problems of piezoelectric media with defects [5]. Wang has obtained the general solutions of governing equations to three-dimensional axisymmetric problems in transversely isotropic piezoelectric media [6]. Williams used the mathematical procedure for analyzing stress singularities in infinite wedges and successfully applying to the analysis of stress distribution at the vicinity of a crack tip [7,8]. Zak and Williams used Eigen functions for analyzing stress singularity field at a crack tip perpendicular to a bimaterial interface [9]. They found that a real part of Eigen value is within the

range of 0 to 1, and expressed a relationship between stress distribution and the order of stress singularity at the crack tip. Aksentian determined Eigen values and Eigen vectors at the singular point in plane intersecting a free edge of the interface in three dimensional dissimilar joints [10].

Hartranft and Sih introduced the Eigen function expansions method in order to study the purely elastic 3D problem [11]. Bazent and Estenssoro, and Yamada and Okumura developed a finite element analysis for solving Eigen value equation to determine directly the order of stress singularity and the angular variation of the stress and displacement fields [12,13]. This Eigen analysis was used to evaluate the order of singularity at a point where a crack meets a free surface in an isotropic material. Then, this Eigen analysis based on a finite element was adapted by Pageau, Joseph and Biggers to use for analyzing the inplane deformation of wedges and junctions composed of anisotropic materials [14]. The stress and displacement fields were obtained from Eigen formulation for real and complex orders of stress singularity. Pageau and Biggers applied to analyze the joints including fully bonded multi-material junctions intersecting a free edge as well as materials containing crack intersecting a free edge [15]. This study showed that the order of singularity in the three-dimensional stress field could be accurately determined with a relatively small number of elements. Pageau and Biggers determined the order of stress singularity and the angular variation of the displacement and the stress fields around the singular points in plane intersecting a wedge front in the three-dimensional anisotropic material structures using the two dimensional displacement formulation under a plane strain assumption [16].

The effects of order of singularity near the vertex of 3D transversely isotropic piezoelectric bonded joints from a continuum mechanics point of view are not clear until now. Therefore, the effect of stress singularity field at a vertex on an interface of transversely isotropic piezoelectric single-step bonded joints is analyzed in this present study.

II. THE GOVERNING EQUATION

In the absence of body forces and free charges, the equilibrium equations of piezoelectric materials are expressed as follows [17]:

$$\sigma_{ij,j} = 0, \qquad d_{i,i} = 0 \tag{1}$$

The constitutive relations are shown as follows:

$$\sigma_{ij} = c_{ijkl}\varepsilon_{kl} - e_{kij}E_k, \qquad d_i = e_{ikl}\varepsilon_{kl} - \chi_{ik}E_k \tag{2}$$

The elastic strain-displacement and electric field-potential relations are presented as follows:

$$\varepsilon_{ij} = \frac{1}{2}\left(u_{j,i} + u_{i,j}\right), \qquad E_i = -\psi_{,i} \tag{3}$$

where i, j, k, l = 1, 2, 3 and σ_{ij}, d_i, ε_{ij}, u_i, E_i, and ψ are the component of stress, electric displacement, strain, elastic displacement, eclectic field and electric potential respectively. Eq. (2) expressed in terms of elastic stiffness constant c_{ijkl} (measured in a constant electric field), the piezoelectric constant e_{ikl} and electric permittivity (dielectric constant) χ_{ik} (measured at a constant strain).

For transversely isotropic material, taking z-axis parallel to the poling axis of the material, by convention, the constructive relation is expressed in the following form.

$$\{\sigma\} = [c]\{\varepsilon\} - [e]\{E\}, \qquad \{d\} = [e]^T\{\varepsilon\} - [\chi]\{E\} \tag{4}$$

where $\{\sigma\}$ and $\{\varepsilon\}$ are the stress and strain which are the mechanical field variables, $\{d\}$ and $\{E\}$ are the electric displacement and electric field respectively, $[c]$ is the elastic constant, and $[e]$ and $[\chi]$ are the piezoelectric and electric permittivity (dielectric) constant respectively.

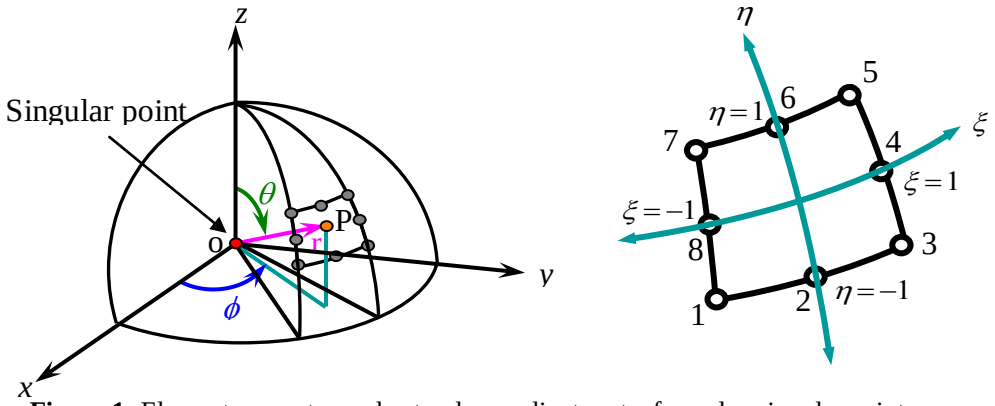

Figure 1: Element geometry and natural co-ordinates at a free edge singular point

Fig. 1 represents the geometry of a typical case where a singular stress state occurs at the point o. The region surrounding the singular point is divided into a number of quadratic pyramidal elements with a summit o, with each element being located in spherical coordinates r, θ, and ϕ by its nodes 1 to 8. A point P in the element can be located using the singular transformation by the following relations.

$$r = r_o\left(\frac{1+\alpha}{2}\right)^{1/p} \qquad or, \qquad \rho = \frac{r}{r_o} = \left(\frac{1+\alpha}{2}\right)^{1/p} \tag{5}$$

$$\theta = \sum_{i=1}^{8} H_i\theta_i \qquad and \qquad \phi = \sum_{i=1}^{8} H_i\phi_i \tag{6}$$

where p Eigen value, $\rho = r/r_o$, r the distance from the singular point, and H_i indicates the shape function, which is written as;

$$H_1 = -\frac{1}{4}(1-\eta)(1-\xi)(\eta+\xi+1) \qquad H_2 = \frac{1}{2}(1-\eta)(1-\xi^2)$$

$$H_3 = -\frac{1}{4}(1-\eta)(1+\xi)(-\eta+\xi-1) \qquad H_4 = \frac{1}{2}(1-\eta^2)(1+\xi)$$

$$H_5 = \frac{1}{4}(1+\eta)(1+\xi)(\eta+\xi-1) \qquad H_6 = \frac{1}{2}(1+\eta)(1-\xi^2)$$

$$H_7 = \frac{1}{4}(1+\eta)(1-\xi)(\eta-\xi-1) \qquad H_8 = \frac{1}{2}(1-\eta^2)(1-\xi) \tag{7}$$

θ and ϕ are the nodal values of the angular coordinates and α, η, and ξ are natural coordinates of the element whose ranges are shown in Fig.1.

The elastic displacement and electric potential field in the element is expressed as follows:

$$\left(\bar{u}-\bar{u}_o\right) = \left(\frac{1+\alpha}{2}\right)\left[\sum_{i=1}^{8} H_i\left(\bar{u}_i-\bar{u}_o\right)\right], \text{ and } \quad \left(\bar{\psi}-\bar{\psi}_o\right) = \left(\frac{1+\alpha}{2}\right)\left[\sum_{i=1}^{8} H_i\left(\bar{\psi}_i-\bar{\psi}_o\right)\right] \tag{8}$$

where $\bar{u}_o$ and $\bar{u}$ represents the elastic displacement vector of the vertex o and the point P respectively, and $\bar{u}_i$ represents the elastic displacement vector of the node i (i = 1, 2, …, 8). Similarly $\bar{\psi}_o$ and $\bar{\psi}$ represents the electric potential vector of the vertex o and the point P respectively, and $\bar{\psi}_i$ represents the electric potential vector of the node i (i = 1, 2, ……, 8). In order to simplify the notation, the following equation can be defined.

$$u = \left(\bar{u}-\bar{u}_o\right), \qquad u_i = \left(\bar{u}_i-\bar{u}_o\right), \text{ and } \quad \psi = \left(\bar{\psi}-\bar{\psi}_o\right), \qquad \psi_i = \left(\bar{\psi}_i-\bar{\psi}_o\right) \tag{9}$$

Using the Eq. (5), Eq. (8) can be expressed as follows:

$$u_k = \rho^p\left[\sum_{i=1}^{8} H_i u_{ki}\right] \quad (k = r,\theta,\phi), \text{ and } \quad \psi = \rho^p\left[\sum_{i=1}^{8} H_i\psi_i\right] \tag{10}$$

The Jacobean matrix relating the spherical coordinates to the natural coordinates is given below:

$$[\mathbf{J}]=\begin{bmatrix} \frac{\partial r}{\partial \alpha} & \frac{\partial \theta}{\partial \alpha} & \frac{\partial \phi}{\partial \alpha} \\ \frac{\partial r}{\partial \xi} & \frac{\partial \theta}{\partial \xi} & \frac{\partial \phi}{\partial \xi} \\ \frac{\partial r}{\partial \eta} & \frac{\partial \theta}{\partial \eta} & \frac{\partial \phi}{\partial \eta} \end{bmatrix}=\begin{bmatrix} \frac{r_o}{2p}\rho^{1-p} & 0 & 0 \\ 0 & \sum_{i=1}^{8} H_{i,\xi}\theta_i & \sum_{i=1}^{8} H_{i,\xi}\phi_i \\ 0 & \sum_{i=1}^{8} H_{i,\eta}\theta_i & \sum_{i=1}^{8} H_{i,\eta}\phi_i \end{bmatrix} \tag{11}$$

Eq. (11) shows that there is no dependence between the radial coordinate and the angular coordinate. From Eq. (11) a sub-matrix is extracted as follows:

$$[\mathbf{J}_1]=\begin{bmatrix} \frac{\partial \theta}{\partial \xi} & \frac{\partial \phi}{\partial \xi} \\ \frac{\partial \theta}{\partial \eta} & \frac{\partial \phi}{\partial \eta} \end{bmatrix}=\begin{bmatrix} \sum_{i=1}^{8} H_{i,\xi}\theta_i & \sum_{i=1}^{8} H_{i,\xi}\phi_i \\ \sum_{i=1}^{8} H_{i,\eta}\theta_i & \sum_{i=1}^{8} H_{i,\eta}\phi_i \end{bmatrix} \tag{12}$$

The strain and electric potential equation is obtained from Eq. (5)~ Eq. (7) and Eq. (10), Eq. (12) by using the chain rule of differentiation.

The strain in a spherical coordinate system:

$$\varepsilon_{rr}=\frac{\partial u_r}{\partial r}=\frac{p\rho^{p\lambda-1}}{r_o}\left[\sum_{i=1}^{8} H_i u_{ri}\right]$$

$$\varepsilon_{\theta\theta}=\frac{\partial u_\theta}{r\partial\theta}+\frac{u_r}{r}=\left(\frac{\rho^{p-1}}{r_o}\right)\left\{\sum_{i=1}^{8} H_i u_{ri}+\left[J_1(1,1)\right]^{-1}\left[\sum_{i=1}^{8}\frac{\partial H_i}{\partial\xi}u_{\theta i}\right]+\left[J_1(1,2)\right]^{-1}\left[\sum_{i=1}^{8}\frac{\partial H_i}{\partial\eta}u_{\theta i}\right]\right\}$$

$$\varepsilon_{\phi\phi}=\frac{u_\theta}{r}\cot\theta+\frac{1}{r\sin\theta}\frac{\partial u_\phi}{\partial\phi}+\frac{u_r}{r}=\left(\frac{\rho^{p-1}}{r_o}\right)\left\{\sum_{i=1}^{8} H_i u_{ri}+\cot\theta\left[\sum_{i=1}^{8} H_i u_{\theta i}\right]\right.$$
$$\left.+\frac{\left[J_1(2,1)\right]^{-1}}{\sin\theta}\left[\sum_{i=1}^{8}\frac{\partial H_i}{\partial\xi}u_{\phi i}\right]+\frac{\left[J_1(2,2)\right]^{-1}}{\sin\theta}\left[\sum_{i=1}^{8}\frac{\partial H_i}{\partial\eta}u_{\phi i}\right]\right\}$$

$$\gamma_{\theta\phi}=\frac{1}{r\sin\theta}\frac{\partial u_\theta}{\partial\phi}+\frac{\partial u_\phi}{r\partial\theta}-\frac{u_\phi}{r}\cot\theta$$
$$=\left(\frac{\rho^{p-1}}{r_o}\right)\left\{-\cot\theta\left[\sum_{i=1}^{8} H_i u_{\phi i}\right]+\left[J_1(1,1)\right]^{-1}\left[\sum_{i=1}^{8}\frac{\partial H_i}{\partial\xi}u_{\phi i}\right]+\left[J_1(1,2)\right]^{-1}\left[\sum_{i=1}^{8}\frac{\partial H_i}{\partial\eta}u_{\phi i}\right]\right.$$
$$\left.+\frac{\left[J_1(2,1)\right]^{-1}}{\sin\theta}\left[\sum_{i=1}^{8}\frac{\partial H_i}{\partial\xi}u_{\theta i}\right]+\frac{\left[J_1(2,2)\right]^{-1}}{\sin\theta}\left[\sum_{i=1}^{8}\frac{\partial H_i}{\partial\eta}u_{\theta i}\right]\right\}$$

$$\gamma_{r\phi}=\frac{1}{r\sin\theta}\frac{\partial u_r}{\partial\phi}+\frac{\partial u_\phi}{\partial r}-\frac{u_\phi}{r}=\left(\frac{\rho^{p-1}}{r_o}\right)\left\{(p-1)\left[\sum_{i=1}^{8} H_i u_{\phi i}\right]\right.$$
$$\left.+\frac{\left[J_1(2,1)\right]^{-1}}{\sin\theta}\left[\sum_{i=1}^{8}\frac{\partial H_i}{\partial\xi}u_{ri}\right]+\frac{\left[J_1(2,2)\right]^{-1}}{\sin\theta}\left[\sum_{i=1}^{8}\frac{\partial H_i}{\partial\eta}u_{ri}\right]\right\}$$

$$\gamma_{r\theta}=\frac{\partial u_r}{r\partial\theta}+\frac{\partial u_\theta}{\partial r}-\frac{u_\theta}{r}=\left(\frac{\rho^{p-1}}{r_o}\right)\left\{(p-1)\left[\sum_{i=1}^{8} H_i u_{\theta i}\right]\right.$$

$$+\left[J_1(1,1)\right]^{-1}\left[\sum_{i=1}^{8}\frac{\partial H_i}{\partial \xi}u_{ri}\right]+\left[J_1(1,2)\right]^{-1}\left[\sum_{i=1}^{8}\frac{\partial H_i}{\partial \eta}u_{ri}\right]\Bigg\} \tag{13}$$

The electric potential in a spherical coordinate system:

$$E_r=-\frac{\partial \psi}{\partial r}=-\left(\frac{p\rho^{p-1}}{r_o}\right)\left[\sum_{i=1}^{8}H_i\psi_i\right]$$

$$E_\theta=-\frac{\partial \psi}{r\partial \theta}=-\left(\frac{\rho^{p-1}}{r_o}\right)\left\{\left[J_1(1,1)\right]^{-1}\left[\sum_{i=1}^{8}\frac{\partial H_i}{\partial \xi}\psi_i\right]+\left[J_1(1,2)\right]^{-1}\left[\sum_{i=1}^{8}\frac{\partial H_i}{\partial \eta}\psi_i\right]\right\}$$

$$E_\phi=-\frac{1}{r\sin\theta}\frac{\partial \psi}{\partial \phi}=-\left(\frac{\rho^{p-1}}{r_o}\right)\left\{\frac{\left[J_1(2,1)\right]^{-1}}{\sin\theta}\left[\sum_{i=1}^{8}\frac{\partial H_i}{\partial \xi}\psi_i\right]+\frac{\left[J_1(2,2)\right]^{-1}}{\sin\theta}\left[\sum_{i=1}^{8}\frac{\partial H_i}{\partial \eta}\psi_i\right]\right. \tag{14}$$

The superscript -1 on the matrix $[J_1]$ represents the inverse matrix. Eq. (13) and Eq. (14) now can be summarized as follows:

$$\{\boldsymbol{\varepsilon}^*\}=\sum_{i=1}^{8}[\mathbf{B}_i]\{\mathbf{u}_i^*\}=[\mathbf{B}]\{\mathbf{u}^*\} \tag{15}$$

where $\{\boldsymbol{\varepsilon}^*\}^T=\{\varepsilon_{rr}\quad \varepsilon_{\theta\theta}\quad \varepsilon_{\phi\phi}\quad \varepsilon_{r\theta}\quad \varepsilon_{r\phi}\quad \varepsilon_{\theta\phi}\quad E_r\quad E_\theta\quad E_\phi\}$

$$\{u_i^*\}^T=\{u_{ri}\quad \bar{u}_{\theta i}\quad \bar{u}_{\phi i}\quad -\bar{\psi}_i\}$$

$$[\mathbf{B}]=\frac{1}{r_o}\rho^{p-1}\left(p[\mathbf{B}_a]+[\mathbf{B}_b]\right)$$

$$[\mathbf{B}_{ia}]=\begin{bmatrix} H_i & 0 & 0 & 0\\ 0 & 0 & 0 & 0\\ 0 & 0 & 0 & 0\\ 0 & H_i & 0 & 0\\ 0 & 0 & H_i & 0\\ 0 & 0 & 0 & 0\\ 0 & 0 & 0 & H_i\\ 0 & 0 & 0 & 0\\ 0 & 0 & 0 & 0 \end{bmatrix}, \text{ and } [\mathbf{B}_{ib}]=\begin{bmatrix} 0 & 0 & 0 & 0\\ H_i & A_1 & 0 & 0\\ H_i & H_i\cot\theta & A_2 & 0\\ A_1 & -H_i & 0 & 0\\ A_2 & 0 & -H_i & 0\\ 0 & A_2 & A_1-H_i\cot\theta & 0\\ 0 & 0 & 0 & 0\\ 0 & 0 & 0 & A_1\\ 0 & 0 & 0 & A_2 \end{bmatrix} \tag{16}$$

Also A_1 and A_2 are written as;

$$A_1=\left[J_1(1,1)\right]^{-1}\left[\frac{\partial H_i}{\partial \xi}\right]+\left[J_1(1,2)\right]^{-1}\left[\frac{\partial H_i}{\partial \eta}\right], \text{ and } A_2=\frac{\left[J_1(2,1)\right]^{-1}}{\sin\theta}\left[\frac{\partial H_i}{\partial \xi}\right]+\frac{\left[J_1(2,2)\right]^{-1}}{\sin\theta}\left[\frac{\partial H_i}{\partial \eta}\right] \tag{17}$$

Eq. (15) ~ Eq. (17) represents the strains, and therefore the stresses are proportional to ρ^{p-1}. The case where $0 < p < 1$ defines a singular stress state at the vertex of the element. The element depicted in Fig.1 must satisfy the principle of virtual work in order to be in equilibrium, that is

$$\int_{\Omega} \sigma_{ij}^{*} \delta\varepsilon_{ij}^{*} d\Omega = \int_{\Gamma} T_i^{*} \delta u_i^{*} d\Gamma + \int_{\Omega} f_i^{*} \delta u_i^{*} d\Omega \tag{18}$$

Where T_i^* represents the traction at the outer boundary. This equation can be transformed into a matrix form with the help of Eq. (5)~ Eq. (7) as follows:

$$\int_{-1}^{1}\int_{-1}^{1}\int_{-1}^{1} r_o^2 \rho^2 \left(\delta\{\varepsilon^*\}^T \{\sigma^*\}\right) \sin\theta |\mathbf{J}| d\alpha d\xi d\eta = \int_{-1}^{1}\int_{-1}^{1} r_o^2 \left(\delta\{\mathbf{u}^*\}^T \{\mathbf{H}\}^T \begin{Bmatrix} \sigma_{rr} \\ \sigma_{r\phi} \\ \sigma_{r\theta} \\ d_r \end{Bmatrix} \right) \sin\theta |\mathbf{J}_1| d\xi d\eta \tag{19}$$

where $|J|$ and $|J_1|$ represent the determinant of the matrices [**J**] and [$\mathbf{J_1}$] respectively and $\{\sigma^*\}^T$ is represented by the following equation.

$$\{\boldsymbol{\sigma}^*\}^T = \{\sigma_{rr} \quad \sigma_{\theta\theta} \quad \sigma_{\phi\phi} \quad \tau_{r\theta} \quad \tau_{r\phi} \quad \tau_{\theta\phi} \quad d_r \quad d_\theta \quad d_\phi\} \tag{20}$$

The relation between stress and electric displacement with strain and electric field is as follows:

$$\{\boldsymbol{\sigma}^*\} = [\mathbf{D}]\{\boldsymbol{\varepsilon}^*\} \tag{21}$$

where **[D]** represents the material constants matrix.

The Eigen equation was formulated for determining the order of stress singularity as follows [14]:

$$\left(p^2 [\mathbf{A}] + p[\mathbf{B}] + [\mathbf{C}]\right)\{\mathbf{U}\} = \{0\} \tag{22}$$

where

$$\{\mathbf{U}\} = \begin{Bmatrix} u_r \\ u_\theta \\ u_\phi \\ \psi \end{Bmatrix}, \text{ and}$$

$$[\mathbf{A}] = \sum_S \left([\mathbf{k}_a - \mathbf{k}_{sa}]\right), \quad [\mathbf{B}] = \sum_S \left([\mathbf{k}_b - \mathbf{k}_{sb}]\right), \quad [\mathbf{C}] = \sum_S \left([\mathbf{k}_c - \mathbf{k}_{sc}]\right)$$

In Eq. (22), p represents the characteristic root, which is related to the order of singularity, λ, as $\lambda = 1\text{-}p$. **[A]**, **[B]** and **[C]** are matrices composed of material properties, and **{U}** represents the elastic displacement and electric potential vector.

$$[\mathbf{k}_a] = \int_{-1}^{1}\int_{-1}^{1} [\mathbf{B}_a]^T [\mathbf{D}][\mathbf{B}_a] \sin\theta |J_1| d\xi d\eta$$

$$[\mathbf{k}_b] = \int_{-1}^{1}\int_{-1}^{1} \left([\mathbf{B}_a]^T [\mathbf{D}][\mathbf{B}_b] + [\mathbf{B}_b]^T [\mathbf{D}][\mathbf{B}_a]\right) \sin\theta |J_1| d\xi d\eta$$

$$[\mathbf{k}_c] = \int_{-1}^{1}\int_{-1}^{1} [\mathbf{B}_b]^T [\mathbf{D}][\mathbf{B}_b] \sin\theta |J_1| d\xi d\eta$$

$$[\mathbf{k}_{sa}] = 2\int_{-1}^{1}\int_{-1}^{1} [\mathbf{H}]^T [\mathbf{SD}][\mathbf{B}_a] \sin\theta |J_1| d\xi d\eta$$

$$[\mathbf{k}_{sb}] = \int_{-1}^{1}\int_{-1}^{1}\left(2[\mathbf{H}]^T[\mathbf{SD}][\mathbf{B}_b] + [\mathbf{H}]^T[\mathbf{SD}][\mathbf{B}_a]\right)\sin\theta|J_1|d\xi d\eta$$

$$[\mathbf{k}_{sc}] = \int_{-1}^{1}\int_{-1}^{1}[\mathbf{H}]^T[\mathbf{SD}][\mathbf{B}_b]\sin\theta|J_1|d\xi d\eta$$

Eq. (22) now expressed as follows

$$\left(-p[\mathbf{B}]-[\mathbf{C}]\right)\{\mathbf{U}\} = p^2[\mathbf{A}]\{\mathbf{U}\} \tag{23}$$

Finally, letting $\{\mathbf{V}\} = p\{\mathbf{U}\}$, the characteristic equation can be transformed into the standard Eigen problem.

$$\begin{bmatrix} -[\mathbf{A}]^{-1}[\mathbf{B}] & -[\mathbf{A}]^{-1}[\mathbf{C}] \\ [\mathbf{I}] & [0] \end{bmatrix}\begin{Bmatrix}\{\mathbf{V}\}\\ \{\mathbf{U}\}\end{Bmatrix} = p\begin{Bmatrix}\{\mathbf{V}\}\\ \{\mathbf{U}\}\end{Bmatrix} \tag{24}$$

III. RESULTS AND DISCUSSIONS

Fig. 2 represents a model for 3D two-phase transversely isotropic piezoelectric dissimilar joints used in the present analysis. The stress singularity line and singularity point on interface of the joint are shown in the figure. The angle θ is equal to 180º and the angle ϕ for upper material and lower material are 90º and 360º respectively. In Eigen analysis, a mesh division for the joint is needed for the analysis. The mesh developed on ϕ-θ plane is shown in Fig. 3, where the surface of a unit sphere is divided into $\phi \times \theta$ = 10º×10º.

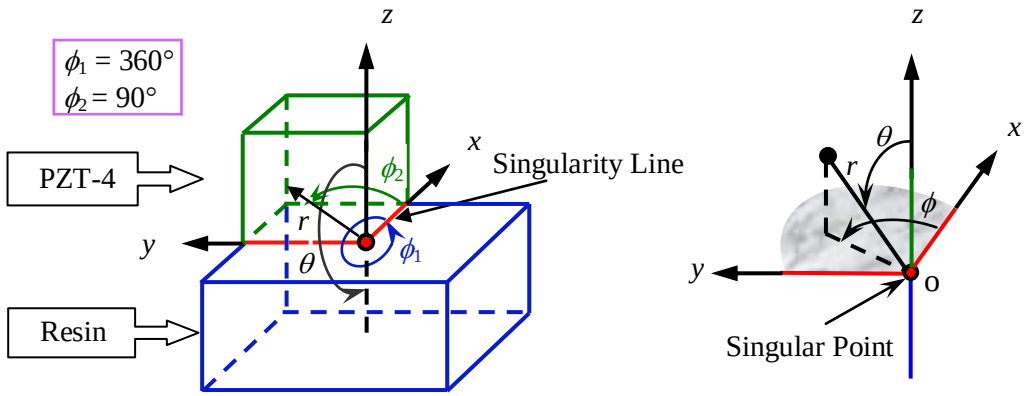

Figure 2: Singular point of 3D piezoelectric single-step bonded joint in *x*, *y*, *z* plane

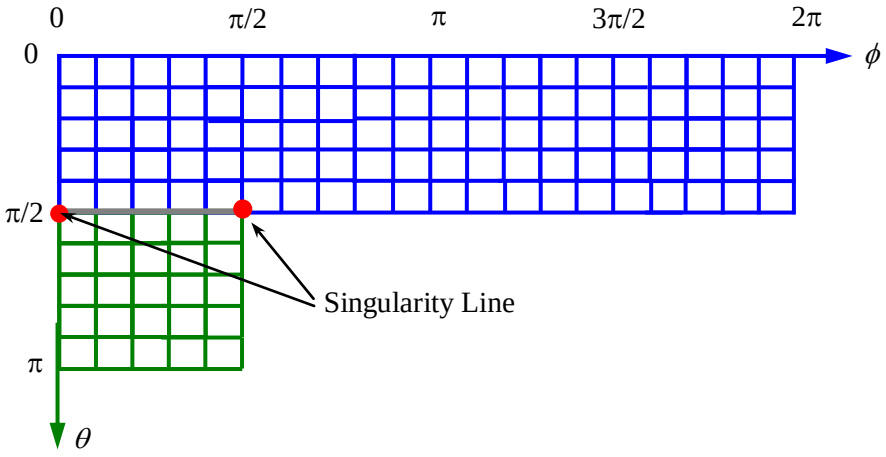

Figure 3: A mesh on developed ϕ-θ plane

Table 1. Material properties of piezoelectric materials

Material	Elastic Constant, 10^{10} N/m^2					Piezoelectric Constant, C/m^2			Dielectric Constant, 10^{-10} C/Vm	
	c_{11}	c_{12}	c_{13}	c_{33}	c_{44}	e_{31}	e_{33}	e_{15}	χ_{11}	χ_{33}
Resin	5.56	3.41	3.41	5.56	1.08	0.0	0.0	0.0	37.9	37.9
PZT-4	13.9	7.78	7.43	11.3	2.56	-6.98	13.8	13.4	60.0	54.7

In this analysis, first of all, Eigen values and Eigen vectors are investigated by Eigen analysis when two different materials are bonded. The order of singularity λ, at the vertex and at a point on the singularity line for the model shown in Fig. 2 is calculated. Solving Eigen equation yields many roots p and Eigen vectors corresponding to each Eigen value are obtained. However, if the root p is within the range of $0 < p < 1$, this fact indicates that the stress field has singularity. The values of the order of singularity at the singularity corner and line for transversely isotropic piezoelectric bonded material are shown in Table 2.

Table 2. Order of singularity for Resin and PZT-4

Material	Order of singularity				
PZT-4 and Resin	λ	1	2	3	4
	λ_{line}	0.3494	0.0895	0.0264	----
	λ_{vertex}	0.4304	0.0291	0.0081	0.0023

The angular functions of elastic displacement and electric potential equation are expressed by the following equitation.

$$u_j(r, \theta, \phi) = b_j(\theta, \phi) r^{1-\lambda}, \text{ and } \quad \psi(r, \theta, \phi) = q(\theta, \phi) r^{1-\lambda} \quad (j = r, \theta, \phi) \tag{25}$$

By differentiating the above equations, get the angular function of strain and electric field equation respectively. The stress and electric displacement distribution equations in the stress singularity region can be expressed as follows.

$$\sigma_{ij}(r, \theta, \phi) = K_{ij} r^{-\lambda} f_{ij}(\theta, \phi), \text{ and } \quad d_i(r, \theta, \phi) = F_i r^{-\lambda} l_i(\theta, \phi) \quad (i, j = r, \theta, \phi) \tag{26}$$

Where r represents the distance from the stress singular point, $b_j(\theta, \phi)$ the angular function of elastic displacement, $q(\theta, \phi)$ the angular function of electric potential, $f_{ij}(\theta, \phi)$ the angular function of stress distribution, $l_i(\theta, \phi)$the angular function of electric displacement, K_{ij} the intensity of singularity, F_i the intensity of electric field, and λ the order of stress singularity. Angular functions of stress components obtained from Eigen analysis in Eq. (22) are examined.

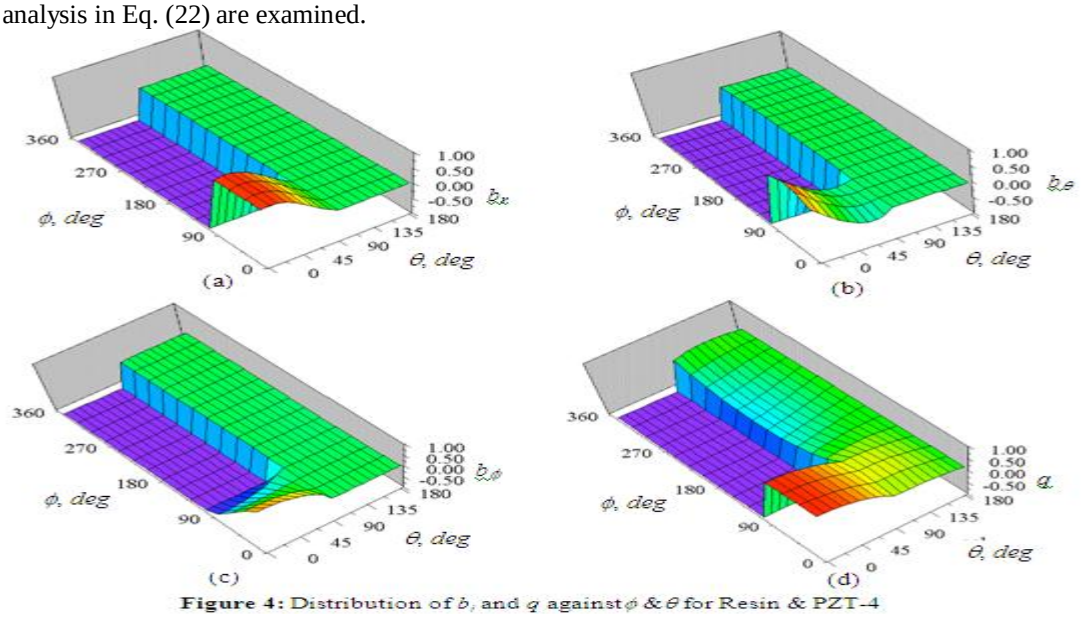

Figure 4: Distribution of b_r and q against ϕ & θ for Resin & PZT-4

Fig. 4 shows the distribution of angular function of elastic displacement and electric potential at $\lambda_1 = 0.4304$. Plots (a), (b) and (c) represent the elastic displacement and plot (d) represent the electric potential. All figures are plotted by using the Eq. (25). All of these plots show that the angular functions are continuous at the interface of the bonded joint. The interface of the joint is at $\theta = 90^{o}$. Resin is exist in the region of $\phi = 0°$ to 360°, $\theta = 90°$ to 180° and PZT-4 is exist in the region of $\phi = 0°$ to 90°, $\theta = 0°$ to 90°. The distribution of angular function of stress against ϕ and θ for $\lambda = 0.4304$ is plotted by using the Eq. (26) and the graphs are shown in the figure below:

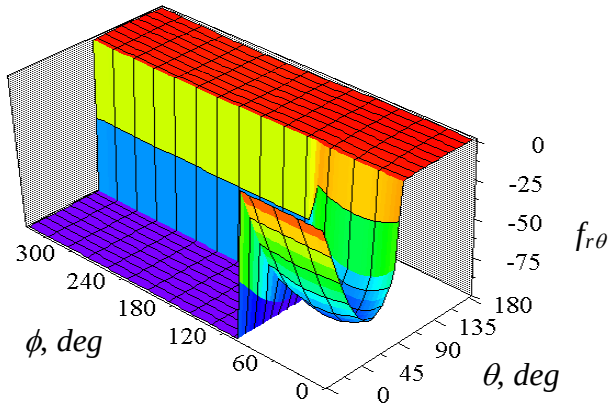

Figure 5: Distribution of $f_{r\theta}$ against ϕ and θ for Resin & PZT-4

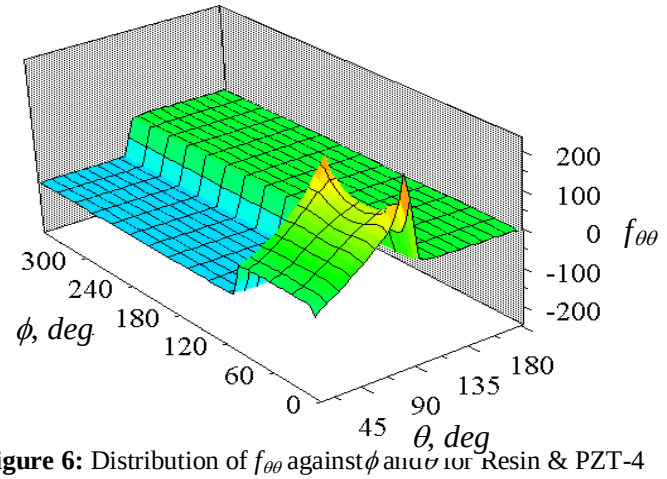

Figure 6: Distribution of $f_{\theta\theta}$ against ϕ and θ for Resin & PZT-4

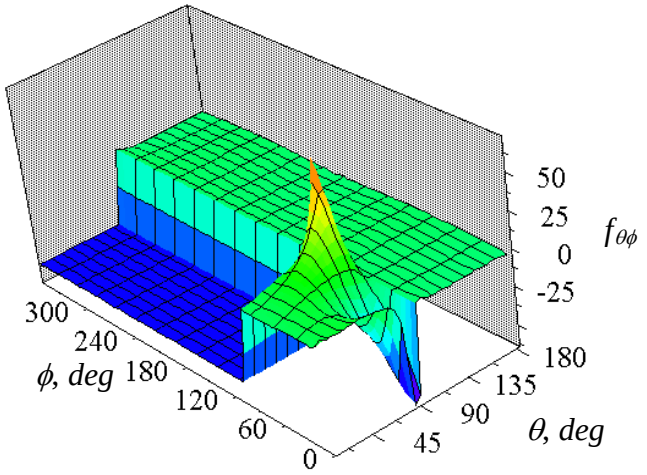

Figure 7: Distribution of $f_{\theta\phi}$ against ϕ and θ for Resin & PZT-4

Fig. 5~7 show the 3D distribution of angular function of stress in ϕ-θ plane for λ = 0.4304. All these graphs show the angular function of stress have the larger value at the interface edge of the bonded joint. The distribution of angular function of electric displacement against ϕ and θ for λ = 0.4304 is plotted by using the Eq. (26) and the graphs are shown in the figure below:

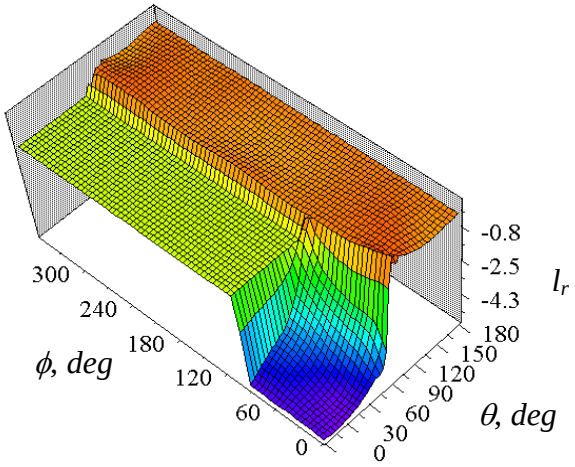

Figure 8: Distribution of l_r against ϕ and θ for Resin & PZT-4

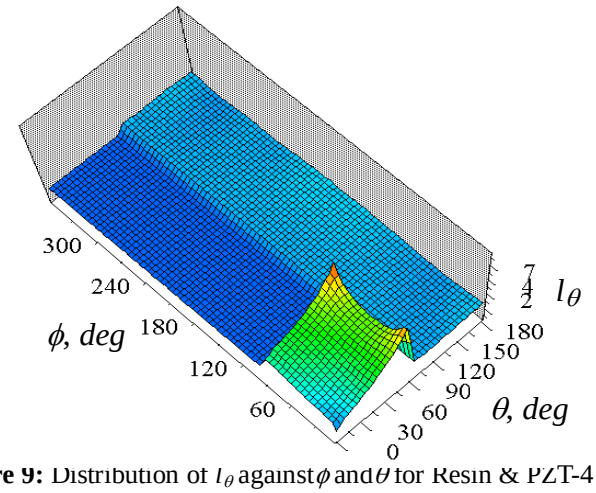

Figure 9: Distribution of l_θ against ϕ and θ for Resin & PZT-4

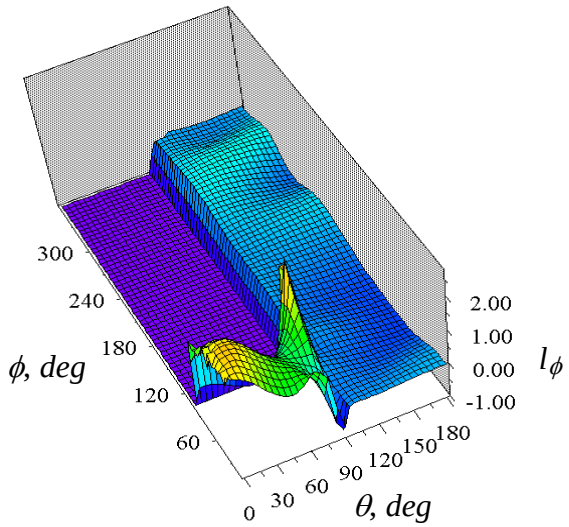

Figure 10: Distribution of l_ϕ against ϕ and θ for Resin & PZT-4

Fig. 8~10 show the 3D distribution of angular function of electric displacement in ϕ-θ plane for $\lambda = 0.4304$. All these figures show the angular function of electric displacement is continuous at the interface of the bonded joint. These figures also show that the larger value of angular function of electric displacement near the interface edge than the in

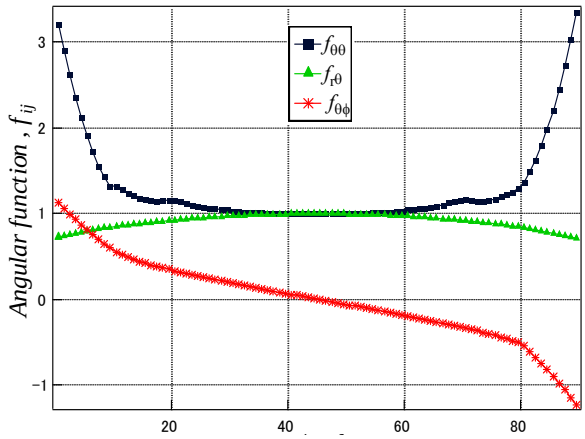

Figure11: Distribution of normalized f_{ij} against ϕ at $\theta = 90°$ for Resin & PZT-4

The normalized angular function of stress is shown in Fig. 11 for $\lambda = 0.4304$. The angular function of stress against the angle ϕ at $\theta = 90°$ is plotted. The stress singularity lines are at the free edge of the material joint. The figure shows that the value of angular function of stress increases rapidly near the interface edge than the inner portion of the joints. The values of $f_{r\theta}$ and $f_{\theta\theta}$ is normalized by their value at $\phi = 45°$ and $f_{\phi\theta}$ is normalized by their value at $\phi = 2.5°$. Near interface edge of the joint has the largest value of angular function of stress. So there is a possibility to debond and delamination occurs near the interface edge of the single-step bonded joint.

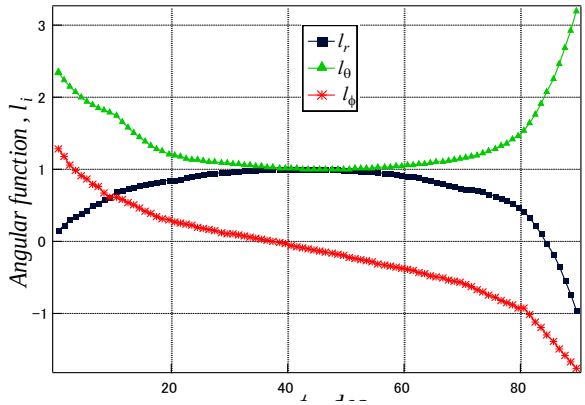

Figure12: Distribution of normalized l_i against ϕ at $\theta = 90^o$ for Resin & PZT-4

The normalized angular function of electric displacement is shown in Fig. 12 for $\lambda = 0.4304$. The angular function of electric displacement against the angle ϕ at $\theta = 90^o$ is plotted. This figure also shows that the value of angular function of electric displacement increases rapidly near the free edge than the inner portion of the joints. The value of l_r and l_θ is normalized by their value at $\phi = 45°$ and l_ϕ is normalized by their value at $\phi = 3.5°$. The angular function of electric displacement has the larger value near the interface edge than the inner portion of the joint. So there is another possibility to debond and delamination occurs near the interface edge of the single-step bonded joint.

IV. CONCLUSIONS

An Eigen equation formulation near the vertex of transversely isotropic piezoelectric single-step bonded joint was presented. Angular functions for singularity corner were derived from Eigen analysis based on

a finite element method. From the numerical results, the following conclusions can be drawn for the piezoelectric single-step bonded joints.
(a) The order of singularity at the singularity corner is larger than that of the line.
(b) Larger value of the angular function occurs at the interface edge in the material joint than the inner portion of the joint.
(c) It is suggested that delamination of the interface may occur at the interface edge of the piezoelectric material joints.

V. ACKNOWLEDGMENTS

I would like to express my deep and sincere gratitude to Prof. Hideo Koguchi, Nagaoka University of Technology, Japan. I am deeply grateful to Takahiko Kurahashi, Nagaoka University of Technology, Japan for his detailed and constructive comments throughout this work.

Notations

σ_{ij}	Stress, N/m^2
ε_{ij}	Strain, m/m
d_i	Electric displacement, C/m^2
E_i	Electric field, N/C
c_{ijkl}	Elastic constant, N/m^2
e_{ilkl} (e_{kij})	Piezoelectric cnstant, C/m^2
χ_{ik}	Electric permittivity, C^2/Nm^2
H	Interpolation function
p	Characteristic root
λ	Order of singularity
u_i	Elastic displacement
ψ	Electric potential

REFERENCES

[1] Ding, H. and Chenbuo, On the Green's functions for two-phase transversely isotropic piezoelectric media, *Int. J. of Solids and Structure*, 34(23), 3041-3057, 1997.
[2] Ming, H. Z., Ping Z. F. and Ya P. S, Boundary integral-differential equations and boundary element method for interfacial cracks in three-dimensional piezoelectric media, *Engineering Analysis with Boundary Elements*, 28, 753-762, 2004.
[3] Wang, Z. and Zheng, B., The general solution of three-dimensional problems in piezoelectric media, *Int. J. of Solids and Structure*, 32(1), 105-115, 1995.
[4] Attaporn, W. and Koguchi, H., Intensity of stress singularity at a vertex and along the free edges of the interface in 3D-dissimilar material joints using 3D-enriched FEM, *CMES*, 39(3), 237-262, 2009.
[5] Sosa, H. A., Plane problems in piezoelectric media with defects, *Int. J. of Solids and Structure*, 28, 491-505, 1991.
[6] Wang, Z. K., Penny-shaped crack in transversely isotropic piezoelectric materials", *Acta Mechanica Sinica*, 10, 1-8, 1994.
[7] Williams, M. L., Stress singularities resulting from various boundary conditions in angular corners of plates in extension, *ASME J. of Applied Mechanics*,19, 526, 1952.
[8] Williams, M. L., On the stress at the base of stationary crack", *ASME J. of Applied Mechanics*, 24, 109-114, 1957.
[9] Zak, A. R. and Williams, M. L., Crack point stress singularities at a bi-material interface, *J. of Applied Mechanics, Brielf Notes*, 142-143, 1963.
[10] Aksentian, O. K., Singularities of the stress-strain state of a plate in the neighborhood of an edge, *PMM*, 31(1), 178-186, 1967.
[11] Hartranft, R. J., and Sih, G. C., The use of Eigen function expansions I the general solution of three-dimensional crack problem, *J. of Mathematical Mechanics*, 19, 123-138, 1969.
[12] Bazent, Z. P. and Estenssoro, L. F., Surface singularity and crack propagation, *Int. J. of Solids and Structure*, 15, 405-426, 1979.
[13] Yamada, Y. and Okumura, H., Analysis of local stress in composite materials by 3-D finite element, *Proceeding of the Japan-U.S. Conference*, Tokyo, Japan, 55-64, 1981.
[14] Pageau, S. S., Joseph, P. F. and Biggers, Jr. S. B., Finite element analysis of anisotropic materials with singular inplane stress fields, *Int. J. of Solids and Structure*, 32, 571-591, 1995.
[15] Pageau, S. S. and Biggers, Jr. S. B., Finite element evaluation of free-edge singular stress fields in anisotropic materials", *Int. J. Numer. Methods in Engineering*, 38, 2225-2239, 1995.
[16] Pageau, S. S. and Biggers, Jr. S. B., A finite element approach to three-dimensional singular stress states in anisotropic multi-material wedges and junctions, *Int. J. of Solids and Structure*, 33, 33-47, 1996.
[17] Liew, K. M. and Liang, J., Modeling of 3D piezoelectric and elastic bimaterials using the boundary element method, *Computational Mechanics*, 29, 151-162, 2002.
[18] XU, J. Q., and Mutoh, Y., Singularity at the interface edge of bonded transversely isotropic piezoelectric dissimilar

material, *JSME International Journal, Series A*, 44(4), 556-566, 2001.

[19] Ou, Z. C., and Xijia, Wu., On the crack-tip stress singularity of interfacial cracks in transversely isotropic piezoelectric bimaterials, *Int. J. of Solids and Structure*, 40, 7499-7511, 2003.

American Journal of Engineering Research (AJER)
e-ISSN : 2320-0847 p-ISSN : 2320-0936
Volume-02, Issue-09, pp-100-102
www.ajer.org

Research Paper Open Access

Efficient Power Allocation Strategy Based Co-Operative Networks

Srinivas MRSP, U Mahender, P.V.S. Srinivas
[1]*PG Scholar, Department of Computer Science and Engineering, TKR College of Engineering and Technology Hyderabad, A.P-500 097, India*
[2]*Assistant Professor, Department of Computer Science and Engineering, TKR College of Engineering and Technology Hyderabad, A.P-500 097, India*
[3]*Professor& Head, Department of Computer Science and Engineering TKR College of Engineering and Technology Hyderabad, A.P-500 097, India*

Abstract: - Here the networks based on the cooperative phenomena used for improving the potential of the system followed by the followed by the capacity of the network oriented with reliability of the effective transmission of the data in a well efficient fashion. There is a huge research going on this particular technology where from the ancient times and increasing the efficiency of the system but till now there is no particular method each and every method is effective with its particular strategy based phenomena but none of them are satisfied each and every properties of the system respectively. Here the cooperative based strategy is well efficient in terms of the network related to the three node oriented phenomena in a well efficient manner and also the and also applied in the network oriented strategies related to the AD HOC and also the scheme oriented with the relay fashion respectively which are mainly dependent on the antennas of the single parameters in a well respective fashion. Here there is some of the limiting condition which is mentioned in above statement that is due to the lack of knowledge on the present communication oriented system followed by its particular analysis in a very respective fashion. Here in this paper a method is designed with a well effective strategy and also with an oriented framework where strategy of the power allocation based phenomena with respect to the structural aspect in a well respective fashion in terms of the accurate power constraints of the node followed by the respective MIMO based strategy in a well efficient manner respectively. Experiments are conducted on the present method and its analysis based on the performance oriented strategy in a well efficient manner is displayed in the present phenomena respectively.

Keywords: - *Multiple input multiple output, Single input multiple output, Multiple input single output, Single input single output, Network cooperation, Allocating power, Optimization, Power strategy Forward and boost respectively.*

I. INTRODUCTION

With the rapid advancement in the technology there is a huge increase in the usage of the systems with respect to the wireless based aspects in a well oriented fashion respectively [1]. There are many of the technologies related to the major wireless aspect. Here the network based on the cooperative phenomena which has got a huge investigation in the recent early years in the around 1970's in a well respective fashion where there is a concept orientation takes place on the channels on behalf of the relay nodes respectively [2][3]. Recently there is a huge interest in the networks based on the cooperative oriented strategy based on the wireless oriented scenario in a well efficient manner for the accurate transmission of the data in a well effective fashion respectively. There are some of the problems related to the above based strategy and some of them includes scheduling of the optimal throughput, Maximization of the lifetime network, Routing distributed phenomena in a well effective manner, Design oriented strategy of the protocol based on the MAC based strategy in a well efficient fashion has to be studied and overcome the performance degradation strategy in a well efficient manner [6][7]. Therefore there is extensively lot of research going on the present strategy in a well effective manner

related to the improving of the performance base strategy of the networks based on the cooperative scenario followed by the performance optimization in a well respective fashion.

II. METHODOLOGY

In this paper a method is designed with a well effective strategy where the design architecture is based on the effective framework mainly used for the purpose of the effective allocation of the power is a major strategy respectively [4][5]. Here the present designed architecture is described in the below shown figure oriented with the effective diagrammatical approach in a well defined strategy. Here the present method is effective and efficient in terms of the analysis followed by the accurate outcome towards the entire system respectively. There is a huge challenge for the present method where it is suppose to accurately study the concept related to this particular phenomena in a well respective fashion and in order to improve the degraded performance of the entire system and also the improvement in the entire system outcome in a well oriented fashion respectively [8].

BLOCK DIAGRAM

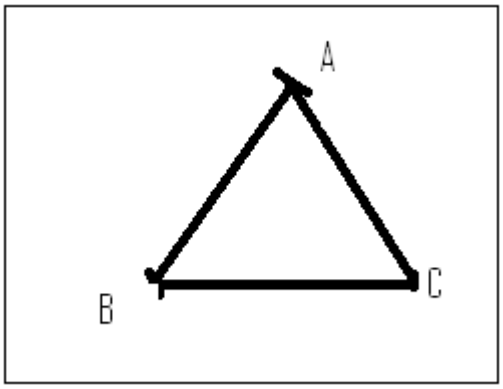

Figure: 1 shows the representation of relay based three node oriented system respectively

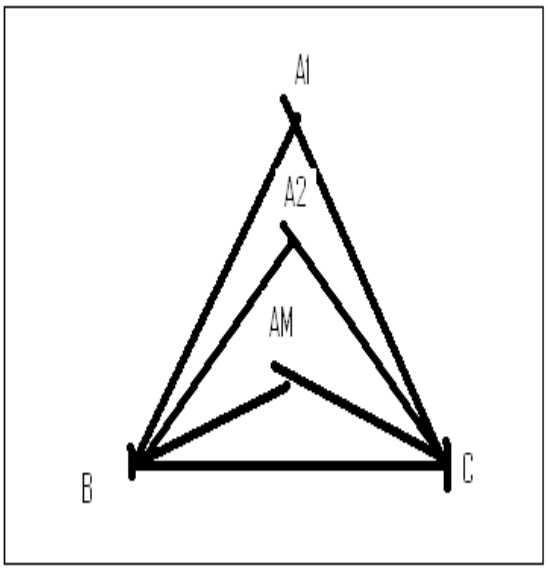

Figure shows the cooperation based network respectively

III. EXPECTED RESULTS

In this paper a lot of analysis has been done on the present system where number of experiments has been conducted on large number of the data sets in a well effective fashion respectively. Here the present method is designed with an effective strategy where it completely overcomes the drawbacks of the several previous existing techniques in a well efficient manner respectively. There is a huge challenge for the present designed strategy in which it is supposed to combat each and every minute problem related to the several

previous existing techniques and control the degraded performance of the previous techniques and efficiently improved in such a way that there should be an accurate outcome towards the entire system response. A comparative analysis is made between the present method to that of the several previous existing techniques and it is displayed in the below graphical representation in a well efficient manner respectively.

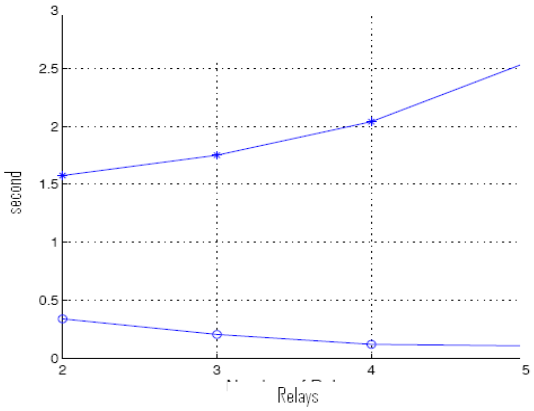

Figure shows the graphical representation of power allocation strategy respectively

IV. CONCLUSION

In this paper a method is designed with an efficient strategy oriented framework where the main criteria is to work on the strategy based on the power allocation based phenomena in a well efficient manner respectively. Here the design strategy include the research oriented phenomena on the MIMO based allocation of the power in a well respect fashion where the effective analysis is made on multiple outcome oriented with the CN based phenomena in a well efficient fashion to solve the problem related to the allocation of the power in a well oriented fashion respectively. There are some of the design specific oriented parameters result generalization here the setting is based on the strategy of the three node based phenomena in a well efficient fashion over the relays based on the multiple strategy based on the constraints oriented with effective power strategy respectively. Here the accurate analysis of the allocation of the power is a major concern and remains as the unknown oriented phenomena. There is a huge amplification of the system in terms of the performance oriented phenomena n a well efficient manner where a lot of gain concerned due to the relay oriented cooperation.

REFERENCES

[1] E. M. Yeh and R. A. Berry, "Throughput optimal control of cooperative relay networks," IEEE Trans. Inf. Theory, vol. 53, no. 10, pp. 3827– 3833, Oct. 2007.
[2] P. Liu, Z. Tao, S. Narayanan, T. Korakis, and S. S. Panwar, "CoopMAC: A cooperative MAC for wireless LANs," IEEE J. Sel. Areas Commun. vol. 25, no. 2, pp. 340–354, Feb. 2007.
[3] A. Behbahani, R. Merched, and A. M. Eltawil, "Optimizations of a MIMO relay network," IEEE Trans. Signal Process., vol. 56, no. 10, pp. 5062–5073, Oct. 2008.
[4] B. Khoshnevis, W. Yu, and R. Adve, "Grassmannian beamforming for MIMO amplify-and-forward relaying," IEEE J. Sel. Areas Commun. vol. 26, no. 8, pp. 1397–1407, Oct. 2008.
[5] W. Guan, H. Luo, and W. Chen, "Linear relaying scheme for MIMO relay system with QoS requirements," IEEE Signal Process. Lett. vol. 15, pp. 697–700, 2008.
[6] Z. Fang, Y. Hua, and J. D. Koshy, "Joint source and relay optimization for non-regenerative MIMO relay," in Proc. IEEE Workshop Sensor Array Multi-Channel Signal Processing, Waltham, WA, Jul. 12-14, 2006, pp. 239–243.
[7] Y. Fu, L. Yang, W.-P. Zhu, and Z. Yang, "A convex optimization design of relay precoder for two-hop MIMO relay networks," in Proc. IEEE ICC, Cape Town, South Africa, May 23-27, 2010.
[8] Y. Rong, "Non-regenerative multicarrier MIMO relay communications based on minimization of mean-squared error," in Proc. IEEE ICC, Dresden, Germany, Jun. 14-18, 2009, pp. 1–5.

American Journal of Engineering Research (AJER)
e-ISSN : 2320-0847 p-ISSN : 2320-0936
Volume-02, Issue-09, pp-103-109
www.ajer.org

Research Paper Open Access

Effect of NGBFS and CBA as fine aggregate on the chloride permeability of concrete

İsa Yüksel[1], Ozan Demirtaş[2]
[1]*Department of Civil Engineering ,Bursa Technical University, Bursa, Turkey*
[2]*4D Architecture & engineering Services Ltd., Zonguldak, Turkey*

Abstract: - This paper presents the results of an investigation which was about influence of non-ground Coal Bottom Ash (CBA) and Non-Ground Granulated Blast-Furnace Slag (NGBFS) as fine aggregate on rapid chloride permeability of concrete. Series of Rapid Chloride Permeability Test (RCPT) were conducted with concrete specimens containing NGBFS and CBA in varying percentages from 10 to 50% with the step of 10% of fine aggregate by weight. Two basic series concrete specimens were prepared in laboratory. The first series (G) was contained NGBFS, the second series (B) was contained CBA as fine aggregate. Test results indicated that NGBFS or CBA improves the resistance to chloride ion penetration to some extent. 30% and 10% replacement ratios were selected as optimum replacement ratios for G and B series. It was concluded that GBFS was more impressive then CBA for blocking chloride ion movements.

Keywords:- *Aggregate, Chloride permeability, Coal bottom ash, Concrete, Granulated blast-furnace slag.*

I. INTRODUCTION

Chloride attack is accepted one of the principal cause for concrete degradation. Chloride ions were generally known as the most harmful agent for reinforced concrete. Mostly, low level of chloride ions can be tolerated in durable concrete. However, excessive chloride levels cannot be tolerated and it may occur over the service life by reason of external chloride sources. Mineral admixtures such as ground blast furnace slag or ground fly ash were currently used to improve durability of cement and concrete. At the same time, researches are in progress on the use of non-ground industrial by-products or industrial wastes such as non-ground granulated blast furnace slag (NGBFS) and coal bottom ash (CBA) in concrete as fine aggregate. Rapid Chloride Permeability Test (RCPT) approach was a relatively simple and quick test for measuring the permeability of concrete indirectly. This test shows quickly the general behavior of concrete permeability that is an important parameter for concrete durability. Production of durable concrete is a critical issue in order to gain economic, ecologic and technical advantages for the future of the concrete industry.

The objective of presented study was to make a comparative investigation of the influence of NGBFS and CBA on rapid chloride permeability of concrete. A series of RCPT is conducted on concrete specimens incorporated NGBFS and CBA in varying percentages by weight as fine aggregate.

II. PREVIOUS WORK

Usually it is not possible to prevent chloride entrance in concrete. Chloride penetration into concrete is a critical issue in the process of corrosion of reinforcing steel bars. The problem is particularly acute in a marine environment, in bridges and roadways subjected to deicing salts, and in parking garages into which salt is transported from salted roadways [1]. The chloride ingress depend on the sorptivity and chloride diffusivity of concrete, ability of concrete to bind chlorides, water/cement ratio, chloride diffusivity of aggregates, alkalinity of the binder, degree of exposure to chloride source, temperature, carbonation, hydrostatic head. Chloride ions can destroy the passive oxide film on reinforcement steel in concrete, even at high alkalinities [2]. The amount of chloride required to initiate rebar corrosion depends on the pH of the solution in contact with the reinforcement steel.

Chloride binding capacity of the concrete should be high to Show high resistance to environmental harmful agents. There are many researches [3-7], about chloride binding capacity of concrete and effects of ground supplementary materials on it. Aggregates can also affect the transport properties of concrete [8]. However, very limited data exist on the role of aggregate in chloride ion ingress. Page et al [9] concluded that chlorides can be transported through the aggregate as well as through the surrounding cement paste in the concrete. Emiko et al [10] found that volume of the lightweight aggregate have reasonable effects on penetrability properties of lightweight aggregate concrete. The concrete diffusivity was influenced by many parameters such as the interfacial zone property between aggregate particles and bulk cement paste as well as the microstructure of the cement paste itself (porosity and pore structure)[11]. Rock type of coarse and fine aggregate was one of the most important factors which determine the diffusivity of concrete. The geometry of the pathways for the penetration of aggressive species was necessarily more complicated in concrete[12]. Two complementary approaches have been introduced for evaluating the influence of interfacial transition zone (ITZ) on transport properties of concrete. Results obtained by Garboczi et al. [13] and Bourdette et al. [14] have clearly emphasized the fact that the concrete transport properties were influenced by the connectivity of ITZ and the excess in tortuosity introduced by increasing the aggregate content in the mixture. Bourdette et al. [14] indicated that the effective diffusion coefficient of chloride ions was 6 to 12 times greater in the ITZ than in the bulk cement paste. Poon et al.[15] showed that fly ash having very similar properties with bottom ash has dual effect in concrete. The first one of these effects was being a micro-aggregate and the second was being a pozzolana. They demonstrated that fly ash had improved the interfacial bond between the paste and the aggregates in the concrete. Such concrete has lower chloride diffusivity than the equivalent plain cement concrete or concrete prepared with lower fly ash contents. According to Polden and Peelen [16] concretes made with blast furnace slag cements and fly ash cements show lower chloride penetration so these concrete types have higher electrical resistance. Oh et al. [17] defines high performance concrete as the concrete having high resistance to chloride penetration as well as high strength. They have approved the positive effects of silica fume, fly ash (FA) or slag cement concretes on the property of chloride resistance. It was reported that water-binder ratio, maximum size aggregates, aggregate particle distribution and aggregate-paste volume ratio also affect the chloride ingress. Hooton and Titherington [18], Aldea et al. [19] were also found out that usage of supplementary cementing materials like slag to produce high performance concrete for both accelerated and ambient curing conditions provide high chloride resistance to chloride penetration. There are few researches about the usage of GBFS or CBA in concrete. Yüksel et. al. [20] used non-ground GBFS as fine aggregate replacement alone and they observed that GBFS improves the chloride resistance of concrete. Ghafoori and Bucholc [21], Basheer and Bai [22] were also used bottom ash as fine aggregate replacement. They reported that bottom ash increases the chloride permeability due to its high water absorption rate but decreases the chloride transport coefficient because of high binding capacity of chlorides. They also showed that it was possible to produce concrete types with bottom ash which have low permeability and high chloride resistance if a low dosage of super plasticizer or chemical admixtures reducing water requirement.

The chloride diffusion coefficient is an important parameter in order to predict the service life of concrete structures. However, the transport of chloride ions through concrete is a complex subject and there are many groups of methods to calculate the diffusion coefficient. Natural diffusion methods, migration methods, and resistivity methods could be shown as examples of these groups of methods. Migration methods which are used in this study imply the application of an electrical field through the concrete. The RCPT method is in group of migration methods. It is a standardized accelerated method. Castellote and Andrade [23] arranged methods to calculate the diffusion coefficient according to three different importance factors. Their ranking is as follows: R1/M > M6 > R1 > D3 > M4 > M1 >D2 > M3 = M5, where M1 is describes the test procedure described in ASTM C1202-97.

III. EXPERIMENTAL STUDY

III. I. Materials

A commercially available CEM I 42.5 N type cement conforming requirements of EN 197-1 was used. Two fractions (0-4 mm and 4-7 mm) of river aggregate was used as fine and coarse aggregate. NGBFS was provided from Ereğli Iron & Steel Works Company in Kdz. Ereğli, Turkey. Particle size distribution for both of NGBFS and CBA were shown on Table 1. Physical properties of the aggregate, NGBFS, and CBA were shown in Table 2. Chemical composition of NGBFS was shown in Table 3 that results were provided from R&D laboratories of the Ereğli Iron & Steel Works Company. Fly ash (FA) was used as mineral admixture which was classified as V-type according to Turkish Standard EN 197-1 and it was also classified as F-type according to ASTM C 618. Chemical composition of CBA was shown in Table 3. Other important properties of CBA used in

this study were tested in R&D laboratories of Turkish Cement Manufacturers' Association. They were shown in Table 4. It should be noted that activity index was high and free CaO content was zero. A hyper-plasticizer which is 0.7 % of cement by weight was used to give a proper workability for the concrete mixtures

Table 1. Particle size distribution of NGBFS and CBA

Sieve size (mm)	Passing (%)	
	NGBFS	CBA
8.00	-	-
6.70	-	-
4.75	-	-
4.00	99.38	94.03
3.35	98.20	91.90
2.36	92.16	86.23
1.70	77.10	76.97
1.18	62.26	61.70
0.60	17.72	36.63
0.30	4.94	-
0.212	2.84	-
0.10	0.80	6.57
0.075	0.44	3.80
0.045	0.12	1.07

Table 2. Physical properties of aggregate, NGBFS, CBA and FA

Property	Aggregate (0-7 mm)	NGBFS	CBA	FA
Loose unit weight (kg/m3)	1930	1052	620	870
Compact unit weight (kg/m3)	1950	1236	660	1110
Specific gravity	2.68	2.08	1.39	1.87
Clay lumps and friable particles (%)	5.00	-	2.40	-
Very fine particles (%)	4.00	3.00	7.00	-
Organic impurities (with NaOH sol.)	Light yellow	Light yellow	-	-

Table 3. Chemical composition of NGBFS and CBA (%)

	SiO_2	CaO	MgO	Al_2O_3	SO_3	MnO	P_2O_3	Fe_2O_3	K_2O
NGBFS	35.09	37.79	5.50	17.54	0.66	0.83	0.37	-	-
CBA	57.90	2.00	3.20	22.60	-	-	-	6.50	0.604

Table 4. Properties of CBA (%)

Property	Value	Property	Value
Loss on ignition	1.67	45μ sieve residue (by weight. %)	25.8
SO_3^-	0.08	7 day strength activity index	76.9
Cl^-	0.0064	28 day strength activity index	85.7
Free CaO	0.00	90 day strength activity index	100

III. II. Method

Two series (G, B) of concrete specimens were produced in the laboratory. Mix proportions of these series were presented in Table 5. NGBFS was replaced 0-4 mm fine aggregate in G series, and CBA was replaced 0-4 mm fine aggregate in B series. The replacement ratio was changed from zero to 50% with the steps of 10%. Also, a reference specimen (R) group was produced for comparison of results. Each subgroup was

constituted with three specimens and the arithmetic average of individual results was considered. The shape of specimens was cylindrical having 200 mm length and 100 mm dimension. All specimens were de-molded after 24 hour and kept in water for the next 27 days. Then they were cut into three slices having 50 mm length. These slices were stored in laboratory where the temperature was 18±3 oC and relative humidity was changed in between 50 to 60 %. RCPT was conducted at the 90th day by following the test procedure described in ASTM C1202-97. RCPT method covers the determination of the electrical conductance of concrete. It consists of monitoring the amount of electrical current passed through cylinders during a 6-h period. A potential difference of 60 V DC was maintained across the ends of the cylinder, one of which is immersed in a sodium chloride solution, the other in a sodium hydroxide solution. The total charge passed has been found to be related to the resistance of the specimen to chloride ion penetration. At the end of experiment, electrical current (in amperes) versus time (in seconds) graphs were drawn. The area underneath the curve was integrated in order to obtain total charge passed during the test period. The total charge passed was taken as a measure of the electrical conductance of the concrete.

Table 5. Mix proportions of series (kg/m^3)

Code	Replacement ratio (%)	Cem.	Water	FA	Chem. Admix.	C.A. (4-7)	F.A. (0-4)	NGBFS	CBA
R	0	350	167	35	2.45	1120	720	0	0
G10	10	350	167	35	2.45	1120	648	72	0
G20	20	350	167	35	2.45	1120	576	144	0
G30	30	350	167	35	2.45	1120	504	216	0
G40	40	350	167	35	2.45	1120	432	288	0
G50	50	350	167	35	2.45	1120	360	360	0
B10	10	350	167	35	2.45	1120	648	0	72
B20	20	350	167	35	2.45	1120	576	0	144
B30	30	350	167	35	2.45	1120	504	0	216
B40	40	350	167	35	2.45	1120	432	0	288
B50	50	350	167	35	2.45	1120	360	0	360

FA: Fly ash; C.A.: Coarse aggregate; F.A.: Fine aggregate

IV. RESULTS AND DISCUSSION

Test results with error bars for G series were shown in Fig. 1. Charge passed from specimens was continuously decreased in between 0 to 30 % replacement ratios. The maximum decrease was observed as 27.7 % at the 30% replacement ratio. This shows that GBFS replacement decreases rapid chloride permeability. However, charge passed from specimens was increased in between 30 to 50 % replacement ratios. The total charge passed from the specimen was increased to the same level of reference specimen (no replacement) at 50 % replacement ratio. As a result, even 50 % replacement doesn't change rapid chloride permeability of concrete with respect to reference concrete. 30 % replacement ratio can be selected the optimum replacement ratio for G series concrete.

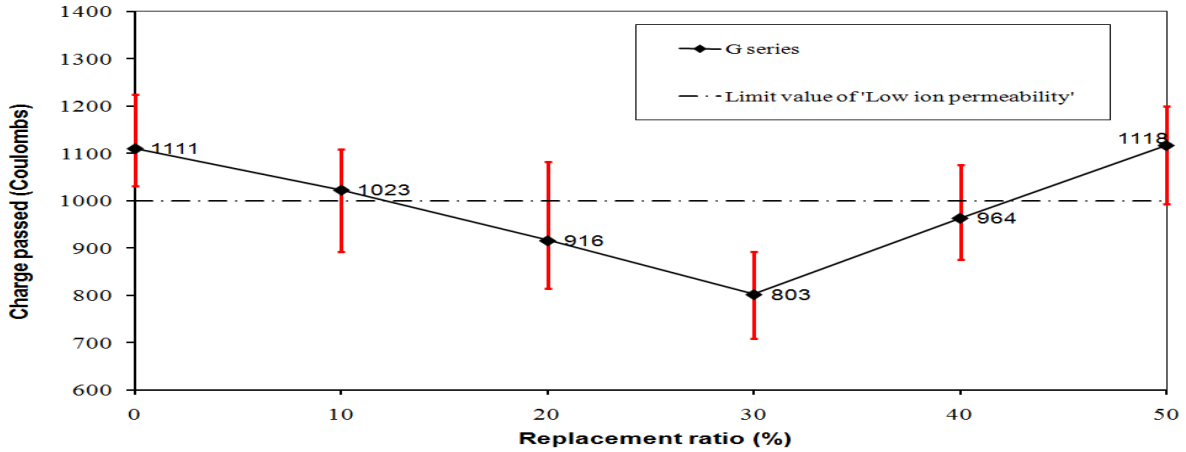

Figure 1: RCPT test results of G series

B series has a different behavior as compared to G series (Fig. 2). A slight (13.1 %) decrease in total charge passed through specimens was observed at the 10 % replacement ratio. Then a gradual increase was observed in between 10 to 40 % replacement ratios. Lastly, a sharp (28.9 %) increase was observed after the 40 % replacement ratio. This trend shows that 10 % was the best ratio for B series concrete. However, as compared to the chloride permeability of reference concrete (0 % replacement), 40 % was also an acceptable replacement ratio since the charge passed on this level (1064 Coulomb) was less than that of reference concrete.

The reason of decreases observed in chloride permeability can be explained with the chloride binding capacity of the replaced materials and the structure of the concrete. Both of these materials have high chloride binding capacity when they were used in concrete. Since reactivity of blast furnace slag is depends on particle diameter and we used it as in non-ground form we do not expect extra hydration products. The differences in terms of surface characteristics, particle shape, particle strength, porosity and permeability of NGBFS and CBA from natural fine aggregate are getting important at this stage. Normal concrete shows a dense structure composed of irregular grains and the hydrated products attach to the aggregate surface strongly. For the low replacement ratios such as 10 or 20%, the concrete has compact and dense structure similar to the normal concrete. However, in the case of increased replacement ratios the microstructure of concrete changes its network structure. Yüksel and Genç [24] investigated compressive, flexural and split tensile strength, water absorption, and microstructure of concrete containing NGBFS or CBA as fine aggregate in different replacement ratios. They concluded that NGBFS and/or CBA decreases tensile and compressive strength of concrete and the rate of decrease depend on the type of replacement material. The transition zone between aggregate and cement paste was getting relatively weak than as in the control concrete. CBA decreases the strength more than NGBFS since CBA contains lumped particles which are not present in NGBFS. Also the SEM analyses and water absorption tests showed that the replaced concrete was more porous than the reference normal concrete. When aggregate is replaced by either NGBFS or CBA, water absorption ratios of concretes are increases.

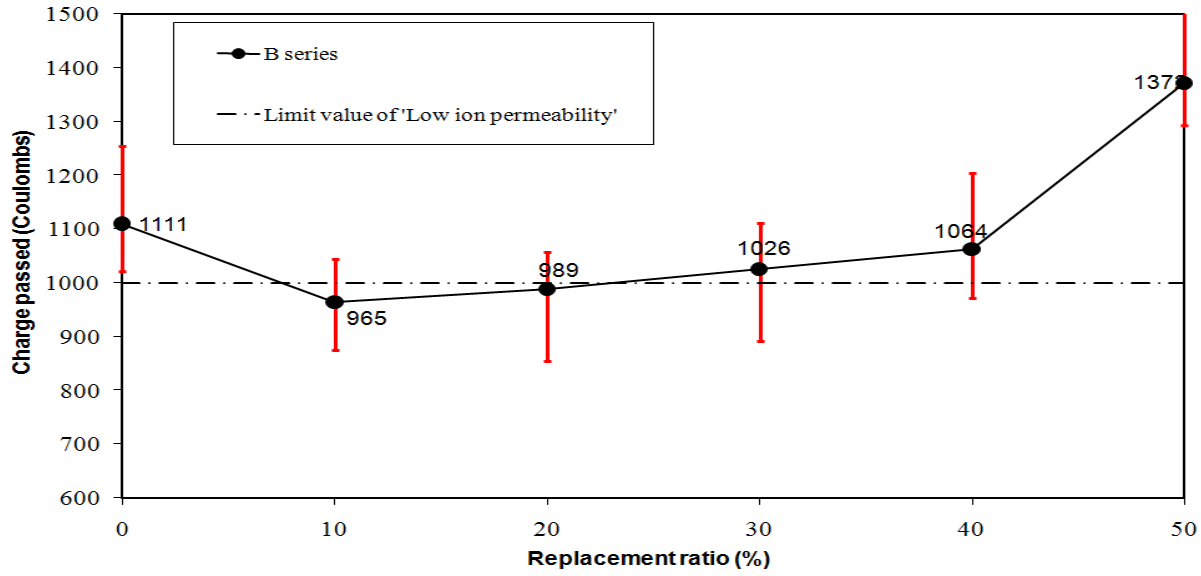

Figure 2: RCPT test results of B series

Non-reacted particles of NGBFS or CBA were efficient to fill up the large capillary pores at low levels of replacement. The new pore system enhanced impermeability of concrete. Generally, the permeability of concrete is influenced by the volume, size, and continuity of the pores. However, for the high level of replacement ratios, since the structure of concrete was changed from compact to porous, the strength is decreased and permeability is increased. Delagrave et al [12] indicated that aggregates modify the microstructure and the transport properties of mortars. This modification can be attributed to the presence of numerous interfacial transition zones. Aggregates in cement pastes act as solid inclusions increasing the tortuosity of the matrix while the presence of numerous interfacial transition zones tends to facilitate the movement of chloride ions.

The concrete produced with NGBFS and CBA as fine aggregate has high permeability than the normal concrete at a high replacement ratio. The increase found in chloride permeability at high replacement ratio such as 50 % can be explained with the diffusivity. The rate of chloride ion ingress into concrete was influenced by both the diffusivity of the cement paste fraction and by the diffusivity of the aggregate. Hobbs [25] states that highly permeable aggregate could increase the chloride ion diffusivity of concrete by a factor of ten.

Measured slump values of fresh concrete are changing 6 cm to 12 cm in G series, and as replacement ratio increases the slump value is increases too. Contrary, measured slump values were decreased in B series due to high absorption capacity of CBA. Andrade et al [26] stated that w/c ratio of the concrete cannot be taken as exact because of the high porosity of the bottom ash. The water absorbed internally by the bottom ash is released to the concrete over time, being part of the production process with the concrete still in the fresh state. Therefore, mixing process was not so easy as compared to reference specimen and large capillary pores were existed for high replacement ratio such as 40 or 50 % replacement. This case affected chloride permeability of concrete. Sharp increase observed in chloride permeability at 50 % replacement in B series can be explained with this event. High slump values measured in G series for replacement ratio higher than 30 % can also results in more capillary pores and high permeability.

Chloride ion penetrability based on charge passed was classified according to the qualitative terms in the ASTM C 1202 – 97. Chloride ion penetration obtained in this study was shown in Table 6. It was found that NGBFS or CBA improves the resistance against chloride ingress. While chloride ion penetrability of normal concrete (R) was “low”, the same parameter of G20, G30, G40, B10, B20 subgroups were “very low”. NGBFS or CBA contributes to concrete chloride ion penetration.

Table 6. Classification of chloride ion permeability of all series with respect to ASTM C1202-97

Code	Charge passed (Coulombs)	Chloride ion penetrability
R	1111	Low
G10	1023	Low
G20	916	Very Low
G30	803	Very Low
G40	964	Very Low
G50	1118	Low
B10	965	Very Low
B20	989	Very Low
B30	1026	Low
B40	1064	Low
B50	1372	Low

V. CONCLUSION

Based upon evaluation of the results following conclusions can be drawn.

(1) Chloride permeability was decreased at low replacement ratios then increased again at high replacement ratios. The decreases observed at low replacement levels depend on chloride binding capacity of GBFS and CBA.

(2) The increased chloride permeability at high replacement levels could be explained with the transport properties of concrete. Since the concrete was more porous and permeable on high replacement ratios movement of chloride ions facilitated. Then chloride binding capacities of GBFS or CBA were not adequate to obstruct chloride ion movements.

(3) NGBFS was more effective then CBA to block chloride ions movement. 30 % and 10 % replacement ratios could be selected as optimum replacement ratios for NGBFS and CBA respectively.

(4) Use of industrial by-products as fine aggregate in concrete exposing chloride ions will help to produce durable and environmental friendly concretes.

VI. ACKNOWLEDGEMENTS

This study is a part of the research project (ICTAG I687) which is financially supported by the Scientific and Technological Research Council (TUBITAK) of Turkey. Authors are gratefully acknowledged for their support.

REFERENCES

[1] Y. Xi, Z P Bazant, Modeling chloride penetration in saturated concrete, *J. Mater. Civ. Eng.*, 11*(1)*, 1999, 58-65.

[2] S. Mindess, J.F. Young, D. Darwin, Concrete (Pearson Education, 2003).

[3] R.K. Dhir, M.A.K. El-Mohr, T.D. Dyer, Chloride binding in GGBS Concrete, *Cement and Concrete Research*, 26(12), 1996, 1767–1773.

[4] C. Arya, Factors influencing chloride-binding in concrete, *Cement and Concrete Research*, 20(2), 1990, 291–300.

[5] G.K. Glass, N.R. Buenfeld, The influence of chloride binding on the chloride induced corrosion risk in reinforced Concrete, *Corrosion Science*, 42(2), 2000, 329–344.

[6] T. Ishida, P.O. Iqbal, H. T. L. Anh, Modeling of chloride diffusivity coupled with non-linear binding capacity in sound and cracked concrete, *Cement and Concrete Research*, 39(10), 2009, 913–923.

[7] R. Luo, Y. Cai, C. Wang, X. Huang, Study of chloride binding and diffusion in GGBS Concrete, *Cement and Concrete Research*, 33*(1)*, 2003, 1–7.

[8] B.B. Sabir, S. Wild, M.A. O'Farrell. Water sorptivity test for mortar and concrete, *Materials and Structures*, 31*(212)*, 1998, 568-574.

[9] C.L. Page, P. Lambert, P.R.W. Vassie, Investigations of reinforcement corrosion: The pore electrolyte phase in chloride-contaminated concrete, *Materiaux et Constructions*, 24*(142)*, 1991, 243–252.

[10] L. Emiko, T.H. Wee, T. Tamilselvan, Penetrability of lightweight aggregate concrete, *Magazine of Concrete Research*, 62*(3)*, 2010, 201–209.

[11] B.H. Oh, S.Y. Jang, Prediction of diffusivity of concrete based on simple analytic equations, *Cement & Concrete Research*, 34*(3)*, 2004, 463–480.

[12] A. Delagrave, J.P. Bigas, I.J. Olliver, Influence of the interfacial zone on the chloride diffusivity of mortars, *Advanced Cement Based Materials*, 5*(3-4)*, 1997, 86-92.

[13] E.J. Garboczi, L.M. Schwartz, D.P. Bentz, Modeling the influence of the interfacial zone on the DC electrical conductivity of mortar, *Advanced Cement-Based Materials*, 2*(5)*, 1995, 169-181.

[14] B. Bourdette, E. Ringot, J.P.Ollivier, Modeling of the transition zone porosity, *Cement & Concrete Research*, 25*(4)*, 1995, 741-751.

[15] C.S. Poon, L. LAM, Y.L. Wong, A study on high strength concrete prepared with large volumes of low calcium fly ash, *Cement & Concrete Research*, 30*(3)*, 2000, 447-455.

[16] R.B. Polden, W.H.A. Peelen, Characterization of chloride transport and reinforcement corrosion under cycling wetting and drying by electrical resistivity, *Cement & Concrete Composites*, 24(5), 2002, 427-435.

[17] B.H. Oh, S.W. Cha, B.S. Jang, S.Y. Jang, Development of high performance concrete having high resistance to chloride penetration, *Nuclear Engineering and Design*, 212*(1)*, 2002, 221-231.

[18] R.D. Hooton, M.P. Titherington, Chloride resistance of high performance concrete subjected to accelerated curing, *Cement &Concrete Research*, 34*(9)*, 2004, 1561-1567.

[19] C.M. Aldea, F. Young, K. Wang, S.P. Shah, Effects of curing conditions on properties of concrete using slag replacement. *Cement &Concrete Research*, 30*(3)*, 2000, 465-472.

[20] İ. Yüksel, Ö. Özkan, T. Bilir, Use of granulated blast-furnace slag as fine aggregate in concrete, *ACI Materials Journal*, 103*(3)*, 2006, 203-208.

[21] N. Ghafoori, J. Bucholc, Investigation of lignite-based bottom ash for structural concrete, *Journal of Materials in Civil Engineering*, 8*(3)*, 1996, 128-137.

[22] P.A.M. Basheer, Y. Bai, Influence of furnace bottom ash on properties of concrete, *Proceedings of the Institution of Civil Engineers Structures & Buildings*, 156*(1)*, 2003, 85-92.

[23] M. Castellote, C. Andrade, Round-Robin Test on methods for determining chloride transport parameters in concrete, *Materials and Structures*, 39*(10)*, 2006, 955–990.

[24] İ. Yüksel, A. Genç, Properties of concrete containing non-ground ash and slag as fine aggregate, *ACI Materials Journal*, 104*(4)*, 2007, 397-403.

[25] D.W. Hobbs, Aggregate influence on chloride ion diffusion into concrete, *Cement & Concrete Research*, 29*(12)*, 1999, 1995-1998.

[26] L.B. Andrade, J.C. Rocha, M. Cheriaf, Influence of coal bottom ash as fine aggregate on fresh properties of concrete, *Construction and Building Materials*, 23*(2)*, 2009, 609-614.

American Journal of Engineering Research (AJER)
e-ISSN : 2320-0847 p-ISSN : 2320-0936
Volume-02, Issue-09, pp-110-117
www.ajer.org

Research Paper Open Access

"Technical Properties of Pond Ash - Clay Fired Bricks – An Experimental Study"

Prashant G. Sonawane, Dr. Arun Kumar Dwivedi
1 - Project Engineer; Galaxy Ventures, 247, I- Floor, Shagun Chowk, Pimpri, Pune, Maharashtra State, India, 411017;
2 - Professor & Head of the Department, Department of Civil Engineering, SSVPS BSD College of Engineering, Deopur, Dhule, Maharastra State, India, 424 005;

Abstract: In the thermal power plants the coal is burnt to heat the water for making the steam, which in turn is used to run the turbines. The pond ash is a waste product from the boilers. It is mainly obtained from the wet disposal of the fly ash, which when get mixed with bottom ash is disposed off in large pond or dykes as slurry. The pond ash is being generated in an alarming rate. The generation of the pond ash is posing a lot of threat to environment and thus its sustainable management has become the thrust area in engineering research. As the pond ash is relatively coarse and the dissolvable alkalies present in it are washed with water, its pozzolanic reactivity becomes low and hence it is not preferred as part replacement of cement in concrete as in the case of fly ash.
In this research work an attempt is made to find out the possibility of using pond ash in burnt clay bricks. The part of the clay is replaced by pond ash in different composition and the bricks are made in conventional method at a brick manufacturing plant. The bricks are fired in a traditional way as per usual practice in the area and the final products with different composition of pond ash are tested in laboratory; for tolerance in dimension, water absorption, compressive strength, initial rate of absorption and weathering. The results of all the tests on brick samples with different % of pond ash are compared with clay bricks and the effect on different characteristics of bricks due to addition of pond ash are studied.

Keywords: *– Burnt Clay Bricks, Compressive Strength, Fly Ash, Pond Ash, Pond Ash – Clay Fired Bricks, Silica*

I. INTRODUCTION

The pond ash is a waste product from boilers, where the coal is burnt to heat the water for preparing the steam, which is a common process in most of coal based thermal power plants. It is mainly obtained from the wet disposal of fly ash. The fly ash gets mixed with bottom ash and disposed off in large pond or dykes as slurry. It is also termed as ponded fly ash and contains relatively coarse particles. The large areas of land are used to store such a mixture of pond ash resulting in land degradation near the thermal power plants. As the pond ash is being produced at an alarming rate, hence the efforts are required to safely dispose it and if possible find ways of utilizing it. In the pond ash the dissolvable alkalies present are washed with water. The metal oxides, sulphur, siliceous & aluminous materials with less pozzolonic properties than fly ash, are some main constituents of pond ash. These ash produced, if disposed off unscientifically, can cause environmental risks i.e. air pollution, surface water and groundwater pollution and thus its safe disposal is indispensable.
In fact, the pond ash is a mixture of fly ash and bottom ash. The main difference between pond ash and fly ash is in their particle size. The pond ash being coarser and less pozzolonic and hence is not being accepted as pozzolona. Some of the physical properties of pond ash are described in Table -1.

Table – 1 : Physical Properties of Pond Ash

Sr.No.	*Properties*	**Pond Ash**
1.	Lime Reactivity of Pond ash	0.66
2.	Specific Gravity	2.16
3.	Bulk density in Loose State	824 kg/m^3
4.	Bulk density in Compacted State	990 kg/m^3
5.	Atterberg's Limits Liquid Limits percentage	 47.3
6.	Grain size distribution Sand % Silt % Clay %	 72 28 NIL
7.	IS Classification	SP-SM

The chemical compositions of fly ash & pond ash generally lie in same range except in their particles size as shown in Table – 2.

Table - 2 : Chemical Compositions of Fly ash & Pond ash

Constituent	**Fly ash (%)**	**Pond ash (%)**
Silica (SiO_2)	49 – 67	67.40
Alumina (Al_2O_3)	16 – 29	19.44
Iron Oxide (Fe_2O_3)	4 – 10	8.5
Calcium Oxide (CaO)	1 – 4	2.7
Magnesium Oxide (MgO)	0.2 – 2	0.45
Sulphur (SO_3)	0.1 – 2	0.30
Loss of Ignition	0.5 – 3	3.46

II. LITERATURE REVIEW

Pandey and Agarwal (2002) manufactured the pond ash bricks and normal clay bricks. One part by weight of hydrated lime and sand was added to about eight parts by weight of pond ash. The compressive strength in bricks is mainly due to Mullite ($3Al_2O_3.2SiO_2$). The main aim of this work was to synchronize mullite ($3Al_2O_3.2SiO_2$) generation in the bricks. Four categories of bricks of differing proportion were made. The burning of these bricks was carried out at different temperatures viz. 200°, 800° and 1200°C and thereafter tested for apparent porosity, bulk density, weight, compressive strength and water absorption. It is concluded that, based on the superior quality, strength and aesthetic merits, mixed pond-ash clay bricks have a greater potential for wider acceptance of the consumers.

Sarkar et al (2007) did experiments by using the pond ash in combination with local clay for making the bricks. The clay were mixed with the two different ashes in the range 10 to 90 weight %, hydraulically pressed and fired at 1000^{o}C. The fired products were characterized for various quality properties required for bricks. The properties of the optimal compositions were compared with conventional red clay bricks including the developed microstructures and the comparative study generally showed that the ash-clay bricks were of superior quality to the conventional products.

Vaka et al (2007) reported an experimental work on fly ash utilization and development of low density red clay bricks. The bricks with different compositions of fly ash, red clay and organic matter, were made and tested for bulk density, water absorption, porosity, shrinkage and crushing strength. The fly ash and red clay content used in bricks was up to 50 and 70% respectively. The organic matter was varied from 0 to 10 %. The bricks made of 40 % fly ash have shown good physical properties. The crushing strength of the brick increased with increase in fly ash content and the brick strength decreased with increase in clay content. The properties of bricks that are fired at 700^{0}C, 800^{0}C and 900^{0}C were obtained. The higher firing temperatures offered greater shrinkage. The bricks developed in the study possess crushing strength up to 16.40 MPa.

Vidya et al (2013) conducted an experimental investigation on pond ash burnt clay bricks. The raw materials used for making the bricks were pond ash, fly ash, lime, gypsum and sand. The modular brick samples of size 230 mm x 110 mm x 75 mm were casted as per IS 12894-2002 using various mix proportions. The four number of mix combinations were arrived by changing the pond ash and lime proportion. The properties of bricks such as compressive strength, water absorption, weight density, efflorescence test were conducted in laboratory. The compressive strength of the bricks observed varying from 9.2 to 7.6 N/mm^2.

III. EXPERIMENTATION

The experimentation is done to study the effect of pond ash in clay-pond ash burnt bricks. The clay is replaced with pond ash. The pond ash for this purpose is collected from Eklahare Thermal Power Station at Nashik, Maharashtra. The pond ash is mixed with the local clay, which is being used for making the bricks in a local brick Kiln at outskirt of Dhule city. The mixtures of clay and the pond ash with different percentage by weight are prepared. The total number of nine mixtures with different proportions of pond ash is selected for experimentation, varying from 0% to 30%. These mixtures are mixed thoroughly by adding the appropriate amount of water, are used to make the clay-pond ash bricks. The special wooden mould of size 230 x 100 x 75 mm size are used for molding the bricks, with a marking 0 – 9, for differentiating the bricks of different proportions of pond ash. The bricks with different % of pond ash blends marked with specific numbers in their frog to identify them at the time of testing are prepared with the help of local laboures working in the Kiln who are trained for this job. The prepared bricks are then air dried in an open atmosphere for 4 - 5 days. About 1400 bricks in total are made. Thereafter, these bricks are fired in a central portion of the open Kiln of capacity 40000, which is then fired for around 15 days, in a traditional way as practiced around Dhule. All the bricks are taken out from the Kiln as per usual procedure, cooled and thereafter transported to the material testing laboratory. The average size of the brick after burning and cooling was measured as 220 x 95 x 70 mm. The flow chart of the process is given in the Figure - 1.

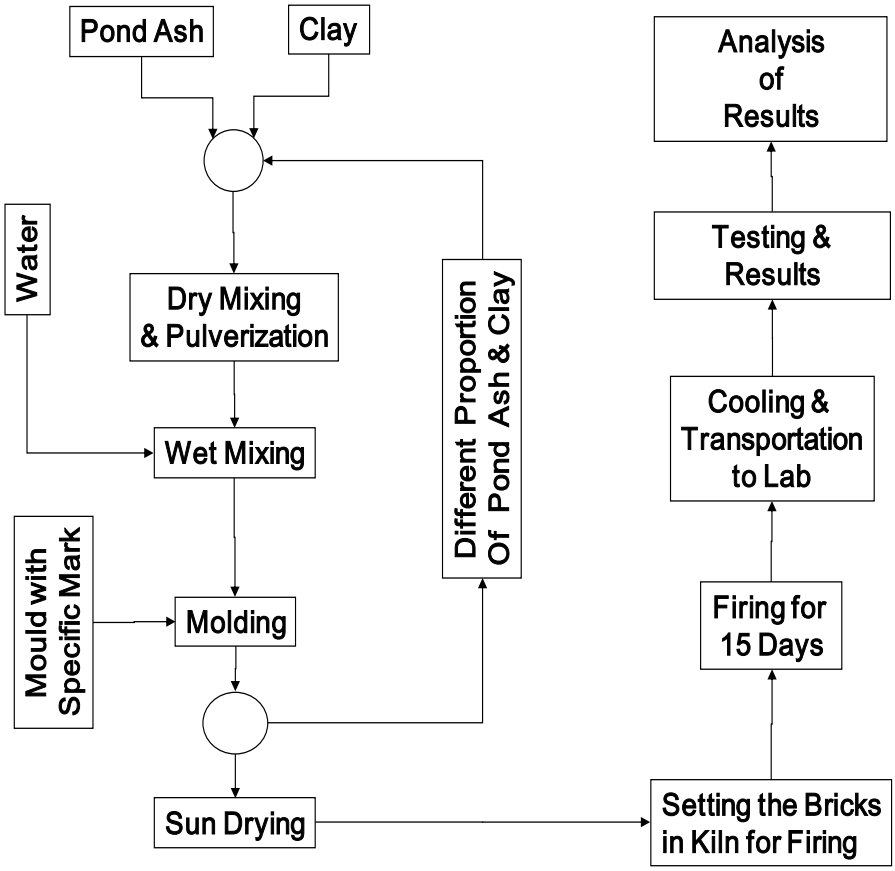

Figure - 1 : Flow Chart Showing Experimental Procedure

IV. RESULTS

Dimension and Tolerance

The bricks are of non-modular type. The dimension and tolerance test is conducted on bricks of all types made with different % of pond ash. As per BIS 1077 : 1992, for non modular size bricks of size 230 x 110 x 70 mm, the permitted tolerance for 20 bricks in row, is 4600 ± 80 mm in length in 2200 ± 40 mm width and in 1400 ± 40 mm in height. The permitted tolerance in terms of % is 1.739 in length, 1.818 in width and 2.857 in height. It is observed that for pond ash more than 20%, the dimensions are beyond the tolerance limit. It can be seen that the bricks are swelling as the % of pond ash is increasing. The % of swelling is more in height as compared to length and width.

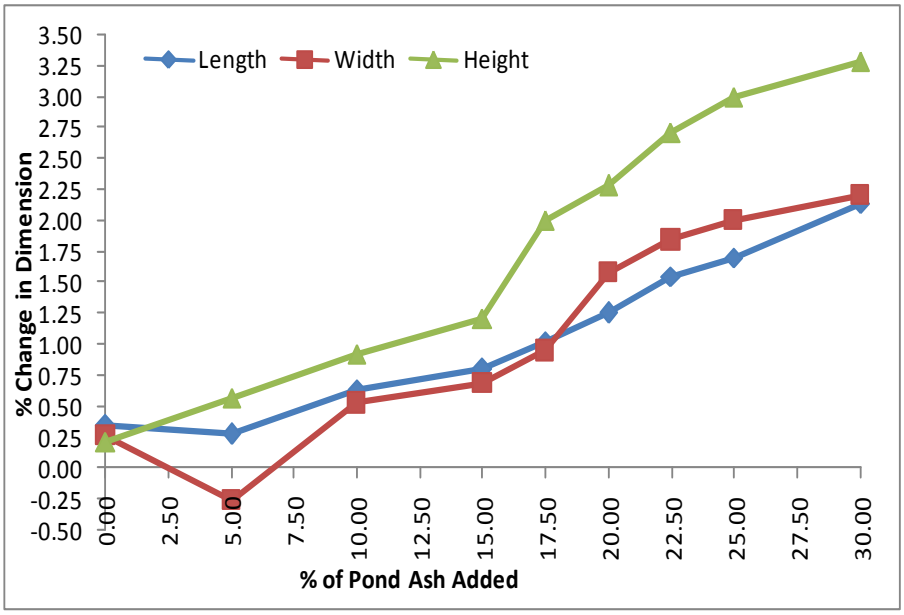

Figure - 2 : Variation in Dimension with % of Pond Ash Added

DRY DENSITY -

The plot of dry densities versus pond ash percentage as shown in Figure – 3, exhibit that the dry density decreases with increase in pond ash percentage.

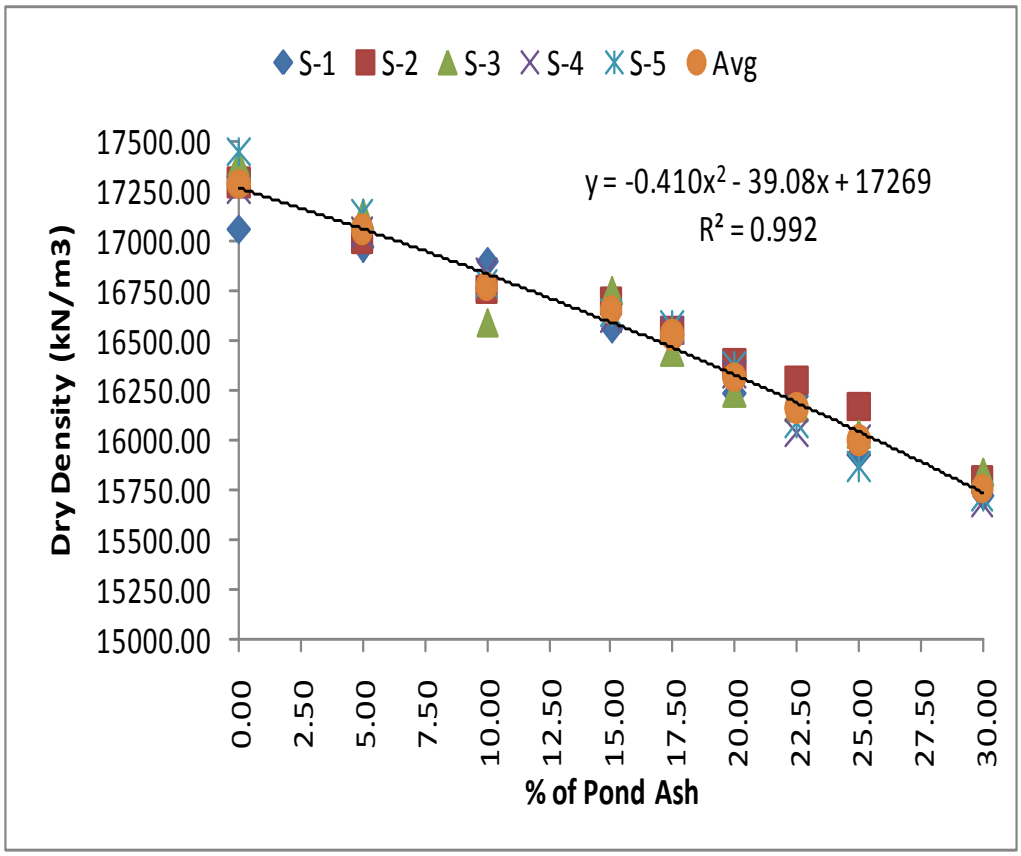

Figure - 3 : Variation in Dry Density with % of Pond Ash Added

WATER ABSORPTION -

A plot of water absorption in % versus the % of pond ash in bricks is shown in Figure - 4, which shows a positive relationship, i.e. the water absorption (%) increases with pond ash % in bricks.

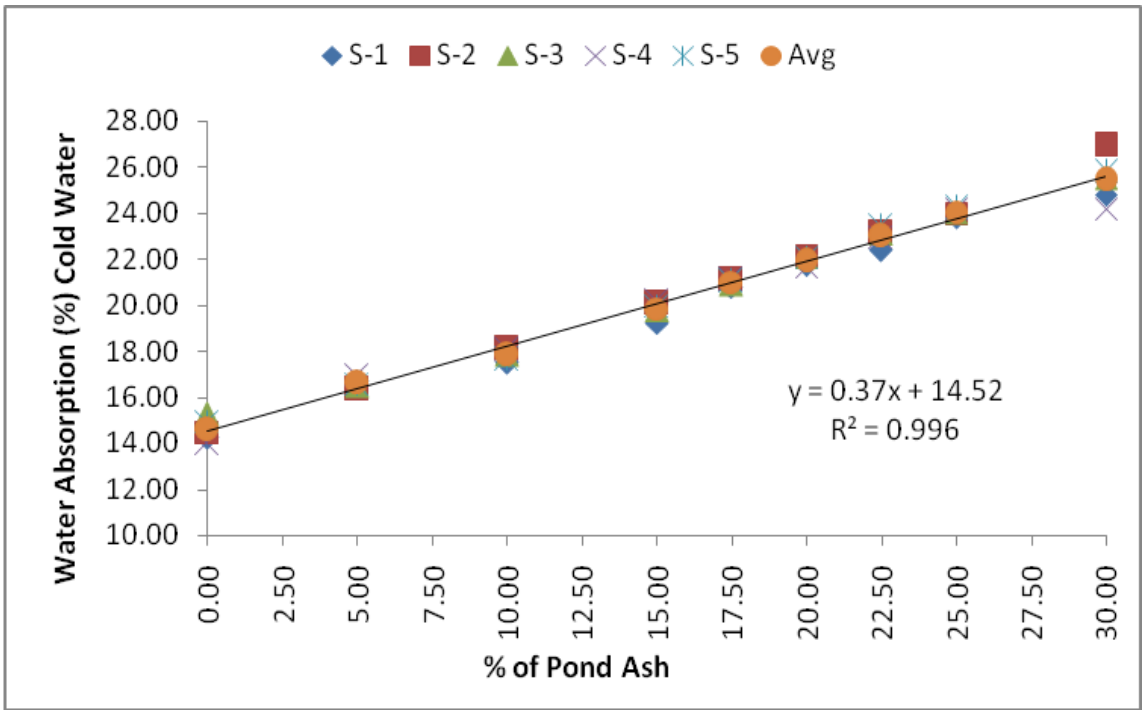

Figure – 4 : Water Absorption (Cold Water) versus Pond Ash % in Bricks

The water absorption % of brick samples after immersing for five hours in boiling water is calculated as per procedure. A plot of water absorption in % versus the % of pond ash in bricks exhibits a positive relationship as in previous case; however, in this case the water absorption % is observed more than that what is observed in cold water.

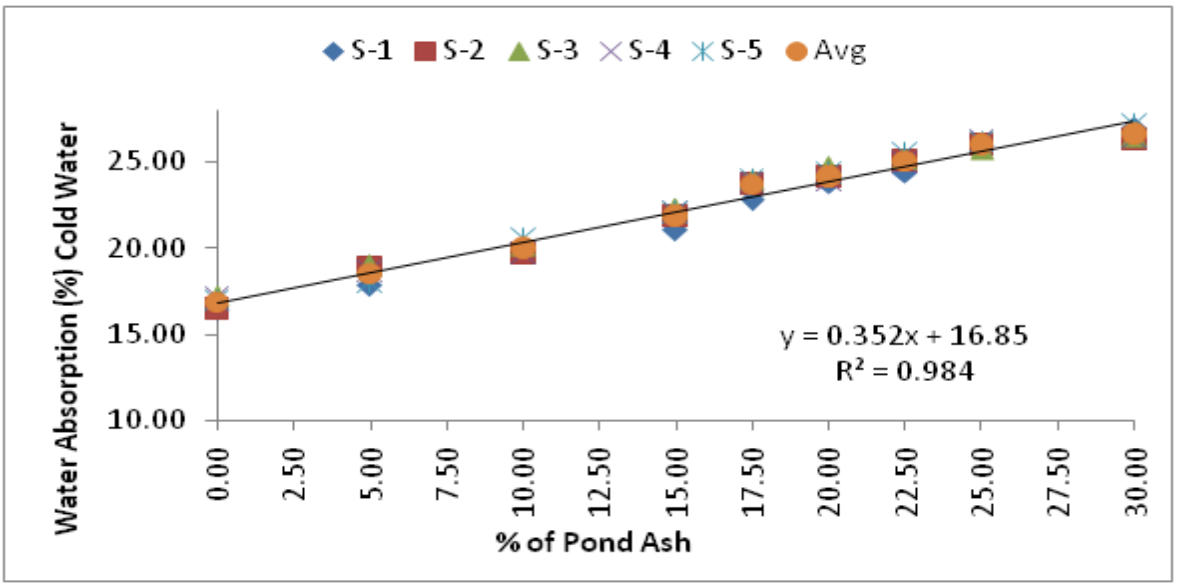

Figure - 5 : Water Absorption (Hot Water) vs Pond Ash % in Bricks

INITIAL RATE OF ABSORPTION (IRA)

The initial rate of absorption test is conducted by immersing 1 cm height of brick in water at room temperature for one minute. The test is conduct on three number of brick samples. The IRA is calculated in gm/cm^2/minute by finding the difference between the wet and dry weight of sample dividing by the plan area of the brick. The IRA value for different % of pond ash in bricks is shown in Figure – 6 which shows that the IRA value increases with increase in % of pond ash in brick.

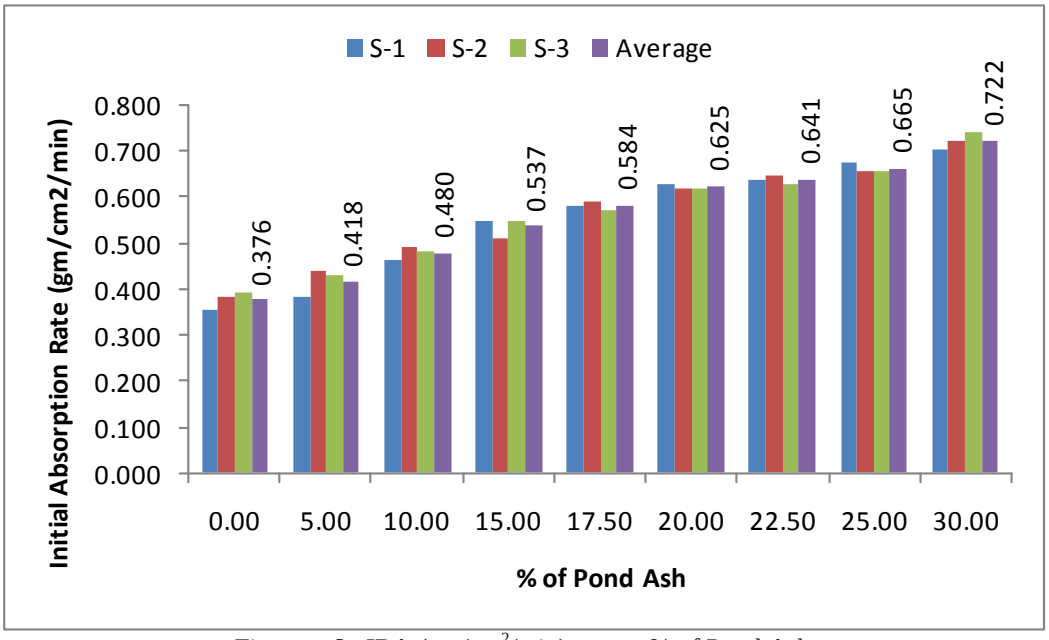

Figure – 6 : IRA (gm/cm^2/min) versus % of Pond Ash

COMPRESSIVE STRENGTH

The test for compressive strength is conducted on five brick samples of each set of bricks. The bricks are prepared and tested for compressive strength in compression testing machine (CTM). The average dimension of brick is taken to find out the area of the brick to calculate the stress at failure.

A plot of compressive strength versus the % of pond ash in bricks, shows that there is an increase in compressive strength with pond ash % in brick up to 15 ~ 17.5% and thereafter the compressive strength decreases.

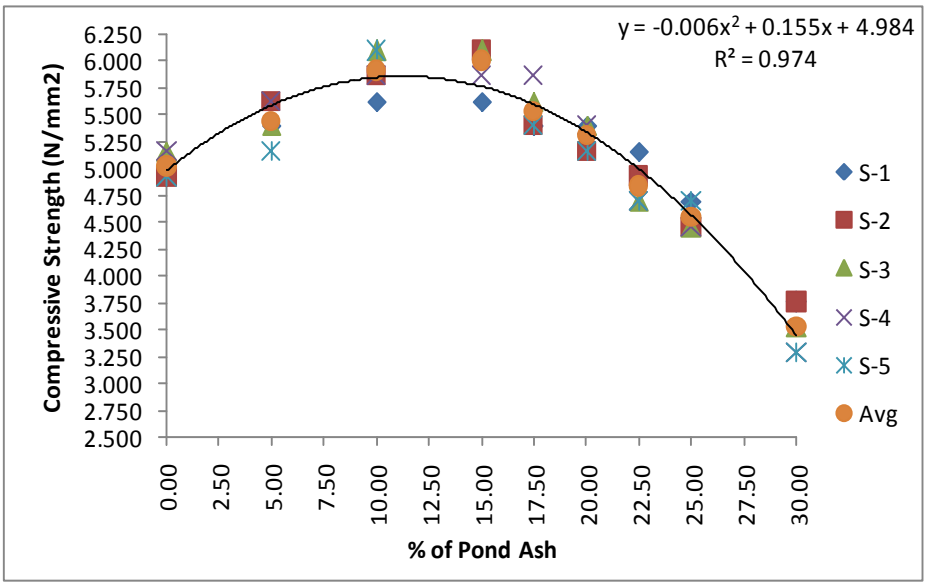

Figure - 7 : Compressive Strength versus Pond Ash % in Bricks

WEATHERING TEST –

The weathering test of the bricks is not conducted as per procedure due to some difficulties during experimentation. The experiment is performed only on one brick. The loss in weathering in each cycle is calculated in percentage with respect to the original dry weight of the sample for each composition of brick. The loss in weathering in percentage versus % of pond ash is shown in Figure 8, which shows that loss in weathering is minimum at 15%.

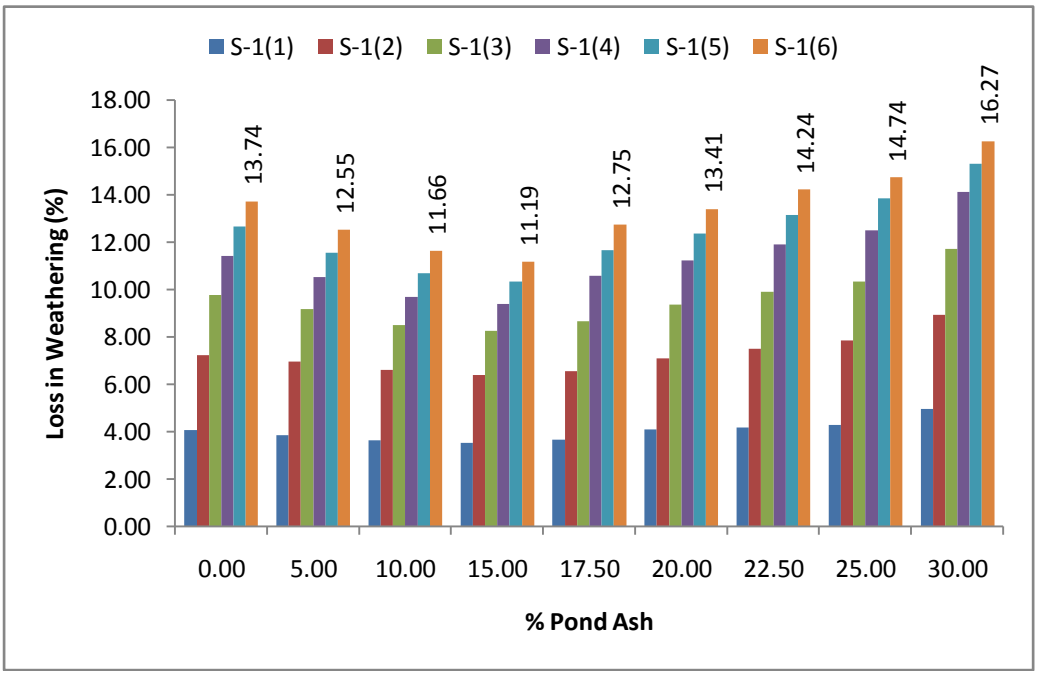

Figure – 9 : Loss in Weathering (%) versus % of Pond Ash

V. CONCLUSIONS

The following conclusions are drawn from the various tests conducted on clay – pond ash brick samples prepared with various percentage of pond ash.

- The result of tolerance test on dimension shows that for clay – pond ash bricks in which the % of pond ash is beyond 20, the dimensions are exceeding the tolerance limit. It is observed that the bricks are swelling as the % of pond ash is increasing. The % of swelling is more in height as compared to length and width.
- The dry density of the bricks decreases with increase in % of pond ash. The decrease in dry density for bricks with pond ash 5.00, 10.00, 15.00, 17.50, 20.00, 22.50, 25.00 and 30.00% are 1.35%, 2.99%, 3.68%, 4.40%, 5.64%, 6.54%, 7.48% and 8.89% respectively.
- The % of water absorption increases with increase in pond ash in bricks, when immersed in cold water for 24 hours. The water absorption percentage varies from 14.59% for clay brick (with no pond ash) to 25.46% for clay – pond ash brick with 30% pond ash.
- In case of boiling water test the pattern of water absorption % is same as that of cold water test. However in this case, the % of water absorption is more as compared to cold water test. In this case the % of water absorption varies from 16.86% for clay brick (with no pond ash) to 26.66% for clay – pond ash brick with 30% pond ash.
- The results of the compressive strength test on brick shows that there is an increase in compressive strength with pond ash % in brick up to 15 ~ 17.5% and thereafter the compressive strength decreases. More precisely, it is evident that the average compressive strength of brick increases up to 19.626 % corresponding to % of pond 15 in pond ash-clay bricks and thereafter falls rapidly with increase in % of pond ash. A decrease of in compressive strength by 29.907% is observed corresponding to 30% pond ash.
- The result of IRA test shows that the IRA value increases with increase in % of pond ash in brick. The IRA value for clay bricks is 0.375 gram/cm^2/minute, whereas it varies from 0.415 gram/cm^2/minute for pond ash clay brick with 5% pond ash to 0.722 gram/cm^2/minute with 30% pond ash.
- The weathering test is done on one brick sample of each composition, which shows that that loss in weathering is minimum at 15%.

LIMITATIONS & FUTURE SCOPE OF STUDY -

There are many limitations while preparing the bricks for experimentation and testing the bricks in the laboratory. The properties of pond ash-clay bricks depends mainly upon the main ingredients i.e. clay and pond ash and in present case the firing temperature. In the present case, the firing of the brick samples prepared with different composition of pond ash is done in traditional way in uncontrolled manner.

The effect of firing temperature on different composition of bricks may be studied and the conclusion based on that may be more logical and useful. This will require the additional facility of high temperature furnaces of bigger sizes.

The BIS code does not provide the procedure for conducting the IRA test and weathering test. The procedure which is mentioned in ASTM is followed partially for getting the results.
The surface porosity and pore size may be determined by using the modern techniques such as scanning electron microscopy (SEM) and the results of water absorption test may be correlated.
The tests for determining the tensile strength, flexural strength and the stress strain characteristics should be conducted for finding out the structural characteristics of the bricks.

REFERENCES

[1] Bhattacharji Ujjwal and Kandpal Tara Chandra (2000), "Potential of fly ash utilisation in India", Energy, 27(1), 151-166.
[2] BIS-1077-1982 (1996), "Indian Standard Common Burnt Clay Bricks Specifications – Fifth Revesion", Bureau of Indian Standard, New Delhi, Second Reprint.
[3] Demir Ismail (2008), "Effect of organic residues addition on the technological properties of clay bricks", Waste Management, 622–627.
[4] Jamal A. and Sidhrath S. (2008), "Value Added Constructional Bricks from Overburden of Open Cast Coal Mines", Journal of Scientific & Industrial Research, 67(1), 445-450.
[5] KUMAR Virender (2004), "Compaction and Permeability Study of Pond Ash amended with Locally Available Soil and Hardening Agent", Journal of the Institution of Engineers, India, Civil Engineering Division, ISSN 0020-336X, 85(i), 31-35.
[6] Kute Sunil and Deodhar S.V. (2003), "Effect of Fly Ash and Temperature on Properties of Burnt Clay Bricks", Journal of Institution of Engineers (India) CV, 84(1), 82 – 85.
[7] Lingling Xu , Guo Wei, Wang Tao, Yang Nanru (2005) "Study on fired bricks with replacing clay by fly ash in high volume ratio", Construction and Building Materials, 19(3), 243–247.
[8] Nirvan G. (2008), *"It's Time to Go in for Green Bricks now"*, The Hindu, On-line Edition, September 6th, 2008.
[9] Pandey Piyush Kant and Agrawal Raj Kumar (2002), "Utilization of Mixed Pond Ash in Integrated Steel Plant for Manufacturing Superior Quality Bricks", Bulletin - Material Science, 25(5), 443-447.
[10] Okunade Emmanuel Akintunde (2008), *"Engineering properties of locally manufactured burnt brick pavers for agrarian and rural earth roads"*, Department of Civil Engineering, University of Ado-Ekiti, Ado-Ekiti, Ekiti State, Nigeria, Gale, Cengage Learning , Science Publications, 2008.
[11] Raimondo Mariarosa, Dondi Michele, Gardini Davide, Guarini Guia and Mazzanti Francesca (2009), "Predicting the initial rate of water absorption in clay bricks", Construction and Building Materials, 23(i), 2623-2630.
[12] Sarkar R., Singh N., Das S.K. (2007), "Effect of addition of pond ash and fly ash on properties of ash-clay burnt bricks", Waste Management and Research,25(6), 66-71.
[13] Vaka Muralimohan Vaka, Padamata Rajendra Prasad, Sujatha V and Sarveswararao S. (2007), "Fly Ash Utilization and Development of Low Density Red Clay Bricks", Materials Engineering and Sciences Division, AIChE Conference.
[14] Vidhya K., Kandasamy S., Malaimagal Sanjana U., Karthikeyan S.R., Basha G.S., Junaid Tariq H. (2013), "Experimental Studies on Pond Ash Brick", International Journal of Engineering Research and Development , 6(5), 06-11.

American Journal of Engineering Research (AJER)
e-ISSN : 2320-0847 p-ISSN : 2320-0936
Volume-02, Issue-09, pp-118-126
www.ajer.org

Research Paper Open Access

A Novel Approach for Image Steganography Using Dynamic Substitution and Secret Key

Saeed Ahmed Sohag, Dr. Md. Kabirul Islam, Md. Baharul Islam
[1](*Department of Computer Science and Engineering, Daffodil International University, Bangladesh*)
[2](*Department of Multimedia Technology and Creative Arts, Daffodil International University, Bangladesh*)

Abstract: - Steganography is a system that hides information in an application cover carrier like image, text, audio, and video. Considerable amount of work has been carried out by different researchers on this subject. Least Significant Bit (LSB) insertion method was more suspicious and low robustness against attacks. The objectives of this study were to analyse various existing system and implement a dynamic substitution based Image Steganography (IS) with a secret key. Our proposed method is more difficult to attack because of message bits are not inserted in to the fixed position. In our method, the message bits are embedded into deeper layer depending on the environment of the host image and a secret key resulting increased robustness. The robustness specially would be increased against those intentional attacks which try to reveal the hidden message.

Keywords: - *I-security, Steganpgraphy, secret key, secure transmission*

I. INTRODUCTION

It is the study of techniques for hiding the existence of a secondary message in the presence of a primary message. The primary message is referred to as the carrier signal or message; the secondary message is referred to as the payload signal or message. The word steganography is derived from the Greek words ‘stegos’ meaning ‘cover’ and ‘grafia’ meaning ‘writing’ [1] defining it as ‘covered writing'. IS means information hidden exclusively inside an image. The main difference between steganography and cryptography is cryptography hide the content of the message and steganography focuses on keeping the existence of a message secret [2]. If there are more similarities between the cover image and the stego-image, it will be harder for an attacker to find out that the stego-image has important secret data hidden inside it. In recent years, enormous research efforts have been invested in the development of digital IS techniques.

In this paper, we have proposed a dynamic approach of substitution in IS where message will be embedded depending on the environment of the host image and a secret key not on the fixed position and also adjust a near bit to improve the quality of the image. It becomes more important as more people join the cyberspace revolution. Privacy and anonymity is a concern for most people on the internet. IS allows for two parties to communicate secretly and covertly. It allows for copyright protection on digital files using the message as a digital watermark. One of the other main uses for image steganography is for the transportation of high-level or top-secret documents between international governments. While it has many legitimate uses, it can also be quite nefarious. It can be used by hackers to send viruses and Trojans to compromise machines, and also by terrorists and other organizations that rely on covert operations to communicate secretly and safely. Military communications system make increasing use of traffic security technique which, rather than merely concealing the content of a message using encryption, seek to conceal its sender, its receiver or its very existence. Similar techniques are used in some mobile phone systems and schemes proposed for digital elections. So we prepare and implement it for efficient and secured information transformation. The objectives of the study are to analyse various existing system and implement a dynamic substitution based image steganography with a secret key. This paper has been organized as literature review, proposed work, experiment result following by discussion and conclusion.

When a stenographic system is developed, it is important to consider what the most appropriate cover Work should be, and also how the stegogramme is to reach its recipient. For example, it is possible that an image stegogramme could be sent to a recipient via email. Alternatively it might be posted on a web forum for all to see, and the recipient could log onto the forum and download the image to read the message. In terms of development, Steganography is comprised of two algorithms, one for embedding and one for extracting. The embedding process is concerned with hiding a secret message within a cover work, and is the most carefully constructed process of the two. A great deal of attention is paid to ensuring that the secret message goes unnoticed if a third party were to intercept the cover Work. The extracting process is traditionally a much simpler process as it is simply an inverse of the embedding process, where the secret message is revealed at the end. The entire process of steganography for images can be presented in figure 1.

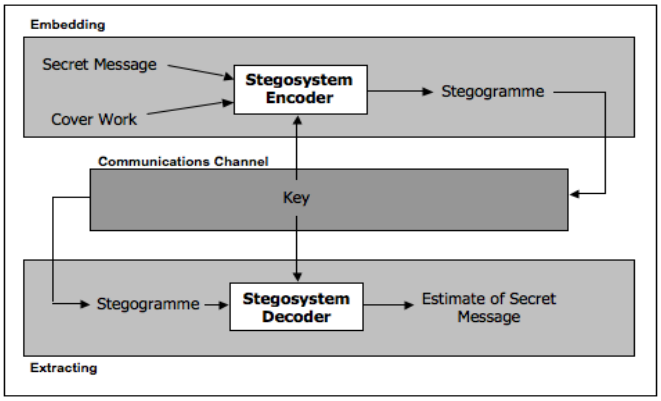

Figure 1: Block diagram of steganography process

Two inputs are required for embedding process. One is secret message that usually a text file that contains the message for transform. And cover work is used to construct a stegogramme that contains a secret message.

1.1. Stego-system

A stego-system (steganographic system) in image steganography refers to a system capable of hiding a secret message within an image, such that no third-parties are aware that the message exists. The image that is output from this process is known as a stegogramme, and great care is taken to ensure that this looks as innocent as possible so that the secret message has the best chance of reaching its intended recipient. However, the stego-system not only refers to encoding the message, it also refers to the system that makes it possible to read the message when it reaches its recipient. The two sub-systems are referred to as the stego-system encoder and the stego-system decoder respectively.

1.1.1. The Encoder

The stego-system encoder is the heart of the steganographic system. It makes it possible to embed a secret message within some cover medium. In the case of image steganography, the encoder will read in a cover image cm;n (where m and n refer to the height and width dimensions of c), and will embed a message m by tweaking carefully selected values of the cover image ci. Exactly which ci values are tweaked depends on the specific embedding algorithm, and it is this decision process that makes each stego-system unique. That is to say that replacing the image data with the message data has no direct impact on the overall perceptibility of the image, therefore meaning the message is hard to detect - at least with the naked eye. Figure 2 shows a graphical representation of the elements and processes typically associated with a stego-system encoder. Stego-systems such as these are referred to as secret key stego-systems. Of course, how many values are tweaked in c to produce the stegogramme depends on the length of the message l(m).

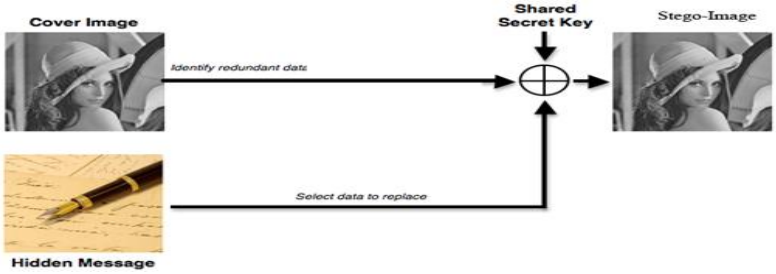

Figure 2: The general design of a basic stego-system encoder

1.1.2. The Decoder

The stego-system decoder allows the receiver of the stegogramme to obtain an estimate of the secret message m0. A good stego-system ensures that the estimate will be as close to the original message m as possible. Figure 3 shows a graphical representation of the elements and processes associated with a common stego-system decoder. As we can see, both the stegogramme and shared secret key k are used to identify the regions that hold the message data. When both of these elements are provided, each mi can be retrieved such that the complete binary sequence m0 can be constructed. The message data can then be converted to an alternative form (typically ASCII) so that it can be read.

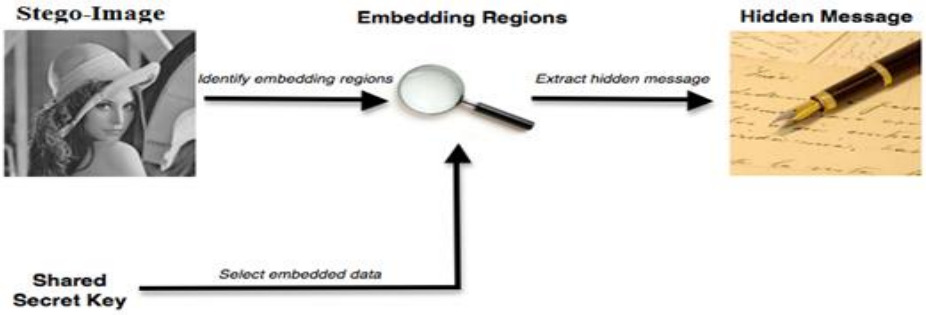

Figure 3: The general design of a basic stego-system decoder

II. RESEARCH BACKGROUND

Image steganography takes the advantage of limited power of human visual system (HVS). Here, unlike watermarks which embed added information in every part of an image, only the complex parts of the image holds added information. Straight message insertion will simply encode every bit of information in the image. More complex encoding can be done to embed the message only in "noisy 'areas of the image that will attract less attention [3]. The least significant bit (LSB) insertion method [4-12] is probably the most well known image steganography technique. The main advantage of this method is that human eye is not able to notice the change; however unfortunately, it is extremely vulnerable to attacks, such as image manipulation. JPEG image format due to its good characteristics (having both reasonable quality and small size) is the most common image format for web and local usages. JPEG uses discrete cosine transform (DCT) to transform successive 8×8 pixel blocks of the image into 64 DCT coefficients. Here, LSBs of the quantized DCT coefficients are used as redundant bits. The modification of even a single DCT coefficient affects all 64 image pixels. As the modifications happen in the frequency domain rather than spatial domain, there is no visual attack against it. Recently, several steganographic techniques for data hiding in JPEGs have been developed [13-15]. All these techniques manipulate the quantized DCT coefficients to embed the hidden message.

The theory of substitution technique is that simply replacing either a bit or a few bits in each sample will not be noticeable to the human eye or ear depending on the type of file. This method has high embedding capacity but it is the least robust. The obvious advantage of the substitution technique is a very high capacity for hiding a message. Obviously, the capacity of substitution techniques is not comparable with the capacity of other more robust techniques like spread spectrum technique that is highly robust but has a negligible embedding capacity (4bps) [16].

1.2. Optimum Pixel Adjustment Procedure

The Optimal Pixel Adjustment Procedure (OPAP) reduces the distortion caused by the LSB substitution method. In OPAP method the pixel value is adjusted after the hiding of the secret data is done to improve the quality of the stego-image without disturbing the data hidden [17]. This procedures is simple, easy retrieval and improved image quality.

1.3. Inverted Pattern Approach (IP)

This inverted pattern (IP) LSB substitution approach uses the idea of processing secret messages prior to embedding. In this method each section of secret images is determined to be inverted or not inverted before it is embedded. In addition, the bits which are used to record the transformation are treated as secret keys or extra data to be re-embedded [18].

1.4. Hiding Streams of 1s and 0s

The usual steganographic methods fetch few bits from the secret data to be embedded. But this method fetches the 1s or 0s present consecutively for hiding. This is an innovative steganographic method where the

data to be hidden is converted to binary. The number of 1s and 0s are counted and stored in the pixels of the cover image in this method. The number of 1s is stored in the odd columns of the pixel and the number of 0s is stored in the even columns [19].

1.5. Pixel Value Differencing (PVD)

Pixel Value Differencing is able to provide a high quality stego image in spite of the high capacity of the concealed information. That is, the number of insertion bits is dependent on whether the pixel is an edge area or smooth area. In edge area the difference between the adjacent pixels is more, whereas in smooth area it is less. While human perception is less sensitive to subtle changes in edge areas of a pixel, it is more sensitive to changes in the smooth areas. This method hides the data in the target pixel by finding the characteristics of four pixels surrounding it [20].

1.6. The PVD Method

This method also uses the concept of hiding the data using the difference between the pixel values. Unlike the previous method, this method hides the data in the difference between two adjacent pixel values. This method gives the stego images of better quality than the traditional method while maintaining a high embedding capacity [19].

1.7. The Mod Method

In this method embedding is done by subtracting any remainder obtained by dividing with 10 and adding the data to be hidden. This is demonstrated by let the pixel be 'p' and data be less than 10 say'd' then new pixel formed is

$$p_1 = p - \text{remainder}(p/10) + d \quad (1)$$

Similarly mod100 method divides the pixel by 100, remainder obtained is subtracted and the data is added to it to get the new pixel. The data hidden will simply be equal to the remainder obtained by dividing the new pixel by 10 or 100 accordingly. This is a method where the data is hidden in the difference between the adjacent pixels, so that mere extraction of few LSB bits will never give the data hidden. Also there is the key file without which extraction of data becomes impossible [19]. Besides there are different methods such as 2D block DCT [21-22], without parity bit [23], spread spectrum [24-26], genetic and wavelet [27], edge detection [7, 28-30], biometric [31] already researched and implemented. A lot of survey [32-40] on image stegonography has done by researchers.

III. MATERIALS AND METHODS

As we know in samples LSBs are more suspicious, thus embedding in the bits other than LSBs could be helpful to increase the robustness. Furthermore, discovering which samples are modified should be uncharted. To reach to the level of ambiguity, the algorithm will not use a predefined procedure to modify the samples but will decide, according to the environment, in this case the host file; as such it will modify indistinct samples of image files, depending on their values and bits status. Thus, some of the samples which algorithm determines they are suitable for modifying will modify and other samples may not change. This ambiguity in selecting samples will thus increase security and robustness of the proposed system. So embedding the bits in deeper layer depending on the environment of the cover image and alter other bit when required will increase the robustness of image steganography and also decrease the alteration complexity. In addition, when not possible in any sample it will ignore them.

3.1. The Embedding Process

In this dynamic technique of substitution based image steganography, first the number of 1 bits of the pixel in cover image is count. If this value is greater than or equal to one and less than the total number of bits in the sample bits then the host is a candidate for substitution. Number of message bits, use as key value. Then number of 1 in sample and secret key value are add and then mod by 8. This value is the position substitution. Now the bit value of that position and the message bit is X-ORed and if this result is 0 then no need to substitution. But if this result is 1, then substitute the bit positioned by message bit and adjust a near bit that equals to the message bit by altering that bit to keep the number of 1's are same as was in the host. The process of message embedding through stego-system encoder is shown in Figure 4. To embed the message into the cover image follows the step below:

Step 1: Covert the message into bits. Here length of message bits used as key.
Step 2: Count the number of 1's in the sample host image, n.

Step 3: If n is greater than or equal to one and less than number of all the bits of the stego sample, then it is a candidate for bit embedding otherwise ignore the sample
Step 4: Calculate p = (n+S_k) mod 8, here S_k means the secret key and 8 is the number of bits in one pixel.
Step 5: Calculate r=h_p xor m_b (h_p= bit of the host sample in position p and m_b is the message bit to embed)
Step 6: If r is equal to zero then need not modify and adjust the bit of the sample otherwise change h_p by m_b and adjust a near bit that is equal tomb by altering it.
Step7: Repeat the steps 2 to 6 until all the bits of the message is completed to embed.

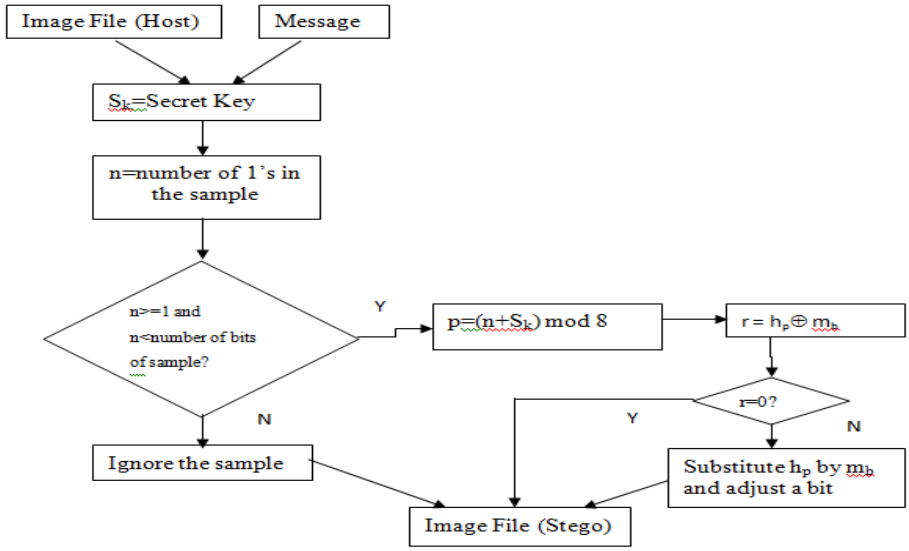

Figure 4: Message embedding process

Message Extraction Process

To get the message from the stego-image, first count the number of 1 bit in the stego-image. If this value is greater than or equal to one and less than the total number of bits in the sample bits then the stego is a candidate for getting the embedding bit of the message otherwise escape the sample. The position of the bit is calculated by (counted value + secret key) mod 8 in the stego-image that is the embedding message bit.

Step 1: Count the number of 1's from the stego-image, n
Step 2: If n is greater than or equal to one and less than number of all the bits of the stego sample, then it is a candidate for bit extraction otherwise ignore the sample
Step 3: Calculate p = (n+ S_k) mod 8, here S_k is the Secret key and 8 is the number of bits in one pixel.
Step 4: Extract the bit S_p (S_p = bit of the stego sample in position p)
Step 5: Repeat the steps 1 to 4 until all the bits (equal to S_k) of the message is extracted
The process of message extract is shown by the flowchart in the Figure 5.

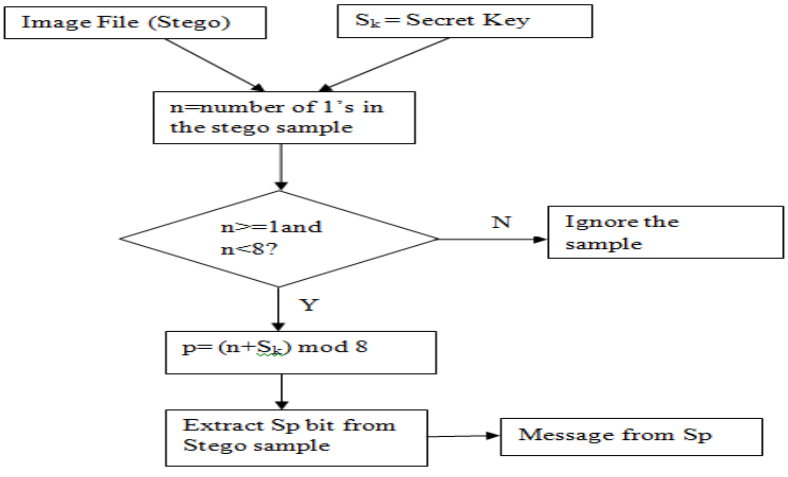

Figure 5: Message extraction process

IV. RESULT AND DISCUSSION

We have implemented the proposed method by using MATLAB R2007b. First we took three cover images (namely Lena, Baboon, Cartoon) of size 256X256 and a message. Then message is converted in to bits and this number of bits acts as the secret key. The images are also converted into series of bits and message bits are inserted in to this cover images according to our method (Dynamic substitution based Image steganography). After embedding the message into the cover images, we have got the stego-images that are closely similar with cover images shown in Figure 6.

Embedded Message: Daffodil University is one of the best private universities in Bangladesh.

Extraction message from Stego-images: Daffodil University is one of the best private universities in Bangladesh.

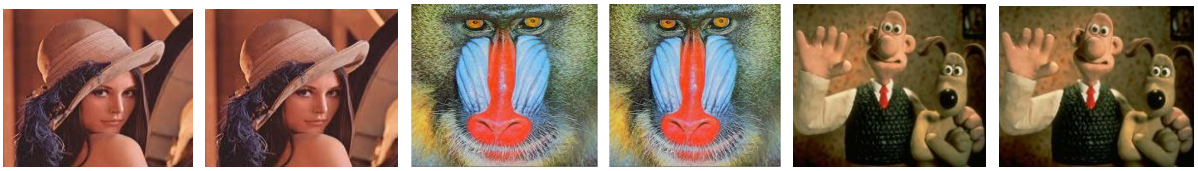

(a) (b) © (d) (e) (f)

Figure 6: Cover image and stego-image (a) Cover image: Lena (b) Stego-image: Lena (c) Cover image: Baboon (d) Stego-image: Baboon (e) Cover image: Cartoon (f) Stego-image: Cartoon

4.1. Comparison between LSB Method and Proposed Method

In LSB having low robustness against attacks which try to reveal the hidden message. But in our proposed method it is difficult to attack, because message bits are not inserted in to the fixed position. It is low robustness against distortions with high average power in LSB. But in our method we adjust pixels bits after insert the message bits that is high robust against distortions. Secret key generation process is easy and provides additional security of the stego-system.

4.2. PSNR Calculation

PSNR is one of metrics to determine the degradation in the embedded image with respect to the host image. Values over 36dB in PSNR are acceptable in terms of degradation, which means no significant degradation is observed by human eye.

Peak signal-to-noise ratio, often abbreviated PSNR, is an engineering term for the ratio between the maximum possible power of a signal and the power of corrupting noise that affects the fidelity of its representation. Because many signals have a very wide dynamic range, PSNR is usually expressed in terms of the logarithmic decibel scale. PSNR is most commonly used to measure the quality of reconstruction of lossy compression codec's (e.g., for image compression). The signal in this case is the original data, and the noise is the error introduced by compression. When comparing compression codec's, PSNR is an *approximation* to human perception of reconstruction quality. Although a higher PSNR generally indicates that the reconstruction is of higher quality, in some cases it may not. One has to be extremely careful with the range of validity of this metric; it is only conclusively valid when it is used to compare results from the same codec (or codec type) and same content.

As a performance measurement for image distortion, the well-known Peak-Signal-to-Noise Ratio (PSNR) which is classified under the difference distortion metrics can be applied on the stego images. It is defined as:

$$PNSR = 10\log 10\left(\frac{C_{max^2}}{MSE}\right) \quad (2)$$

Where *MSE* denotes Mean Square Error which is given as:

$$MSE=\frac{1}{MN}\sum_{x=1}^{M}\sum_{y=1}^{N}(S_{xy}-C_{xy})^2 \quad (3)$$

Where x and y are the image co-ordinates, M and N are the dimensions of the image, S_{xy} is the generated stego-image and C_{xy} is the cover image. Also 2 C_{max}^2 hold the maximum value in the image. PSNR values falling below 30dB indicate a fairly low quality, i.e., distortion caused by embedding can be obvious; however, a high quality stego-image should strive for 40dB and above. MSE and PSNR figures provided in this thesis were calculated after quantization (i.e. after converting floating-point pixel values to integer), but before clipping of the intensity range.

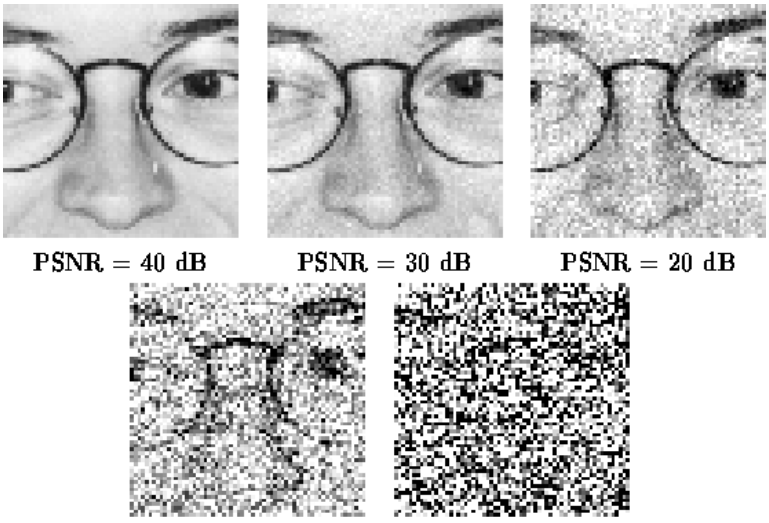

Figure 5: Illustration of the PSNR measure

Table I represents the PSNR comparison of LSB substitution and our method using cover image Lena, Baboon and Cartoon.

Table I: Comparison of image steganography algorithms

Cover Image	LSB	Dynamic Substitution
Lena	44.0216	44.7638
Baboon	37.8642	38.7295
Cartoon	43.9901	44.7354

V. CONCLUSION

Many techniques are used to hide data in various formats in steganography. The most widely used mechanism on account of its simplicity is the least significant bit. Least significant bit or its variants are normally used to hide data in a digital image. The other bits may be used but it is highly likely that image would be distorted. However, in the present the bits used were not in fixed position. The LSB technique used in the present study is simple; it generally causes noticeable distortion when the number of embedded bits for each pixel exceeds three. In Optimal Pixel Adjustment Procedure (OPAP) method the pixel value is adjusted after the hiding of the secret data is done to improve the quality of the stego image without disturbing the data hidden. In inverted pattern (IP) method each section of secret images is determined to be inverted or not inverted before it is embedded. The secret key is generated automatically after embedding. The usual steganographic methods fetch few bits from the secret data to be embedded. But this method fetches the 1s or 0s present consecutively for hiding. This is an innovative steganographic method where the data to be hidden is converted to binary. The number of 1s and 0s are counted and stored in the pixels of the cover image in this method. The number of 1s is stored in the odd columns of the pixel and the number of 0s is stored in the even columns. In this method embedding is done by subtracting any remainder obtained by dividing with 10 and adding the data to be hidden. Similarly mod100 method divides the pixel by 100, remainder obtained is subtracted and the data is added to it to get the new pixel. The data hidden will simply be equal to the remainder obtained by dividing the new pixel by 10 or 100 accordingly. Message capacity and stego-image quality are two important criteria in evaluating a steganogarphic method. This new approach of dynamic substitution based image steganography has high robustness against attacks which try to reveal the hidden message and low robustness against distortions with high average power. The proposed method will embed the message bits in the deeper layers of samples and alter a bit near the substitute bit to decrease the error and if not possible then ignore them and improved security, reliability, and efficiency. So, using the proposed method, message bits could be embedded into vague and deeper layer depending on the environment of the host sample robustness. Our future work will cover against all kinds of intentional and unintentional attacks to increase the robustness of the image steganography. Our experimental results have shown that the proposed method provides good image quality and large message capacity as well as increase in the system immunity. It is very sensitive to any kind of filtering or manipulation of the stego-image. Scaling, rotation, cropping, addition of noise, or lossy compression to the stego-image will destroy the message. Our future work will be recovering it.

REFERENCES

[1] M Ozaki, Y. Adachi, Y. Iwahori, and N. Ishii, Application of fuzzy theory to writer recognition of Chinese characters, *International Journal of Modelling and Simulation, 18(2),* 1998, 112-116.

[2] H. Wang, S. Wang, Cyber warfare: Steganography vs. Steganalysis, *Communications of the ACM, 47(10),* 2004

[3] C. Stanley, *Pairs of Values and the Chi-squared Attack*, Master's thesis, Department of Mathematics, Iowa State University, 2005

[4] M. A. F. Al-Husainy, Message Segmentation to Enhance the Security of LSB Image Steganography, *International Journal of Advanced Computer Science and Applications, 3(3),* 2012, 57-62

[5] N. Santoshi, B. L. Rao, A Secure and Lossless Adaptive Image Steganography with Mod-4 LSB Replacement Methods Using Image Contrast, *International Journal of Scientific & Engineering Research, 3(8),* 2012, 1-9

[6] M. Kavitha, K. Kadam, A. Koshti, P. Dungha, Steganography Using Least Signicant Bit Algorithm, *International Journal of Engineering Research and Applications (IJERA), 2(3),* 2012, 338-341

[7] N. Jain, S. Meshram, S. Dubey, Image Steganography Using LSB and Edge – Detection Technique, *International Journal of Soft Computing and Engineering (IJSCE), 2(3),* 2012, 217-222

[8] S. Singh, G. Agarwal, Use of image to secure text message with the help of LSB replacement, *International Journal of Applied Engineering Research, 1(1),* 2010, 200-205

[9] R. Kaur, B. Singh, I. Singh, A Comparative Study of Combination of Different Bit Positions in Image Steganography, *International Journal of Modern Engineering Research (IJMER), 2(5),* 2012, 3835-3840

[10] B. Karthikeyan, S. Ramakrishnan, V. Vaithiyanathan, S. Sruti, M. Gomathymeenakshi, An Improved Steganographic Technique Using LSB Replacement on a Scanned Path Image, *International Journal of Network Security, 15(1),* 2013, 314-318

[11] V. Tyagi, A. Kumar, R. Patel, S. Tyagi, S. S. Gangwar, Image Steganography using Least Significant Bit with Cryptography, *Journal of Global Research in Computer Science, 3(3),* 2012, 53-55

[12] N. Tiwari, M. Shandilya, Evaluation of Various LSB based Methods of Image Steganography on GIF File Format, *International Journal of Computer Applications, 6(2), 2010,* 1-4

[13] J. Fridrich, M. Goljan, D. Hogea, Attacking the Out Guess, Proc. ACM Workshop Multimedia and Security2002, ACM Press

[14] A. Westfeld, High Capacity Despite Better Steganalysis (F5–ASteganographic Algorithm), *Information Hiding. 4th International Workshop on Information hiding,* New York, 2001, 289–302

[15] N. Provos, Defending Against Statistical Steganalysis, Proc.10th USENIX Security Symposium, Washington, 2001

[16] S. K. Pal, P. K. Saxena, S. K. Mutto, The Future of Audio Steganography, *Pacific Rim Workshop on Digital Steganography*, Japan, 2002

[17] C.K. Chan, L.M. Chen, Hiding data in images by simple LSB substitution, *Journal of Pattern Recognition, 37(3),* 2004, 469–474

[18] C. H. Yang, Inverted pattern approach to improve image quality of information hiding by LSB substitution, *Journal of Pattern Recognition, 41*, 2008, 2674–2683

[19] R. Amirtharajan, R. Akila, P. Deepikachowdavarapu, A Comparative Analysis of Image Steganography, *International Journal of Computer Applications, 2(3),* 2010, 41-47

[20] Y. R. Park, H. H. Kang, S. U. Shin, K. R. Kwon, An Image Steganography Using Pixel Characteristics, CIS 2005, Part II, Springer-Verlag Berlin Heidelberg LNAI 3802, 2005, 581– 588

[21] K. B. S. Kumar, K. B. Raja, R. K. Chhotaray, S. Pattnaik, Steganography Based on Payload Transformation, *International Journal of Computer Science, 8(2)*, 2011, 241-248

[22] M. Singh, R. Sharma, D. Garg, A New Purposed Issue for Secure Image Steganography Technique Based On 2-D Block DCT and DCT, *International Journal of Advanced Research in Computer Science and Software Engineering, 2(7)*, 2012, 29-34

[23] C. N. Yang, J. Ouyang, L. Harn, Steganography and authentication in image sharing without parity bits, *Journal of Optics Communications, 285*, 2012, 1725–1735

[24] L. M. Marvel, C. G. Boncelet, C. T. Retter, Spread Spectrum Image Steganography, *IEEE Transactions on Image Processing, 8(8)*, 1999, 1075-1083

[25] S. Goyat, A Novel Technique Used For Image Steganography Based On Frequency Domain, *International Journal of Engineering Research & Technology (IJERT), 1(7),* 2012, 1-15

[26] G. S. Sravanthi, B.S. Devi, S. M. Riyazoddin, M. J. Reddy, A Spatial Domain Image Steganography Technique Based on Plane Bit Substitution Method, *Global Journal of Computer Science and Technology Graphics & Vision, 12(15),* Version 1.0, 2012

[27] E. Ghasemi, J. Shanbehzadeh, N. Fassihi, High Capacity Image Steganography using Wavelet Transform and Genetic Algorithm, *Proc. of International Multi Conference of Engineers and Computer Scientists*, March 16-18 2011, Hong Kong
[28] S. Arora, S. Anand, A Proposed Method for Image Steganography Using Edge Detection, *International Journal of Emerging Technology and Advanced Engineering, 3(2)*, 2013, 296-297
[29] A. A. Ali, A. H. S. Saad, New Image Steganography Method by Matching Secret Message with pixels of Cover Image (SMM), *International Journal of Computer Science Engineering and Information Technology Research (IJCSEITR), 3(2*), 2013, 1-10
[30] A. M. A. Shatnawi, A New Method in Image Steganography with Improved Image Quality, *Journal of Applied Mathematical Sciences, 6(79)*, 2012, 3907 – 3915
[31] A.Cheddad, J. Condell, K. Curran, P. M. Kevitt, Biometric Inspired Digital Image Steganography, *15th Annual IEEE International Conference and Workshop on the Engineering of Computer Based Systems*, 2008
[32] A. Cheddad, J. Condell, K. Curran, P. M. Kevitt, Digital image steganography: Survey and analysis of current methods, Journal *of Signal Processing, 90*, 2010, 727–752
[33] G. Kaur, A. Kochhar, Transform Domain Analysis of Image Steganography, *International Journal for Science and Emerging Technologies with Latest Trends" 6(1)*, 2013, 29-37
[34] J. Kaur, S. Kumar, Study and Analysis of Various Image Steganography Techniques, *International Journal of Computer Science and Technology, 2(3)*, 2011, 535-539
[35] B. Li, J. He, J. Huang, Y. Q. Shi, A Survey on Image Steganography and Steganalysis, *Journal of Information Hiding and Multimedia Signal Processing , 2(2)*, 2011, 142-172
[36] M. Kumari, A. Khare, P. Khare, JPEG Compression Steganography & Cryptography Using Image-Adaptation Technique, *Journal of Advances Information Technology, 1(3)*, 2010, 141-145
[37] N. Hamid, A. Yahya, R. B. Ahmad, O. M. Al-Qershi, Image Steganography Techniques: An Overview, *International Journal of Computer Science and Security (IJCSS), 6(3)*, 2012, 168-179
[38] M. Kharrazi, H. T. Sencar, N. Memon, Performance study of common image steganography and steganalysis techniques, *Journal of Electronic Imaging 15(4), 2006*
[39] M. S. Prasad, S. Naganjaneyulu, G. Krishna, C. Nagaraju, A Novel Information Hiding Technique for Security by Image Steganography, *Journal of Theoretical and Applied Information Technology, 8(1),* 2009, 35-39
[40] N. Tiwari, M. Shandilya, Evaluation of Various LSB based Methods of Image Steganography on GIF File Format, *International Journal of Computer Applications, 6(2), 2010*, 1-4

American Journal of Engineering Research (AJER)
e-ISSN : 2320-0847 p-ISSN : 2320-0936
Volume-02, Issue-09, pp-127-132
www.ajer.org

Research Paper Open Access

Brain Image Segmentation Technique Using Gabor filter parameter

Dr. Debmalya Bhattacharya[*], Mrs. Jibanpriya Devi[#], Ms. Payal Bhattacherjee[~]
School of Electrical Engineering
Vel Tech Dr. RR & Dr. SR Technical University
Avadi, Chennai-600062, Tamil Nadu

Abstract: - This paper imparts the recognition of Gabor filter techniques using nine different types of brain images. This paper is based on the identification analysis on the output of noisy and filtered images by using Gabor filter technique. This technique is acquiring the noisy images is built on the three types of images: Gaussian, Poisson and Speckle. In conclusion an algorithm is established that implement all the types of filtering technique on the input image and arithmetic parameters are calculated as per the comparison between output and input images. These arithmetic parameters are exhibit distinctly and they are compared for both the noisy and filtered images. For the calculation of the performance of Gabor filters mathematical parameters like signal to noise ratio, correlation coefficient and Structure similarity are used and the MATLAB codes required in calculating these parameters are developed. These parameters are used to calculate the image quality of the output image obtained from Gabor filter technique, based on the values of these parameters the results of all the output images is discussed.

I. INTRODUCTION

This paper work is carried out to study the analysis of Gabor filtered output images and the noisy images. For this analysis, we are examining the values of various quality parameters like SNR, Correlation and SSIM. For acquiring the noisy images, we are using three types of noises, Gaussian, Poisson and Speckle noises. For all the images, we are choosing a specific area of the original images and this area is different in the segmentation propose. For segmentation analysis, we are using the comparison of three output images as: Original image segmentation, Gabor filtered output segmentation and noised output segmentation.

These three output images are having the same dimensions for their comparison. The several parameters of the Gabor filter involve a major role in selecting the output image. The size, phase, orientation and frequency of the output image are selected by the Gabor filter. The image features are determined by applying an proper Gabor filter with adaptively chosen size, orientation, frequency and phase for each pixel.

An image property called phase divergence is used for the selection of the appropriate filter size.Essential features related to the change in brightness, texture and position are extracted for each pixel at the selected size of the filter. 2-D Gabor filter is easier to tune the direction and radial frequency band-width, and easier to tune center frequency, so they can instantly get the best resolution in spatial domain and frequency domain. Gabor filter outputs can be designed as Gaussian's and establish algorithm for choosing optimal filter specification.

II. GABOR FILTERS

In image processing, a **Gabor filter**, is a linear filter used for edge detection. Frequency and orientation representations of Gabor filters are similar to those of the human visual system, and they have been found to be particularly appropriate for texture representation and discrimination. In the spatial domain, a 2D Gabor filter is a Gaussian kernel function modulated by a sinusoidal plane wave. The Gabor filters are self-similar: all filters can be generated from one mother wavelet by dilation and rotation.

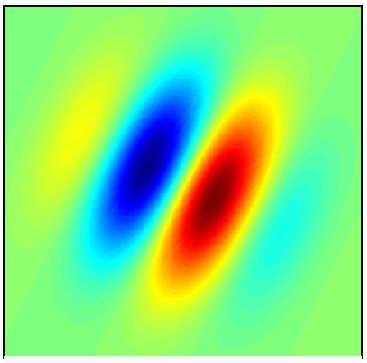

A two-dimensional Gabor filter

Its impulse response is defined by a harmonic function multiplied by a Gaussian function. Because of the multiplication-convolution property (Convolution theorem), the Fourier transform of a Gabor filter's impulse response is the convolution of the Fourier transform of the harmonic function and the Fourier transform of the Gaussian function. The filter has a real and an imaginary component representing orthogonal directions. The two components may be formed into a complex number or used individually.

Complex

$$g(x, y; \lambda, \theta, \psi, \sigma, \gamma) = \exp\left(-\frac{x'^2 + \gamma^2 y'^2}{2\sigma^2}\right) \exp\left(i\left(2\pi\frac{x'}{\lambda} + \psi\right)\right)$$

Real

$$g(x, y; \lambda, \theta, \psi, \sigma, \gamma) = \exp\left(-\frac{x'^2 + \gamma^2 y'^2}{2\sigma^2}\right) \cos\left(2\pi\frac{x'}{\lambda} + \psi\right)$$

Imaginary

$$g(x, y; \lambda, \theta, \psi, \sigma, \gamma) = \exp\left(-\frac{x'^2 + \gamma^2 y'^2}{2\sigma^2}\right) \sin\left(2\pi\frac{x'}{\lambda} + \psi\right)$$

where

$$x' = x\cos\theta + y\sin\theta$$

and

$$y' = -x\sin\theta + y\cos\theta$$

In this equation, λ represents the wavelength of the sinusoidal factor, θ represents the orientation of the normal to the parallel stripes of a Gabor function, ψ is the phase offset, σ is the sigma of the Gaussian envelope and γ is the spatial aspect ratio, and specifies the ellipticity of the support of the Gabor function.

A Gabor filter is a linear filter whose impulse response is defined by a harmonic function multiplied by a Gaussian function. Because of the multiplication-convolution property (Convolution theorem), the Fourier transform of a Gabor filter's impulse response is the convolution of the Fourier transform of the harmonic function and the Fourier transform of the Gaussian function. Gabor filters are directly related to Gabor wavelets, since they can be designed for number of dilations and rotations. However, in general, expansion is not applied for Gabor wavelets, since this requires computation of biorthogonal wavelets, which may be very time-consuming. Therefore, usually, a filter bank consisting of Gabor filters with various scales and rotations is created. The filters are convolved with the signal, resulting in a so-called Gabor space. This process is closely related to processes in the primary visual cortex. The Gabor space is very useful in e.g., image processing applications such as iris recognition and fingerprint recognition. Relations between activations for a specific spatial location are very distinctive between objects in an image. Furthermore, important activations can be extracted from the Gabor space in order to create a sparse object representation. The Gabor Filters have received considerable attention because the characteristics of certain cells in the visual cortex of some mammals can be approximated by these filters. In addition these filters have been shown to posses optimal localization properties in both spatial and frequency domain and thus are well suited for texture segmentation problems. Gabor filters have been used in many applications, such as texture segmentation, target detection fractal dimension management, document analysis, edge detection, retina identification, and image coding and image representation. A Gabor filter can be viewed as a sinusoidal plane of particular frequency and orientation, modulated by a Gaussian envelope.

$h(x, y)$ □$s(x, y)g(x, y)$
$s(x, y)$: Complex sinusoid
$g(x, y)$: 2-D Gaussian shaped function, known as envelope

$$s(x, y) = e^{-j2\pi(u_0 x + v_0 y)}$$

$$g(x, y) = \frac{1}{\sqrt{2\pi}\sigma} e^{-\frac{1}{2}\left(\frac{x^2}{\sigma_x^2} + \frac{y^2}{\sigma_y^2}\right)}$$

Where $s(x, y)$ is a complex sinusoid, known as the carrier, and $g(x, y)$ is a 2-D Gaussian-shaped function, known as the envelope.

The real part and imaginary part of this sinusoid are the parameters and define the spatial frequency of the sinusoid in Cartesian coordinates. This spatial frequency can also be expressed in polar coordinates as magnitude Fo and direction Wo:

$$F_0 = \sqrt{{u_0}^2 + {v_0}^2}$$

i.e.

$$\omega_0 = \tan^{-1}\left(\frac{v_0}{u_0}\right)$$

$$u_0 = F_0 \cos\omega_0$$

$$v_0 = F_0 \sin\omega_0$$

III. MATERIALS AND METHODS IMAGES AS INPUTS

Gabor filters needs some types of images as the input. These images require the process of computer algorithms as per the input image. These computer algorithms yield two types of images from Computer Algorithm: noisy image and magnitude image. The magnitude image is comparing with the noisy image, which gives the advantages of Gabor filters in various parameters. There are ten original standard images:-

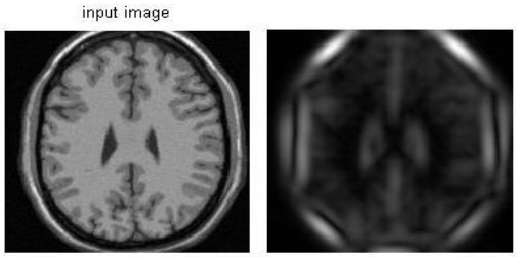

Noises Gaussian noise- This type of noise adds normal distributed noise to the original image. The noise is independent of the image it is applied to. The value of the pixel is altered by the additive Gaussian noise as Where n is the noise, being distributed normally with variance v. the noisy pixels which are generated are anywhere between black and white, distributed according to the Gaussian curve. The width of the curve is adjusted with the mean and the variance parameter.

Poisson noise- Poisson noise is generated from the data instead of adding artificial noise to the data. If I, the original image, is double precision, then input pixel values are interpreted as means of Poisson distributions scaled up by. Poisson noise generates a noise sequence of integer numbers having a Poisson probability distribution,

Speckle noise- Speckle adds multiplicative noise to the image according to the following formula: where n is an array with the size of an array with the size of the original image, filled with random values resulting from a normal distribution (Gaussian distribution) with mean 0 and are controlled by the variance. With this type of noise, noise generation is dependent on the original image, hence the product in the formula. Quality metrics there are various quality metrics in our work. By evaluating the values of those parameters we can compare the values of the noisy and the magnitude images of the output. The values of those parameters lead to best results as per the details of various values by comparing the noisy and the magnitude output values. These are the various working parameters:

SNR- SNR stands for signal to noise ratio. SNR is defined as the ratio of the net signal value to the RMS noise. Where the net signal value is the difference between the average signal and background values, and the RMS noise is the standard deviation of the signal value.

Correlation- The operation called correlation is closely related to convolution. In correlation, the value of an output pixel is also computed as a weighted sum of neighboring pixels. The correlation coefficient matrix represents the normalized measure of the strength of linear relationship between variables correlation coefficient. Correlation indicates the strength and direction of linear relationship between 2 signals and its value lie between +1 and -1. The correlation is 1 in the case of a linear relationship, -1 in the case of a decreasing linear relationship and some value in between for all other cases, including the degree of linear dependence between the 2 signals. The closer the coefficient is to either -1 or +1, the stronger the correlation between the signals.

SSIM- SSIM stands for structural Similarity. The SSIM index is a method for measuring the similarity between two images. The SSIM index is a full reference metric, in other words, the measuring of image quality based on an initial uncompressed or distortion-free image as reference. SSIM is designed to improve on traditional methods like PSNR and MSE, which have proved to be inconsistent with human eye perception. The SSIM metric is calculated on various windows of an image.

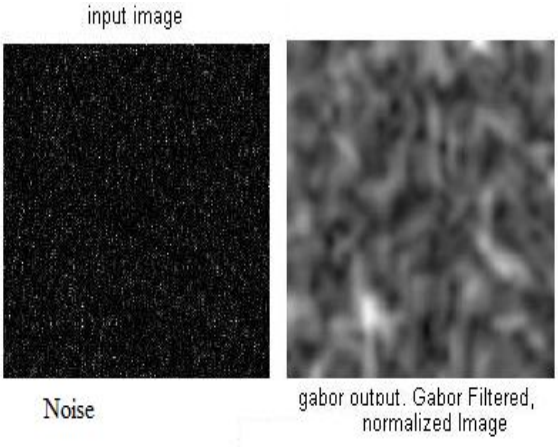

IV. WORKING ALGORITHM USING MATLAB

This working Algorithm is the way of doing our work. This is a step by step procedure that how we implement the images and how we evaluate the working parameters. The main algorithm, followed in order to fulfill the aim of our work, is as follows:

Step 1: Read the original standard image.
Step 2: Apply the Gabor Filter to the original standard image and storing the mainly outputs for the Noisy image and the Magnitude image.
Step 3: Resize the output noisy and output magnitude images as per the original standard image size as the size of the original image may be. To evaluate various parameters from the original and the output image it is necessary to maintain the same size of the images.
Step 4: Before calculating the values of the various parameters, it is necessary to convert that output image to 1-Dimensional image because that standard image doesn't work by using the parameters formula in their original form.
Step 5: Calculate the value of the quality metrics parameters by using the MATLAB command: SNR (I, J), Correlation (I, J), [mssim ssim_map] = ssim_index (I, J) his command gives the values of the SNR, Correlation and SSIM where I is the original image and J is the output image.
Step 6: After run of all the parameters, all the values of parameters are calculated by changing the Variances and changing the frequency of the Gabor filters. The best value results are collected and plotted all with respect to their particular Variances.
Step 7: The result analysis shows that Segmentation result of image with noise and without noise shows less different.

V. RESULTS

Image Analysis of segmentation with noise with Gabor filter

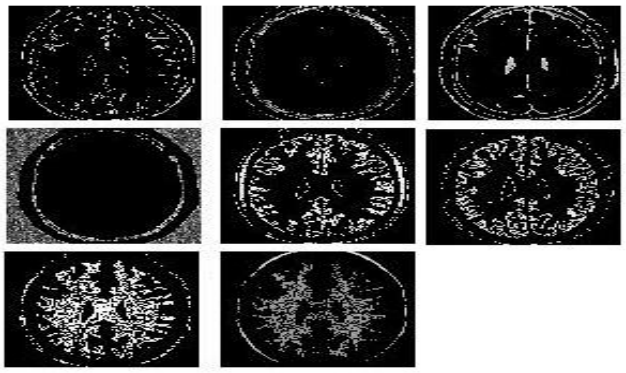

Noisy Image Segmentation

Image Analysis of segmentation without noise with Gabor filter

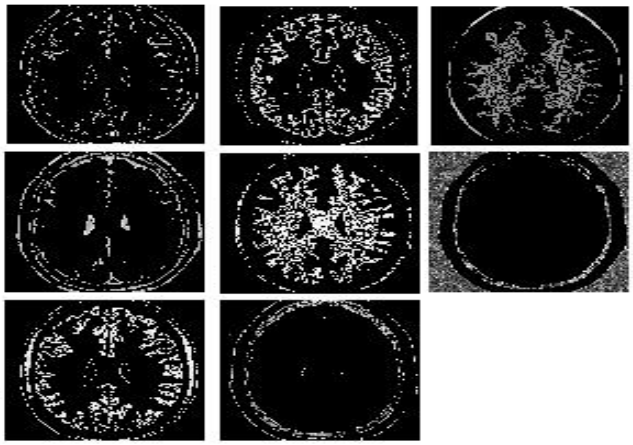

Image Segmentation without noise

VI. EFFECT OF GABOR FILTER FOR IMAGE SEGMENTATION

These are the comparison of Image segmentation for various images. There are nine segmentation results for every image. These are the segmentation of Original image and the best values output for Noisy and filtered images.

Number of iteration applied to every image is not less than 100 counts.

Segmented image similarity is around 84% as compare between the original input images.

Time taken for iteration process is less different between noisy image and noiseless images.

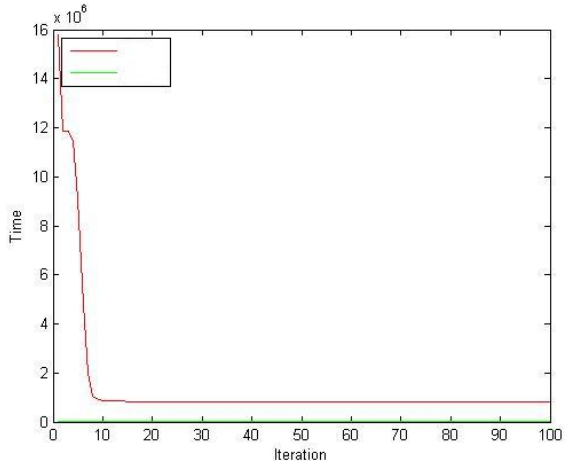

REFERENCE

[1] Hans G. Feichtinger, Thomas Strohmer: "Gabor Analysis and Algorithms", Birkhäuser, 1998; ISBN 0-8176-3959-4

[2] Karlheinz Gröchenig: "Foundations of Time-Frequency Analysis", Birkhäuser, 2001; ISBN 0-8176-4022-3

[3] John Daugman: "Complete Discrete 2-D Gabor Transforms by Neural Networks for Image Analysis and Compression", IEEE Trans on Acoustics, Speech, and Signal Processing. Vol. 36. No. 7. July 1988, pp. 1169–1179

[4] "Online Gabor filter demo". Retrieved 2009-05-25.

[5] Movellan, Javier R. "Tutorial on Gabor Filters". Retrieved 2008-05-14.

[6] "Procedural Noise using Sparse Gabor Convolution". Retrieved 2009-09-1

[7] J. G. Daugman. Uncertainty relation for resolution in space, spatial frequency, and orientation optimized by two-dimensional visual cortical filters. *Journal of the Optical Society of America A*, 2(7):1160–1169, July 1985.

[8] 3D surface tracking and approximation using Gabor filters, Jesper Juul Henriksen, South Denmark University, March 28, 2007

[9] Daugman, J.G. (1980), "Two-dimensional spectral analysis of cortical receptive field profiles", *Vision Res.* **20** (10): 847–56,PMID 7467139

[10] J.P. Jones and L.A. Palmer. An evaluation of the two-dimensional gabor filter model of simple receptive fields in cat striate cortex. J. Neurophysiol., 58(6):1233-1258, 1987

Mrs. Jiban Priya Devi finished BE in 2008 from Anna University, Chennai & M.Tech in 2010 from Anna University. Currently she is working as Assistant Professor in Vel Tech Technical University, Avadi, Chennai. Her area of research interest is Signal & Image processing.

Dr. Debmalya Bhattacharya is working as Associate Professor in Vel Tech Technical University Chennai. He has published several papers on DSP & Wireless communication in National and International Journals. His current research interests are DSP, Antenna Design & Wireless Communications and Renewable Energy Sources.

Ms. Payal Bhattacherjee finished BE in 2008 from Anna University, Chennai & M.Tech in 2011 from Sathyabama University. Currently she is working as Assistant Professor in Vel Tech Technical University, Avadi, Chennai. Her area of research interest is Signal & Image processing

American Journal of Engineering Research (AJER)
e-ISSN : 2320-0847 p-ISSN : 2320-0936
Volume-02, Issue-09, pp-133-139
www.ajer.org

Research Paper Open Access

Stabilization of Dune Sand with Ceramic Tile Waste as Admixture

Dr. N. K. Ameta, Dr. Wayal A. S., Puneet Hiranandani
[1]*Professor, Civil Engineering Department, M.B.M. Engineering, JNV University Jodhpur, Rajasthan, India*
[2]*Associate Professor, Civil & Env. Engineering, V.J.T.I, Matunga, Mumbai, India*
[3]*M.Tech. student, M.B.M.Engineering, JNV University Jodhpur, Rajasthan, India*

Abstract: - The Dune-Sand has nil cohesion and thus has a very low compressive strength. The stabilization of Dune-Sand is of prime importance since it can be used for various construction works and highways, airfields and helipads projects. The investigation reported herein presents a study of stabilization of Dune- Sand with Ceramic Tiles Wastage as admixture. All the California Bearing Ratio tests were conducted at maximum dry density and optimum moisture content as arrived from Standard Proctor Test. Direct shear tests were also performed. The main objective of this experimental study was to obtain an economical stabilized mix of ceramic tiles wastage and dune sand so that largely and cheaply available dune-sand be used for various construction purposes.

Keywords**:** *- Dune sand, Ceramic tiles, stabilization, C.B.R., Shear.*

I. INTRODUCTION

Utilization of immense reserve of dune sand, the huge mass remained unnoticed, untouched from centuries, where life itself requires courage to move ahead to survive, in the absolute scarcity of basic needs. Soil stabilization is the alteration of one or more soil properties, by mechanical or chemical means, to create an improved soil material possessing the desired engineering properties. Soils may be stabilized to increase strength and durability or to prevent erosion and dust generation.

The properties of a soil may be altered in many ways among which a few are chemical, thermal, mechanical and other means. Stabilization is being used for a variety of engineering works such as construction of all-weather roads and air-field pavements including helipads, where the main aim is to increase the strength or stability of soil by making best use of the locally available materials. Engineers are responsible for selecting or specifying the correct stabilizing method, technique, and quantity of material required.

There is a great scope of stabilization of Dune-Sand with the admixture of Ceramic Tiles Wastage for construction of pavements, airfields and helipads. The main aim of the present work is to develop a mix composition which can be economically used for stabilization of dune sand in any type of environment. The laboratory studies have been done on dune sand using ceramic tiles wastage. The test specimens were prepared in the laboratory by direct mixing of the ceramic tiles wastage in dune sand.

The ceramic tiles wastage can be easily available from various construction sites and manufacturing units. If this wastage can be used efficiently then we can obtain an economical mix of dune sand and ceramic tiles wastage as a construction material. On the other hand, the problem of the disposal of ceramic tiles wastage can be overcome by using it for stabilization of dune sand. Many researchers like Ameta et al. (2008), Jain O.P. et al. (1979), Kevin M.(1978) and Wayal A.S et al.(2012) have worked on stabilization of soils.

II. MATERIALS USED FOR STUDY

2.1 Dune-Sand

The Great Indian Desert known as Thar Desert in the west of Rajasthan bordering Pakistan covers over 60% of its area and includes 12 of its 32 districts. The Thar Desert is one of the most densely populated desert environments in the world, occupying an area of 2,10,000 sq. kms., covering 61.3% of the Rajasthan State and

6.3% of the country as a whole.

Jodhpur district is a part of Thar Desert. The Dune Sand used in the present study was brought from location near Jajiwal-Banar villages, at about 20-25 km away from Jodhpur on Jodhpur-Jaipur road. Dune sand has nil cohesion and has poor compressive strength and hence need stabilization. Dune sand is coarse grained, uniform clean sand as per Unified Soil Classification system. Particles size ranges between 75 □ to 1.0mm i.e. fine coarse sand, round to angular in particle shape as per Indian Standard Classification System.

2.2 Ceramic Tiles

A ceramic tile is an inorganic, nonmetallic solid prepared by the action of heat and subsequent cooling. Ceramic materials may have crystalline or partly crystalline structure, or may be amorphous. Because most common ceramics are crystalline, the definition of ceramic is often restricted to inorganic crystalline materials.
The word "ceramic" comes from the Greek word (kermos) which means "potter's clay". The earlier ceramics were pottery objects made from clay, either by itself or mixed with other materials, hardened in fire. Later ceramics were glazed and fired to create a coloured, smooth surface. The potters used to make glazed tiles with clay; hence the tiles are called as "ceramic tiles".
The raw materials to form tile consist of clay minerals mined from the earth's crust, natural minerals such as feldspar that are used to lower the firing temperature, and chemical additives for the shaping process.

2.3. Ceramic Tiles Wastage

A lot of ceramic tiles wastage is produced during formation, transportation and placing of ceramic tiles. This wastage or scrap material is inorganic material and hazardous. Hence its disposal is a problem which can be removed with the idea of utilizing it as an admixture to stabilize dune sand, so that the mix prove to be very economical and can be used as subgrade in low traffic roads or village roads.

III. TEST PROGRAM AND PROCEDURE

The laboratory investigation on dune sand stabilization with ceramic tiles wastage as admixture was performed. The ceramic tile wastage was brought from some construction site. The ceramic tiles were of Kajaria Company. The dune sand had similar characteristics which are found in various areas of Jodhpur district. Hence sand from one location near Jajiwal-Banar Villages, at about 20-25 kms away from Jodhpur on Jodhpur-Jaipur Road was brought for the study.

The objective of the present study is to evaluate the use of dune sand as a construction material after stabilizing it with ceramic tiles wastage particles as admixture. The present study has been undertaken with the following objectives:

1. To study the effect of ceramic tiles wastage particles of varying size (4.75mm. 2mm, 1.18mm and .425mm) on Proctor density and OMC of dune sand.
2. To study the changes in CBR value of dune sand by mixing ceramic tile wastage of varying size in different proportions in unsoaked and soaked conditions.
3. To study the changes in shear stress of dune sand mixed with ceramic tiles wastage of varying size in different proportions.

3.1 Test Programme

The test programme included the preliminary tests for dune sand and mix compositions of dune sand with ceramic tiles wastage. Following tests were carried out :

1. Determination of particle size distribution of dune sand.
2. Standard Proctor Test for determining maximum dry density and optimum moisture content. (For dune sand and mix composition with ceramic tiles wastage).
3. CBR Test to determine CBR values for dune sand and mix compositions with ceramic tiles wastage.
4. Direct Shear Test to determine shear stress of dune sand and mix compositions with ceramic tiles wastage.

Table 1 : Particle Size Distribution of Dune Sand

S.No.	Sieve Size (mm)	Weight retained (gm)	% weight retained	Cumulative % weight retained	Cumulative % weight passing	% Finer
1.	2.0	8.0	0.8	0.8	99.2	99.2
2.	1.0	4.0	0.4	1.2	98.8	98.8
3.	.600	3.0	0.3	2.2	98.1	98.1
4.	.425	3.0	0.3	2.2	97.8	97.8
5.	.300	6.0	0.6	2.8	97.2	97.2
6.	.150	894.0	89.4	92.2	7.8	7.8
7.	.075	73.0	7.3	99.5	0.5	0.5
8.	Pan	5.0				

3.1.1 Standard Proctor Test Or Proctor Compaction Test

The result tabulated in the Table 1 shows that on increment of the ceramic tiles wastage in the dune sand, the maximum dry density (M.D.D.) of the mix composition increases. On the other hand, on increasing particle size of the ceramic tiles wastage the maximum dry density (M.D.D.) increases. The optimum moisture content (O.M.C.) also increased from 12 to 16 percent. The maximum dry density variations of mix compositions are shown in Figure1.

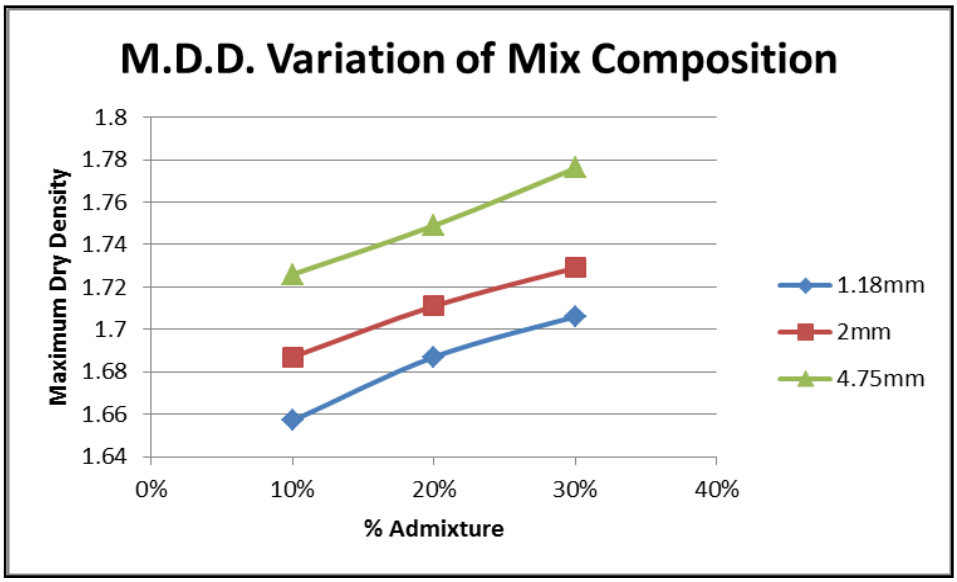

Figure 1: M.D.D. Variations Of Mix Compositions

3.1.2 California Bearing Ratio (CBR Test)

CBR Tests were conducted to determine CBR values of stabilized dune sand. Different proportions of ceramic tiles wastage were mixed in dune sand to perform the tests. 5 kg of soil was taken and mixed properly with proportion of ceramic tiles wastage and water equal to optimum moisture content obtained already by Standard Proctor Test.

The mix was compacted in 2250 ml CBR mould (150 mm diameter and 127.3 mm height) using light compaction. The mix was compacted in three equal layers; each layer being given 56 uniformly distributed blows of 2.6 kg rammer. Top surface of the specimen was finished properly to make it even for loading test. The next day, the samples were tested for the determination of CBR values in soaked condition.

For obtaining the CBR values of unsoaked & soaked samples penetration tests were done. The mould, containing the specimen was mounted on the testing machine and a surcharge weight equal to 5 kg (two spacer discs) was placed on the top of specimen before starting the penetration test. After setting the plunger on the surface of specimen and setting the load and penetration measuring dial gauge to read zero the load was applied. Load readings at every 0.5 mm were noted and a graph was drawn between the load (ordinate) and penetration (abscissa). In most of the tests the curve was either straight or convex upwards in the initial portion. In such cases the test load corresponding to 2.5 mm and 5.0 mm were read from the curve. If, in case the curve, in its initial portion comes to be concave upwards, in those cases the corrected origin point is to be shifted to the point of greatest slope with the penetration axis.

Test results obtained show that CBR value increases with increase in ceramic particle size. The CBR value for same size ceramic particles in mix composition increases with increase in percentage of ceramic particles. The tables and graphs are shown in the coming pages.

IV. COMPARATIVE STUDY

We have graphically represented the variations in C.B.R. values in the graphs below for both unsoaked and soaked conditions. On the graph, at abscissa (x-axis) ceramic particles percentage of sand varying from 5% to 30% at an interval of 5% has been marked and on ordinance (y axis) C.B.R. values have been plotted for mix compositions of ceramic tiles wastage passing 4.75mm, 2.0mm, 1.18mm and 425□ .

From graphs it can be seen that on increment of particle size of admixture, the C.B.R. value of the mix composition increases. Also as the quantity or percentage of admixture increases, the C.B.R. value of the mix

composition increases. Hence it can be concluded that to use the mix compositions in base and sub base constructions, the C.B.R. values can be increased or decreased as needed.
Variations in C.B.R. values at different percentages of mix composition at different size also show that increase in C.B.R. values is more at unsoaked condition than that compared with soaked condition.

Table 2: CBR Value Variation in Mix Compositions in Unsoaked Conditions

Admixture (%)	CBR(%)			
	Mix composition			
	425 µ Sieve	1.18 mm Sieve	2 mm Sieve	4.75 mm Sieve
5	1.255	1.674	1.883	2.511
10	2.197	2.511	2.824	3.766
15	3.138	3.452	3.766	4.394
20	3.452	3.766	4.08	5.021
25	4.08	4.394	5.021	6.277
30	4.394	5.021	5.963	6.591

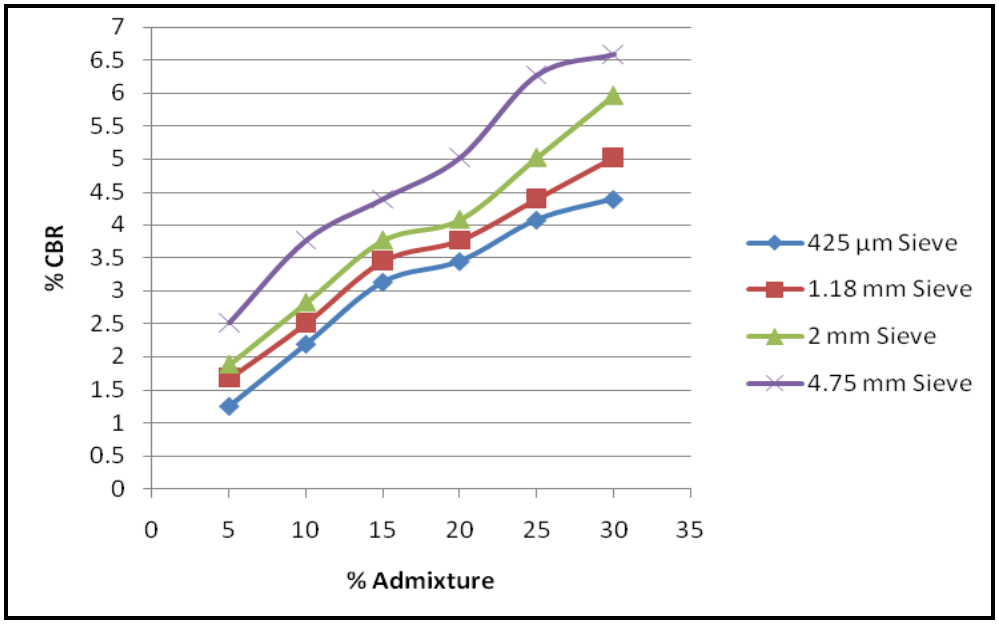

Figure2: CBR Value Variation in Mix Compositions in Unsoaked Conditions

Table 3: CBR Value Variation in Mix Compositions in Soaked Conditions

Admixture (%)	CBR (%)			
	Mix composition			
	425 µ Sieve	1.18 mm Sieve	2 mm Sieve	4.75 mm Sieve
5	1.046	1.255	1.464	1.674
10	1.255	1.464	1.674	1.883
15	1.673	1.883	2.197	2.511
20	2.197	2.511	2.72	3.138
25	2.301	2.511	2.72	3.138
30	2.511	2.929	3.347	3.452

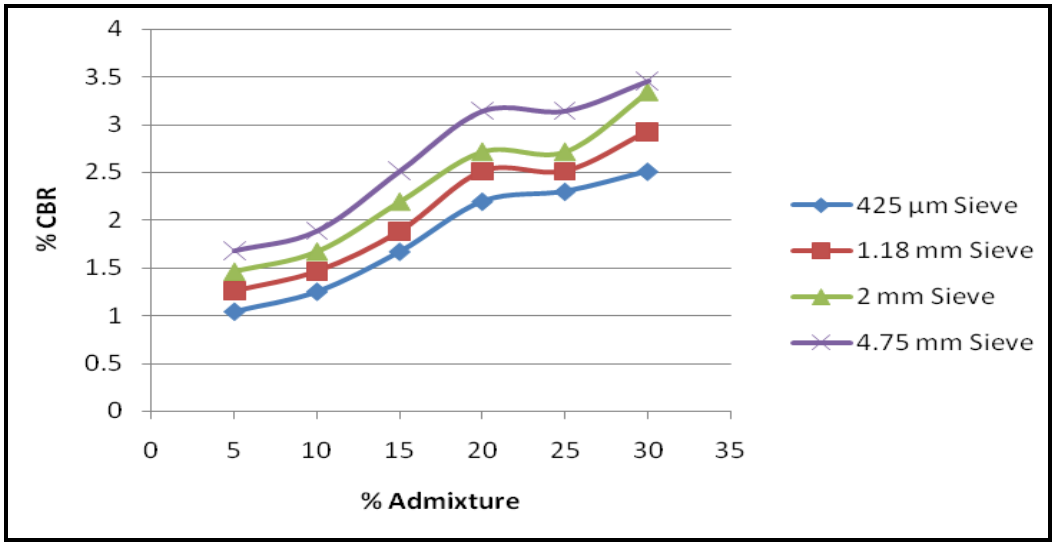

Figure 3: CBR Value Variation in Mix Compositions in Soaked Conditions

V. DIRECT SHEAR TEST

Direct shear tests were performed on mix composition of ceramic particles of size passing sieve 4.75 mm, 2.0 mm and 1.18 mm with 10%, 20% and 30% of sand. Tests were carried out with a strain controlled shear apparatus at rate of 1.25 mm/min to determine failure stress and angle of internal friction ( ) of different mix composition.

From the results obtained it can be concluded that angle of internal friction varies with increase in size of ceramic tiles wastage in mix composition. On the other hand for the same size of ceramic tiles wastage, the angle of internal friction increases with increase in percentage or quantity of ceramic tiles wastage.
Variation of failure stress and angle of internal friction of 4.75mm, 2mm and 1.18mm sieve size at 10%, 20% and 30% admixture has been presented graphically and tabulated in following tables.

5.1 Comparative Study

A comparative study of variation of stresses has been made from the test results in preceding tables. For variation of shear stress graphs showing on x-axis normal stress 0.1 kg /cm2, 0.2 kg/cm2, 0.3 kg /cm2 and on y-axis corresponding shear stress at 10%, 20% and 30% admixture of 1.18 mm,2.0 mm and 4.75 mm sieve have been presented and tabulated in following tables .

It has been found from the study that on keeping normal stress as constant, as the particle size or the quantity of the admixture increases, the shear stress value of the mix composition increases. Also for the same particle size of admixture ,the shear stress values of the mix composition increases as the normal stress increases.

Table 4 : Variation of shear stress for 10% Admixture of 4.75mm, 2 mm and 1.18mm sieve.

Normal Stress(kg/cm2)	Shear Stress (kg/cm^2) Mix composition		
	1.18mm pass sieve	2mm pass sieve	4.75mm pass sieve
0.1	0.1518	0.1848	0.2178
0.2	0.2244	0.2706	0.3168
0.3	0.2970	0.3564	0.4158

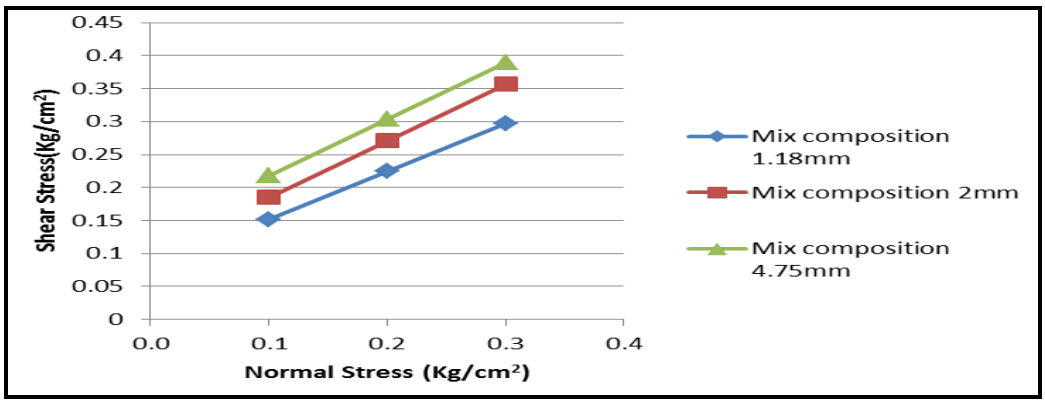

Figure 4 : Variation of shear stress for 10% Admixture of 4.75mm, 2 mm and 1.18mm sieve.

Table 5: Variation of shear stress for 20% Admixture of 4.75mm, 2 mm and 1.18mm sieve.

Normal Stress(kg/cm2)	Shear Stress (kg/cm²) Mix composition		
	1.18mm pass sieve	2mm pass sieve	4.75mm pass sieve
0.1	0.2046	0.2442	0.2838
0.2	0.3036	0.3630	0.4224
0.3	0.4026	0.4618	0.5610

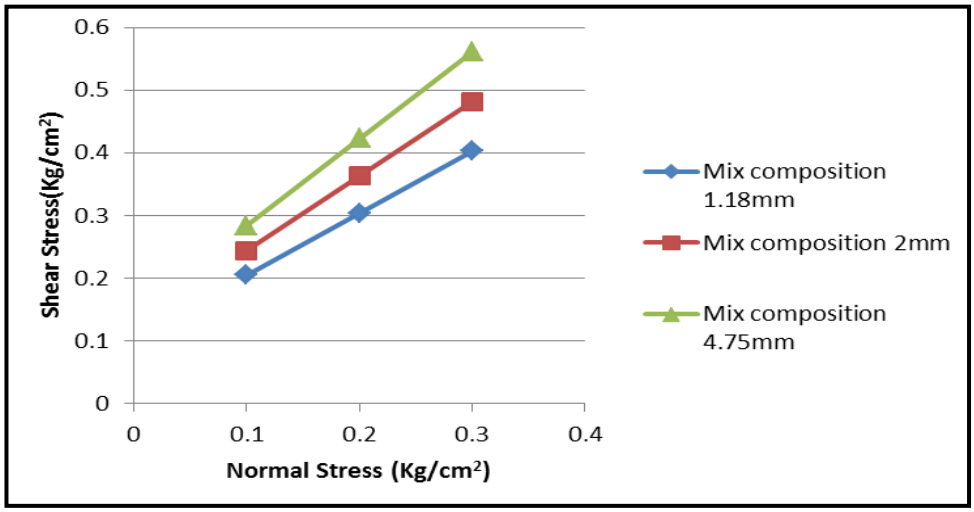

Figure 5: Variation of shear stress for 20% Admixture of 4.75mm, 2 mm and 1.18mm sieve.

Table 6 : Variation of shear stress for 30% Admixture of 4.75mm, 2 mm and 1.18mm sieve.

Normal Stress(kg/cm2)	Shear Stress (kg/cm²) Mix composition		
	1.18mm pass sieve	2mm pass sieve	4.75mm pass sieve
0.1	0.2376	0.2838	0.3366
0.2	0.3564	0.4224	0.5016
0.3	0.4752	0.5610	0.6666

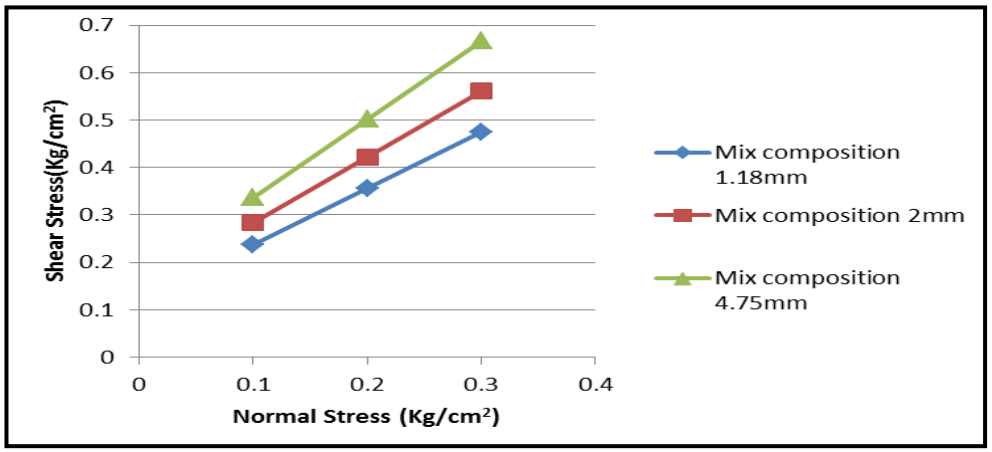

Figure 6 : Variation of shear stress for 30% Admixture of 4.75mm, 2 mm and 1.18mm sieve.

VI. CONCLUSIONS

The investigations were carried out with the view of exploring the possibilities of stabilizing dune sand with ceramic tiles wastage as admixture. Various experiments were performed on mix compositions of dune sand with ceramic tiles wastage as admixture and it was found that with increasing percentage and particle size of admixture the stabilization of dune sand was achieved.

The main conclusions drawn from the investigations performed are:

1. The maximum dry density of mix-composition of dune sand and ceramic tiles wastage as admixture increases on increasing particle size of admixture. Also for same particle size of admixture the M.D.D. increases on increasing the quantity of admixture (increment from 10% to 30%).
2. A linear increment was observed in CBR values in both unsoaked and soaked conditions. CBR tests were performed on mix compositions of dune sand and ceramic tiles wastage as admixture. Ceramic tiles wastage passing sieve size 4.75 mm, 2.0 mm, 1.18 mm and 425 μ of varying percentages 5%, 10%, 15%, 20%, 25% and 30% were mixed with dune sand. For unsoaked condition, CBR values are greater than that of soaked condition for same particle size and quantity of admixture.
3. In the Direct Shear Test, angle of internal friction (shearing resistance) Φ increases with increase in size of ceramic tiles wastage in mix composition. The Shear Tests were performed for mix compositions of dune sand with ceramic tiles wastage passing sieve size 4.75 mm, 2.0 mm and 1.18 mm of varying percentages 10%, 20% and 30%. The angle of internal friction (shearing resistance) Φ also increases with the quantity of the ceramic tiles wastage.
4. On the basis of the experiments performed it has been concluded that loose dune sand transform after stabilization into a strong rigid mass.

REFERENCES

[1]. Ameta N.K. and Abhay Shivaji Wayal : "Effect of Bentonite on Permeability of Dune Sand". E.J.G.E., Vol. 13 – Bundle A, 2008.
[2]. Ameta N.K., D.G.M. Purohit and Abhay Shivaji Wayal : "Characteristics, Problems and Remedies of Expansive Soils of Rajasthan, India". E.J.G.E., Vol. 13- Bundle A, 2008.
[3]. Ameta N.K., Purohit D.G. M and Wayal A.S., "Behavior of Square Footing on Dune Sand Reinforced with Nylon Fibre" April 2009, International Journal of Geotechnical Engineering, Volume 3, Issue 2, pp 313-317.
[4]. Jain, O.P. and Jain, B.K. "Earthwork Brick Properties" Nem Chand and Brothers Publishing Company. Journal of S.M.F.D., ASCE, Vol. 105, GTI, Paper No. 14335, Jan 1979.
[5]. K.R. Arora "Soil Mechanics and Foundation Engineering", Standard Publishers and Distributors, New Delhi.
[6]. Kevin, M: "Micro Characteristics of Chemical Stabilized Granular Materials". Journal of GT, Proceedings of ASCE, Vol. 104, No. GT7, 1978.
[7]. Wayal A.S., Ameta N. K., Purohit D.G. M., "Dune sand stabilization using bentonite and lime", JERS, Volume III, Issue I, Jan-March 2012, pp 58-60.Ameta N.K. and Abhay Shivaji Wayal : "Effect of Bentonite on Permeability of Dune Sand". E.J.G.E., Vol. 13 – Bundle A, 2008.

American Journal of Engineering Research (AJER)
e-ISSN : 2320-0847 p-ISSN : 2320-0936
Volume-02, Issue-09, pp-140-161
www.ajer.org

Research Paper Open Access

MHD Natural convection in the localized heat sources of an inclined trapezoidal Nanofluid-filled enclosure

M. A. Mansour, A.Y. Bakier, M. A. Y. Bakeir
Department of Mathematics, Faculty of Sciences, Assiut University, Assiut, Egypt

Abstract: - The effects of magnetic force, acting vertically downward on natural convection within a nanofluid filled tilted trapezoidal enclosure saturated with an electrically conducting fluid have been investigated numerically. The bottom wall of the enclosure is subjected to a constant cold temperature and the top wall experiences a heat source whereas the remaining sidewalls are kept adiabatic. The physical problems are represented mathematically by different sets of governing equations along with the corresponding boundary conditions. By using approximations of finite difference method, the non-dimensional governing equations are discritized. For natural convection the influential parameters are Rayleigh number Ra, the rotational angle of the enclosureΦ and the Hartmann number Ha, through which different thermo-fluid characteristics inside the enclosure are obtained. In the present study, the obtained results are presented in terms of streamlines, isotherms and average Nusselt number along the heat source. The result shows that with increasing Ha, the diffusive heat transfer become prominent even though Rayleigh number increases. Optimum heat transfer rate is obtained at higher values of Ra in the absence of magnetic force.

Keywords: - *magneto-hydrodynamics, inclination angle, nanofluid, Rayleigh number, solid volume fraction.*

I. INTRODUCTION

Magnetohydrodynamic (MHD) flow and especially when associated with heat transfer have received considerable attention recent years because of their wide variety of application in engineering areas such as crystal growth in liquid, cooling of nuclear reactor, electronic package, microelectronic devices, solar technology, etc. in case of free convection of an electrically conducting fluid in presence of magnetic field, there are two body force, buoyancy force and Lorentz force. They interact with each other an influence on heat and mass transfer, so it is important to study the detailed characteristics of transport phenomena in such a process to have a better product with improved design. A porous medium consists of a solid matrix with an interconnected void. This solid matrix is either rigid or deformable [1-2]. Porous materials such as sand and crushed rock underground saturated with water, which, under the influence of local pressure gradients, migrates and transports energy through the material. Natural convection heat transfer in a cavity saturated with porous media in the presence of magnetic field is a new branch of thermo-fluid mechanics.

The heat transport phenomenon can be described by means of the hydrodynamics, the convective heat transfer mechanism and the electromagnetic field as they have a symbiotic relationship [3–7]. The flow within an enclosure consisting of two horizontal walls, at different temperatures, is an important circumstance encountered quite frequently in practice. In all the applications having this kind of situation, heat transfer occurs due to the temperature difference across the fluid layer, one horizontal solid surface being at a temperature higher than the other. If the upper plate is the hot surface, then the lower surface has heavier fluid and by virtue of buoyancy the fluid would not come to the lower plate. Because in this case the heat transfer mode is restricted to only conduction. But if the fluid is enclosed between two horizontal surfaces of which the upper surface is at lower temperature, there will be the existence of cellular natural convective currents, which are called as Benard cells. For fluids whose density decreases with increasing temperature, this leads to an unstable situation. Benard [8] mentioned this instability as a “top heavy” situation. In that case fluid is completely stationary and heat is transferred across the layer by the conduction mechanism only. Rayleigh [9] recognized that this unstable situation must break down at a certain value of Rayleigh number above which convective motion must be

generated. Jeffreys [10] calculated this limiting value of Ra to be 1708, when air layer is bounded on both sides by solid walls.

The symbiotic interaction between the fluid velocity field and the electromagnetic forces give rise to a flow scenarios; the magnetic field affects the motion. Natural convection in an enclosure saturated with porous medium plays a significant role in many practical applications. Among those, geophysical systems: heat exchange between soil and atmosphere, dynamics of terrestrial heat flow through aquifer; compacted beds for the chemical industry, high performance insulations for cryogenic containers, sensible heat storage beds, food processing, grain storage, solar power collectors, flows over heat exchanger pipes, cooling of electronic systems, cooling of radioactive waste containers and the post-accidental heat removal in nuclear reactors have become increasingly important to the engineers and scientists. In this analysis, the effects of permeability and different thermal boundary conditions on the natural convection in a square porous cavity by using Darcy–Forchheimer model [11] and Darcy–Brinkman-Forchheimer model [12, 13] have been studied numerically. The tilted position of the enclosure [14–16] has a significant influence on the natural convection. Mahmud and Fraser [17] examined the flow, temperature and entropy generation fields inside a square porous cavity under the influence of magnetic field using Darcy model. The momentum equation including Navier–Stokes inertia term and Brinkman viscous diffusion term derived for the porous media in the presence of magnetic field makes the present works discernible. The main attribute for choosing the trapezoidal shape cavity is to enhance the heat transfer rate as it could be said intuitionally due to its extended cold top surface. Contextually the present study will focus on the computational analysis of the influence of magnetic field on the natural convection in a trapezoidal enclosure saturated with porous medium of constant porosity.

Nanotechnology has been widely used in industry since materials with sizes of nanometers possess unique physical and chemical properties. Nano-scale particle added fluids are called as nanofluid which is firstly introduced by Cho [18]. Use of metallic nanoparticles with high thermal conductivity will increase the effective thermal conductivity of these types of fluid remarkably. Because nanofluid consists of very small sized solid particles, therefore in low solid concentration it is reasonable to consider nanofluid as a single phase flow [19]. There are many numerical studies on natural convection flow of nanofluid in different geometries. The computational studies are much disputed, because the majority results have reported an enhancement in heat transfer due to the presence of nanoparticles [20–23]. It seems that the first numerical study of natural convection of Copper (Cu)–water nanofluid in a two dimensional enclosure was done by Khanafer et al. [20]. The nanofluid in the enclosure was assumed to be in single phase. It was found that for any given Grashof number, the average Nusselt number increased with the solid volume concentration parameter. Mahmoudi et al. [21] investigated numerically the effect of position of horizontal heat source on the left vertical wall of a cavity filled with Cu–water nanofluid. Their results showed that the presence of nanoparticles at low Ra was more pronounced; also when the heat source was located close to the top horizontal wall, nanofluid was more effective. Oztop and Abu-Nada [22] considered natural convection in partially heated enclosures having different aspect ratio and filled with nanofluid. They found that the heat transfer was more pronounced at low aspect ratio and high volume fraction of nanoparticles. Aminossadati and Ghasemi [23] considered the effect of apex angle, position and dimension of heat source on fluid flow and heat transfer in a triangular enclosure using nanofluid. They found that at low Rayleigh numbers, the heat transfer rate continuously increases with the enclosure apex angle and decreases with the distance of the heat source from the left vertex. Natural convection in trapezoidal enclosures has been the subject of interest for many studies due to its important application in various fields such as electronic components and solar collectors. Although, there are some valuable studies on natural convection in trapezoidal enclosures using pure fluid [24–26], only a few works considered the effect of nanofluid [27, 28]. But no attempt was made to optimize the problem. This can be done by using the Entropy Generation Minimization technique as introduced by Bejan [29]. However, there are only a few studies that consider the second thermodynamic laws in the presence of nanofluids [30–31]. Shahi et al. [30] numerically studied the entropy generation and natural convection in a square cavity with a vertical heat source which is filled with copper–water nanofluid. They have considered entropy generation and heat transfer for a wide range of the Rayleigh number, solid volume fraction parameter and different positions of the heat source. The present study will focus on the computational analysis of the influence of magnetic field on the nanofluid in natural convection in a tilted trapezoidal enclosure saturated with porous medium of constant porosity.

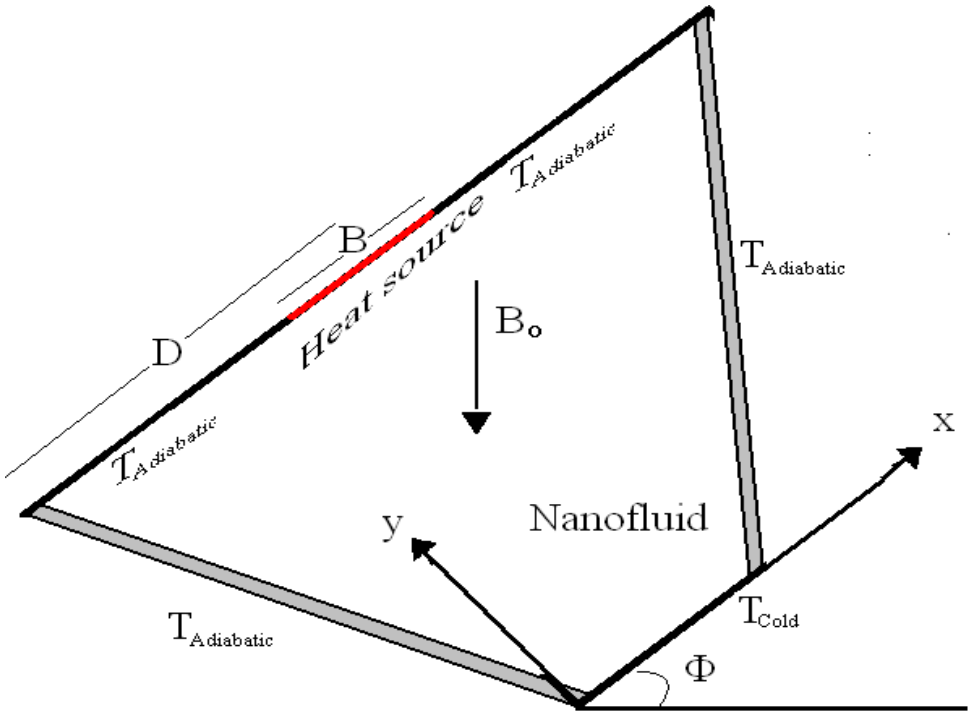

Fig. 1. Schematic diagram of physical problem.

II. MATHEMATICAL MODEL

Fig. 1 shows the flow model used. Consider same assumptions mentioned, then the governing equations of momentum is deducted as (Mamun et al. (2010), Basak et al. (2009) and Mansour et al. (2010)). Moreover, using the same dimensionless transforms (Eq. (12)); the governing equations can be formulated as:

Continuity equation,

$$\frac{\partial U}{\partial X}+\frac{\partial V}{\partial Y}=0 \tag{1}$$

Momentum equation,

$$\frac{\partial \psi}{\partial y}\frac{\partial \Omega}{\partial X}-\frac{\partial \psi}{\partial x}\frac{\partial \Omega}{\partial Y}=\frac{\mu_{nf}}{\rho_{nf}\alpha_f}\left(\frac{\partial^2\Omega}{\partial X^2}+\frac{\partial^2\Omega}{\partial Y^2}\right)$$
$$+Ha^2\,\mathrm{Pr}\frac{\sigma_{nf}}{\sigma_f}\frac{\rho_f}{\rho_{nf}}\left[\cos\Phi\frac{\partial^2\psi}{\partial Y^2}+\sin\Phi\frac{\partial\psi}{\partial Y\partial X}\right]$$
$$+Ra\,\mathrm{Pr}\frac{\rho_f}{\rho_{nf}}\left[1-\varphi+\frac{(\rho\beta)_s}{(\rho\beta)_f}\varphi\right]\left(\cos\Phi\frac{\partial\theta}{\partial Y}+\sin\Phi\frac{\partial\theta}{\partial X}\right) \tag{2}$$

Where Ha (= $\beta_0 W(\sigma/\mu)^{0.5}$) is Hartmann number, σ electrical conductivity and Φ is the inclination angle.

$$\Omega=\frac{\partial V}{\partial X}-\frac{\partial U}{\partial Y}=-\nabla^2\psi \tag{3}$$

$$\frac{\partial \psi}{\partial Y}\frac{\partial \theta}{\partial X}-\frac{\partial \psi}{\partial X}\frac{\partial \theta}{\partial Y}=\frac{\alpha_{nf}}{\alpha_f}\left(\frac{\partial^2\theta}{\partial X^2}+\frac{\partial^2\theta}{\partial Y^2}\right) \tag{4}$$

The boundary conditions are

Bottom wall : $\psi=0,\theta=0$ (5 a)

Top wall : $\psi=0,\theta=1;\ D-B/2<X<D+B/2$ (5 b)

Otherwise : $\psi=0,\frac{\partial\theta}{\partial n}=0$ (5 c)

Sides' walls: $\psi = 0, \frac{\partial \theta}{\partial n} = 0$ (5 d)

where *n* is a vector perpendicular to the side wall.

Numerical method and validation

Equations (1)-(4) subject to the boundary conditions (5) are solved numerically by using the finite difference methodology. Then all these analyses are implemented in a FORTRAN program. The solution procedure is iterated until the following convergence criterion is satisfied:

$$\sum_{i,j} | \chi_{i,j}^{new} - \chi_{i,j}^{old} | \leq 10^{-7}$$

where χ is the general dependent variable. Prior to the simulations (Ching-Chang Cho et al., 2012), a grid –independence analysis has been performed to determine the mesh size which achieved the optimal compromise between the computational cost of the solution procedure and the numerical accuracy.

The finite difference method uses four sets of grids: 882, 1922, 3362, and 5202. There is a good agreement was found for 1922 nodes as shown in table 1. In order to verify the accuracy of present method, the obtained results in special cases are compared with the results obtained by Walker and Homsy (1978), Gross et al. (1986), Manole and Lage (1992). Table 3 shows a good agreement was found between the present results and the results obtained by the previous works in the test case. These favorable comparisons lend confidence in the numerical results to be reported subsequently.

Table 1 Grid independency results

	Nu_m	θ_{max}	ψ_{max}	ψ_{min}
882	5.602	0.183	0.682	-1.290
1922	5.593	0.185	0.706	-1.292
3362	5.768	0.181	0.777	-1.292
5202	6.054	0.173	0.877	-1.292

Table 2. Thermo-physical properties of water and nanoparticles.

	Pure water	Copper (Cu)
$\rho(kgm^{-3})$	997.1	8933
$C_p(Jkg^{-1}K^{-1})$	4179	385
$k(Wm^{-1}K^{-1})$	0.613	401
$\beta(K^{-1})$	21×10^{-5}	1.67×10^{-5}
σ	0.05	$5.96\text{x}10^{7}$

Table 3. Comparison of ψ_{max}.

Ra	Haajizadeh et al. [38]	Grosan et al. [36]	Present
	ψ_{max}	ψ_{max}	ψ_{max}
10	0.078	0.079	0.0799
10^3	4.880	4.833	4.8266

III. RESULTS AND DISCUSSION

Metamorphosis of thermo-fluid fields have described. There exists a counter circulating cell in Fig. 2, where the core of the vortex lays in the left upper region of the cavity near the heat source, D=-0.5, and therefore fluid has crowded in the left half of the enclosure. As the inclination angle increases, the fluid motion increases which mean the obvious effect of buoyancy force. Hydrodynamic boundary layer along all walls except for the right inclined sidewall. Isotherms are polarized in the left-upper corner. Therefore the thermal boundary layer is very small in the inclined sidewall. It's observed stratification for temperature field. The effect of magnetic force is multiple with buoyancy force because they experience in the same direction. For inclination angle greater than 45° the flow tends to stretch diagonally. Fig. 3 shows the nano case; the hydro-field for circulating cell has been zoned from the extreme left-upper corner due to the existence of nanoparticles through the fluid, and the geometric attributes for this corner. It can be observed a week rotation clockwise has been formed as a counter effect of duple governing force which producing the circulating cells extensively regions in

the cavity. So in this corner the viscous force is prominent. As the inclination angle increases, the resultant force decays because the buoyancy force is not being still work at the same destination of magnetic force. Thereby the effect of viscous force has been destroyed. Increasing of the inclination angle the primary circulation cell are stretching diagonally until it is becoming 90 where the magnetic force is perpendicular to buoyancy force. The buoyancy force gets the flow move upward for away from the left-upper corners. On other hand, Ha generates the viscous diffusion flow. These two phenomena make three circulating cells, the strength of them increases as flow moves toward the right side. Flow comes from the cold wall to hot wall thereby diffusion currents are overwhelmed by convection currents. The extreme left portion resulting good thermal performance, while the extreme right region represents diffusion dominated zone where the motion is very strong since it's only subjected to the normal magnetic field. It's noticed that there are two circulating cells in the ends which are in the anti-clockwise direction, so that the circulating cell entrapped with them is in the clockwise direction. By continue, the primary vortex grasps with other circulating cells. All of them expand paralleling to the secondary diagonal direction. Temperature keeps invariant during the round. Until the angle = 90, a huge disturbance happens because of the appearance of diffusion heat transfer in the right part. The effects of heat source location, heat source length and Hartmann number are showed in Figs. 4-6. The core of vortex follows D's movement it is noticeable there is no similarity even if the heat source location in the bisection way because Ha effect is regular along the top surface. In the same direction the effect buoyancy force acting from the source. It is observed the similarity between each pairs of corresponding cases such as the two cases of D=-0.5 and 1.5. As B increases the circulating cell has stretched horizontally and then the hydrodynamic boundary layer decreases. Also the stratification in the isotherms increases indicating the strong influence of viscous diffusion. It is observed that the temperature gradients increase as B increases at the vicinity of tilted left surface, where the inclination angle =45 the thermal boundary layers very tinny along this surface invoking the supremacy of convection heat transfer. For low Ha the motion is regularly at whole the cavity where a singular circulating cell and counter clockwise direction of motion. As Ha increases the circulating cell squeezes toward the nearest side to the heat source. Because the intensity of magnetic force increases the resulting recirculation cell experience the retarding motion. The diffusion current starts to dominate the convection current. As the magnetic force triumphs over buoyancy force, the core of the vortex shifts toward the source. By increasing of Ha, a core of circulating cell is shifted resulting formulation a stagnation point in the left upper corner. Also, temperature lines switch toward the left side decelerating the formulation of thermal boundary layer. At Ha =100, multicellaur formulation is appeared in the cavity. The weaker zone is shifted and the major vortex is entrapped by two minor vortices so the diffusion flow becomes more prominent. The oscillating thermal boundary layer represents the dominancy of diffusion heat flux. Figs. 7-9 display the effect of Ha, D and B in the nano case. The symmetry in streamlines in Fig. 7 which appears two contour rotating vortices is due to symmetrical dynamic flow and symmetrical boundary condition. At the absence of magnetic force the strength of circulating cell is high relatively. Thermal boundary layer in the left side has more effect than the right side. As Ha increases the core of vortex stretched toward the source. Increasing Ha also leads to increase temperature gradient and increase heat transfer rate consequently. Comparing with Fig. 4, considering the change in the inclination angle, it is observed the relation between D and buoyancy force which appears its effect in generation of vortices and the relation between D and temperature gradient reflecting the effective range of diffusion heat transfer and size of thermal boundary layer. Variation of B explains the link between heat source and the idiosyncratic attributes for thermo-flow application. As B increases the fluid motion tends to take the anti-clockwise direction, therefore at B=2 there exists three cores. Two of them are produced by the stretch happening in the counter circulation cell. For isotherms, the changing of B is related to the stratification of temperature lines which ensures the dominancy of diffusion heat transfer. For moderate value of Ha=5, Figs 10 and 11 show the effect of solid volume fraction in various titled positions. By studying the scenario of change horizontally, it confirms the argument of Fig. 2 the vertically studying, for the familiar position the increase of solid volume fraction get the flow more be symmetric. But for other inclination positions, it is observed a shipment of core of vortices are generated and rigorous develop of plumage has been happened. The left circulating cell decays and minor vortices have grasped to the major vortex which expanded diagonally. Isotherms tend to cluster in the right portion as the inclination angle increases respect to the buoyancy force. The vertical scenario shows that the increase of the angle leads to increase the diffusion current. For Figs. 12 and 13, increases in Ha result in increase the polarization of the core of circulating cells toward the source, which appears by horizontal change. Also it leads to increase the diffusion current adding to convection current. The vertical scenario shows at the absence of magnetic force, increasing in Ra makes the flow unsymmetrical. Also it strengthens the counter circulation cell and increases the convection heat transfer. Fig. 14 shows the symmetrical behavior of local Nusselt number. As B decreases, the heat transfer rate increases, moreover, the temperature gradients increases. Fig. 15 offers the symmetrical behavior of Nu –local- around the D, which strengthens the heat transfer rate. Figs 16 and 17 ensure the previous argument about Figs. 14 and15. It shows

the effect of inclination angle on the heat transfer generally. Fig. 18 deduces that Nu_m slightly decreases as the solid volume fraction increases except for B=0.2 because the greatest value of temperature gradient and heat transfer rate. It is showed that Nu_m increases as B decreases. Fig. 19 and 20 show the average Nusselt number increases with the solid volume fraction for constant parameters' motion except for Ha which decreases the Nu_m. When Ra is the only variable in the Nu_m-φ relation, Nu_m increases linearly with φ and Ra enhances it. As the inclination angle increases in Fig. 21, Nu_m increases. The relation between Nu_m-φ is irregular; however Nu_m increases with φ linearly for the small angles. Nu_m increases with Ra as an exponentially behavior in Fig. 22 where Ra changes in logarithm way. Ha do not affect Nu_m for small Ra; otherwise, it has a huge effect for high Ra values. Figs. 23 -27 show relations V-X and temperature-X. Vertical velocity tends to be symmetrical for { φ, B , Ha} changes, while temperature tends to be more smooth for both Ha and Ra changes. At X=0.5, the maximum value for velocity when Ha=0 while for temperature when Ha=20. The global maximum temperature at B=2.

IV. CONCLUSION

Magneto-hydrodynamics (MHD) is the science of the motion of electrically conducting fluids under the influence of applied magnetic forces. A numerical study has been achieved for the natural convection cooling of a heat source mounted inside a trapezoidal cavity filled by Cu–water nanofluid in the presence of vertical magnetic field. It was observed that the increasing in inclination angle enhances the buoyancy force while the effect of viscous force has been vanished. At maximum inclination angle, the left part of the enclosure has good thermal performance but the right represents diffusion dominated zone where the motion is subject to the magnetic force. Increase of B produces a strong influence of viscous diffusion. In the left inclined surface, once the inclination angle equal 45 the flow invokes the supremacy of convection heat transfer. As Ha increases the temperature gradients increases, hence heat transfer rate increases. At Ha=100 the oscillating thermal boundary layer refers to the dominancy of diffusion heat flux. There is a strong relation between the heat transfer location and the temperature gradient in nanofluid which reflects the effective range of diffusion heat transfer and size of thermal boundary layer. It is noticed that as the solid volume fraction increases the diffusion currents increase. But as Ra increases the convection currents increase specially in the absence of magnetic force.

REFERENCES

[1] M.A.H. Mamun, Md.T. Islam, Md.M. Rahman, Natural convection in a porous trapezoidal enclosure with magneto-hydrodynamic effect, Nonlinear Analysis: Modelling and Control, 2010, Vol. 15, No. 2, 159–184.

[2] J. Bear, Dynamics of Fluids in Porous Media, American Elsevier publishing company, Inc., New York, 1972.

[3] D.A. Nield, A. Bejan, Convection in Porous Media, 3rd ed., Springer, New York, 2006.

[4] Transport Phenomena in Porous Media, D.B. Ingham, I. Pop (Eds.), Elsevier, Oxford, 2005.

[5] Hanbook of Porous Media, K. Vafai (Ed.), 2nd ed., Taylor & Francis, Boca Raton, 2005.

[6] Emerging Topics in Heat and Mass Transfer in Porous Media, P. Vadasz (Ed.), Springer, New York, 2008.

[7] I. Pop, D.B. Ingham, Convective Heat Transfer: Mathematical and Computational Modeling of Viscous Fluids and Porous Media, Pergamon, Oxford, 2001.

[8] H. B´enard, Formation p´eriodique de centres de giration `a l'arri`ere d'un obstacle en mouvement, C. R. Acad. Sci., 147, pp. 839–842, 1908.

[9] L. Rayleigh, On convection currents in a horizontal layer of fluid when the higher temperature is on the underside, Philos. Mag., 6(32), pp. 529–546, 1946.

[10] H. Jeffreys, Some cases of instabilities in fluid motion, P. Roy. Soc. Lond. A Mat., 118, pp. 195–208, 1928.

[11] N.H. Saied, I. Pop, Non-Darcy natural convection in a square cavity filled with a porous media, Fluid Dyn. Res., 36, pp. 35–43, 2005.

[12] F.Marcondes, J.M.Medeiros, J.M. Gurgel, Numerical analysis of natural convection in cavities with variable porosity, Numer. Heat Tr. A-Appl., 40, pp. 403–420, 2001.

[13] P. Nithiarasu, K.N. Seetharamu, T. Sundararajan, Numerical investigation of buoyancy driven flow in a fluid saturated non-Darcian porous medium, Int. J. Heat Mass Tran., 42, pp. 1205–1215, 1999.

[14] E. Baez, A. Nicolas, 2D natural convection flows in tilted cavities: Porous media and homogeneous fluids, Int. J. Heat Mass Tran., 49, pp. 4773–4785, 2006.

[15] A.C. Baytas, I. Pop, Natural convection in a trapezoidal enclosure filled with a porous medium, Int. J. Eng. Sci., 39, pp. 125–134, 2001.

[16] F.C. Lai, I. Pop, Natural Convection in a Truncated Circular Sector of Porous Medium, Int. Commun. Heat Mass, 17, pp. 801–811, 1990.
[17] S. Mahmud, R.A. Fraser, Magnetohydrodynamic free convection and entropy generation in a square porous cavity, Int. J. Heat Mass Tran., 47, pp. 3245–3256, 2004.
[18] Cho SUS. Enhancing thermal conductivity of fluids with nanoparticles. ASME Fluids Eng Division 1995;231:99–105.
[19] Xuan YM, Li Q. Heat transfer enhancement of nanofluid. Int J Heat Fluid Flow 2000;21:58–64.
[20] Khanafer K, Vafai K, Lightstone M. Buoyancy-driven heat transfer enhancement in a two-dimensional enclosure utilizing nanofluids. Int J Heat Mass Transfer 2003;46:3639–53.
[21] Mahmoudi AH, Shahi M, Raouf A, Ghasemian A. Numerical study of natural convection cooling of horizontal heat source mounted in a square cavity filled with nanofluid. Int Commun Heat Mass Transfer 2010;37:1135–41.
[22] Oztop HF, Abu-Nada E. Numerical study of natural convection in partially heated rectangular enclosures filled with nanofluids. Int J Heat Fluid Flow 2008;29:1326–36.
[23] Aminossadati SM, Ghasemi B. Enhanced natural convection in an isosceles triangular enclosure filled with a nanofluid. Comput Math Appl 2011;61:1739–53.
[24] Natarajan E, Basak T, Roy S. Natural convection flows in a trapezoidal enclosure with uniform and non-uniform heating of bottom wall. Int J Heat Mass Transfer 2008;51:747–56.
[25] Basak T, Roy S, Singh A, Balakrishnan AR. Natural convection flows in porous trapezoidal enclosures with various inclination angles. Int J Heat Mass Transfer 2009;52:4612–23.
[26] Varol Y, Oztop HF, Pop I. Natural convection in right-angle porous trapezoidal enclosure partially cooled from inclined wall. Int Commun Heat Mass Transfer 2009;36:6–15.
[27] Saleh H, Roslan R, Hashim I. Natural convection heat transfer in a nanofluid-filled trapezoidal enclosure. Int J Heat Mass Transfer 2011;54: 194–201.
[28] Nasrin R, Parvin S. Investigation of buoyancy-driven flow and heat transfer in a trapezoidal cavity filled with water–Cu nanofluid. Int Commun Heat Mass Transfer 2012;39:270–4.
[29] Bejan A. Entropy generation through heat and fluid flow. New York: Wiley; 1982.
[30] Mahmoudi AH, Shahi M, Talebi F. Entropy generation due to natural convection in a partialy open cavity with a thin heat source subjected to a nanofluid. Numer Heat Transfer A 2012;61:283–305.
[31] Shahi M, Mahmoudi AH, Honarbakhsh Raouf A. Entropy generation due to natural convection cooling of a nanofluid. Int Commun Heat Mass Transfer 2011;38:972–83.
[32] M. Mahmoodi, S. M. Hashemi, Numerical study of natural convection of a nanofluid in C-shaped enclosures, International Journal of Thermal Sciences 55 (2012) 76-89.
[33] Brinkman HC. The viscosity of concentrated suspensions and solutions. J. Chem. Phys. 1952;20:571–81.
[34] Maxwell JC. A treatise on electricity and magnetism. 2nd ed. Cambridge: Oxford University Press; 1904. p. 435–41.
[35] M.A. Mansour, A.J. Chamkha, R.A. Mohamed , M.M. Abd El-Aziz , S.E. Ahmed, MHD natural convection in an inclined cavity filled with a fluid saturated porous medium with heat source in the solid phase. Nonlinear Anal. 15(2010) 55–70.
[36] T. Grosan , C. Revnic, I. Pop, D.B. Ingham, Magnetic field and internal heat generation effects on the free convection in a rectangular cavity filled with a porous medium. Int. J. Heat Mass Transf. 52(2009)1525–1533.
[37] B.V. Ratish Kumar, P.V.S.N. Murthy, P. Singh, Free convection heat transfer from an isothermal wavy surface in a porous enclosure. Int. J. Numer. Meth. Fluids 28(1998) 633–661.
[38] M. Haajizadeh , A.F. Ozguc and C.L. Tien, Natural convection in a vertical porous enclosure with internal heat generation, Int. J. Heat Mass Transfer, 27(1984) 1893–190.

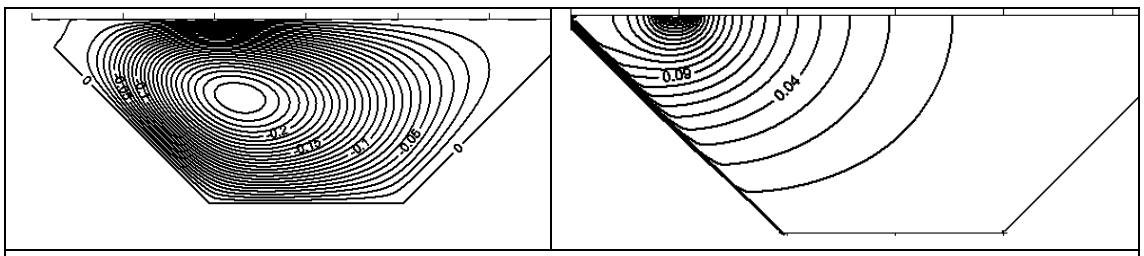

$\Phi = 0$

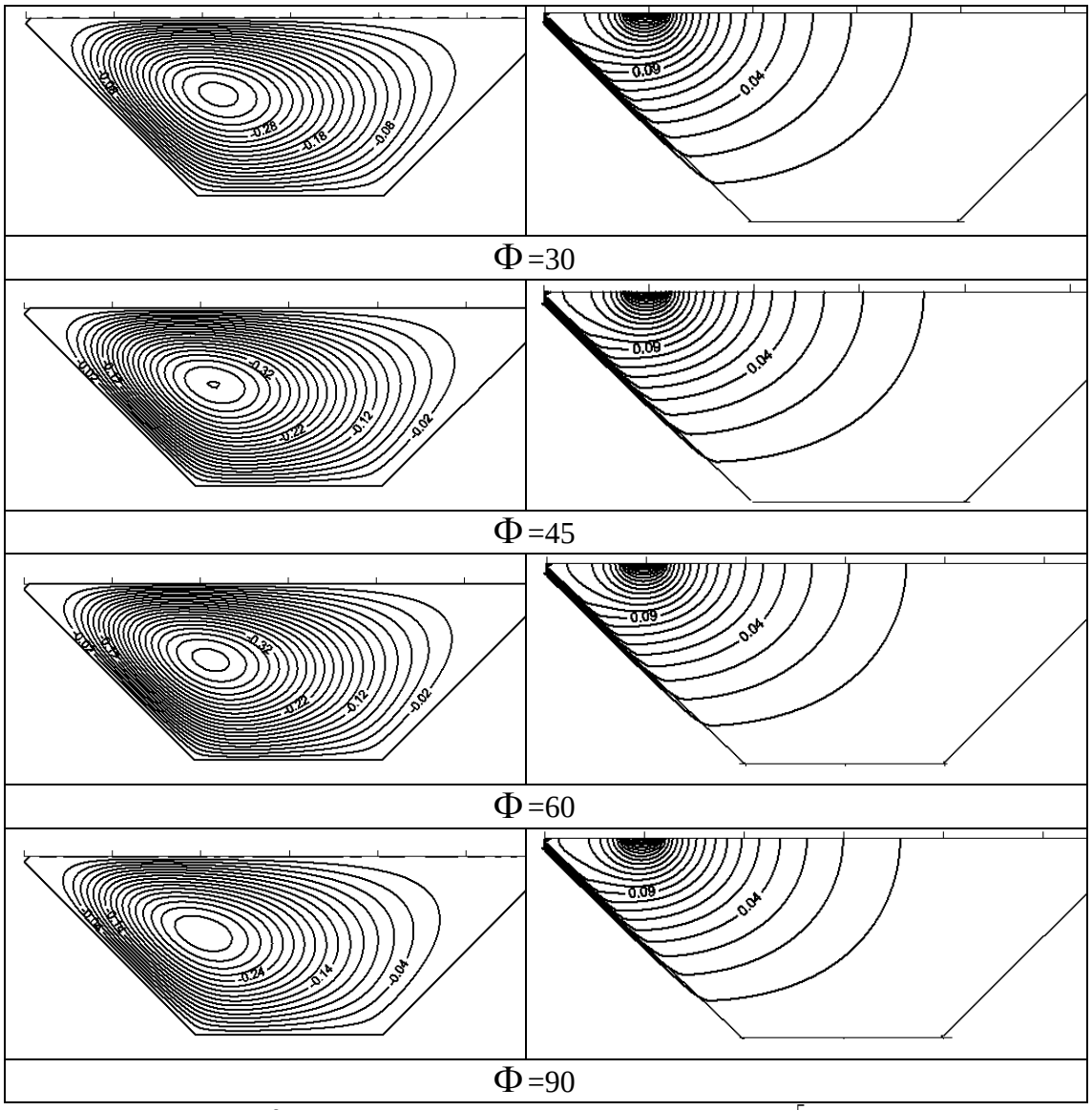

Fig 2 Streamlines (left) and isotherms (right) with Ha=5, Ra=10^5, B=0.2, D=-0.5, φ =0.

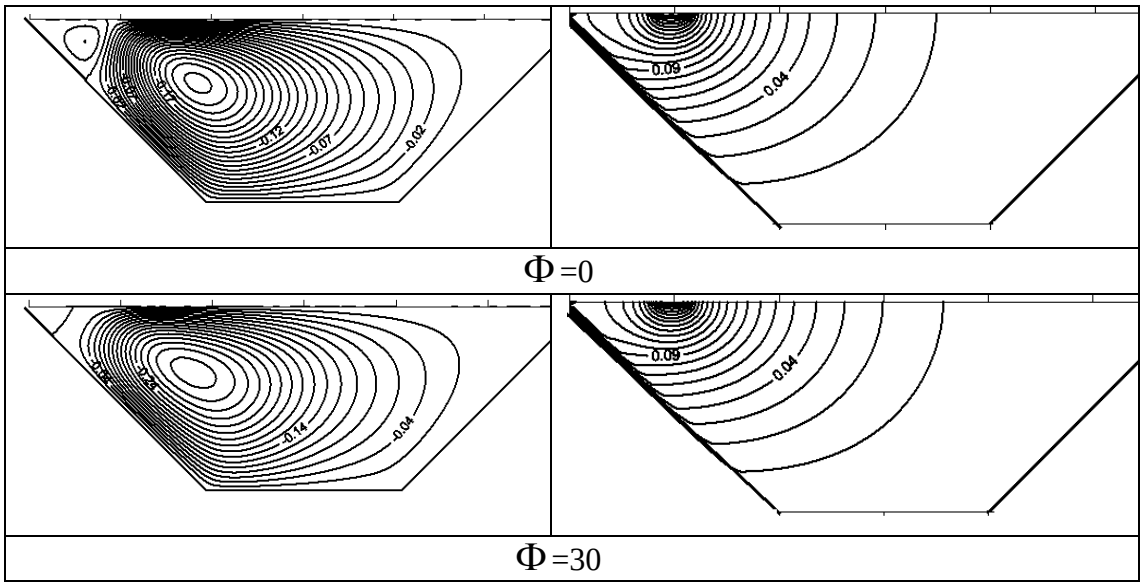

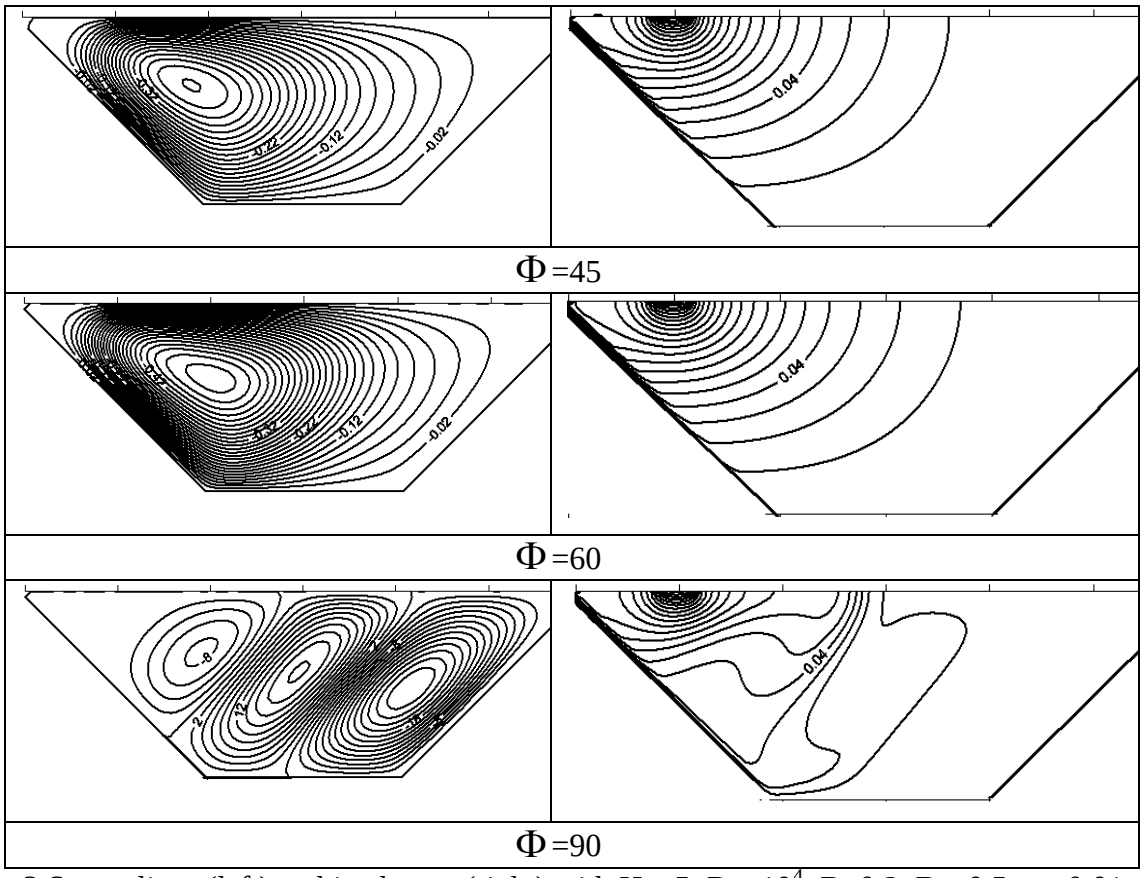

Fig 3 Streamlines (left) and isotherms (right) with Ha=5, Ra=10^4, B=0.2, D=-0.5, φ =0.01.

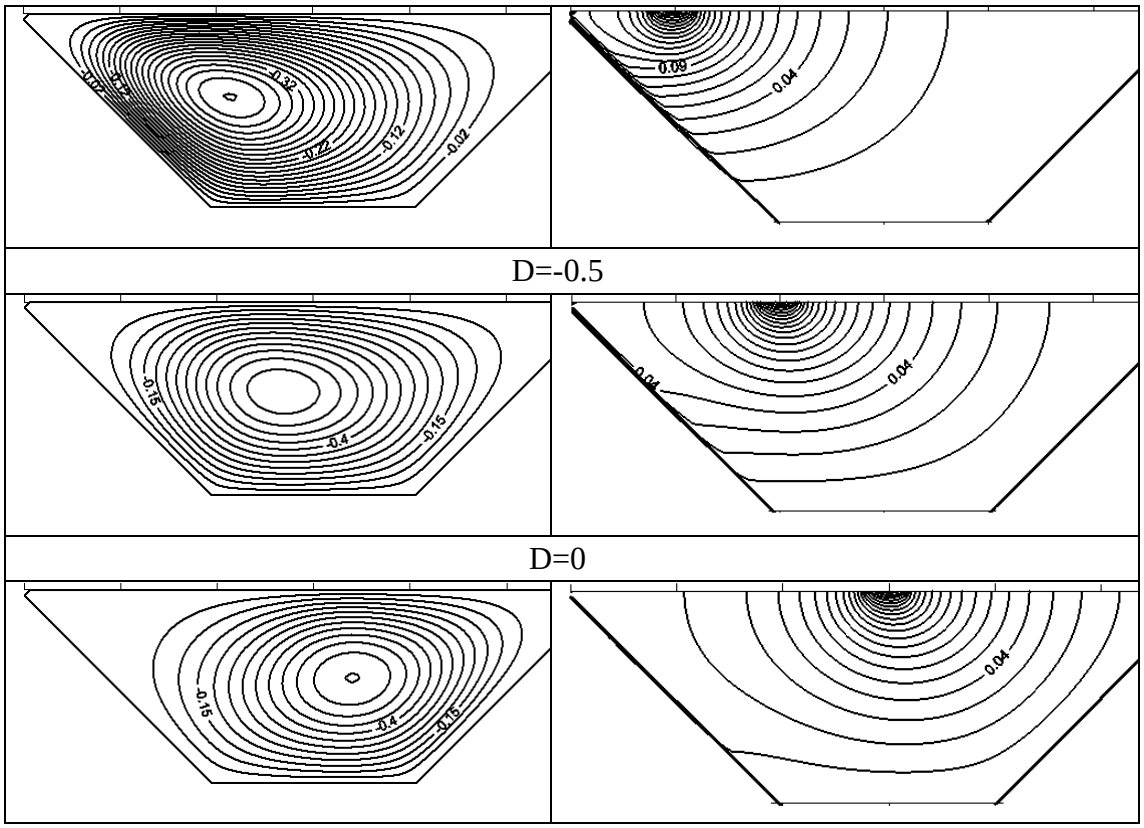

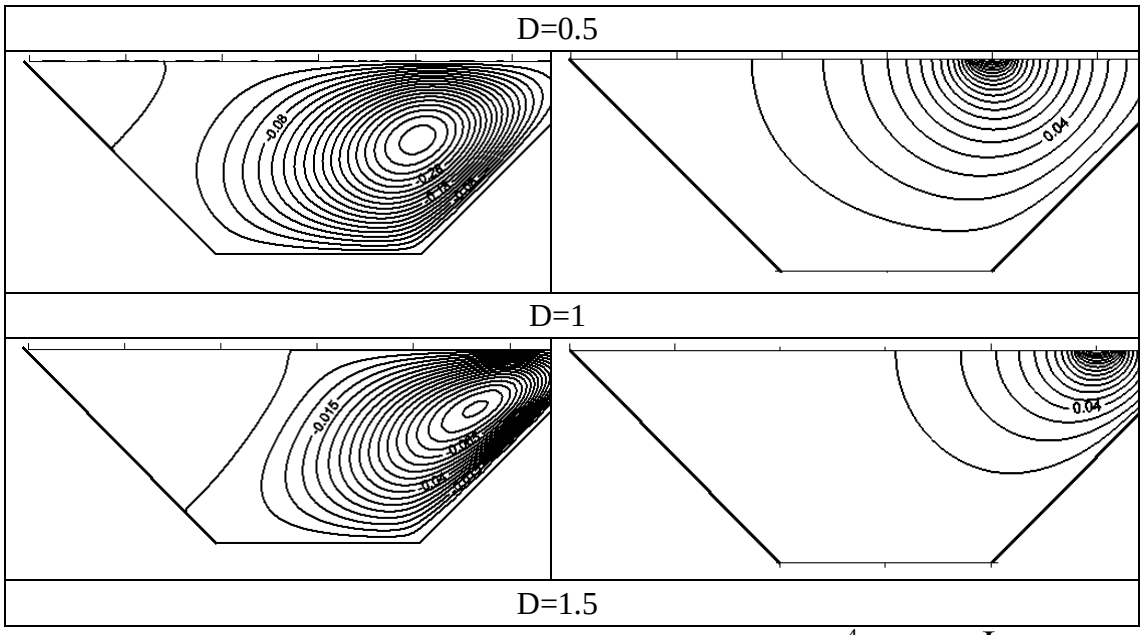

Fig 4 Streamlines (left) and isotherms (right) with Ha=5, Ra=10^4, B=0.2, Φ=45, φ=0.

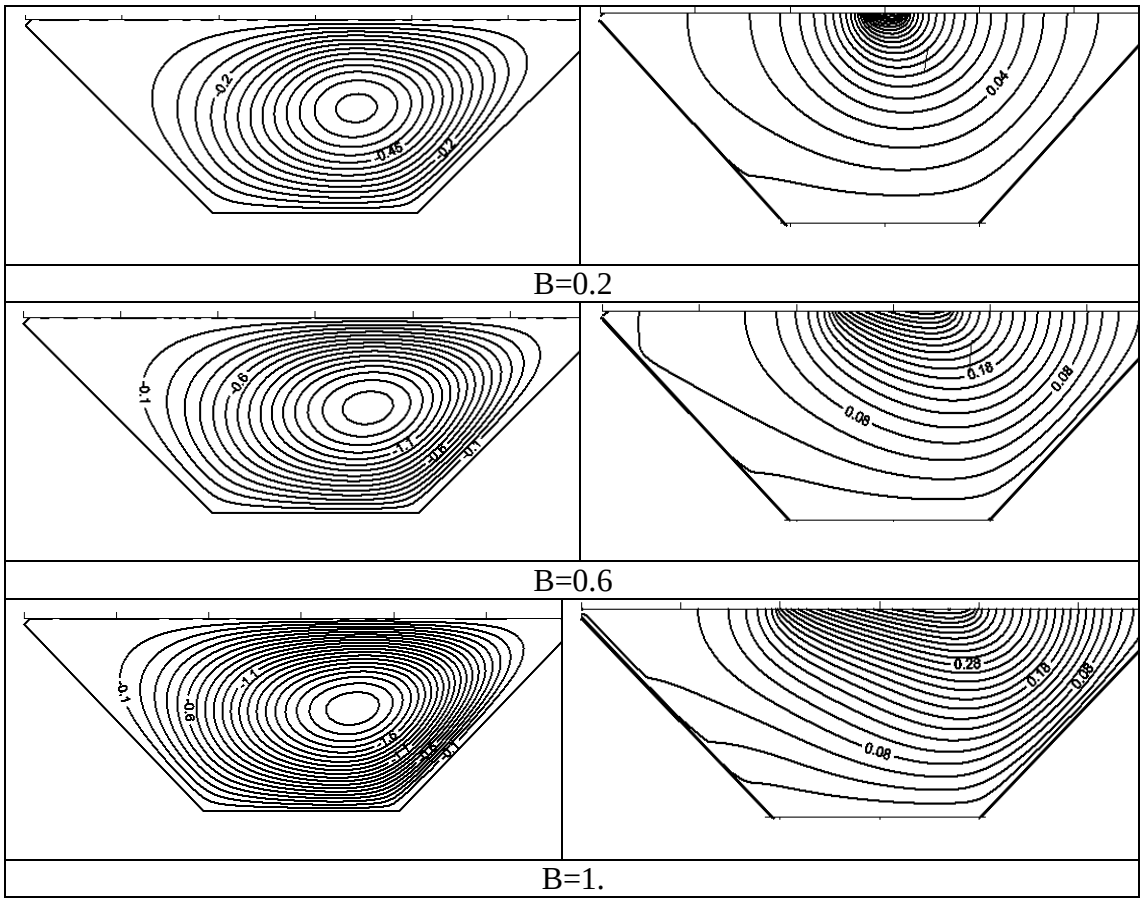

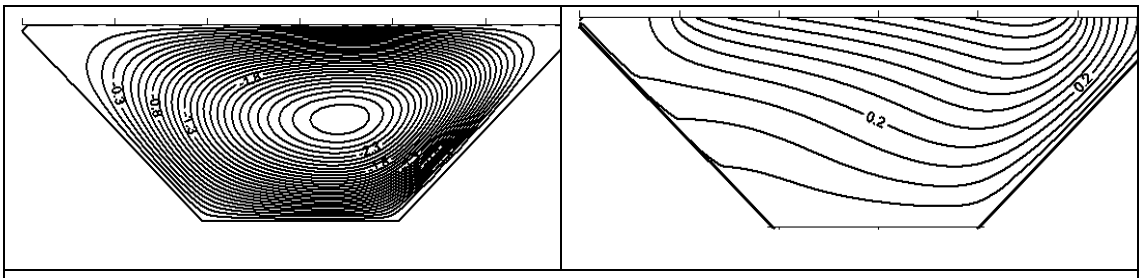

B=2.

Fig 5 Streamlines (left) and isotherms (right) with Ha=5, Ra=10^4, D=0.5, Φ=45, φ=0.

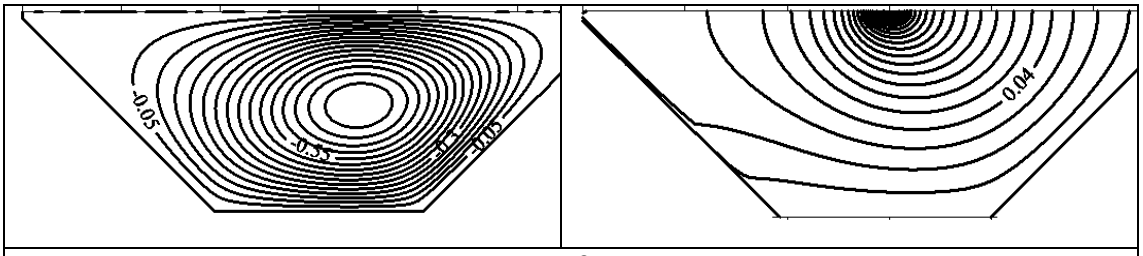

Ha=0

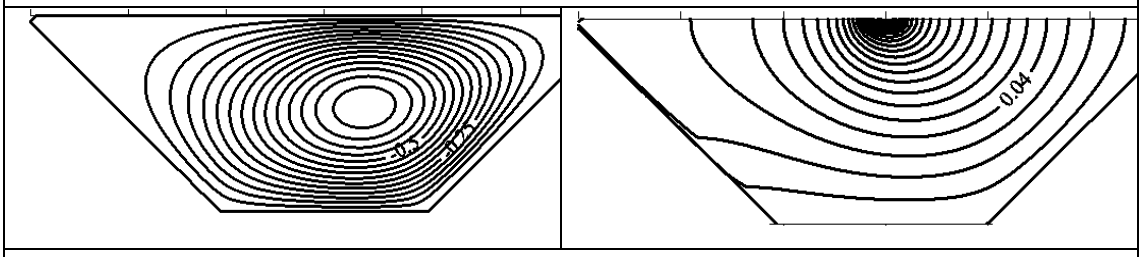

Ha=5

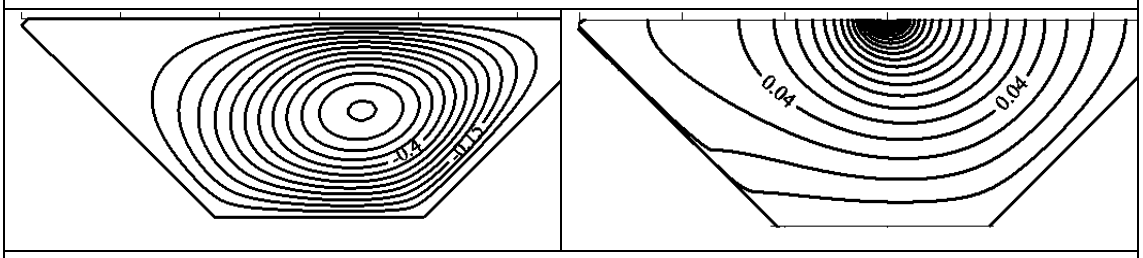

Ha=10

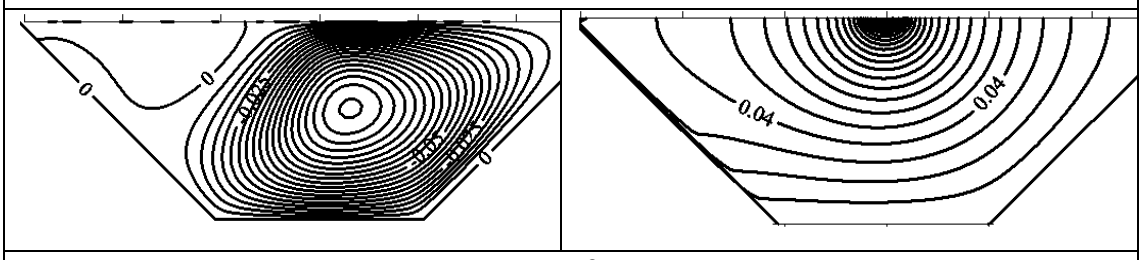

Ha=50

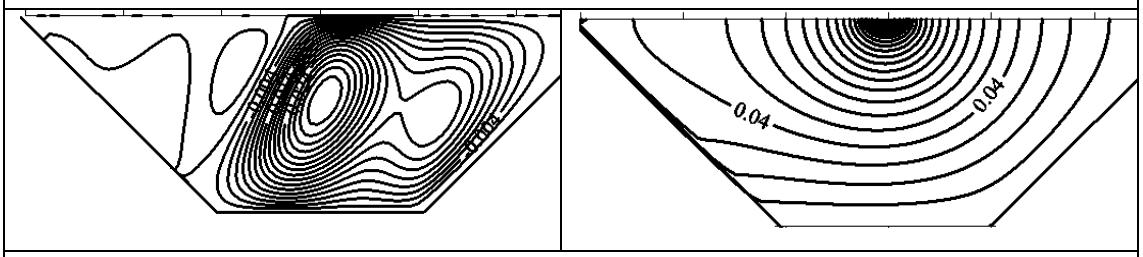

Ha=100

Fig 6 Streamlines (left) and isotherms (right) with B=0.2, Ra=10^4, D=0.5, Φ=45, φ=0.

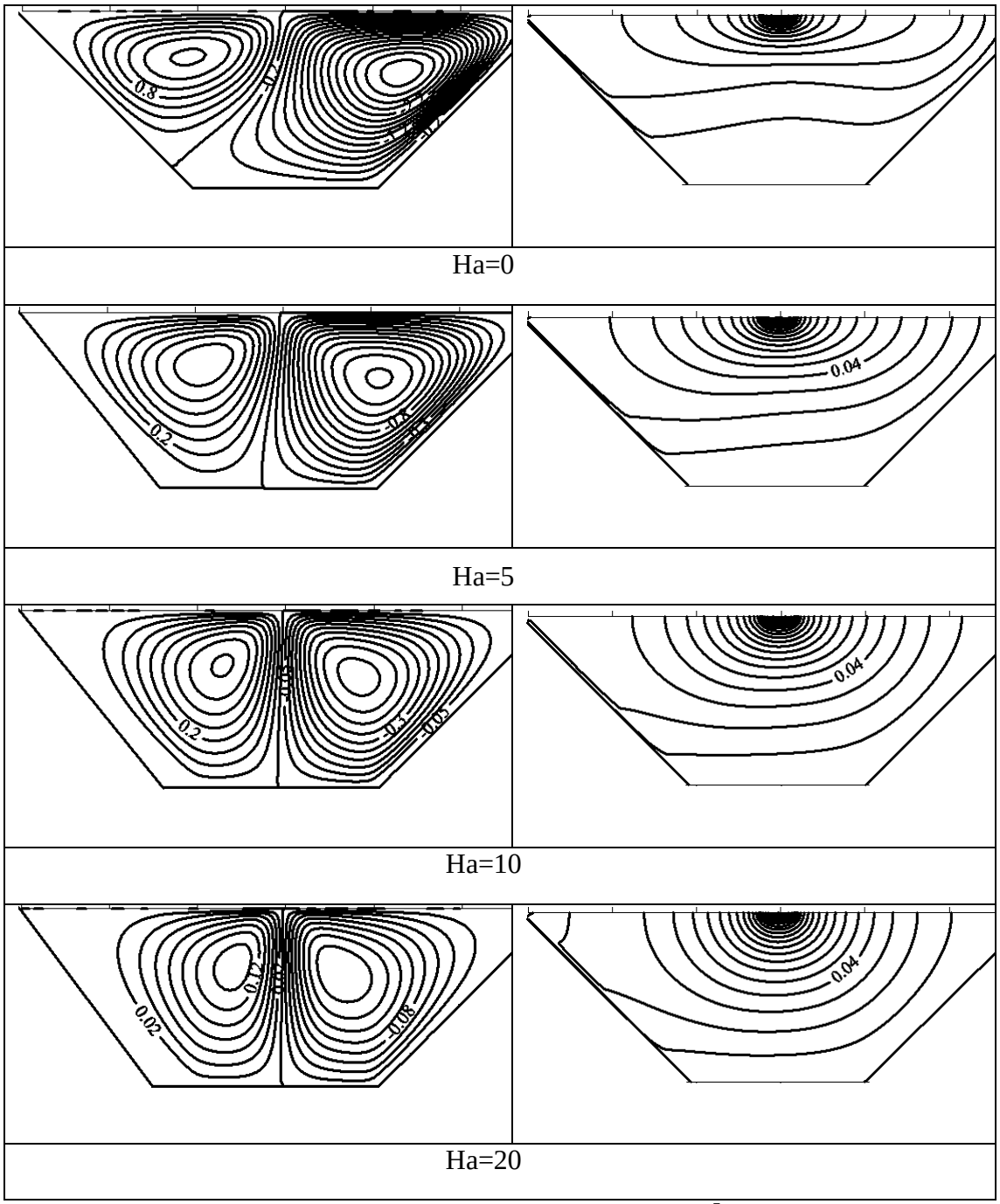

Fig.7 Streamlines (left) and isotherms (right) with Φ=0, Ra=10^5, B=0.2, D=0.5, φ=0.01.s

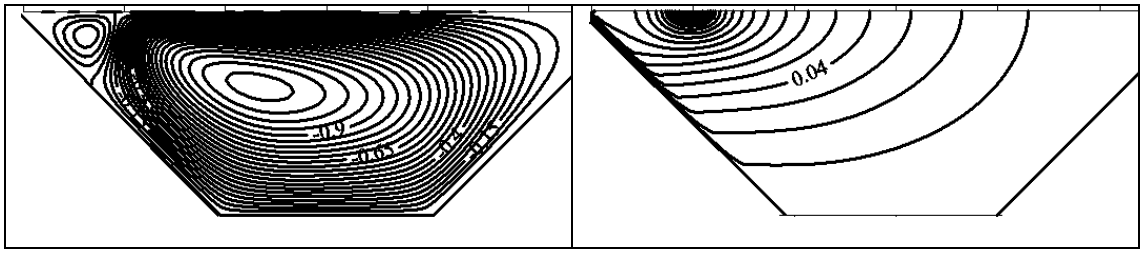

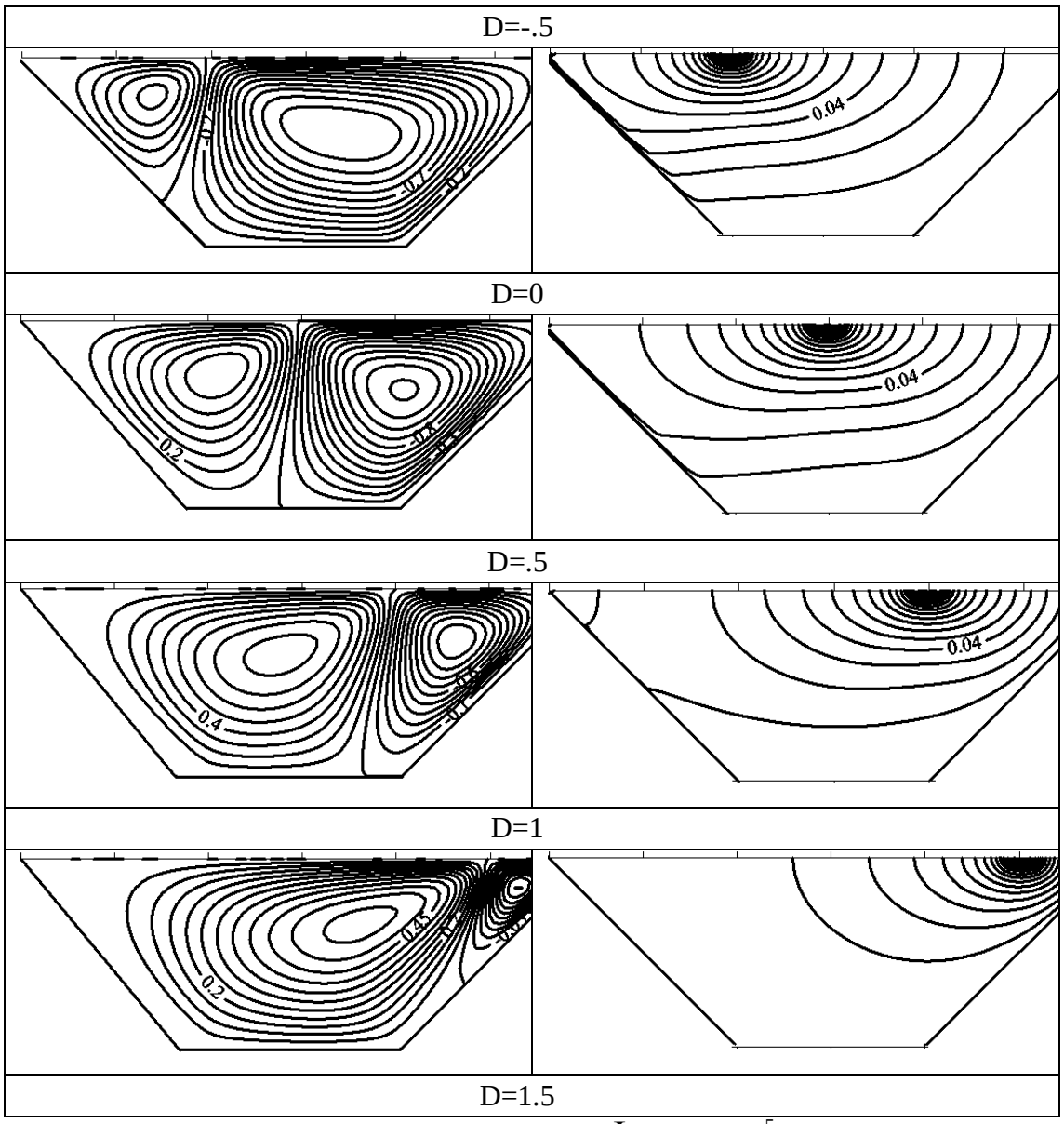

Fig.8 Streamlines (left) and isotherms (right) with Φ=0, Ra=10^5, B=0.2, Ha=5, φ=0.01.

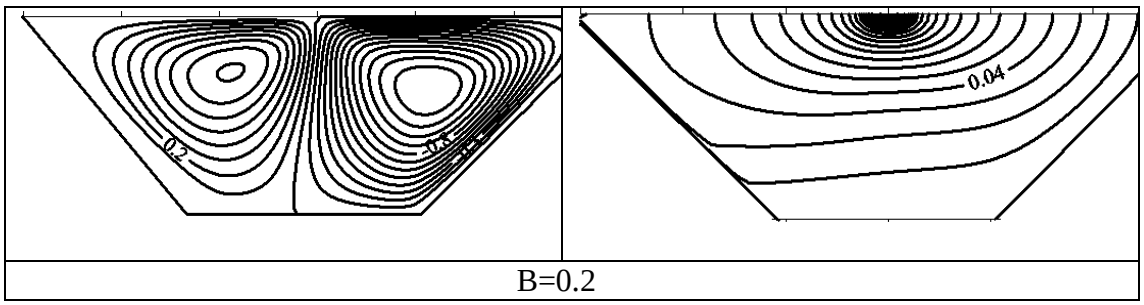

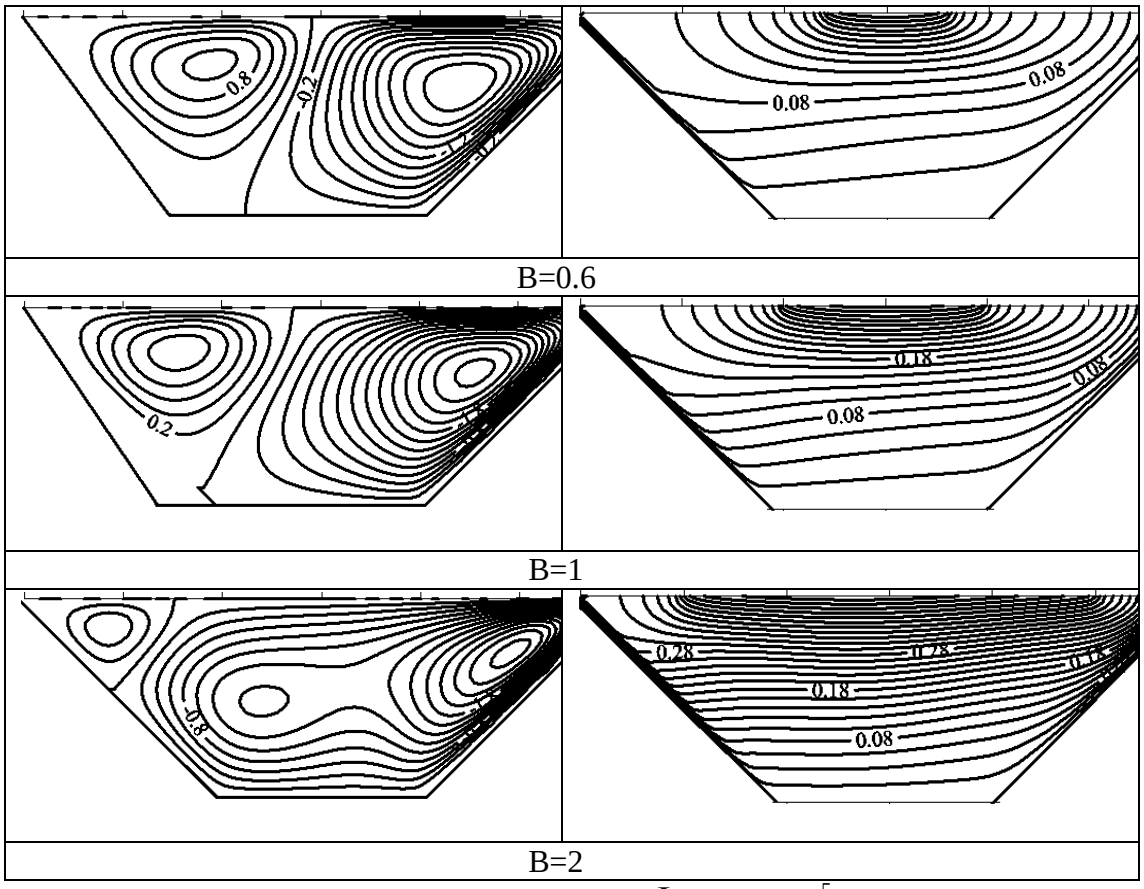

Fig.9 Streamlines (left) and isotherms (right) with Φ =0, Ra=10^5, D=0.5, Ha=5, φ =0.01.

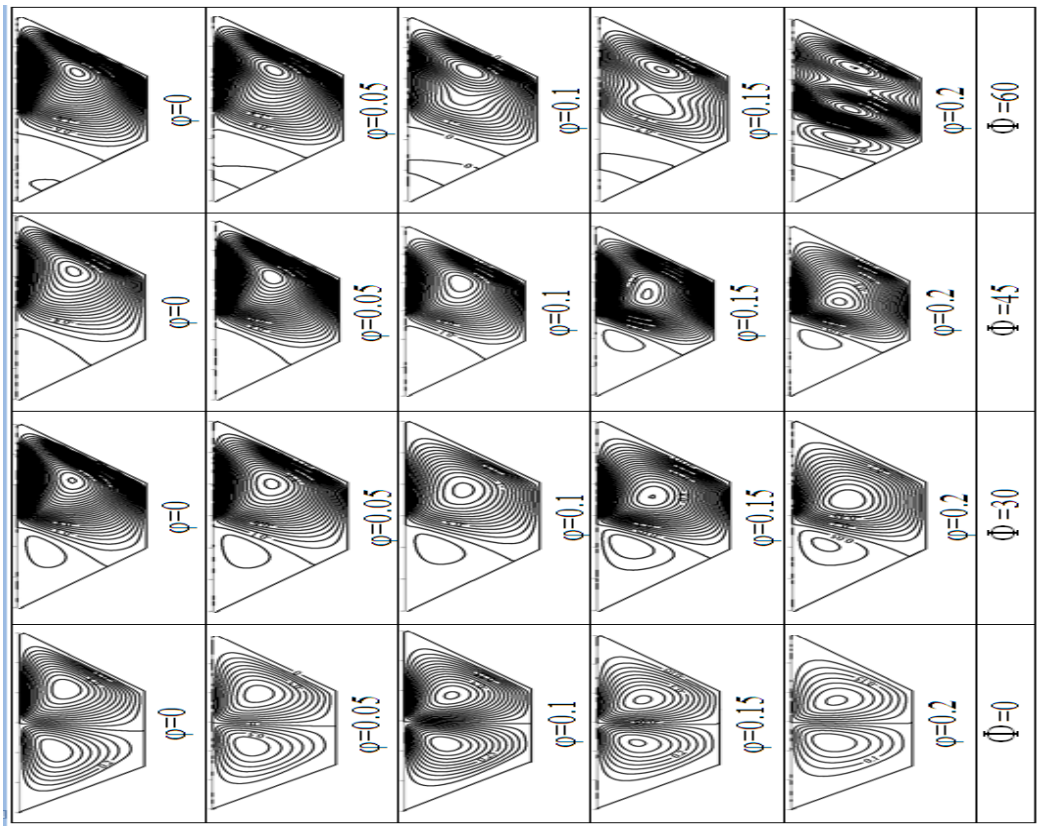

Fig.10 Streamlines B=0.2, Ra=10^5, D=0.5, Ha=5

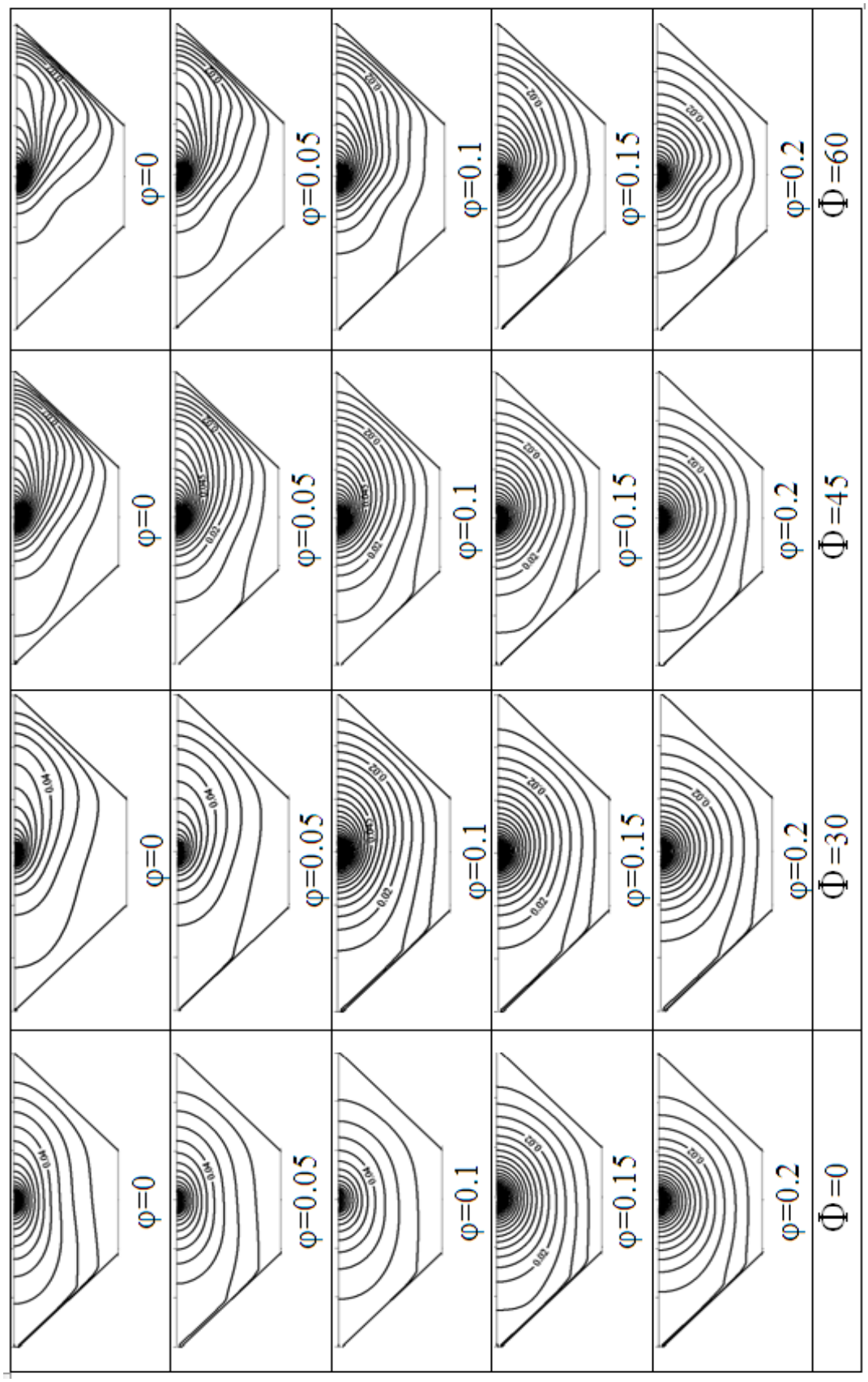

Fig 11 Isotherms B=0.2, Ra=10^5, D=0.5, Ha=5.

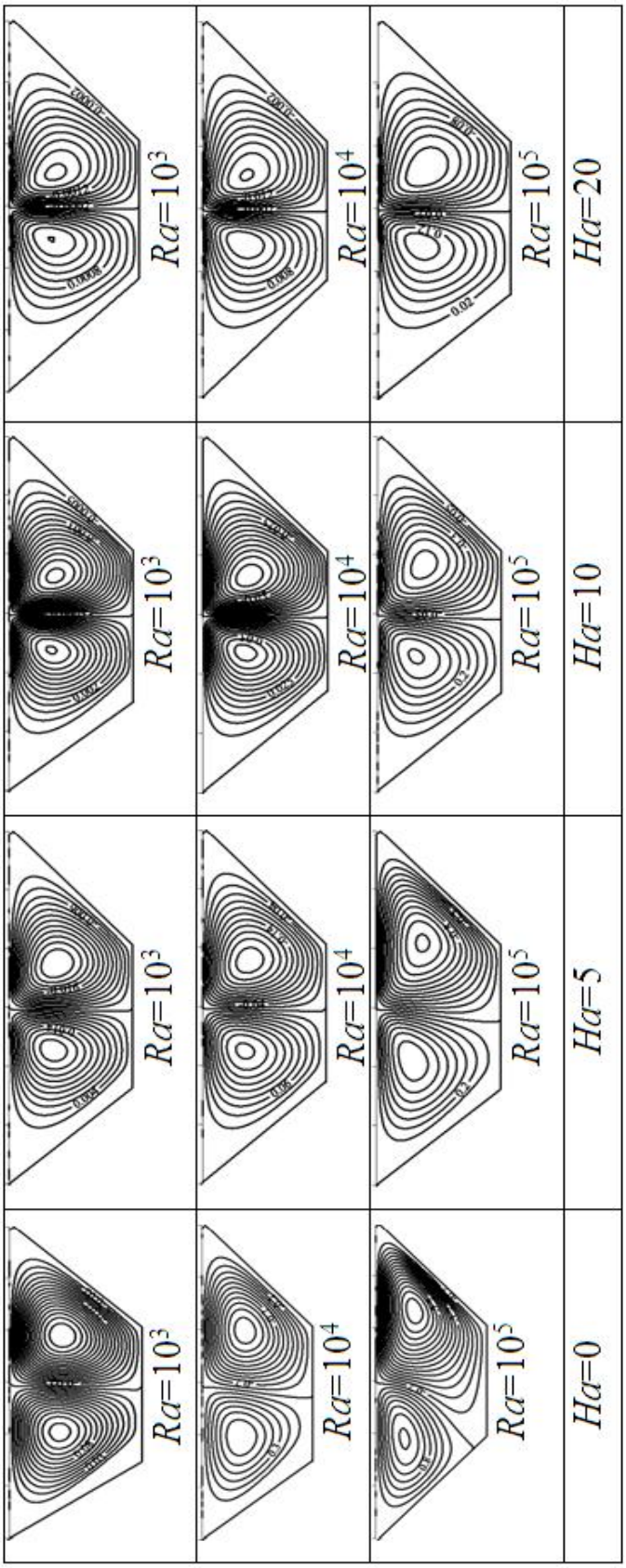

Fig 12 Streamlines B=0.2, Φ=0, D=0.5, φ=0.01.

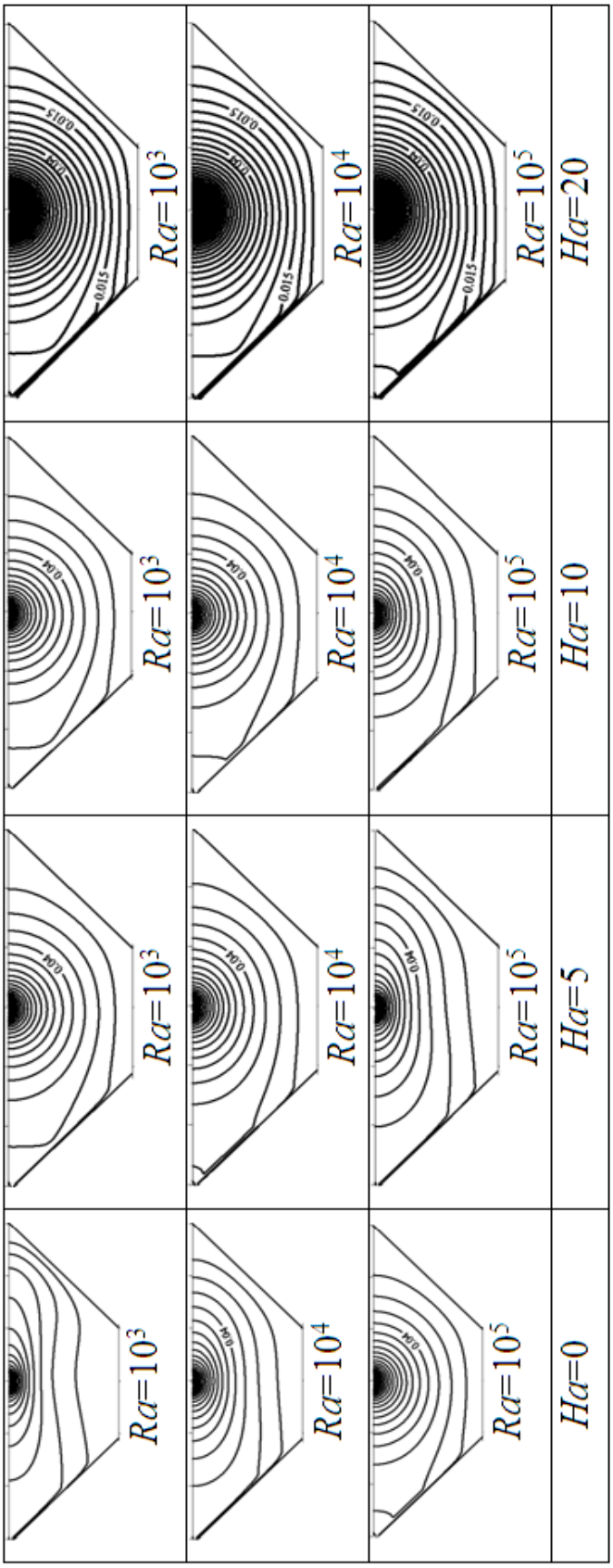

Fig.13 Isotherms B=0.2, Φ=0, D=0.5, φ=0.01.

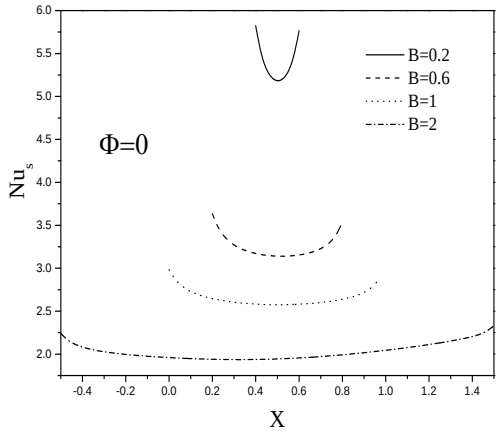

Fig. 14 Variation of local Nusselt number along the heat source for different heat source lengths.

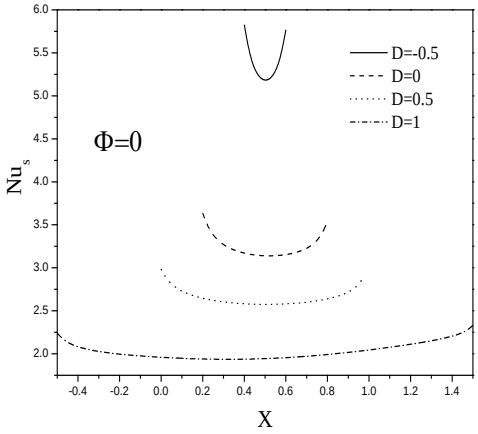

Fig. 15 Variation of local Nusselt number along the heat source for different heat source locations.

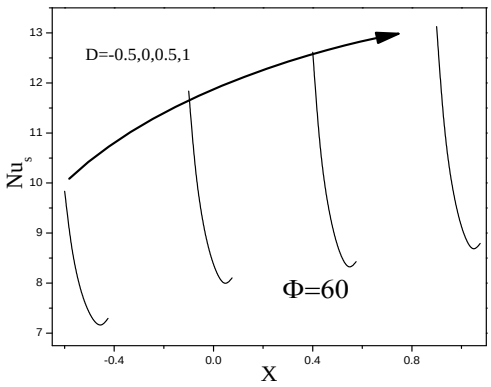

Fig. 16 Variation of local Nusselt number along the heat source for different heat source lengths.

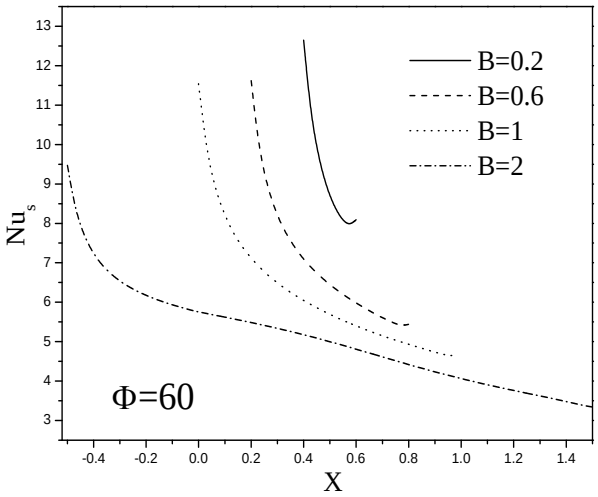

Fig. 17 Variation of local Nusselt number along the heat source for different heat source lengths.

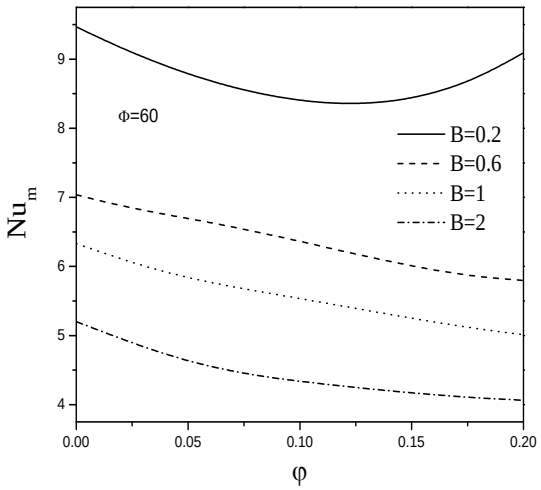

Fig. 18 The effect of distinct heat source lengths on variation of average Nusselt number with solid volume fraction.

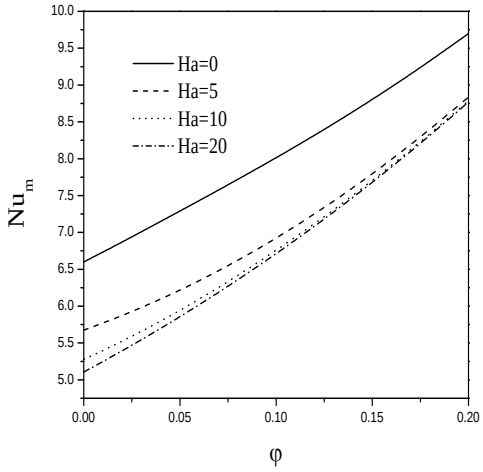

Fig. 19 The effect of distinct Hartmann numbers on variation of average Nusselt number with solid volume fraction.

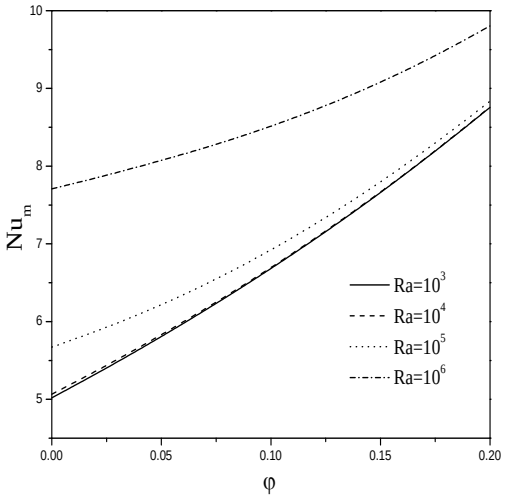

Fig. 20 The effect of distinct Raylei-gh numbers on variation of average Nuss-elt number with solid volume fraction.

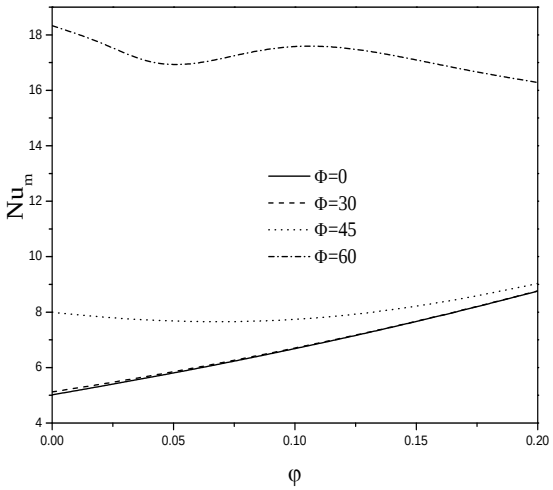

Fig. 21 The effect of various tilted positions on variation of average Nusselt number with solid volume fraction.

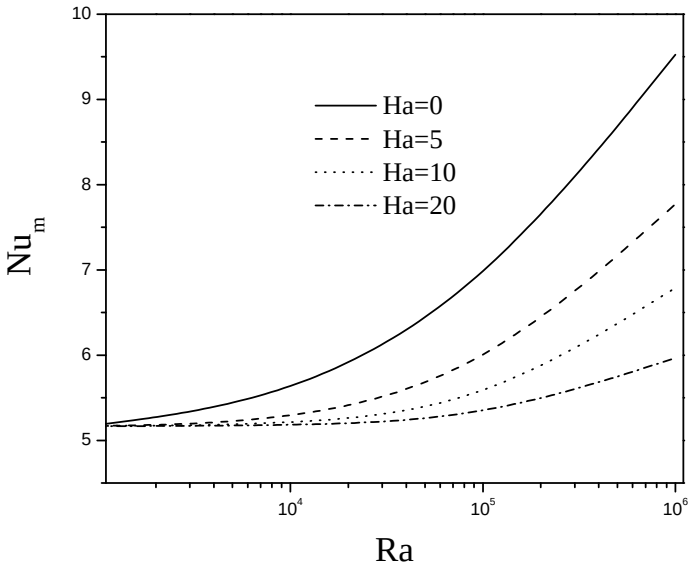

Fig. 22 The effect of distinct Hartmann numbers on variation of average Nusselt number for different Rayleigh numbers.

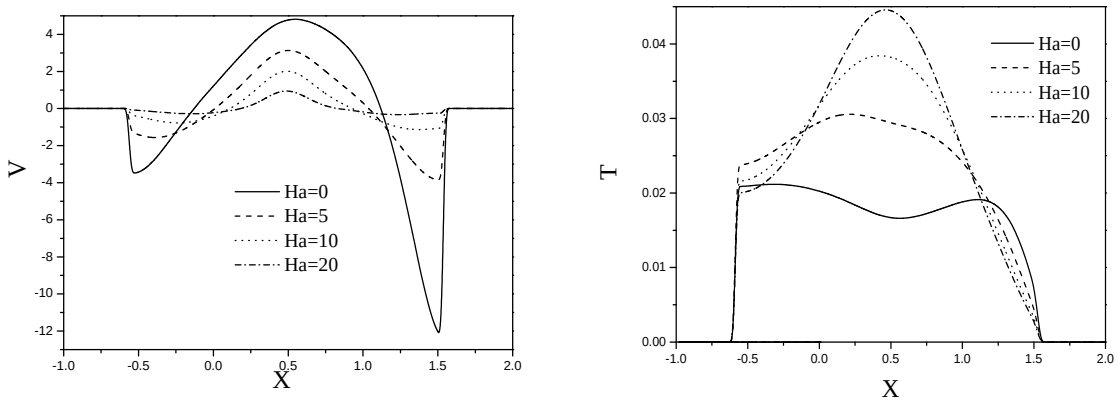

(a) (b)

Fig. 23 The effect of distinct Hartmann numbers on variation of (a) vertical velocity and (b) dimensionless temperature along the middle horizontal axis.

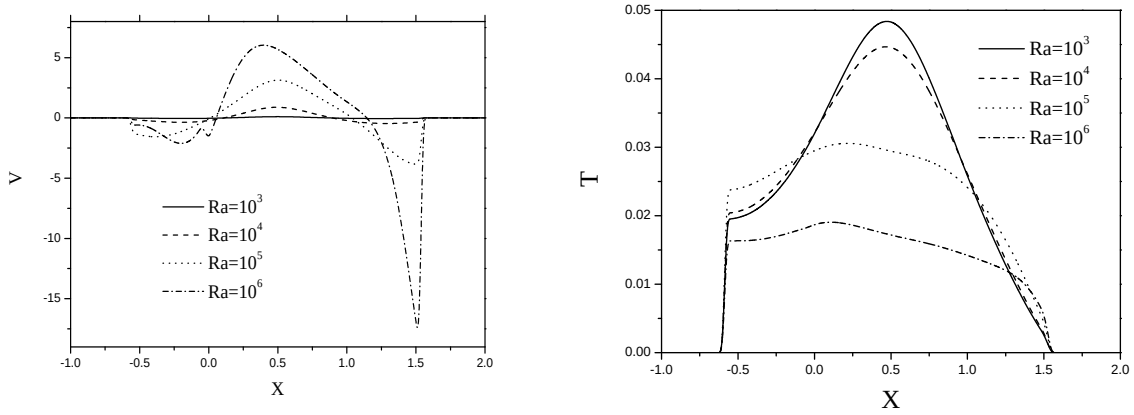

(a) (b)

Fig. 24 The effect of distinct Hartmann numbers on variation of (a) vertical velocity and (b) dimensionless temperature along the middle horizontal axis.

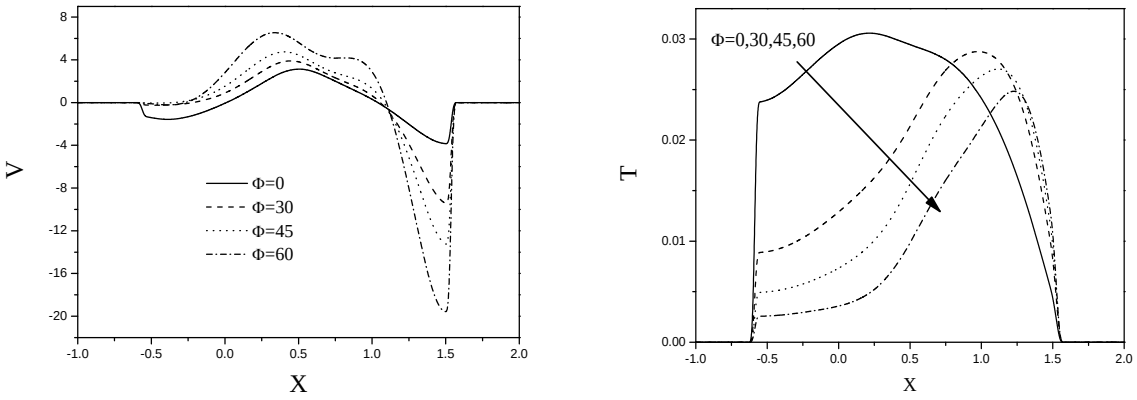

(a) (b)

Fig. 25 The effect of different tilted positions on variation of (a) vertical velocity and (b) dimensionless temperature along the middle horizontal axis.

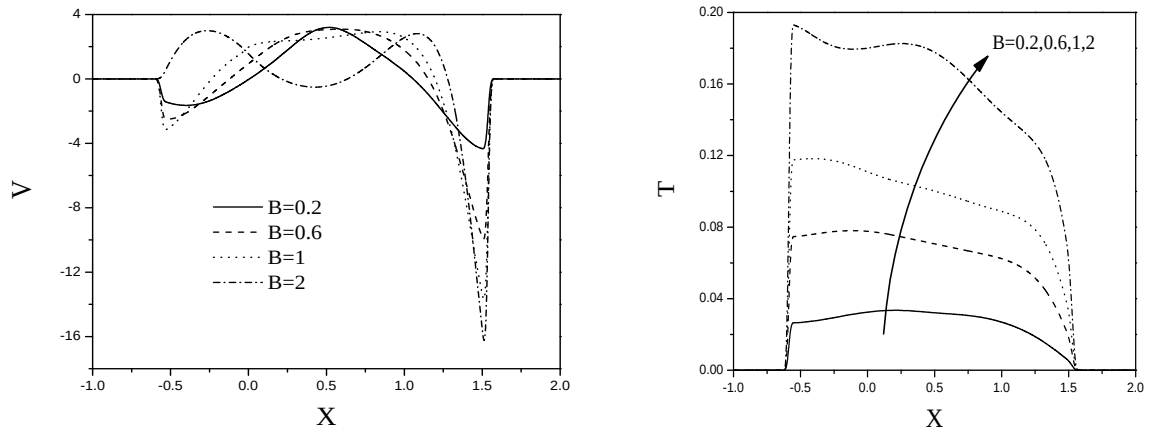

(a) (b)

Fig. 26 The effect of distinct heat source lengths on variation of (a) vertical velocity and (b) dimensionless temperature along the middle horizontal axis.

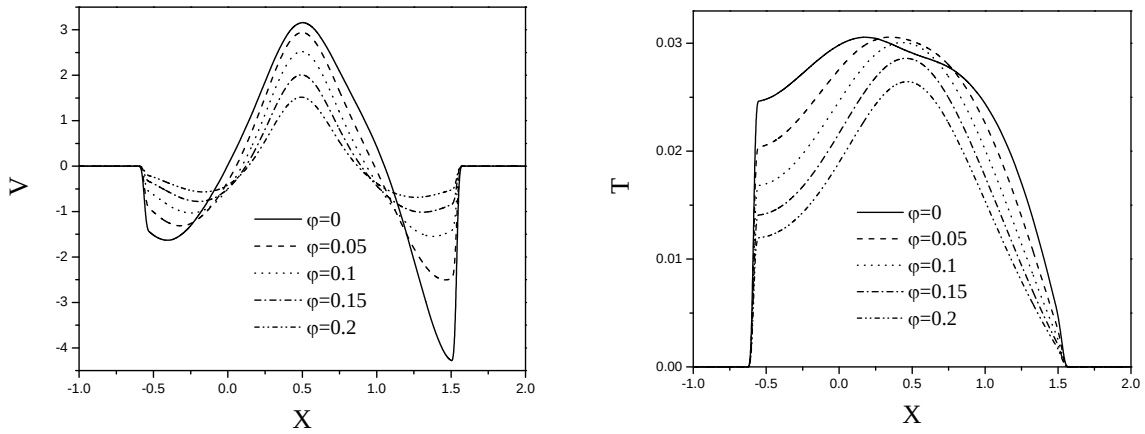

(a) (b)

Fig. 27 The effect of distinct solid volume fractions on variation of (a) vertical velocity and (b) dimensionless temperature along the middle horizontal axis.

American Journal of Engineering Research (AJER)
e-ISSN : 2320-0847 p-ISSN : 2320-0936
Volume-02, Issue-09, pp-147-153
www.ajer.org

Research Paper Open Access

Experimental Study of Turbidity Control by Coagulation for Salt Gradient Solar Pond

S P Shekhawat[1], Dr N V Halegowda[2], and Dr M Husain[3]
[1]*Research Scholar, North Maharashtra University, Jalgaon, India,*
[2]*Principal, Adsul College of Engineering, Ahmadnagar, India,*
[3]*Professor, SSBT's College of Engineering & Technology, Bambhori, Jalgaon, India.*

***Abstract*: -** Salt Gradient Solar Pond (SGSP) is futuristic energy option for Indian conditions. India's solar energy potential is immense. It has a long coastal line that can provide salt water for SGSP. The turbidity has a great influence on radiation transmission in SGSP water. In the present study, it is observed that the effectiveness of Aluminum Sulfate (Alum) in reducing the turbidity in the experimental SGSP is investigated. The optimum dose is worked out. It is hoped that the present work will assist the researchers in the solar energy and will provide them useful scientific data base.

***Keywords*: -** *Coagulation, Radiation, Salt Gradient Solar Pond, Turbidity*

I. INTRODUCTION

Mankind is not threatened with an energy crisis due to the exhaustion of oil, gas, and coal reserves if it masters the technologies for using renewable energy [1]. On May 26 2010, California, US President Barak Obama declared, "The nation that leads the clean energy economy will be the nation that leads the global economy" [2]. Now it is an urgent need for the scientists and technocrats to explore alternative sources of renewable energy. The dawn of twenty-first century has brought two major challenges for the human civilization i.e. energy crises and environmental degradations. Interestingly, both the issues are deeply interlinked. The alternative energy is the only reliable option to solve the problem of environmental degradation and energy crises. The conventional energy is rapidly depleting and civilization has come to a critical juncture.

A Salinity-Gradient Solar Pond (SGSP) is a combined solar energy collector and heat storage system reliant upon an aqueous solution of salt at varying densities to suppress natural convection and store thermal energy [3]. The SGSP consists of three different zones; the upper convective zone (UCZ) with uniform low salinity; a non-convective zone (NCZ) with a gradually increasing density; and a lower convective zone (LCZ), called the storage zone, having uniform density as shown in Figure 1.

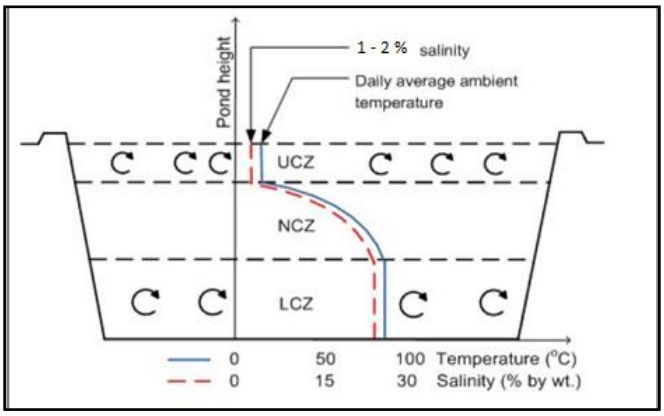

Figure 1. Schematics of a Salt Gradient Solar Pond.

Srinivasan has reported that the thermal efficiency of a solar pond is strongly dependent upon the clarity of the pond. Clarity is reduced by the presence of algae or dust [4]. Wind born turbidity and microbial growth in water are the principal sources of clarity loss in pond [4]. Clarity as such is a qualitative term. Wang and Yagoobi first used the term turbidity to quantify the same and used Nephelometric Turbidity Units (NTU) to express the it [5].

Turbidity is a complex phenomenon contributed by several natural and artificial sources. It is defined as a phenomenon of orthogonal scattering and absorption of visible light due to colloidal solids in fluid [6]. Researchers Many researchers have been extensively studied the effect of turbidity and its impact on thermal performance of SGSP. The water turbidity control of pond water is still a challenging problem during the operation period of solar ponds since its transparency is easy to get worsen in the open environment [7],[8],[9,[10].

Wang and Seyed-Yagoobi introduced turbidity in their radiation transmission model, and indicate that water turbidity plays a critical role in the thermal performance of solar ponds[11]. High turbidity levels can prevent ponds from storing energy. Therefore, the turbidity levels within the pond must be regularly monitored and kept as low as possible. Coagulation-flocculation is a well known phenomenon to remove turbidity. Coagulation in water is a four stage phenomenon as described by following schematics:

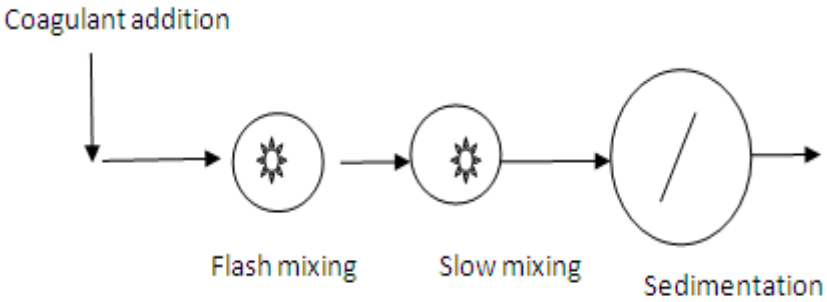

Figure 2: Coagulation Process

It was reported that alum, a low-cost chemical, has the ability to well depress the breeding of algae and bacteria, largely reduce the turbidity of seawater and keep it a long-lasting limpidity [12]. Therefore, it can be applied in the solar pond on a large scale as an efficient and economical turbidity reduction chemical. alum when added to water reacts with the natural alkalinity to form insoluble aluminum hydroxide. The rapid mixing is done with an objective of dissolving the alum in water and mixing it with the entire volume. The slow mixing is done to bring in contact the insoluble molecules together which get polymerized and form floc. The floc comes in contact with colloidal particles and forms larger floc. However in case of SGSP, there are density gradients prevailing. Hence mixing is not permitted. Thus coagulation in SGSP is a simplified two step process:

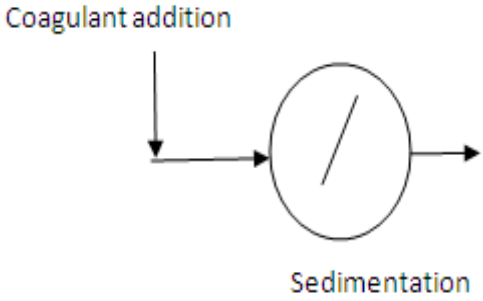

Figure 3: Simplified Coagulation Process

II. SCOPE OF SGSP IN INDIA

Salt gradient solar ponds have great scope in India. This is because the sea water which is an economical raw material to establish a SGSP is available in ample in India due to its long coastal line. Solar energy which is the driving force for solar pond, is available is India in abundance due to its geographical placement and clear sky. Over and above this, India has technical expertise in this area due to its great scientists and engineers who have worked in this field. In Kutch area of Gujarat one commercial SGSP has worked successfully for several years during early 90s. Experimental SGSPs have worked successfully at Indian Institute Technology, Delhi, Indian Institute of Science, Bangalore and Birla Institute of Technology, Ranchi. Thus India has a great scope of harnessing solar energy through s SGSP.

Estimation of SGSP potential in India:
Power requirement of India = 120000 MW
Solar radiation (Average) = 200 W
Thus land area of SGSP required to harness desired
level of energy = $120000*10^6/200$
= $600 *10^6$ m^2.
However, SGSP has conversion efficiency around 20%.
Thus actual area required = $600 *10^6/20\% = 3000* 10^6$ m^2 = 3000 sq km only.

When a thermal or nuclear power plant is established, they occupy area not only for construction and waste disposal, but also for safety and pollution control purpose. Their effective area coverage is significantly large. However data regarding actual land area covered by thermal power plants and nuclear power plants is not found in literature.

India has ambitious plan gaining manufacturing expertise, especially in solar thermal technology, to be able to deliver 2000 MW off-grid applications during 2017-2022 [13]. Solar Pond is one of the important options for off-grid solar thermal applications as mention in directions, innovations and strategies for renewable energy in Vision – 2020 by The Energy and Resource Institute (TERI) [14].

III. COAGULATION STUDIES

The experimental studies are carried out at Shrama Sadhana Bombay Trust's College of Engineering and Technology, Bambhori, Jalgaon, MS, located in Jalgaon city (21.05N, 75.57E, at 250 m from mean sea level) of India. The location is having tropical climate. The study is carried out in the months of April to August. April has clear sky and very high radiation with mild winds. May also has the same parameters associated with high winds. The high winds are responsible for large dust loads. In June the climate turns with the arrival of monsoon. The sky is cloudy with heavy winds. Sometimes sky is clear too with high radiation. In July and August the wind velocity again reduces. Sky is almost covered. Due to rains the landscape soil becomes moist and wind carries less dust load.

Figure 4: Experimental Pond

Turbidity Control and Alum
The present study has investigated the efficiency of alum in reducing the turbidity in the experimental pond. The experimental methodology is described in following steps:

- Stock alum solution is prepared by dissolving laboratory grade alum in to water having strength of 1mg/mL.
- Artificial turbidity is created in the pond by using clay. Clay is first dissolved in water buckets. The large size particles are allowed to settle down for 6 hours. The supernatant is poured in the experimental pond. Then it is mixed with the tank content using large size rods.
- The turbidity of the tank water is measured. It is adjusted to the desired level (~2 NTU) by adjusting the quantity of supernatant being poured.
- Now the tank is added with alum solution. Taking into account the volume of tank, 5 mg/L alum is added (1 mL of alum solution contains 1 mg of alum).
- The turbidity is allowed to settle for 24 hours.
- Now, samples of water are collected from top 10cm, 1 m depth and 1.5 m depth. The samples are examined for turbidity level under Nephelo-turbidity meter.

- The tank is emptied and refilled with tap water. Artificial turbidity to the *same* desired level is again created in the tank as described above.
- The tank is dosed with 10 mg/L alum. The entire process is repeated.
- Similar process is done with alum dose varying from 10 mg/L to 60 mg/L with steps of 10 mg/L.
- Again, artificial turbidity is created by the process described above. This time the desired level is kept as 4NTU.
- The entire process of removal is followed.

IV. RESULTS AND DISCUSSIONS

Turbidity removal is a complex process. Turbidity itself is a complex parameter. It includes a combination of concentration of suspended particles in a particular size range, their shape, their hydro-philicity, their color and many other parameters. These parameters cannot be measured with desired accuracy. Hence turbidity removal cannot be mathematically modeled. It can be only described by the experimental data. The experimental results are presented in following graphs.

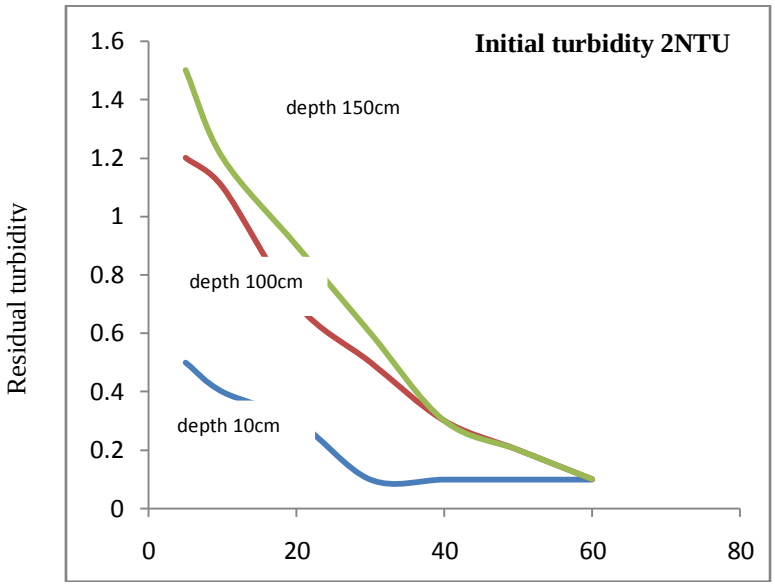

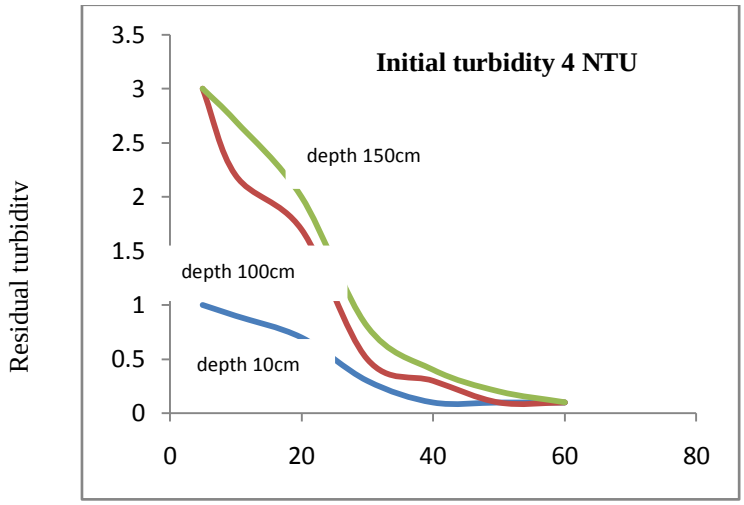

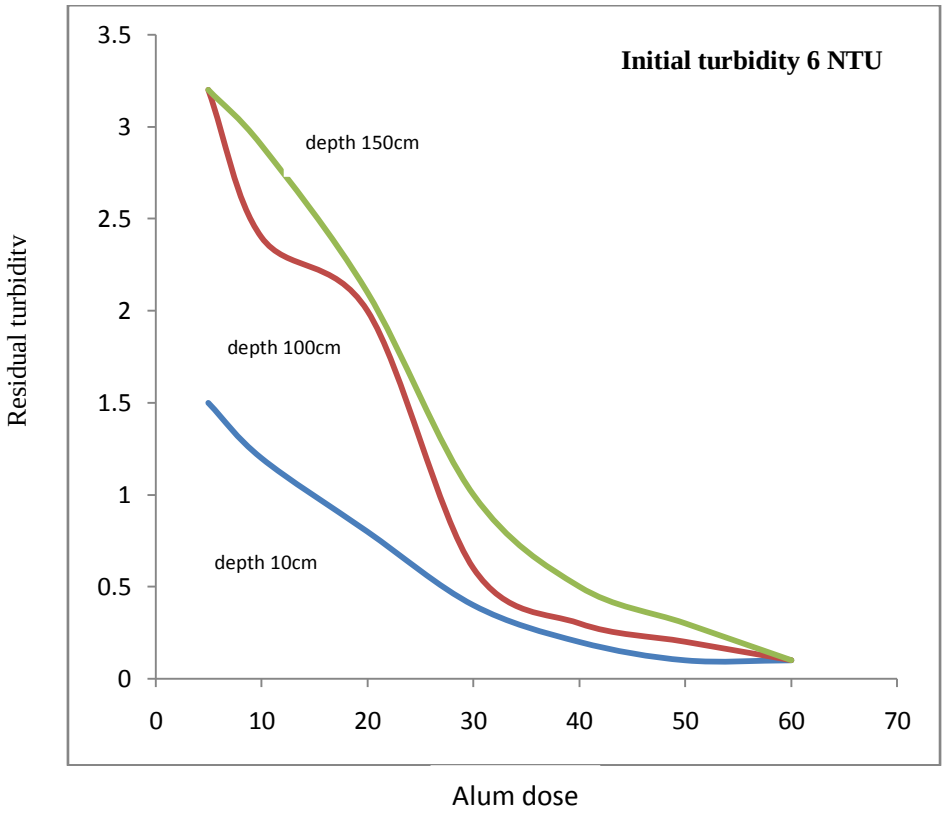
Initial turbidity 6 NTU
depth 150cm
depth 100cm
depth 10cm
Residual turbidity
Alum dose
0
0.5
1
1.5
2
2.5
3
3.5
0
10
20
30
40
50
60
70

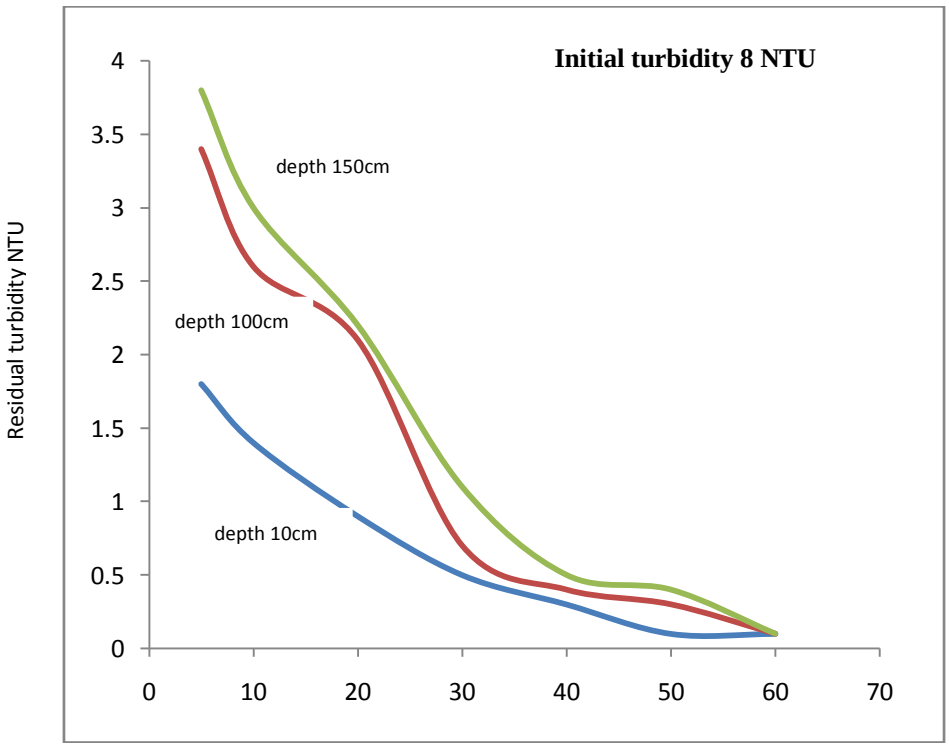
Initial turbidity 8 NTU
depth 150cm
depth 100cm
depth 10cm
Residual turbidity NTU
Alum dose
0
0.5
1
1.5
2
2.5
3
3.5
4
0
10
20
30
40
50
60
70

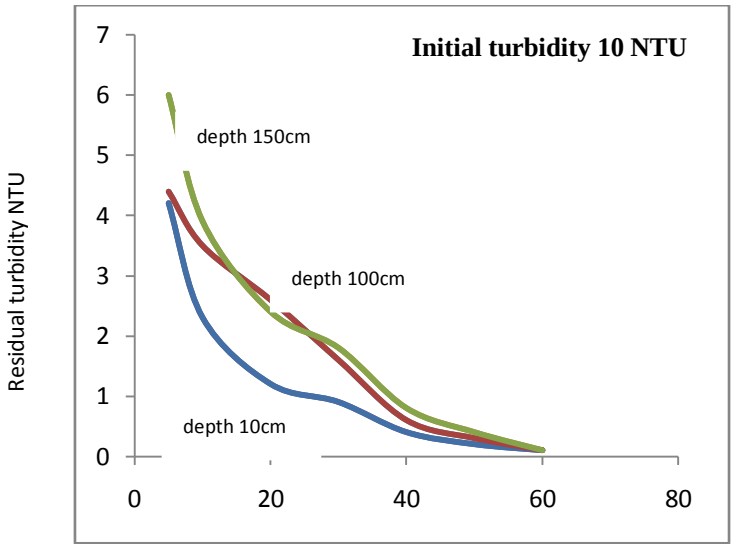

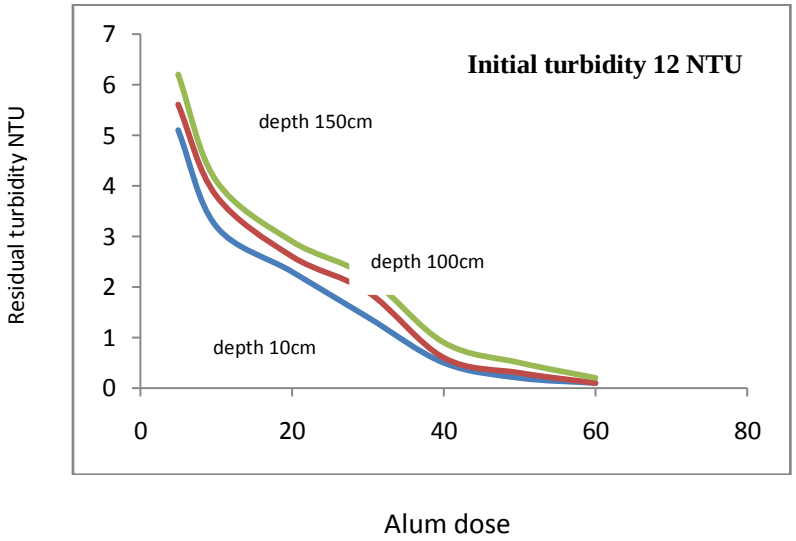

The above results lead to the following interpretations:

- Alum is an effective coagulant for removal of turbidity.
- Alum dose cannot remove turbidity below 0.1 NTU. This is an important observation. In fact this means that pond designers must consider minimum 0.1NTU turbidity in water while estimating the thermal performance and efficiency for realistic estimations.
- The turbidity of top layer is reduced first and then it travels downward.
- Alum dose up to 50 mg/L can effectively reduce turbidity as high as 12 NTU.
- Alum dose does not increase in proportion to the turbidity. This is due to the complexities involved in the removal mechanism. In fact the alum removal process cannot be accurately modelled. Therefore data base is useful information for pond operators to control turbidity.
- The information generated by this experimental study will be a useful guideline for future pond researchers, pond designers and pond operators.
- It is observed that as turbidity level and depth of the pond increases, transmission of solar radiation reduces. It is also clear that turbidity due to dust or wind born debris adversely affects the solar radiation transmission of the pond or performance of the pond.

V. CONCLUSIONS

SGSP's are open to atmosphere. They essentially accumulate wind born turbidity. The present work has estimated the rate of turbidity accumulation and observed that the turbidity can be effectively removed by using alum for coagulation process. Alum dose in the range 50 mg/L can effectively reduce the turbidity of water. The turbidity cannot be reduced to zero level, yet it can be brought down to minimum permissible level.

VI. ACKNOWLEDGEMENTS

This work is supported by the Shram Sadhana Bombay Trust's, College of engineering and Technology, Jalgaon, India under Shram Sadhana Research Promotion Scheme. The authors wish to thanks the Management, Principal and Director of Research and Development of the institute for support and encouragement.

REFERENCES

[1] D. S. Strebkov, "Solar Power Engineering in the Future World: A View from Russia", Applied Solar Energy, Vol. 48, No. 2, 2012,pp. 71–75, ISSN 0003701X.
[2] Sun and Wind Energy, 2010, no.7, p. 8.
[3] Hull J R, K V Liu, W T Sha, J Kamal, and C E Nielsen, " Dependence of ground heat loss upon solar pond size and perimeter insulation: calculations and experimental results", Solar Energy, 33, 661-666., 1984
[4] Srinivasan J., "Solar pond technology", Sadhana, Vol. 18, Part 1, March 1993, pp. 39-55.
[5] Wang J and S Yagoobi , "Effect of Water Turbidity on Thermal Performance of a Salt Gradient Solar Pond", Solar Energy, 54(5), 301-308.,1994
[6] APHA, AWWA and WPCF, "Standard Methods for the Examination of Water and Wastewater", 16th edition, 1985.
[7] Atkinson, J.F., Harleman, D.R.F., A wind-mixed layer model for solar ponds. Solar Energy 31, 243–259, 1983.
[8] Nan Li , Fang Yin , Wence Sun , Caihong Zhang , Yufeng Shi, "Turbidity study of solar ponds utilizing seawater as salt source", Solar Energy 84 , 289–295, 2010
[9] Hassab, M.A., Tag, I.A., Kamaland, W.A., Al-Noaimi, F.M., "Problems encountered in operating salt gradient solar pond in the Arabian Gulf region", Solar Energy 43, 169–181., 1989
[10] Hull J R , " Computer simulation of solar pond thermal behavior", Solar Energy, 25,33-40.,1980
[11] M. A. Punyasena, C. D. Amarasekara, J. R. P. Jayakody, P. A. A. Perera, Construction and Commissioning of a Large-area Salt-gradient Solar Pond at Palatupana Salterns in Southern Sri Lanka. Proceedings of the 19th Technical Session of the Institute of Physics - Sri Lanka, 65, 2003
[12] Wang J and S Yagoobi , " Effect of Water Turbidity and Salt Concentration Levels on Penetration of Solar Radiation Under Water", Solar Energy, 52(5), 429-438, 1995
[13] Report of World Energy Council, 2010.
[14] R. K. Pachauri and Pooja Mehrotra, " Vision 2020: Sustainability of India's Material resources", TERI, New Delhi

American Journal of Engineering Research (AJER)
e-ISSN : 2320-0847 p-ISSN : 2320-0936
Volume-02, Issue-09, pp-154-162
www.ajer.org

Research Paper Open Access

IBC Secured Key Partition for A Peer-To-Peer Network

Suneeta peddireddy, Lokesh A, Prapulla C
Suneeta Peddireddy is with Asst.Professor,RajivGandhi Institute of Technology,Bengaluru-560032.
Lokesh A is with Asst.Professor, M S Engineering College, Bengaluru-560064
Prapulla C is with M.Tech III SEM CS&E, M S Engineering College, Bengaluru-560064.

Abstract: - For identity verification and authentication purposes we introduced an Identity based cryptography (IBC) into peer-to-peer (P2P) . However problems on secure private key issuing could not be addressed by current IBC-based solution. In this paper we present a IBC infrastructure setup phase, a peer registration solution using Shamir's (k, n) secret sharing scheme, and a secure key issuing scheme, which adopts key generate center (KGC) and key privacy authorities (KPAs) to issue private keys to peers securely in order to enable the IBC systems to be more acceptable and applicable in real-world P2P networks[1]. We use Byzantine fault tolerance protocol to develop a scheme to authenticate KPAs and to maintain a security of KPAs. This has theoretical analysis and experimental results that shows performance is effective and is able to support large scale network.

Keywords: - *Peer-to-Peer, Secured key issuing, Secrete key sharing, fault tolerance*

BACKGROUND

P2P networks are extremely vulnerable to large spectrum of attacks , with its self-organized and self-maintenance nature. This is mainly due to the lack of certification service responsible for identity verification and for authentication purposes.

We can solve some of the problems by verifying the authenticated nodes identities and by issusing public keys to the nodes for certification using traditional certificate-based public key infrastructure.PKI based on security protocol is difficult to deployed as many nodes that store certificates to each node may become invalid quickly as node churn is highly frequent in P2P network. Practically it is difficult to implement as each node requires more space to store public key certificates. If overlay nodes have a common shared key for secure communication then secured P2P overlay communication is efficient. In dynamic P2P overlay network achieving such an efficiency is difficult as a new key must be generated every time a node membership changes occurs in order to preserve secrecy.

Suneeta peddireddy is with Asst.Professor, Rajiv

I. INTRODUCTION

In Securing Key issuing trust level that is to be placed on third party is important .In regular transmission of data that the users supplies information must be blinded which is also called as blinding. The third party provides a partial private key which is called as blinded. That key is passed on many other third party. Once the users gets the key the users can unblind the keys and retrieve the information. Here the secured key is divided into several parts and any three of the key part can be used by the user to retrieve the information

II. SYSTEM DESIGN

We have four section namely system setup,peer registration, secure keying and system maintenance. In system setup phase we describe how KGC and KPA work in the beginning of the system. In Peer Registration phase and secure keying phase we describe how a peer joins the system . In system maintenance phase the maintenance of KPAs takes place

The requirements of the system are :

- Secure peer registration:

It must be able to a methodology to mitigate attacks such as man-in-middle attack, collusion attacks during peer registration phase.

- Robust system maintenance :

The system must provide a online method to add new substitution of KPAs remove, identify malicious KPAs.

- Secure key issuing :

The key that is being issued must be secure that will secure the keys without secure channel and defend attacks of all types.

The software requirements analysis (SRA) step of a software development process yields specifications that are used in software engineering. If the software is "semi automated" or user centered, software design may involve user experience design yielding a story board to help determine those specifications. If the software is completely automated (meaning no user or user interface), a software design may be as simple as a flow chart or text describing a planned sequence of events. There are also semi-standard methods like Unified Modeling Language and Fundamental modeling concepts. In either case some documentation of the plan is usually the product of the design.
A software design may be platform-independent or platform-specific, depending on the availability of the technology called for by the design

Design Considerations

There are many aspects to consider in the design of a piece of software. The importance of each should reflect the goals the software is trying to achieve. Some of these aspects are:

- **Compatibility** –The software is able to operate with other products that are designed for interoperability with another product. Since our software is developed on java it is compatible with other products.
- **Packaging** - In java many packages are available. Thus we have used various packages which made coding simpler.
- **Reliability** - The software is able to perform a required function under stated conditions for a specified period of time. Hence the software reliable.
- **Reusability** -The modular components designed capture the essence of the functionality expected out of them and hence the modules are reusable.
- **Robustness** - The software is able to tolerate unpredictable or invalid input.
- **Usability** - The software has user friendly interface which makes its usability easy.

III. RESULT

4.1 Creating Peer Node

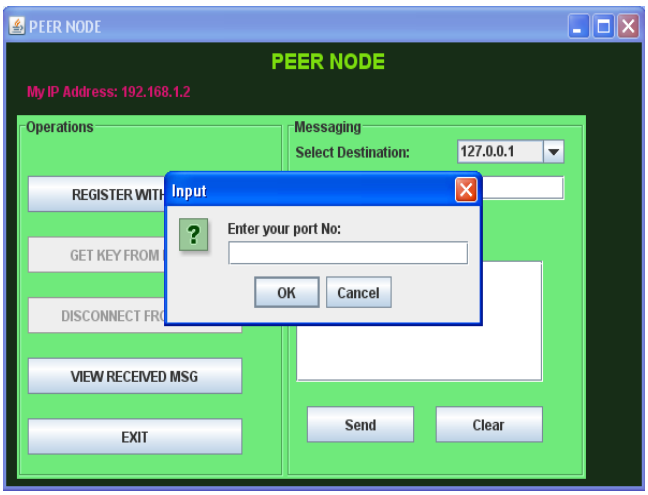

4.1: Creating Peer Node

4.2 Register The Peer Node

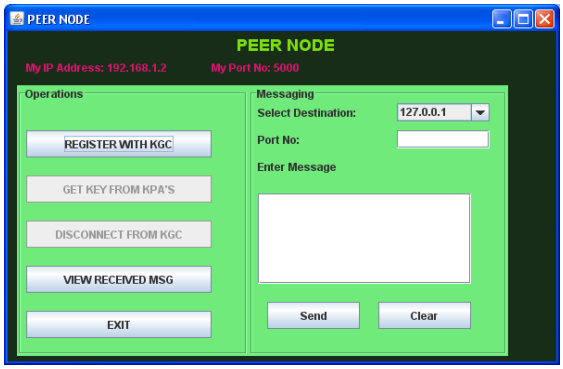

4.2.1: Register The Peer Node

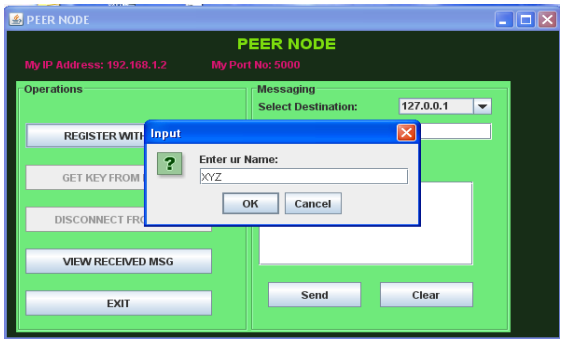

4.2.2: Giving name to peer node

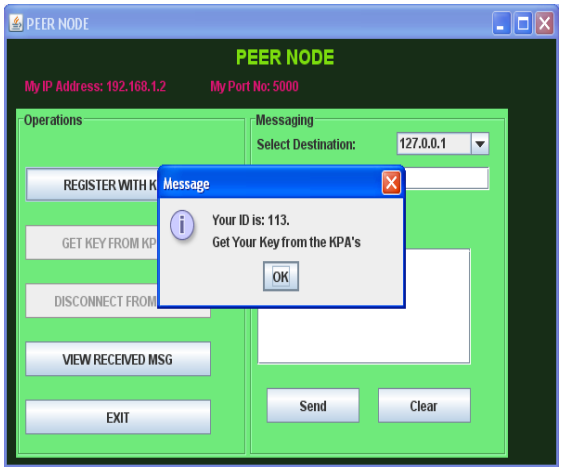

4.2.3: ID is received

4.3 Key Generation Centre

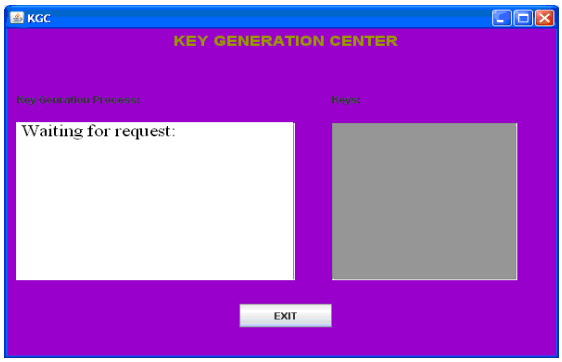

4.3.1: Key Generation Center waiting for request

4.4 Key Generation Process

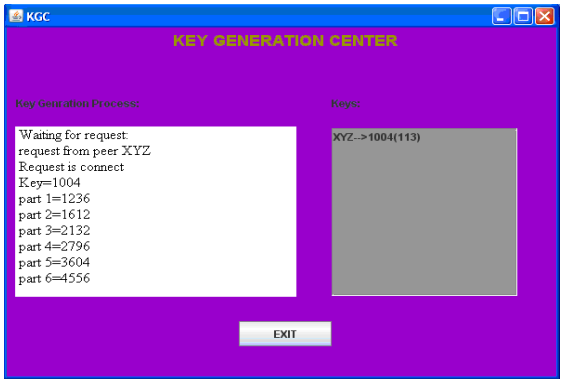

4.4.1: Key Generation Process

4.5 Key Privacy Authority

4.5.1 : Key Privacy Authority

4.6 Key generation centre with key parts

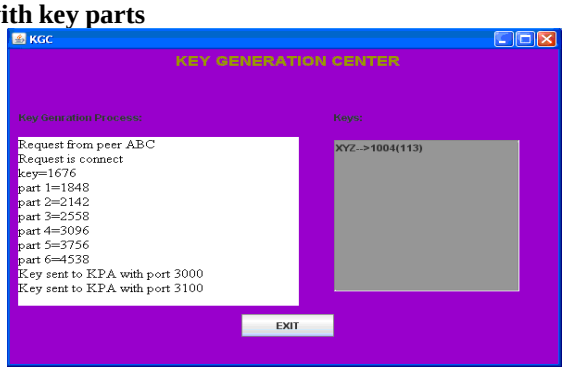

4.6.1: Key generation centre with key parts

4.7 KPA with a key part

4.7: KPA with a key part

4.8 Get Key from KPAs

4.8.1: Get Key from KPAs

4.9 Retrieving the key

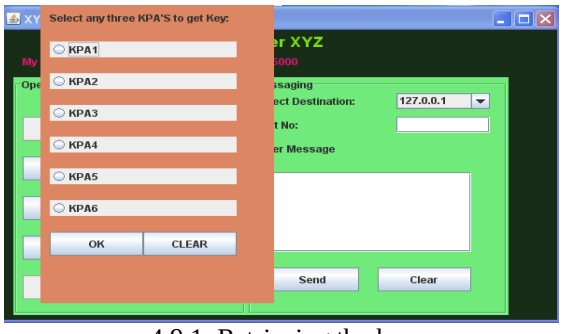

4.9.1: Retrieving the key

4.10 Entering ID of the peer node

4.10.1: Entering ID of the peer node

4.11 Using the key parts

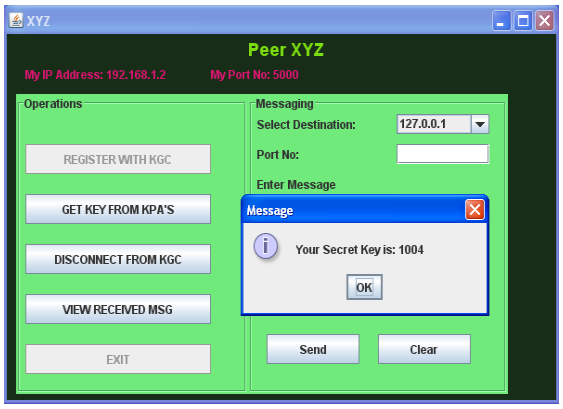

4.11.1: Using the key parts

4.12 Sending Message to Receiver Peer

4.12.1: Sending Message to Receiver Peer

4.13Confirmation

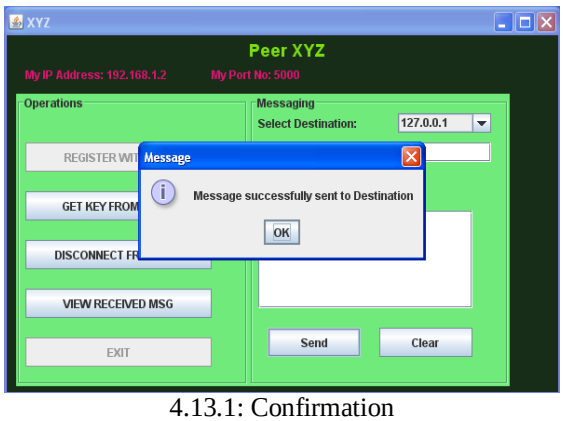

4.13.1: Confirmation

4.14 Receiving a Message

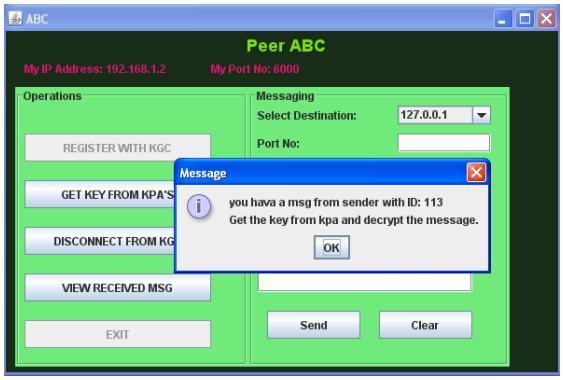

4.14.1: Receiving a Message

4.15 Selection of KPAs

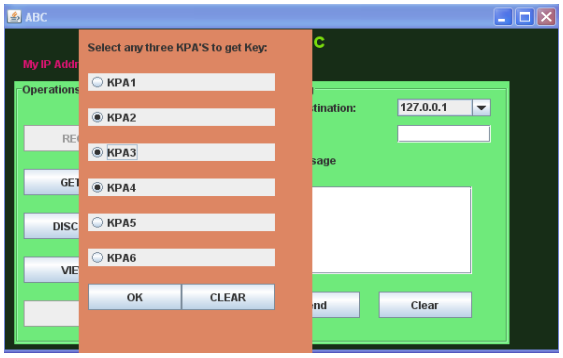

4.15.1: Selection of KPAs

4.16 Entering the peer's ID

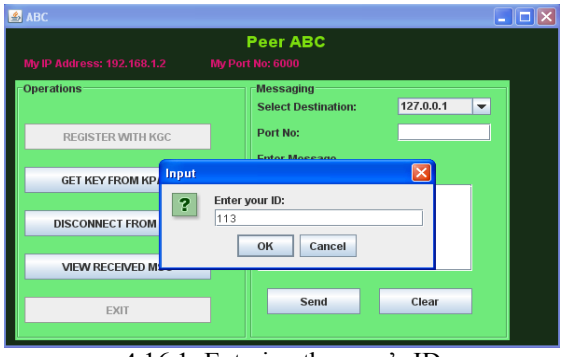

4.16.1: Entering the peer's ID

4.17 Decryption

4.17.1: Decryption

4.18 Key display

4.18 Key display

4.19 Disconnected from KGC

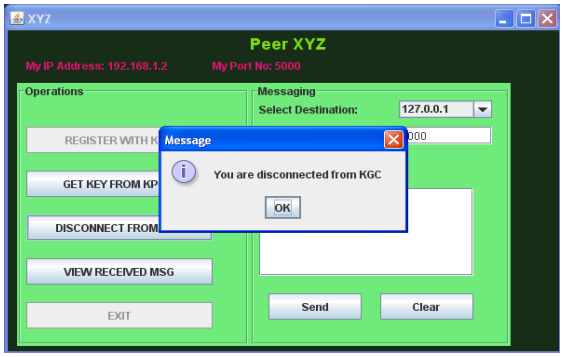

6.19.1: Disconnected from KGC

4.20 KGC after disconnection

4.20.1: KGC after disconnection

4.21 KPA after disconnection

4.21.1: KPA after disconnection

IV. CONCLUSION & ENHANCEMENT

We have developed a secure key issuing scheme for P2P networks using IBC, SKIP. SKIP provides a peer registration service using Shamir's (k,n) secret sharing scheme. We develop a secure key issuing protocol, which adopts KGC and KPAs to issue private keys to peers securely.

Our future work includes developing a scheme to authenticate KPAs, remove malicious ones and finding out alternate ones to join in the system using the BFT protocol.

REFERENCES

[1] Cong Tang, Ruichuan Chen, Zhuhua Cai, Anming Xie, Jianbin Hu∗ , Liyong Tang, Zhong Chen, "SKIP: A Secure *K*ey *I*ssuing Scheme for *P*eer-to-Peer Networks", in Institute of Software, Peking University, China,2010,

[2] E. Sit and R. Morris, "Security considerations for peer-to-peer distributed hash tables," in *IPTPS*, 2002, pp. 261–269.

[3] Shamir, "Identity-based cryptosystems and signature schemes," in *CRYPTO*, 1984, pp. 47–53.

[4] D. Boneh and M. K. Franklin, "Identity-based encryption from the weil pairing," in *CRYPTO*, 2001, pp. 213–229.

[5] Lee, C. Boyd, E. Dawson, K. Kim, J. Yang, and S. Yoo, "Secure key issuing in id-based cryptography," in *ACSW Frontiers*, 2004, pp. 69–74.

[6] R. Gangishetti, M. C. Gorantla, M. L. Das, A. Saxena, and V. P. Gulati, "An efficient secure key issuing protocol in idbased cryptosystems," in *ITCC (1)*, 2005, pp. 674–678.

[7] Saxena, "Threshold ski protocol for id-based cryptosystems," in *IAS*, 2007, pp. 65–70.

[8] Z.-L. Lu, G.-H.; Zhang, "Wheel of trust: A secure framework for overlay-based services," *ICC*, pp. 1148–1153, 2007.

[9] Stoica, R. Morris, D. R. Karger, M. F. Kaashoek, and H. Balakrishnan, "Chord: A scalable peer-to-peer lookup service for internet applications," in *SIGCOMM*, 2001, pp. 149–160.

[9] E. K. Lua, "Securing peer-to-peer overlay networks from Sybil attack," in *ISCIT'07*, Sydney, Australia, 2007.

[9] S. Ryu, K. R. B. Butler, P. Traynor, and P. D. McDaniel, "Leveraging identity-based cryptography for node id assignment in structured p2p systems," in *AINA Workshops (1)*, 2007, pp. 519–524.

[10] L. M. Aiello, M. Milanesio, G. Ruffo, and R. Schifanella, "Tempering kademlia with a robust identity based system," in *Peer-to-Peer Computing*, 2008, pp. 30–39.

[11] Shamir, "How to share a secret," *Commun. ACM*, vol. 22, no. 11, pp. 612–613, 1979.

American Journal of Engineering Research (AJER)
e-ISSN : 2320-0847 p-ISSN : 2320-0936
Volume-02, Issue-09, pp-163-170
www.ajer.org

Research Paper Open Access

Design the High Gain and Low Power Amplifier for Radio over Fiber Technology at 2.4 GHz

A. Salleh, N. R. Mohamad, M. Z. A Abd Aziz, M. N. Z Hashim, M. H. Misran, M. A. Othman

[1,2,3,4,5,6]*Center for Telecommunication Research & Innovation (CeTRI), Faculty of Electronic & Computer Engineering(FKEKK), Universiti Teknikal Malaysia Melaka (UTeM), Hang Tuah Jaya, Melaka, Malaysia*

Abstract:- This paper describes the high performance design a power amplifier for Radio over Fiber (RoF) Technology at 2.4 GHz using Agilents HBFP-0450 transistor. Based on wireless network RoF technology has been proposed as a promising cost effective solution to meet ever increasing user bandwidth and wireless demands. In this network, a central station (CS) is connected to numerous functionally simple Radio Access Point (RAP) via an optical fiber. The only components required at the passive RAP are Electro Absorption Modulator (EAM) and antenna where EAM is used as a remote transceiver. There are practical limitations on the power that can produce by the passive RAP which can affect the dynamic range. In order to improve the dynamic range of passive pico cell RAP power amplifier is placed at the front end of RAP for the downlink transmission which operate in active mode. The central station (CS) is connected to numerous functionally simple RAP via an optical fiber in the RoF network. The design is based on the conjugate matching method which able to achieve the maximum gain. The performance of the design simulation done using Agilent Advanced Design System (ADS) software . The design has shown an acceptable behavior with gain of 13.172 dB. At the 1-dB compression point the output power is approximately 16.108 dB and the Power Added Efficiency (PAE) is 24.915 %.

Keywords: *- Power Amplifier, Radio Access Point, Radio over Fiber, Advanced Design System (ADS), Gain*

I. INTRODUCTION

RoF is refers to a technology whereby light is modulated by a radio signal and transmitted over an optical fiber link to facilitate wireless access [1]. RoF is a well established technology that used intensively worldwide for delivering radio signal from a CS to RAPs via an optical fiber [2]. Recently, wireless communication is becoming an integral part of today's society. The proliferation of mobile and other wireless devices coupled with increased demand for broadband services are putting pressure on wireless systems to increase capacity. To achieve this, wireless systems must have increased feeder network capacity, operate at higher carrier frequencies, and cope with increased user population densities. However, raising the carrier frequency and thus reducing the radio cell size leads to costly radio systems while the high installation and maintenance costs associated with high-bandwidth silica fiber render it economically impractical for in-home and office environments [3]. With such advantages of optical fiber as low loss, large bandwidth and transparent characteristics, RoFs system can simultaneously support multi-standard applications including cellular services and Wireless Local Area Networks (WLANs) [4]. 2.4 GHz frequency is one most commonly used license free frequencies which based on IEEE802.11 standard for WLAN. RoF systems are expected to play an important role in future wireless communication and phased array antenna sensor systems [5-8].

In the new concept of wireless architecture using this technology, all the signal processing associated with the base station, usually found in the RAP or remote antenna unit (RAU), can now be moved to the CS. Consequently, the RAP becomes a small module that only consists of an electroabsorption modulator (EAM), filter, amplifier and an antenna. Fig. 1 shows the basic diagram of RoF [9]. In practice, some loss of simplicity may need to be traded for increased range. The benefits of such a system result directly from the shift of complexity away from the antenna unit to the CS. In other words, centralization can be used to aid

simplification. In the passive RAP, EAM is used as a remote transceiver. The only components required at the RAP are the EAM and an antenna.

There are practical limitations on the amount of power that can produce by the RAP which can affect the dynamic range. Firstly, there are limits to the amount of RF modulated optical power that can be produced economically when linearly modulating a semiconductor laser which this is the source of power ultimately used by the RAP. Secondly, there is a threshold power beyond which the EAM optical waveguide saturates (typically less than 10 mW) [1]. Other limitations arise from the coupling efficiency between the input or output fibers and the EAM waveguide. Apart from the limiter radio range, another potential problem with passive optical link is intermodulation distortion, especially since the EAM is operated without bias. However, analogue optical links are noted for their broadband capability, which allows several radio systems to be supported simultaneously. Inter-system interference is therefore an important issue if there is overlap between signals from one system and the harmonics of another. Such a situation arises for example between GSM900 and DCS1800. Second order distortion is therefore the main limitation of dynamic range in this situation [1]. A power amplifier is placed between the EAM and the antenna in order to improve the dynamic range of passive pico cell (RAP). Pico cells use low power and low capacity base stations that are small, light, relatively low cost and easy to install [2]. Pico cell has a coverage range up to 100 m. To achieve this distance, the RAP needs to operate in active mode, by inserting RF amplifier between optoelectronic photo detector and antenna for downlink path, and inserting LNA between the antenna and optoelectronic modulator [9]. Fig. 2 shows the simple diagram representation of an active optical RAP. Due to a bi-directional amplifier is needed to provide amplification in both transmit and receive directions, the microwave circulators or similar devices will be needed to provide separate uplink and downlink signal paths between the EAM and the antenna. Likely the power amplifier of general RF system, amplifier design for RoF involves many tradeoffs between noise figure, gain, linearity, impedance and matching network [10].

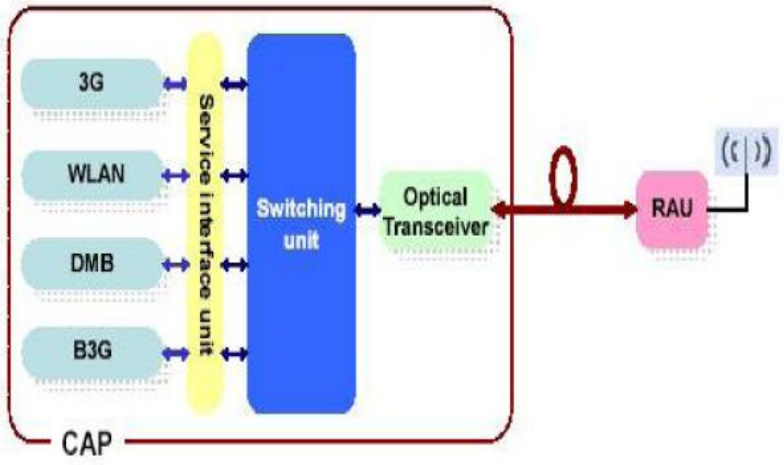

Figure 1: RoF system block diagram

The power amplifier is the critical element in transmitter units of communication systems, is expected to provide a suitable output power at a very good gain with high efficiency and linearity [11]. The output power from a power amplifier must be sufficient for reliable transmission. High gain reduces the number of amplifier stages required to deliver the desired output power and hence reduces the size and manufacturing cost. High efficiency improves thermal management, battery lifetime and operational costs. Good linearity is necessary for bandwidth efficient modulation. However these are contrasting requirements and a typical power amplifier design would require a certain level of compromise. There are several types of power amplifiers which differ from each other in terms of linearity, output power or efficiency. Parameters which quantify the various aspects of amplifier performance such as output power, gain, 1-dB compression point, intermodulation distortion, efficiency and are discussed in the next section. In this paper, the major goal is to design and simulate a power amplifier using the ADS software at 2.4 GHz based on RoF requirements. The analysis is based on S-parameters which are used to determine stability, maximum gain and matching network.

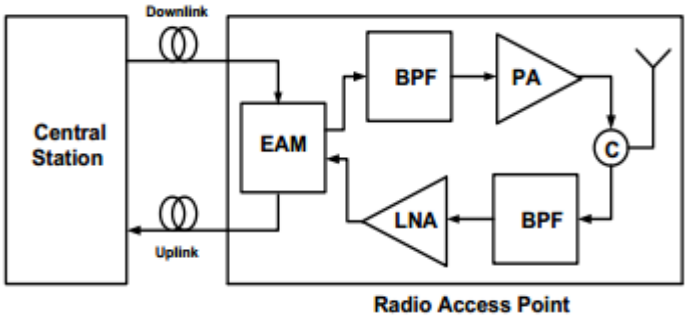

Figure 2. Active Optical Radio Access Point

II. DESIGN METHODOLOGY

Designing a power amplifier consist of different steps which based on conjugate matching method. The maximum gain or conjugate matching method is in the single stage amplifier design. This method will be realized when the overall gain given by a transistor, G_o provide a conjugate match between the amplifier source or load impedance and the transistor as shown in Fig. 3. A critical step in any power amplifier design is the selection of transistor. The transistor used in the current design is Agilent HBFB-0450. This product is based on a 25 GHz transition frequency fabrication process, which enables the products to be used for high performance, medium power, and low noise applications up to 6 GHz. The microwave bipolar transistor is usually of the non type and are often preferred over GaAs field effect transistor (FET) at frequencies below 2 to 4 GHz because of the higher gain and lower cost [12]. Table 1 shows the specifications of the power amplifier (PA) design. The operating frequency of the amplifier is at 2.4 GHz. The target of this project is that design the low power of PA which for short range application (pico cell). The output power of pico cell is less than 1 Watt (30 dBm) and the maximum output power produced at WLAN 2.4 GHz is 20 dBm [13].

First of all a DC simulation must be done to find the optimal bias and bias network for the system. From the transistor datasheet, it concern to choose the biasing point which produced the best performance in term of gain. The gain of the transistor is depending on the S parameter at the operating frequency. Biasing is a process to obtain the transistor static IV curves for desired operation such as class A, class B, class C, or class AB. The biasing point at V_{CE}= 3 V and I_C = 50 mA is selected because have higher gain compare to the others biasing point. The higher value of S_{21} (dB) can give a higher gain. Next, S-parameter simulations is done to find the exact value of the S-parameters and evaluate the stability of the model at the operating point. When embarking on any amplifier design it is very important to spend time checking on the stability of the device chosen, otherwise the amplifier may well turn into an oscillator. The main way of determining the stability of a device is to calculate the Rollett's stability factor (K) based on a set of S-parameters for the device at the frequency of operation [12]. There are two stability parameters K and $|\Delta|$ is used to indicate that whether a device is likely to oscillate or not or whether it is conditionally or unconditionally stable.

The input and output matching network are designed to make sure that maximum power is delivered when the load is matched to the line and power loss in fed is minimized. The single stub method is used for matching network. In the single stub matching that uses a single open circuited or short circuited of transmission line (stub), connected either in parallel or in series with the transmission feed line at the certain distance from the load as shown in Fig. 4. The important factors in the selection of a particular matching network include complexity, bandwidth, implementation and adjustability. Finally the whole system is optimized to achieve the better output power, efficiency and gain.

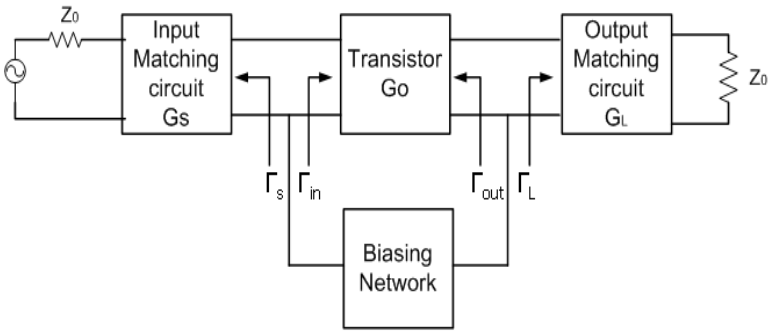

Figure 3. Model of single stage microwave power amplifier

Table I: Power Amplifier Specifications

Parameters	Values
Operating	2.4 GHz
Output Power, P_{out}	< 30 dBm
Gain, G	> 10 dB
Transistor	Agilent HBFB-0450
Matching Network	Single Stub

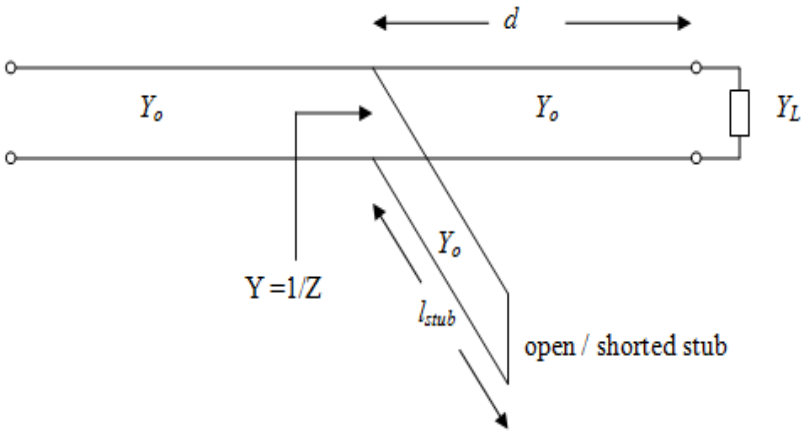

Figure. 4. Single Stub Tuning

III. RESULT AND ANALYSIS

The first step towards designing the class A power amplifier was to select a suitable bias point for the operation. The transistor should be biased for class A operation and maintained comfortably inside the rectangle limited by the nonlinearity borders which are the collector-emitter voltage, Knee voltage, V_k, and collector-base breakdown, V_{BR}. Transistor I-V curves with the optimal load line for the class A operation is shown in Fig. 5. The bias point at the optimal condition is V_{ce} = 2.45 V and I_c = 40.35 mA. The I-V curves also help to see a safety region which condition that the device can be expected to operate without self-damage due to thermal heating. The performance of transistor at the optimal bias value is summarized in Table 2. The maximum output power of this transistor is 16.22 dBm which the transistor can be used for pico cell application (less than 20 dBm).

The main way of determining the stability of a device is to calculate the Rollett's stability factor (K), which is calculated using a set of S-parameters for the device at the frequency of operation.. The stability can be determined from the value of K and Δ. The simulation of stability is shown in Fig. 6. The system is the unconditional stability due to $|\Delta| < 1$ and $K > 1$ which mean that the amplifier is stable for all passive sources and load impedance. After the stability of the transistor have been determined, and the stable regions for the reflection coefficient for source and load (Γ_S and Γ_L) have been located on the Smith chart, the input and output matching section can be designed. Simulation maximum gain will be realized when matching sections provide a conjugate match between the amplifier source or load impedance and the transistor. Fig. 7 shows the simulation of effective gain. The results of effective gain between calculation and simulation almost the same. Available gain is a ratio between the power available from the output of the transistor and the power available from the source. The maximum value is occurring when the input of the power amplifier is conjugate-matched to the source. The Maximum Available Gain (MAG) is the highest possible value of transducer gain in case when both the input and output ports are conjugate-matched. MAG can be defined only if the transistor unconditionally stable.

$$K = \frac{1-|S_{11}|^2-|S_{22}|^2+|\Delta|^2}{2|S_{12}.S_{21}|} = 1.014 \text{ where } |\Delta| = S_{11}.S_{22} - S_{12}.S_{21} = 0.543\angle -77.35°$$

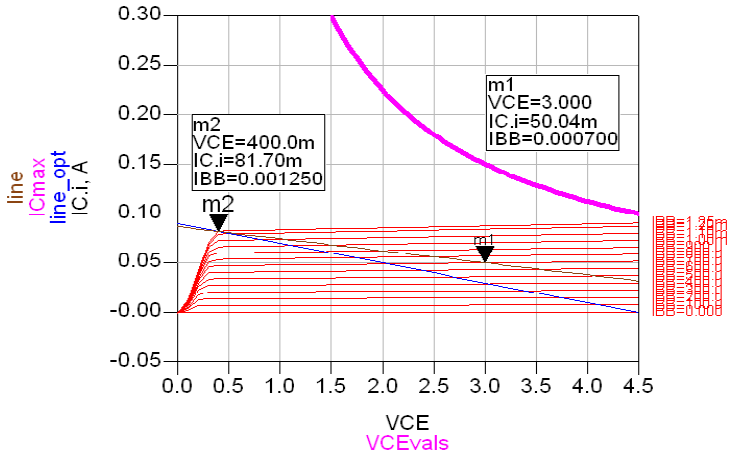

Figure. 5 I-V curves.

Table 2: Performance of Transistor at Optimum Bias Point.

Parameter	Values
Output Power, P_{out}	16.22 dBm
Efficiency, η	41.84%
DC Power, P_{dc}	100.1 mW
V_{ce}	2.45 V
I_c	40.85 mA
R_L	50.183 Ω

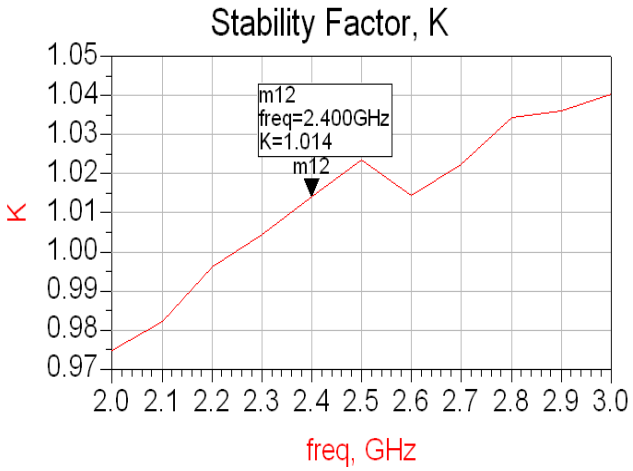

Fig. 6. Simulation of stability factor, K .

The single stub matching technique is used to obtain the input and output matching. From this matching technique, the distance, d and length of stub, ℓ are acquired which open circuit shunt stub is used to find the length of stub. Fig 7 shows the schematic of the input and output matching. The distance and length of stub which obtained from the Smith chart are converted to micro-strip line. The transformation to the micro-strip lines (MLIN and MLOC) are obtained by using an ADS Line calculator, LineCalc. The shunt tuning is especially easy to fabricate in microstrip or stripline form. The matching network can easily be determined using the Smith chart. For the shunt- stub case, the basic idea is to select the distance, *d* so that admittance, Y, seen looking into the line at *d* from the load is of the form Y_0 + jB. Then the stub susceptance is chosen as –jB, resulting in the matching condition.

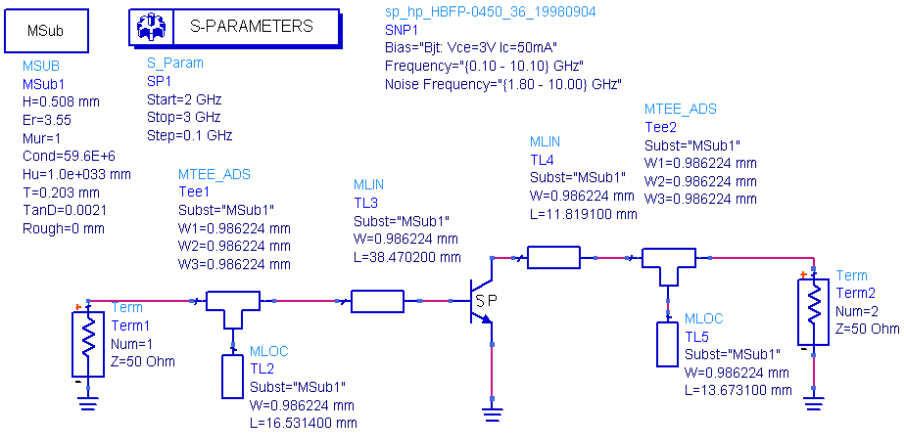

Figure. 7. Schematic of Input and Output Matching

The optimization of input and output matching is needed to improve the performance of the amplifier. The width and length of micro-strip line are tuned until the magnitude of S_{11} and S_{22} approximately to zero which for the perfect matching. The magnitude of both S-parameters are referred to the reflection coefficient, Γ at the input and output. Fig. 8 shows the comparison of gain before and after optimization. From the observation, all the parameter presented the improvement. For example, the gain of amplifier was increased from 12.89 dB to 13.172 dB. The aim of optimization is to improve the performance of an amplifier such as the gain, input and output return loss. For example, in the simulation using ADS software, tune parameter is used to tune the input (magnitude of S_{11}) and output matching (magnitude of S_{22}). Both of magnitudes are referred to the reflection coefficient, Γ which for the perfect matching, the value of Γ should be equal to zero.

The single tone harmonic balance simulation was done to plot the transducer power gain, the PAE, input power, P_{in}, and output power, P_{out}. Fig. 9 shows the transducer power gain versus frequency. The gain increases a frequency increases until 2.6 GHz. Then, after that frequency, the gain decreases as a frequency increases. At a 1-dB compression point, the gain is 9.012 dB at 2.4 GHz. The input 1-dB compression point is defined as the power level for which the input signal is amplified 1 dB less than the linear gain. When a power amplifier has operated in its linear region, the gain is a constant for a given frequency. However when the input signal power is increased, there is a certain point beyond which the gain is seen to decrease. Fig. 10 shows the relationship between PAE and frequency. PAE is directly proportional to output power, it takes a maximum value of 32.132 at 11 dBm input power and it takes a value of 24.951 at the 1-dB compression point. Fig. 11 shows the P_{out} vs. frequency which the response has same characteristic with the Fig 10. The output power is about 16.108 at 1-dB compression point.

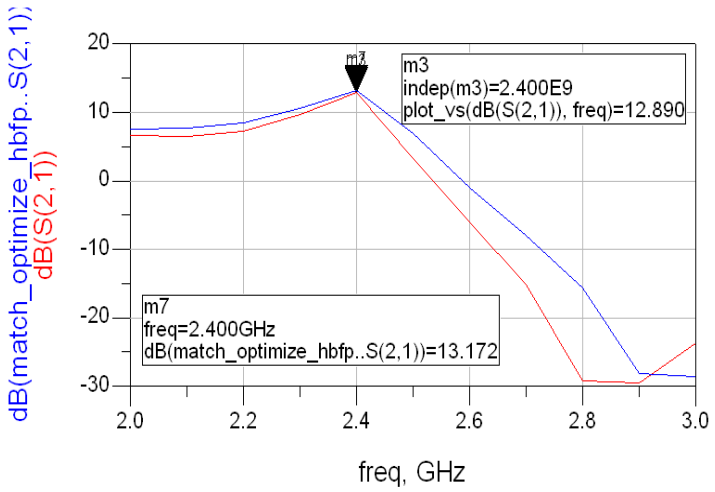

Figure. 8. Comparison of gain before and after optimization.

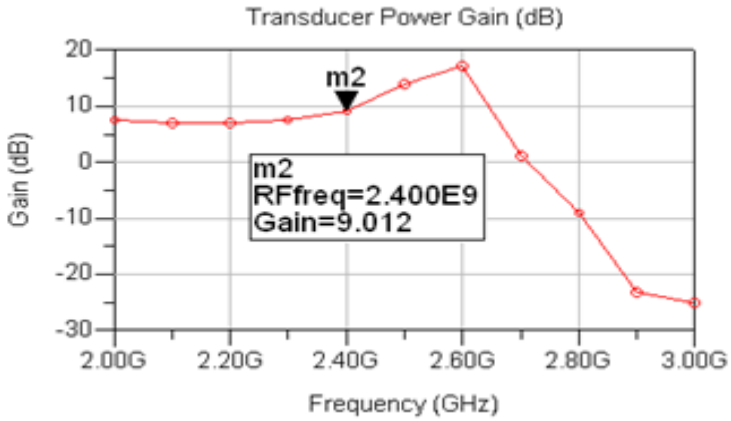

Figure. 9. Transducer power gain versus frequency

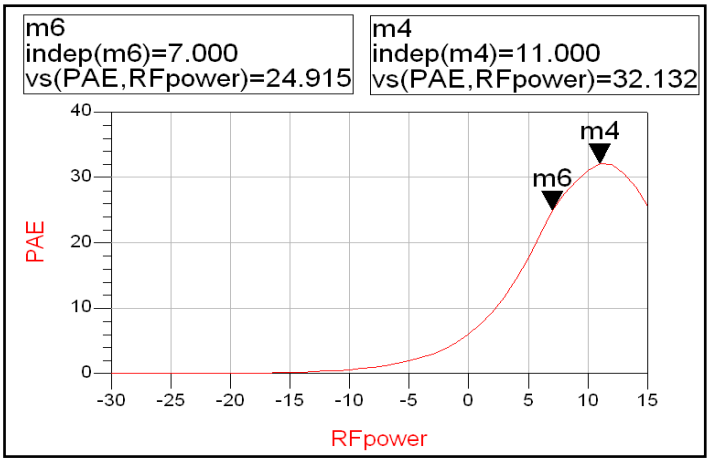

Figure. 10. Power Added Efficiency Vs. Input Power

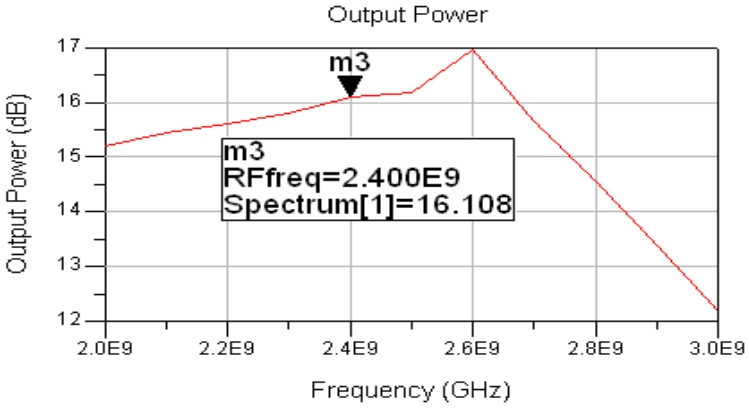

Figure. 11. Output power vs. frequency

IV. CONCLUSION

In this paper proposed designs and analysis power amplifier in the RAP at 2.4 GHz for RoF. In order to achieve that, an ADS model for the transistor, given from freescale, has been used in the designing process. The selection of transistor is the most critical part in the power amplifier design. From that, S-parameter at the operating frequency (2.4 GHz) is used to determine stability, maximum gain and matching network. Many aspects of the PA were considered when presenting the final results, as the power gain, output power, linearity, efficiency, PAE. At the optimal bias point for class A operation, the maximum output power is about 16.22 dBm and the PAE is approximately 41.84 %. Then, the power transducer gain after optimization of matching network is about 13.172 dB. The performance final implementation of power amplifier was examined using one tone

and two tone simulations. At the 1-dB compression point the output power is found approximately 16.108 dB, the PAE is 24.915 %, and transducer power gain is 9.019 dB. All the results are meeting the requirement for a low power amplifier with operating in Class A and can be used for short range application (pico cell). So an interesting future work would be to improve the performance of the system and achieve a higher gain. The load pull technique can be used to determine the load impedance required for maximizing efficiency. From the two tone simulation, the other parameters also can be computes such as the intercept point and intermodulation.

V. ACKNOWLEDGEMENTS

The author would like to thank Universiti Teknikal Malaysia Melaka (UTeM) which has financially supported this research to be accomplished.

VI. REFERENCES

[1] P P Smyth, Optical Radio – A review of a Radical New Technology For Wireless Access Infrastructure, In: Peter Smyth. Mobile and Wireless Communication: Key Technologies and Future Applications. London. : The Institution of Electrical Engineers. 2004.

[2] Vanblaricum, M.L. , Photonic Systems for Antenna Applications, IEEE Antenna Propag. Mag, 36(5), pp. 30-38, 1994.

[3] A. Salleh, M. Z. A Abd Aziz, N. R. Mohamad, M. A. Othman, Z. Zakaria, M. H. Misran, "Design of Low Noise Amplifier for Radio over Fiber Technology at 5.2 GHz", IOSR Journal of Electonics and Communication Engineering , vol. 5, issue 3, pp. 65-69, 2013.

[4] Hyo-Soon Kang, Myung-Jae Lee and Woo-Young Choi, Multi Standard Radio over Fiber Systems using CMOS-Compatible Si Avalanche Photodetector, Asia Pacific Microwave Photonics Conference, pp. 302–35, 2008.

[5] Hamed Al-Raweshidy, Shozo Komaki, Radio over Fiber Technologies for Mobile Communications Networks, Artech House, Boston, 2002.

[6] P.K.Tang, L.C.Ong, B.Luo,A.Alphones and M.Fujise, Transmission of Multiple Wireless Standards over a Radio-over-Fiber Network, IEEE Microwave Symposium Digest ,2004.

[7] Sangil Kim, Hodeok Jang et al, Performance Evaluation for UWB Signal Transmission with Different Modulation Schemes in MultiCell Enviroment Distributed Using ROF Technology, 2004.

[8] Gurprakash Singh and Arokiaswami Alphones, OFDM Modulation Study for Radio-over-Fiber System for Wireless LAN (IEEE802.11a), 4th International Conference on Information, Communications & Signal Processing , 2003.

[9] Razali Ngah, Teguh Prakoso & Tharek Abdul Rahman, Coverage Range and Cost Comparison of Remote Antenna Unit Designs for In building Radio over Fiber Technology, ITB J. ICT Vol. 2, No. 1, 2008.

[10] Pengcheng Xiou, Zhigong Wang, 5.2GHz CMOS Narrow Optical Receiver for Radio over Fiber,Proc. of International Conference on Communications, Circuits and Systems, pp. 1937-1941, 2006.

[11] Muthuswamy Venkataramani, Efficiency Improvement of WCDMA Base Station Transmitters using Class-F power amplifiers, Virginia Polytechnic Institute and State University, Feb 2004.

[12] D. M. Pozar, Microwave and RF Design of Wireless Systems, John Wiley & Sons, Inc., 2001.

[13] Westbrook, L.D. and Moodie, D.G., 'Simultaneous bidirectional analogue fibre optic transmission using electroabsorption modulator', Electronic Letts. 32(19), pp. 1806 -1807, September 1996.

American Journal of Engineering Research (AJER)
e-ISSN : 2320-0847 p-ISSN : 2320-0936
Volume-02, Issue-09, pp-171-189
www.ajer.org

Research Paper Open Access

The Use of Alternate Ligno-cellulosic Raw Materials Banana *(Musa sapientum)* Ankara *(Calotropis procera)* and Pineapple *(Ananas comosus)* in Handmade Paper & their Blending with Waste Paper.

Atul Kumar[1], Brij Pal Singh[2], Rakesh Kumar Jain[3], and Ashwini Kr. Sharma[1]
1: Kumarappa National Handmade Paper Institute, Sanganer, Jaipur, (Rajasthan) ,India; 2: Deenbandhu Chhotu Ram University of Science and Technology, Murthal, Sonepat (Haryana),India; 3: Central Pulp and Paper Research Institute, Saharanpur, (UP), India;

Abstract: - The studies were made to established suitability of lingo-cellulosic raw materials namely leaf fibre **Banana (Musa Sapientum),** bast fibre **Ankara (Calotropis Procera), &** leaf fibre **Pineapple (Ananas Comosus)** for making pulps for handmade paper industry. This should help in providing a cost effective, good quality cellulosic raw material as an alternate to cost prohibitive traditionally used cotton hosiery waste traditionally used for manufacturing good quality handmade paper & it's products. This will help in improving the cost economics & competitiveness of the Indian paper industry in the global market besides addressing the problems of environment & global warming. The aim of the research was to study the extraction, morphology, chemical composition and pulping of these fibres and relate these properties to the composite properties obtained with these fibres as reinforcement with short fibres viz. waste paper. For the pulp production to be feasible it is essential to use suitable pulping methods, which maximize the yield of pulp and introduce as low damage as possible to the fibres. The different pulping methods were applied to these fibre to get optimized strength properties papers. The Studies thus carried out provide useful information about the nature of these raw materials, suitable pulping & bleaching process to produce an eco-friendly handmade paper and converted products. The research work provides a good quality cost effective lingo-cellulosic raw material for handmade paper industries with a possibility of replacement of the expensive and traditionally used cotton hosiery waste. The paper thus produced using environmental friendly pulping and bleaching process is characterized for its strength properties like tensile, tear, bursting, folding endurance and other parameters. The effluents generated from pulping and bleaching of above ligno-cellulosic waste materials were characterized for various pollution parameters like Residual Alkali, BOD, COD etc. The research work thus carried out in the present research has of great importance for handmade paper industry not in India but also in developing and developed countries in other parts of the world. Further the study will be useful in providing opportunities for employment generation and income enhancement among the rural masses.

Keywords: - *Alkaline Peroxide Pulping (APP), Alkaline Sulphite Pulping (ASP), Bast fibres, BOD, COD, Leaf fibre, RCF, TAPPI*

I. INTRODUCTION

Handmade paper making is one of the traditional industries of India, though it's invention is claimed by Chinese dated back to 105 A.D. by T'sai Luin, but recent researches showed that the papers were used in India dated back 325 BC when Budhism took place here [1]. However, prior to this period, the palm leaves were the medium of writing in India. 'Papyrus' from which the world 'Paper' has been derived, on the bank of Nile river in Egypt, has been the medium of communication in Egypt[2].

1.1 Scenario in India:

As per estimates, there are nearly more than 500 handmade paper units scattered all over India producing nearly 50,000 tonnes of handmade paper and board. The Indian handmade paper industry had grown remarkably in the recent past wherein the production of handmade paper industry has reached to a turnover of Rs 250,000 million. Due to increased literacy, industrialization and modernization, the per capita consumption of the paper and paper board has increased remarkably from 4.5 kg in the year 2000 to nearly 9.0 Kg in the recent past. This industry provides employment to about 15,000 people and most of them are situated in the rural areas[3].

With the growing trend of environmental friendliness, demand of handmade papers made out of natural fibers is rising. Moreover, the rising cost of traditionally used cellulosic raw materials like cotton rags and hosiery waste, being used in handmade papermaking is also forcing the industry to search for additional cellulosic raw materials for production of handmade paper and board which are available as waste biomass in different parts of the world. This should help in providing more opportunities for cost effective, locally available lignocellulosic raw materials / agro residues like Banana, Ankara, Pineapple, etc. there by addressing the problem of environment and the issue of global warming in a right prospective.

Handmade paper sector is considered to be eco-friendly, utilizing non woody and waste raw materials in its manufacturing process. The durability of the paper is high with exclusive look and texture. The paper is available in a saga of rich varieties, designs, shapes and colors. Most of the handmade paper units in India have been traditionally using cotton hosiery waste as the main source of raw material, which produce paper with excellent strength characteristics.

1.2 Share in Export Market:

China is holding the maximum share of 27% in the export of handmade paper and paper products while India is at Number 2 position with a share of 24% . Thailand and Philippines are the next competitors in the handmade paper and paper products export. Data is depicted in Table -1 &Fig- 1.

II. OBJECTIVE OF THE STUDY

2.1 The aim of the research: The aim of the research was to study the morphology, chemical composition and pulping of these fibres and relate these properties to the composite properties obtained with these fibres as reinforcement with short fibres viz. waste paper. For the pulp production to be feasible it is essential to use suitable pulping methods, which maximize the yield of pulp and introduce as low damage as possible to the fibres.

2.2 Different Pulping Method: The different pulping methods were applied to these fibre to get optimized strength properties papers. The Studies thus carried out provide useful information about the nature of these raw materials, suitable pulping & bleaching process to produce an eco-friendly handmade paper and converted products.

III. METHODOLOGY OF THE STUDY

3.1 Proximate / Chemical analysis and Fibre length & Dia of Banana, Ankara and Pineapple Fibres:

The trimmed sample of fibres were grilled in dust making machine and screened, since no diffusion limitations were observed for the particle size in preliminary studies. Samples were dried, homogenized in a single lot to avoid differences in composition among aliquots, and stored.

Characterization experiment involved the following parameters: 1% NaOH solubility (Tappi 212 om-98), hot water solubility (Tappi 207 cm-93), ash (Tappi-211, om-85), alcohol-benzene extractives (Tappi 204 cm-97), cellulose (Tappi 203-om-93), Klason lignin (Tappi T 222 om-98) and holocellulose (Wise et al., 1946) contents. All treatments in this study were in a completely randomized design with five replications (variation coefficient less than 5%. less than 1% for holocellulose and cellulose contents).The results are depicted in Table-2 & Graph-1.

For determination of fiber length, 100 individual fiber were measured from each variety. Statistical analyses were performed using PROJECTINA Microscope and the differences among varieties were compared. The means were separated on the basis of least significant difference at 0.05 probability level. The results are depicted in Table-3 & Graph-2.

3.2 Pulping of the Fibres:

Pulp is a fibrous material resulting from complex manufacturing processes that involve the chemical and / or mechanical treatment of various types of plant material. Pulp is one of the most abundant raw materials worldwide which is used predominantly as a major component in the manufacture of paper and paperboard, and with increasing importance also in the form of a wide variety of cellulose products in the textile, food, and pharmaceutical industries. It is self-evident that the competitiveness of pulp and its products produced thereof can only be maintained through continuous innovations at the highest possible level. In context of handmade

paper, cotton waste and hosiery waste being the basic raw materials for paper making in India, pulping of these selected raw materials were subjected to following pulping processes.
3.2.1 Atmospheric Temperature & Pressure Pulping.
3.2.2 Alkaline Pulping.
3.2.3 Alkaline Peroxide Pulping.
3.2.4 Alkaline Sulphite Pulping.

Concerned to the global environment, utilization of these lignocellulosic raw materials has become a major focus in the handmade paper / paper board production. The preparation of pulps from plant fibers normally requires the use of the digester for the fiberization and delignification processes. This research concerns the development of a pulping process, suitable which can be performed under atmospheric temperature & pressure. In this process, the only sodium hydroxide used as a pulping chemical to delignify the fibres, without the use of digester. The cooking conditions were milder than the methods used in the other said pulping processes, and subsequently resulted in pulps with higher yields and good physical properties. [4]

Alkali treatments refers to the application of alkaline solutions such as NaOH, Ca(OH) 2 or ammonia. Among these, treatment with NaOH has been used for delignification of these pseudo stem, bast and leaf fibres. The alkali treatment causes swelling, leading to an increase in internal surface area, a decrease in the degree of polymerization, a decrease in crystallinity, separation of structural linkages between lignin and carbohydrates, and disruption of the lignin structure. As a consequence, the lignin is dissolved from the raw material, being separated in the form of a liquor rich in phenolic compounds that represents the process effluent. The inconvenient of this technique is that it also degrades part of the hemicellulose. [5]

Hydrogen peroxide treatment utilizes alkaline solutions at temperatures 95º C, which promote a fast decomposition of H2O2. As a consequence, more reactive radicals such as hydroxyl radicals (HO) and superoxide anions (O2–) are produced, which are responsible for lignin degradation. This technique is used for bleaching and delignification purposes (to improve the brightness of pulp as it reacts with colored carbonyl-containing structures in the lignin). However, total chlorine free pulp may be obtained by this delignification process. [6]

Similarly to the alkaline treatment, during the lignin solubilization by hydrogen peroxide part of the hemicellulose is also removed from the material structure.

Alkaline Sulphite treatment is another way to remove the lignin content of lignocellulosic materials. Lignin attacks as a scavenger during this pre-treatment because it consumes most of sulphite during the degradation of the carbohydrate content. As a consequence, low alkali amounts are available for cellulose degradation. However, this treatment may also attacks the cellulose and hemicellulose components besides the lignin molecule. Cellulose degradation has been attributed partly to a direct reaction of with the glycosidic linkage and partly to a free radical mediated oxidation of hydroxyl groups in glucose. Some advantages of this treatment are that the effluent after concentrating can be use as adhesive chemicals for other industries. [7]

Conditions involved in the pulping processes:
3.2.1 Atmospheric Temperature and Pressure Pulping

After cutting the raw materials into suitable size, ie 1 -1.5 inches it was subjected to above said method with different % of NaOH. The raw materials were soaked at room temperature and pressure with 8%, 10% and 12% of sodium hydroxide and left for 24 hours with the bath ratio 1:8 as depicted in Table 5.

Strength Characteristics

After washing, the fibers were beaten in laboratory valley beater. The pulps were beaten up to ~300 ml CSF (Canadian Standard Freeness) and laboratory sheets of 60 GSM were formed in hand sheet former. The sheets were conditioned for 24 hours at 27 $\pm$1ºC and 65$\pm$2 % relative humidity. After conditioning, the physical strength properties were evaluated as per the Standard Test Methods viz TAPPI, BIS, IS & ISO:2471. The results are recorded in Table 6 and Graph-3.

Results and Discussion

The physical strength properties of these fibres at atmospheric temperature and pressure showed that these fibres can be used for making handmade paper by using NaOH simply without any external source of heat. The pulp thus produced can be used for making variety of handmade papers / paper boards. This method can be useful for the that type of industry people who do not have the cooking utensils like digesters or can not afford to have digesters.

3.2.2 Alkaline Pulping:

After cutting the raw materials into suitable size ie 1-1.5 inches, it was subjected to alkaline pulping method. The raw materials were cooked at 100° C temperature with 8%, 10% and 12% of sodium hydroxide and cooked for three hours with the bath ratio 1:8. The conditions are depicted in Table 7.

Strength Characteristics

After washing, the fibers were beaten in laboratory valley beater. The pulps were beaten up to ~300 ml CSF (Canadian Standard Freeness) and laboratory sheets of 60 GSM were formed in hand sheet former. The sheets were conditioned for 24 hours at 27 $\pm$1ºC and 65$\pm$2 % relative humidity. After conditioning, the physical strength properties were evaluated as per the Standard Test Methods viz TAPPI, BIS, IS & ISO:2471. The results are recorded in Table 8 & Graph-4.

Results and Discussion

The physical strength properties of these fibres at 100 degree temperature showed a remarkable changes in their strength properties that can be seen in above table. Also the effluent generated is under control. The tensile and folding strength increased remarkably, also the other strength properties like tear and burst also improved. So these fibres can be used for making handmade papers by using NaOH in digester. The pulp thus produced can be used for making variety of handmade papers / paper boards, particularly specialty papers . This method can be useful for the industry people who have the cooking utensils like digesters or even they do not have digesters simply go for open digestion.

3.2.3 Alkaline Peroxide Pulping:

After cutting the raw materials into suitable size ie 1-1.5 inches, it was subjected to alkaline peroxide pulping method. The raw materials were cooked at 95° C temperature with 8%, 10% and 12% of sodium hydroxide and 2% hydrogen peroxide for three hours with the bath ratio 1:8. The conditions are depicted in Table 9. But before pulping following pretreatment were followed to get better results.

Pretreatment with chelating agent

The plant materials like banana, ankara and pineapple contains metal ions like iron, manganese etc. which if present may decompose hydrogen peroxide and form complex with the metallic ions affecting the brightness and permanence of paper.

Therefore to avoid the interference of metallic ions pretreatment of raw material with chelating agent EDTA (Ethylene diamine tetra acetic acid disodium salt) was carried out. The following conditions were applied:

EDTA: 0.05 %, pH: 4 to 5, Time: 30 Mints, Temperature: Room temperature

After chelation, these raw materials were cleaned by de-mineralized water. After washing, the raw material were cooked with different doses of chemicals ie 8%, 10% and 12% of NaOH and 2% H2O2. The materials were pulped with APP process under the conditions recorded in Table 9.

The experiments on pulping of raw materials, carried out with Alkaline Peroxide process as per the following procedure.

Strength Characteristics

After washing, the fibers were beaten in laboratory valley beater. The pulps were beaten up to ~300 ml CSF (Canadian Standard Freeness) and laboratory sheets of 60 GSM were formed in hand sheet former. The sheets were conditioned for 24 hours at 27 $\pm$1ºC and 65$\pm$2 % relative humidity. After conditioning, the physical strength properties were evaluated as per the Standard Test Methods viz TAPPI, BIS, IS & ISO:2471. The results are recorded in Table 10 &Graph-5.

3.2.3.1 Utilization of Banana, Ankara & Pineapple pulp for manufacturing of Tissue paper and its application in Archival use

The pulp thus produced from Alkaline Peroxide pulping of Banana, Ankara & Pineapple (Exp- 8% NaOH & 2% H2O2) were further explored for making archival tissue paper (11 GSM) & other grammage paper (25, 40 GSM). The results of the strength properties and age of the Banana, Ankara & Pineapple papers are shown in Table 11 &Graph-6.

Results & Discussion:

From the result shown in table 11, it was observed that the strength properties are increased reasonably in all the parameters as the peroxide was used the better delignification occurred. In some of the properties banana fibre showed better results than the other fibres. The banana fibre has some inherent characters like

lustrous, fine structure and clean texture make a super quality fibre / pulp over the others. From the results shown in Table 11, it has been observed that the tissue paper produced from banana possess reasonably higher strength properties, double fold no. (250) coupled with the high age (650 years) making it very much suitable for archival application for the preservation of old documents and manuscripts.

The other paper of higher GSM (25 & 40) produced from Banana, Ankara & Pineapple because of their specific peculiar texture coupled with the other features viz. higher age, very high strength properties made its suitable for high end application & value added hand craft products viz. lamp shades, greeting cards specially stationary items & other gift items etc.

3.2.4 Alkaline Sulphite Pulping:

After cutting the raw materials into suitable size ie 1-1.5 inches, it was subjected to alkaline sulphite pulping(ASP) method. The raw materials were cooked at 120° C temperature with 8%, 10% and 12% of total chemical out of which 70% NaOH and 30% Na2SO3 were maintained for three hours with the bath ratio 1:8. The conditions are depicted in Table 12.

Strength Characteristics:

After washing, the fibers were beaten in laboratory valley beater. The pulps were beaten up to ~300 ml CSF (Canadian Standard Freeness) and laboratory sheets of 60 GSM were formed in hand sheet former. The sheets were conditioned for 24 hours at 27 $\pm$1ºC and 65$\pm$2 % relative humidity. After conditioning, the physical strength properties were evaluated as per the Standard Test Methods viz TAPPI, BIS, IS & ISO:2471. The results are recorded in Table 13 & Graph-7.

Results & Discussion:

From the result shown in table - 13 it was observed that the strength properties are increased with all respect as compared to APP and other pulping process reasonably. Again in some of the properties banana fibre showed better results than the other fibres at low chemical dosages particularly in case of tensile and burst strength.

It was observed that the pulp produced from this process there is requirement of brightness for making high quality papers like archival tissue papers. To over come of this property a bleaching experiment was conducted with 2% of hydrogen peroxide.

The bleached pulp obtained as above and the bleach effluent was characterized for strength characteristics (Table-14) and pollution loads in respect of COD & BOD respectively. Whereas the spent pulping liquor obtained after the alkaline sulphite pulping and washing the unbleached pulp were mixed and evaporated to a solids concentration of 30% w/w for its application in various industries.

3.2.4.1 Bleaching Studies

The unbleached pulp obtained by Alkaline Sulphite pulping of these raw materials with total chemical of 8% Alkaline Sulphite Process were bleached with 2% hydrogen peroxide under following
Hydrogen Peroxide-2 %, NaOH-1 %, EDTA 0.15 %, Consistency-8-9 % Temperature 60-70° *C*,Time-1 hr

The bleached pulp obtained as above and the bleach effluent was characterized for strength characteristics (Table-14) and pollution loads in respect of COD & BOD respectively. Whereas the spent pulping liquor obtained after the alkaline sulphite pulping and washing the unbleached pulp were mixed and evaporated to a solids concentration of 30% w/w for its application in various industries. The Physical strength & optical properties of the bleached pulp from Alkaline Sulphite Pulping (Total 8% chemicals) followed by peroxide bleaching process (~300 ml freeness) were recorded in Table-15.

Results & Discussion:

The bleached pulp of 8% treated pulp shows little bit of increase in strength properties. Of course the brightness of the pulp is increased remarkably. From the results shown in Tables. 10, 11, 13 & 15, it is observed that the strength & optical properties of the pulp produced from alkaline peroxide pulping and alkaline sulphite pulping process followed by peroxide bleaching were superior in respect of Tensile, Tear, Burst & Double fold with a reasonable brightness value wherein it was possible to achieve a brightness 48.60% ISO, 44.11% ISO & 43.41% ISO in case of Banana, Ankara & Pineapple pulp produced from alkaline sulphite pulping followed by peroxide bleaching which was higher compared to other pulping processes.

3.3 Blending Studies

3.3.1 Fibre strength in RCF Pulp blended with these fibre at different pulping condition:

In this section of study, the pulp which were cooked with 8% of chemical in Pulping at atmospheric temperature and pressure process, Alkaline Pulping, Alkaline Peroxide Pulping and Alkaline Sulphite Pulping

process were taken for the blending with the RCF pulp. The results of these pulp sheets at this condition have remarkable strength properties which is suitable for making any kind of handmade paper and paper products. These result are once again depicted in table-16,17,18 and 19, respectively & RCF in table-20 to understand the result in better way.

3.3.1.1. Physical and optical strength properties of the pulps from Pulping at atmospheric temperature and pressure process- Blended with Recycled fibre (RCF).

The recycled fibre beaten up to the level of ~300 CSF and it was blended with the pulps of Banana, Anakra and Pinapple which were cooked with 8% of NaOH for 24 Hrs at Room Temp. The result are depicted in table-21.

Strength Characteristics:

After blending, the fibres were run in laboratory valley beater without any load, and laboratory sheets of 60 GSM were formed in hand sheet former. The sheets were conditioned for 24 hours at 27 $\pm$1ºC and 65$\pm$2 % relative humidity. After conditioning, the physical strength properties were evaluated as per the Standard Test Methods viz TAPPI, BIS, IS & ISO:2471. The results are recorded in Table 21 & Graph-8.

Results and Discussion:

The physical strength properties of these blended fibres sheet showed a remarkable changes ie increase in their strength properties that can be seen in above table. The tensile and folding strength increase, also the other strength properties like tear and burst also improved. So RCF can be used for making handmade papers by using these lignocellulosic raw material pulp. The paper sheets thus produced can be used for making variety of handmade papers / paper boards. This is useful method to industry who do not have Digester.

3.3.1.2. Physical and optical strength properties of the pulps from Alkaline Pulping Process Blended with Recycled fibre (RCF).

The recycled fibre beaten up to the level of ~300 CSF and it was blended with the pulps of Banana, Anakra and Pinapple which were cooked with 8% of NaOH for 3 Hrs at 100° C. The result are depicted in table-22.

Strength Characteristics:

After blending, the fibres were run in laboratory valley beater without any load, and laboratory sheets of 60 GSM were formed in hand sheet former. The sheets were conditioned for 24 hours at 27 $\pm$1ºC and 65$\pm$2 % relative humidity. After conditioning, the physical strength properties were evaluated as per the Standard Test Methods viz TAPPI, BIS, IS & ISO:2471. The results are recorded in Table 22 &Graph-8.

Results and Discussion:

The physical strength properties of these blended fibres sheet showed a remarkable changes ie increase in their strength properties that can be seen in above table. The tensile and folding strength increased remarkably, also the other strength properties like tear and burst also improved. So RCF can be used for making handmade papers by using these lignocellulosic raw material pulp. The paper sheets thus produced can be used for making variety of handmade papers / paper boards. This can be useful for the industry people who are using RCF as a raw material.

3.3.1.3. Physical strength and optical properties of the pulp from Alkaline Peroxide Pulping Process Blended with Recycled Fibre (RCF).

The recycled fibre beaten up to the level of ~300 CSF and it was blended with the pulps of Banana, Anakra and Pinapple which were cooked with 8% of NaOH and 2% H2O2% (Hydrogen Peroxide) for 3 Hrs at 95° C. The results are depicted in table-23.

Strength Characteristics:

After blending, the fibres were run in laboratory valley beater without any load, and laboratory sheets of 60 GSM were formed in hand sheet former. The sheets were conditioned for 24 hours at 27 $\pm$1ºC and 65$\pm$2 % relative humidity. After conditioning, the physical strength properties were evaluated as per the Standard Test Methods viz TAPPI, BIS, IS & ISO:2471. The results are recorded in Table 23 &Graph-10.

Results and Discussion:

The physical strength properties of these blended fibres sheet showed a remarkable changes ie increase in their strength properties that can be seen in above table. The tensile and folding strength increased remarkably, also the other strength properties like tear and burst also improved. So RCF can be used for making

handmade papers by using these lignocellulosic raw material pulp. The paper sheets thus produced can be used for making variety of handmade papers / paper boards, particularly specialty papers . This can be useful for the industry people who are using RCF as a raw material.

3.3.1.4. Physical strength and optical properties of the pulp from Alkaline Suiphite Pulping (ASP) Process Blended with Recycled Fibre(RCF).

The recycled fibre beaten up to the level of ~300 CSF and it was blended with the pulps of Banana, Anakra and Pineapple which were cooked with 8% of Total chemical (Out of which NaOH-70% and Na2SO3 (Sodium Sulphite) for 3 Hrs at 120° C. The results are depicted in table-24.

Strength Characteristics:

After blending, the fibres were run in laboratory valley beater without any load, and laboratory sheets of 60 GSM were formed in hand sheet former. The sheets were conditioned for 24 hours at 27 $\pm$1ºC and 65$\pm$2 % relative humidity. After conditioning, the physical strength properties were evaluated as per the Standard Test Methods viz TAPPI, BIS, IS & ISO:2471. The results are recorded in Table 24 & Graph-11.

Results and Discussion:

The physical strength properties of these blended fibres sheet showed a remarkable changes ie increase in their strength properties that can be seen in above table. The tensile and folding strength increased remarkably, also the other strength properties like tear and burst also improved remarkably. So RCF can be used for making handmade papers by using these lignocellulosic raw material pulp depends upon their availability in that particular region. The paper sheets thus produced can be used for making variety of handmade papers / paper boards, particularly specialty papers . This can be useful for the industry people who are using RCF as a raw material.

IV. FIGURES AND TABLES

Table 1. Export Scenario of Handmade Paper in World

COUNTRY	EXPORT IN RS CRORES	% AGE SHARE
INDIA	366	24
PHILIPPINES	127	8
NEPAL	15	1
CHINA	411	27
OTHERS	435	28
TOTAL	1546	
	341.07 MILLION US $	

Source: Report on “Market research in Indian Handmade Paper Industry” by M/S Sycom Projects Consultants Pvt. Ltd. New Delhi.

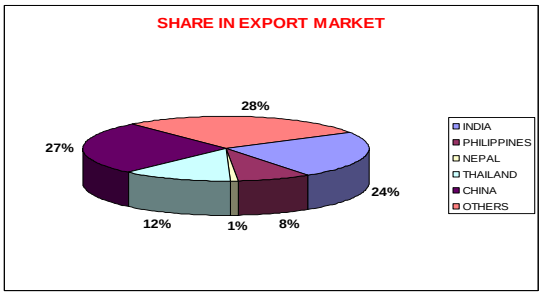

Figure 1. Percentage share of countries in export

Table-2 Proximate / Chemical analysis of Banana, Ankara and Pineapple Fibres:

Particulars	Banana fibre	Ankara fibre	Pineapple fibre
NaOH solubility,1%	18.01	16.90	17.33
Hot Water Solubility,%	7.91	7.30	2.56

Alcohol-Benzene Solubility %	24.04	23.90	12.10
Ash, %	2.45	4.10	1.00
Pentosan, %	10.32	8.90	5.50
Lignin, %	11.90	7.10	7.85
Holocellulose,%	84.11	89.50	92.81
Alpha cellulose, %	82.00	79.00	86.41

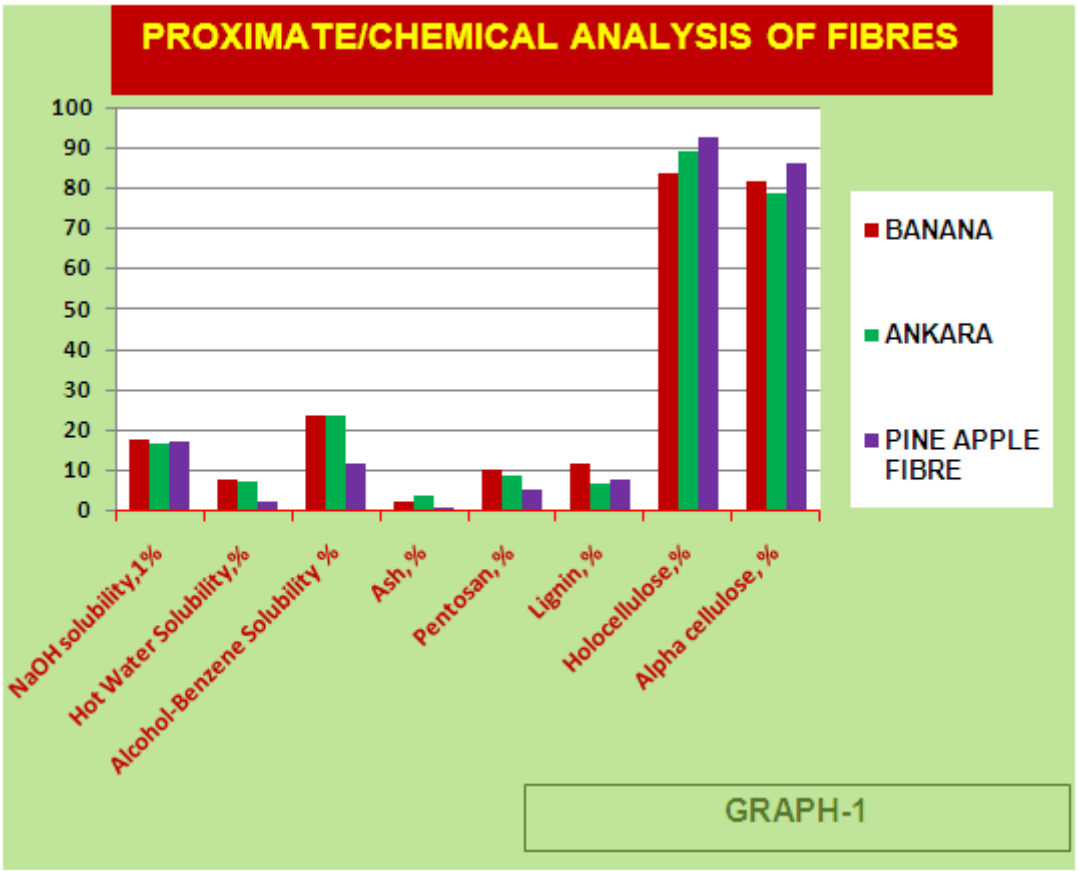

Table-3 Length and Dia of Banana, Ankara and Pineapple Fibres:

Common name (Scientific name)	Fibre Length (mm)		Fibre Dia (µm)	
	Avg	Range	Avg	Range
Banana (*Musa sapientum*)	3.00	1.8~15	24.00	16~32
Ankara (*Calotropis procera*)	3.56	2~20	25.00	15~40
Pineapple (*Ananas comosus*)	9.11	6~25	28.00	25~40

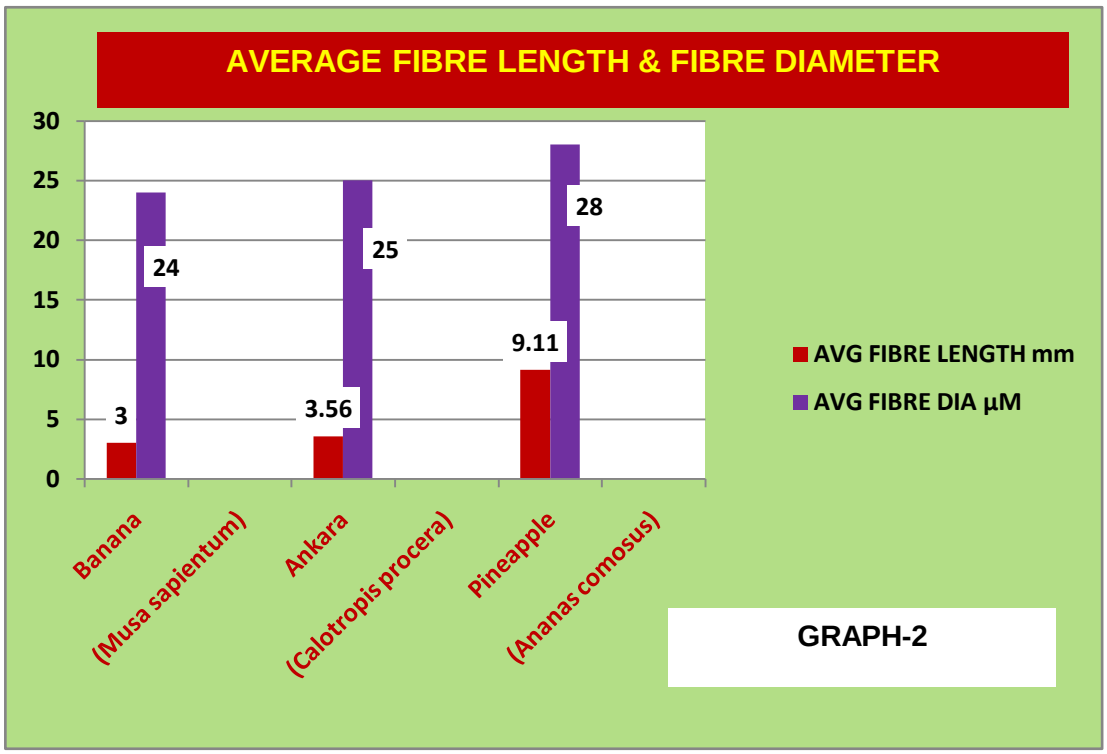

Table 5 Pulping condition of fibres at atmospheric temperature and pressure:

S. No.	Characteristics	Banana			Ankara			Pineapple		
1.	**Cooking conditions**									
	Soaking Time, Hrs.	24			24			24		
	NaOH %	8	10	12	8	10	12	8	10	12
	Temperature ° C	RT	RT	RT	RT	RT	RT	RT	RT	RT
	Pressure	Atm	Atm	Atm	Atm	Atm	Atm	Atm	Atm	Atm
	Bath ratio	1:8	1:8	1:8	1:8	1:8	1:8	1:8	1:8	1:8
2.	**Black liquor analysis**									
	Residual active alkali after digestion, gpl	Nil	Nil	0.10	Nil	Nil	0.12	Nil	Nil	0.15
3.	**Pulp Yield%**	86.91	85.11	84.90	84.89	83.23	82.78	89.90	86.19	85.12

RT-Room Temperature
Atm-Atmospheric Pressure

Table 6 Physical and optical strength properties of the pulp from Pulping at atmospheric temperature and pressure process (At ~ 300 ml freeness)

S.No.	Characteristics	Banana			Ankara			Pineapple		
	CSF, ml	**~300**			**~300**			**~300**		
	NaOH %	8	10	12	8	10	12	8	10	12
1.	Tensile Index, (Nm/g)	29.23	32.61	35.21	28.20	30.91	34.30	35.20	38.81	41.20
2.	Tear Index ,($mN.m^2/g$)	1.96	2.01	2.15	1.78	1.94	2.02	2.10	3.71	3.44
3.	Burst Index, ($Kpa.m^2/g$)	1.90	2.10	2.40	1.81	2.00	2.21	2.51	3.00	3.51
4.	Double Fold, No.	1270	1450	1700	1200	1420	1630	1700	1810	2100
5.	Brightness (%) ISO	41.50	40.10	38.00	36.50	35.95	35.00	35.90	34.40	33.31

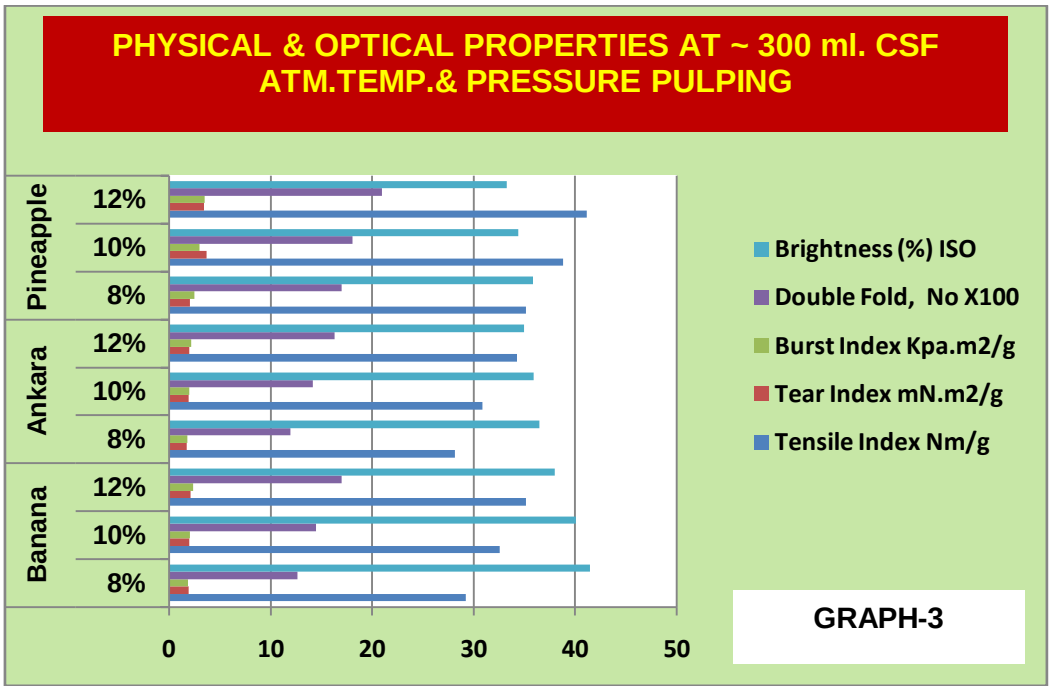

Table 7 Pulping conditions of Banana, Ankara and Pineapple fibers (Alkaline Pulping)

S.No.	Characteristics	Banana			Ankara			Pineapple		
1.	**Cooking conditions**									
	NaOH, %	8	10	12	8	10	12	8	10	12
	Time, Hrs	3	3	3	3	3	3	3	3	3
	Temperature °C	100	100	100	100	100	100	100	100	100
	Bath Ratio	1:8	1:8	1:8	1:8	1:8	1:8	1:8	1:8	1:8
2.	**Effluent Characteristics**									
	Residual active alkali after digestion, gpl	1.00	1.15	1.50	1.12	1.30	1.72	1.25	1.55	1.94
	BOD (Biological Oxygen Demand) **ppm**	1220	1380	1500	1300	1450	1730	1300	1450	1730
	COD (Chemical Oxygen Demand) **ppm**	6000	7700	8100	7000	8100	8700	7100	8200	8800
3.	Pulp Yield ,%	86.66	85.21	84.42	86.65	85.11	84.12	89.60	87.40	86.31

Table 8 Physical and optical strength properties of the pulps from Alkaline Pulping Process (At~ 300 ml freeness).

S.No.	Characteristics	Banana			Ankara			Pineapple		
	CSF,ml	**300**			**300**			**300**		
1.	Tensile Index, (Nm/g)	72.03	75.65	77.71	71.00	71.89	72.80	72.10	73.20	74.15
2.	Tear Index (mN. m^2/g)	4.86	4.91	5.14	4.80	4.82	4.98	4.90	5.10	5.66
3.	Burst Index, (Kpa.m^2/g)	4.10	4.98	5.12	3.80	4.01	4.51	3.97	4.81	4.97
4.	Double Fold , No.	8500	8600	8650	8400	8450	8500	9500	9700	9800
5.	Brightness ,(%) ISO	41.00	40.00	40.00	36.00	35.00	35.00	41.60	41.10	40.00

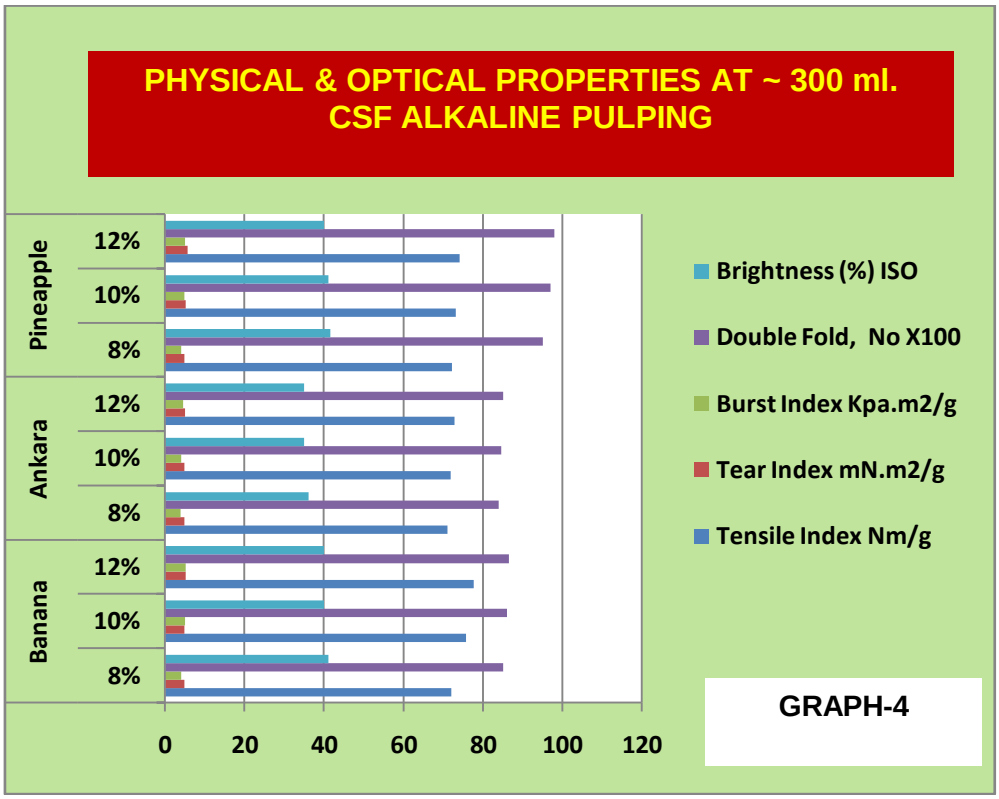

Table 9 Pulping conditions of Banana, Ankara and Pineapple fibers (Alkaline Peroxide Pulping)

S. No.	Characteristics	Banana			Ankara			Pineapple		
1.	**Cooking conditions**									
	NaOH %	8	10	8	8	8	12	8	8	12
	H2O2%	2	2	2	2	2	2	2	2	2
	Time, Hrs	3	3	3	3	3	3	3	3	3
	Temperature ° C	95	95	95	95	95	95	95	95	95
	Bath ratio	1:8	1:8	1:8	1:8	1:8	1:8	1:8	1:8	1:8
2.	**Effluent Characteristics**									
	Residual active alkali after digestion, gpl	1.12	1.25	1.59	1.20	1.39	1.81	1.32	1.65	2.00
	BOD(Biological Oxygen Demand), **ppm**	1800	2000	2300	2300	2300	2600	2320	2350	2630
	COD (Chemical Oxygen Demand), **ppm**	7000	8000	8000	8000	8000	9000	8050	8070	9050
3.	**Pulp Yield%**	80.20	78.89	75.00	75.00	74.50	73.11	84.10	83.00	82.21

Table 10 Physical strength and optical properties of the pulp from Alkaline Peroxide Pulping Process (At ~ 300 ml freeness).

S. No.	Characteristics	Banana			Ankara			Pineapple		
	CSF, ml	~300			~300			~300		
1.	Tensile Index (Nm/g)	85.50	86.10	86.65	80.31	81.11	82.10	86.20	87.70	88.11
2.	Tear Index (mN. m^2/g)	5.05	5.45	6.71	5.00	5.10	5.59	6.00	6.60	6.90
3.	Burst Index (Kpa.m^2/g)	6.31	6.51	6.80	6.26	6.31	6.53	6.50	7.50	7.88
4.	Double Fold , No.	10000	10110	10600	9910	9950	10000	17970	18000	18850
5.	Brightness (%) ISO	48.00	46.50	45.00	38.00	37.00	36.00	47.50	44.00	39.90

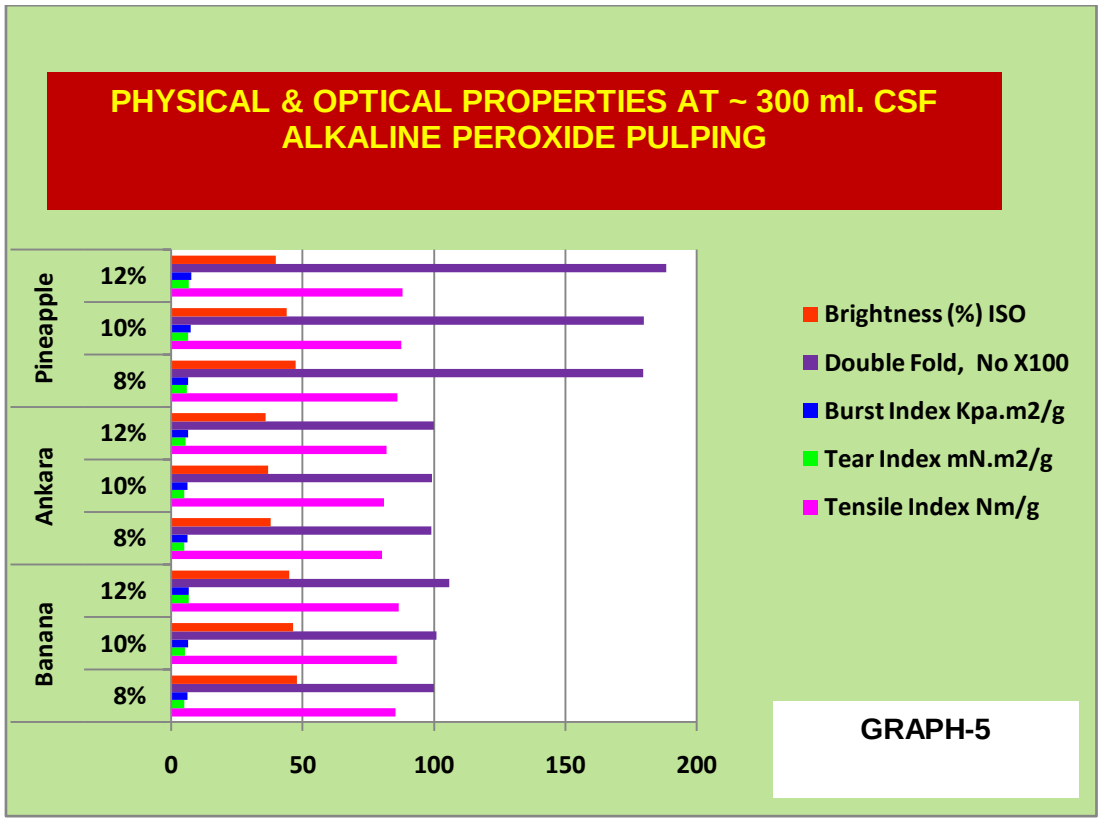

Table 11 Physical and optical strength properties of different GSM Tissue Papers developed from these fibres at ~300 ml freeness

S. N.	Characteristics	Banana			Ankara			Pineapple		
		8%NaOH+2% H2O2			8%NaOH+2% H2O2			8%NaOH+2% H2O2		
	GSM	~11	~25	~40	~11	~25	~40	~11	~25	~40
1.	Tensile Index (Nm/g)	52.76	60.00	65.12	32.50	35.97	40.12	60.30	63.21	69.16
2.	Tear Index (mN.m^2/g)	4.64	6.10	7.71	2.72	6.00	6.70	5.00	6.70	7.75
3.	Burst Index, (Kpa.m^2/g)	2.46	3.87	4.00	2.25	3.95	3.90	3.00	4.30	4.50
4.	Double Fold ,No.	250	600	1000	17	451	800	250	655	1000
5.	Brightness (%) ISO	48.00	48.50	48.50	46.00	47.60	48.00	47.00	46.50	46.00
6.	Age, Years (Average)	-	650	-	-	452	-	-	650	-

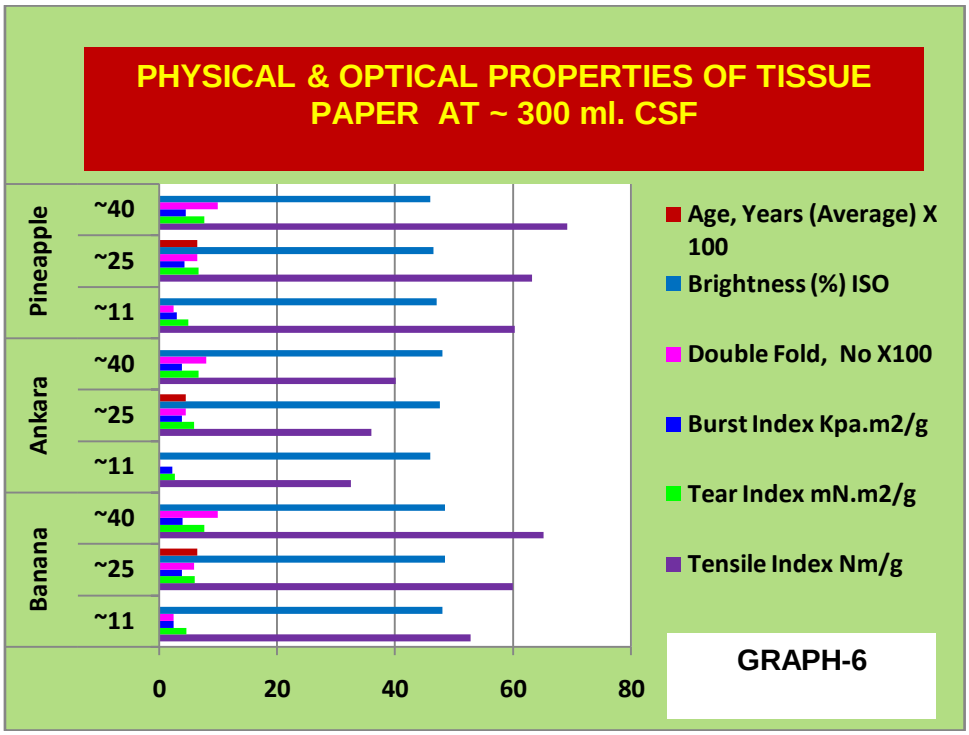

Table 12 Pulping conditions of Banana, Ankara and Pineapple fibers (Alkaline Sulphite Pulping).

S. N.	Characteristics	Banana			Ankara			Pineapple		
1.	**Cooking condition**									
	Total Chemical	8%	10%	12%	8%	10%	12%	8%	10%	12%
	NaOH	70%	70%	70%	70%	70%	70%	70%	70%	70%
	Na2SO3	30%	30%	30%	30%	30%	30%	30%	30%	30%
	Time Hrs	3	3	3	3	3	3	3	3	3
	Temperature ° C	120	120	120	120	120	120	120	120	120
	Bath ratio	1:8	1:8	1:8	1:8	1:8	1:8	1:8	1:8	1:8
2.	**Black liquor analysis**									
	Residual active alkali after digestion, **gpl**	0.72	1.29	1.73	1.02	1.47	1.98	1.07	1.56	2.00
	BOD (Biological Oxygen Demand), **ppm**	2300	2350	2500	2400	2500	2700	2450	2530	2710
	COD (Chemical Oxygen Demand), **ppm**	8000	8500	9100	8700	8900	9100	8750	8920	9160
3.	Yield,%	79.50	78.51	74.80	74.10	73.00	71.51	83.00	82.00	80.30

Table 13 Physical strength and optical properties of the pulp from Alkaline Suiphite Pulping (ASP) Process (At ~ 300 ml freeness).

S.No.	Characteristics	Banana			Ankara			Pineapple		
	CSF	**300**			**300**			**300**		
1.	Tensile Index, (Nm/g)	84.91	85.30	85.90	79.01	80.51	81.30	86.33	86.45	87.28
2.	Tear Index (mN. m^2/g)	5.35	5.95	6.90	5.00	6.51	6.78	6.00	6.76	7.00
3.	Burst Index, (Kpa.m^2/g)	6.10	6.50	6.70	5.70	6.00	6.10	6.20	6.81	7.15
4.	Double Fold, No.	9100	10100	10700	9000	9210	9800	16200	18430	19000
5.	Brightness (%) ,ISO	39.00	38.49	38.00	38.12	38.00	37.77	39.41	38.90	36.44

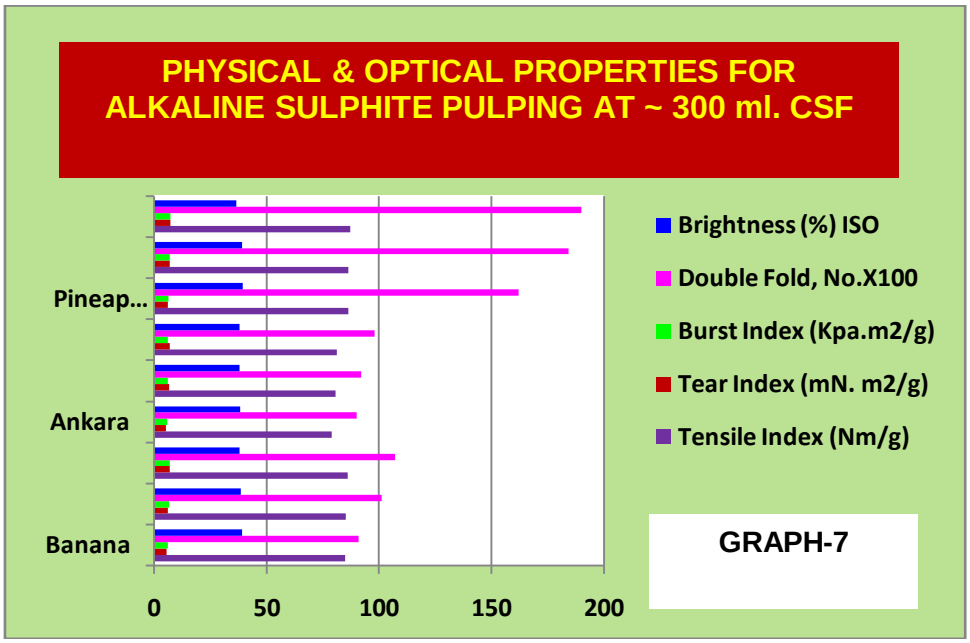

Table 14 Effluent Characteristics of Banana, Ankara and Pineapple fibers (8% Alkaline Sulphite Pulping) after the bleaching.

Characteristics	**Banana**	**Ankara**	**Pineapple**
Effluent Characteristics			
BOD (Biological Oxygen Demand), **ppm**	60	80	82
COD (Chemical Oxygen Demand), **ppm**	640	800	810
Pulp Yield,%	79.00	73.50	82.52

Table 15 Physical strength & optical properties of the bleached pulp from Alkaline Sulphite Pulping (Total 8% chemicals) followed by peroxide bleaching process (~300 ml freeness)

S.No.	Characteristics	Banana	Ankara	Pineapple
1.	Tensile Index (Nm/g)	84.98	79.50	86.73
2.	Tear Index (mN. m^2/g)	5.45	5.17	6.10
3.	Burst Index (Kpa.m^2/g)	6.18	5.90	6.22
4.	Double Fold ,No.	9,120	9040	16210
5.	Brightness (%) ISO	48.60	44.11	43.41

Table-16: Physical and optical strength properties of the pulp from Pulping at atmospheric temperature and pressure process (At ~ 300 ml freeness):

S.No.	**Characteristics**	**Banana**	**Ankara**	**Pineapple**
	CSF, ml	**~300**	**~300**	**~300**
	NaOH %	8	8	8
1.	Tensile Index (Nm/g)	29.23	28.20	35.20
2.	Tear Index(mN.m^2/g)	1.96	1.78	2.10
3.	Burst Index (Kpa.m^2/g)	1.90	1.81	2.51
4.	Double Fold,No.	1270	1200	1700
5.	Brightness (%) ISO	41.50	36.50	35.90

Table 17. Physical and optical strength properties of the pulps from Alkaline Pulping Process (At ~ 300 ml freeness).

S.No.	Characteristics	Banana	Ankara	Pineapple
	CSF,ml	**300**	**300**	**300**
1.	Tensile Index (Nm/g)	72.03	71.00	72.10
2.	Tear Index (mN.m^2/g)	4.86	4.80	4.90
3.	Burst Index (Kpa.m^2/g)	4.10	3.80	4.17
4.	Double Fold ,No.	8500	8400	9500
5.	Brightness (%) ISO	41.00	36.00	41.60

Table 18. Physical strength and optical properties of the pulp from Alkaline Peroxide Pulping Process (At ~ 300 ml freeness).

S. No.	Characteristics	Banana	Ankara	Pineapple
	CSF, ml	**~300**	**~300**	**~300**
		100%B	100%A	100%P
1.	Tensile Index (Nm/g)	85.50	80.31	86.20
2.	Tear Index (mN. m^2/g)	5.05	5.00	6.00
3.	Burst Index (Kpa.m^2/g)	6.31	6.26	6.50
4.	Double Fold , No.	10000	9910	17970
5.	Brightness (%) ISO	48.00	38.00	47.50

Table 19. Physical strength and optical properties of the pulp from Alkaline Suiphite Pulping (ASP) Process (At ~ 300 ml freeness) .

S.No.	Characteristics	Banana	Ankara	Pineapple
	CSF	**300**	**300**	**300**
		100%B	100%A	100%P
1.	Tensile Index (Nm/g)	84.91	79.01	86.33
2.	Tear Index (mN. m^2/g)	5.35	5.00	6.00
3.	Burst Index (Kpa.m^2/g)	6.10	5.70	6.20
4.	Double Fold, No.	9100	9000	16200
5.	Brightness (%) ISO	39.00	38.12	39.41

Table 20. Physical strength and optical properties of the pulp of RCF(At ~ 300 ml freeness).

S.No.	Characteristics	RCF
	CSF	**300**
		100%
1.	Tensile Index (Nm/g)	21.4
2.	Tear Index (mN. m^2/g)	3.61
3.	Burst Index (Kpa.m^2/g)	2.20
4.	Double Fold, No.	15.00
5.	Brightness (%) ISO	45.00

Table 21. Physical and optical strength properties of the pulps from Pulping at atmospheric temperature and pressure process (At ~ 300 ml freeness) Blended with Recycled fibre (RCF).

S.N.	Characteristics	Banana(B)			Ankara(A)			Pineapple(P)		
	CSF, ml	300			300			300		
		100% B	100% RCF	80% RCF +20%B	100% A	100% RCF	80% RCF +20%A	100%P	100% RCF	80% RCF +20%P
1.	Tensile Index (Nm/g)	29.23	21.4	24.91	28.20	21.4	23.62	35.20	21.4	25.00
2.	Tear Index (mN. m^2/g)	1.96	3.61	2.10	1.78	3.61	1.91	2.10	3.61	2.89
3.	Burst Index (Kpa.m^2/g)	1.90	2.20	2.11	1.81	2.20	2.00	2.51	2.20	2.53
4.	Double Fold, No.	1270	15.00	200	1200	15.00	180	1700	15.00	300
5.	Brightness (%) ISO	41.50	45.00	43.00	36.50	45.00	40.00	35.90	45.00	41.00

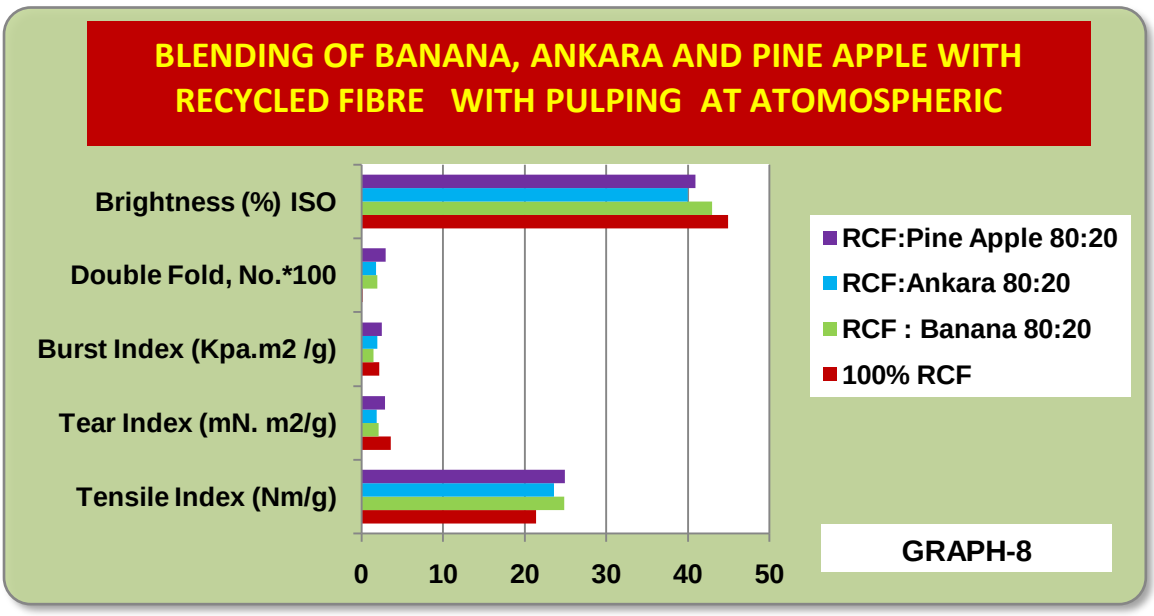

Table 22. Physical and optical strength properties of the pulps from Alkaline Pulping Process (At ~ 300 ml freeness) Blended with Recycled fibre (RCF).

S. N.	Characteristics	Banana(B)			Ankara(A)			Pineapple(P)		
	CSF, ml	300			300			300		
		100% B	100% RCF	80% RCF +20%B	100% A	100% RCF	80% RCF +20%A	100%P	100% RCF	80% RCF +20%P
1.	Tensile Index (Nm/g)	72.03	21.4	35.16	71.00	21.4	34.60	72.10	21.4	42.33
2.	Tear Index (mN. m^2/g)	4.86	3.61	4.51	4.80	3.61	4.42	4.90	3.61	4.80
3.	Burst Index (Kpa.m^2/g)	4.10	2.20	3.14	3.80	2.20	3.00	4.17	2.20	3.96
4.	Double Fold, No.	8500	15.00	451	8400	15.00	408	9600	15.00	500
5.	Brightness (%) ISO	41.00	45.00	42.00	36.00	45.00	44.00	41.60	45.00	43.00

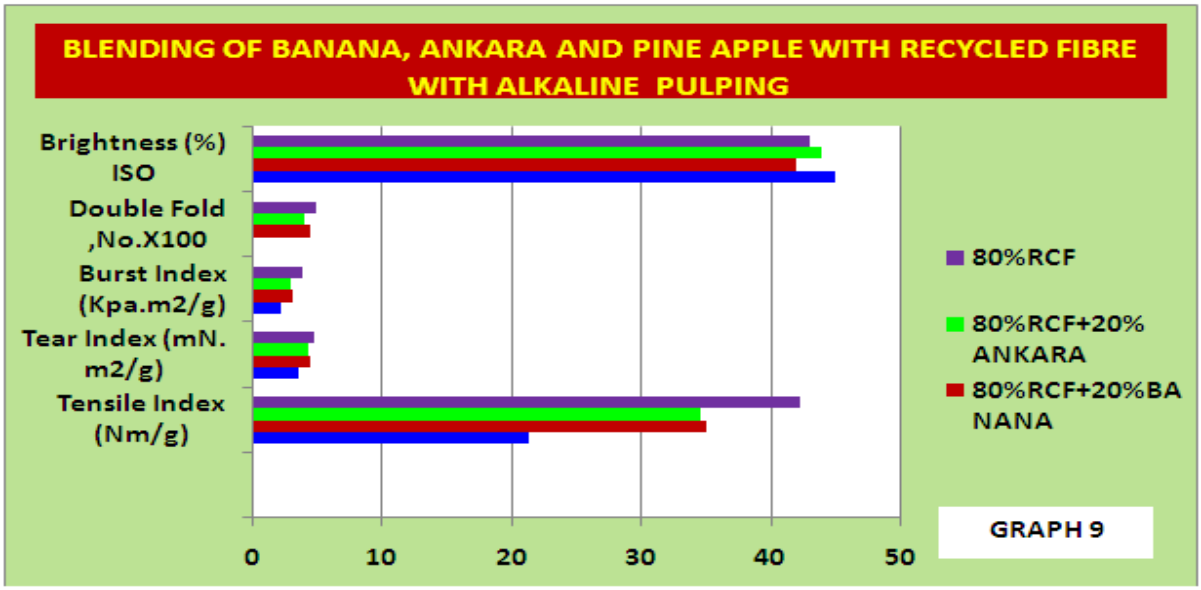

Table 23. - Physical strength and optical properties of the pulp from Alkaline Peroxide Pulping Process (At ~ 300 ml freeness) Blended with Recycled Fibre (RCF).

S. No.	Characteristics	Banana(B)			Ankara(A)			Pineapple(P)		
	CSF, ml	~300			~300			~300		
		100%B	100% RCF	80% RCF +20%B	100%A	100% RCF	80% RCF +20%A	100%P	100% RCF	80% RCF +20%P
1.	Tensile Index (Nm/g)	85.50	21.4	39.61	80.31	21.4	41.03	86.20	21.4	42.21
2.	Tear Index (mN. m^2/g)	5.05	3.61	4.81	6.20	3.61	4.71	6.00	3.61	4.91
3.	Burst Index (Kpa.m^2/g)	6.31	2.20	5.00	6.26	2.20	4.12	6.50	2.20	5.51
4.	Double Fold , No.	10000	15.00	760	17900	15.00	700	17970	15.00	790
5.	Brightness (%) ISO	48.00	45.00	46.00	38.00	45.00	40.00	47.50	45.00	46.00

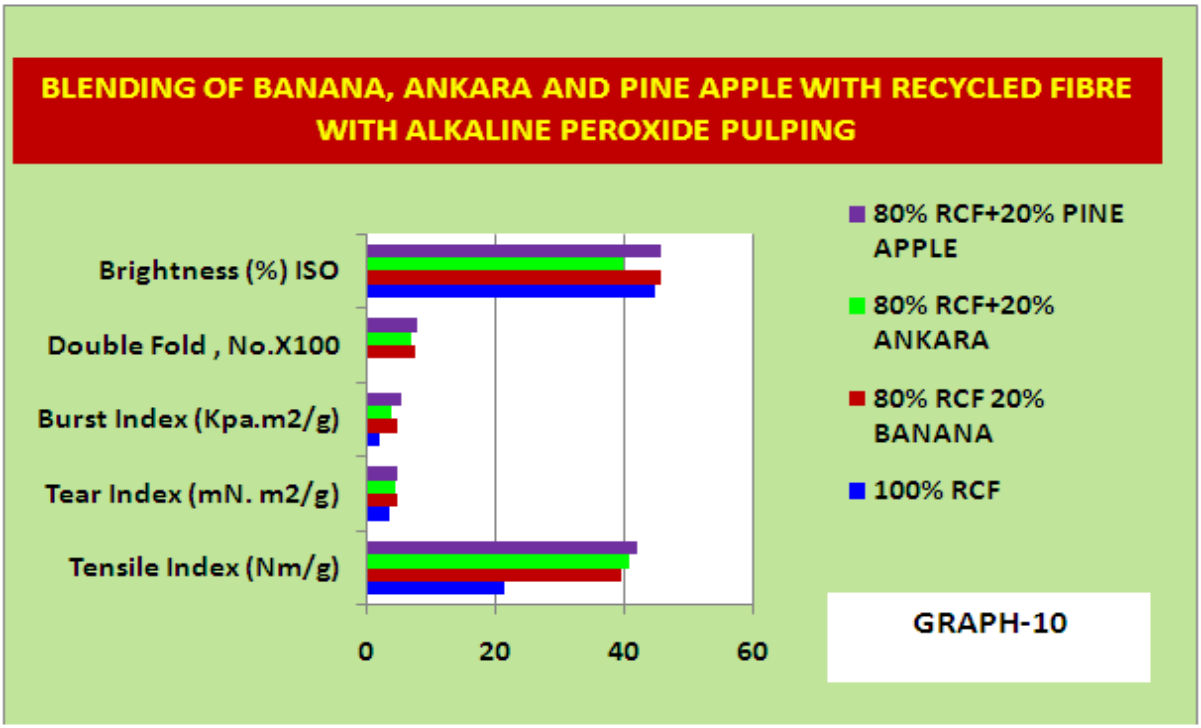

Table 24. - Physical strength and optical properties of the pulp from Alkaline Suiphite Pulping (ASP) Process (At ~ 300 ml freeness) Blended with Recycled Fibre (RCF).

S.N.	Characteristics	Banana(B)			Ankara(A)			Pineapple(P)		
	CSF	300			300			300		
		100% B	100% RCF	80% RCF +20%B	100%A	100% RCF	80% RCF +20%A	100%P	100% RCF	80% RCF +20%P
1.	Tensile Index (Nm/g)	84.91	21.4	41.11	79.01	21.4	40.00	82.33	21.4	43.81
2.	Tear Index (mN. m^2/g)	5.35	3.61	4.53	5.00	3.61	4.91	6.00	3.61	5.10
3.	Burst Index (Kpa.m^2/g)	6.10	2.20	5.01	5.70	2.20	4.71	6.20	2.20	5.41
4.	Double Fold, No.	9100	15.00	600	9000	15.00	570	16200	15.00	700
5.	Brightness (%) ISO	39.00	45.00	40.00	38.12	45.00	41.00	39.41	45.00	41.00

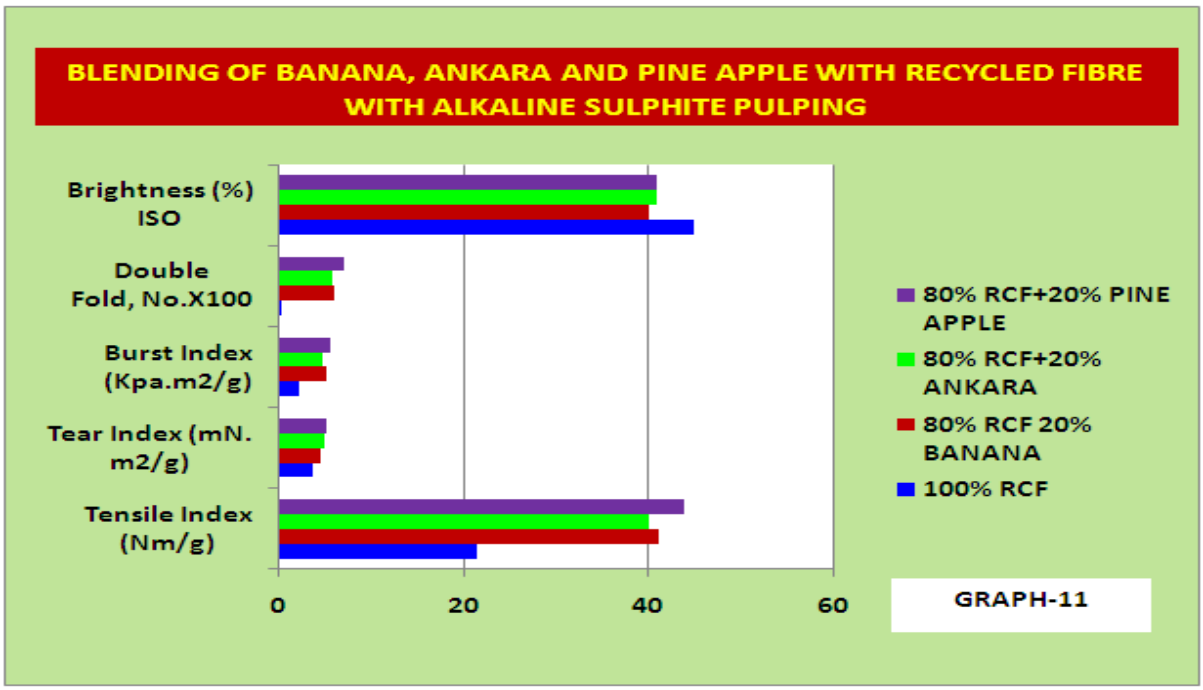

V. CONCLUSION

- These non-wood fibers have tremendous variations in chemical and physical properties. Of particular importance for pulping are fibre length, lignin content and cellulose content. Fiber length-Nonwood fibers average 3 mm (banana) and can be as long as 9 mm (pine apple). Lignin content-Lignin content of fibers is lower than that of any woody pulp. The low lignin content indicates that these fibres will require very mild pulping conditions. Cellulose content-Cellulose content of these fibers is 80% and higher.
- The raw materials used most commonly in handmade industry are the off cut of the textile industry ie hosiery waste in white colour as well as in mixed colours, cotton rags, off cut from HMPI, and recycled secondary fibres. Global trends towards sustainable development have brought to the light that natural, renewable, biodegradable raw materials, among them bast fibres, leaf fibres continue in extending their use in handmade paper industries.
- Recent new trend of applications of green fibres and related products permit to draw the following conclusions: Fast growing population as well as eco and health awareness create large space for future expansion of other than rag fibres. The change of consumer's taste also attract the handmade paper makers for the production and processing of these fibres in handmade paper industry.
- Due to fast progress in research and development, leaf and bast fibres are used for the production of non-wood pulps. This can help to stop forest depletion, flood of non biodegradable waste, environmental degradation. This can also rise living standard of rural areas in many part of globe.
- **Recycling** of natural fibre-reinforced composites is relatively easy and convenient. This fact makes one of the most important factors in forecasting the future **growth of production and consumption** of these materials.
- When preparation of natural fibers from the point of view of their homogeneity and quality would be improved, a new **big potential market** for natural fibers can emerge.
- Beating / Pulping of these raw materials is based on the use of non-polluting chemicals such as NaOH, peroxides, sulphite. It has been avoided to use harmful chemicals like sulphate, chlorine and chlorine compounds for the delignification processes. There is no any major pollution or negative impact on environment.
- The another very good use of these pulps are as to blend it with RCF(Recycled Fibre Pulp). As evident from the results depicted in tables 22, 23 and 24 that the strength properties increased remarkably in many parameters. Here, it may also recommended that these fibre can replace imported long fibre wood pulp sheets which are being imported by big paper mills.

REFERENCES

Journal Papers

[1] Gupta H. K., Kumar A., Agrawal, S. (2001). "Role Of Handmade Paper Units In Improving Paper Quality And Efficiency Of Recycled Waste Paper Based Mills," *IPPTA Journal* 13(4),Pages-47-51

[2] Panda, A., Singh, S. N., Bhoomiah, M. And Khandekar, V. "Handmade Paper Making In India: Prospects, Possibilities And Problems," Paper-Ex-1995,International Seminar On Pulp And Paper Industry, New Delhi,Pages-157-187.

[3] Sharma, A. K. And Satyapal "An Overview Of Indian Handmade Paper Industry," Handmade Paper And Product Souvenir, Paperex-2011, New Delhi, India Atmospheric Pulping Of Non-Woody Fibers

[4] Takanori NOMURA*, Makoto TAKADA*, Masato OKA*, Hirokazu MATSUBARA*, Taketoshi OHIRA* And Shunichi SHINAGAWA***: Gifu Prefectural Research Institute Of Industrial Product Technology, 777, Maeno, Mino Gifu 501-3716, Japan**: National Institute Of Materials And Chemical Research (NIMC), 1-1, Higashi, Tsukuba, Ibaraki 305-8565, Japan

[5] MULTIFUNCTIONAL ALKALINE PULPING, DELIGNIFICATION AND HEMICELLULOSE EXTRACTION GABRIELE SCHILD, HERBERT SIXTA* And LIDIA TESTOVA** Kompetenzzentrum Holz Gmbh, St.-Peter-Str. 25, A-4021 Linz, Austria*Lenzing AG, Werkstraße 1, A-4860 Lenzing, Austria **Department Of Forest Products Technology, Helsinki University Of Technology, Vuorimiehentie1, 02015 Espoo, Finland; December 4, 2009 (CELLULOSE CHEMISTRY AND TECHNOLOGY).

[6] Studies On The Mechanism Of Alkaline Peroxide Delignification Of Agricultural Residues J. Michael Gould, Northern Regional Research Center, Agricultural Research Service, U.S. Department Of Agriculture, Peoria, Illinois 61604 Accepted For Publication June 5, 1984 (BIOTECHNOLOGY AND BIOENGINEERING, VOL. 27, MARCH 1985).

[7] Handbook Of Pulp- Edited By Herbert Sixta Copyright © 2006 WILEY-VCH Verlag Gmbh & Co. Kgaa, Weinheim ISBN: 3-527-30999-3

[8] Saravana Bavan D And GC Mohan Kumar (2010) Potential Use Of Natural Fiber Composite Materials In India *Journal Of Reinforced Plastics And Composites* 29: 3600 Http://Jrp.Sagepub.Com/Content/29/24/3600

Books/Reports

[9] Hunter, D. Paper Making: The History and Technique of an Ancient Craft, Dover Publication Inc. New York.

[10] Rydholm. A. S. (1985). *Pulping Processes*, Intersciences Publishers, New York.

[11] Strengthening of Handmade Paper industry in India (IND/90/037/A/01/37). Technical Report , Second Mission-based on the work of S. B. Green, Chief Technical Advisor ,UNODO, Vienna.

[12] Strengthening of Handmade Paper industry in India (IND/90/037/A/01/37). UNDP-KVIC Project Reports, Market Survey Report and Various Fellowship Reports.

[13] *The Wealth of India: Raw Materials*, CSIR, New Delhi, India.

[14] Indian Standard Writing and Printing Papers Specification(Third Revision)IS 1848 :1991.

[15] Author in the book HANDMADE PAPER FROM RAG TO RICHES (ISBN No. 8180695301, ISBN 13 9788180695308, Publisher- Concept Publishing Company- Year 2009) written and compiled by Shri Luxmi Das, Ex-Chaiman KVIC, Mumbai and Secretary All India Handmade paper Association, New Delhi.Improved Process for Conversion of Shredded Currency Waste into Different Varieties of Handmade Papers/R.K. Jain, A.K. Sharma, Baleshwer Prasad, Atul Kumar. Mohd. Esa Khan and Saakshy Agarwal.Development of Specialty Papers for Archival Applications/R.K. Jain, A.K. Sharma, Atul Kumar and M.E. Khan.Bhimal / Beol Fibre (Grewia Oppsitifolia Roxb.) for Handmade Paper Making/Atul Kumar and Saakshy Agarwal.

[16] Author for U.G. Course on Handmade Paper run by Indira Gandhi National Open University,(IGNOU) New Delhi on the following topics.Block-2, UNIT-2 Availability of Raw Materials, Atul KumarBlock-2, UNIT-3 Selection / Collection / Classification and Storage of Raw Materials, Atul Kumar

[17] Utilization of Dhaincha(Sesbania Bispinosa) and Aka (Hibiscus Macrophyllus) Fibres for Handmade Paper and Board making. Atul Kumar, A. K. Sharma, Satya Pal, G.Hussain- Souvenir on Handmade Paper published by Directorate of HMPFI-KVIC-Mumbai in Paperex-2011 December, New Delhi)

[18] Pulping and physical strength properties of bodha and carrot grass as raw material for handmade paper making Indian Journal of Weed Science 40 (1&2) : 92-94, 2008, Atul Kumar, R.K. Jain, A.K. Sharma and Sushil Kumar1,Kumarappa National Handmade Paper Institute, Sikarpura Road, Sanganer, Jaipur (Rajasthan),1-National Research Centre for Weed Science, Adhartal, Jabalpur (Madhya Pradesh)

Thesis

[19] A Review of Literatures Related of Using Kenaf for Pulp Production (Beating, Fractionation, and Recycled Fiber)-Published by Canadian Center of Science and Education (Modern Applied Science) Vol. 4, No. 9; September 2010,by Ahmad Azizi Mossello (Corresponding author) Institute of Tropical Forestry and Forest Products, University Putra Malaysia, Malaysia Department of Desert Region Management, College of Agriculture, Shiraz university, Shiraz, Iran, Jalaluddin Harun & Paridah Md Tahir Institute of Tropical Forestry and Forest Products, University Putra Malaysia, Malaysia Hossein Resalati Faculty of Forestry and Wood Technology , Gorgan University of Agricultural and Natural Resources, Iran.

American Journal of Engineering Research (AJER)
e-ISSN : 2320-0847 p-ISSN : 2320-0936
Volume-02, Issue-09, pp-190-197
www.ajer.org

Research Paper Open Access

Mathematical Modelling Of Cyanide Inhibition on Cassava Wastewater Treatment

E. Onukwugha[1] and A.O. Ibeje[*]
Department of Civil Engineering, Federal Polytechnic, Nekede, Owerri, Nigeria Department of Civil Engineering, Imo State University, P.M.B. 2000, Owerri, Nigeria.

Abstract: - Anaerobic Baffled Reactors (ABR) is used to evaluate the extent of cyanide inhibition of cassava wastewater treatment. The reactor has aspect ratio of 4:1:1. Kinetic analyses of specific growth rate μ_{max} and half saturation constant k_s are evaluated for the reactor. For non-inhibited cassava wastewater treatment, Monod model yields μ_{max} = **10.87 day^{-1};** and $k_s = 0.87\ mgCODL^{-1}$. Coefficient of determination R^2 is used to verify the model to yield value of 0.917 for Monod model. For inhibited cassava wastewater treatment, the inhibition constant k_i is evaluated from the reactor as $1.172 * 10^{-5} mgCyanide/L^{-1}$. This clearly indicates that the extent of cyanide inhibition of cassava waste water treatment is minimal.

Key Words: - *Cyanide inhibited, Treatment, Cassava Wastewater, Monod model and Reactor*

I. INTRODUCTION

Cassava (Manihot esculenta crantz, also known as manioc or yucca) is one of the leading food and feed plants in the world: it ranks fourth among staple crops with a global production of about 160 milllion tons per year (1). Most of these are grown in three regions, West Africa, and the Congo basin, tropical South America, and South East Asia (2), while in Western countries it is not commonly used, because of the presence of cyanoglucosides (linamarin and lotaustralin). Cassava roots contain cyanogenic glucosides (the precursors of HCN) in various concentrations depending on the variety and growing conditions (3). This cyanide is released during peeling, slicing and crushing. The bound cyanide is converted to free cyanide during the milling operation. About 40% to 70% of the total cyanide appears in the water used to wash the starch from the disintegrated tissue (4). The press water, although produced in relatively low volumes (250 – 300 litres per tonne of roots), is the main problem because of its high biological oxygen demand (BOD) of 25,000 – 50,000 mg/l with a typical cyanide concentration in excess of 400 mg/l (5). Cyanide, being an acidic component will naturally have an inhibiting action on the biological degradation of cassava wastewater. This effect on the environment is yet to be addressed properly in developing countries due to inadequate equipment and lack of research materials. The objectives of this study are to formulate an improved mathematical model to describe cassava wastewater treatment taking into account its inhibition characteristic and to determine the extent of inhibition caused by cyanide, on the degradation of cassava wastewater.

II. MATERIALS AND METHODOLOGY

The Reactor

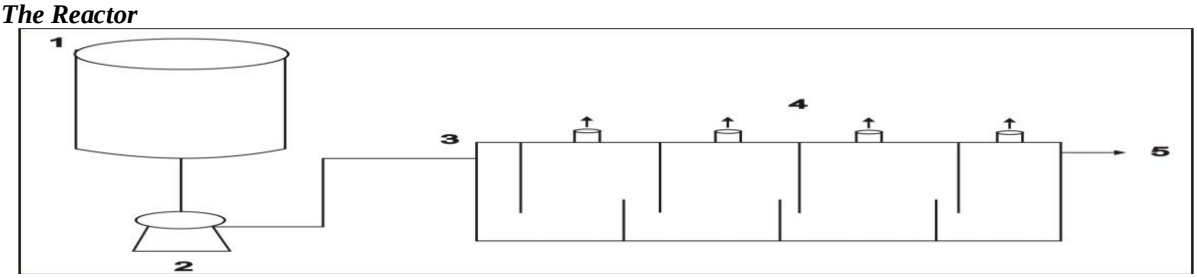

Figure 1: Scheme of the ABR. 1. Feed Tank; 2. Peristaltic Pump; 3. Influent; 4. Sampling Ports; 5. Effluent.

The laboratory scale ABR was constructed from 6mm thick stainless steel, with external dimensions of lengths, widths, depths and working volumes as shown in table 1. Figure 1 shows a schematic diagram of the reactor. The reactor was divided into different number of equal compartments by vertical baffles with each compartment of the reactor having downcomer and riser regions created by a further vertical baffle. The widths of upcomers were multiples of the widths of downcomer. The lower parts of the downcomer baffles were angled at 45^0 in order to direct the flow evenly through the upcomer. This produced effective mixing and contact between the wastewater and anaerobic sludge at the base of each riser. Each compartment was equipped with sampling ports that allowed biological solids and liquid samples to be withdrawn. The operating temperature was maintained constant at $35\pm0.5°C$ by putting the reactor in a water bath equipped with a temperature regulator. The influent feed was pumped using variable speed peristaltic pump. The outlet was connected to a glass U-tube for level control and to trap solids.

Start-up of ABR

Start-up without seed sludge was rather difficult and time consuming for suspended growth anaerobic reactors. The following 3 steps were taken: (i) the reactor was filled with cassava wastewater and allowed to rest for 15 days (ii) the sludge bed was allowed through a process of sludge accumulation by settling and sludge improvement and (iii) after 15 days, feeding of the wastewater was resumed at a flow rate of 5.33litres per day and HRT of 6days with a very low organic loading rate (OLR) of $0.067kgCOD/m^3.day$. The resumed wastewater feeding helped the development of sludge bed at the bottom of individual chambers of the ABR. This process of feeding the system followed by two weeks rest is based on the experiment made in Kanpur (India) for the start-up of a UASB plant without inoculum (6).

Characterization of Wastewater

The cassava wastewater from a cassava processing factory at Imo Polytechnic Umuagwo in eastern Nigeria was used as feed. The supernatant of the wastewater after the simple gravity settling, used in the investigation, had low TSS, as approximately 90% of the solids were removed. The supernatant wastewater was diluted to achieve the COD concentration required for each loading rate with water. In order to achieve pH and alkalinity adjustment, the supernatant was neutralized by NaOH and $NaHCO_3$. A COD:N:P ratio of 300:5: 1 was kept during operation using NH_4C1 and K_2HPO_4. The micro-nutrient deficiency was added occasionally to correct growth conditions according to (7).

Procedure for Experiment 1 (Non-Cyanide Inhibited Treatment)

The wastewater was collected twice a day from the cassava processing plant, and it was intermittently mixed to feed the reactor with a consistent quality. The wastewater came from processing cassava specie (bogot) that had no cyanide content (Table 2). The wastewater was fed to the reactor with the help of a variable speed peristaltic pump. The ABR was operated at various hydraulic retention times (HRTs) by varying the flow rate of influent wastewater (Q_{inf}), thereby varying the organic loading rate (OLR). The wastewater flowed from the downcomer to the upcomer within an individual chamber through the sludge bed formed at the bottom of the individual chambers. After receiving treatment in the particular chamber, wastewater entered the next chamber from the top. Due to the specific design and positioning of the baffle, the wastewater is evenly distributed in the upcomer and the vertical upflow velocity (V_{up}) could be significantly reduced. The treated effluent was collected from the outlet of the 3rd compartment (C3). The reactor was kept in a temperature controlled chamber maintained at 35 ^OC.

Procedure for Experiment 2 (Cyanide Inhibited Treatment)

After the start-up stage has been completed; the steady-state operation was conducted. The ABR was operated at various cyanide concentrations by using influent wastewater from different cassava species as listed in table 1. The steady-state performance was evaluated under hydraulic retention time of 3 to 10 days. (Organic loading rate of 1.60 to 5.33 g-COD (l day). At any given loading rate, the bioreactor was continuously operated until steady-state condition is achieved, when effluent COD, VSS and gas production rate in bioreactor become constant. Then samples were collected and subjected to the analysis of the following parameters, i.e. influent and effluent COD, suspended solids and volatile suspended solids, according to standard methods.

Model Formulation

Nomenclature

S_i = Substrate concentration in the influent (mgl^{-1}); S_e= Substrate concentration in the effluent (mgl^{-1}); k_s= Half

saturation constant (mgl^{-1}); μ = Specific growth rate of organism (per day); μ_{max} = Maximum specific growth rate of organism (per day); X = concentration of active biomass (mg/L); r_A = Rate of utilization of substrate (mg/l.day) ; K_i = the inhibition constant and I = the noncompetitive (Cyanide) inhibitor concentration (mgl^{-1}).

Monod Model for ABR

The Monod model is described as

$$r_A = \frac{ds}{dt} = \frac{Q}{V}(S_i - S_e) = \mu . X \qquad (1)$$

$$= \frac{\mu_{max} S_e}{K_s + S_e} X$$

$$\frac{XV}{Q(S_i - S_e)} = \frac{K_s}{\mu_{max}} \frac{1}{S_e} + \frac{1}{\mu_{max}} \qquad (2)$$

Applying experimental results to Equations (2), graph will be plotted. In this, graph $XV/(S_i-S_e)$ is plotted against $1/S_e$

Cyanide-inhibited Monod Model for ABR

Monod kinetics with substrate inhibition are assumed (Andrews, 1969), i.e.

$$\mu_g = \frac{\mu_{max}}{1 + \frac{K_s}{S_e} + \frac{I}{K_i}} \qquad (3)$$

Substituting Equation 3 into Equation 1, by replacing μand μ_g gives

$$\frac{ds}{dt} = \frac{Q}{V}(S_i - S_e) = x . \mu \qquad (4)$$

$$= x \left[\frac{\mu_{max}}{1 + \frac{K_s}{S_e} + \frac{I}{K_i}} \right] \qquad (5)$$

$$= \frac{x\mu_{max}}{1 + \frac{K_s}{S_e} + \frac{I}{K_i}} \qquad (6)$$

i. e. $$\frac{Q}{V}(S_i - S_e) = \frac{x\mu_{max}}{1 + \frac{K_s}{Se} + \frac{I}{K_i}} \qquad (7)$$

Taking inverse of both sides of the Equation;

$$\frac{1}{\frac{Q}{V}(S_i - S_e)} = \left[\frac{x\mu_{max}}{1 + \frac{K_s}{Se} + \frac{I}{K_i}} \right]^{-1} \qquad (8)$$

$$\frac{V}{Q(S_i - S_e)} = \frac{1 + \frac{K_s}{Se} + \frac{I}{K_i}}{x\mu_{max}} \qquad (9)$$

$$xV\mu_{max} = Q(S_i - S_e)\left[1 + \frac{K_s}{Se} + \frac{I}{K_i}\right] \qquad (10)$$

$$\frac{xV}{Q(S_i - S_e)} = \frac{1 + \frac{K_s}{Se} + \frac{I}{K_i}}{\mu_{max}} \qquad (11)$$

Linearising equation 11 gives:

$$\frac{xV}{Q(S_i - S_e)} = \frac{1}{\mu_{max}} + \frac{K_s}{\mu_{max}} . \frac{1}{S_e} + \frac{1}{\mu_{max} K_i}(I) \equiv y = c + mx \qquad (12)$$

$$\frac{xV}{Q(S_i - S_e)} = \text{plot on } y - \text{axis}; \quad I = \text{plot on x axis}; \quad \frac{1}{\mu_{max} K_i} = \text{slope}$$

And: $$\frac{1}{\mu_{max}} + \frac{K_s}{\mu_{max}} . \frac{1}{S_e} = \text{intercept}$$

Table 1: Cassava Species of Varying Cyanide Concentrations

Variety	Total Leaves Cyanide (µg/g)	Free Leaves Cyanide (µg/g)	Total Roots Cyanide (µg/g)	Free Roots Cyanide (µg/g)	Total Cyanide Content Ratio in Leaves and Roots
Java Brown	490	33(6.7)	185	9(4.9)	2.6
Datu	541	19(3.5)	120	9(7.5)	4.5
Bogot	456	21(4.6)	n.d.	n.d.	n.d.
Lakan	189	13(6.9)	45	0.4(1.0)	4.2

n.d. = not detected; Source: (8).

III. RESULTS AND DISCUSSION

Model Calibration

From linear regression (Figure 2);

$$y = mx + c$$
$$\mathbf{y = 0.078x + 0.092}$$

By comparison with equation 2;

$$\frac{1}{\mu_{max}} = c = \text{intercept; i.e. } \mu_{max} = \frac{1}{c} = \frac{1}{0.092} = \mathbf{10.87/day}$$

and;

$$\frac{K_s}{\mu_{max}} = m = \text{slope; i.e. } K_s = \mu_{max} * m$$
$$\therefore K_s = 10.87 * 0.078 = \mathbf{0.87 mgCOD/L}$$

Substituting μ_{max} and k_s into equation 1 gives;

$$r_A = \frac{ds}{dt} = \frac{Q}{V}(S_i - S_e) = \frac{\mu_{max} * S_e}{K_s + S_e} = \frac{\mathbf{10.87 * S_e}}{\mathbf{0.87 + S_e}}$$

From linear regression equation (Figure 3);

$$y = mI + c$$
$$\mathbf{y = 96909I + 6.267}$$

By comparison with equation 12 and substituting μ_{max} from experiment 1 gives;

$$\text{slope} = m = \frac{1}{\mu_{max} K_i};\ K_i = \frac{1}{m\mu_{max}} = \frac{1}{96909 * 21.74}$$
$$= \frac{1}{85308.993} = \mathbf{1.172 * 10^{-5}}$$

Substituting k_s from experiment 1 into equation (12) gives;

$$\frac{xV}{Q(S_i - S_e)} = \frac{1 + \frac{K_s}{S_e} + \frac{I}{K_i}}{\mu_{max}} \equiv \frac{xV}{Q(S_i - S_e)} = \frac{1 + \frac{\mathbf{2.37}}{S_e} + \frac{I}{\mathbf{1.172 * 10^{-5}}}}{21.74}$$

Thus, the new kinetic model for cassava wastewater ABR is

$$\frac{V}{Q(S_i - S_e)} = 3{,}924.80 + 0.109 S_e^{-1}$$

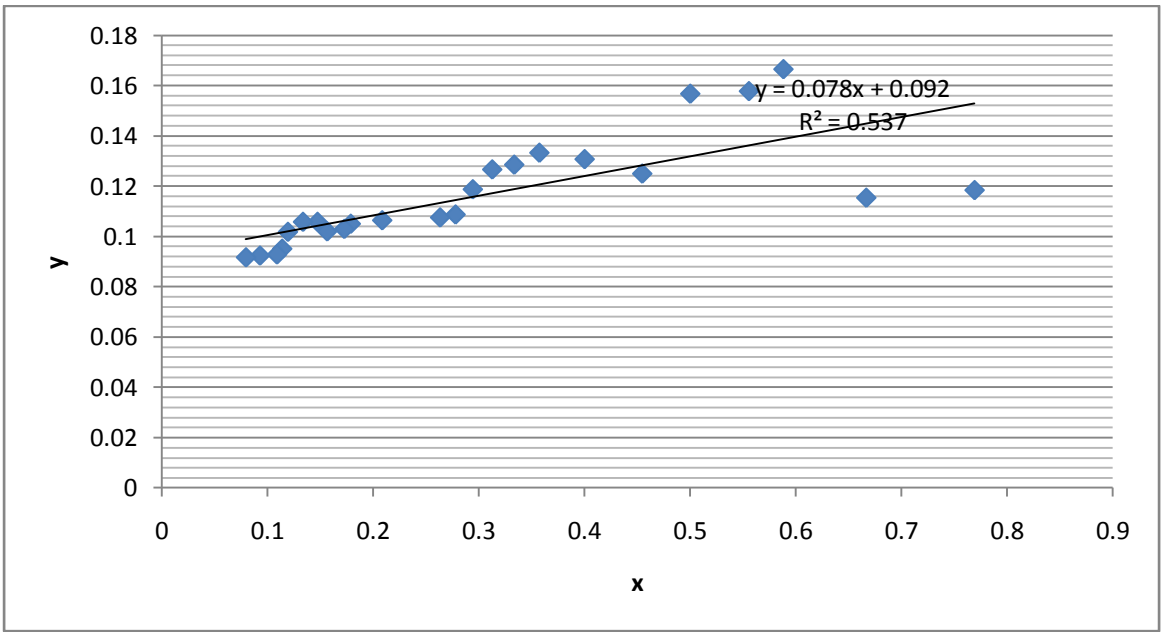

Figure 2: A Plot of $y = \frac{xv}{Q(S_i - S_e)}$ (L.d/mg) Versus $x = \frac{1}{S_e}$(L/ mg)

Table 2: Computations for Monod Model (Experiment 1)

S/N	$x_i = SV_i - SV_e$ (mg/ L.d)	$\frac{Q(S_i - S_e)}{V}$ (mg/ L.d)	$\frac{V}{Q(S_i - S_e)}$ (mg/ L.d)	$y = \frac{x.V}{Q(S_i - S_e)}$ (mg/ L.d)	S_e (mg/L	$x = \frac{1}{S_e}$ (L/ mg)
1	0.9	7.6	0.1315789	0.1184211	1.3	0.7692308
2	0.9	7.8	0.1282051	0.1153846	1.5	0.6666667
3	1.5	9	0.1111111	0.1666667	1.7	0.5882353
4	1.5	9.5	0.1052632	0.1578947	1.8	0.5555556
5	1.6	10.2	0.0980392	0.1568627	2	0.5
6	1.6	12.8	0.078125	0.125	2.2	0.4545455
7	1.7	13	0.0769231	0.1307692	2.5	0.4
8	1.8	13.5	0.0740741	0.1333333	2.8	0.3571429
9	1.8	14	0.0714286	0.1285714	3	0.3333333
10	1.9	15	0.0666667	0.1266667	3.2	0.3125
11	1.9	16	0.0625	0.11875	3.4	0.2941176
12	2	18.4	0.0543478	0.1086957	3.6	0.2777778
13	2	18.6	0.0537634	0.1075269	3.8	0.2631579
14	2	18.8	0.0531915	0.106383	4.8	0.2083333
15	2.1	20	0.05	0.105	5.6	0.1785714
16	2.1	20.4	0.0490196	0.1029412	5.8	0.1724138
17	2.1	20.6	0.0485437	0.1019417	6.4	0.15625
18	2.2	20.8	0.0480769	0.1057692	6.8	0.1470588
19	2.2	20.8	0.0480769	0.1057692	7.5	0.1333333
20	2.3	22.6	0.0442478	0.1017699	8.4	0.1190476
21	2.3	24.2	0.0413223	0.0950413	8.8	0.1136364
22	2.3	24.8	0.0403226	0.0927419	9.2	0.1086957
23	2.4	26	0.0384615	0.0923077	10.8	0.0925926
24	2.4	26.2	0.0381679	0.0916031	12.6	0.0793651

Table 3: Computations for Cyanide-Inhibited Monod Model (Experiment 2)

S/N	$\frac{Q(S_i - S_e)}{V}$ (mg/ L.d)	$\frac{V}{Q(S_i - S_e)}$ (mg/ L.d)	x_i	$y = \frac{x.V}{Q(S_i - S_e)}$ (mg/ L.d)	I (mg/L)
1	250	0.004	2.2	0.0088	8500
2	400	0.0025	1.4	0.0035	3600
3	500	0.002	0.6	0.0012	1250
4	782.17	0.0013	0.2	0.0002557	250
5	800	0.0013	0.6	0.00075	750
6	849.98	0.0012	1	0.0011765	1100
7	849.98	0.0012	1.4	0.0016471	1550
8	899.95	0.0011	1.7	0.001889	1800
9	900.01	0.0011	2	0.0022222	2100
10	900.02	0.0011	2.2	0.0024444	2350
11	899.99	0.0011	2.4	0.0026667	2550

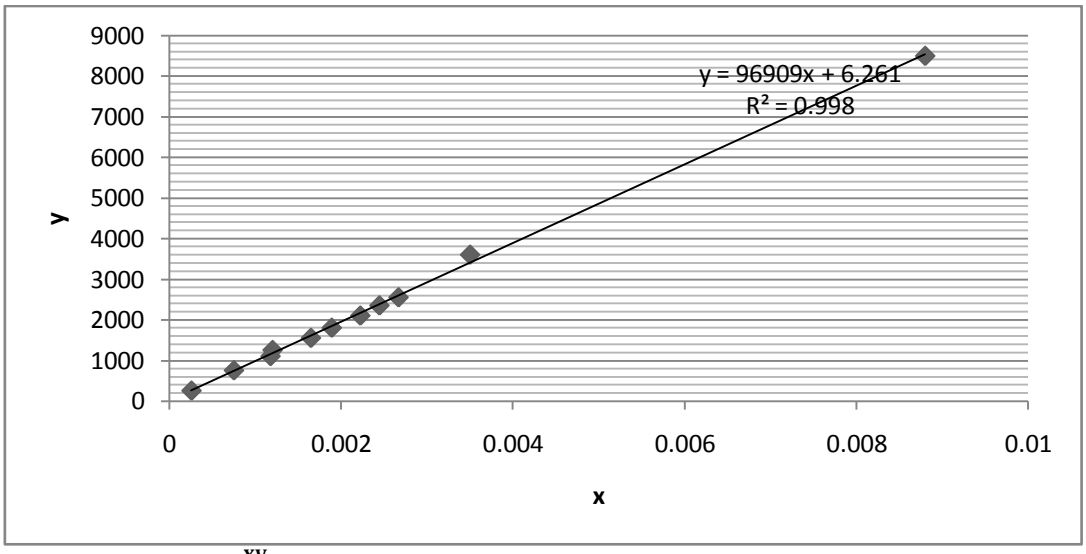

Figure 3: A Plot of $y = \frac{xV}{Q(S_i - S_e)}$ (L.d/mg) Versus I(L/ mg) for Cyanide Inhibited Monod Model

Model Verification

Table 4: Simulation for Monod Model

Observed y $\frac{x_i.V}{Q(S_i - S_e)}$ (mg/L.d)	Simulated y' $\frac{x_i.V}{Q(S_i - S_e)}$ (mg/L.d)
0.1184211	0.11456
0.1153846	0.114208
0.1666667	0.137882
0.1578947	0.135333
0.1568627	0.131
0.125	0.127455
0.1307692	0.1232
0.1333333	0.119857
0.1285714	0.125214
0.1266667	0.116375
0.11875	0.114941
0.1086957	0.113667
0.1075269	0.112526
0.106383	0.10825
0.105	0.105929
0.1029412	0.105448
0.1019417	0.104188
0.1057692	0.103471
0.1057692	0.1024
0.1017699	0.101286
0.0950413	0.100864
0.0927419	0.100478
0.0923077	0.099222
0.0916031	0.09819

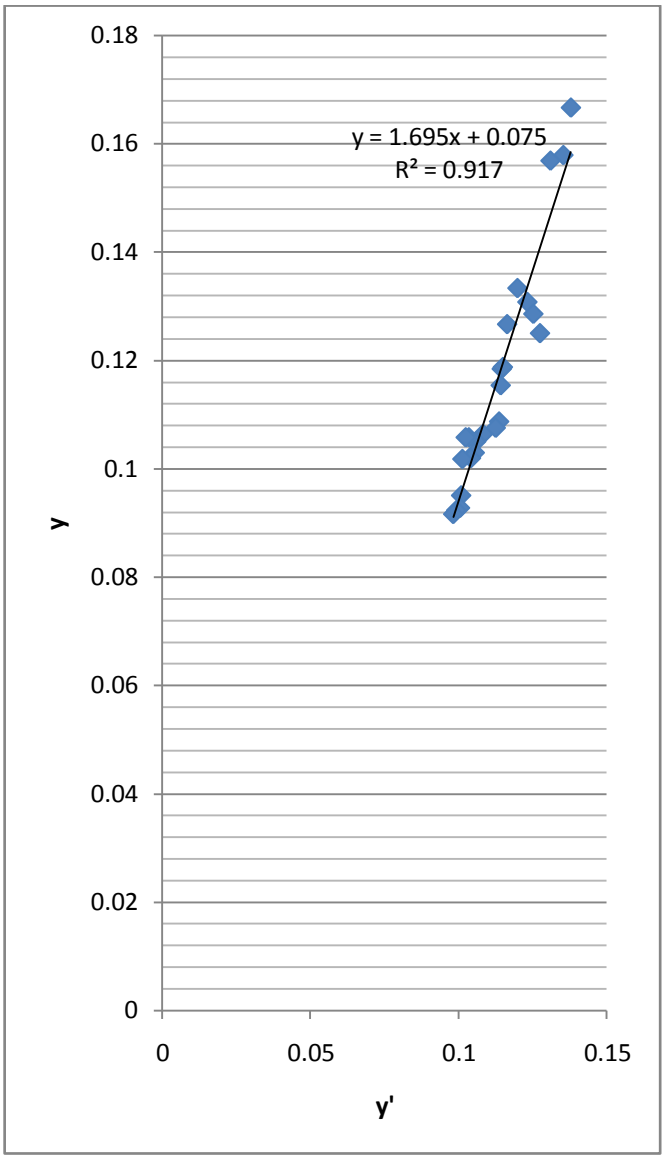

Figure 4: A Scatter plot of Observed y versus Simulated y' for Monod Model

The coefficient of determination, R^2 for reactor 1 in Monod Model yielded 0.916, suggesting a satisfactory fitting of the developed model.

IV. CONCLUSIONS

For inhibited cassava wastewater treatment, the inhibition constant $\mathbf{k_i}$ was evaluated from reactor as $\mathbf{1.172 * 10^{-5} mgCyanide/L^{-1}}$. This clearly indicates that the extent of cyanide inhibition of cassava wastewater treatment is minimal. Despite the fact that the mathematical model proposed for design purposes was found to be suitable though some deviations between experimental and theoretical data were observed,

there is an urgent need to generate models for larger scale reactors and to model reactor behaviour when hydrolysis is at the rate-limiting step. The improvement of the model, without it becoming too complicated and impracticable for practical applications, is a challenge to be confronted in future researches.

REFERENCES

[1] Lawrence, J.H. and Moore, L.M. (2005). United States Department of Agriculture Plant Guide. Cassava, Manihot esculenta Crantz. USDA: Washington, DC, 2005, http://plants.usda.gov/plantguide/doc/pg_maes.doc (accessed March 24, 2008).

[2] Kawano, K. (2003). Thirty years of cassava breeding for productivity – Biological and social factors for success. Crop Science, 43: 1325-1335.

[3] Nartey, N. C. (1973). Influence of hydrodynamic conditions on naphthalene dissolution and subsequent biodegradation. Biotechnol. Bioeng. 57, 145 – 154.

[4] Cooke, R.D. and Maduagwu, E.N. (1978). The effects of simple processing on the cyanide content of cassava chips. Journal of Food Technology, 13: 299-306.

[5] Gomes, G. and Valdivieso, M. (1984). Effects of sun drying on a concrete floor and ovendrying on trays on the elimination of cyanide from cassava whole root chips. J. Food Technol. 19:703-710

[6] Draaijer, H., Maes, J.A., Schaapman, J.E. and Khan, A. (1992). Perf0rmance of 5MLD UASB Reactor For Sewage Treatment at Kanpor, India, Water Sci, Technol. 23(7), 123-133

[7] Angenent, L. T., Abel, S. J. and Sung, S. (2002). Effect of an organic shock load on the stability of an anaerobic migrating blanket reactor. J. Environ. Eng., 128 (12): 1109-1120.

[8] Hasyimoto, A.G., Roman, L. and Hruska, U.S. (1982). "Methane from cattle waste effects of temperature, hydraulic retention time, and influent substrate concentration on kinetic parameter, Biotcch, Bioeng. 26, 2039-2052.

.

American Journal of Engineering Research (AJER)
e-ISSN : 2320-0847 p-ISSN : 2320-0936
Volume-02, Issue-09, pp-198-203
www.ajer.org

Research Paper Open Access

Estimation Of The Electric Power Potential Of Human Waste Using Students Hostel Soak-Away Pits.

Onojo, O.J, Chukwudebe, G.A, Okafor, E.N.C, Ononiwu, G.C., Chukwuchekwa, N., Opara, R. O., Dike, D. O.
Department Of Electrical And Electronic Engineering, Federal University Of Technology Owerri.

Abstract: - With the growing demand for electric power supply in Nigeria, there is a need to look into all possible means of electricity generation especially renewable ones. It is an established fact that methane gas is a major product of the anaerobic digestion of human waste and the combustion of this gas can be used to generate electricity. This paper presents a carefully articulated approach to the technique of estimating the amount of electricity that can be generated from a specified amount of human waste. The analysis of the acquired data from a student's hostel pit toilet at the Federal University of Technology, Owerri, shows that the available biomass waste in tonnes per day from the case study area is 3.66 tonnes and the biogas accruable bi-monthly is 154.76kg capable of running a 5KW biogas generator for six (6) days.

Keywords: - *biomass, biogas, renewable, anaerobic, digesters, waste.*

I. INTRODUCTION

Scientific interest in the manufacturing of gas produced by the natural decomposition of organic matter was first reported in the 17th century by Robert Boyle and Stephen Hale, who noted that flammable gas was released by disturbing the sediment of streams and lakes[Ferguson, 2006]. In 1808, Sir Humphrey Davy determined that methane was present in the gases produced by cattle manure [Cruazon, 2007]. The first anaerobic digester was built by a leper colony in Bombay, India, in 1859. In 1895, the technology was developed in Exeter, England, where a septic tank was used to generate gas for the sewer gas destructor lamp, a type of gas lighting. Also in England, in 1904, the first dual-purpose tank for both sedimentation and sludge treatment was installed in Hampton. In 1907, in Germany, a patent was issued for the Imhoff tank, an early form of digester.

Through scientific research, anaerobic digestion gained academic recognition in the 1930s. This research led to the discovery of anaerobic bacteria, the microorganisms that facilitate the process. Further research was carried out to investigate the conditions under which methanogenic bacteria were able to grow and reproduce [Humanic, 2007]. This work was developed during World War II, during which in both Germany and France, there was an increase in the application of anaerobic digestion for the treatment of manure.

1.0 Processes of Biogas production

There are four key biological and chemical stages of anaerobic digestion:

1. Hydrolysis
2. Acidogenesis
3. Acetogenesis
4. Methanogenesis

In most cases, biomass is made up of large organic polymers. For the bacteria in anaerobic digesters to access the energy potential of the material, these chains must first be broken down into their smaller constituent parts. These constituent parts, or monomers, such as sugars, are readily available to other bacteria. The process of breaking these chains and dissolving the smaller molecules into solution is called hydrolysis. Therefore, hydrolysis of these high-molecular-weight polymeric components is the necessary first step in anaerobic

digestion. Through hydrolysis the complex organic molecules are broken down into simple sugars, amino acids, and fatty acids.

Acetate and hydrogen produced in the first stages can be used directly by methanogens. Other molecules, such as volatile fatty acids (VFAs) with a chain length greater than that of acetate must first be catabolised into compounds that can be directly be used by methanogens [Boone, Mah, 2006].

The biological process of acidogenesis results in further breakdown of the remaining components by acidogenic (fermentative) bacteria. Here, VFAs are created, along with ammonia, carbon dioxide, and hydrogen sulfide, as well as other byproducts. The process of acidogenesis is similar to the way milk sours. The third stage of anaerobic digestion is acetogenesis. Here, simple molecules created through the acidogenesis phase are further digested by acetogens to produce largely acetic acid, as well as carbon dioxide and hydrogen.

The terminal stage of anaerobic digestion is the biological process of methanogenesis. Here, methanogens use the intermediate products of the preceding stages and convert them into methane, carbon dioxide, and water. These components make up the majority of the biogas emitted from the system. Methanogenesis is sensitive to both high and low pH and occurs between pH 6.5 and pH 8[Martin, 2007]. The remaining, indigestible material the microbes cannot use and any dead bacterial remains constitute the digestate.

A simplified generic chemical equation for the overall processes outlined above is represented in equation 2.14.

$$C_6H_{12}O_6 \rightarrow 3CO_2 + 3CH_4 \qquad (1.0)$$

1.1 Biomass Power Generation

People living in countries with flush-toilets and running water produce a huge amount of wastewater daily. This is full of organic compounds that store usable energy in their chemical bonds. Several methods can be employed to harvest it for example; engineers can extract methane through anaerobic (oxygen-free) digestion, or produce electricity using microbial fuel cells.

Rural areas usually have large supplies of material crop residues and animal wastes-theoretically suitable for conversion into a usable source of energy. The process that appears to hold the greatest immediate potential for utilization of these materials as sources of fuel is anaerobic fermentation. This process, also called anaerobic digestion, converts complex organic matter to methane and other gases. It has advantages that recommend it for serious consideration:

1. It is the simplest and most practical method known for treating human and animal wastes to minimize the public health hazard associated with their handling and disposal; and
2. The residue left after removal of the gas is a valuable fertilizer that contains all the essential nutrients present in the raw materials.

The fact that organic material, rotting under conditions where it is out of contact with air, will produce a flammable gas has been known for centuries, particularly in the phenomenon of marsh gas. The occasional dancing flames of this gas (ignited, perhaps, by stray sparks from a nearby fire), seen at night, have given rise to the legends of the "will-o'-the-wisp," or fool's fire. Although it is not certain when it was first recognized that manure, if allowed to decompose in a sealed pit, would also produce a flammable gas, we know that the gas from a "carefully designed" septic tank was used for street lighting in Exeter, England, in 1895 [McCabe, Eckenfelder, 1957]. The experience must have been successful enough to encourage others, for, in the 1920s, several devices were built and used in England, specifically for the purpose of generating this gas,' which is primarily methane, the simplest organic compound of carbon and hydrogen. The process has also been utilized where energy supplies have been reduced, as in France, Algeria, and Germany during and after World War II, when methane thus produced was used to run automobiles.

In countries hampered by low natural abundance or inadequate distribution of energy supplies, methane-generating equipment has often been adapted to meet rural needs. Family-size methane-generating units have been used in diverse climates and cultures. In India, concern over the loss of cow dung for fertilizer, because of its traditional use as fuel, sparked early experiments to develop a system to provide fuel without destroying the dried dung. These experiments were initiated in 1939 at the Agricultural Research Institute in New Delhi. An account of that experience states: "The experiments resulted in the designing of a simple and easy-to-operate gas plant in which dung is fermented to yield a combustible gas which can be used as a fuel and the dung residue can be utilized as manure". The work in India continued and expanded with the encouragement of the Khadi and Village Industries Commission. In 1961 the Gobar Gas Research Station was started in Ajitmal, Etawah (Uttar Pradesh), and in 1971 it published a variety of designs for gas plants. In the years since experiments first began in India, many thousands of such plants have been built in that country most of them in rural areas and serving from one to several families.

The interest in this anaerobic digestion process is not as easily chronicled for other developing countries as it is for India, with the exception, perhaps, of Taiwan. There, experiments with the generation of working fuel from pig manure began about 1955 and developed into a program supported by the government [Ju-tung, 1965]. To date, about 7,500 such devices have been built in Taiwan as permanent adjuncts to pig-

raising operations on small and medium-size farms, although reports indicate that perhaps only half that number is actually in operation [Chan, 1983].

There are scattered reports of the use of methane generation from waste materials in other countries. Installations have been reported in Uganda [Jefferies, 1964], and Bangladesh [Chan, 1983].

Since 1971 some experiments have also been carried out on the islands of the South Pacific; a pilot project was installed on a small farm in Fiji and a successful demonstration project was operated at Port Moresby, Papua New Guinea.

Finally, in the United States and Western Europe, interest in the use of anaerobic digestion to provide fuel and safe "natural" fertilizer for small-scale use has been growing steadily for a number of years and numerous pamphlets have appeared that give more-or-less detailed instructions for building digesters [Garg, 2009].

Thus, extraction of energy from wastes by anaerobic digestion is decades old, and the general technology is well-known. It has not, however, been confined to small-scale use. Large-scale municipal digesters are used in the treatment of municipal sewage sludge, with the evolved gases satisfying part of the energy needs of the municipal treatment plant.

Common materials used for methane generation are often defined as "waste" materials, e.g., crop residues, animal wastes, and urban wastes including night soil. Some of these materials are already used in developing countries as fuels and/or fertilizers. Use of these materials for methane generation, as illustrated in Fig.1.0, will allow additional value to be gained from them while the previous benefits are still retained.

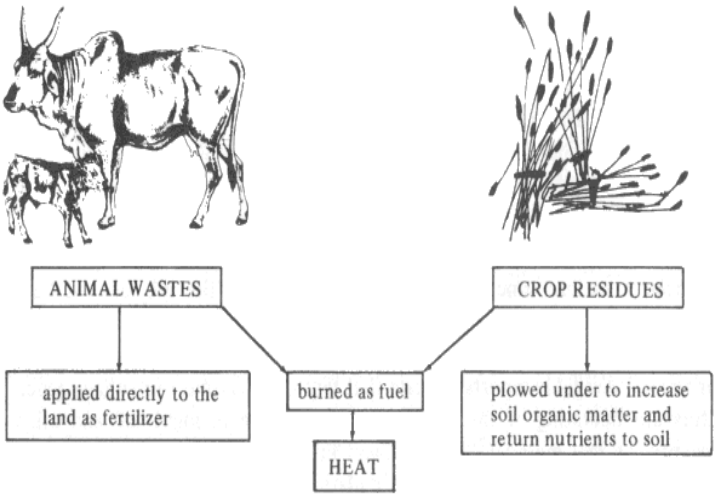

Fig.1.0: Use of Biomass as Energy Source.

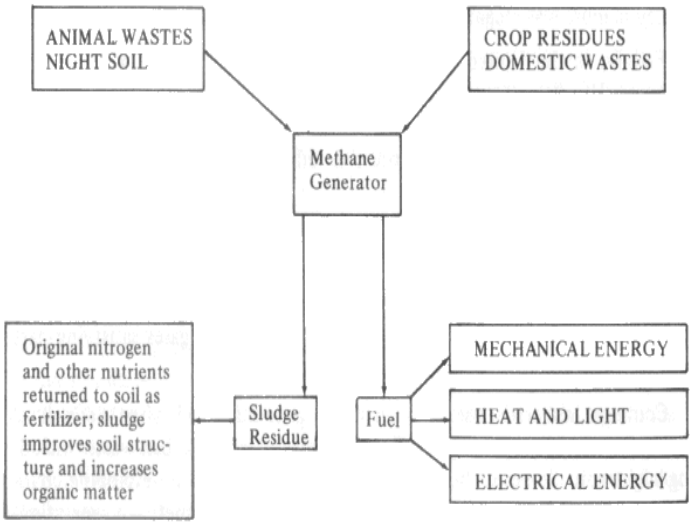

Fig.2.0: Process of Methane Generation.

In the past several years, an increasing amount of research has focused on developing and improving on these methods, as harnessed sewage power could help water treatment plants produce enough power to meet all their own consumption and even serve as a fuel source in developing countries where supplies are currently unreliable. It is necessary to know how much usable energy raw sewage holds. This was the question posed by the authors of a study published in a journal of *Environmental Science & Technology* [Mukhopadhyay, 2004]. Their answer was that wastewater likely holds a lot more than was previously thought of by Elizabeth Heidrich, a PhD student at Newcastle University in England and lead author of the new study, studied microbial fuel cells devices that generate electrical current by capturing the electrons freed as bacteria break down organic matter in wastewater. As she was preparing her doctoral research project she decided to determine how much energy engineers could count on wastewater to provide. Heidrich found only one study, published in 2004, which had tried answer to the question. The authors had tested a sample of raw municipal sewage collected from a Toronto treatment plant and, using calorimetry (the measurement of heat absorption and emission), calculated the internal chemical energy of the sample to be 6.3 kilojoules per liter. They also correlated the amount of energy found in the sample to its Chemical Oxygen Demand (COD), a commonly used indirect measurement of dissolved organic compounds. Based on this correlation, they estimated that, in all, the wastewater produced in 2004 by the world's 6.8 billion people contained a continuous supply of energy somewhere in the range of 70 to 140 Giga Watts. (One large nuclear plant produces around 1 Giga Watt). But the results of this study which Heidrich notes have been cited multiple times in the microbial fuel cell literature are problematic.

Before a sample can be tested in a calorimeter it has to be dry, and in this case the authors had dried their sample by leaving it overnight in an oven heated to 103 degrees Celsius. And because the boiling points of several organic liquids including methanol, ethanol and formic acid found in sewage are lower than 103 degrees, it is expected that there would be losses. These losses would mean the authors had not accounted for all the energy contained in the sample. So, in a similar study, the researchers collected their own samples one from a plant that treats domestic, household wastewater and another from a facility that treats "mixed" wastewater containing chemicals disposed of by industrial facilities. Instead of using an oven they freeze-dried the samples before testing them in a calorimeter. They found that the industrial sample held about 16.8 kilojoules per liter, whereas the domestic sample contained 7.6 - 20 percent more than the previous study had reported for its domestic sample. Perhaps more importantly, given that wastewater samples are highly variable, it was found that the commonly used COD measurement does not actually correlate to energy content, and thus is an unreliable metric. Had they relied on the same calculation methods employed in the previous study, they would have found only around half the energy contained in each of their samples. Thus, the older estimate likely is a "substantial underestimation."

Heidrich's method has its own limitations: The freeze-drying step takes weeks, so it cannot be relied on as a routine testing method. And although the process preserves more organic matter than does oven drying, it still causes some energetic molecules to be lost. Regardless, Heidrich notes, the study's result has immediate real-world implications. Up until this research, domestic municipal wastewater was seen as something that cannot really generate energy, so it was considered not worth the effort. Now, that thought has changed.

With an accelerating world shortage of power and rising costs of fuels, many places have started utilizing bio wastes. San Antonio generates electric power from human faeces while San Francisco is generating power from pet droppings and several large US farms utilize pig litter. Suffolk in the UK has a power plant generating 12.7 MW of energy and consumes 125,000 tonnes of poultry litter per year and encouraged by its success is now planning a human waste plant in Northampton shire. The UN is also sponsoring a project for power from poultry wastes in Bangladesh [Sujata, 2010].

Power from human wastes will be especially valuable in urban areas but all farm wastes can be effectively used. The world's 7 billion people produce about 14 million tonnes of faeces every day and 25% of this has the potential power to produce roughly 40,000 MW of energy. India with one seventh of the world population could therefore add some 6,000 MW to her slow growing power capacity. Furthermore as the technology is quite simple and cheap much of this potential can be made available very quickly.

Rwanda has installed 20 human waste power generating plants of 500 kW each at some of their big prisons where many thousands convicted of genocide are incarcerated. These now provides about half of their electricity requirements. For this initiative, Rwanda earned the Ashden Award for Sustainable Energy with a cash component of $50,000. If Rwanda can achieve this, it is very clear that it is necessary to intensify research in this area around the world. The biogas system includes the gas production process, the use of the gas produced, and the use of the sludge remaining after fermentation is complete.

1.3 Biogas Production and Use

The production of methane during the anaerobic digestion of biologically degradable organic matter depends on the amount and kind of material added to the system. The efficiency of production of methane depends, to some extent, on the continuous operation of the system. As much as $1000m^3$ of gas (containing 50-

70 percent methane) can be produced from 1000m^3 of volatile solids added to the digester when the organic matter is highly biodegradable (e.g., night soil or poultry, pig, or beef-cattle faecal matter) for a period of 30 days [Sujata, 2010]. Combustion of about 30litres (1 ft^3) of gas will release an amount of energy equivalent to lighting a 25-watt bulb for about 6 hours [Sujata, 2010].

In general, lower gas-production rates result when the wastes are less biodegradable. In developing countries, an important consideration will be the differences in the quantity and quality of waste material produced from various sources; for example, the quality and quantity of animal manure is influenced by the diet and general health of the animals. The use to which the gas is put depends upon removal of non-combustible components (such as carbon dioxide) and corrosive components (such as hydrogen sulphide). Among the many potential uses of digester gas are hot-water heating, building heating, room lighting, and home cooking. Gas from a digester can be used in gas-burning appliances if they are modified for its use. Conversion of internal-combustion engines to run on digester gas can be relatively simple; thus the gas could also be used for pumping water for irrigation. Past experiences have shown that where methane is generated in significant quantities in rural areas of developing countries, its use is primarily for lighting and cooking.

The gas produced by digestion of organic waste is colourless, flammable, and generally contains approximately 60 per cent methane and 40 per cent carbon dioxide, with small amounts of other gases such as hydrogen, nitrogen, and hydrogen sulphide. It has a calorific value of more than 500 Btu/ft^3 (18,676kJ/m^3). Methane itself is a non-toxic gas and possesses a slight but not unpleasant smell; however, if the conditions of digestion produce a significant quantity of hydrogen sulphide, the gas will have a distinctly unpleasant odour.

1.4 Biogas Resource Evaluation

The production of methane during the anaerobic digestion of biologically degradable organic matter depends on the amount and kind of material added to the system. The efficiency of production of methane depends on the continuous operation of the system. As much as 1000*l* of gas (containing 50-70 per cent methane) can be produced from 1000*l* of volatile solids(1000kg/m^3) added to the digester when the organic matter is highly biodegradable (e.g., night soil or poultry, pig, beef-cattle faecal matter or human municipal waste).

1.5 Biomass Sources in FUTO

The biomass in FUTO ranges from cow dung, green leaves and municipal solid waste (MSW). With the number of students living in the school's hostel, some amount of human waste can be generated.
It was gathered from the director of Estate and Works Department, that the septic tanks are usually dislodged every two months. The dimensions of the septic tanks used at the various hostels were received from the Physical Planning and Development (PP and D) Unit in the Senate building. This enabled the calculation of the volume of the waste every two months.
The cost at which the dislodgement is done was found from the Dean of Student Affairs to be fifty thousand naira per pit. This value is required by the software for the effective implementation of the cost analysis.

1.6 Calculations on Biogas Resources

The following analytical results were obtained from the anaerobic digestion of biomass wastes using human wastes to produce methane:
Since 1kWh = 3415btu, a simple gas turbine has a fuel consumption of 3415/0.34 =10000Btu/kWh, where 0.34 is the plant factor.
Net heating value of methane = 21433Btu/pound
Thus the methane consumption in a simple gas turbine would be:
10000/21433 = 0.47pounds/kWh = 0.21kg/kWh
1000litres = 1m^3
22.4litres = 1*mol*
Molar mass of methane is 16g per mole
Therefore 16/1mol ×1000l/m^3×1/22.4l = 714g/ m^3
Volume of human waste from hostel A = 43.2 m^3
Volume of human waste from hostel B = 43.2 m^3
Volume of human waste from hostel C = 43.2 m^3
Volume of human waste from hostel D = 43.2 m^3
Volume of human waste from hostel E = 43.2 m^3
Volume of human waste from PG hostel = 3.75m^3
Total volume = 43.2 × 5 + 3.75 = 219.75m^3 = 219.75 m^3
219.75 m^3 × 0.714 = 154.76kg

If 1000 litres of human waste produces 700 litres of biogas, 219.75 m^3 will produce 153.83 m^3 of biogas (since 70% of biogas can be produced from any given mass of human waste)[Martin, 2007]. Energy produced from 154.76kg of biogas will be 154.76kg /0.21kg/kWh = 736,95kWh
Recommending a 5kW biogas generator, the generator can run for 736.95/5 = 147.39, 147.39/24h = 6.14 i.e. approximately six days.
The density of human waste is approximately equal to the density of water = 1000kg/ m^3.
Mass of human waste = 1000 × 219.75 = 219750kg
Since the hostels' septic tanks are dislodged after every two months, the mass per month = 109875kg
The mass per day = 3662.5kg. The available biomass waste in tonnes per day is given as: 3662.5/1000 = 3.66 tonnes per day and this will vary according to when students are around in school.

II. CONCLUSION

From the results obtained from this research, there is a clear indication that human waste is capable of being a source of biogas which can be converted to a useful amount of electric energy. This type of energy source is renewable and this makes it environmentally friendly. The sludge which is usually the waste from the anaerobic digestion process can also be a very useful source of natural manure. Animal droppings can produce larger amounts of biogas than human waste because of their high fiber content. Therefore, it will not be out of place to recommend that large poultry farms and cattle ranches be put in place to support the biogas production process in the school.

REFERENCES

[1] Biomass-Renewable Energy from Plants and Animals. Retrieved from www.eia.gov/kids/energy drenergyservices.com/wasteenergy.html
[2] Boone, D., Mah, R. (2006) Transitional bacteria in anaerobic digestion of biomass, New York: Mc-Graw Hill, Pp 35.
[3] Chan, L.G. (1983) Waste Utilization in Rural Industrialization, Papua Guinea: University of Papua Guinea.
[4] Chaniotakis, E. (2001), M.Sc. Thesis on Energy Systems and the Environment, Department of Mechanical Engineering University of Strathclyde.
[5] Cruazon, B., History of anaerobic digestion, web.pdx.edu. 2007.
[6] Energy from Human Waste. Retrieved from www.pubs.acs.org/stoken/presspac/presspac/full/10.1021/es103058w
[7] Fergusen, T., Mah, R. (2006) Methanogenic bacteria in anaerobic digestion of Biomass, New York: Mc-Graw, , Pp49.
[8] Garg, A.C., M. A. Idani, T. P. Abraham (2009), Organic Manures, Bulletin No.32, New Delhi: Indian Council of Agricultural Research.
[9] Humanik, F. et al. Anaerobic digestion of animal manure, epa.gov. 2007 Hybrid Renewable Energy System; Wikipedia, the free encyclopedia.Hydro power, micro hydro power, small hydro turbine. Retrieved from http//www.micro-hydro-power.com
[10] Jefferies, C. et al. (1964). A review of Colonial Research, New York: McGraw, Pp 44-67.
[11] Jedlicka, D.A., Comments on the Introduction of Methane Generation in Mexico with Emphasis on Diffusion of Back-yard Generators for use by Peasant Farmers, U.S.A.: University of Northern Iowa, 1974.
[12] Ju-tung, Y (1965) Notes on Raising Pigs to gain Wealth, Taipei: Feng Nien She. Kaldellis, J.K. Kondili E, E. and Filios, A. (2006), Sizing a Hybrid Wind Diesel Stand-alone system on the Basis of Minimum Long Term Electricity Production Cost, Applied Energy, Vol. 83,. Pp. 1384-1403.
[13] Ma, S., H. Yin, D. M. Kline, (2006) Efficient System Design and Sustainable Finance for China's Village Electrification Program, Conference Paper NREL/CP-710 -39588.
[14] Martin, A.D. (2007) "Understanding Anaerobic Digestion," Presentation to the Environmental Services Association
[15] McCabe, J. Eckenfelder. (1957) Biological Treatment of Sewage and Industrial Wastes, Anaerobic Digestion and Solids-Liquids Seperation, Papers presented at the Conference on Anaerobic Digestion and Solids Handling, Sponsored by Manhattan College, New York: Reinhold Publishing Company.
[16] Mukhopadhyay, K. (2004), An assessment of a biomass gasification based Power plant in Sunderbans. Biomass and bioenergy 27(3), pages 253-264.
[17] Sujata, G. (2010) Biogas comes in from the cold, New Scientist Conference, London: Sunita Harrington, Pp14.

American Journal of Engineering Research (AJER)
e-ISSN : 2320-0847 p-ISSN : 2320-0936
Volume-02, Issue-09, pp-204-207
www.ajer.org

Research Paper Open Access

Estimation of the Current Occasion Parameters Using Successive Sampling Approach

A.E. Anieting, and V. O. Ezugwu
Department of mathematics and statistics
University of uyo, P.M.B.1017,uyo, Nigeria

Abstract: - In this study, successive sampling was used to determine the current estimate of the mean, minimum variance, estimate of change between the two successive occasions and estimate of average over the period of the two occasions. The Data used were based on the number of persons per school deployed by National Youth Service Corps scheme, Akwa Ibom State, Nigeria. The estimates of change and estimate of average over time give their optimum variance when $\rho = 0$ and $\mu = 1$ under varying values of ρ and μ . Also the variance where found to be smaller in the second occasion as compared to the variance in the first occasion

Keywords: - *Successive Sampling, Average overtime, Unmatched portion*

I. INTRODUCTION

Successive Sampling is used extensively in applied sciences, sociology and economic researches. Many survey these days are repetitive in character. Government agencies like the National Bureau of Statistics and other research based institutes collect information regularly on the same population to estimate some population parameters for the current occasion . When the same population is sampled repeatedly, say that a first sample has been taken (on one occasion) from a poplation of N units and a second sample is to be taken (on another occasion) on the same population, there is thus an opportunity of making use of the information contained in the first sample. The problem is how best to learn from past experience and use it for improving precision of future estimates. Estimates can be made not only for the existing time period (current estimates) but also of the change that has taken place since the previous occasion and of the average over a given period. This is what successive sampling entails. The theory of successive sampling appears to have started with the work of Jessen (1942). He utilized the entire information collected in the previous occasion and obtained two estimates, one was the sampling mean based on new sample only and the other was a regression estimate based on the sample units observed on both occasions by combining the two estimates . Yates (1949) extended jessen's scheme to the situation where the population of the variable is estimated on each one of the h≥ 2 occasions from a rotational sample design. Kullduf(1963) modified Jessen's scheme of the sampling by selecting the unmatched sample from the units not selected on the first occasion. He considered in details the optimum choice of the matching fraction under the most general form of cost function apart from fixed costs. Sen (1972) generalized Jessen's work by using a double sampling multivariate ratio estimate using P-auxilliary Variable (p>1) from the matched portion of the sample. Expressions for optimum matching fraction and the combined estimate and its error have also been derived. Okafor (1987) compared some estimators of the population total in two –stage successive sampling using auxiliary variable. Artes, Rueda and Arcos (2005) worked on successive sampling using a product estimate but they considered the case when the auxiliary variables are negatively correlated and double sampling product estimate from the matched sample was presented . Expressions for optimum estimator and its variance have been derived . Trivedi and Shukla (2008) looked into the efficient estimator in successive sampling using post stratification .They stated that it is often seen that the population having large number of elements remains unchanged in several occasions but the value of units change . In their work they introduced an estimator under successive survey , the estimator is unbiased and efficient over post stratification estimation. The intention of this paper is to estimate current mean ,the changes over time and the average over the periods of the number of 'corpers' deployed in Akwa Ibom State, Nigeria.

II. DATA USED

The data used for this study is from the records of the number of persons posted by National Youth Service Corps Scheme to serve in different schools in Akwa Ibom State , Nigeria. The scheme is a one year compulsory scheme for graduates from Nigeria to serve in different part of the country after their graduation from a Bachelor Degree programme. Corper is the name given to those who participate in the scheme.

III. METHODOLOGY

A population is sampled over two occasions for making current estimates and also for estimating changes in the population characteristics. On the first occasion a random sample of size n units is taken from a finite population of size N units. On the second occasion a random sub sample of size m =n$\boldsymbol{\lambda}$, ($0 \leq \boldsymbol{\lambda} \leq \mathbf{1}$) is retained from the first occasion sample and another independent random sample of size u(u =n-m), is selected from the population to supplement . A number of alternatives can be made about replacement policy on the structure of the sample on each occasion . For estimating change from one occasion to the next , it may be best to retain the sample on each occasion , a new sample on each occasion (that is entire independent sample) is drawn if average of change is our target and if it is desired to estimate the mean on each occasion and also the change from one occasion to the next, it may be best to retain part of the sample and draw the remainder of the sample afresh. It should be noted that high positive correlation always exist between observations made on the same unit at two occasions that are successive. For simplicity we shall denote by Y and X the measurement on the second and first occasions respectively.

IV. RESULTS

From the data used, a random sample of 50 schools was selected from a population of 490 schools on each occasion ,this comprises of 30 unmatched schools and 20 matched schools.

i.e n=50; $\boldsymbol{\lambda}$=0.4; μ= 0.6; $S^2{}_x$ =4.79; $S^2{}_y$=3.58; b=0.95; ρ =0.93

$\hat{\mu}_{2m}$ = $\bar{y}'$-b ($\bar{x}'$-$\bar{x}$) =5.67

The minimum variance unbiased estimator is used for the estimation because of the assumption of the equal variability at both occasions. We use the variance obtained by pooling the variances from the matched samples on the first and second occasions as an estimate of the population variance . The pooled variance is therefore

σ^2 = (m-1) $S^2{}_y$ +(m-1) $S^2{}_x$ /2 (m-1) = 4.19

The variance for the matched portion is

V ($\hat{\mu}_{2m}$) = σ^2[1+ (1-$\boldsymbol{\lambda}$) 1-2ρ)/n = 0.04

Estimation of optimum variance is

V($\hat{\mu}_2$) = σ^2/2n [1+$\sqrt{2(1-\rho)}$] =0.06

Mean at the second occasion is

$\widehat{M}_2$ = 1/1-$\mu^2\rho^2$ [$\lambda\mu\rho$ ($\bar{x}^{''} - \bar{x}'$) +$\boldsymbol{\lambda}\bar{y}'$+ μ (1-μ$\rho^2$) $\bar{y}^{''}$]= 3.94

V ($\widehat{M}_2$) = (1-μρ^2) σ^2/ (1-$\mu^2\rho^2$)n =0.059

The optimum variance of the mean at the second occasion is

V ($\widehat{M}_2$) = σ^2 [1+ $\sqrt{1-\rho^2}$] /2n =0.056

Mean at the first occasion is

$\widehat{M}_1$ = 1/1-$\mu^2\rho^2$ [$\lambda\mu\rho$ ($\bar{y}^{''} - \bar{y}'$) +$\boldsymbol{\lambda}\bar{x}'$+ μ (1-μ$\rho^2$) $\bar{x}^{''}$]= 3.53

Estimate of change is

$\hat{\Delta}$ = $\widehat{M}_2 - \widehat{M}_1$ = 0.41

V ($\hat{\Delta}$) = 2σ^2 (1-ρ)/ n(1-μρ) = 0.027

V ($\hat{\Delta}_1$) = 2(1- $\rho\boldsymbol{\lambda}$) $\boldsymbol{\sigma^2}$ /**n** = 0.105

Thus gain in efficiency of using sampling on two successive occasions is

[V ($\hat{\Delta}_1$)/ V ($\widehat{M}_2$) -1] × 100%=77.9 %

Estimate for average over time is

$\hat{\sum}$/ 2 = $\widehat{M}_2 + \widehat{M}_1$ /2 =3.735

V ($\hat{\sum}$) =0.104

V($\hat{\sum}$/ 2) = 0.026

From table 1, minimum variance as well as maximum precision is achieved when ρ=1. This implies that there is a perfect positive relationship between the first and the second sampling occasions. From tables 2 and 3, variance estimates of change give the same values at $\rho = 0\ and\ \mu = 1$. Therefore to enhance precision, μ should be considerable small and ρ considerably high. From tables 4 and 5 , the variance estimates of the sum shows that the same estimate was obtained when ($\rho = 0\ and\ \mu = 1.$), the said estimate happens to be the

minimum value when compared to others at different values of ρ. To enhance precision therefore, independent samples should be taken on each occasion

V. CONCLUSION

Based on the collected data utilized in the analysis of this study, we have been able to achieve the intention of this work which was to estimate the current mean and this was found to be 4 approximately with variance 0.059 and a standard error of 0.243. The minimum variance as well as maximum precision was achieved in table 1 when $\rho = 1$ because at this point the value was 0.052 which is minimum the values of ρ. The estimate of average of change overtime was 3.735 with variance of 0.026 and a standard error of 0.161. the relative efficiency or gain between the successive occasions was 77.9%.

REFERENCES

[1] Artes E.,Rueda M. and Arcos (2005) Successive Sampling using Product Estimate When the auxiliary variables are negatively correlated; Applied Science and Environment

[2] Cochran W. G. (1977) Sampling Technique (third edition). John Wiley and Sons

[3] Jessen R. J. (1942) Statistical investiagation of a sample survey for farm facts. Iowa agricultural experiment statistical research bulletin.pg 304

[4] Kullduff. G, (1963). Some problem of optimum allocation for sampling on two occasion. Review international statistical institute vol.31,24-57

[5] Manish T. and Shukla D. (2008) Efficient Estimator in successive sampling using post stratification

[6] Okafor (1987) Comparison of estimators of population totals in two-stage successive sampling using auxiliary information survey method

[7] Sen (1972) Successive sampling P-auxilliary variables. Ann Mathematical Statistics

Appendix

Table 1. Table for variance of current estimate with different values of ρ

ρ	V ($\widehat{M}_2$)
0.0	0.0838
0.2	0.083
0.4	0.08
0.6	0.075
0.8	0.067
1.0	0.052

Table 2. Table for estimate of change with different values of μ

μ	V ($\widehat{\Delta}$)
0.0	0.012
0.2	0.014
0.4	0.019
0.6	0.027
0.8	0.046
1.0	0.168

Table 3 Table for estimate of change with different values of ρ

ρ	V ($\widehat{\Delta}$)
0.0	0.168
0.2	0.152
0.4	0.132
0.6	0.105
0.8	0.064
1.0	0

Table 4 Table of average over time with varying μ

μ	V ($\widehat{\sum}$)
0.0	0.323
0.2	0.273
0.4	0.236
0.6	0.208
0.80	0.185
1.0	0.168

Table 5 Table of average over time with varying ρ

ρ	V ($\widehat{\sum}$)
0.0	0.168
0.2	0.180
0.4	0.190
0.6	0.197
0.8	0.204
1.0	0.210

American Journal of Engineering Research (AJER)
e-ISSN : 2320-0847 p-ISSN : 2320-0936
Volume-02, Issue-09, pp-208-213
www.ajer.org

Research Paper Open Access

Evaluating of Mashhad urban development plans from compact city viewpoint

Mohammad rahim Rahnama, Ali Homaeefar, Toktam Piruz
Associate Professor Geography and Urban Planning department, Ferdowsi University, Mashhad, Iran
PhD Scholar Department of Geography and Urban Planning, Ferdowsi University, Mashhad, Iran
PhD Scholar Department of Geography and Urban Planning, Ferdowsi University, Mashhad, Iran

Abstract: - There are many problems especially in large cities due to producing of urban development plans in different time, on the other hand; changing traditional to strategies approach is other reason for creating today problems. Therefore, one of the main factors of sustainability development principles is smart growth by emphasis on compactly. Mashhad metropolitan need, presentation sustainable development pattern in urban development plans due to complex structure and important position. Due to, are prepared development plans in various times, should be adapted with sustainable development principles and compact city indicators. In this research at first were studied indicators of smart growth pattern, after that was evaluated development and comprehensive plans based on these principles.
Finding of research show, although there is mentioned viewpoint in urban development plans but haven't succeeded in order to achieving smart growth. On the other hand, Mashhad Middle West area is one of the main districts that smart growth principles are nearly, but it isn't success completely.

Key word: - *Compactly, smart city, Mashhad comprehensive and development plan*

I. INTRODUCTION

The concept of "smart growth" emerged in the early 1990's, driven by "new guard" urban planners, architects, developers, community activists, and historic preservationists (Masnavi, 2004: 90). It accepts that growth and development will continue to occur, and so seeks to direct that growth in an intentional, comprehensive way (Krizak, 2010:190). Smart growth principles are directed at developing sustainable communities that are good places to live, to do business, to work, and to raise families (Hal, 2010:30). Some of the fundamental aims for the benefits of residents and the communities are increasing family income and wealth, improving access to quality education, fostering livable, safe and healthy places, stimulating economic activity (both locally and regionally), and developing, preserving and investing in physical resources. There is a need to distinguish between smart growth "principles" and smart growth "regulations". The former are concepts and the latter their implementation, that is, how federal, state, and municipal governments choose to fulfill smart growth principles (vahidi, 2010). One of the earliest efforts to establish smart growth forward as a regulatory framework were put forth by the American Planning Association (Kafashi , 2010) . In 1997, the APA introduced a project called Growing Smart and published "Growing Smart Legislative Guidebook: Model Statutes for Planning and the Management of Change (Rahnam, 2009: 41)." The U.S. Environmental Protection Agency defines smart growth as "development that serves the economy, the community, and the environment (Kamali, 2012). It changes the terms of the development debate away from the traditional growth/no growth question to how and where should new development be accommodated (zebar dast , 2005 : 190) .

At first the growth of Mashhad is calm, but after that growth sharply due to some extra factors. So was created urban mechanism phenomenon. Thus city growth horizontal and raid of its growth is faster than growth population. This issue has been led to some problems such as: environmental, social and etc. Smart growth strategies could be effected for achieving urban sustainable. Therefore the main question is what is development plan adapted to smart growth?

1.1. Research purpose

Total purpose is, evaluating urban development plans according to growth indicators.
Thus suboriented aims are:

1- Studying population density changes in urban development plan that effect to smart and compact growth.
2- Studying of aims of development plan ,also comparing with urban compactly growth factors

II. THEORETICAL PRINCIPLE

Urban compact and smart growth is an urban planning and transportation theory that concentrates growth in compact walk able urban centers to avoid sprawl. It also advocates compact, transit-oriented, walk able, bicycle-friendly land use, including neighborhood schools, complete streets, and mixed-use development with a range of housing choices. The term 'smart growth' is particularly used in North America. In Europe and particularly the UK, the terms 'Compact City' or 'urban intensification' have often been used to describe similar concepts, which have influenced government planning policies in the UK, the Netherlands and several other European countries (masnavi , 2012: 90) .

Smart growth values long-range, regional considerations of sustainability over a short-term focus. Its goals are to achieve a unique sense of community and place; expand the range of transportation, employment, and housing choices; equitably distribute the costs and benefits of development; preserve and enhance natural and cultural resources; and promote public health (Mehyari, 2005: 203).

Smart growth is related to, or used in combination with the following concepts:

- New Urbanism
- New Community Design
- Sustainable Development
- Traditional Neighborhood Development
- Resource Stewardship
- Land Preservation
- Preventing urban sprawl
- Creating Sense of Place
- Development Best Practices
- Preservation Development

The smart growth approach to development is multifaceted and can encompass a variety of techniques. For example, in the state of Massachusetts smart growth is enacted by a combination of techniques including increasing housing density along transit nodes, conserving farm land, and mixing residential and commercial use areas. Perhaps the most descriptive term to characterize this concept is Traditional Neighborhood Development, which recognizes that smart growth and related concepts are not necessarily new, but are a response to car culture and sprawl. Many favor the term New Urbanism, which invokes a new, but traditional way of looking at urban planning.

There are a range of best practices associated with smart growth, these include: supporting existing communities, redeveloping underutilized sites, enhancing economic competitiveness, providing more transportation choices, developing livability measures and tools, promoting equitable and affordable housing, providing a vision for sustainable growth, enhancing integrated planning and investment, aligning, coordinating, and leveraging government polices, redefining housing affordability and making the development process transparent.

Related, but somewhat different, are the overarching goals of smart growth, and they include: making the community more competitive for new businesses, providing alternative places to shop, work, and play, creating a better "Sense of Place," providing jobs for residents, increasing property values, improving quality of life, expanding the tax base, preserving open space, controlling growth, and improving safety.
There are 10 accepted principles that define smart growth:

1. Mix land uses
2. Take advantage of compact building design
3. Create a range of housing opportunities and choices
4. Create walk able neighborhoods
5. Foster distinctive, attractive communities with a strong sense of place
6. Preserve open space, farmland, natural beauty, and critical environmental areas
7. Strengthen and direct development towards existing communities
8. Provide a variety of transportation choices
9. Make development decisions predictable, fair, and cost effective

10. Encourage community and stakeholder collaboration in development decisions

III. STUDYING OF EFFECTIVE URBAN DEVELOPMENT PLANS IN MASHHAD METROPOLITAN

In 40 decade in Iran was started, preparing comprehensive plan due to accruing some changes that created some problems such as increasing population , rural migration to cities , urban sprawl development . Until now has been produced three comprehensive based on special position of Mashhad. They are: 1- first plan is Khazeni; second plan is Morazán and third plan is as metropolitan development plan (comprehensive). Also, it has been prepared before end of previous plan by Farnahad consultant engendering (2007-2027).
On the other, there wasn't district development plan and urban contribution plan while preparing first & second plan (mentioned above). Thus, Khazeni & Morazán plans don't comprehensive and regional regards. So, they hadn't succeeded due to this reason.

3.1. Khazeni comprehensive plan (1967- 1992)

This plan according to current condition has been led to horizontal development. But increasing population has been more than city development. Thus, city has been expanded more than forecasted. Therefore the, the approach had been "expanded city" due to population density. Density population was 75 people in hectare.

3.2. Morazán comprehensive plan(1992- 2017)

By comparing proposed density in previous plan, there was compactly approach in this plan. But, forecasting of population wasn't true, so city growth as horizontally. The population in 2007 was 2.247.000 people. Also, density population was 60 people in hectare.
Although, there was horizontal development and hadn't achieve proposed population, but there was compact city influence nearly rather than Khazeni plan. On the other hand, second plan was succeeded more than first plan to reach "sustainable development" strategies due to old fabric renovation and maximum using from vacant capacity in order to infill development .

Table 1: forecasted population in future plan of Morazán plan

Proposed development area		1989	2002	2017	Area (hectare)	Density
City boundary		1480000	2460000	2800000	18500	151
Continues development	North east	190000	280000	350000	1750	200
	West	-	100000	700000	3500	200
	South	-	20000	150000	750	200
Total		1670000	2860000	4000000	24500	163
New cities		-	200000	1400000	-	-
Total		1670000	3060000	5400000	-	-

Source: Mashhad comprehensive plan, 1994

3.3. Development plan (comprehensive plan) of Mashhad district (Farnahad consultant engineering- 2006) and Mashhad conurbation plan (2008)

Centralization development plan of Mashhad have created some problems such as: physical, economical, social and environmental issue. These problems have been led to other problems for example, imbalance of population, services and etc. these problems have been led to imbalance natural capacity. So city has been grown sprawl. So, the important issue in planning Mashhad district, creating balance between environment and other population and activities centers. Thus the main strategies by sustainable approach, is creating balance in studied area. Also decentralization is other and main approach is research. So, should be prevented horizontal development. Also increase population density.

3.4. Farnahad Development plan (comprehensive plan) (2007-2027)

Was cleared basic mistakes of the end periods in Morazán plan. The basic precaution is mistakes, so was reviewed at the end of period. On the other hand, density population is due to expanding of boundary of city. Also it hasn't relation to proposal of plan . Could be considered 81 people in hectare as basic population density for starting research.

In this plan was suggested macro aims, they were:
1- giving unique religious identify , historical and cultural in world scale
2- achieving sustainable development principle by globalization approach
3- improving quality of urban environment
4- sustainable preservation from resident healthy and their security

In order to, infill development policy for achieving "compact city" concept was important aim in plan (Farnahad, 2006).
Density of population should be achieved to 130 people in hectare that was created compact viewpoint.
Existence boundary and proposed boundary in Farnahad plan 2027 were 30558 & 55502 hectare. So mentioned plan has regarded compactly phenomenon rather than Morazán plan.

3.5. Detail plan of Mashhad middle west area -2011(Parsomash consultant engineering)
Middle West area has especially condition in Mashhad. Also, its area 4011.5 hectare. These districts have structure and functional importance in Mashhad. Important factors are:
1- appropriate local position
2- easy access to other districts
3- there is high level services in this area
4- there is urban and extra urban land- uses
5- there is various functional area & high population

The roles of Middle West area from viewpoint comprehensive plan are:
1- completing spaces of different land-uses (complex entertainment & purchase location with cultural activities
2- prospecting of especial physical structure according to their position
3- creating capacity of macro lots in order to improving spatial quality and increasing security of studied area

Figure 1: Middle West area position of Mashhad

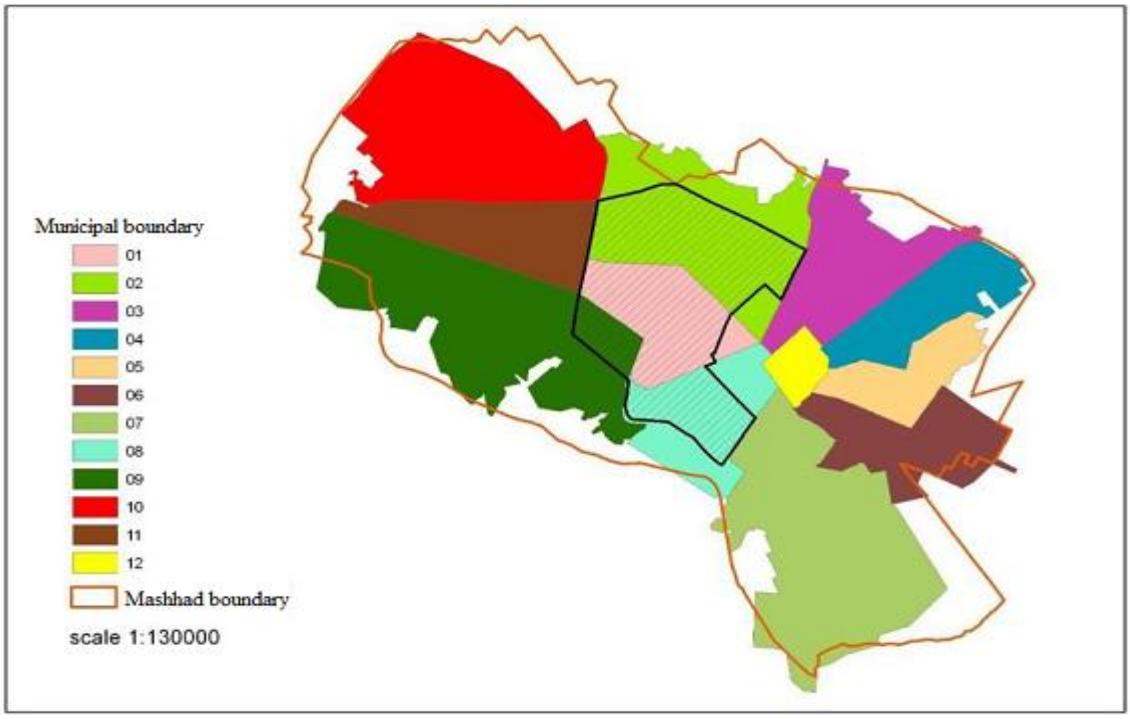

Density population was 129 people in hectare. Also it would be increased to 200 people in hectare. Proposed population was calculated for end of time plan (Parsomash, 2011, 45). So, based on its position mentioned density is false. But, didn't achieved the aims of compact city due to, don't emphasis on functional goals.
Attracting of population is different due to strategies and above policies such as: increased density, distribution of population, urban services, services per capita and etc. undoubted , studied area have potential for increasing

of population that should be planned based on comprehensive plan strategies for distribution of them (Parsomash, 2011, 44- 48) . Middle West of Mashhad has better function in some factors such as: residential density, complex locations and etc. Totally, this plan has been succeeded in order to achieving "compact city pattern" concept.

Table 2: existence and proposed boundary, population and density based on each plan

Plan	Area			population			density		
	existence	Proposed	End of plan	Start of plan	Proposed	End of plan	existence	Proposed	End of plan
Kazeni (1967- 1992)	3200	17000	33000	0.409	1.465	1.9	128	86.1	57
Morazán (1992- 2017)	33000	24500	30000	1.9	4	2.427	57	163	81
Farnahad (2007-2027)	30000	30558		2.247	3.8		81	130	
Mid-west area	4011			0.518	0.802		129	200	

IV. RESULTS

- Totally, in proposed Khazeni plan vast agriculture areas were in legal boundary. So, the city has been grown horizontal. But in other issues such as: residential density and complex functional areas was better. Indeed, comprehensive khazeni plan has been led to horizontal growth. Thus, mentioned plan hasn't succeeded for compact city concept.
- Besides that Morazán plan, although has forecasted the most population, but also didn't succeeded for presenting compact city pattern. On the other hand, second plan was succeeded more than first plan to reach "sustainable development" strategies due to old fabric renovation and maximum using from vacant capacity in order to infill development .
- Current comprehensive plan has compact city policy in functional and physical structure. Moreover, current plan has been more prosperous than other plan for achieving mentioned phenomena. In the same way detail plan determine comprehensive plan position. Therefore, in order to creating harmonic and sustainable city should be study about them.
- Development pattern of Middle West detail plan has attempted, to achieving compact city concept items. The proposed population was 800.000 people for studied area. Also, there are 650.000 people now. So in this matter, mentioned plan don't succeed. But in other elements is better that other plan such as: residential density in hectare and complex land-uses.

Therefore, should be prepared urban development plan and district development plan at the same time. Totally, development pattern of compact city in Mashhad should be provided quantitative and quality indicators of "compact city". Also, it is ideal that all will improve of the quantitative and qualities. On the other hand, should be attempted that achieve maximum factors of sustainability and compact city. So, should be produced compactly indicators from above plans.

REFERENCES

[1] J. Bowen, K., and Modares. (1388). City and environment. (M. Tabibian, Translator), Tehran: Tehran University Press.
[2] J. Krizak. (1388). Guide for planning of sustainable development. (H. Hatami race, and S. Amirian, Translator) Tehran: Wheel spillway.
[3] Rahnama, M. The. (1387). Physical principles and models of assessment forms. Mashhad: Mashhad University Jihad publications.
[4] Zebar dast , Esfandiar, 1383, Optimum city size, Urban and Architectural Research Center
[5] Shakeri, M. and others, on issues of urban planning, Jihad, Mashhad University Press, 1389
[6] Kafashi, M. (1389). The concept of compact cities and sustainable urban form. Tehran
[7] Kamali. (1390). Sustainable Development
[8] Masnavi, MR, 1381, a new paradigm of sustainable development and urban (city-wide compact city), Journal of Ecology (3)
[9] Parsomash Consulting Engineers, August 1388, Mid-Western model of development and detailed design, development studies and prerequisite for model development, Volume I
[10] Parsomash Consulting Engineers, August 1388, Mid-Western model of development and detailed design, development studies and prerequisite for model development, Volume 2

[11] Parsomash Consulting Engineers, August 1388, Mid-Western model of development and detailed design, review and analysis of housing, Volume VI
[12] Parsomash Consulting Engineers, February 1389, and the detailed design of mid-western development model, the development model development, Volume XII, Second Edition
[13] Farnahad Consulting Engineers, in October 1384, comprehensive plan , the second volume of Mashhad, public recognition of the region, the Department of Housing and Urban Development
[14] Farnahad Consulting Engineers, December 1384, Development Plan (Comprehensive) District Mashhad, Volume VIII, of the city of Mashhad, Department of Housing and Urban Development, Second Edition
[15] Farnahad Consulting Engineers, September 1384 Development Plan (Comprehensive) District Mashhad, Volume IX, programs, plans and projects
[16] Farnahad Consulting Engineers, September 1384 Development Plan (Comprehensive) District Mashhad, Volume IX, programs, plans and projects , second edit
[17] Farnahad Consulting Engineers, July 1388 Development Plan (Comprehensive) Metropolis Mashhad, Development Vision, Goals, Strategies and Policies, Third Edition
[18] Farnahad Consulting Engineers, April 1388 Development Plan (Comprehensive) basic studies and human activity (population), First Edition
[19] Farnahad Consulting Engineers, May 1389, a development plan for the city of Mashhad, Mashhad Metropolitan Development Plan, First Edition
[20] Farnahad Consulting Engineers, September 1388, analysis of the condition of existing plans and programs;
[21] Farnahad Consulting Engineers, 1388 Development Plan of Mashhad, Mashhad reference bank locations, man-made environment, urban development plans
[22] (GIS)
[23] Mehdizadeh, J., strategic planning, urban development, department of Architecture and the Department of Housing and Urban Development, 13
[24] Mehyari , 1388 , http://www.javanemrooz.com
[25] V, G. (1389). The city is compact, sustainable urban form. Conference on sustainable urban development
[26] Hall, Peter, Pfeiffer,. (1388). Urban Future 21 th century. (L. sadeqi, & N.. Safai, Translator), Tehran: Iranian Society of Consulting Engineers
[27] .http://fa.wikipedia.org
[28] http://yissr.blogfa.com. http://www.smart-cities.eu/
[29] Elkin, T .et al. 1991. Reciving the City: Towards Sustainable Urban development, Friends of the Earth, London.
[30] Crane, R. and Daniere A. (1996): "Measuring access to basic services in global cities: descriptive and behavioral approaches" Journal of
[31] the American Planning Association,Vol. (2)
[32] Gordon,P,Harry,W.Richarson(1997)Are Compact Cities a Desirable Planning Goal, Journal of the American Planning Association
[33] Ewing, R (1997) Is Los Angeles-Style Sprawl Desirable?, Journal of the American Planni Association
[34] Glaster,G,et.al., (2001) Wrestling Sprawl to the Ground: Defining and Meaturing an Elusive Concept, Housing Policy Debate,Volume 12,
[35] Issue 4
[36] Tsai, Yu-Hsin (2005) Quantifying urban form: Compactness versus Sprawl, Urban Studies, Vol.42, No1

American Journal of Engineering Research (AJER)
e-ISSN : 2320-0847 p-ISSN : 2320-0936
Volume-02, Issue-09, pp-214-223
www.ajer.org

Research Paper Open Access

Evaluating sustaiable development factors on stress residential (case study: Mashhad Sarshur neighborhood)

Mohammad Rahim Rahnama, Ali Homaeefar
[1] Associate Professor Geography and Urban Planning department, Ferdowsi University, Mashhad, Iran
[2] PhD Scholar Department of Geography and Urban Planning, Ferdowsi University, Mashhad, Iran

Abstract: - The discussion of urbanity evolutions and populational movements in recent several years has caused to increase in, countly urban population in 55 last years, from five millions and nine hundred to fifty-four million persons since 1335 to 1390, i.e about 10-times increas. This quick growth has caused that urbanity problems in one human chalenge encounter with social indicators and neighborhood identity from various dimensions, which are sustainable development indicators.
In this study, It is tried to use opinions of neighborhood residents with resulting neighborhoodsustainable developmentindicatorswhile use of prior investigations related to subject.
The method of this research is "describtional-correlational". The information gathering method has been obtaind by refer to resources and texts.
Other required information have been accomplished by questionary tool based on questions and research purposes. Statistical society in related to questionary including Sarshur neighborhood residents. Sample valume in residents (household supervisor), equal to 279 people, has been used for data analysis and determined based on Cochran formula. The aim of investigation is to determine the effect of neighborhood sustainable indicators on residental mental health and to reduce their stress rate.
Since cities and neighborhood's residents have fundumental role to success development plan, so notice to their mental aspects is important.
Studied variable are neighborhood sustainable development parameters and resident's stress. The findings of this study show that decreased in residental's stress by enhancing neighborhood sustainable developmentindicators such as: neighborhood identity, partnership, security, legibility and neighborhood's vitalist.

Key words: - *neighborhood sustainable development, neighborhood identity, partnership, security, resident's stress.*

I. INTRODUCTION

Unlike per capita GDP or standard of living, both of which can be measured in financial terms, it is harder to make objective or long-term measurements of the quality of life experienced by nations or other groups of people. Researchers have begun in recent times to distinguish two aspects of personal well-being: Emotional well-being, in which respondents are asked about the quality of their everyday emotional experiences the frequency and intensity of their experiences of, for example, joy, stress, sadness, anger, and affection and life evaluation, in which respondents are asked to think about their life in general and evaluate it against a scale. Such and other systems and scales of measurement have been in use for some time. Research has attempted to examine the relationship between quality of life and productivity (nur bala, 2002: 5).
In recent decade evaluating of life condition is important due to creating urban issues. today the modern method is led to created some problems such as : density , crowded , pollution (Zahedi , 2002 : 20) . Improving human urban quality is necessary for governments (Ganji, 2002: 67).

1.1.The investigation functional purposes

- The effecy of neighborhood sustainable development indicators on residents mental health.
- Determination of environmental stressors elements.

II. RESEARCH HYPOTHESIS

It seems that to perform given strategies in neighborhood sustainable development theory can decrease in rate of stress in residents.

2.1.neighborhood sustainable development

Urban neighborhoods have less important role to organize pattern of urban residency because of its historical importance. Meanwhile, it has been emphasized to their recovery in recent several decades in steady development theory frame.

For urban sustainable development, it is required to plan (due to environmental and social reasons) in neighborhood level. All social, economical, political and physical activities in neighborhood level can be accounted as sustainable development intiative. Topic of neighborhood communication and its development have been noticed in frame of sustainable development subject since late of 190s because of relatively long prehistory in texts and scientific literatures as subject of neighborhood sustainable development concept.

The bases of persian-language investigation in this field is relatively weaker than urbansustainable development domain. The research commonly have stated, in analysis of stability in neighborhood level, that there are social integration increase, incorporation, dependance to neighborhood, hygine andnvironmental health, diversity, neighborhood identity and economical stability and house value.(Efroymson,ThanhHa,Thu Ha,2009&CHIRAS, WANN,2003&Robertson,McIntosh, James Smyth2010)

To evaluation of stability in neighborhood level, urban system in supposed as form of open system which our neighborhood is it's subsystems. In this communication system, it is studied sustainability evaluation in neighborhood level by assuming neighborhood as a comprehensive system. Therefore, it has not been noticed this metropolis elements which have effect on neighborhood sustainability.

Sustainable development in neighborhood level means "Enhancement of life quality in city" which include all features and environmental, cultural, political, organizational, social and economical components without creation of barrier for future generation.

This barrier is decrease of natural resources and increase of neighborhood lack.(Urban Conferences, Berlin, July 2007)

It can be considered principals and scales in frame of theories and existing internal and external experiences for neighborhood sustainable development; These principals and scales are included:

Economical and access indicator: rent and low price of house, easy access to services and public transportation and existing of pedestrian route and bicycle route in neighborhood, easy access to inside of neighborhoods parking lot.

Environmental indicator: lack of traffic, noise pollution, air and environmental pollution and existing of green space in neighborhood.

Neighborhood identity indicator: dependency to neighborhood, corporation of residents in neighborhood affairs, neighborhood legibility.

Social indicator: houses security, lack of unsuitable individuals inside neighborhood, allies security, neighborhood illumination, lack of privacy corners, increase in social interaction.

In respect to most of investigations which has been just focused on environmental and economical subject, in this study, ht has been tried to focus and discuss neighborhood identity and social concern.

2.2. Identity

The concept of identity word in domains and various achools has definitions and differences. Moien dictionary has defined identity as: what cause to identify person. I.e what cause to distinguish one person from another one, So, identity is not mentioned in vacum. Of course, there is self and othera, otherwise identification doesen't have mean. Amid dictionary knows identity as object and person fact which consists of his/her quintessential attributes. Also, it has meant identity as personality, essence, existence. Identity is meant by Oxford dictionary as what and who is person

Identity is mean-building process based on one cultural feature or continuation comples of cultural features which have been given priority to other meaning resources.(castelz,22,1380)

People appose against to be individual process and social analysis, they tend to present in communication organizations which creat dependancy over time and finally in many cases public and cultural identity. Of the greatest theorists in field of social identity theory is George Herbert Mead. In Mead viewpoint, each person forms his/her identit via organization of other individual attitude in frame of social or group organized attitudes. In another words, the picture which each person makes of him-/herrself and sense to him-/herself is attitudee

feedback which others give him/her.(Mead,1964,22)
The most important element to state neighborhood sustainable development is interests and benefits and dependancies which provide correlation and that resident of neighborhood united.(Hashemi, 491,2002)
The problem of today cities is not only environmental inadequency, traffic problems and other urbanity problems, the important problem of these cities is sense of non-identity and lack of dependancy to city and neighborhood from residents and citizens. Neighborhood identity is process of interaction, assossiation, environmental dependancy and collective integration which generate in typical time and place conditons.(Ma´asoumi,1389)
Neighborhood identity shows mutual effect of physical and social elements.(Robertson, McIntosh & Smyth,2010)

Identity sense and dependency to a place results in individual association with knows human as components of place. This assumes one role for place in the mind based on its experiences of symbols, meaning and functions this role is unique and different and it becomes important and respectful as result of place. One place forms the possibility of occurrence one social relation and common experience among people, dependency sense and correlation.

2.3. Partnership

Public participation is base of urban sustainable development. The project which was define by World Hygiene Organization, this is based on two principals: the parts coordination and public participation. (Mohammadzade ASL, 35, 1385)

The public participation can be known as meaning of participation and active, deliberate and voluntary, organized and effective presense of individual, groups, and urban organizations in urban life cultural, social and economical activities to accomplish in urban collective purposes. Although partnership as form of one organized activity and as mean of all-aspects interference of people in cultural, social, economical. And political process, which is effected by them, is stated since 1960's, but global experiences show that in 1980'stowards. It is noticed to development plans and also urban development, so that at present, public participation is success code of urban development project and one of evaluation acales of urban management function and its pillars (counsil and municipality).(pardaraz,1383)

In city-building encyclopedia, public participation to build city has been stated as instrument for society members to participate in design and edit politics which have effected on their life environment. The most basic stimulus in public participation is increasingly complication of urban life.(Ahmadi,46,1380)
United Nation research institute knows partnership as organized tries in order to increase in resources and disciplinal institute in determined social conditions from certain groups and movements which are deprived from such control for social development. On this basis, it can be observed partnership in field of political, econmical, social and metal partnership.

On the basis of this definition, it is very important to be able deprived and isolated groups to enter them in partnership process to make decision and supervision on affairs about self.
In order to explanation necessity of public participation usage in urban design and planning, it can be pointed to some advantages and disadvantages use of partnership as whole:

- **Increase in public knowledge level**;

people participate in planning and city-building activities causes to enhance their public knowledge level. Via this, the people can be familiar with features and limitations of planning and design; and this causes to be more real their demands and expectations, therefor, the purposes of designs and plans will furthur match with realities.

- **Creation of social resposibility and dependancy to society**;

"public participation creats one real sense about collective responsibility and dependacy to society. This causes to participate people in partnership and performing designs".(Dutta,1992). Coaction and collaboration mentalitywhich is accomplished by public participation , causes to decrease in tension and inconsistency among people and it is increased in sensitivity and sympathy sense of people relative to affairs improvement.

- **Acceptance of designs and plans by people**;

one of the main codes of designs and plans success in their acceptance from people which the final aim of all designs and plans. When it isn't accepted one design or plan by people, it is actually encountered with unsuccess, although it would be good design. Public participation in planning process can cause to accept designs and plans from people. "They will use the results of their share to decision-making. Since they accustom with demands and bio-methods, so they furthure coordinate."(Mokhber,1365)

2.4.Security

Security is complicated world which has extensive application as functionally. From the most inner thoughts and human senses to the most important problems amonng goverments contain security concept.

Oxford dictionary translates security as follow: free from concerns and safe against dangers and also contractional scales to gaurantee a country, person and thing safes which have value. Also, Moien and Amid dictionries have translated security as to be safe, safty, calm and relaxation.

Urban space has the most communication with people and life environmen, so it has important role for part identity an calmness sense for citizens. It seems that in present century, urban unsuitable environments have created many problems for citizens security and they are effective in social damages growth. By development of these damages, security is removed and it causes to enhance crimes and people act warily in social actions and it becomes double fear and prestiment by each happen, as a results, it is created unsafe sense. Social security is calmness and serenity which each society is required to provide for society and its members in the economical, political and judjment fields. Therefore, social security is not anything except manner of people calmness from fear, threat, stress an immune of life, wealth, honor, identity and belief from each threat and agression.

It has been given in 8th article of human rights and citizen announcement in France, 1973 that: security is included support which has been granted by society for individuals and Hs members to survive life & rights.(Mahboubi Manesh,6,1385)

Malformation in uraban space is introduction of unsafe and young population dense in larg cities in danger for urban stability security. The main metropolis problems is increasingly urban-rural immigration and small city to larg city immigration, boarder-sitting and urban poor population which can be resulted in security instability.(Ficker,344,1971)

One of the most important threating elements is people presence in public spaces, fear and unsafe sense. Places and public spaces unsafe disturb exhilaration and health in routine life, and it imposes huge expenses on society because of creation of barrier on cultural growth and public participation.(Eftekhari,8,1381).

The criterions of oe urban safe space can be suitable illumination, visible sense, public care, access to help and enough sight, environment legibility and keeping and preventing of disturbance and vandalysm.

2.5.Stress

Stress word is derived english language and it hasn't any accurate equivalent in farsi except pressure, and it gives extensive manning. Stress means pressure. This is the word which has been borrowed from physics and today, it has public application to state psychosomatics pressure.(Iran Panah,1377)

Stress was meant difficulty, hardness and disaster since 18th century. Hans selye(Austrian sychologist) was founder of scientific investigations about stress and he is the first man who explained the relation between stress and diseases. He defined relation between stress and diseases. He defined stress as rate of weans and Teas metabolism due to life pressures. Ofcourse, stress word is not called only to precedure in this phenomenon in human body, but also it is called as stressors stimulate under this name,(Shamloo,1362)

Psychologists say on the average, what is resulted in stress is gathering life events which disturb individual consistency with existing condition. In their viewpoint, stress is important phrase which is for describtion of situation or recognition that cause to creat mental pressure. Nevertheless, stress is more extensive concept from physical and material pressure and each stimulus that creats tension in human and makes reaction inside him/her, it is recognized as stressors factor. This factor may be one event, condition, situation or problem. The created tension and respond to this tension creat process which is called stress. In psychology term, stress can be accounted as environmental stimulus one reaction against environmental stimulus or inter-stimulus interaction and reaction.(Riggio,1955,Translation by Hossein Zade,1383)

Stress or mental pressure mean force which is enforced from inter and outer elements on person and has effect on his/her behavior. In another word, it is sort of behavioral disorder which is created by putting person in unknown or insuitable situations.(Byrne &Espnes,2007)

III. MODELS OF ENVIRONMENTAL STRESSORS

3.1.Adaptability model

one model which explain the effect of environmental stressors factors, is adaptabillity. This model emphasizes on the effect of environmental stressors elements on human physiological aspects which have adjustable ability. Caplan was given this theory, this theory state that human has this ability to close interaction in various environmental conditions. People can appose uncomfortable conditions in special time domain. Thi model studies exposure to stress condition by human which is resulted in accustom process.(Evans & Cohen,578,1986)

3.2.Control model

There is considerable evidence that human beings have a srong need for environmental mastery and a sense of self-efficacy. Negative consequences associated with lack of control include negative effect, cognitive

deficits, and reduced motivation to behave instrumentally when the opinion is available. Actual or perceived control over a stressors generally leads to fewer negative consequences than exposure to stressors that are uncontrollable. This is particularly true if the individual believes that control has the potential to modify his or her experience of the stressors.(Evans & Cohen,578,1986)

3.3.Predictability

A number of scholars have noted the tendency of environmental stressors like noise to disrupt or interfere with ongoing behaviors. Unpredictable stressors are more distrancting and make concentration on tasks more difficult poulton has emphasized that distraction is the principal mechanism of task decrements noted in noise. Distraction has physiological consequences as well, related to the orienting reflex, which tiggers a state of mental alertness and vigilance. Predictability is also related to patterns of environmental stimulation. Setting that are unfamiliar or highly ambiguous or difficult to interpert may be stressors. When one cannot discern the meaning or function of an object or a setting, confusion as well as stress may occur.(Evans & Cohen,578,1986)

3.4.Systems models

The psychological perspective on stress, as discussed earlier, emaphasizes the dynamic balance between environmental demands and the organism's ability to cope with those demands. Congruence or the extent of fit between person and environment has been used explain stress. Stress occurs when environmental opportunities are insufficient in affording important personal or group needs and goals. Stress is an outcome of incongruence between person and environment.(Evans & Cohen,578,1986)

IV. ENVIRONMENTAL STRESSORS

Infact, everything that is furthur under pressure and results in life and mental analysis is called stressors. The control of environmental important problems such as (to become warm earth, change climate, air pollution or accident and disastes) has been stated as large challemge.(Homburg,2006)

Number of social and physical features in neighborhood may act as stressors. Physical aspects of neighborhood include large number of empty buildings in order to conclude this place is not safe and suitable place for living; this can cause to make stress, lack of green places may decrease in the effect of nutural environment on stress reduction. Tendency and attitude to neighborhood environment as unsafe, wild and irregular environment can creat stress sense as direct and indirect with fear in individuals. Violence and disorder in social and individual level is accompanied by neighborhoods with depression and distress. Infact, the stressorsresulting in neighborhood unit have effect on individual tendency relative to their life environment.(Mair,2010)

4.1. Stressors can be devided into 4 cases

Economical elements: inflation, lack of economical security, fear of poverty and unemployment, material problems to be married.

- Cultural elements: fade of scientific, literatural, art values, dominance of force cultures as a result strange disease comprehension
- Departmental elements: lack of job, dominance of relations on criteria, complicated Brocracy, lack of control and evaluation mechanisms.
- Plitical elements: unclear the person participation in self-determination, lack of security sense about life and result and believes, sense of pressure in freedom and independanceof counry.(Soltani,1381)

V. RESEARCH METHOD

Type of research is "describtional and correlation". Describtional research isn't often experimental type and deal with nutural position an dummy which are available now or it has happened before. In this method, it can be analyzed human behavior as nuturaly and in real conditions which is occurred in different situation of life.(Negahban & Mostajabi,1384)

Describtional or non-experimental research inclde 5 groups: mensurational, correlational, post-evental, actional, case study.(Bandar Abad,1390)

The method of gathering information has obtained via refer to texts and resources. Another required information has been accomplished by research questions and puposes via questionary tool.

Thorndike theory says: if there would be anything, yhen it has quantity; and what has quantity, it is measurable. In some cases which there are some features that can't be measured such as rate of satisfaction and stress, the only way to gather data and only suitable tool is use of questionary. So it can measure hidden feature.(Negahban & Mostajabi,1384)

It has been raised some question to design questionary in several level by method of error and test; some

unrelated questions have been omitted and then 50 questionaries give to residents as pre-test, after analysis, it is added and omitted some questions by suggestion of residents.
In first time, it was responded 300 questionaries by residents, but the result dosen'tmatch with research hypotheses, thus it was designed questionariy for second time in order to prove hypotheses and it was distributed 279 ones among residents.
The method of scoring was based on 5 degree lickert scale which included: very low=1, low=2, medium=3, high=4 and very high=5.

To design a goodquestionariy, it must be first recognize the purpose compeletely, then it must be considered som questions to accomplish that purpose.(Negahban & Mostajabi,1384)
Stattistical society in relation with questionariy includs residents of Sarshur neighborhood which it has been sample randomly. Sample volume in residents (Household supervisor) in equal to 279 persons which it has been determined by Cochran formula. Also, it has been used spss software to analysis data.
The studide variables about neighborhood sustainable development is as independent variable and residents stress is the depndent variable.

Neighborhood sustainable development: sustainable development in neighborhood level means "anhancement of life quality in city" whichh includs environmental,cultural, political, organizational, social and economical features and components without any obstacle for future generation. This onstacle cause in local lacks.(Urban Conferences, Berlin, July 2007)
Environmental stress: this is a negative emotional reaction which is created by threaten one element in physical environment.(www.urbanity.ir)
It has been accounted stability of research attitude spectrums by Cronbakh alpha stability test and it has been shown in table1.

Table 1: stability rate (Cronbakh alpha) of questionariy attitude spectrums.

Rate of Cronbakh alpha coefficient	Number of spectru	Research spectrums
o.701	10	environmental Stress
0.707	10	Neighborhood Sustainable development
0.803	14	stress

VI. STUDIED AREA

Sarshur has been located in central sector of Mashhad city. Sarshur has been located near the holy shrine. So has important position in this city. Also, it has located in old fabric. On the other hand famous carpet bazaar of Iran.
Sarshur neighborhood is on of the main six neighborhood in Mashhad that its position is west of holy shrine . Also, Khosravi & Akhund Khorasani Avenue have located around the neighborhood.

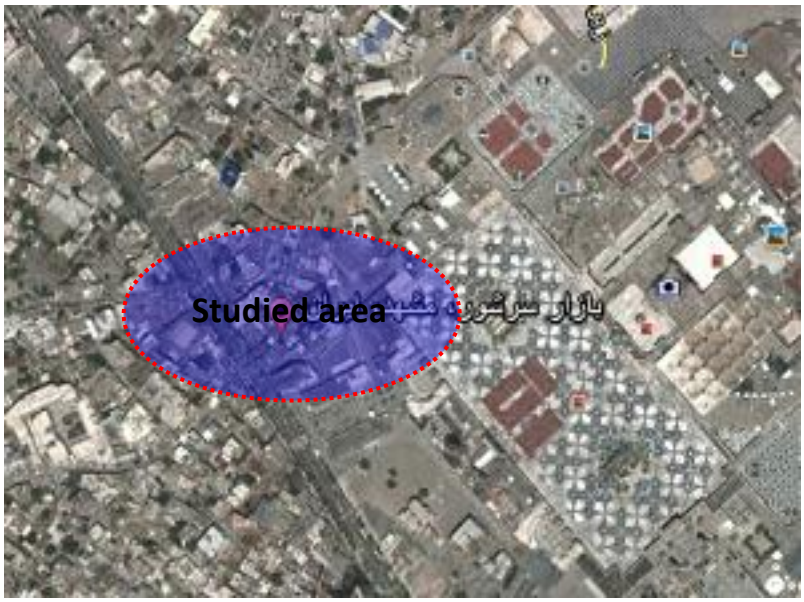

Figure 1 : Sarshur neighborhood

VII. FINDING RESEARCH

Indicators which have been studied in this part, are included:

- Economical and access indicator: rent and low price of house, easy access to services and public transportation and existing of pedestrian route and bicycle route in neighborhood, easy access to inside of neighborhoods parking lot.
- Environmental indicator: lack of traffic, noise pollution, air and environmental pollution and existing of green space in neighborhood.
- Neighborhood identity indicator: dependency to neighborhood, corporation of residents in neighborhood affairs, neighborhood legibility.
- Social indicator: houses security, lack of unsuitable individuals inside neighborhood, allies security, neighborhood illumination, lack of privacy corners, and increase in social interaction.

Table 2: frequency distribution related to environmental stress spectrum.

Environmental stress	frequency	Percent
Low	19	6.8
Medium	158	56.6
High	102	36.6
Total	279	100

On the basis of above table from total studied respodents, most of them had stated that their environmental stress is in medium level (56.6%). Then, there are persons who have high environmental stress in 36.6% and 6.8% of them had low environmental stress.

Table 3: frequency distribution related to neighborhood sustainable development spectrum.

neighborhood sustainable development	frequency	percent
Low	109	39.1
Medium	153	54.8
High	17	6.1
Total	279	100

On the basis of this table data from all studied respondents, most of them had stated that their neighborhood sustainable development is in medium level (54.8%), then, there are people who believed that their neighborhood has had very low development (39.1%) and 6.1% of individual believe that they had high neighborhood sustainable development.

Table4: correlation test and variable regression analysis of neighborhood sustainable development access and respondent environmental stress.

	R	R2	R2 Ad	Standard error	B Coefficient	Beta	T	F	Sig
Correlationsocial dimension ofneighborhood sustainable developmentand environmental stress.	0.542	0.294	0.291	4.42	-1.469	-0.542	-10.732	115.170	0.000

In order to study the relation betweenneighborhood sustainable developmentaccess and individual environmental stress, it has been used regression statistical technic. Based on results, there is high correlation (R=0.516) between access and individual environmental stress. The value R^2=0.276 shows that anticipation

variable has had medium effect on observed changes in sample population as rate of neighborhood sustainable development.

Table 5:correlation test and variable regression analysis of to neighborhood sustainable development identity variable and respondent environmental stress.

	R	R^2	R^2 Ad	Standard error	Coefficient B	Beta	T	F	Sig
Correlationneighborhood sustainable development identity and environmental stress.	0.511	0.261	0.258	4.52	-1.489	-0.511	-9.895	97.913	0.000

In order to study the relation between neighborhood sustainable development identity and individual environmental stress, it has been used regression statistical technic. Based on results, there is high correlation (R=0.511) between identity and individual environmental stress. The value R^2=0.261 shows that anticipation variable has had medium effect on observed changes in sample population as rate of individual neighborhood sustainable development.

Table 6: correlation test and variable regression analysis in social dimension of neighborhood sustainable development and respondent environmental stress.

	R	R^2	R^2 Ad	Standard error	Coefficient B	Beta	T	F	Sig
Correlationneighborhood sustainable development access and environmental stress.	0.516	0.267	0.264	4.51	-1.087	-0.516	-1.037	100.731	0.000

In order to study the relation between neighborhood sustainable development social and individual environmental stress, it has been used regression statistical technic. Based on results, there is high correlation (R=0.542) between social and individual environmental stress. The value R^2=0.294 shows that anticipation variable has had medium effect on observed changes in sample population as individual neighborhood sustainable development rate.

Table 7:correlation test and variable regression analysis between neighborhood sustainable development environmental dimension and respondent environmental stress.

	R	R2	R2 Ad	error Standard	Coefficient B	Beta	T	F	Sig
Correlationenvironmental dimension and environmental stress.	0.478	0.228	0.225	4.62	-2.055	-0.478	-9.050	81.908	0.000

In order to study the relation between neighborhood sustainable development environmental dimension and individual environmental stress, it has been used regression statistical technic. Based on results, there is high correlation (R=0.478) between environmental dimensionand individual environmental stress. The value R^2=0.228 shows that anticipation variable has had medium effect on observed changes in sample population as rate of individual neighborhood sustainable development.

The research finds demonestrate that the variables e.g economical, social, and environmental dimensions and sub-indicators such as security, partnership, identity and to be low pollutions rate are effective to decrease in residents stress.

The effect of economical indicator in case study shows that easy access to public transportation andreduction of house price and its rent can help to decrease stress.

It can be decreased in stress in social dimension in individual by improve some factors such as: sub-indicators of houses security, lack of people with un suitable appearance inside neighborhood, allies security, neighborhood illumination, lack of vacancy corners, dependancy to neighborhood, residents participation in neighborhood affaairs, and neighborhood legibility in respect to generalization to security and confidence among residents and to creat residents resposibility relative to each other and to their neighborhood.

The effect of environmental indicator in studied domain showed that reduction of noisepollution, air and environmentalpollution, reduction of traffic rate and increase green space cane reduce residents stress.

VIII. CONCLUSION

Following change in conditions and elements to expand develop urban part in recent years. Human construction of residental neighborhoods have special place to form cities. While urban sustainable development has devoted main part of recent years urbanism literature, to set to principals and critoria of neighborhood sustainable development require many investigation.

This study has been designed and performed by purpos of neighborgood sustainable development indicators effect on neighborhood resident stress and exploit measurment method. The results are based on gathered data analysis of samples with 279 persons of Mashhad Sarshur neighborhood residents. The obtained results show that there is reverse relation between neighborhood sustainable development and residents stress, so the more sustainable development, the les rate of residents stress. Generally, the respondants know to equal rate of sustainablity in case study in all indicators or in medium level. At last on the basis of small different in rate of sustainability and stress related to each indicator in studied neighborhood, residents know less sustainability related to security and social indicators. As a result, they have the stress in relation with this indicator and they have known sustainability in the field of environmental domain, so they had less stress due to environmental reasons and third stressor has been for them and at last economical element has been devoted according to residents and according to residents as instability in second rate and it is second stressor. In respect to this finding, it has been given some strategies to increase in security, decrease in economical expense and to be high neighborhood identity and public participation and to less environmental problems.

8.1.Roposing of strategise

- Respect to cases to enhance security such as various times of activity, provide illumination and use of lightening in social supervision to enhance security, choosing sector police among residents typically young people.
- Issue some laws in order to keep citizens rights during walking, biking, to enhance walking spaces quality and quantity such as: creat suitable cobble in spaces, increase in green space next to such spaces, to equipt such spaces in suitable urban furniture, existing of services user next to such spaces, to create spaces in order to bicycle rent, lawful planning about urban waste-water chanel, water, electricity, gas, telephone and other municipality services about pedestrain spaces, biking citizens in outdoor spaces as aesthetics principals and created obstacles in spaces.
- To give participate strategies in order to enhance residents social activities with based-neighborhood approach such as to motive and form inter neighborhood and inside-neighborhood NGOS, possibility of residents communication via internet, to creat equipments to perform groups decisions and to promote culture of participation in public matches.
- Control and more supervision on traffic problems and widen street and struct under-way bridges to decrease in traffic and to increase in number of pedestrain bridges.

REFERENCES

[1] AbdollahiSabet,Mohammad Mehdi, To edit criteria and sustainability indicators in residental neighborhood, Urban management magazine,1386.

[2] Administrative engineers, Mahmoud Mahboodi, The procedure of people participation attraction in the field of

improvement and repair old structure, 1383.
[3] Bandar Abad, Alireza, research method, 1390.
[4] Barak Pour, Naser, Sustainable identity in residental neighborhoods, Municipality magazine, #25, 1380.
[5] Barton,Hugh,etal(2003)."ShapingNeighbourhoods:Aguideforhealth,sustainability and vitality".SponPress,London and New York.
[6] Byrne,D.G&Espens,G.(2008)occupationalstressandcardiovasculardiseas.journal of occupational Health psychology.
[7] Custelz, M, Information era; economic, society and culture (identity power), translated by: Ahmad Aligholian, Hassan Chawoshian, second volume, Tehran, new design, 1380.
[8] DanChiras& DaveWann,(2003),Superbia "31 ways to create Sustainable neighborhoods" , New Society Publishers,2003.
[9] Daphna Oyserman ,Kwang-Il Yoon, Neighborhood Effects on Racial–Ethnic Identity: The Undermining Role of Segregation, Springer Science+Business Media, LLC 2009.
[10] David Lipe, Mapping Neighborhood Identity in Seattle's Cascade District, Professor Manish Chalana,URBDP 587, Winter 2007.
[11] Debra Efroymson& Tran ThiKieuThanh Ha & Pham Thu Ha(2009), Public Spaces "How They Humanize Cities", HealthBridge - WBB Trust Dhaka, October 2009.
[12] Douglas Robertson & Ian McIntosh & James Smyth "Neighbourhood Identity: The Path Dependency of Class and Place", Department of Applied Social Science, University of Stirling, UK & Department of History and Politics, University of Stirling, UK, Version of record first published: 21 Jan 2010.
[13] Dutta , A.K & Jena , P.K (1992)"People`s Participation in Development Process - Role of Education"; ITPI Journal , Sep.1992.
[14] Eftekhari, Asghar, Struction and secrity, magazine of strategical studies, Fifth year,#1, Spring 1381.
[15] Ficker. B & Herbert S. H. urban crisis, 461 p,New York : Macmillan, 1971.
[16] FulongWu,Neighborhood attachment, social participation, and willingness to stay in China's low-income communities, Bartlett School of Planning, University College London, 2012.
[17] GaryWEvans&SheldonCohen,EnvironmentalStress,PrograminSosialEcology,UniversityofCalifornia&CarnegieMellon,University,Pittsburg, Pennsylvania,1986.
[18] Homburg, Andreas. Stolberg Andreas, Explaining pro-environmental behavior with a cognitive theory of stress Philipps-University, Marburg, Germany, May 2006.
[19] Hoodsani, Hanieh, The improvement of spatial struture of urban neighborhoods in frame of case study neighborhood sustainabile development, the art university of TarbiatModaress, 1384,
[20] Iran Panah, Akbar, Oxford English to persian dictionary, Moshdeh publication,1377.
[21] Kathi Wilson, JohnEyles, AnneEllaway, SallyMacintyre, LauraMacdonald, Health status and health behaviours in neighbourhoods: A comparison of Glasgow, Scotland and Hamilton, Canada, Health & Place 16 (2010) 331–338.
[22] Ma'asoumi, Salman, Local development in parallel Tehran metropolis sustainability, 1390.
[23] MahboobiManesh, Hosssein, Short contemplation about social damage as public security problem, fasle danseh,8th year, 3th number,1385.
[24] Mair, Christina. DiezRoux, AnaV .D.Morenoff, Jeffrey Neighborhood stressors and social support as predictors of depressive symptoms in the Chicago Community Adult Health Study, Health & Place journal, USA, 2010.
[25] Mala Rao, Francoise Barten and coworker, Urban Planning, Development and Non-communicable Diseases, Planning Practice and Research, Vol. 26, No. 4, pp. 373–391, August 2011.
[26] Mark Livingston, Nick Bailey and Ade Kearns, People'sattachment to place the influence of neighborhood deprivation, Published for the Joseph Rowntree Foundation by the Chartered Institute of Housing, Glasgow University 2008.
[27] Mead. G. Herbert , On social psychology, University of Chicago Press, 1964 - Psychology - 358 pages.
[28] Mohammad ZadehAsl, Nazi, Study of comparison households social welfare indicatores in 22 region of Tehran, Iran statistic center, 1386.
[29] Mokhber, Abbas, Local planning and rural development, Translated by Plan & budget organization, Tehran, 1365.
[30] Negahban, Alireza and FaridMostajabi, The guidance of research method by help of questionary, organization of university publications, 1384.
[31] Pakzad, Jahanshah, Thoughts in urbanism3, Tehran, Shahidi publication, 1388.
[32] Shamloo, Saeed, Mental hygine, Chehr publication, 1362
[33] Soltani, Iraj, Scientific strategies to decrease in stress among managers an employers, 13 period, #129, Fall 1381.
[34] Stura Benjamin, Stress of civililization new disease, translated by ParirokhDadsetan, Roshd publications,1386.
[35] The White House Office of Faith-Based and Neighborhood Partnerships, A Partnership Guide for Faith-Based and Neighborhood Organizations,2009.
[36] Urban Conferences, Barlin, July 2007.
[37] Zieleniec, Andrzej, Space and social theory, Bridget Fowler, University of Glasgow, SAGE Publications Ltd, 2007.
[38] Engineering & Community development department, Neighborhood participation meeting program ordinance, City of Oakland park "A city on the move", 2009.

American Journal of Engineering Research (AJER)
e-ISSN : 2320-0847 p-ISSN : 2320-0936
Volume-02, Issue-09, pp-224-227
www.ajer.org

Research Paper Open Access

Measurement of Natural Radioactivity in Soil Along the Bank of River Kaduna – Nigeria.

Abdullahi, M. A., Mohammed, S.S. and Iheakanwa, I. A.
Department of Applied Science, College of Science and Technology
Kaduna Polytechnic, Kaduna – NIGERIA

***Abstract*: -** Gamma-ray spectrometry of natural radioactivity was carried out in soil along the bank of river Kaduna Nigeria using EDXRF techniques. The activity concentration in Bq/kg for ^{40}K and ^{232}Th were calculated from the % weight of K and Th determined in the soil samples. The mean activity concentration of ^{40}K was found to be 1168.13 ±94.67Bq/kg in range between 810.62 ± 21.91 to 1765.32 ± 31.30 Bq/kg. The mean activity concentration of ^{232}Th was found to be 18.76 ± 2.51Bq/kg in range between 8.12 ± 2.44 to 33.70 ± 6.90 Bq/kg. The highest values of ^{40}K and ^{232}Th were found in samples obtained from GRA 2 and this can be attributed to the increase anthropogenic activities going on in the area. The mean activity concentration of ^{40}K in the study area is higher than world average value while that of ^{232}Th is lower than world average value.

***Keywords*: -** *Natural Radioactivity, Radionuclides, Activity Concentration, Bq/kg, ^{40}K and ^{232}Th.*

I. INTRODUCTION

A knowledge of various radionuclide in soil and rocks plays an important role in health physics and geo-scientific research. The naturally occurring radionuclide ^{226} Ra, ^{232}Th and ^{40} K are the main sources of radiations in soil and rocks from which traditional building materials are derived. These radionuclides pose exposure risk externally due to their gamma-ray emissions and internally due to radon and its progeny which emit particles[1]. Even though depend on the local geological conditions and as such they vary from place to place.

In many developing countries like Nigeria soils are affected by mine waste disposal, acid deposition, sewage, sludge and other anthropogenic activities. Radioactive materials can enter water in several ways by being deposited in surface water from the air, by entering ground water or surface water from the ground through erosion, seepage, or human activities such as mining, farming, storm water and industrial activities and by dissolving from underground mineral deposits as water flows through them [2]. The environment contains in abundance of man made and natural radionuclide as well as polluting heavy metals. Their accumulation and the inevitable impact on human health is a matter of serious international concern. There are several ways in which humans can come into contact with this radionuclide: inhalation from the passing cloud external exposure in contaminated soil surface and ingestion due to food chain transfer of radionuclide. The types of diseases that can occur include leukemia, thyroid, bone, breast, lung and others. As at 1988, there were 237 confirmed cases of illness resulting from this incident as well as 31 fatalities in the Soviet Union [3]. Similarly, in Nigeria over 400 children died of lead poisoning in Zamfara State due to artisanal mining activities [4].

The International Basic Safety Standards (BSS) for protection against ionizing radiation and the safety of radiation sources [5] specify the basic requirement for the protection of health and the environment from ionizing radiation. These are based on the latest recommendations of the International Commission on Radiological Protection on the regulation of Practices and interventions [6]. The BSS is applied to both natural and artificial sources of radiation in the environment and the consequences on living and non-living species.

Irradiation of the human body from external sources is mainly by gamma radiation from radionuclides of the ^{235}U and ^{232}Th decay series and from ^{40}K. These radionuclides may be present in the body and irradiate various organs with alpha and beta particles as well as gamma rays [7,8,9].

In this research, the activity concentration of ^{40}K and ^{232}Th in soil samples obtained from five locations along the bank of river Kaduna Nigeria were determined using EDXRF techniques.

II. MATERIALS AND METHOD

Ten (10) soil samples were collected at five (5) different locations along the bank of river Kaduna, Nigeria namely; Gamji Recreational Area (GRA), Kabala Costain (KC), Nasarawa (NS), Unguwan Rimi (UR) and Zango (Zg) as shown in figure -1, at 10cm depth using a mechanical digger. The 10cm depth was carefully chosen as the appropriate depth to obtain the samples in line with the facts established that these pollutants are highly absorbed to clayed materials and organic matters in the study areas[10].

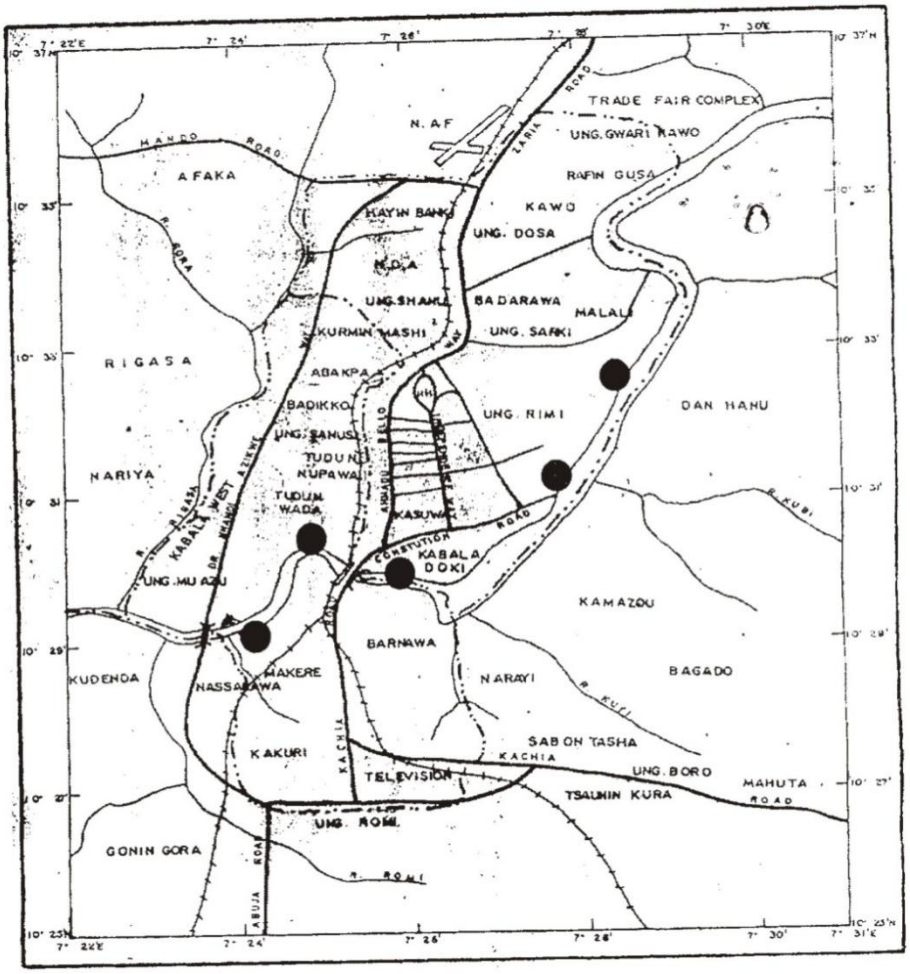

LEGEND

	Road
	Railway line
	Local governemnt boundary
	River Kaduna
	Sampling location

Figure- 1: Map of kaduna metropolis showing the sampling locations

The Ten (10) soil samples collected from the sampling locations were pretreated by oven drying them at a regulated temperature of 50^0c for 48 hours. After drying, a series of mesh size 35µm was used to remove large undesirable particle sizes [10]. The dry test samples were analyzed using the energy dispersive X-ray florescence (EDXRF) minipal (4) model to determine the concentration of the metals pollution in the soil samples.

The activity concentration in Bq/kg for ^{40}K and ^{232}Th were calculated from % weight of K and ppm (mg/kg) of Th using IAEA 2003 conversion of radio element concentration to specific activity (1%k in soil = 313Bq/kg of ^{40}K and 1ppm of Th in soil = 4.06 Bq/kg of ^{232}Th).

III. RESULT AND DISCUSSION

The soil samples collected were analysed using EDXRF where the percentage weight of all the elements present in the sample were obtained. The percentage weight of Th was converted to mg//kg (ppm) as shown in table 1.

Table 1: % weight of K and concentration Th mg/kg

S/No	Location	%K	Th ppm (mg/kg)
1	GRA 1	3.5 ± 0.08	4.60 ± 0.7
2	GRA 2	5.64 ± 0.01	8.30 ± 1.7
3	KC 1	4.71 ± 0.01	4.70 ±1.1
4	KC 2	3.08 ± 0.08	2.00 ± 0.6
5	NS 1	3.06 ± 0.08	3.06 ± 0.6
6	NS 2	2.59 ± 0.09	7.60 ± 0.8
7	UR1	3.83 ± 0.09	3.40 ± 0.6
8	UR 2	4.49 ± 0.09	4.20 ± 0.8
9	ZG 1	3.58 ± 0.08	4.70 ± 0.6
10	ZG2	2.4 ± 0.0	3.1 ± 0.7

The activity concentration of ^{40}K and ^{232}Th in Bq/kg were calculated based on IAEA 2003 conversion factor. Inferential statistics was used to compare the activity concentration of ^{40}K and ^{232}Th across the sampling locations. The one way ANOVA at the 5% level of significance was applied for the analysis. The mean activity concentration of ^{40}K and ^{232}Th are shown on table- 2.

Table 2: Activity concentration for ^{40}K and ^{232}Th in Bq/kg

S/No	Location	^{40}K	^{232}Th
1	GRA 1	1095.50 ± 25.04	18.68 ± 2.84
2	GRA 2	1765.32 ± 31.30	33.70 ± 6.90
3	KC 1	1474.23 ± 31.30	19.08 ± 4.47
4	KC 2	964.404 ± 25.04	8.12 ± 2.44
5	NS 1	957.78 ± 25.04	14.62 ± 2.44
6	NS 2	810.62 ± 21.91	30.86 ± 3.25
7	UR1	1198.79 ± 28.17	13.0 ± 2.44
8	UR 2	1405.37 ± 28.17	17.05 ± 3.25
9	ZG 1	1120.54 ± 25.04	19.08 ± 2.44
10	ZG2	888.92 ± 25.04	12.57 ± 2.4
	Mean	1168.13	18.76
	StdErr	94.67	2.50

Activity Concentration of ^{40}K

From the result of the analysis the mean activity concentration of ^{40}K is 1168.13± 94.67 Bq/kg in range between 810.62 ± 2191 to 1765.32± 31.30Bq/kg with the highest activity concentration in GRA 2 as shown in Fig. 1.

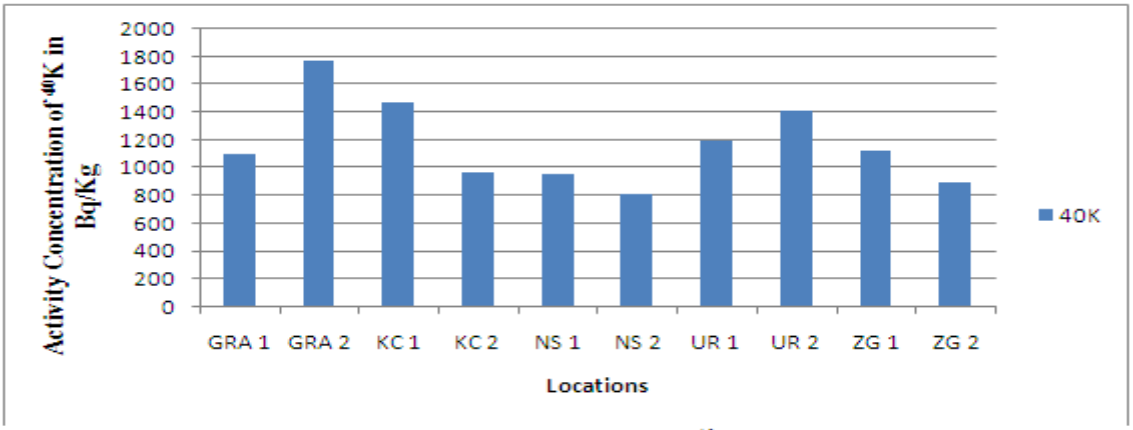

Fig. 1: Plot of Activity Concentration of ^{40}K by Location

The mean activity concentration of ^{40}K obtained in this study is higher than 997.57 Bq/kg obtained from gold bearing soil [11] 641Bq/kg in Zaria Nigeria [12] 682 Bq/kg in Ghana [13] and world average value of 420 Bq/kg[8]. The high activity concentration of ^{40}K in the area can be attributed to anthropogenic activities and geochemical setting of the area.

Activity Concentration of ^{232}Th.

The mean activity concentration of 232Th in the samples was 18.76 ± 2.50 Bq/kg in range between 8.12± 2.44 to 33.70 ± 6.90 Bq.kg. the highest activity concentration was obtained from GRA2 as shown in Fig 2.

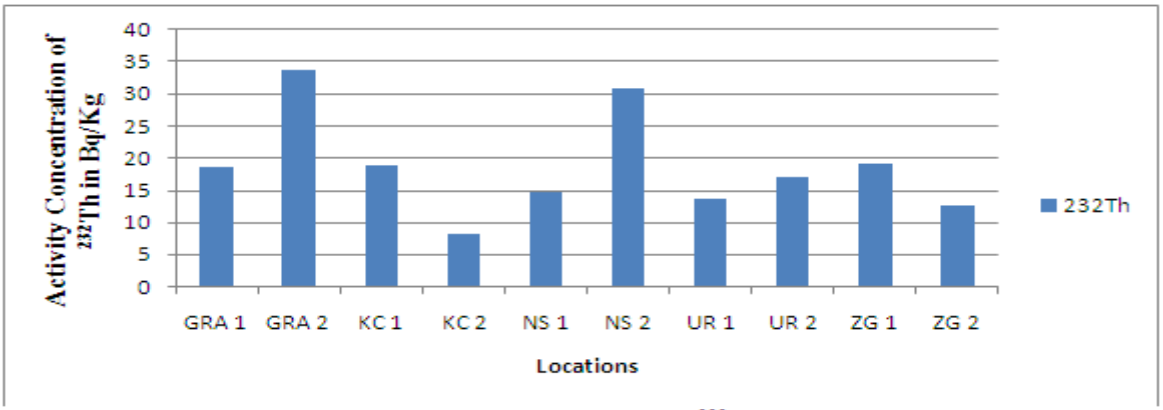

Fig.2: Plot of Activity Concentration of ^{232}Th by Location

The values obtained from this study are lower than 62.69Bq/kg obtained in gold bearing soil [11] 34 Bq/kg in Zaria Nigeria [12] 21 Bq/kg in Ghana [13] and the world average value of 45 Bq/kg [8].
The high activity concentration of 33.70 ± 6.90 Bq/kg obtained from GRA2 can be attributed to anthropogenic activities in the area.

IV. CONCLUSION

The activity concentrations in Bq/kg of ^{40}K and ^{232}Th were measured from the % weight of K and Th determined using EDXRF techniques from soil samples collected along the Bank of River Kaduna, Nigeria the result showed that ^{40}K has a mean activity concentration of 1168.13 ± 94.67 Bq/kg with minimum and maximum values of 810.62 ± 21.91 and 1765.32 ± 31.30 Bq/kg. The mean activity concentration of ^{232}Th is 18.76 ± 2.5 Bq.kg in range between 8.12 ± 2.44 to 33.70 ± 6.90 Bq/kg. The highest values of both ^{40}K and ^{232}Th were obtained in GRA 2. The ANOVA (0.000100.5) showed that there is a significant difference in the relative abundance of ^{40}K and ^{232}Th in the sampling locations. In other words in all the locations the activity concentration of ^{40}K is more than that of ^{232}Th.

REFERENCES

[1] Muhammad, I., Tufail, M., and Mirza S.M. (2000). Measurement of natural radioactivity in Marble found in Pakiston using Na1 (TI) gamma-ray spectrometer. Elsellier. J. Env. Radioactivity 51. 255 – 265.
[2] Beck H. (1980). Exposure Rate conversion factors for Radionuclides Deposited on the ground, EML– 3778 Environmental measurement Laboratory, New York
[3] Anspaugh L.R., Catlin R.J. and Goldman M., (1988). The global impact of the Chernobyl reactor accident science, 242, 1513–1519.
[4] Weekly Trust Newspaper, Nigeria Saturday 3rd December, (2011)
[5] IAEA, (1996). International Basic Safety Standard for Protection against Ionising Radiation and for the Safety of Radiation Sources. Safety Series No 115, IAEA Vienna.
[6] ICRP, (2007). Recommendations of the International Commission on Radiological Protection. ICRP Publication 103, Pergamon Press, Oxford.
[7] Cember, H., (1996). Introduction to Health Physics. 3rd Edn., McGraw-Hill, New York.
[8] UNSCEAR, (2000). Exposures from natural sources of radiation. Report to General Assembly Annex B, New York.
[9] IAEA, (2005). Naturally occurring radioactive materials (iv). Proceeding of an International Conference held in Szezyrk, IAEA TEC DOC-1472, Poland.
[10] Kabata–Pendias A., (1993). Behavioral properties of trace metals in soils. Applied Geochemistry 2,3
[11] Nasir R. Zakari I.Y., and Abdullahi M.A., (2013). Distribution of Gamma Emitting Radionuclides Goldmine Kaduna State Nigeria. Res. J. of Sci. Engineering and Tech 6(17) 3255 – 3258.
[12] Muhammad, A.M., I.F. Isa, S.P. Mallam and S.A. Arabi, (2010). Determination of absorbed and effective dose rate from natural background radiation around a nuclear research facility. Am. J. Environ. Sci., 7(2): 173-177.
[13] Darko, E.O., G.K. Tettea and E.H.K. Akaho, (2005).Occupational radiation exposure to norms in goldmine. J. Radiat. Protect. Dosimet., 114(4): 538-545.

American Journal of Engineering Research (AJER)
e-ISSN : 2320-0847 p-ISSN : 2320-0936
Volume-02, Issue-09, pp-228-233
www.ajer.org

Research Paper Open Access

On the choice of importance of Resampling schemes in Particle Filter

Mr. J.Joseph Ignatious, Dr.S.Abraham Lincon,
Department of Electronics and Instrumentation Engineering,
Annamalai University, Annamalai Nagar, India.

Abstract: **-** Particle filter is a powerful tool for tracking of targets in any system .The systems which are non-linear and non Gaussian are commonly occur in practice. This paper investigates various resampling algorithms which are available on particle filter .Many tracking methods have been developed but still there are difficulties in continuous tracking of the target. This work aims on the preference of resampling algorithms in tracking .The performance of resampling is evaluated in terms of their MSE value of SIR filter with that of resampling schemes**.**

Index Terms: **-** *SIR Filter, Mean Square Error(MSE), Resampling, Particle filter*

I. INTRODUCTION

The main strength of the particle filters is that they can be used in filtering even in problems where we cannot compute the distribution analytically. It is only needed to be known proportionally. Importance sampling is a technique for getting samples from analytical distributions. The idea is to get samples from another distribution, like normal distribution, and then assign the weight according to the real distribution. This estimation of the filtering distributions is done in every time instant from the beginning. The weight of the particles are calculated as follows:

$$\omega^{(i)}(k) = \omega^{(i)}(k-1)\frac{p(y(k)|x^{(i)}(k)p(x(k)|x^{(i)}(k))}{p(x^{(i)}(k)|x^{(i)}(k),y(k))}$$

where $\omega^{i}(k)$ is weight of the particle, x(k) one possible system state sampled from the proposal distribution, $p(x(k)|x^{i}(k-1))$ is its prior probability and y(k) are the observation, $p(y(k) \mid x^{i}(k))$ is its likelihood and $p(x^{i}(k)|x^{i}(k-1), y(k))$ is the value of the density function of this particle's proposal distribution. Then the weights are normalized so that their sum equals unity. The new weights are:

$$\tilde{w}^{(i)}(k) = \frac{\omega^{(i)}(k)}{\Sigma^{n}_{j=1}\omega^{(i)}(k)}$$

From these equations it can be known, how the prior distribution differs from the real one. It would be fine if samples match better with the real distribution. For example regular particle filters such as bootstrap and SIR filters use prior distribution for the particle in the prediction stage. If prior distribution is far from the real one it is very likely that many particles end up to the low likelihood area and will not be in the resampling stage. The main techniques of increasing particles in the resampling stage are increasing the number of the particle sample size, prior editing and auxiliary variable. Easiest way to get more particles to the resampling stage is by simply increasing proposal sample size technique. If we have more proposals it is likely that more of them will get in to high likelihood area .In prior editing, the proposals are computed one by one. If the likelihood of the observation for the proposal is high enough than the threshold value, we accept the proposal. Otherwise it is rejected. This is continued until we have N accepted proposals, which allows us to get more proposals from the particles in high likelihood area and none from the particles in low likelihood area to get more particles to the resampling stage which makes the future estimates more accurate. We compare the estimation and prediction

performance of the SIR filters with that of resampling schemes based on the following metrics. MSE is defined by

MSE = $\frac{1}{N}\sum_{n=1}^{N} Xn - \widetilde{Xn}$

The analysis in this paper is related to the Sample Importance Resampling (SIR) type of PFs. However, the analysis is compared to various resampling schemes. First, in Section 2 we provide a brief review of the resampling operation. Then in section 3 we focus on the performance and analysis of several techniques that have been proposed to implement the resampling step and the summary of our work is outlined in section 4.

II. REVIEW OF RESAMPLING SCHEMES.

Besides prediction stage, particle filter also needs resampling stage . In this stage the particles with high weights are multiplied and the ones with low weight disappear. Even though the resampling decreases the number of the particles at current time instant, it also makes the future estimates more accurate. That is because after resampling ,there are more particles to describe high likelihood area. Resampling can be performed with numerous different algorithms like Multinomial resampling, Systematic resampling, Residual resampling, Stratified sampling or Deterministic sampling. Algorithms differ in terms of computational complexity, variance of the of the number of particles and bias. The above mentioned sampling techniques used for simulations in this paper since they are the best unbiased resampling algorithms . These resampling algorithms determine how many copies of each weighted particles made to represent unweighted particles at the next point in time.

2.1 SIR Particle Filter

The Sampling-Importance Resampling (SIR) is motivated from the bootstrap techniques. Bootstrap technique is a collection of computationally intensive methods that are based on resampling from the observed data [1], [2], [3]. The intuition of bootstrapping is to evaluate the properties of an estimator through the empirical cumulative distribution function (cdf) of the samples instead of the true cdf.. The resampling step is aimed to eliminate the samples with small weights and duplicate the samples with importance weights. The steps of SIR proceeds as follows:

Draw Np random samples $\{x^{(i)}\}_{i=1}^{Np}$ from proposal distribution q(x);

Calculate importance weights ω (i) $\propto$ p(x)/q(x) for each sample x(i);

Normalize the importance weights to obtain $\widetilde{w}$(i);

Resample with replacement N times from the discrete set $\{x^{(i)}\}_{i=1}^{Np}$ where the probability of resampling from each x(i) is proportional to $\widetilde{w}$(i). Resampling usually (but not necessarily) occurs between two importance sampling steps. In resampling step, the particles and associated importance weights {x(i), $\widetilde{w}$(i)} are replaced by the new samples with equal importance weights (i.e.) = $\widetilde{w}$(i)=1/Np). Resampling can be taken at every step or only taken if regarded necessary.

• As justified in [4], resampling step plays a critical role in importance sampling since

(i) if importance weights are unevenly distributed, propagating the "trivial" weights through the dynamic system is a waste of computing power;

(ii) when the importance weights are distorted, resampling can provide chances for selecting "important" samples and restore the sampler for the future use, though resampling doesn't necessarily improve the current state estimate because it also introduces extra Monte Carlo variation.

• Resampling schedule can be deterministic or dynamic [5], [6]. In deterministic framework, resampling is taken at every k^{th} time step (usually k = 1). In a dynamic schedule, a sequence of thresholds (that can be constant or time-varying) are set up and the variance of the importance weights are monitored; resampling is taken only when the variance is above the threshold.

2.2 Multinomial resampling

[7]: The procedure reads as follows

- Produce a uniform distribution u ~ U(0, 1), construct a cdf for importance weights calculate s= $\sum_{j=1}^{i} \widetilde{w}$(i)
- Find s_i such that $s_{i-1} \le u < s_i$, the particle with index *i* is chosen; Given {x(i), $\widetilde{w}$(i) }, for j = 1, ,Np, generate new samples x(j) by duplicating x(i) according to the associated $\widetilde{w}$(i);
- Reset ω (i) = 1/Np.

Multinomial resampling uniformly generates Np new independent particles from the old particle set. Each particle is replicated Ni times (Ni can be zero), namely each x(i) produces Ni particles.

Note that here $\sum_{i=1}^{Np} Ni = Np$

E[Ni] = Np $\tilde{w}$(i), Var[Ni] = Np $\tilde{w}$(i) (1 − $\tilde{w}$(i)).

2.3. Residual resampling

[8]: Liu and Chen [5] suggested a partially deterministic resampling method calculates the number of times each particle is replicated except that it avoids when residual particles need to be resampled. The number of replications of a specific particle is determined by truncating the product of the number of particles and the particle weight The selection procedure is as follows [5]:

- For each i = 1, • • • ,Np, retain k_i = [Np ω (i)] copies of $x^{(i)}$ n ;
- Let Nr = Np − k1 − … − kNp , obtain Nr from {$x^{(i)}$n} with probabilities proportional to Np $\tilde{w}$(i)− k*i* (*i* = 1,… ,Np);
- Reset ω (i) = 1/Np.

Residual resampling procedure is computationally cheaper than the conventional SIR and achieves a lower sample variance, and it doesnot introduce additional bias. Every particle in residual resampling is replicated.

2.4. Systematic resampling (or Minimum variance sampling)

This resampling**[9]** takes the previous method one step further by deterministically linking all the variables drawn in the sub-intervals. The procedure proceeds as follows:

- u ~ U(0, 1)/Np; j = 1;m = 0;i = 0;
- do while u < 1
- if m > u then • u = u + 1/Np; output x(i)
- else, pick k in {j,… ,Np}
- i = x(k), m = m + ω (i)
- switch (x(k), ω (k)) with (x(j), ω (j))
- j = j + 1, end if, end do

The systematic resampling treats the weights as continuous random variables in the interval (0, 1), which are randomly ordered. The number of grid points {u+k/Np} in each interval is counted . Every particle is replicated and the new particle set is chosen to minimize Var[Ni] = E[(Ni −E[Ni])^2].

2.5 Stratified Sampling

[10];The idea of stratified sampling is to distribute the samples evenly (or unevenly according to their respective variance) to the sub regions dividing the whole space. Let g (statistics of interest) denote the Monte Carlo sample average of a generic function g(x) ∈ RNx , which is attained from importance sampling. Suppose the state space is decomposed into two equal, disjoint strata (subvolumes), denoted as a and b, for stratified sampling, the total number of Np samples are drawn from two strata separately and we have the stratified mean

g = 1/ 2 (g_a + g_b), and the stratified variance

$$Var[g] = \frac{Var_a[g] + Var_b[g]}{4}$$

$$= \frac{Var_a[g] + Var_b[g]}{2NP}$$

where the second equality uses the facts that Vara[g] =2/Np Vara[g] and

[Vara[g] = 2/Np Varb[g]. In addition, it can be proved that NpVar[g] = Var[g]

$$= N_P Var[\dot{g}] + \frac{(Ea[g] + Eb[g])^2}{4}$$

$$\geq N_P Var[\dot{g}]$$

Hence, the variance of stratified sampling Var g` is never bigger than that of conventional Monte Carlo sampling Var[g], whenever Ea[g] ≠ Eb[g]. In general, provided the numbers of simulated samples from stratified a and b are Na and Nb ≡ Np−Na, respectively, becomes

$$Var[\dot{g}] = \frac{1}{4}\left(\frac{Var_a[g]}{Na} + \frac{Var_b[g]}{N_P}\right)$$

the variance is minimized when

Na/Np = σa / (σa + σb) and the achieved minimum variance is

$$Var[\dot{g}]min = \frac{(\sigma a + \sigma b)^2}{4Na}$$

Table –I shows different popular montecarlo methods.

Table-I

Author	Sampling method	Applied
Rubin	SIR	On/off line
-	Stratified sampling	On/off line
Gordon	Bootstrap	Online
-	QMC	On/offline
Bolic	RSR	On/offline

III. UNIVARIATE NON-STATIONARY GROWTH MODEL AND RESULTS

To illustrate some of the advantages of SIR Particle Filter with various resampling schemes mentioned in this paper.,Let us now consider an example[11], in which we estimate a model called Univariate Nonstationary Growth Model (UNGM), which is previously used as benchmark .what makes this model particularly interesting in this case is that its highly nonlinear and bimodal, so it is really challenging for traditional filtering techniques. The dynamic state space model for UNGM can be written as

$$x_n = \alpha x_{n-1} + \beta \frac{x_n}{1+x_{n-1}^2} - 1 + \cos(1.2(n)) + w_n$$

$$Y_n = x_n^2 / 20 + v_n, \qquad n = 1,\ldots\ldots,N$$

Table-II shows the comparison of root mean square error(RMSE) of SIR particle filter with that of The cosine term in the state transition equation simulates the effect of time-varying noise. From the above equation we choose α=0.5,β=25,γ=8.For N=100 particles ,the mean square error(MSE) curves of the estimated results of SIR particle filter is compared with different resampling schemes are shown in Figures and Table below.

Table-II

Resampling Schemes	ob	fob
SIR	2.839	2.132
Multinomial	-1.535	0.3845
Residual	-0.712	0.5523
Deterministic	0.802	0.594
Systematic	0.196	0.647

*ob- observation ,*fob-filtered observation

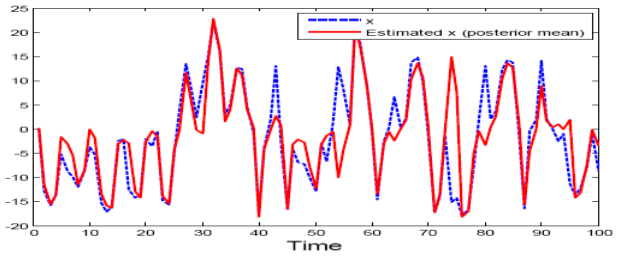

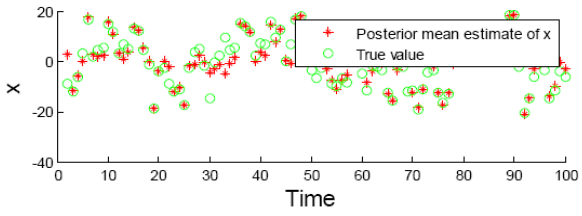

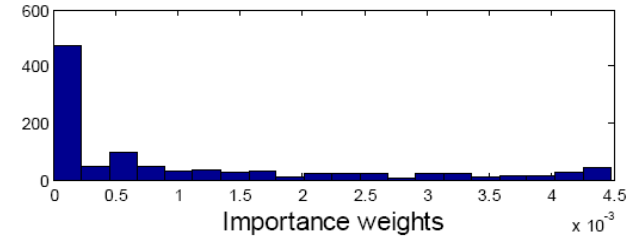

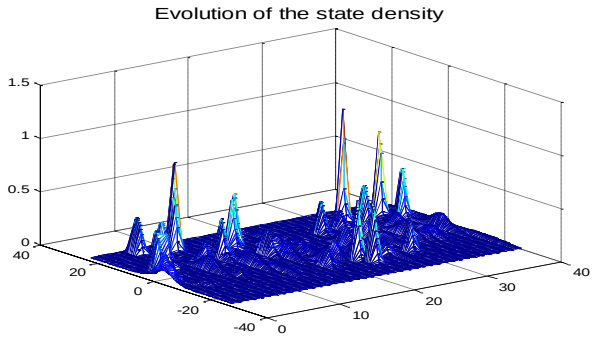

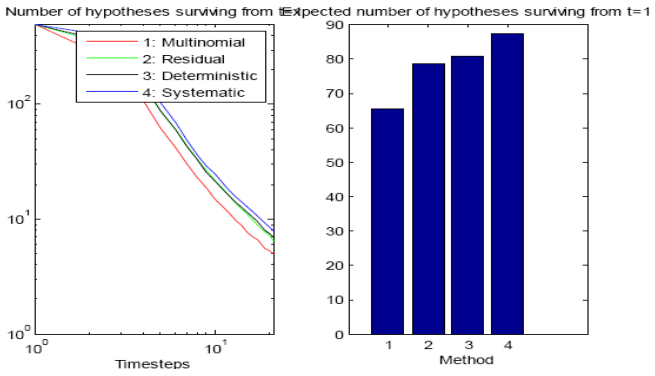

IV. CONCLUSION

The purpose of this work is to examine the application of particle filters in radar systems that use different resampling schemes. The performance of the algorithms were investigated in Matlab simulation . In practical applications of sequential Monte Carlo methods, residual, stratified, multinominal and systematic resampling are generally found to provide comparable results. Due to lack of complete theoretical analysis of its behavior, systematic resampling is often preferred because it is the easiest method to implement. From a theoretical point of view however only the residual and stratified resampling methods (as well as the combination of both) may be shown to dominate the basic multinomial resampling approach, in the sense of having lower covariance for all configurations of the weights.

REFERENCES

[1] G. A. Einicke and L. B. White, "Robust extended Kalman filter," IEEE Trans. Signal Processing, vol. 47, no. 9, pp. 2596– 2599, Sept. 1999.
[2] W. R. Gilks and C. Berzuini, "Following a moving target – Monte Carlo inference for dynamic Bayesian models," J. Roy. Statist. Soc., Ser. B, vol. 63, pp. 127–1546, 2001.
[3] B. Manly, Randomization, Bootstrap and Monte Carlo Methods in Biology, 2nd ed., CRC Press, 1997
[4] J. S. Liu and R. Chen, "Blind deconvolution via sequential imputation," J. Amer. Statist. Assoc., vol. 90, pp. 567–576, 1995.
[5] "Sequential Monte Carlo methods for dynamical systems," J. Amer. Statist. Assoc., vol. 93, pp. 1032–1044, 1998.
[6] J. S. Liu, R. Chen, and T. Logvinenko, "A theoretical framework for sequential importance sampling with resampling," in Sequential Monte Carlo Methods in Practice, A. Doucet, J. F. G.
[7] de Freitas, N. J. Gordon, Eds. Berlin: Springer Verlag, 2001.
[8] Multiple Imputation for Nonresponse in Surveys, New York: Wiley, 1987.

[9] T. Higuchi, "Monte Carlo filter using the genetic algorithm operators," J. Statist. Comput. Simul., vol. 59, no. 1, pp. 1–23, 1997.
[10] "Monte Carlo filter and smoother for non-gaussian nonlinear state space models," J. Comput. Graph. Statist., vol. 5, no. 1, pp. 1–25, 1996.
[11] W. H. Press and G. R. Farrar, "Recursive stratified sampling for multidimensional Monte Carlo integration," Computers in Physics, vol. 4, pp. 190–195, 1990
[12] M. S. Arulampalam, S. Maskell, N. Gordon, and T. Clapp, "A tutorial on particle filters for online nonlinear/non-Gaussian Bayesian tracking," IEEE Transactions on Signal Processing, vol. 50, no. 2, pp. 174–188, 2002

J.Joseph Ignatious received his BE degree in Electronics and communication Engineering in April. 2005, in Nov. 2002 he received the ME degree in Process control and Instrumentation from Annamalai University, Chidambaram. He has since Feb. 2011 been pursuing the PhD degree at the division of Instrumentation Engineering Annamalai University .

S. Abraham Lincon obtained his B.E degree is Electronics and Instrumentation Engineering in the year 1984 and received M.E. degree in Power System Engineering in 1987 and another M.E degree in Process Control and Instrumentation Engineering in 2000 from the Annamalai university, Chidambaram. Presently he is working as a professor of the Department of Instrumentation Engineering in Annamalai University. His areas of research are Process Control, Fault Detection and Diagnosis and Multivariable Control.

American Journal of Engineering Research (AJER)
e-ISSN : 2320-0847 p-ISSN : 2320-0936
Volume-02, Issue-09, pp-234-243
www.ajer.org

Research Paper Open Access

Analysis Of Convective Plane Stagnation Point Chemically Reactive Mhd Flow Past A Vertical Porous Plate With A Convective Boundary Condition In The Presence Of A Uniform Magnetic Field.

Adeniyan, A., Adigun, J. A
[1]*Department of Mathematics, University of Lagos, Lagos.*
[2]*Department of Physical Sciences, Bells University of Technology, Ota.*

Abstract: - The numerical investigation of a stagnation point boundary layer flow , mass and heat transfer of a steady two dimensional , incompressible , viscous electrically conducting, chemically reacting laminar fluid over a vertical convectively heated , electrically neutral flat plate exposed to a transverse uniform magnetic field has been carried out to examine the influence of the simultaneous presence of the effects of a convective boundary condition, chemical reaction, heat transfer and suction or injection. The governing coupled partial differential equations have been reduced to a set of coupled nonlinear ordinary differential equations by means of the similarity transformation , which has been solved using the classical fourth order Runge-Kutta method alongside with a shooting technique. The computational results have been presented by means of the table and discussed graphically. It has been observed that pertinent and invaluable engineering parameters such as the Skin-friction coefficient, the plate temperature distribution, the velocity , temperature and concentration profiles are appreciably influenced by flow parameters such as the magnetic field, convective heat parameters , Prandtl number, Sherwood number, Nusselt number, etc .

Keywords: - *convective boundary condition, work due to pressure, hydromagnetics, chemical reaction, porous plate, suction/ injection*

I. INTRODUCTION

Study of flow, heat and mass transfer of a boundary layer flow in the presence of oblique or transverse magnetic field has aroused the interest of many a researcher over the years and more recently consequent upon its immediate applications in extrusion of plastic and paper sheets, polymer spinning of fibres, cooling of nuclear reactors, cooling of moderately large sheets in electrically conducting liquids and molten metals, forest fire alarms, geophysical and petrochemical industries, vapour deposition on surfaces. The quality control in industrial and engineering processes is very essential for standard final products wherein the chemical deposition on surfaces is significant.

Crane [1] appeared to be the first among his pioneering contemporaries whose research incorporated the study of steady two-dimensional flow of a Newtonian fluid driven by a linearly stretching elastic flat plate. Ishak et al [2] studied the stretching sheet due to the presence of magnetic field with emphasis on buoyancy and power law effects. Nield and Bejan [3], Ingham and Pop [4] and a few others have also researched into the subject matter. Recently, a significant number of electrically conduction fluids such as liquid metals, water mixed with a little acid and others in the presence of a magnetic field on the flow and heat transfer of a viscous and incompressible fluid past a moving surface or a starching sheet in a quiescent fluid show considerable response to the influence of heat transfer rate, work done by pressure at the surface and the magnetic field. In order to accurately predict the flow, mass and heat transfer rate it is necessary to take into account not only the effect of viscosity and magnetic field but also that due to the work due to pressure at bthe surface. Chamkha [5] and Abo-Eldahab [6] considered the problem related to hydromagnetic three-dimensional flow on a stretching surface while Ishak et al [7] studied the effects of a uniform transverse magnetic field on the stagnation point

flow towards a stretching sheet. Very recently, Anjali Devi and Thiyagarajan [8] investigated the effects of a transverse magnetic field on the flow and heat transfer characteristics over a stretching surface by assuming that the magnetic strength is non-linear, and he obtained similarity solution. Ibrahim and Makinde [9] examined chemically reacting MHD boundary layer flow of heat and mass transfer past a low-heat-resistant sheet moving vertically downwards in a viscous electrically conducting fluid permeated by a uniform transverse magnetic field. Adeniyan and Adigun [10] examined the effects of a chemical reaction on stagnation point MHD flow over a vertical plate with convective boundary conditions but neglected the energy due to pressure force which provides the motivation for this work. Problems of this type have invaluable applications in geothermal energy extraction and underground storage system. The effects of various thermo-magneto physical parameters on the velocity, temperature and concentration profiles are considered and discussed through tables and graphs.

II. PROBLEM FORMULATION

We consider a vertical porous plate wholly immersed in a two-dimensional stagnation point flow of a chemically reacting and electrically conducting incompressible viscous laminar MHD stream. The magnetic field of magnitude B_0 is strategically positioned in a direction which is transverse to the porous plate. We took an assumption that the magnetic Reynolds number is very small so that the Hall current effects and the induced magnetic field are negligible. T_w *and* C_w represent the wall temperature and species concentration respectively while T_∞ *and* C_∞ stand for the ambient temperature and species concentration. The flow,. Heat and mass transfer equations relevant for the model are:

$$\frac{\partial u}{\partial x}+\frac{\partial v}{\partial y}=0 \tag{1}$$

$$u\frac{\partial u}{\partial x}+v\frac{\partial v}{\partial y}=-\frac{1}{\rho}\frac{\partial p}{\partial x}+\gamma\frac{\partial^2 v}{\partial y^2}-\frac{\sigma}{\rho}\beta_0^2 u \tag{2}$$

$$\frac{\partial T}{\partial x}+v\frac{\partial T}{\partial y}=\alpha\frac{\partial^2 T}{\partial y^2}+\frac{1}{C_P}u_e\frac{du_e}{dx}(u_e-u) \tag{3}$$

$$u\frac{\partial C}{\partial x}+v\frac{\partial C}{\partial y}=D_m\frac{\partial^2 C}{\partial y^2}-kr(C-C_\infty) \tag{4}$$

Outside the boundary layer, use is made of the inviscid flow assumptions to eliminate the first term on the right of eqn. (2) to obtain a new form posited as

$$u\frac{\partial u}{\partial x}+v\frac{\partial u}{\partial y}=u_e\frac{du_e}{dx}+\gamma\frac{\partial^2 u}{\partial y^2}-\frac{\sigma}{\rho}\beta_0{}^2(u-u_e) \tag{5}$$

Boundary Conditions

$$u(x,0)=ax, v(x,0)=\pm V_0, u(x,\infty)=u_\infty=ax \tag{6a}$$

$$\left.\begin{aligned} -k\frac{\partial T}{\partial y}(x,0)&=h_f(T_f-T(x,0)), \quad T(x,\infty)=0\\ C(x,0)&=C_w, \qquad\qquad C(x,\infty)=0\end{aligned}\right\} \tag{6b}$$

Where $T_w=T(x,0)$.

In eqns. $(1)-(6b)$ above, the velocity field **q**= ($u(x,y), v(x,y)$) where u *and* v are the components of the velocity along and normal to the plate respectively. $T(x,y)$ is the temperature field, ɣ is the kinematic viscosity,

$\alpha = \frac{k}{\rho C_P}$ is the thermal diffusivity, p is the fluid pressure, ρ is the fluid density, k is the thermal conductivity, σ is the electrical conductivity of the fluid , Kr is the reaction rate constant of the first order homogeneous and irreversible reaction, $\boldsymbol{B} = (0, B_0)$, is the imposed magnetic field, D_m is the mass diffusivity, C_P is the specific heat at constant pressure and the left hand side of the vertical plate surface say, is heated by convection from hot fluid at temperature $T_f > T_w > T_\infty$, which provides a heat transfer coefficient h_f while the right hand of the plate is filled with electrically conducting fluid for y ≥ 0. In terms of the steam function $\psi(x, y)$, the velocity components

$$u = \frac{\partial \psi}{\partial y}, \quad v = -\frac{\partial \psi}{\partial x} \tag{7}$$

automatically satisfy eqn. (1) upon the use of the set of transformation and dimensionless quantities given by eqn. (8) below.

$$\left.\begin{aligned} \eta &= y\sqrt{\frac{a}{\gamma}}, \quad \psi(x,y) = x\sqrt{a\gamma}\, f(\eta), \\ Pr &= \frac{\gamma}{\alpha}, \qquad Bi = \frac{h_f}{k}\sqrt{\frac{\gamma}{\alpha}} \\ \phi(\eta) &= \frac{C - C_\infty}{C_w - C_\infty}, \qquad \theta(\eta) = \frac{T - T_\infty}{T_f - T_\infty}, \\ M = \frac{\sigma B_0^{\,2}}{\rho a}, \; K &= \frac{K_r}{a}, \qquad Sc = \frac{\gamma}{D_m}, \; Ec = \frac{x^2 a^2}{C_p (T_w - T_\infty)} \end{aligned}\right\} \tag{8}$$

By means of eqn. (8), Using the similarity transformation in (8), equations (2), (3) and (4) are reduced to:

$$f''' + ff'' - (f')^2 + 1 - M(f' - 1) = 0 \tag{9}$$

$$\theta'' + PrEc(1 - f') + Prf\theta' = 0 \tag{10}$$

$$\phi'(\eta) + Scf(\eta)\phi'(\eta) - ScK\phi(\eta) = 0 \tag{11}$$

subject to the transformed boundary conditions:

$$f'(0) = 0, f(0) = F_w, \; -\theta'(0) = B_i(1 - \theta(0)), \; \phi(0) = 1 \tag{12a}$$

$$f'(\infty) = 1, \theta(\infty) = 0, \phi(\infty) = 0. \tag{12b}$$

Where the prime denotes differentiation with respect to η, Pr is the Prandtl number, Sc is the Schmidt number, M is the magnetic parameter , Ec is the Eckert number and the dimensionless reaction rate constant $K = \frac{K_r}{a}$.

The dimensionless suction parameter $F_w = -V_o\sqrt{a\gamma}$ and V_o is the suction velocity .

The physical quantities of relevance are Skin-friction C_f , the Nusselt number Nu and the Sherwood number Sh, which are respectively proportional to $f''(0), -\theta'(0)$ and $-\phi'(0)$.

The system of equations (9) – (12b) is a coupled system of non-linear boundary value ordinary differential equations and it is difficult to solve by known available analytical methods. Nevertheless the equations are solved using a reliable classical fourth order Runge-Kutta integration method with a shooting technique implemented on a computer written in Maple(15), Heck[11].

RESULTS AND DISCUSSION

Our results illustrate the influence of Prandtl number (Pr), Schmidt number (Sc), Biot number(Bi), Magnetic parameter(M), Reaction rate parameter(K), Eckert number(Ec) and Suction (Fw) which are in agreement with earlier communications [7, 9, 10] on the Skin friction coefficient as well as the heat and mass transfers at the plate surface.

Table 1 shows the numerical results for various parameter variations

Pr	Sc	Bi	M	K	Ec	F_w	$f''(0)$	$-\theta'(0)$	$-\phi'(0)$
0.72	0.24	0.1	0.1	0.2	0.5	0.1	1.330132	0.058220	0.399302
2.71	0.24	0.1	0.1	0.2	0.5	0.1	1.330132	0.039792	0.399302
5.00	0.24	0.1	0.1	0.2	0.5	0.1	1.330132	0.026291	0.399302
7.10	0.24	0.1	0.1	0.2	0.5	0.1	1.330132	0.017352	0.399302
0.72	0.62	0.1	0. 1	0.2	0.5	0.1	1.330132	0.058220	0.610665
0.72	0.64	0.1	0.1	0.2	0.5	0.1	1.330132	0.058220	0.619710
0.72	0.78	0.1	0.1	0.2	0.5	0.1	1.330132	0.058220	0.679378
0.72	0.24	0.5	0.1	0.2	0.5	0.1	1.330132	0.180330	0.399302
0.72	0.24	1.0	0. 1	0.2	0.5	0.1	1.330132	0.244408	0.399302
0.72	0.24	10.0	0.1	0.2	0.5	0.1	1.330132	0.359320	0.399302
0.72	0.24	0.1	0.5	0.2	0.5	0.1	1.476360	0.060357	0.402593
0.72	0.24	0.1	1.0	0.2	0.5	0.1	1.640784	0.062441	0.405929
0.72	0.24	0.1	2.0	0.2	0.5	0.1	1.927601	0.065442	0.410972
0.72	0.24	0.1	0.1	0.4	0.5	0.1	1.330132	0.058220	0.448650
0.72	0.24	0.1	0.1	0.5	0.5	0.1	1.330132	0.058220	0.471947
0.72	0.24	0.1	0.1	1.0	0.5	0.1	1.330132	0.058220	0.577494
0.72	0.24	0.1	0.1	0.2	1.0	0.1	1.330132	0.031796	0.399302
0.72	0.24	0.1	0.1	0.2	5.0	0.1	1.330132	0.179595	0.399302
0.72	0.24	0.1	0.1	0.2	10.0	0.1	1.330132	0.443834	0.399302
0.72	0.24	0.1	0.1	0.2	0.5	0.5	1.578868	0.051241	0.463431
0.72	0.24	0.1	0.1	0.2	0.5	1.0	1.923517	0.078772	0.549008
0.72	0.24	0.1	0.1	0.2	0.5	2.0	2.698494	0.087938	0.734407
0.72	0.24	0.1	0.1	0.2	0.5	-0.5	1.010300	0.027260	0.311802
0.72	0.24	0.1	0.1	0.2	0.5	-1.0	0.797568	0.019326	0.248298
0.72	0.24	0.1	0.1	0.2	0.5	-2.0	0.511852	0.135360	0.151000

We observed that the magnitude of Nusselt number which represents the heat transfer is decreased with an increase in the Prandtl number. An increase in the Sherwood number which stands for the mass transfer rate is noticed when the Schmidt number is increased. Furthermore, an increased variation in the Biot number produces a corresponding increase in the Nusselt number.

It is also of note that the Skin friction coefficient, which shows the level of viscous drag in the boundary layer, the Nusselt and Sherwood numbers are all increased with an increase in the Magnetic parameter. An increase in the reaction rate parameter produces a corresponding increase in the Sherwood number.

When the Eckert number is increased, a increase in the Nusselt number is observed. The table also shows that the skin friction together with the heat and mass transfer rate at the porous plate surface increase with increasing magnitude of fluid Suction(F_w) at the plate surface.

Effects of parameter variation on velocity profiles

The effects of various parameters on velocity profiles in the boundary layer region are depicted in Figures 1 to 2. It is observed that the velocity starts minimum value of zero at the plate surface and increases exponentially to a free stream value of unity located far from the plate surface, satisfying the far field boundary conditions for all parameter values. In **Figure 1** , the magnetic parameter(M) enhanced the fluid velocity thereby increasing the velocity boundary layer thickness.

Moreover, it is interesting to note that in **Figure 2.** , the effect of increasing the magnitude of fluid suction (F_w) at the plate surface increases the fluid velocity and also further thickens the velocity boundary layer thickness. Reverse is the case for the response due to increase in injection or fluid blowing (-F_w) as seen in t**able 1**.

Effects of parameter variation on temperature profile

It is observed in **Figure 3**, that the thermal boundary layer thickness decreases with an increase in the Prandtl number. The opposite is observed in the fluid temperature as it is seen that the temperature increases with increasing Prandtl number. Nevertheless **Figures 4** and **5** revealed that there is an increase in the thermal boundary layer and rise in fluid temperature as the values of Biot and Eckert number are increased respectively. Lastly, in **Figure 6**, we obtained a slightly similar result to that of **Figure 3**, in terms of decreased thermal boundary layer but there is a decrease in the fluid temperature as the magnitude of the suction is increased.

Effects of parameter variation on concentration profile

Generally, the species concentration in the fluid has a maximum value at the plate surface and decreases exponentially to the free stream zero value far from the plate. In the case of concentration boundary layer, we have observe a decrease with an increase in Schmidt number, rate constant and increasing magnitude of suction (see **figures 7** to **9**).

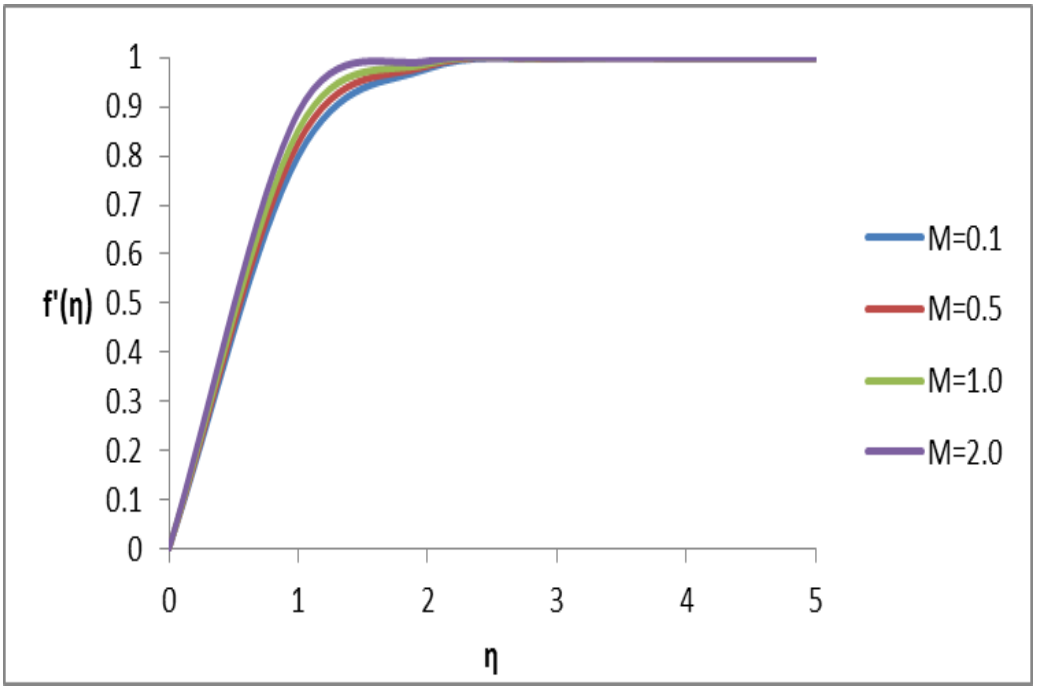

Figure 1: Effect of Magnetic parameter on the velocity profile for Pr=0.72, Sc = 0.24, Bi=0.1, K = 0.2, Ec=0.5 and $F_w = 0.1$.

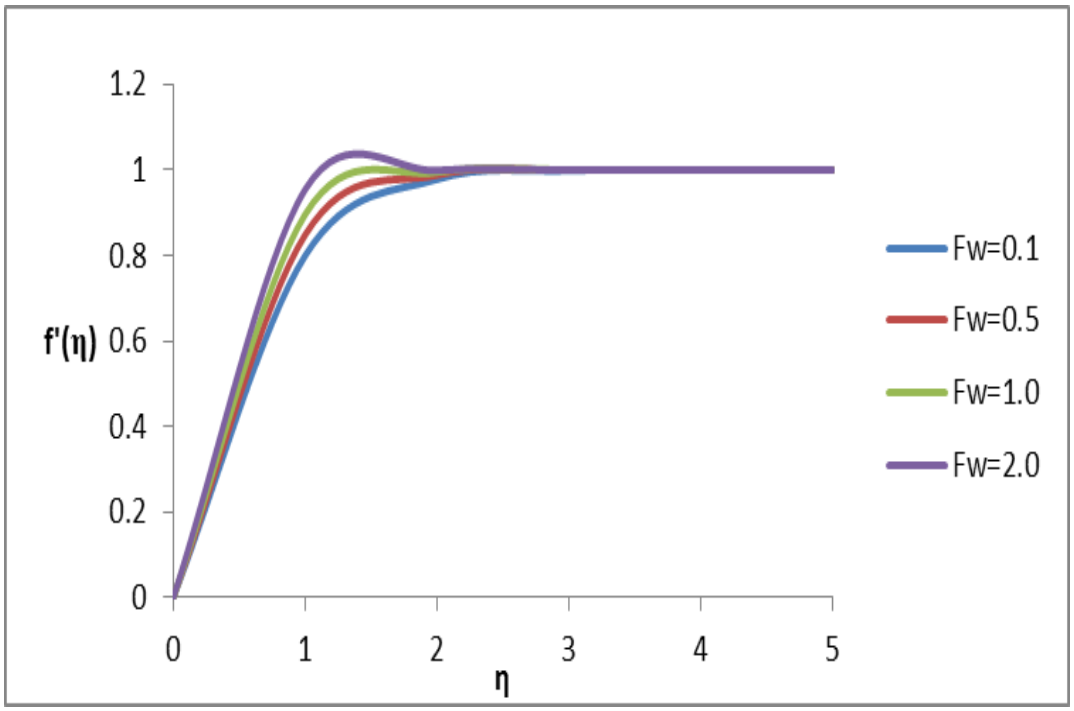

Figure 2: Effect of Suction on the velocity profile for Pr=0.72, Sc = 0.24, Bi=0.1, M = 0.1, K = 0.2 and Ec=0.5.

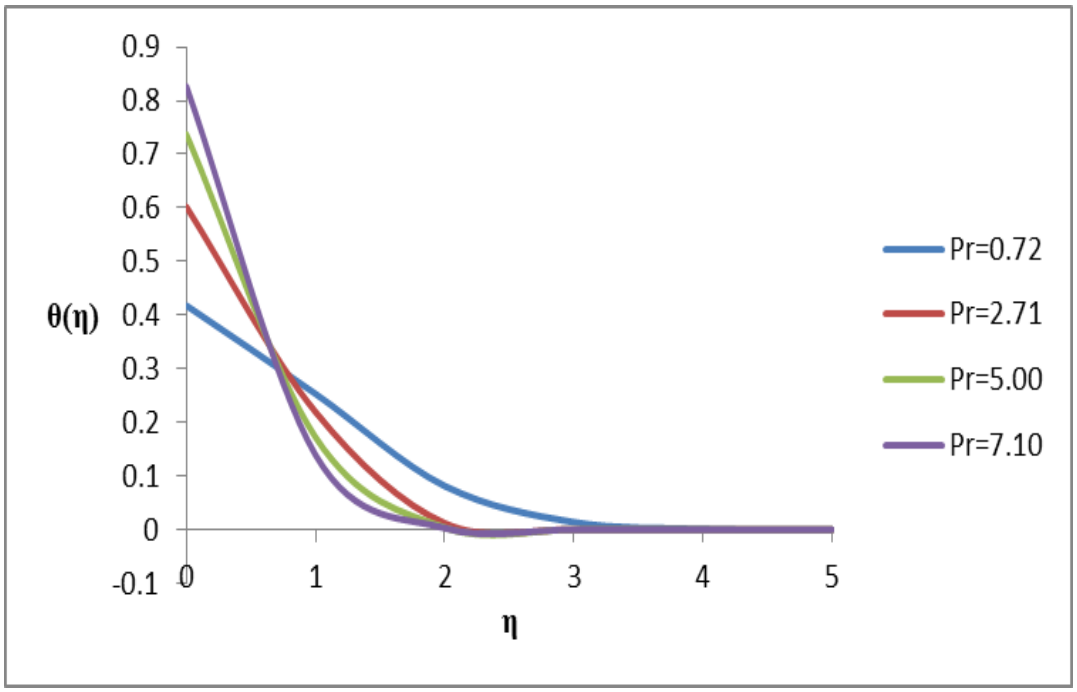

Figure 3: Effect of Prandtl number on the temperature profile for Sc = 0.24, Bi=0.1, M = 0.1, K = 0.2, Ec=0.5 and $F_w = 0.1$.

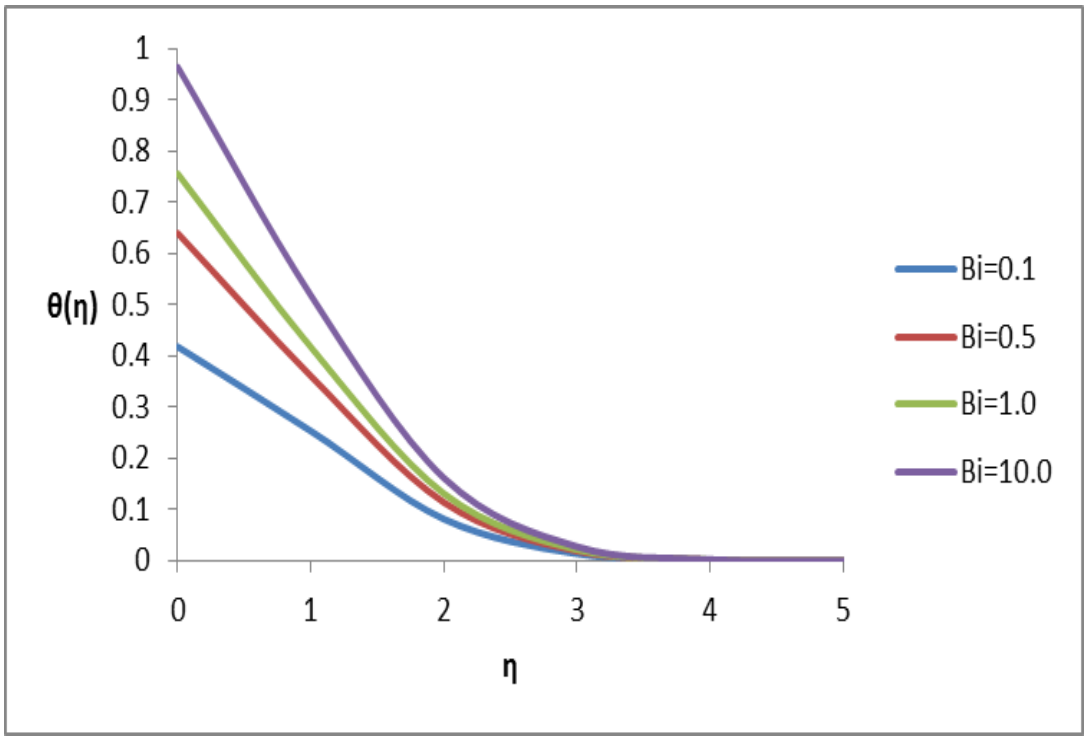

Figure 4: Effect of Biot number on the temperature profile for Pr=0.72, Sc=0.24, M = 0.1, K = 0.2, Ec=0.5 and $F_w = 0.1$.

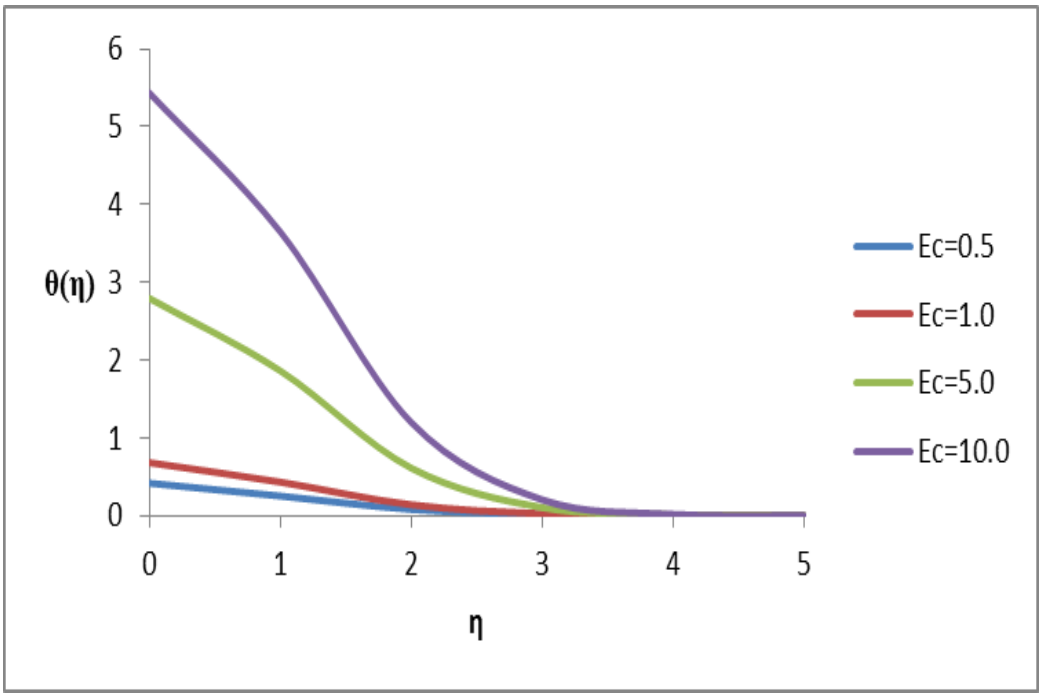

Figure 5: Effect of Eckert on the temperature profile for Pr=0.72, Sc = 0.24, Bi=0.1, M = 0.1, K = 0.2, Ec=0.5 and $F_w = 0.1$.

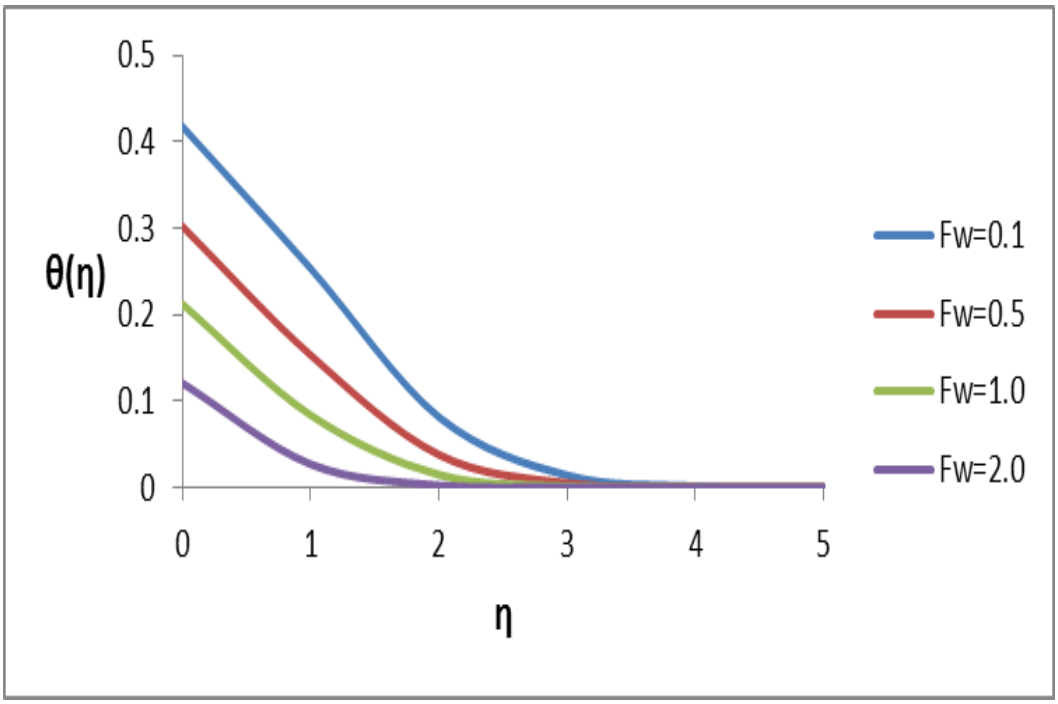

Figure 6: Effect of Injection on the Temperature profile for Pr=0.72, Sc = 0.24, Bi=0.1, M = 0.1, K = 0.2, and Ec=0.5.

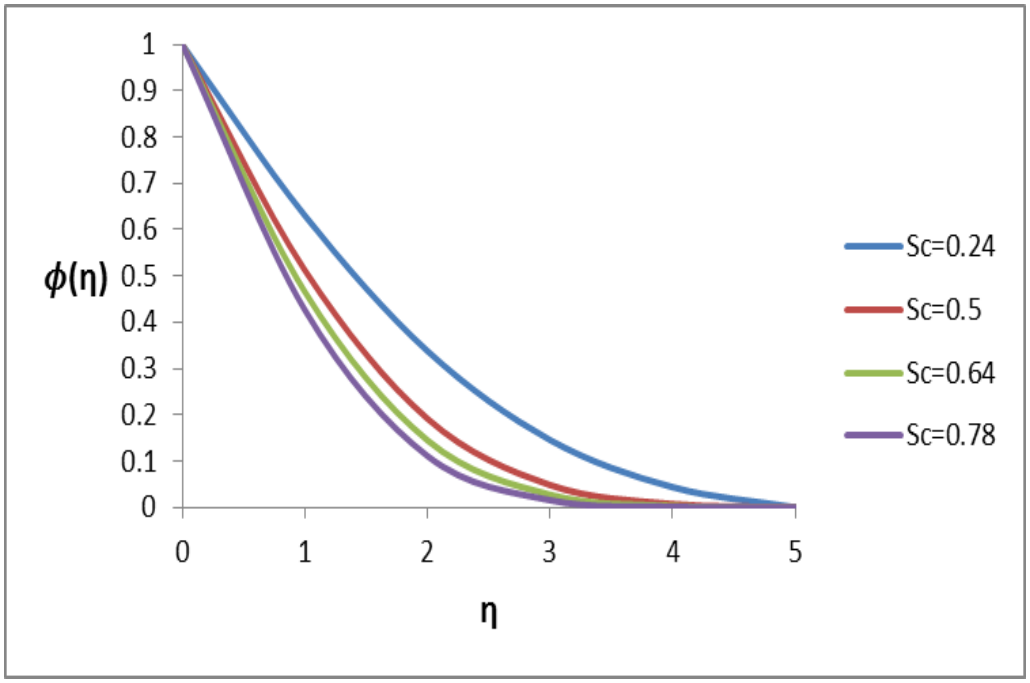

Figure 7: Effect of Schmidt number on the concentration profile for Pr=0.72, Bi=0.1, M = 0.1, K = 0.2, Ec=0.5 and $F_w = 0.1$

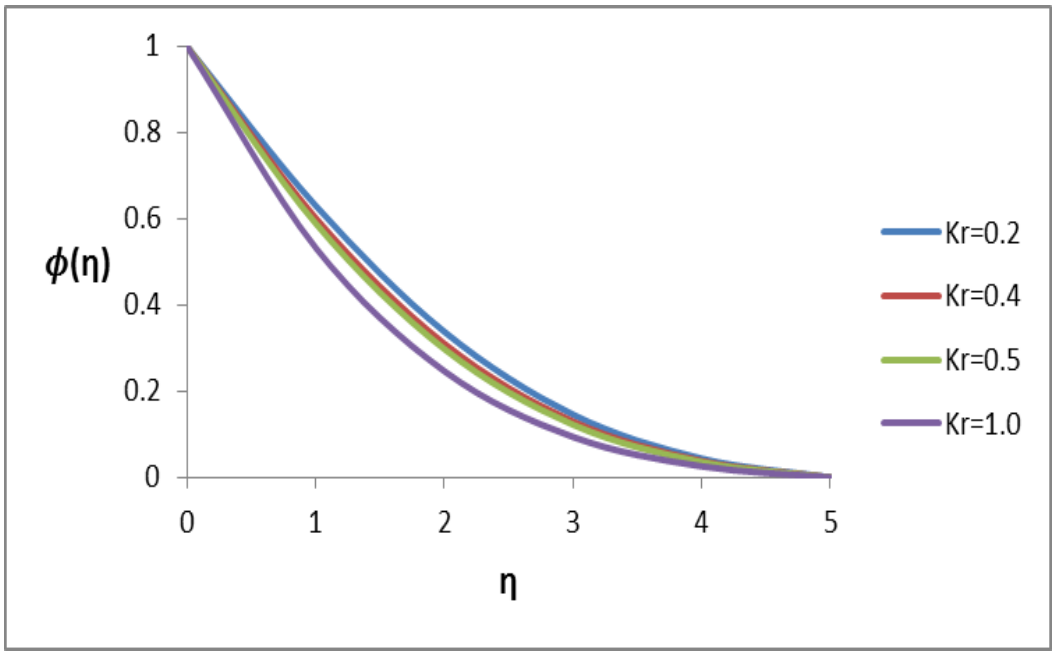

Figure 8: Effect of Reaction rate on the concentration profile for Pr=0.72, Sc = 0.24, Bi=0.1, M = 0.1, Ec=0.5 and $F_w = 0.1$.

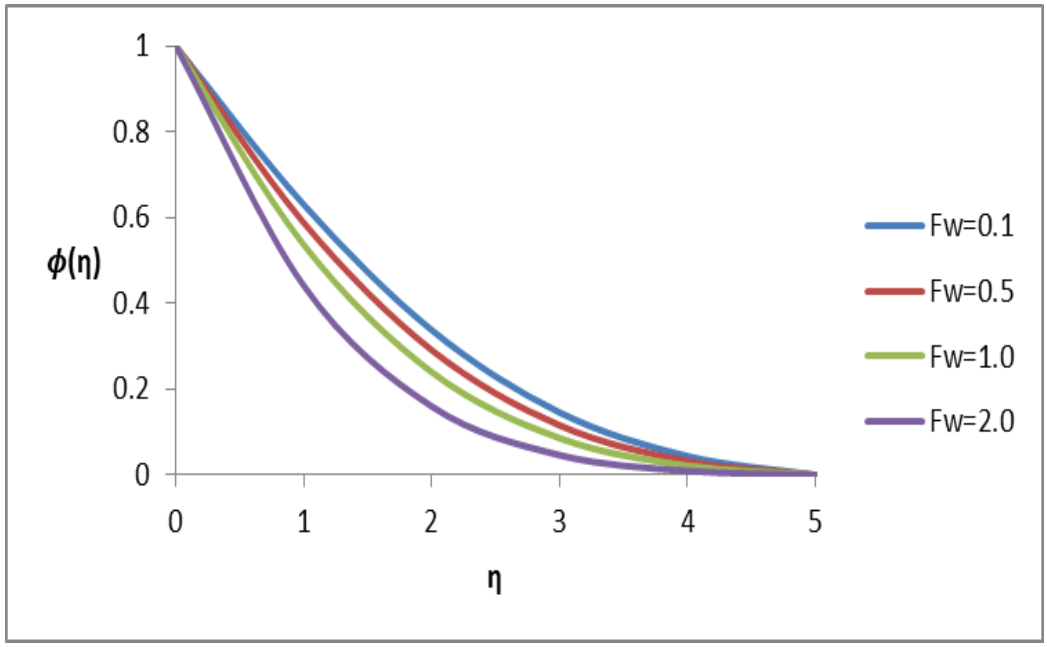

Figure 9: Effect of Injection on the concentration profile for Pr=0.72, Sc = 0.24, Bi=0.1, M = 0.1, K = 0.2, and Ec=0.5.

CONCLUSION

This paper studies the effects of chemical reaction and magnetic field on the convective stagnation point MHD flow over a plate which is vertically placed and with convective boundary conditions. The non-linear and coupled governing differential equations have been solved numerically using the fourth order Runge-Kutta shooting technique. Numerical results have been presented whilst the velocity, temperature and concentration profiles illustrated graphically and interpreted for the physical meanings. Our results show that the convective boundary conditions, the stagnation point, chemical reaction and the magnetic field have significant effects on the heat and mass transfer rate, velocity boundary layer thickness and the thermal boundary layer thickness respectively.

REFERENCES

[1] Crane, L..J. (1970). Flow past a Stretching Plate. J. Applied Math. Phys. (ZAMP), 21:645-647.

[2] Ishak, A., Nazar R., Pop I.(2008) Hydromagnetic Flow And Heat Transfer Adjacent To A Stretching Vertical Sheet, Heat and Mass Transfer, 44:921-927.

[3] Nield, D.A, Bejan, A.(1999). Convection in porous media. 2nd Ed. Springer, N.Y.

[4] Ingham, D.B, Pop, I. (1998). Transport phenomena in porous media. I, Pergamon, Oxford.

[5] Chamkha, A.J (1999). Hydromagnetic three-dimensional free convection on a vertical stretching surface with heat generation or absorption. Int J Heat Fluid Flow 20:84-92

[6] Abo-Eldahab, E.M (2005). Hydromagnetic three-dimensional flow over a stretching surface with heat and mass transfer. Heat Mass Transfer 41:734–743

[7] Ishak, A., Nazar, R., Pop, I. (2006) Magnetohydrodynamic stagnation-point flow towards a stretching vertical sheet. Magnetohydrodynamics 42:17–30

[8] Anjali Devi, S.P, Thiyagarajan, M. (2006) Steady non-linear hydromagnetic flow and heat transfer over a stretching surface of variable temperature. Heat Mass Transfer 42:671–677

[9] Ibrahim, S.Yand Makinde ,O.D. (2011).Chemically reacting Magnetohydrodynamics (MHD) boundary layer flow of heat and mass transfer past a low-heat-resistant sheet moving vertically downwards. Scientific Research and Essays, 6(22): 4762-4775.

[10] Adeniyan, A, Adigun J.A.(2012) Effects of chemical reaction on stagnation point MHD flow over a vertical plate with convective boundary condition in the presence of a uniform transverse magnetic field. The International J. of Engineering and Science(THE IJES), 2:310-313.

[11] Heck, A. (2003). Introduction to Maple , 3rd Edition, Springer-Verlag, New York Inc.

American Journal of Engineering Research (AJER)
e-ISSN : 2320-0847 p-ISSN : 2320-0936
Volume-02, Issue-09, pp-244-246
www.ajer.org

Research Paper Open Access

Assessing the Impact of Heavy Metal Exposure in Green Leafy Vegetables in Singrauli District of Madhya Pradesh, India

Dr. Vinod Kumar Dubey, Shalini Singh
**1.Main and Corresponding author, Professor, Applied Chemistry Division, Deptt. Of Chemistry, SGS Govt. P.G. Autonomous (NAAC Accredited) College, SIDHI-486661 (M.P.) India*
2. Assistant Professor, SIT College, Jamodi, SIDHI -486661 (M.P.) India

Abstract: - The green leafy vegetables such as Brassica (*Brassica campestris*) and Cabbage (*Brassica oleraca*) randomly collected from market and from agricultural fields in and around Singrauli city were analyzed for heavy metals Fe, Zn, Cd, Cr, Cu and Pb. Nearly 18 % samples of Palak from market had high level of Cd than the permissible limit of 1.5 mg/kg. 25 % sample of Brassica had high Pb and 27 % sample of Cabbage had high Zn than the permissible limit of 2.5 mg/kg. as per Indian standard of Food adulteration act. Heavy metals in the randomly collected samples were in the order of Fe > Zn> Pb>Cu>Cd where as in vegetables collected from agricultural fields around Singrouli City were in the order of Zn > Pb > Cu > Fe>Cd. The metal content in vegetable from agricultural areas indicate high level of soil contamination and accumulation of Pb and Cd in vegetable.

Keywords: - *Heavy Metals, Palak, Yellow Sarson and Cabbage*

I. INTRODUCTION

Metal contaminated soils are potentially harmful to plants, animal and humans. Toxic substances such as heavy metals have increased in Natural water and agriculture soils particularly in industrialized areas. Atmospheric deposition of heavy metals in soil and or in vegetables growing near industrial areas have been investigated[(1)] which indicate high concentration of heavy metals in leafy vegetables. Majority of soil contamination is through atmospheric deposition of heavy metals from sources such as metaliferous mining, smelting and other industrial activities. The heavy metals being immobile get accumulated in the soil endangering crops and vegetable[(2)].

Potential risk to population subgroups living on an consuming vegetables grown on large urban sites were assessed and was considered that young children are highly exposed[(3)]. The potential cancer risk from Cd and Ni are adzdressed as a result of occupational inhalation exposure[(4)].

Heavy metals may enter the body through inhalation of dust, direct ingestion of soil and consumption of food plant grown in metal contaminated soil[(5,6)]. Potentially toxic metals are also present in commercially produced foods stuffs[(7)]. Exposure to potentially toxic metals form dust inhalation or soil ingestion is usually modeled simply as the concentration of a contaminant measured in the soil multiplied by the quantity of dust inhaled or soil digested[(8)]. Municipal sludge is a valuable organic manure and soil conditioner and has been used as a fertilizer over decades but at the same time sludge may contain heavy metals and organic pollutants, which are harmful to crops and microorganism in soil therefore in current investigation metal analysis was carried out in randomly collected fresh samples of green leafy vegetable such as Brassica *(Brassica campestris)* and cabbage *(Barassica aleracea)* from vendors and agricultural filled.

II. MATERIALS AND METHODS

2.1 Collection and Preparation of Leafy Vegetable Sample :

A total of 45 vegetable samples were collected from places in and around Singrauli disttrct of M.P. during the period from February to April 2012 to assess the heavy metal contamination. The samples procured form market and agricultural filled included Brassica and Cabbage Vegetable samples were collected and then washed with running tap water to remove soil and dirt followed by distilled water. All samples were dried at 70^0

C for about 48-72 hours, then cooled to ambient temperature, crushed by means of a pestle and mortar and sieved. The sieved samples were stored in airtight sealed plastic bags until required for analysis.

2.2 Determination of heavy meals in Leafy Vegetables

One gram oven dried sieved sample was digested by wet digestion method with concentrated HNO_3 (15 ml.) and $HClO_4$ (5 ml.) in the ratio 3:1[(9)]. The samples were digested on a hot plate at a temperature corresponding to 100^0 C for 3-4 hours heating was done till it dried up completely and whitish brown dry mass was obtained.

It was then cooled and the precipitate/digest mixture was extracted in acid water mixture (Concentrated HCl : distilled water in the ratio 1:1) and filtered through whatman filter paper no. 42, valume was made up to 50 ml. The filtrate was analyzed for metal content using atomic absorption spectrophotometer. The instrument was calibrated using standard solution of Cr, Fe, Ni, Pb, Zn and Cd. The various metals along with their sensitivity limit (µg ml^{-1}) are as follows- Cr : 0.05, Fe : 0.05, Ni : 0.04, Pb : 0.06, Zn : 0.008 and Cd : 0.009.

III. RESULT

3.1 Metals in random samples of green leafy vegetables:

In randomly collected samples of Palak *(Beta vulgaris)*, Cabbage *(Brassica oleracea)* and yellow sarson *(Brassica campestris)* from 45 different vendors within the city of Waidhan and Morba heavy metals Fe, Zn, Pb, Cr and Cd analyzed showed great variation (Fig, 1). In Palak Zn varied from 25 to 68.88 mg/kg., Cd varied from 0.23 to 3.45 mg/kg., Fe varied from 6 to 12.8 mg/kg. Where as Cr and Ni were below detection limit in all the vegetables analysis showed that the trend for the heavy metals in Palak samples was in the order Fe>Zn>Pb>Cu>. In cabbage Fe ranged from 0 to 3928 mg/kg., Zn varied form 2.3 to 59.9 mg/kg., Pb was from 0.05 to 5.6 mg/kg., Cd was from 1.06 to 6.98 mg/kg. Where as Cr and Ni were below detection limit in all and the trend was Fe>Zn>Pb/Cu>Cd. In yellow sarson Cd ranged from 0.89 to 37.8 mg/kg., Zn from 27 to 70.2 mg/kg., Fe was from 1.08 to 45.2 mg/kg., Pb was from 9.3 to 51 mg/kg. Where as Cr and Ni were again below detection limit in all the samples.

Amongst the various heavy metals analyzed for different green leafy vegetables is similar trend in metal content was observed i.e. Fe>Zn>Pb>Cu>Cd, however their values in all vegetables were different. Fe was found highest in Palak with a mean of 24 ± 3.5 mg/kg. followed by cabbage with a mean of 17.45 ± 3.3 mg/kg. as yellow sarson as 17.35 ± 3.3 mg/kg, Zn was highest in yellow sarson with a mean of 35.6 ± 4.03 mg/kg. followed by Palak with a mean of 24 ±.5 mg/kg. and Cabbage having 16.3 ± 5.04 mg/kg. Cd was highest in Cabbage with a mean of 23.5 ± 66 mg/kg. followed by Palak with mean of 18.75 ± 5.3 mg/kg. and minimum in Brassica i.e. 17.35 ± 3.3 mg/kg. Cu was maximum in case of Palak with a mean of 56.25 ± 5.5 mg/kg. followed by Cabbage with a mean of 5.3 ± 0.52 mg/kg. and 3.95 ± 0.37 mg/kg. was for yellow sarson which was least.

3.2 Metals in random samples of green leafy vegetable collected from agricultural filed :

Vegetables were collected from different agricultural field around Singrauli city to study the metal concentration in the fresh farm produce fig. (II). In yellow sarson maximum concentration of Fe was found in sample of village Tamai (44.48 mg/kg) where as lowest concentration was reported in sample from village Judi (2.5 mg/kg) Cd concentration was highest in sample from village Bilaungi (37.8 mg/kg) followed by samples from Tamai (8.99 mg/kg) and village Madhauli (1.44 mg/kg) where as lowest concentration was reported in sample from village Judi (1.2 mg/kg.). Zn was maximum in sample from village Tamia (422 mg/kg) followed by sample from Judi and Madhauli villages (44.8 mg/kg and 53.4 mg/kg). Cu was maximum in sample from village Tamai (82.2 mg/kg) and minimum in samples from Judi village (2.5 mg/kg). Pb was maximum in samples from village Tamai (171 mg/kg) where as lowest was reported in samples from Bilaunji (3.26 mg/kg). Analysis trend showed that the order of metal content in Brassica was Zn>Pb>Cu>Fe>Cd.

Palak had maximum Fe concentration in samples from Tamai (23.36 mg/kg) followed by samples from village Judi, Madhauli and Khutar (7.77 mg/kg, 7.76 mg/kg and 3.7 mg/kg) respectively. Cd was maximum in sample from village Tamai (6.45 mg/kg) followed by sample from village Khutar (0.6 mg/kg) and Madhauli (0.55 mg/kg). Zn was maximum in village Tamai (247 mg/kg) followed by village Khutar (95.2 mg/kg) and Madhauli (47.78 mg/kg), Pb was reported to be maximum in village Tamai (82 mg/kg) followed by village Balaunji, Khutar and Judi (27.78 mg/kg, 17.66 mg/kg and 10.16 mg/kg) respectively. Cu was maximum in sample from village Tamai (40.12 mg/kg) followed by Bilaunji (16.86 mg/kg) and Khutar (6.2 mg/kg) trend in metal content was Zn>Pb>Cu>Fe>Cd.

Cabbage had Showed maximum Fe concentration in sample from village Judi (7.85 mg/kg) followed by Tamai (6.77 mg/kg) and Madhauli (4.56 mg/kg). Zn was maximum in sample from village Judi (47.42 mg/kg) followed by village Bilaunji 28.79 mg/kg) and village Madhauli (27.16 mg/kg). Cd was highest in

sample form village Bilaunji (0.66 mg/ks) followed by village Tamai (0.3 mg/kg) where as in other villages like Judi, Khutar and Madhauli it was bellow detection limit. Cu was maximum in samples from village Judi (16.4 mg/kg) and minimum in sample from Madhauli (8.3 mg/kg). Pb was reported to be maximum in village Judi (60.5 mg/kg) followed by sample from village Tamai (34.85 mg/kg) and village Khutar (30 mg/kg) trends observed in the heavy metal content was Pb>Zn>Cu>Fe>Cd. The study showed that the concentration of metals in different samples form different villages were different, indicating varied metal uptake. In all vegetables from different places it was formed that village Tamai had high concentration of Fe, Zn, Cu and Pb, samples from village Bilaunji had higher concentration of Cd whereas Cr and Ni were below detection limit.

IV. DISCUSSION

The rsult indicate that the metal content in the randomly collected samples of Brassica, Cabbage and spinach (Palak) were in the order of Fe>Zn>Pb>Cu>Cd, Where as in vegetable collected from agricultural filled around Waidhan city the order of metal content in general was Zn>Pb>Cu>Fe>Cd. The metal content in all the vegetable was above as defined by nutritiondata.com and elook.org, nearly 18 % samples of Palak from market had high level of Cd than the permissible limit of 1.5 mg/kg. 25 % sample of Brassica had high Pb and 27 % sample of Cabbage had high Zn than the permissible limit of 2.5 mg/kg as per Indian standard of food Adulteration Act.

The peak of the harvest was chosen keeping in consideration that the metal concentration in Plants varies with their age and season. A major cause for the occurrence of high content of metals in leafy vegetables is due to the presence of higher content of metals in the soil in which these vegetable are growing as these places were located near to industries and or high content is also due to irrigation by metal contaminated water released from the industries in the vicinity. A major pathway of soil contamination is through atmospheric deposition of heavy metals form point sources such as metalliferous mining, smelting and industrial activities. Other non point sources of contamination affecting predominantly agricultural soil are due to various inputs such as fertilizer, pesticides sewage sludge, organic manure, and compost **(10)**. Additionally foliar uptake of atmospheric heavy metals from emission gas also been identified as an important pathway of heavy metals contamination in vegetable crops. Several studies have shown that vegetable, particularly leafy crops, grown in heavy metal contaminated soil have higher concentration of heavy metals than those grown in uncontaminated soil **(11,12)**.

REFERENCES

[1] J. Gzyl, "Ecological impact and remediation of contaminated sites around lead smelter in Poland", J. Geochan. Explore, 53 (1995) page 251-258

[2] M. Athar, S. Vohra, "Heavy metals and environment" New Age International Publishers Ltd, New Delhi (1995)

[3] J. A. Ryan, R. L. Chaney, "Issue of risk assessment and its utility in development of soil standards". In Proceeding of 3rd international symposium on Biogeochemistry of Trace elements Paris, ICOBTE (1995), page 253

[4] A. R. Goyer, T.W. Clarkson, "Toxic effects of metals", New York McGraw Hill (2001), page 811-868

[5] K. Cambra, T. Martinez, A Urzclai, E. Alonso, "Risk analysis of a Farm area near a Pb and Cd contaminated industrial site", Journals of Soil contain, (1999), page 527-540

[6] S. Dudka, W. P. Miller, Permissible concentration of As and Pb in Soil based on risk assessment water air soil Poll. 113 (1999), Page 127-132

[7] DEFRA (Department of Environment, Food and Rural Affairs), Total Diet Study Al, As, Cd, Cr, Cu, Pb, Hg, Ni, Se, Sn, and Zn London, The Stationary Office (1999).

[8] J. Konz, K. Lisi, E. Friebele, Exposure Factors Handbook EPA/600/8-89/043, Washington DC, US Environment Protection agency, Office of the Health and Environmental Assessment 1989

[9] Hseu, Zeng-yei "Evaluating heavy metals continents in the 9 compost using four digestion methods", Bio-resource Technology, 95 (2004) page 53-59

[10] B. Singh, Heavy metals in soils sources, chemical reactions and forms in Geo Environment. Proceeding of 2nd Australia and New Zealand, conference on Environmental Geotechniques, New Castle South Wales, Eds. D. Smith S. Fityus and M Allman (2001) page 77-93

[11] G. Guttormsen, B. R. Singh, A. S. Jeng, Cadmium Concentration in the Vegetable Crops Grown in Sandy soil as affected by Cd Levels in Fertilizer and Soil PH Fert. Res. 41 (1995) page 27-32

[12] R. H. Dowdy, W. E. Larson, The Availability of Sludge-Borne Metals to Various Vegetable Crops, J. Environ., Qual. 4 (1995) page 278-283

American Journal of Engineering Research (AJER)
e-ISSN : 2320-0847 p-ISSN : 2320-0936
Volume-02, Issue-09, pp-247-250
www.ajer.org

Research Paper Open Access

The Certified Written Press As An Element of The Information Society: Case of Algeria.

Dr. Khaled Rouaski[1], Dr. Rachid Toumache[2] and Mss.Sabah Fadel[3]
[1]*High National School of Statistics and Applied Economics, Algeria,*
[2]*High National School of Statistics and Applied Economics, Algeria,*
[3]*University of Algaria III ,*

Abstract: - The rapid evolution of information technologies and communications in the recent ten years has transformed developed countries into societies of information. The new technologies are in the heart of a debate in developing countries which also aim to take profit of the inheriting advantages. The daily press follows this evolution. For instance, it is transformed, and feeds in its turn, via its online editions, the wide web of digital networks. The observation of this adaptability permits to avoid the confusion between technical support (electronic tubes replace stain tubes) and informative continent. Computing is built upon the contraction of the word information and the words mathematics and electronics. The confusion, at this level, should be ended. The written information, in terms of daily newspaper, supported by paper, stores all its propulsive force. The daily written press' past has a bright future as long as it's real dynamic is resuscitated. There a strong link between the information society and the delivery function of the written press (quality of delivering), it doesn't exist a unique function of delivering newspapers. In this context, the role of messengers should be examined and assessed relatively to the universal norms of delivery. From this, since its creation in 1922 in France, in order to control the issuance, then the distribution of the paid press (the association for the control and the distribution of the media) the OJD which has seven bureaus (the bureau of the paid press is the older and the most important); in 2007, it counts some 1,100 adherents titles; and certified by more than 4.7 billion copies, 900 titles of paid press 'main stream'; 85% of the distribution of the French press, 99% of French titles with more than 100,000 copies, to gain share of the advertising market. The advertising market does not give, in fact, the same value to the different means of distribution. However, the distribution certified by the OJD serves the editors to build their advertising tariffs and to announcers, also to their media agencies, to accept their evolutions. Hence, the obligation to have normalized indicators, similar from a title to another and timely. In France, nearly 5 billion Euros are invested in the press each year. For Algeria, the written press market knew a remarkable development during the last years, more than 141 daily newspapers, but four newspapers (El Khabar ,El Watan , Echourouk El Yaoumi , Ennahar El Djadid) certified by the association for the control of the media, the OJD. This gave birth to the private messaging in the landscape of the Algerian press. The aim of our work is to assess the results of the Algerian written press experience certified in the field of delivery.

Keywords: *- Mass Media, Newspapers, certified press, paid press, Diffusion Theory.*

I. INTRODUCTION

The rapid evolution of information and communication technologies during the last ten years has transformed the advanced countries into information societies. The new technologies are amidst a debate between developing countries, desiring taking advantage of the associated technologies. The daily press follows this evolution. Obviously, it transforms, and feeds on its turn, by its online editions, the wide web of digital networks. The observation of this ability permits to avoid the confusion between technical support (electronic pipes replace the stain pipes) and informative content. Computing is built on the contraction of the word information and the words mathematics and electronics.

The confusion, at this stage, should be ended. The written information, in the form of daily newspaper, supported by papers, holds all its propulsive force. The past of the written daily press has a big future, requiring

its real dynamic to be resuscitated. It exist a strong relationship between information society and the function of distributing of the written press (distribution quality), and there is not only one way to distribute newspapers. In this context, the role of messaging deserves to be examined.

The written press market in Algeria has known a remarkable development during the last few years, giving birth to new private messaging in the Algerian press. The aim of our work is to assess the results of the Algerian written press experience certified in the distribution (El Khabar, El Watan, Echorouk El Yaoumi, Ennahar El Djadid).

II. METHODOLOGY

a. Définitions of the Concepts

The Certified Paying Press: The certification of the paid press by the Association for the Control of the Publishing Media (OJD) which was created in 1922 in France initially in order to control publishing, then the diffusion of the pays press. The OJD has seven bureaus; the one of the Paid Press is the older and most important. In 2007, it had 1,100 adherent newspapers/magazines ; certified more than 4.7 billion issues ; 900 paid print press « mainstream media » ; 85% of French press diffusion ; 99% of French press having more than 100,000 issues.; 85 % of the French press diffusion, 99 % of French titles having more than 100.000 copies.

It follows a-three step procedure: declaration of the editor, control and minutes. For the paid press, the quality of control lies on the double analysis of both physical traceability and financial accounting; that's what makes it original and guarantees its performance. In addition to the accounting (balance sheet, results, closing book, balance of suspicious customers, …), the main checked points are the selling by subscription and the selling by issue; control the number and the breakdown of different types of subscriptions or purchase by issue, in order to be classified in the minute.

Medias of the paid press are classified into two big branches due to their function and their readers: the"mainstream" press and the"technical and professional" press. In each branch, the issues are ranked by the nature of their content (news, women, magazines, cars, people,).

The OJD combines the titles of the paid press, publications benefiting from a joint commission number or justifying a paid diffusion above 50% of their total diffusion. The paid diffusion takes into account only the effective bought copies. Whatever the origin (subscription, selling by number, portage …), the price could not be 50% below that mentioned in the issue.

Individual paid diffusion: individual bought copies by subscription or by a purchase at a point of selling.

Paid diffusion by a third person in number: It comprises purchase by quantity and the subscriptions by numbers in the limit of 50% of the individual paid diffusion.

Unpaid diffusion: all the copies not responding to the paid diffusion criteria may be retained in the unpaid diffusion, except the archiving and the justifications in the broader sense.

Useful issue by number: The number of finished copies returned to the editor for not being in circulation.

The paid diffusion: Subscriptions paid by the receiver subscriber: These subscriptions are subscribed and paid by the receiver (legal person or entity, public institution, association,) or directly by the editor, or via a library or a sales agent.

These individual subscriptions are available for a determined period or not (free period given by certain intermediaries), at a price not inferior to 50% of the subscription one, indicated on the issue.

Sales by issue paid by the purchaser: Sales by issue represent the number of copies sold directly to the customers by the editor, by the press messaging, via sales agent (depositors of press, libraries', libraries at stations, sellers, …), at a price that cannot be 50% inferior to the price mentioned in the issue. Every issues sold taken on unsold are reckoned separately.

Free Distribution: These are copies distributed for free, by post, by portage, on a sales area, on an event or by any other mean.

b. The different means of distribution

If we rely on the paper based issues – the online press is of a particular case and cannot treated on the same way – we reckon 4 methods by which press companies may reach their readership : the postal subscription, portage, purchase by a reader, purchase by a third party.

III. RESULTS

For the case of Algeria, during the recent years, the written press market has achieved a remarkable evolution, and we can summarize the results of that Algerian written press experience certified via a comparison with other countries on different means of diffusion as follows:

Postal subscription: It represents actually a changing percentage following families of press and also countries. As for French daily press (including the seventh-day newspapers), its share is approximate 14%. But, in the case

of Algeria, in 2011, it represents 0% for the 4 newspapers certified by the OJD (El Khabar, El Watan, Echorouk, Ennahar El Djadid).

Bearing in mind that its development supposes investments in terms of prospection and promotion, it is admitted that this system presents the most advantages for the editor. Surely (the sales are stable), rational (the problem of unsold copies is put aside) and financially securing (the product is prepaid). Despite this, its shares are decreasing. This trend takes on the conditions under which is delivered : organizations of tours, in adapted hours of delivery, lack of distribution during Saturday afternoon and on Friday, recurrent irregularities of the postal services, difficulties of the post offices to support a growing weight of copies. The regional daily press in France uses a little of this mode of diffusion, but we reckon there to many imbalances following the regions or the titles. Hence, the postal subscription represents 36% of the sales for La Montagne, 22% for La Dépêche du Midi, 18% for Ouest-France, and 16% for Sud-Ouest, and only 8% for La Provence, 4% for La Voix du Nord and 3% for Le Télegramme, Les Dernières Nouvelles d'Alsace or Corse matin.

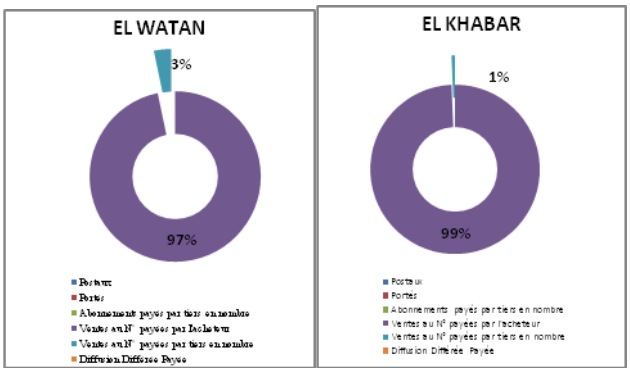

Figure 1: Breakdown by mean of diffusion for El Watan et El Khabar newspapers

The portage:

This mode of diffusion consists in a delivery of the newspaper to the home. Essentially used by daily newspapers and especially regional newspapers, theoretically it has the same advantages as the subscription; two elements distinguish this mode, which the lecturer benefits: the copies are delivered early in the morning to their receivers and risks are less frequent than postal subscription. It also allows retaining readers. In this system, a network of porters is rewarded by the editor, the depositary or the distributor.

The service may be prepaid or paid by week, bi-monthly or monthly by the receiver. It is a form of individual subscription, even if sometimes it takes the form of a sale by issue done under the responsibility of the editor or one of its representatives; this method of diffusion is unequally practices in the world. Heavily used in Ireland (99%), in Japan (93%) or in Central/Northern Europe: 90% in Switzeland, 67% in Germany, 90% in Netherlands, 72% in Sweden … it is considered as abandoned in other countries. The portage rate is 19% in the USA and 13% in United Kingdom for the national press in contrast; local newspapers use this form of distribution a lot – 4% in Spain and 0% in Italy, France and in Algeria.

Purchase by the reader:

We have to assume its history: the most fragile system and the least profitable for press companies is still dominant in our country. It lies on the daily freedom practiced by the act of purchasing. The resulting weaknesses are obvious: very tenuous link compared with other systems between the purchaser and the newspaper, imbalances in the act and place of purchase, high percentage of unsold (in 2011: 17.48% for El Watan, 14.32% for El Khabar, 10.76% for Ennahar El Djadid, 20.14% for Echorouk El Yaoumi). In France (26% in 2001 for national daily newspapers, which we add 11.6% for provincial daily newspapers).

To be efficient, this method of diffusion supposes the existence of sophisticated distribution chain and many sales points. Even if texts regulating the remuneration of press sales agents are in explicitly in reference to fixed-post crier, street vendors and peddler vendors, it appears that this form of sale is permanent?

In 2011, the sales by issue (sales by issue paid by the purchaser and the sales by issue paid by a third party) represented 100% of the total paid diffusion in Algeria for the OJD certified newspapers (Table 1).

In France, it represents 74% of the total paid diffusion of the national daily press and 47% of the regional daily press.

Purchase by a third party:

Newspapers may be purchased in numbers by a person, a company or a group in a promotional

operation, communication or a mean aiming simply at insuring the customers' comfort. In Algeria, sales by quantity to a third party represented 3.3% for El Watan, 0.7% for El Khabar, 0.3% for Ennahar El Djadi, 0.4 for Echorouk El Yaoumi (Table 1). In France, according to the 14th Press Observatory, the sales by quantity to a third party represented 4.3% of the paid diffusion in the French territory in 2003, individual diffusion is obviously 95.7%. Notice that this form of diffusion concerns mostly the national daily press (13.4%) than regional/departmental newspapers because the diffusion by a third party represents only 1.3% of the total paid diffusion.

National Algerian newspaper	Issues	Diffusion in Algeria			
		Subscriptions paid by the receiver subscriber		Sales paid by the purchaser (by number)	Sales paid by a third party (by number)
		Posted	Ported		
EL WATAN	50 199 649	0	0	39 812 095	1 355 191
EL KHABAR	167 016 550	0	0	141 710 098	965 393
ENNAHAR	111 691 540	0	0	99 223 017	300 490
ECHOROUK	190 982 094	0	0	151 443 697	572 373

Table 1: Different means of diffusion for Algerian newspapers certified by the OJD

Unpaid diffusion:

all newspapers have free services. They can respond to individual demands of persons or entities expressed in writing, or sent to assistants of the publishing company, to correspondents of the publication or to administrations during a minimum duration. There may also be issues sent by numbers, here too for a minimum duration, to companies or group of companies which made an order for third party readers (institutions hosting public, universities …). In Algeria, unpaid diffusion represented in 2011 : 0.46% for El Watan, 0.28% for El Khabar, 0.14% for Ennahar El Djadid and 0.30% for Echorouk El Yaoumi. In France, unpaid diffusion represented slightly more than 3% of the daily press total diffusion, whether being national or regional. In constrast, the strategy seems variable following categories of newspapers. Business press uses this mode more than opinion press and more than general press or political one. Hence, in 2004, Les Echos and La Tribune published for free 15.6% and 12.6% respectively, Le Figaro 1.6% and Libération 1.3%.

IV. CONCLUSION

The advertising market does not allow the same value to different means of diffusion. However, the OJD certified diffusion serves editors to build their advertising tariffs and for advertisers, in addition to media agencies, to accept the evolutions. That is why the obligation to have normalized indicators, comparable in time from a newspaper to another. In France, almost 5 billion Euros are invested in the press each year. In Algeria, figures of press advertisement showed more than 600 million Algerian Dinars in 2011.

For this reason, there is a necessity to develop and establish a modern regulatory framework, and implement a complete regulation offering to investors, journalists and readers a climate of certainty and predictability to benefit from international advantages.

It is imperative to certify issue numbers and the distribution of national and regional newspapers in Algeria, to allow to the academicians to do benefiting research to the Algerian written press.

We found evidence that the sales of written press in Algeria, based on the sales by issue (sales' issue paid by the purchaser and the sales by issue paid by a third party) are costly (irregularities in the act and place of purchase, high percentage of unsold copies); in consequence, Algerian newspapers should integrate other distribution methods (portage, subscriptions) to retain their readers and control the costs.

REFERENCES

[1]. L'association Pour Le Controle De La Diffusion Des Media (Ojd), *La vérité des chiffres* (www.ojd.com), P2.
[2]. Emmanuel Delrieux, *Médias et société* (Edition Montchrétien ,11ème Edition).
[3]. Emmanuel Delrieux et Trudel, *Les principes du droit de la communication dans la jurisprudence* du Conseil constitutionnel Legipresse.
[4]. Francis Balle, *La presse en France: la liberté aménagée* (Edition Montchrétien, 11ème édition, 2003), P.302.
[5]. OJD, *Procès Verbal De Contrôle 2011*. (www.ojd .com.)

American Journal of Engineering Research (AJER)
e-ISSN : 2320-0847 p-ISSN : 2320-0936
Volume-02, Issue-09, pp-251-257
www.ajer.org

Research Paper Open Access

Water and Soil Pollution in Punjab with Special Reference to Mandi Gobindgarh & Surrounding Areas

Dr. Shalini Gupta[1], Dr. D S Grewal[2], Ajay Gupta[3]
1. Pro Vice Chancellor, Desh Bhagat University, Mandi Gobindgarh, Punjab, India
2. Dean R & D, Desh Bhagat University, Mandi Gobindgarh, Punjab, India
3. Research Scholar, Desh Bhagat University, Punjab, India

I. INTRODUCION

Mandi Gobindgarh is an industrial town in Fatehgarh District of Punjab, India, located on NH-1 at an equi-distance of 55 kms from Ambala, Ludhiana and Chandigarh. It is the second biggest industrial town in Punjab and its industry includes 475 units generating hazardous waste making it as one among the list of 43 critically polluted industrial hubs of the country on which the ministry had imposed a moratorium. (Indian Express: 09 Dec 2012). The population showed a higher prevalence of symptoms of respiratory problems, angina, cardiovascular and skin diseases. The rural area around the city too stands polluted due to industrial smoke, dust and 'the burning of over 20 million tons of paddy husk by Punjab's farmers' triggered smog.' (Times of India 12 Dec 2012). The Commutative Environment Pollution Index for land (soil and ground water) has been calculated as 62 for Mandi Gobindgarh and it has been declared as critical as per the analysis results of the samples of ground water collected by the Punjab Pollution Board from different localities of the town.

II. NEED FOR THE STUDY

No detailed study on pollution of water and soil in Mandi Gobindgarh and its perforation into surrounding areas have been found studied. None of the related studies has covered the pollution in rural areas of the district or the adjoining rural areas of the industrial town. No study has yet been carried out on macro scale or nano-scale. The detailed impact of all types of pollution on health is also not studied so far, hence this study is conducted.

III. BACKGROUND

There are 89 induction furnaces, 38 cupola furnaces, 1 arc furnace, 247 steel rolling mills, 13 refractories and forging industry each and 3 lead extraction units. It stands the 17th most polluted industrial town in India. (The Tribune India: 9 Dec 2011) 475 units situated in Mandi Gobindgarh that area generating hazardous waste. The main hazardous waste is generated from arc /induction furnaces as dust from air pollution control device. About 3 TPD of hazardous waste is generated by these industries. In addition 9 hospitals operating in Mandi Gobindgarh generate about 20 Kg/day of biomedical waste pertaining to category No.1, 4, 5, 6, 7 and 8 is generated in the town. About 44 T/day of municipal solid waste is generated from the Mandi Gobindgarh town. The Municipal Council has not made any arrangements for proper treatment and disposal of the said waste. Presently, the solid waste is disposed of on 1.25 acre of open land located on Agni Casting Road (link road from G.T. Road on Sirhind Side). The solid wastes in the shape of solid sludge generated from the cooling water recirculation tanks of re-rolling mills are disposed of along the road sides. The e-waste is generally generated from dismantling activities of various electrical/electronic appliances/gadgets such as audiovisual components, televisions, VCRs, stereo equipment, mobile phones and computer components. But till date, no inventory of such waste has been prepared. However, for the proper disposal of such type of waste, the Ministry of Environment & Forest India, has included this waste in the Hazardous Wastes.

A report prepared by the Punjab Pollution Control Board identified various bodies responsible for different actions in different areas of pollution control. These bodies included Punjab Pollution Control Board, Municipality, Police, PWD, Department of Forests, industries, transport, and local bodies and prepared an action plan. It found the following areas need corrective action in order to improve the ground water quality:

(i) Stagnation of M.C. sewage / silage
(ii) Unscientific disposal of municipal solid waste
(iii) Improper disposal of industrial solid waste

IV. OBJECTIVE OF THE STUDY:

1. To study the water and soil pollution in Mandi Gobindgarh and surrounding rural areas.
2. To find out the causes of water and soil pollutants in the area.
3. To measure the impact of soil and water pollution on health of the population of the area.
4. To find out solutions to these pollutants and their effects
5. To evaluate the measures adopted to control/eliminate these pollutants
6. To suggest an Environment Management System.

V. HYPOTHESIS

1. Water and soil of Mandi Gobindgarh town and the surrounding rural areas are highly polluted
2. Pollution is the cause of chronic diseases like Cardiovascular and Gastro diseases in the area.
3. Pollution in urban area is also impacting the surrounding rural area.

VI. DELIMITATION

Area of the study is the town of Mandi Gobindgarh town and surrounding villages of Fatehgarh Sahib District with in 10 Kms of the town. In addition some samples are also obtained from other neighbouring villages to know the actual extent of impact. 397 samples were taken from industry and rural areas.

VII. METHODOLOGY

Research Methodology adopted is exploratory in nature since very limited research has been carried out on pollution in Mandi Gobindgarh and surrounding areas. The methodology involved observation and survey. Techniques used were questionnaire and camera in addition to personal observation. Observations of Mandi Gobindgarh and adjoining areas were conducted by the researcher in detail since she has been the permanent resident of the area for the last 30 years. She visited most part of the area of research to find out the exact details and established contacts with the samples for information. The important pollution sources were photographed with the help of institution's photographers. The survey was conducted through 10 questionnaires. Secondary data was provided by the Punjab Pollution Control Board and the medical Authorities. Both Primary and secondary data was made use of.

Data Collection through Questionnaire

The observations were further extended with 8 sets of questionnaires. In addition records from Medical authorities at Mandi Gobindgarh and Amloh were also obtained through 2 different questionnaires. The questionnaire to the general public and the rural areas was both in English and Punjabi since most of the population is Punjabi speaking. One questionnaire was given to Punjab Pollution Control Board, Patiala. The data and the information so collected through these 10 questionnaires were crosschecked for validity and reliability through cross checking because certain questions were meant for cross-check to check the reliability. Keeping in view the validity requirement, questionnaires were separately prepared for Industry management: industrial labour, farm management: farm labour, urban residents: rural residents respectively. To check the effect of the pollution and the remedial actions taken so far by various agencies; two questionnaires were given to medical authorities at Mandi Gobindgarh and Amloh and one to Punjab Pollution Control Board Patiala. Photography of prominent pollution sources was also obtained.

Samples

Samples were selected from among the residents of Mandi Gobindgarh (113) and over 20 villages (99) around to know their experience of pollution. Also samples were obtained from the persons involved with sources of pollution i.e., industry managements (45), industry labour (48), farmers (49) and farm labour (40). Observations of 397 observers through questions were thus obtained; about 98% of them having the experience of pollution in the area for more than 5 years. Out of these 207 samples were from Mandi Gobindgarh and 190 from adjoining villages. Samples were taken from male as well as female respondents. Samples were selected both from urban and rural areas.

Data Tabulation & Analysis

The obtained data was compiled in Tables and results in tables and graphs. Analysis of the data was done statistically with the help of Wiconxon Tests and Paired Sample Test.

VIII. RESULTS AND ANALYSIS

Observations:

The researcher visited the entire area of Mandi Gobindgarh and adjoining villages to find the actual state of pollution and found that the entire Mandi Gobindgarh area was heavily polluted. The environment degradation in Mandi Gobindgarh and surrounding area is observable and recordable.The rural areas are polluted most due to pesticides and stubble burning. Pesticides are chemicals used to control a whole range of pests and include insecticides, herbicides, fungicides and rodenticides. There are serious environmental problems and health concerns resulting from the use of pesticides. Pesticide residues have been found in breast milk, milk from cattle, and in fruits and vegetables. The mortality rate of milch cattle in this area has been increasing during the monsoon for the past few years. While veterinarians say the increasing mortality rate is a consequence of the excessive use of pesticides and insecticides by farmers in their fields, toxicologists claim that concentration of nitrate in the stalks of crops is the main reason. The affected farmers, however, feel that some poisonous wild growth has been the cause of their death. Locals are voicing forcefully for the government to outlaw pesticides and advocate organic agriculture. After decades of relying on fertilizers, some farmers now say that the benefits have come at too great a cost, slowly siphoning the health of both the soil – sapping nutrients and killing micro-organisms – and the surrounding communities. It has led to a spike in cancer, low sperm counts in men, the early onset of menstruation and an increase of still births in women, as well as other ailments. Presently medical teams are assessing the TB cases in the area under a Central Government project from Ministry of Health.

Carrying out Environmental Impact Assessment (EIA) remains a problem. The researcher found that the major obstacles are the difficulties in obtaining reliable baseline data, the lack of access to modern technological tools like Global Positioning Systems and Geographical Information Systems, a shortage of quality laboratories and little public participation.

The researcher herself visited the entire area of Mandi Gobindgarh and adjoining villages to find out the actual state of pollution and also the action taken on the points by Punjab Pollution Control Board in the Action Plan 2010. The researcher found that entire Mandi Gobindgarh is heavily polluted and did not find any improvement since 2010.

Analysis and Interpretations

All the primary sources i.e., observations, discussions, survey questionnaires, schedules and photography and the secondary sources; the report of Punjab Pollution Control Board, articles and news in local papers and the two field studies reveal that Mandi Gobindgarh and its surrounding areas are polluted. All the air, soil and water in the area are badly affected by the pollution. The presence of all these chemicals are considered an alarming as its prolonged exposure has led to various health ailments. Diseases like TB, heart ailment, skin, breathing problems, allergy, gases, anemia, asthma which did not exist ten years before have now come in a big way.

Population of Mandi Gobindgarh is 155416 in 2012 and of Amloh is 12686. It shows that every person in among ten in Mandi Gobindgarh is sick by one or other disease while the sickness ratio in Amloh just 14 kms from Mandi Gobindgarh is not even 0.5%. For example respiratory diseases, problems are 1000 times more heart problems are more than 400 times and skin 300 times more in 2012 in Mandi Gobindgarh than Amloh. This is all due to heavy amount of pollution in the area. The excessive particulate matter is a potential danger to the residents and it is very essential that it is controlled at war footing. Wilcoxon test for pollution due to water and soil in urban and rural areas was carried out to find out the relationship between pollution and various diseases.

Wilcoxon Test Urban Area for Water

Table 1:Wilcoxon Signed Rank Test Statistics of relationship between water pollution and various diseases in Urban Area Mandi Gobindgarh[b]

	TB - Water	Gastro - Water	Skin - Water
Z	-7.649[a]	-7.620[a]	-4.250[a]
Asymp. Sig. (2-tailed)	.000	.000	.000

a. Based on positive ranks.

b. Wilcoxon Signed Ranks Test

Analysis 1: From table 1 relationship between water pollution and TB, Gastro and Skin diseases in Urban Areas of Mandi Gobindgarh were compared through Wilcoxon Signed Ranks Test. The test showed a

significant impact of water pollution on TB, Gastro and Skin diseases because of z value of 7.649 between water pollution and TB diseases; z value of 7.620 between water pollution and gastro diseases; z value of 4.250 between water pollution and skin diseases. All these values are well above z values 1.96, 2.58 and even 3. It showed that impact of water pollution on TB, Gastro and Skin diseases in urban area of Mandi Gobindgarh is very significant.

Wilcoxon Test Rural Area for Water

Table 2: Wilcoxon Signed Rank Test Statistics of relationship between water pollution and various diseases in Rural Areas surrounding Mandi Gobindgarh[b]

	TB - Water	Gastro - Water	Skin - Water
Z	-4.557[a]	-5.632[a]	-4.901[a]
Asymp. Sig. (2-tailed)	.000	.000	.000

a. Based on positive ranks.

b. Wilcoxon Signed Ranks Test

Analysis 2: From table 2, relationship between water pollution and TB, Gastro and Skin diseases in Rural Areas surrounding Mandi Gobindgarh were compared through Wilcoxon Signed Ranks Test. The test showed a significant impact of water pollution on TB, Gastro and Skin diseases because of z value of 4.557 between water pollution and TB disease; z value of 5.632 between water pollution and gastro diseases; z value of 4.901 between water pollution and skin diseases. All these values are well above z values 1.96, 2.58 and even 3. It showed that impact of water pollution on TB, Gastro and Skin diseases in rural area surrounding Mandi Gobindgarh is very significant.

Wilcoxon Test Urban Area for Soil

Table 3:Wilcoxon Signed Rank Test Statistics of relationship between soil pollution and various diseases in Urban Area Mandi Gobindgarh[b] Urban Test Statistics[b]

	TB - Soil	Heart - Soil	Respiratory - Soil	Skin - Soil
Z	-6.862[a]	-2.907[a]	-6.379[a]	-3.402[a]
Asymp. Sig. (2-tailed)	.000	.004	.000	.001

a. Based on positive ranks.

b. Wilcoxon Signed Ranks Test

Analysis 3: From table 3, relationship between soil pollution and TB, Heart, Respiratory and Skin diseases in Urban Areas of Mandi Gobindgarh were compared through Wilcoxon Signed Ranks Test. The test showed a significant impact of soil pollution on TB, Heart, Respiratory and Skin diseases because of z value of 6.862 between soil pollution and TB diseases; z value of 2.097 between soil pollution and Heart diseases; z value of 6.379 between soil pollution and respiratory diseases and z value of 3.402 between soil and skin diseases. All these values (except of Heart and Soil) are well above z values 1.96, 2.58 and even 3. It showed that impact of soil pollution on TB, Respiratory and Skin diseases in urban area of Mandi Gobindgarh is very significant and significant between Heart diseases and soil.

Wilcoxon Test Rural Area for Soil:

Table 4: Wilcoxon Signed Rank Test Statistics of relationship between water pollution and various diseases in Rural Areas surrounding Mandi Gobindgarh Rural Test Statistics

	TB - Soil	Respiratory - Soil	Skin - Soil	Gastro - Soil	Heart - Soil
Z	-2.429[a]	-6.581[a]	-2.429[a]	-3.429[a]	-2.263[a]
Asymp. Sig. (2-tailed)	.015	.000	.015	.001	.024

a. Based on positive ranks.

b. Wilcoxon Signed Ranks Test

Analysis 4: From table 4, relationship between soil pollution and TB, Heart, Respiratory and Skin diseases in Rural Areas surrounding Mandi Gobindgarh were compared through Wilcoxon Signed Ranks Test. The test

showed a significant impact of soil pollution on TB, Heart, Respiratory and Skin diseases; because of z value of 2.429 between soil and TB; z value of 6.581 between soil pollution and Respiratory diseases z value of 2.429 between soil pollution and skin diseases; z value of 3.429 between soil pollution and gastro diseases and z value of 2.263 between soil and Heart diseases. All these values are well above z values 1.96, and respiratory and gastro diseases have relationship well above the value of 2.58 and even 3. It showed that impact of soil pollution on respiratory and gastro diseasews in rural areas surrounding Mandi Gobindgarh are very significant but significant between TB, heart and Skin diseases.

Paired test: Water Pollution Urban Area

Table 3: Paired Samples correlations test Statistics of relationship between water pollution and various diseases in Urban Areas Mandi Gobindgarh

		N	Correlation	Sig.
Pair 1	Water & TB	113	.120	.204
Pair 2	Water & Gastro	113	.257	.006
Pair 3	Water & Skin	113	-.130	.169

Analysis 3: From table 3 relationship between water pollution and TB, Gastro and Skin diseases in Urban Areas of Mandi Gobindgarh were compared through Paired Test. The test showed a significant impact of water pollution on TB, Gastro and Skin diseases.

Paired test Water pollution Rural Area

Table 4: Paired Samples Correlations Test Statistics of relationship between water pollution and various diseases in Rural Areas surrounding Mandi Gobindgarh

		N	Correlation	Sig.
Pair 1	Water & TB	99	-.089	.378
Pair 2	Water & Gastro	99	.120	.237
Pair 3	Water & Skin	99	.098	.334

Analysis 4: From table 4 relationship between water pollution and TB, Gastro and Skin diseases in Rural Areas surrounding Mandi Gobindgarh were compared through Paired Sample test.. The test showed a significant impact of water pollution on TB, Gastro and Skin diseases.

Paired sample test for Soil Pollution in Urban Area

Table 5: Paired Samples Correlations Test Statistics of relationship between soil pollution and various diseases in urban Areas Mandi Gobindgarh

		N	Correlation	Sig.
Pair 1	Soil & Respiratory	113	.177	.061
Pair 2	Soil & Heart	113	-.449	.000
Pair 3	Soil & TB	113	.038	.688
Pair 4	Soil & Skin	113	-.106	.262

Analysis 5: From table 5 relationship between soil pollution and Respiratory, Heart, TB and Skin diseases in Urban Areas of Mandi Gobindgarh were compared through Paired sample Test. The test showed a significant impact of soil pollution on Respiratory, Heart, TB and Skin diseases.

Paired sample test for Soil pollution in Rural Area

Table 6: Paired Samples Correlations Test Statistics of relationship between soil pollution and various diseases in Rural Areas surrounding Mandi Gobindgarh

		N	Correlation	Sig.
Pair 1	Soil & Respiratory	99	.094	.357
Pair 2	Soil & Skin	99	.034	.736

Pair 3	Soil & Heart	99	.011	.911
Pair 4	Soil & TB	99	.034	.736

Analysis 6: From table 6 relationship between soil pollution and Respiratory, Heart, TB and Skin diseases in rural Areas surrounding Mandi Gobindgarh were compared through Paired sample Test. The test showed a significant impact of soil pollution on Respiratory, Heart, TB and Skin diseases.

This corresponds to the earlier report by Punjab Pollution Control Board in 2011 who initiated measures to control the pollution in which almost all the departments of the Government were involved. Results of the same are yet to be seen. The public however is not yet involved in making them aware of this monster of pollution and to take effective measures to save themselves from the serious ailments which is essentially needed.The quality of input in industry should also be improved and the junk received from foreign war zones should be discontinued.

IX. FINDINGS

This study has been able to cover the research gap of macro study of various pollutants and their effects and has also covered the environment in the adjoining rural areas. The study found Mandi Gobindgarh heavily polluted. The impact of pollution caused by the industry of Mandi Gobindgarh was also felt strongly in surrounding rural areas. Water and soil was found heavily polluted. The detailed impact of all types of pollution on health has also been studied. Relationship to various chronic diseases to pollution through water and soil has also been established. The heart, respiratory, skin, TB Gastro are all effectd by water and soil pollution.

Water is found stagnated in number of vacant plots. Untreated water consists of harmful chemicals and vehicle fluids i.e., motor oil, antifreeze, gasoline, air-conditioning refrigerants, and transmission, brake, hydraulic and windshield-wiper fluids. Soil is found polluted from chemicals, molted and grinded metal, untreated water, factory and domestic refuse and bio-waste

The pollution control by various government agencies is not much effective since the impacted diseases are continuously increasing. All citizens must be made aware of the pollution and its causes and effects and help the pollution control agencies to control the pollution religiously. NGO's and religious institutions' must help to propagate the effects of pollution.The Government and the pollution Control agencies have to work harder than they are doing at present as the spread and increase of pollution is faster and even getting out of control. The citizens themselves have to be aware and stand against this demon to fight united before every one's life goes into danger Zone. Special care is needed to control the effect of pollution on heart and gastro diseases which are continuously increasing at an alarming rate.

The existence of pollution much more than the National level limits is a great cause of concern. This proves the hypothesis that pollution in Mandi Gobindgarh and surrounding areas are highly polluted. The study was able to find the type and amount of pollution in Mandi Gobindgarh in qualitative terms. However the quantitative measure of pollution requires a separate detailed study and special equipment at nano scale. This study will help the various authorities and the persons responsible to check pollution to go into more depth and to be more serious in controlling pollution since the diseases pertaining to heart, skin and lungs are of alarming proportion. All the objectives of the study are thus met by studying the pollution, its extent, causes and impact and evaluating the measure adopted to control the pollution. Solutions and suggestion have been provided to control the pollution and its effects in various fields and an awareness campaign has been started at Desh Bhagat University level through lectures and demonstrations. The major effect on environmental pollution and cause of diseases being nanoparticles; these nanoparticles however still remain to be studied in detail with the help of advance microscopes like SPM, SEM and TEM.

X. RECOMMENDATIONS

Since the environment pollution in Mandi Gobindgarh is much more the limits laid down by national and international standards, there is an urgent requirement to take strong measures to check and control the pollution. An Environmental Impact Assessment (EIA) must be carried out and a dedicated team be detailed by Punjab Pollution Control Board to carry out assessment of pollution at least at the 10 identified points in the industrial area. A reliable base line data is required through the use of Global Positioning System and Geographical Information Systems.A dedicated effort be put up to make the public aware of the effects of pollution and public participation must be encouraged in reducing pollution at their homes and surrounding areas.

Proper effluent treatment plants must be setup and industrial, house hold and medical wastage must have proper dumping ground away from the residential area. Proper channeling of water must be done, sewerages system be approved and allowing the water in plots must be paid punishable. The Govt. administration must coordinate the activities of Punjab Pollution Control Board, Municipality, Police, PWD,

Department of Forest, Industries, Transport and local bodies and estab;ish a proper environment managements system (EMS) and update the action plan. A policy must be framed and proper action plan must be prepared and circulated not only among the departments but also in industry and public to make them more aware. In rural areas the proper sewerages system and water outlets will save water stagnation. The use of fertilizers is required to be controlled immediately. An overall awareness campaign must be started through pamphlets and paper advertisements highlighting the dangers of environmental pollution

XI. CONCLUSION & SUGGESTIONS

The study found Mandi Gobindgarh heavily pollutedwhich in turn has affected surrounding rural areas. Water and soil in addition to air were found heavily polluted causing chronic diseases relating to heart, respiratory, skin, TB Gastro to pollution. Water is found stagnated in number of vacant plots. Untreated water consists of harmful chemicals and vehicle fluids i.e., motor oil, antifreeze, gasoline, air-conditioning refrigerants, and transmission, brake, hydraulic and windshield-wiper fluids. Soil is found polluted from chemicals, molted and grinded metal, untreated water, factory and domestic refuse and bio-waste. The pollution control by various government agencies is not much effective since the impacted diseases are continuously increasing. Detailed study on pollution at micro and nano scale in the area is needed and there is an urgent necessity of having a proper Environment Management System. All citizens must be made aware of the pollution and its causes and effects and help the pollution control agencies to control the pollution religiously. NGO's and religious institutions' must help to propagate the effects of pollution. The Government and the pollution Control agencies have to work harder than they are doing at present as the spread and increase of pollution is faster and even getting out of control.

REFERENCES

[1] Britton RS, Tavill AS, Bacon BR.(1994).Mechanisms of iron toxicity. In: Iron metabolism in health and disease. Brock, J.H., Halliday, J.W., Pippard, M.J., Powell, L.W. (eds.). WB Saunders, London, pp. 311-351.

[2] Brunekreef B, etal (Veenstra 1981). Lead uptake by 1- to 3- year old children living in the vicinity of a secondary lead smelter in Arnhem, The Netherlands. *Environ Res* 25, 441-448, Bush RK, Portnoy JM, Saxon A, Terr AI, Wood RA. (2006). The medical effects of mold exposure.*J Allergy ClinImmunol*117, 326-333.

[3] Calderon J, Navarro ME, Jimenez-Capdeville ME, Santos-Diaz MA, Golden A, Rodriguez-Leyva I, Borja-Aburto V, Diaz-Barriga F. (2001).Exposure to arsenic and lead and neuropsychological development in Mexican children. *Environ Res* 85, 69-76.

[4] Campen MJ, Nolan JP, Schladweiler MC, Kodavanti UP, Evansky PA, Costa DL, Watkinson WP. (2001). Cardiovascular and thermoregulatory effects of inhaled PM-associated transition metals: a potential interaction between nickel and vanadium sulfate. *ToxicolSci*64, 243-252.

[5] Corhay JL, Weber G, Bury T, Mariz S, Roelandts I, Radermecker MF. (1992.), Iron content in human alveolar macrophages. *EurRespir J*, 5, 804-809,

[6] Damstra T. (2002).Potential effects of certain persistent organic pollutants and endocrine disrupting chemicals on the health of children. *J ToxicolClinToxiol*40, 457-465.

[7] Finland M. (1982), Pneumococcal infections. In: Evans AS, Feldman HA, eds. Bacterial infections in humans. Epidemiology and control. New York: Plenum.

[8] Lambert AL, Dong W, Selgrade MK, Gilmour MI.Enhanced allergic sensitization by residual oil fly ash particles is mediated by soluble metal constituents. *ToxicolApplPharmacol*165, 84-93, 2000.

[9] Lanphear BP, Dietrich K, Auinger P, Cox C. (2000), Cognitive deficits associated with blood lead concentrations <10 µg/dL in US children and adolescents. *Pub Health Rep* 115, 521-529.

[10] Prpic-Majic et al (2000), Lead absorption and psychological function in Zagreb (Croatia) school children. *NeurotoxicolTeratol*22, 347-356,

[11] Rahman A, Maqbool E, Zuberi (2002), HS.Lead-associated deficits in stature, mental ability and behaviour in Karachi.*Ann Tropical Med* 22, 301-311.

[12] Raizenne M,et al, (1996)Health effects of acid aerosols on North American children: pulmonary function. *Environ Health Perspect*104, 506-514..

American Journal of Engineering Research (AJER)
e-ISSN : 2320-0847 p-ISSN : 2320-0936
Volume-02, Issue-09, pp-258-264
www.ajer.org

Research Paper Open Access

Drivers for Energy Efficiency in Indian Railway Workshops

Suresh D. Mane, N. Nagesha
[1] *Research Scholar, Asst. Divisional Mechanical Engineer (Rtd.), South Western Railway, Bangalore 560036 Karnataka, India*
[2]*Industrial & Production Engineering Department, UBDT College of Engineering, Davangere 577004 Karnataka, India*

Abstract: - Two major railway coach repair workshops involved in periodical overhauling of broad gauge passenger coaches located in south India has been undertaken for studying the drivers for energy conservation (EC). The study covers a period of six calendar years from 2007 to 2012 and takes into account the various activities in terms of maintenance of coaches and production of components the energy input for both the workshops. Carriage Repair Workshop Hubli (UBLS) Central Workshops Mysore (MYSS) have introduced many an EC measures yielding good results. The extended study was then undertaken to analyse the drivers for energy efficiency in both of these workshops. The main stakeholders in both the workshops viz. the officers and senior section engineers (SSE's) were interviewed separately and their experience on the drivers for EC were sought. Totally seven drivers for EC were arrived at from the discussions with the stakeholders. To rank these seven drivers a questionnaire was devised to capture the data from both of these workshops and weighted average method adopted for ranking. The stakeholders were briefed of the questionnaire so as to make them accustomed to it. 82 respondents from UBLS and 41 respondents from MYSS filled up the forms in all respects which were used for analysis using weighted average method. Results show the similar first three ranking in both the workshops with total weighted average of greater than 0.5. The top ranked driver of both the workshops was dedication of the top management, engineers and staff with a weighted average score of 0.18 and 0.19 respectively from MYSS and UBLS respectively. The driver "awareness and adoption of latest technologies for EC" is a close second with a weighted average of 0.16 and 0.17 respectively from MYSS and UBLS respectively. Capacity utilization is ranked third which again is common for both the workshops. It was found that due to better awareness about environment at MYSS, it was ranked fifth when compared to UBLS wherein it was ranked the last at seventh position. These results clearly indicate that Railways is mainly driven by the dedication of its personnel and its sustenance and improvements on the energy front continue to contribute mainly by them. Indian Railways has 45 such workshops which are major energy consumers catering to the preventive maintenance of its fleet and thus railways need to keep their human resource motivated to contribute towards EC and reduce its carbon footprint.

Keywords: *- Carriage Repair Workshops, Drivers for Energy Efficiency, Energy Conservation, Indian Railways, Weighted Average*

I. INTRODUCTION

Indian Railways (IR) has 53220 number of passenger coaches which are given major attention in the form of periodical overhauling (PoH) at an interval of 18 months at carriage repair workshops [1]. Indian Railways has 45 workshops spread over the nation in its 17 zones to cater to periodic overhauling of all the coaches apart from some catering to the freight stock, locomotives [2]. South Western Railway over Indian Railways has two workshops which are undertaking PoH of passenger coaches one located at Hubli and the other located at Mysore. UBLS is one of the few workshops which have aggressively introduced numerous EC (EC) measures which have given good results and successfully sustained the same. MYSS too has kept pace and has implemented the agenda issued by Railway Board for EC. Major effort has been undertaken by MYSS to replace its aged centralized reciprocating air compressor by state of art microprocessor controlled screw compressor in July 2013, thereby ensuring savings in electricity consumption. UBLS during 2012-13 overhauled 761 coaches, carried out refurbishment of 140 coaches and undertook manufacturing of 2700 bogies and its

subassemblies employing over 3100 staff with 2877 being in the technical staff and others being in ministerial and other supporting categories[3]. The details of various categories of staff at UBLS and MYSS, activities undertaken by both the workshops and the manpower utilization are furnished in table 1 and table 2 below. The workshop has six technical officers who are managing the organisation with the help of 240 engineers (Including Electrical) who are the frontline managers and are responsible for the quality and quantity of daily output.

Table.1 Staff position of UBLS and MYSS as on 01.01.2013

Dept.	UBLS			MYSS		
	Engineers/ Supervisors.	Gr. C & Gr.D	Total	Engineers/ Supervisors	Gr. C & Gr.D	Total
Mech	223	2322	2545	140	1293	1433
Electrical	17	315	332	9	134	143
Stores	30	216	246	4	118	122
Ministerial	19	115	134	5	83	88
Total	289	2968	3257	158	1628	1786

Table.2 Staff deployment by UBLS and MYSS during 2012-13

Sl	Activity	UBLS			MYSS		
		Engineers	Gr. C & Gr. D	Total	Engineers	Gr. C & Gr. D	Total
1	Coach PoH, IoH, RSP	1307	82	1389	1143	28	1171
2	Brake Van mfg (UBLS)	188	10	198	0	0	0
3	Bogie frame & its sub-assembly mfg (UBLS)	490	29	519	0	0	0
4	MW, Outstation Works	174	21	195	104	3	107
5	Toy Train mfg (MYSS)	0	0	0	87	2	89
6	Composite Brake Block Mfg (MYSS)	0	0	0	32	2	34
7	Total	2159	142	2301	1366	35	1401

Mfg. Manufacturing, RSP – Rolling Stock Programme, IoH – Intermediate Overhaul

Deployment of staff at UBLS towards carriage repair activity (which also includes rolling stock programme) is 1307 staff and 82 engineers as evident from table 2. The Production shops include High speed brake van manufacturing, Bogie frame and its sub-assemblies manufacturing and utilize 678 staff and 39 engineers. Maintenance shops in both the workshops not only undertake maintenance of machinery and plant but also take up new developmental activities.

The average cost of overhauling of one broad gauge coach as per 2012-13 inputs cost is Rs 0.95 million which is nearly 10% of the cost of a new coach and the share of energy towards the cost of coach maintenance is miniscule 0.5%. UBLS is one of the oldest workshops in this country and is undertaking diverse activities which include the core activity of coach PoH and also has forayed into fabrication of bogies, its sub assemblies and also manufactures brake van for the freight trains, this workshop has been taken up for detailed study. Earlier study clearly indicated that UBLS has initiated novel measures for EC and sustained the same over the years inspite of increase in the connected load it was considered a fit case to study in detail the drivers for EC. The study undertaken to analyse the drivers for energy efficiency at UBLS divided the respondents into four functional wings viz. coach repair shop, production shops, electrical and maintenance shop which also included the trainers of the workshop. These four groups represent the backbone of the workshops due to their education, experience and above all their contribution in successfully managing the activities on a day to day basis. The study reveals that majority of respondents have more than two decades of experience with a maximum of 42 years which clearly highlights the loyalty towards the organisation and very low attrition rates. MYSS during 2012-13 undertook PoH of 789 coaches including 650 non AC coach PoH [4] apart from manufacturing 1, 04, 865 composite brake blocks and three toy trains. In MYSS the strength of engineers is 138 when compared to 240 of UBLS and as such no division among the engineers was made for the analysis sake. MYSS annually

consumes 1, 03,572 liters of diesel apart from 63,584 units of electricity per month. MYSS during July 2013 has switched over from old reciprocating centralized air compressor unit (90kW) to new state of art microprocessor controlled 90 kW screw air compressor thereby leading to saving of 1250 units of electricity per month.

Table 3. Energy consumed by UBLS and MYSS for year 2011

Sl. No.	Type of Energy Carrier	Application	UBLS	MYSS
1	Diesel in liters	a. D. G. Set	11,000	15,600
		b. Transport vehicles	45,000	50,000
		Total Qty. of Diesel	**56,000**	**65,600**
2	Electricity in kWh	Machines, Cranes	**16,35,771**	**6,85,963**
		a. Coach POH	19380	11,000
3	LPG in kg	b. Production	16150	11,000
		c. Canteen	0	8,500
		Total LPG in Kgs	35,530	30,500
4	Total Energy	**GJ**	**9631**	**6385**

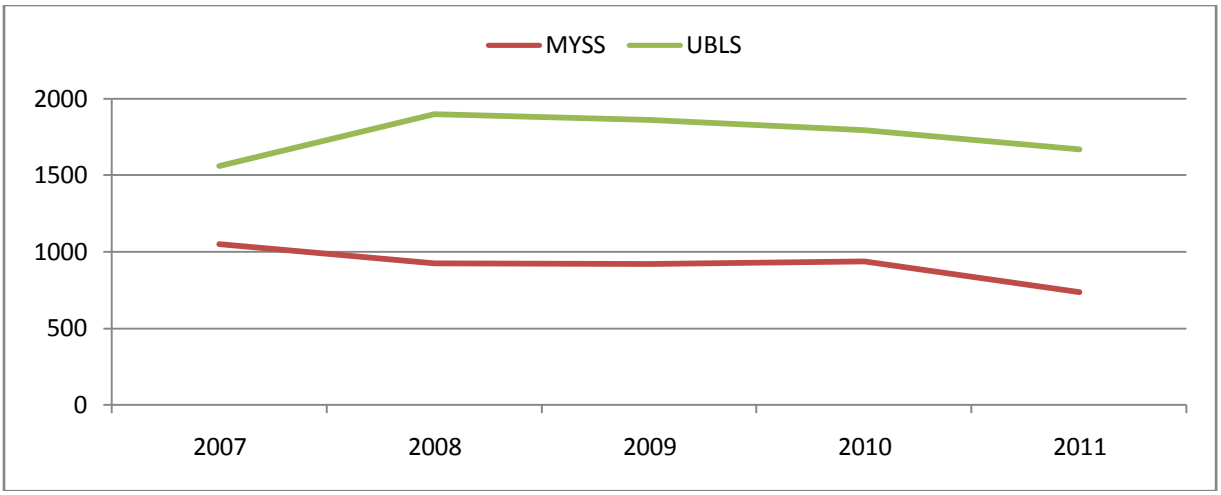

Fig. 1 Annual Electricity Consumption in Thousand kWh by UBLS and MYSS

The study reveals that from illumination point of view, the new technologies like T5 lamps, CFL, light pipe, metal halide lamps, tower lights with timers are already installed and as such there is little scope for improving energy efficiency in illumination area. The trend analysis of the energy consumption and energy bills shows that both the workshops have taken numerous steps to reduce the energy consumption over a period of time and thereby the overall cost of energy is reducing inspite of the increase in the energy costs by electricity distribution companies..

N. Nagesha and P. Balachander in their study [5] on drivers for energy efficiency in small scale industrial sector have considered the various drivers and prioritized the same using weighted averages method. More recently Patrik Thollander et.al [6] studied the various drivers for energy efficiency in energy intensive foundry sector using the survey method and as such we have adopted the method of survey to undertake the study. In order to continue progress in the field of EC, a study was required to determine the factors which lead to promotion of implementation and sustenance of EC measures. These factors can be taken up aggressively by other sister workshops to adopt and improve EC drives in their respective workshops.

II. METHODS AND MATERIAL

The author visited both the workshops over a period of four years and interacted with the team of officers and SSE's who manage the workshops. Based on the expert value judgment of the officers and SSE's

the seven drivers were listed and a common questionnaire framed for both the workshops. In UBLS 90 questionnaires were distributed among the respondents and 82 were received back duly filled in all respects. Six supervisors could not rank the drivers properly and were further guided to ensure that each rating appeared only once in the list. Out of the 82 respondents, 62 are diploma holders in engineering, 18 are engineering graduates and two are post graduates in engineering. The respondents include 4 officers, 44 SSE's and 30 Junior Engineers (JE). The average experience of SSEs is 24 years and that of JEs is 16 years. Initially the respondents were briefed about the questionnaire and were asked to rank the drivers in their functional areas as they perceived them. The questionnaire was administered to 4 out of 6 technical officers and 77 engineers out of 240 engineers of the shops (both mechanical and electrical put together) which cover 35% of the population. Similarly at MYSS the author briefed the respondents about the questionnaire and distributed 50 questionnaires. 42 questionnaires were received back duly filled in all respects.

The questionnaire was briefed to the respondents at both the workshops as they are not familiar with filling such forms and were instructed to rank the drivers from 1 to 7 as per their weight age and ensure that each rank from 1 to 7 was used once and also the details of their qualification and experience is mentioned in the form. The questionnaire was collected and analyzed using weighted average method. The weightage was arrived by adding 1 to 7 which totals to 28 and rank 1 was thus given a weightage of 7/28 = 0.25. Similar calculation yields weightage for rank 2 to 7 as 0.21, 0.18, 0.14, 0.11, 0.07 and 0.04 respectively. The data of the respondents were tabulated in the form of tables for both the workshops separately and also an overall table was prepared capturing the data of 123 respondents. The weighted average for each ranking was calculated and the drivers are ranked based on their weighted average score.

III. RESULTS AND DISCUSSIONS

The consolidated details of the driver analysis in UBLS covering the four groups of carriage Shop, production shops, maintenance shops and electrical wing are presented in tables No.4 below. The table shows the number of respondents choosing different ranks for each of the seven drivers considered in the study, apart from the weighted scores and the ranking for the respective group. 30 respondents out of 82 at UBLS ranked "dedication of management, engineers and staff" as the main driver for energy efficiency improvement which was seconded by 19 other respondents. The driver "awareness and adoption of latest technologies for EC" is a close second in all the four groups under study. It is very essential that unless the engineers are aware of the current technologies, improvements in energy front cannot be brought about. Due to increased awareness the major energy consuming equipment have been optimally loaded to reduce underutilization. This is one of the technical factors being introduced in UBLS. For example instead of having a centralized large capacity compressor like at MYSS, UBLS has gone for decentralization of air compressors, located them in the area where compressed air is required with capacities matching the requirement. As the engineers are all technically qualified and experienced, they do attach importance to EC measures and hence is ranked forth. Top management i.e. zonal railways and railway Board does encourage EC and awards energy efficiency shield to the best performing workshop. Also the officers, engineers with meaningful contribution are recognized and awarded during railway week celebrations annually. Officers from railway board, zonal headquarters review the position of workshops by personal inspections and also encourage EC activities by giving away spot awards. This is one good feature being adopted by railways to improve EC amongst the officers, engineers and staff.

The result analysis finds that all the four groups at UBLS show the similar ranking wherein it was evident that dedication of the top management, engineers and staff was the major driver for implementation and successful maintenance, sustenance of the energy efficiency measures. The ministry of railways i.e. railway board does circulate guidelines for implementing measures for EC and currently an list of 28 items is in force which is being actively pursued by the zonal railways. It is the sheer dedication of all the associates that the EC measures are properly installed, operated and successfully maintained. This was the major driver emerging from the analysis of all the four groups of the workshops. Railways has a dedicated organisation viz. Research, Design and Standards Organisation located at Lucknow in Uttar Pradesh which has a energy management cell and has come out with many a new technologies for energy efficiency for traction and non-traction applications. The awareness and adoption of latest technologies available for EC ranked second and the concern for planet earth, environment protection was ranked at the bottom. The workshop complies with all the statutory requirements of both central and state pollution boards and has got no issues with local pollution; it has never been an issue with the associates. It is evident from the study that as most of the engineers are elderly people who were educated two to three decades ago when environment was not an issue and as such they did not appreciate this driver as compared to the other six drivers. At railway workshops the share of energy as a percentage of total repairs or production cost is insignificant as such it is not considered as a major driving force.

Table. 4 Overall workshops weighted average scores of drivers at Carriage Repair Workshops- Hubli

Rank	1	2	3	4	5	6	7	Total	Weighted	Rank
Value	0.25	0.214	0.179	0.143	0.107	0.071	0.036	Response	Average	
Dedication of Mgt.	30	19	10	8	9	3	3	82	0.19	1
Awareness	12	20	23	10	7	6	4	82	0.17	2
Capacity Utilization	8	12	21	13	13	5	10	82	0.15	3
Top Management	12	6	5	19	12	16	12	82	0.14	5
Education of Associates	10	12	11	12	15	14	8	82	0.15	4
Recognition	3	9	8	15	17	24	6	82	0.12	6
Concern for planet Earth	7	3	3	6	9	15	39	82	0.08	7

Table. 5 Driver wise weighted average of all shops at Carriage Repair Workshops, Hubli

Weighted Average of	Officers & Electrical Shop	Maintenance Shop	Carriage Shop	Production Shop	Overall Workshop
Dedication of Mgt.	0.19	0.21	0.19	0.172	0.19
Awareness	0.17	0.16	0.17	0.161	0.17
Capacity Utilization	0.15	0.15	0.15	0.161	0.15
Top Management	0.14	0.13	0.14	0.156	0.13
Education of Associates	0.15	0.14	0.15	0.152	0.15
Recognition	0.13	0.12	0.13	0.114	0.13
Concern for planet Earth	0.08	0.09	0.08	0.087	0.09

Table. 6 Weighted average scores of drivers in Central Workshops- Mysore

Rank	1	2	3	4	5	6	7	TR	WA	Rank
Value	0.25	0.21	0.18	0.14	0.11	0.07	0.04			
Dedication of Mgt.	9	10	12	2	3	1	4	41	0.18	1
Awareness	7	7	5	10	7	2	3	41	0.16	2
Capacity Utilization	6	10	7	5	6	6	1	41	0.16	3
Top Management	3	4	5	5	9	8	7	41	0.12	6
Education of Associates	2	7	5	13	5	5	4	41	0.14	4
Recognition	3	1	4	3	8	13	9	41	0.10	7
Concern for planet Earth	11	2	3	3	3	6	13	41	0.13	5

TR – Total Responses, WA – Weighted Average

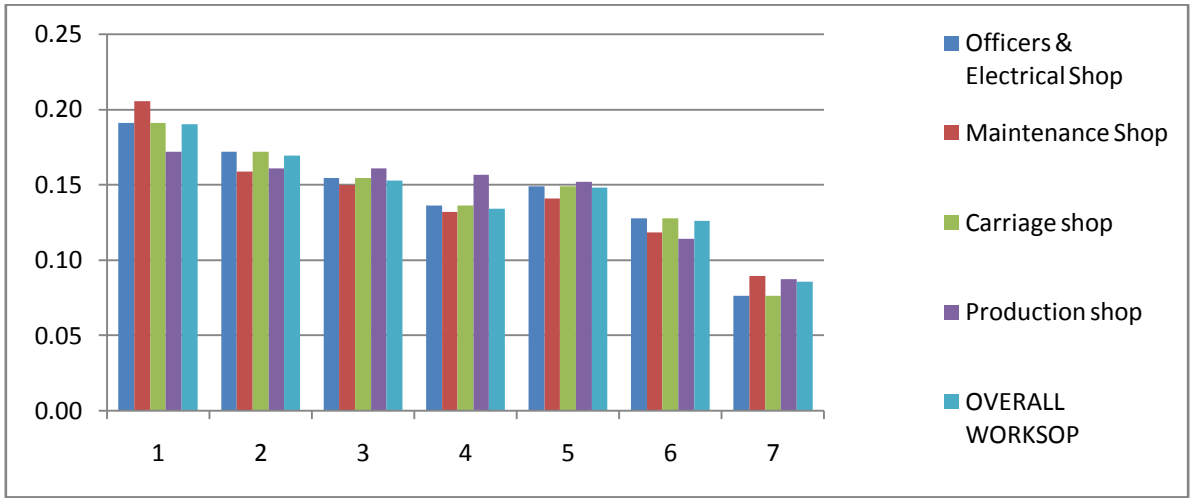

Fig. 2 Relative position of the drivers in the four group's driver wise at UBLS

LEGEND FOR FIGURE 2 AND TABLE 3

1. Dedication of management, Engineers and staff towards EC
2. Awareness & adoption of new technologies available for EC
3. Capacity Utilization of machines and plant
4. Top Management drive viz. by Railway Board and Zonal Railways
5. Education of Associates, Trainings provided
6. Recognition & Motivation of staff by Management towards EC
7. Concern for planet Earth, Environmental protection

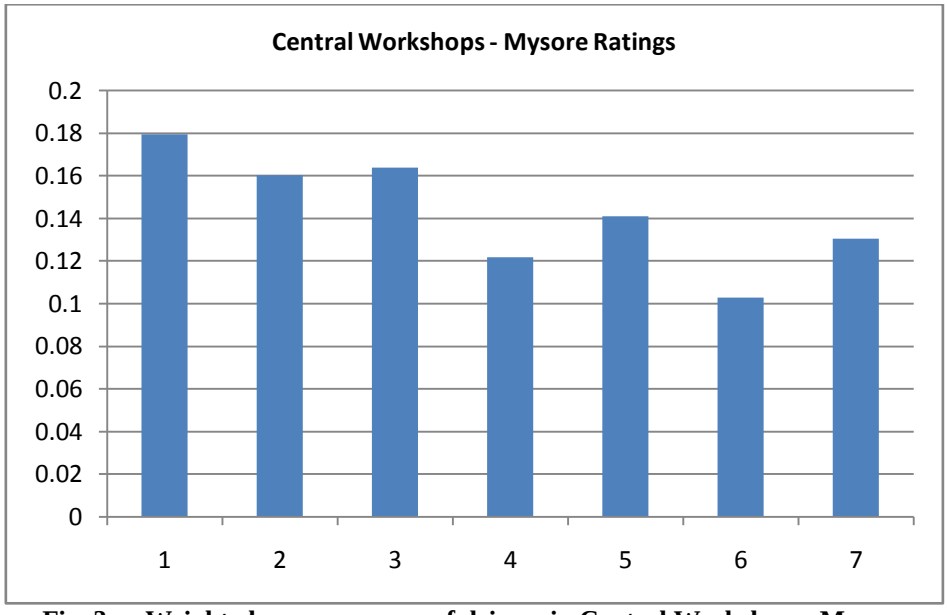

Fig. 3 Weighted average scores of drivers in Central Workshops- Mysore

A comparison of relative position of drivers in the four groups along with the overall workshop is illustrated in figure 1. On the whole all the four groups have the same ranking with dedication being at number 1, followed by awareness, capacity utilization, education, top management, recognition and the last being concern for planet earth. The rankings follow the order of questions except for position four and five which are swapped. The comparative bar chart of drivers in the study groups reinforces the inference deduced after comparing the four groups and it is clearly evident that the overall perceptions of the officers, engineers regarding the drivers to energy efficiency remain similar across the group irrespective of their functional activities.

It is easy to see the linkage among these findings. The lowest rank to environment is due to the fact that these workshops maintain a good quality of ambient air and follow the guidelines laid down by the pollution control boards. Accordingly the earlier activity of casting cast iron brake blocks at UBLS using cupola furnaces has been discontinued in the wake of increased indoor pollution levels. On a larger context the outcomes clearly indicate that railway workshops being government organizations maintain good environment conditions by utilizing clean fuels and procure the best and state of art equipments by way of global tendering process for the high end equipment. Necessary training and exposure to new ideas by way of conferences, workshops shall improve the energy management in all the shops.

IV. CONCLUSIONS

The result analysis finds show the similar first three ranking in both the workshops with total weighted average of greater than 0.5. The top ranked driver of both the workshops was dedication of the top management, Engineers and staff with a weighted average score of 0.18 and 0.19 respectively from MYSS and UBLS respectively. The driver "awareness and adoption of latest technologies for EC" is a close second with a weighted average of 0.16 and 0.17 respectively from MYSS and UBLS respectively. Capacity utilization is ranked third which again is common for both the workshops. It was found that due to better awareness about environment at MYSS, it was ranked fifth when compared to UBLS wherein it was ranked the last at seventh position. This clearly indicates that railways is mainly driven by the dedication of its personnel and its sustenance and improvements on the energy front continue to contribute mainly by them

The compilation of the data and its subsequent analysis has given the above results from which we can conclude that officers and electrical engineers group mention" dedication of management, engineers and staff towards the EC" as the strongest driver with an weighted score of 0.19. This is very apt from the fact that both the workshops have consistently reduced its energy requirements inspite of multifarious activities and also increases in quantities of few activities. Introduction of renewable energy in the form of solar thermal for water heating in canteen, solar PV for illumination of administrative building also has contributed to the energy savings. Study also reveals that in UBLS all the four groups have similar ranking for the drivers. The dedication of all the associates ensures that the energy usage is controlled, regular preventive maintenance of major equipment is undertaken, the health of the equipments are monitored and the subordinate staff are informally counseled for EC. The engineers and staff recruitment are undertaken in a very fair and transparent manner and as such the best get an opportunity to serve the great organisation. All the staff both supervisory and technicians are provided with induction training either for 6 months or for 12 months and as such it is essential that a module on EC should be a part of such training. This will improve the awareness and understanding of the concepts in energy management. Also the engineers and staff have ranked concern for environment at the last which calls for inculcating the importance of environment by way of educating them during their initial induction training.

V. ACKNOWLEDGEMENTS

Authors acknowledge with deep appreciation and gratitude the Chief Workshop Managers of UBLS and MYSS for permitting to undertake the study in their respective workshops and for their invaluable guidance throughout. Special thanks are due to the Divisional Electrical Engineers of both the workshops for their immense contribution in guiding and also in open discussions on the energy front. Thanks are due to all the officers and engineers of the two workshops for their valuable time, support, contribution and co-operation in conducting the study.

REFERENCES

[1] Suresh D. Mane and N. Nagesha, "Energy Conservation and Efficiency Improvement in Indian Railways: A Review", 2009 – Proceedings of National Conference on Advances in Mechanical Engineering, UBDT College of Engineering, Davangere.

[2] Suresh D. Mane and N. Nagesha, "Carriage Repair Workshops on Indian Railways: Study on Energy Conservation Potential" 2013, International Journal of Emerging Technology and Advanced Engineering Vol. 3, Special Issue 3, ICERTSD 2013, pp. 1-8.

[3] Standard Note of Carriage Repair Workshop, Hubli, January 2013.

[4] Standard Note of Central Workshop, Mysore, February 2013.

[5] N. Nagesha and P. Balachandra, "Energy Efficiency and Economic Performance in Small Scale Industry Clusters; An analysis of Influencing Factors, Barriers and Drivers": 2005.

[6] Patrik Thollander, Sandra Backlund, Andrea Trianni and Enrico Cagno, "Beyond Barriers- A Case study of Driving forces for Improved Energy Efficiency in the Foundry Industries in Finland, France, Germany, Italy, Poland, Spain and Sweden", Applied Energy, Vol. , 111, 2013, pp. 636-643.

American Journal of Engineering Research (AJER)
e-ISSN : 2320-0847 p-ISSN : 2320-0936
Volume-02, Issue-09, pp-265-275
www.ajer.org

Research Paper Open Access

Analyzing Public Emotion and Predicting Stock Market Using Social Media

Jahidul Arafat[1], Mohammad Ahsan Habib[2] and Rajib Hossain[3]
[1]Researcher, HT Research and Consultancy, UK.
[2]Department of Information and Communication Technology, Mawlana Bhashani Science and Technology University, Bangladesh
[3]Freelancer, oDesk, Bangladesh

Abstract: - The focus of this research was to build a cloud based architecture to analyze the correlation between social media data and the financial markets. From analytical point of view this study refurbish the viability of models that treat public mode and emotion as a unitary phenomenon and suggest the needs to analyze those in predicting the stock market status of the respective companies. With the aim to justify the correlation between social media and stock market prediction process our result reveals a proportional correspondence of pubic emotion over time with the company's market viabilities. The major significance of this research is the normalization and the conversion process that has utilized vector array list which thereby strengthen the conversion process and make the cloud storing easy. Furthermore, the experimental results demonstrate its improved performance over the factor of emotion analysis and synthesizing in the process of prediction to extract patterns in the way stock markets behave and respond to external stimuli and vice versa.

Keywords: - *Public Emotion, JSON, CSV, Hashtag.*

I. INTRODUCTION

Micro blogging is an increasingly popular form of communication on the web. It allows users to broadcast brief text updates to the public or to a limited group of contacts. In this micro blogging, stock market prediction has attracted much attention from academia as well as business. But can the stock market really be predicted? Early research on stock market prediction [1], [6], [34]-[36] was based on random walk theory and the Efficient Market Hypothesis (EMH) [4]. According to the EMH stock market prices are largely driven by new information, i.e. news, rather than present and past prices. Since news is unpredictable, stock market prices will follow a random walk pattern and cannot be predicted with more than 50% accuracy [2], [34].

However this research focused on to fetch the public emotions associating the several companies of UK and store them into a cloud. It enables the researcher to do further analysis on public sentiments to depict how the emotions change over time. It thereby assists the companies to decide on their stock market operational pattern.

This paper is organized as follows: section 2 presents literature reviews on the public emotional context while section 2.1 defines the public emotion and characteristics of tweets are described in section 2.2. Furthermore, section 3 and its subsequent sections presets technologies incorporated for sentiment management such as Query Generation and Tweet Management Technique and section 3.2 presents the Opinion Detection system that can be applied on tweets. Later section 3.3 portraits several existing software and technologies for analyzing those tweets and depicting the real cause of sentiments. Next to it is section 4 which presents the research's aim with that of the design, implementation, evaluation strategies and outcomes and both the limitations and advantages of it. Recommendation on further development is depicted in section 5. At the end, section 6 presents the degree upon which the research outcomes meet the objectives and section 7 comes out with some concluding remarks.

II. RELATED LITERATURE ON SENTIMENT ANALYSIS

An increasing number of empirical analyses of sentiment and mood are based on textual collections of public user generated data on the web. Sentiment analysis and opinion mining are now a research domain in

their own which sometimes referred to as \subjectivity analysis" | whose methods and applications were extensively surveyed in much details in [10].

Different methodological approaches have been used to extract sentiment from text. Some methods are grounded in natural language processing (NLP) and rely on word constructs (n-grams) found in text to extract sentiment towards a subject (favorable or unfavorable). NLP methods have been used to extract sentiment and opinion from texts such as camera [12] and pharmaceutical reviews [11]. Other techniques of sentiment analysis, rooted in machine learning, use support vector machines (SVM) to classify text in positive or negative mood classes based on pre-classified training sets. SVM has been used to classify noisy customer feedback data [9] and movie reviews using a 5-point scale [8]. A number of hybrid methods that blend NLP and machine learning techniques have also appeared in the literature [15].

Besides the textual content discussed thus far (movie reviews, camera reviews, customer feedback), sentiment analyses have touched on many different kinds of personal online content. Personal websites such as blogs and online journals are often awash with emotive information and have been extensively used to deduct everyday happiness [10], explore trends and seasonality [14], forecast mood [17] and predict sales of books [18] and movies [20]. Some similar analytical tools operate entirely on the web: We Feel Fine5 constantly harvests blog posts for occurrences of the phrases "I feel" and "I am feeling" and provides statistics and visualizations of past and current geo-tagged mood states. A similar online site, Mood views, constantly tracks a stream of Live journal weblogs that are user-annotated with a set of pre-defined moods.

The results generated via the analysis of such collective mood aggregators are compelling and indicate that accurate public mood indicators can be extracted from online materials. Using publicly available online data to perform sentiment analyses reduces enormously the costs, efforts and time needed to administer large-scale public surveys and questionnaires. These data and results present great opportunities for psychologists and social scientists. Yet, while blogs have largely been analyzed for mood patterns, not much research has yet addressed social networking sites and micro blogging platforms. Recently, emotion has been extracted from public communication on Myspace [22], [28] and status updates on Facebook, but this study could not find any large scale sentiment analysis of Twitter, other than a study focused on micro bloggers' response to the death of Michael Jackson [13], [15]. This may be due to the fact that micro blogging and social networking sites are fairly recent forms of online communication (at least when compared to blogs).

Scale may be an issue as well. Sentiment analysis techniques rooted in machine learning yield accurate classification results when sufficiently large data is available for testing and training. Minute texts such as micro blogs may however pose particular challenges for this approach. In fact, the Twitter analysis of Jackson's death mentioned above was performed using a term-based matching technique based on the Affective Norms for English Words (ANEW). ANEW provides pre-existing, norm emotional ratings for nearly 3,000 terms along three dimensions (pleasure, arousal, dominance) [21] and has been recently employed to measure mood of song lyrics, blog posts and U.S. Presidents speeches [26]. Since it doesn't require training and testing, this syntactical approach may enable sentiment analysis for very small text data where machine learning techniques may not be appropriate. Choi and Varian [27] shows that using emoticons as labels for positive and sentiment is effective for reducing dependencies in machine learning techniques.

1.1 Defining Public Emotion

To meet the objective of the study, sentiments or emotions are defined to be of personal positive or negative feeling. Table 1 shows some examples of these.

For example, the following tweet is considered neutral because it could have appeared as a news research headline, even though it projects an overall negative feeling about General Motors: *"RT @Finance Info Bankruptcy filing could put GMon road to profits (AP) http://cli.gs/9ua6Sb #Finance"* [12].
In this research, neutral tweets are not considered for further analysis. Only positive or negative tweets has been utilized for deriving sentiment. Many tweets do not have sentiment, so those referred as tweet of question mark.

Table 1. Tweet Example

Emotion	Query	Tweet
Positive	jquery	dcostalis: Jquery is my new best friend.
Neutral	San Francisco	schuyler: just landed at San Francisco
Negative	exam	jvici0us: History exam studying ugh.

1.2 Characteristics of Tweets

Twitter messages have many unique attributes, which differentiates this research from previous research [14], [29], [30] :

1. Length: The maximum length of a Twitter message is 140 characters.
2. Data availability: Another difference is the magnitude of data available. With the Twitter API, it is very easy to collect millions of tweets.
3. Language model: Twitter users post messages from many different media, including their cell phones. The frequency of misspellings and slang in tweets is much higher than in other domains.
4. Domain: Twitter users post short messages about a variety of topics unlike other sites which are tailored to a specific topic. This differs from a large percentage of past research, which focused on specific domains such as movie reviews.

III. TECHNOLOGIES INCORPORATING THE MANAGEMNT OF SENTIMENT ANALYSIS

1.3 Query Generation and Management Technique in Twitter

1.3.1 Twitter Search API

The Twitter Search API is a dedicated API for running searches against the real-time index of recent Tweets. There are a number of important things to know before using the Search API which is explained below [24].

However, one major limitation of this Twitter API is that it is not complete index of all Tweets, but instead an index of recent Tweets. At the moment that index includes between 6-9 days of Tweets. Moreover, one cannot use the Search API to find Tweets older than about a week. Furthermore, Queries can be limited due to complexity. If this happens the Search API will respond with the error: {"error":"Sorry, your query is too complex. Please reduce complexity and try again."}. In addition to this, search does not support authentication meaning all queries are made anonymously and search is focused in relevance and not completeness. This means that some Tweets and users may be missing from search results [12-15]. That's why, Choi and Varien [27] recommends the Streaming API if research require more completeness in data. But the near operator cannot be used by this Search API. Instead the geocode parameter could be used [5], [7], [23].

The best practices of this API ensure all parameters are properly URL encoded [9]. Include a since_id when asking for Tweets. since_id should be set to the value of the last Tweet has received or the max_id from the Search API response. If the since_id is provided older than the index allows, it will be updated to the oldest since_id available. Furthermore, Java et al. [7] suggests to include a meaningful and unique User Agent string when using this method. It will help to identify the traffic when one use shared hosting and can be used by this study to triage any issues that report. However, it limits the searches to 10 keywords and operators [37].

Constructing a Query: it involves the following three basic steps: (a) Run the search on twitter.com/search. (b) Copy the URL. For example: https://twitter.com/#!/search/%40twitterapi and (c) Replace https://twitter.com/#!/search/ with http://search.twitter.com/search.json?q=. For example: http://search.twitter.com/search.json?q=%40twitterapi [32].

1.3.2 Hashtag

A hashtag is simply a relevant word or series of characters preceded by the # symbol [11]. Hashtags help to categorize messages and can make it easier for other Twitter users to search for tweets [15].

When one search for or click on a hashtag he/she will see all other tweets that use the same hashtag (see Twitter Advanced search option) [21]. Only others who are interested in the same topic thread will likely be using the same hashtag. For example, if one search for "Apple company" then "#Apple" will assit in most for having that company oriented information instead of using "Apple" [12].

1.4 Scripting language for advance searching

JSON (JavaScript Object Notation) is a lightweight data-interchange format [22]. It is easy for humans to read and write. It is easy for machines to parse and generate. It is based on a subset of the JavaScript Programming Language, Standard ECMA-262 3rd Edition - December 1999. JSON is a text format that is completely language independent but uses conventions that are familiar to programmers of the C-family of languages, including C, C++, C#, Java, JavaScript, Perl, Python, and many others. These properties make JSON an ideal data-interchange language [33].

JSON is built on two structures: (a) A collection of name/value pairs. In various languages, this is realized as an object, record, struct, dictionary, hash table, keyed list, or associative array [11, 24]. (b) An ordered list of values. In most languages, this is realized as an array, vector, list, or sequence [25]-[27].

However, the structures that the JSON offer are universal in nature. Virtually all modern programming languages support them in one form or another. It makes sense that a data format that is interchangeable with programming languages also be based on these structures [4], [16], [22].

1.5 Opinion detection in Twitter

1.5.1 Emotion Corpus Based Method

Emotion Corpus Based Method is based on vector space model for calculating document similarity. For the emotion detection in tweets, an emotion corpus that is based on 8 basic classes can be used, E= {Anger, Sadness, Love, Fear, Disgust, Shame, Joy, Surprise}[3]. Each class represents a dimension in the Boolean emotion vector of a tweet. Look for emotion words in a tweet, and if found, set the corresponding class dimension in the emotion vector to 1, otherwise it remains 0 [12], [25].

Tweet: I was on Main Street in Norfolk when I heard about tiger woods updates and it made me feel angry, on 2009-12-11. Emotion vector: (1, 0, 0, 0, 0, 0, 0, 0).

For all the tweets in a chosen time interval, a centroid of all corresponding emotion vector dimensions can be calculated. This centroid is considered as a document for each interval [8]. For a given time interval T that contains N tweets, let V ={v1, v2, . . ., vN} be a set of vectors (with l = 8 dimensions each) generated from these tweets. Define centroid $\bar{v}$ for period T as [16]:

$$\bar{v} = \left(\frac{\sum_{k=1}^{k=N} v_k^1}{N}, \frac{\sum_{k=1}^{k=N} v_k^2}{N} \ldots, \frac{\sum_{k=1}^{k=N} v_k^t}{N}\right) \quad (1)$$

After finding centroid vector for each interval, define the opinion similarity between two intervals T1 and T2 by calculating cosine similarity between their centroid vectors as suggested by [24]:

$$Sim(T_1, T_2) = \frac{\overline{v_1}.\overline{v_2}}{|\overline{v_1}||\overline{v_2}|} \quad (2)$$

1.5.2 Set Space Model

Set Space Model prescribes representing each interval by a single document which is the union of the tweets posted in that particular time interval [11]. After removing the stop words and stemming the terms using Porter stemmer 3, collect all terms in a hash set for each interval as suggested by [24]. Define the similarity between two intervals T1 and T2 by calculating Jaccard Similarity [2]:

$$Sim(T_1, T_2) = \frac{|(Set)T_1 \cap (Set)T_2|}{|(Set)T_1 \cup (Set)T_2|} \quad (3)$$

To find the changes, neither corpus based method nor the set space model alone is suitable [19]. For the corpus based method, a change in the centroid can be misleading when the interval has very few emotion words compared to its neighbors [17]. For the set space model, a change in similarity does not by itself imply an opinion change, because not all of the words are emotion words. In this method, first analyze vector space similarity as suggested by [33]. If detect a possible change, validate it by analyzing the Jaccard Similarity [31].

Tn is a time break, if the followings are satisfied in both corpus based method and set space model:

$$Sim(T_{n-1}, T_n) < Sim(T_{n-2}, T_{n-1}) \quad (4)$$

$$Sim(T_{n-1}, T_n) < Sim(T_n, T_{n+1}) \quad (5)$$

1.6 Twitter Public emotion and opinion analysis: Software and Techniques

1.6.1 Opinion Finder (OF)

Opinion Finder (OF) is a publicly available software package for sentiment analysis that can be applied to determine sentence-level subjectivity [38], i.e. to identify the emotional polarity (positive or negative) of sentences. It has been successfully used to analyze the emotional content of large collections of tweets [19] using the OF lexicon to determine the ratio of positive versus negative tweets on a given day. The resulting time series were shown to correlate with the Consumer Confidence Index from Gallup4 and the Reuters/University of Michigan Surveys of Consumers5 over a given period of time. Weadopt OF's subjective lexicon that has been established upon previous work [3], [6], [20].

Like many sentiment analysis tools OF adheres to a uni-dimensional model of mood, making binary distinctions between positive and negative sentiment [25]. This may however ignore the rich, multi-dimensional structure of human mood. To capture additional dimensions of public mood a second mood analysis tools, labeled GPOMS, that can measure human mood states in terms of 6 different mood dimensions, namely Calm, Alert, Sure, Vital, Kind and Happy can further be used [12], [17], [29].

1.6.2 Google-Profile of Mood States (GPOMS)

GPOMS' mood dimensions and lexicon are derived from an existing and well-vetted psychometric instrument, namely the Profile of Mood States (POMS-bi) [4], [22]. To make it applicable to Twitter mood analysis it can expanded the original 72 terms of the POMS questionnaire to a lexicon of 964 associated terms by analyzing word co-occurrences in a collection of 2.5 billion 4- and 5-grams6 computed by Google in 2006 from approximately 1 trillion word tokens observed in publicly accessible Web pages [6]. The enlarged lexicon of 964 terms thus allows GPOMS to capture a much wider variety of naturally occurring mood terms in Tweets and map them to their respective POMS mood dimensions. Then match the terms used in each tweet against this

lexicon. Each tweet term that matches an n-gram term is mapped back to its original POMS terms (in accordance with its co-occurrence weight) and via the POMS scoring table to its respective POMS dimension. The score of each POMS mood dimension is thus determined as the weighted sum of the co-occurrence weights of each tweet term that matched the GPOMS lexicon [32]-[34].

To enable the comparison of OF and GPOMS time series it can be normalized to z-scores on the basis of a local mean and standard deviation within a sliding window of k days before and after the particular date. For example, the z-score of time series Xt, denoted ZXt ,is defined as [38]:

$$\mathbb{Z}_{X_t} = \frac{X_t - \bar{x}(X_{t\pm k})}{\sigma(X_{t+k})} \quad (6)$$

Where, (Xt±k) and (Dt±k) represent the mean and standard deviation of the time series within the period [t−k, t + k]. This normalization causes all time series to fluctuate around a zero mean and be expressed on a scale of 1 standard deviation

The mentioned z-score normalization is intended to provide a common scale for comparisons of the OF and GPOMS time series [39]. However, to avoid so-called "in-sample" bias, Bayir [4] suggests not to apply z-score normalization to the mood and DJIA time series that are used to test the prediction accuracy of the Self-Organizing Fuzzy Neural Network.

1.6.3 Self-Organizing Fuzzy Neural Network

SOFNN has been developed specifically for regressions, function approximation and time series analysis problems [29]. Compared with some notable fuzzy neural network models, such as the adaptive-network-based fuzzy inference systems (ANFIS), self-organizing dynamic fuzzy neural network (DFNN) and GDFNN, SOFNN provides a more efficient algorithm for online learning due to its simple and effective parameter and structure learning algorithm . In some researches work, SOFNN has proven its value in electrical load forecasting, exchange rate forecasting and other applications [31]-[32].

IV. RESEARCH DESIGN

1.7 Research Aim

The aim of this research is to build a cloud based architecture to further analyze the correlation between social media data and the financial markets.

1.8 Complete Design Artifact

This design artifact presents the structure the way the research and the program will work. It presents a skeleton portraying the blocks and sequence of operations.

1.8.1 The Block Diagram

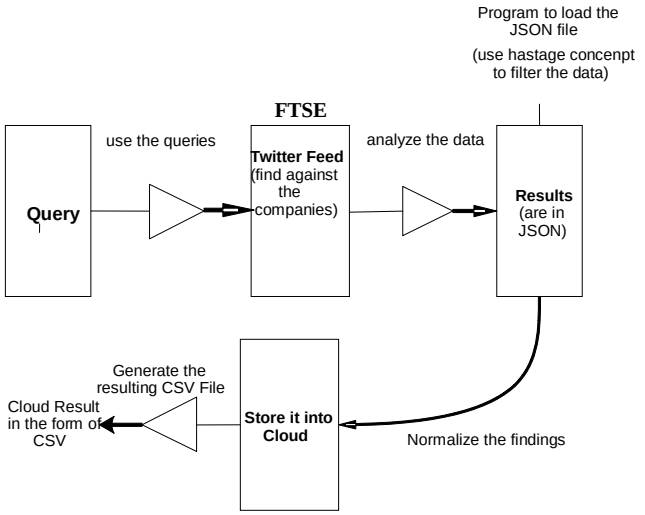

Fig 1: The block diagram

This block diagram is composed of four phases. In the first phase the queries that need to be executed to find out the public mood on the corresponding companies have to be designed and need to be associated in the program. However the structure of these queries will be the same as depicted in the above sections. Once after the queries and their associated codes has been incorporated into the program, the resulting tweeter feed consisting positive, negative or question mark or default feeds will be fetched from the tweeter database. After

gathering the required tweet feed, the data has to be analyzed and the results need to be generated in JSON. For that a program which will load that JSON file is preloaded a prior. After the loading and execution of that program the next step is to normalize all the findings and store into a cloud. For that the program will use a conversion technology to store the outcomes into a CSV file. However, before that when fetching down the tweets or feeds the available hashtag technology of twitter will be used which is further details in section 4.3.2.

1.9 Technologies and methods used for implementation

1.9.1 JSON

This research acknowledges the use of JSON data structures that generates the outputs based on the inputs received from queries and display and store the resultant outcomes into cloud.

1.9.2 The tweet fetching and cloud storing process

To normalize all the finding and store into a cloud this program has used a conversion technology to store the outcomes into a CSV file. However, before that when fetching down the tweets or feeds, the available hangtag technology of tweeter is also used. Moreover to identify the emotional polarity (positive or negative) of sentences lexical analysis was done using the keywords provided by tweeter where "love" for positive feeds, "hate" for negative feeds and "traffic" for question mark feeds, "Hate" or "Traffic" for negative question mark feeds, "love" or "traffic" for positive question mark feeds and "mixed" for all kinds of feeds and "Popular" for the recent and by default feeds were used. Finally the public modes of the corresponding companies were converted and stored in cloud in the form of the separate CSV file for further analysis or comparisons. This CSV file conversion process utilized vector array list for getting data and then put that data into JTable. The associated code of this tweet fetching and CSV file storing process details in the next subsequent sections.

As stated in earlier section, the design of the searching process should have the number of tweets to be searched, the number of pages on which the tweets can be displayed at maximum and the company name for which to search.

V. PROGRAM EVALUATION

The evaluation of this research has outcome with a cluster of seven steps as show below where step 1: the main GUI will be "enabled" to do the rest of the operation. Upon choosing the search option a new dialog box has been opened in step 2, where all the necessary search options i.e. number of tweets to be searched, how many pages in where results to be shown, for which company public emotions to be searched along with the category of tweets to be fetched i.e. positive, negative or question marked is enlisted. Upon selection of all these and clicking on the OK button as tweets associating that particular company has been fetched into a textbox in step 3. Next all these resultant tweets have to be saved in a CSV file. Upon choosing the save and location the file automatically converted into the CSV format in step 4. These process has been repeated for all of the enquired companies that the study focused into. The overall evaluation process of this implementation is depicted in the following series of illustration.

1.10 Survey Results

The entire survey results have been clustered around three sessions as tabulated below to show how the public emotion on a particular company of share market changes over time.

Table 2. Session Duration

Session Duration	1/04/2012 to 10/04/2012	11/04/2012 to 20/04/2012	21/04/2012 to 30/04/2012

1.10.1 Result on HSBC

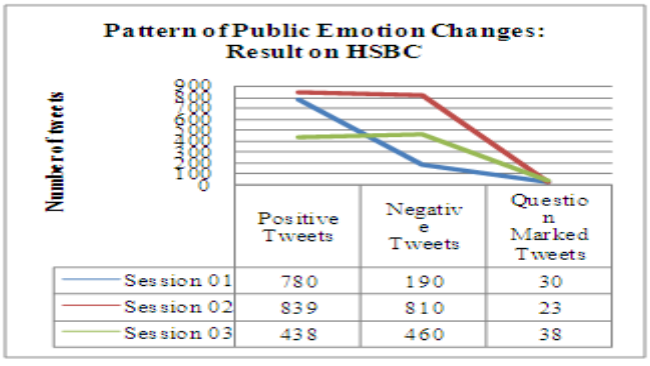

Fig 4: Pattern of public emotion change: result on HSBC

Table 3. Pattern of public emotion change: result on HSBC-Session wise breakdown

	Session 01	Session 02	Session 03
Number of Tweets	1000	1672	936
The oldest one	HSBC offers new deals to first time buyers - HSBC has launched new mortgage products for those with a 10 per...		

1.10.2 Result on GSK

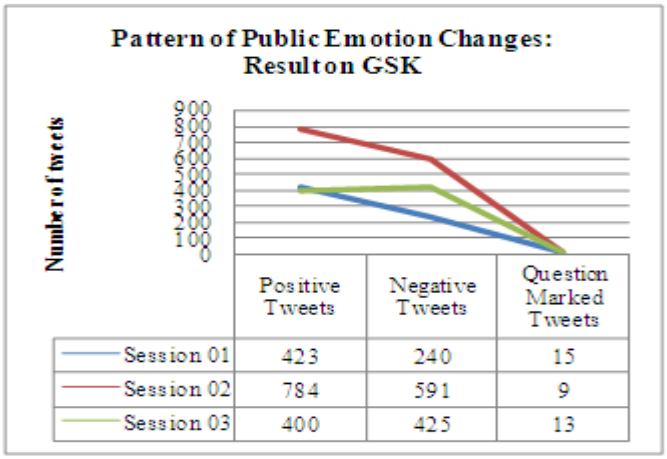

Fig 5: Pattern of public emotion change: result on GSK

Table 4. Pattern of public emotion change: result on GSK-Session wise breakdown

	Session 01	Session 02	Session 03
Number of Tweets	678	1348	837
The oldest one	**GSK** fined measly $90,000 by Argentine court for killing 14 babies in illegal vaccine trials: pewsitter.com/page_1.html#nw… **#FB**		

1.10.3 Result on BAE System

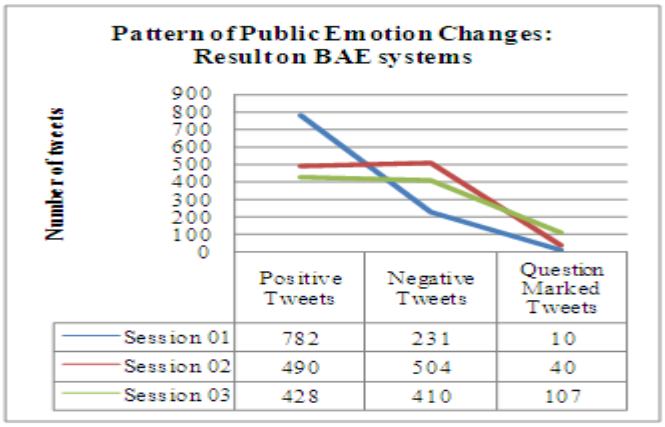

Fig 6: Pattern of public emotion change: result on BAE System

Table 5. Pattern of public emotion change: result on BAE System-Session wise breakdown

	Session 01	Session 02	Session 03
Number of Tweets	1023	1034	945
The oldest one	The Week Ahead: Results due from **BAESystems**, Cable & Wireless, Thorntons ...: Domino's Pizza will roll out more...		

1.10.4 Result on BP

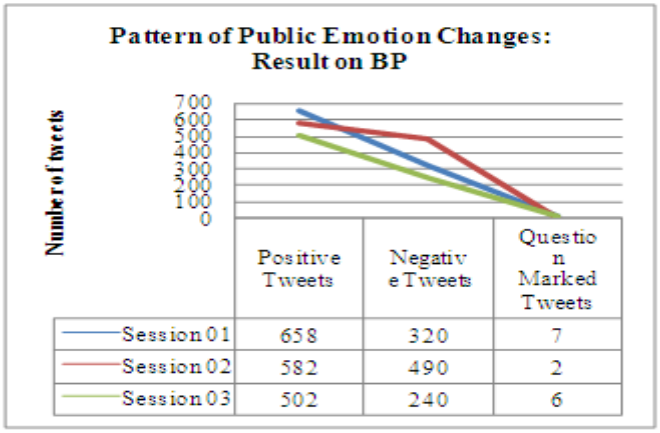

Fig 7: Pattern of public emotion change: result on BP

Table 6. Pattern of public emotion change: result on BP-Session wise breakdown

	Session 01	Session 02	Session 03
Number of Tweets	985	1074	740
The oldest one	**BP** wins exclusion of emails from oil spill trial reut.rs/wuyNMP via @Reuters		

1.10.5 Result on BSysB

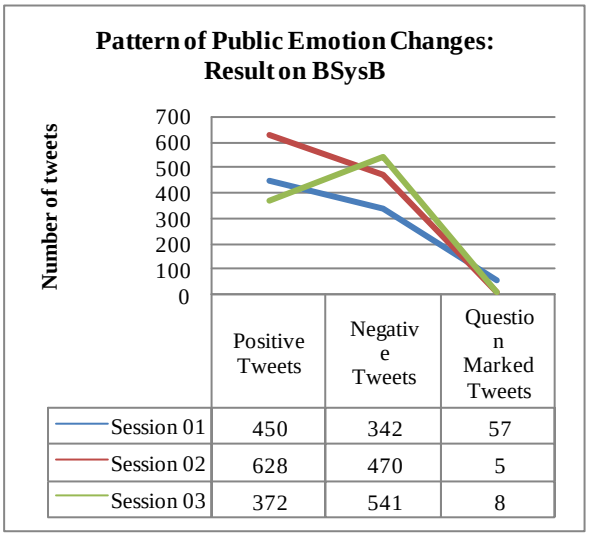

Fig 8: Pattern of public emotion change: result on BSysB

Table 7. Pattern of public emotion change: result on BSysB-Session wise breakdown

	Session 01	Session 02	Session 03
Number of Tweets	849	1103	921
The oldest one	**BSysB**is one track for next business run… great news indeed….!!		

1.10.6 Summary of the Results: Impact of the results on predicting share market causes

All these results tabulated above depict how the public emotions had changed over time on a particular company. The emotion carves and charts presents the time variant fluctuations. This found to be high on positive response in some sessions but high on negative responses in other sessions. Thereby these illustrates the people's

changing nature and thought regarding a particular company. The oldest tweets on each company as depicted above with that of other fetched tweets. All these portraits somehow the reasons behind all the changing emotion dimensions which is further details in section 5.3.

1.11 Main Findings

Fetching the public emotion, analyzing them and enabling those to predict the share market pattern was the prime concern of this research to undertake. The findings of this study illustrates that the mathematical prediction morphology is of significant interest for the present stock market of UK. The experiments indicate that the proposed emotion fetching and analyzing solution enables companies of UK to figure out the social impact of share market vulnerabilities. These further assist the share market leaders to do justification on their market setting while associating the public concern. These would also help the regulatory body of share market to have a holdings on the market setting by configuring market leaders social responses and activities.

1.12 Evaluation

This study has investigated whether public mood measured from large-scale collection of tweets posted on twitter.com is correlated with market prediction. The results show that changes in the public mood state can indeed be tracked from the content of large-scale twitter feeds by means of rather simple text processing techniques and that such changes respond to a variety of socio-cultural drivers in a highly differentiated manner. Changes of the public mood as that the change in the market ground of those companies found to be proportional while incorporating the social media and stock market prediction processes.
Public mood analysis from Twitter feeds on the other hand offers an automatic, fast, free and large-scale addition to this toolkit that may in addition be optimized to measure a variety of dimensions of the public mood state.

5.4 Advantages of the Research

This research has a number of potential implications i.e. here public mood is measured from large-scale collection of tweets posted on twitter.com and correlated through this designed toolkit. The normalization and the conversion process has utilized vector array list which thereby strengthen the conversion process and make the cloud storing an easy.

5.5 Limitations

The concerned time limit restricted the researcher to focus only on the following two dimensions instead of going for analyzing the whole set of stoke market pattern: (a) calculated the share fluctuations in the form of numeric from the posed tweets and (b) graphically depicting how the emotions changes over time. However, inclusion of other research dimensions could strengthen the research outcomes. Furthermore, more lexical analysis could be done on the posted tweets for robust vector analysis and clustering instead of using just the twitter factory defined keywords. Besides, when fetching the tweets it found to have some junk comments written other than using pure English grammatical syntax. In addition, limiting the scope only in twitter rather than utilizing other forms of social media invokes the further constraint to this study.

5.6 Reflection of the objective

The major objective of this research was to fetch the different dimensions of public emotion associating the stock market of UK and store them into a cloud. Along with this, the research aimed to justify whether the sentiment or emotion attached to a specific company changes over time. Execution of this program however reveals a proportional correlation with the company's market viabilities over time. This thereby will assist the companies to evaluate their stakeholder's concerns and set their new stock market strategy while assessing the public sentiments and emotions.

VI. FUTURE WORK

This work was a short term social-economic research and many extents of it could not be explored because of time limitation. Thereby this study suggests the following strategies for the further improvement: (a) Store the tweets or feed into Array. (b) Do lexical analysis on the stored feeds to retrieve the meaning of it (c) To aid to this analysis process all the English words associating the meaning to positive, negative or neutral are recommended to be gathered and stored into three different text file such as hate.txt, question.txt and positive.txt. (e) Read those files using java FileReader function or equivalent function and bring the associating words into Array. (f) Compare those words with the each words in the comment field. (g) Finally, categorize the feeds into associating field of emotion.

Furthermore a Self-Organizing Fuzzy Neural Network can be used to train the program on the basis of past DJIA values. The public mood time series will demonstrate the ability to improve the accuracy of the most

basic models to predict DJIA closing values. Given the performance increase for a relatively basic model such as the SOFNN, this study is hopeful to find equal or better improvements for more sophisticated market models which will associate new sources and a variety of relevant economic indicators. These results will have implications for existing sentiment tracking tools in which individual's evaluate the extent to which they experience positive and negative effect, happiness, or satisfaction with life. However, due to shortage of time it could not be done but suggest that this program will further be evaluated on it. However, such surveys are relatively expensive and time-consuming, and may not allow the measurement of public mood along with the mood dimensions that are relevant to assess particular socio-economic indicators.

VII. CONCLUSION

This study only focused on the stock market of UK to analyze the associating public mode and emotions. Information being fetched on those companies identified the factors and the outcomes reveals the correlation those exists among the people's emotion and market practice of a current organization.

VIII. ACKNOWLEDGMENTS

Our thanks to HTRC, a subsidiary organ of HMRC, London, UK, which has contributed towards completion of this research.

REFERENCES

[1] Li C.T., Wang C.Y., Tseng C.L. and Shou-De L. 2011. A sentiment-based audiovisual system for analyzing and displaying micro blog messages, Proceedings of the 49th Annual Meeting of the Association for Computational Linguistics: Human Language Technologies: Systems Demonstrations, p.32-37, June 21-21,Portland, Oregon.

[2] Guerra P.H.C., Adriano V., Wagner M.J. and Virgílio A. 2011. From bias to opinion: a transfer-learning approach to real-time sentiment analysis, Proceedings of the 17th ACM SIGKDD international conference on Knowledge discovery and data mining, August 21-24, San Diego, California, USA.

[3] Agarwal A., Boyi X., Vovsha L., Owen R. and Rebecca P. 2011. Sentiment analysis of Twitter data, Proceedings of the Workshop on Languages in Social Media, p.30-38, June 23-23, Portland, Oregon.

[4] Bayir M. A., Toroslu I. H., Cosar A., and Fidan G. 2009. Smart miner: a new framework for mining large scale web usage data. In WWW, pages 161–170.

[5] Cao H., Jiang D., Pei J., He Q., Liao Z., Chen E., and Li H. 2008. Context-aware query suggestion by mining click-through and session data. In KDD, pages 875–883.

[6] Diakopoulos N. and Shamma D. A. 2010. Characterizing debate performance via aggregated twitter sentiment. In Conference on Human Factors in Computing Systems (CHI), April.

[7] Java, Song X., Finin T., and Tseng B. 2007. Why we twitter: understanding microblogging usage and communities. In Proceedings of the 9th WebKDD and1st SNA-KDD 2007 workshop on Web mining and social network analysis, pages 56–65. ACM.

[8] Jin W., Ho H. H., and Srihari R. K. 2009. Opinionminer: a novel machine learning system for web opinion mining and extraction. In KDD, pages 1195–1204.

[9] Kwak H., Lee C., Park H., and Moon S. B. 2010. What is twitter, a social network or a news media? In WWW, pages 591–600.

[10] Pang and Lee L. 2007. Opinion mining and sentiment analysis. Foundations and Trends in Information Retrieval, 2(1-2):1–135.

[11] Chang C.C. and Lin C.J. 2011. LIBSVM: A library for support vector machines. ACM Transactions on Intelligent Systems and Technology, 2:27:1–27:27.

[12] Jansen J., Zhang M., Sobel K., and Chowdury A. 2009. Micro-blogging as online word of mouth branding. In CHI EA '09: Proceedings of the 27th international conference extended abstracts on Human factors in computing systems, pages 3859{3864, New York, NY, USA, ACM.

[13] Pang B. and Lee L. 2008. Opinion mining and sentiment analysis. Foundations and Trends in Information Retrieval, 2(1-2):1.

[14] Dodds, P. S., and Danforth, C. M. 2009. Measuring the happiness of Large-Scale written expression: Songs, blogs, and presidents. Journal of Happiness Studies 116.

[15] Gilbert, E., and Karahalios, K. 2010. Widespread worry and the stock market. In Proceedings of the International Conference on Weblogs and Social Media.

[16] Hopkins, D., and King, G. 2010. A method of automated nonparametric content analysis for social science. American Journal of Political Science 54(1):229–247.

[17] Lindsay, R. 2008. Predicting polls with Lexicon. Available Online (accessed on: 22 January, 2012) http://languagewrong.tumblr.com/post/ 55722687/predicting-polls-with-lexicon.

[18] Manning, C. D., Raghavan, P. and Schutze, H. 2008. Introduction to Information Retrieval. Cambridge University Press, 1st edition.
[19] Mei, Q., Ling, X., Wondra, M., Su, H. and Zhai, C.X. 2007. Topic sentiment mixture: modeling facets and opinions in weblogs. In Proceedings of the 16th International conference on World Wide Web.
[20] Ounis, I., MacDonald, C. and Soboroff, I. 2008. On the TREC blog track. In Proceedings of the International Conference on Weblogs and Social Media.
[21] Pang, B. and Lee, L. 2008. Opinion Mining and Sentiment Analysis. Now Publishers Inc.
[22] Velikovich, L., Blair-Goldensohn, S., Hannan, K. and Mc- Donald, R. 2010. The viability of web-dervied polarity lexicons. In Proceedings of Human Language Technologies: The 11th Annual Conference of the North American Chapter of the Association for Computational Linguistics.
[23] Wilcox, J. 2007. Forecasting components of consumption with components of consumer sentiment. Business Economics 42(4):2232.
[24] Johan B., Huina M. and Xiaojun Z. 2011. Twitter mood predicts the stock market. Journal of Computational Science 2, p.1–8.
[25] Asur S., Huberman B.A. 2010, Predicting the Future with Social Media, http://www.arxiv.org arXiv:1003.5699 v.1.
[26] Bergsma S., Dekang L. and Goebel R. 2009. Web-scale N-gram models for lexical disambiguation, in: Proceedings of the Twenty-first International Joint Conference on Artificial Intelligence (IJCAI-09), Pasadena, CA, pp. 1507–1512.
[27] Choi H. and Varian H. 2009. Predicting the Present with Google Trends, Tech. rep., Google.
[28] Dodds P.S. and Danforth C.M. 2009. Measuring the happiness of large-scale written expression: songs, blogs, and presidents, Journal of Happiness (July).
[29] Edmans D. and García O.Y., 2007. Sports sentiment and stock returns, Journal of Finance 62 (4), 1967–1998.
[30] Frey B.S. 2008. Happiness: A Revolution in Economics, MIT Press Books, The MIT Press, June. Available Online (accessed on: 22 January, 2012) http://ideas.repec.org/b/mtp/titles/0262062771.html.
[31] Gilbert, K.K. 2010. Widespread worry and the stock market, in: Fourth International AAAI Conference on Weblogs and Social Media, Washington, DC, pp. 58–65.
[32] Mao H., Zeng X.J., Leng G., Zhai Y. and Keane J.A. 2009. Short and mid-term load forecasting using a bilevel optimization model, IEEE Transactions On Power Systems 24 (2), 1080–1090.
[33] O'Connor, Balasubramanyan R., Routledge B.R. and Smith N.A. 2010. From tweets to polls: linking text sentiment to public opinion time series, in: Proceedings of the International AAAI Conference on Weblogs and Social Media, Washington, DC, May.
[34] Pak, P.P. 2010. Twitter as a corpus for sentiment analysis and opinion mining, in: N. Calzolari, K. Choukri, B. Maegaard, J. Mariani, J. Odijk, S. Piperidis, M. Rosner, D. Tapias (Eds.), Proceedings of the Seventh conference on International Language Resources and Evaluation (LREC'10), European Language Resources Association (ELRA), Valletta, Malta, May, pp. 19–21.
[35] Pang and Lee L. 2008. Opinion mining and sentiment analysis, Foundations and Trends in Information Retrieval 2 (1–2), 1–135.
[36] Prechter R.R. and Parker W.D. 2012, The financial/economic dichotomy in social behavioral dynamics: the socioeconomic perspective, Journal of Behavioral Finance 8 (2) (2007) 84–108.
[37] Schumaker R.P. and Chen H. 2009. Textual analysis of stock market prediction using breaking financial news, ACM Transactions on Information Systems 27 (February (2)) (2009) 1–19.
[38] Zhang X., Fuehres H. and Gloor P.A. 2010, Predicting Stock Market Indicators Through Twitter I Hope It is Not as Bad as I Fear, Collaborative Innovation Networks (COINs), Savannah, GA.
[39] Zhu X., Wang H., Xu L. and Li H. 2008, Predicting stock index increments by neural networks: the role of trading volume under different horizons, Expert Systems with Applications 34 (4) 3043–3054.

American Journal of Engineering Research (AJER)
e-ISSN : 2320-0847 p-ISSN : 2320-0936
Volume-02, Issue-09, pp-276-281
www.ajer.org

Research Paper Open Access

Analysis and Evaluation of Government-Websites' Accessibility: Bangladesh Perspective.

Subhra Prosun Paul, Afzal Hossain, Sharmin Rashid

[1] *East West University, Dhaka,Bangladesh,*
[2] *IIT,University of Dhaka,Dhaka,Bangladesh,*
[3] *IIT,University of Dhaka,Dhaka,Bangladesh,*

Abstract: **-** The Web is a progressively more important resource in many aspects of life: education, employment, government, commerce, healthcare, recreation, and more. It is essential that the web be accessible to people with equal access and equal opportunity to all also with disabilities. An accessible web can also help people with disabilities more actively contribute in society. This paper concentrates on mainly two things; firstly, it briefly examines accessibility guidelines, evaluation methods and analysis tools. Secondly, it analyzes and evaluates the web accessibility of e-Government websites of Bangladesh according to the 'W3C Web Content Accessibility Guidelines'. We also present a recommendation for improvement of e-Government website accessibility in Bangladesh.

Keywords: **-** *Web accessibility, Accessibility guidelines, Assistive tools, e-Government, Accessibility testing and evaluation.*

I. INTRODUCTION AND OBJECTIVES

The use of information and communication technology (ICT) has been playing a vital role in the 21st century due to globalization and the governments of the countries are being encouraged to adapting with the coming future. Likewise the democratic government of Bangladesh has declared the "Vision 2021" in the election manifesto which targets establishment of a resourceful and modern country by 2021 through effective use of information and communication technology - a "Digital Bangladesh". The government of Bangladesh has realized the importance of ICT to improve the delivery of information and services to citizens and business. And now the changes are being seen in many sectors like education, business, and agriculture, healthcare. Besides the government initiatives, private sectors are also keeping their vital roles to fulfill the target of "Vision 2021" by embracing the World Wide Web for delivering information and services to their clients.

Though Web is an exciting technological tool to communicate with people, it does require innovative and easily recognizable design to make it accessible to everyone, including people with disabilities. Most of services and facilities provided in the past decades on behalf of the United Nations or the country governments for the poor or deprived community, it is found that were not equally distributed all the targeted people. That means the persons with disabilities are often discriminated of their basic needs including health care, housing, education, employment and other opportunities. They are the poorest of the poor community. This situation is more or less same in all over the world.

In Bangladesh the estimated number of persons with disabilities is around 10% of its total population [2]. The persons with disability are most neglected part of the country. Disable people cannot participate in the current development stream in spite of the Disabled Welfare Act 2001 [7]. Widespread discrimination against them and their exclusion from mainstream society lead to extensive economic hardship and loss of their creative capabilities. In respect of web accessing facility the situation has been more worsened. Hindering a large amount of people with disabilities in from accessing web, it will cause a delay to achieve the goal of "Digital Bangladesh".

Accessibility in terms of web design generally refers to facilitating the use of technology for people with disabilities with any impairment, no matter what its severity [4]. The researchers analyze primarily five

Bangladesh-government websites' to assess its accessibility. This paper aims to discover to what extent web accessibility is considered by the government's websites of Bangladesh. Therefore, it investigates whether the government websites conform to international accessibility guidelines (W3C WCAG 1.0) [3] or not and if not, what are the reasons behind that. This paper comes to an end giving a recommendation to improve the accessibility.

II. WEB ACCESSIBILITY AND ITS IMPACT

Accessibility can be defined as the quality of a web site that makes it possible for people to use it – to find it navigable and understandable – even when they are working under limiting conditions or constraints [8]. Suppose you have developed a website with versatile & rich features. A large number of users are visiting your sites daily to get your service. Each page of your site has many images suppose users' avatars, products' image etc. Then a blind person or with very low vision how will he able to browse your pages and get the service. Another thing may happen the users sometimes want to browse web pages without downloading images due to very low internet speed. So you should have to provide proper information (e.g. alternative text) in the case of missing images. If your website does not cover this situation or has a limited access into the targeted web users, you have lack of web accessibility. Accessibility is about designing so that **more people** can use your web site **effectively** in **more situations**.

Web accessibility is not a new idea. Despite the extensive web accessibility work accomplished in a few areas, the majority of web site designers and developers were, in the recent past, not aware of accessibility issues at all. This is not the case that they even know the term; actually they think that it will not cause any effect in their business. It is estimated that between 15% and 30% of the total general people (i.e. 750 million) in the world have functional disability to use technology tools [9]. Again in the coming days this figure will increase due to some factors e.g. as we are growing older, most people experience a decrease in vision, hearing, physical abilities, and cognitive abilities [10]. So just think who once was one of your big customers will be lost from you in turn because of the accessibility limitations. Accessible web sites accommodate a wider range of customers and constituents, increasing the number of people who can effectively use your website which will promote your business day by day.

In many countries, the Web is increasingly used for government information and services, education and training, commerce, news, workplace interaction, civic participation, health care, recreation, entertainment, and more. In some cases, the Web is replacing traditional resources. Therefore**,** it is essential that the Web be accessible in order to provide equal access and equal opportunity to people with disabilities. The Web was initially designed as a medium for sharing information, where in addition of accessing information, one can also contribute information. People with disabilities are able to contribute content to the Web by ensuring its accessibility. Moreover an organization that are committed to corporate social responsibility (CSR), providing an accessible website is one way an organization can demonstrate its commitment to rendering equal opportunities.

III. WEB ACCESSIBILITY GUIDELINES

A numerous efforts and works for establishing standard Web Accessibility Guidelines are governed by many web-groups and organization separately or in cooperatively with World Wide Web Consortium (W3C) [8]. In 1997, the World Wide Web Consortium established the Web Accessibility Initiative (WAI – http://www.w3.org/wai) and in 1999 the Web Content Accessibility Guidelines (WCAG) 1.0 were finalized as a Recommendation. Its primary goal was to promote and achieve Web functionality for people with disabilities. However, following the guidelines (by programmers, designers) will also make Web content more available to all users, whatever user agent they are using (e.g., desktop browser, voice browser, mobile phone, automobile-based personal computer, etc.) or constraints they may be operating under (e.g., noisy surroundings, under- or over-illuminated rooms, in a hands-free environment, etc.). Following these guidelines will also help people find information on the Web more quickly [3].

WCAG 1.0 encompasses a series of checklist which are available in a tabular form as in [11]. Each checkpoint has a priority level assigned by the W3C Working Group based on the checkpoint's impact on accessibility. There are total three priority levels for the checklist and their conformance level according to number of priority level satisfied are listed in table 1.

Table I: WCAG 1.0 Priority with Conformance Level

Priority	Description	Conformance Level

[1]	A Web content developer **must** satisfy this checkpoint. Otherwise, one or more groups will find it impossible to access information in the document. Satisfying this checkpoint is a basic requirement for some groups to be able to use Web documents.	"A": all Priority 1 checkpoints are satisfied
[2]	A Web content developer **should** satisfy this checkpoint. Otherwise, one or more groups will find it difficult to access information in the document. Satisfying this checkpoint will remove significant barriers to accessing Web documents.	"Double-A": all Priority 1 and 2 checkpoints are satisfied;
[3]	A Web content developer **may** address this checkpoint. Otherwise, one or more groups will find it somewhat difficult to access information in the document. Satisfying this checkpoint will improve access to Web documents.	"Triple-A": all Priority 1, 2, and 3 checkpoints are satisfied;

IV. WEB ACCESSIBILITY EVALUATION TOOLS

Web accessibility evaluation tools are software programs or online services that are used to check your website's accessibility level under web accessibility guidelines. There is a huge number of accessibility tools for commercial purposes or freely available on the web such as Watch Fire Bobby, AChecker, Cynthia Says, EvalAccess etc. Some good free web-based website accessibility evaluation tools are linked in [15]. A complete list of accessibility evaluation tools is in W3C [13]. These tools are very useful for programmers and designers to determine whether or not their sites follow WCAG. During the design, implementation, and maintenance phases of Web development if these tools are used carefully, it can help the targeted users in preventing accessibility barriers, repairing encountered barriers, and improving the overall quality of Web sites [14].

V. ASSISTIVE TECHNOLOGY

Assistive technologies are hardware or software or combination of both used by persons with disabilities to increase, maintain, and improve the functional capabilities in spite of their physical or mental impairments. Assistive technologies enable people to communicate, receive instruction, learn, play, move about, achieve, and be independent. This can also help the families of people with disabilities and his surroundings to be benefited. Instead of a wife having to read the mail of a person who has visual impairment, he can read it himself using screen reader software. There are different types of assistive technologies for different purposes for example:

- Screen readers: NVDA, JAWS.
- Text enlargers: Zoom Text
- Alternative input devices
- Adaptive keyboards and mice (e.g. one-handed keyboards)
- Voice-recognition systems
- Eye-tracking systems
- Mouth sticks and other mouth/tongue operated devices etc.
- Making websites accessible will help the people with disabilities to access your sites more easily using the assistive technologies.

VI. METHODOLOGY

Our whole investigation limits to evaluating accessibility level i.e. finding out the conformance level of websites by following the process described in W3C Evaluating Accessibility [14]. In the analysis and evaluation process we have tested each website manually as well as automatically with the help of some well-known accessibility tools (W3C Markup Validation Service, AChecker, EvalAcces) and assistive technologies (NVDA, Lynx). Then a total of 50 participants were invited from different age groups of which most of them were with visual disabilities. Based on W3C WCAG 1.0 the researches have prepared some questionnaires and taken feedbacks from the participants. In this research, both qualitative and quantitative methods have been used. To make the evaluation result more accurate, they have also taken an interview of the participants. Additionally, an email or web base survey of the web designers of government websites was conducted for exploring some accessibility issues of such websites.

VII. ANALYSIS AND EVALUATING ACCESSIBILITY

The researchers selected five government websites in Bangladesh for the evaluating of accessibility as a sample. The main aim was to determine the conformance level of government websites' accessibility. Determining conformance level is an approach such that if a website meets accessibility standards e.g. WCAG. As mentioned in section 3 (Table 1) if all priority 1, 2, and 3 checkpoints are satisfied then conformance level

will be "AAA". All priority 1, 2 checkpoints are needed to satisfy conformance level "AA" and conformance level "A" will be determined when all priority 1 meets. According to the procedure of W3C Conformance Evaluation of Web Sites for Accessibility as in [15] we have divided our whole process into some subsections orderly.

7.1. Using Web accessibility evaluation tools

In this stage the researchers did the work in two phases: first validate each of the five websites using W3C Markup Validation Service [17] and then used two online web accessibility tools: AChecker [18] and EvalAccess 2.0 [19].

Phase 1:

Validation is the first step in evaluating web accessibility. If your website doesn't validate to W3C standards, you may preventing assistive technology users from accessing your web pages. Syntax errors that do not affect the visual presentation of your page can hobble screen readers and other assistive technology. When checking with W3C Markup Validation Service the researchers manually put the URL of each websites and listed the result as in Table 2.

Table II: Markup validity check result

SL.	Website	Can able to Check	Errors	Warnings
1	http://www.bangladesh.gov.bd/	Yes	98	29
2	http://www.bangabhaban.gov.bd/	*No	NA	NA
3	http://www.pmo.gov.bd/	Yes	45	43
4	http://www.moedu.gov.bd/	Yes	215	196
5	http://www.mosict.gov.bd/	Yes	123	105

This validator checks the markup validity of Web documents in HTML, XHTML, SMIL, MathML, etc. For the website in SL. 2 the validator could not display the result but leaves an error message "Sorry! This document can not be checked." due to "No Character encoding declared at document level". Besides this a huge number of errors and warning are found for each websites.

Phase 2:

In this phase the researchers adopted two popular open source web accessibility evaluation tools both of which share nearly common features. These tool checks single HTML pages for conformance with accessibility standards to ensure the content can be accessed by everyone. Both are extremely efficient because on a single page listing, they cite the line number of the accessibility violation, show the errant code, give the appropriate remediation, and links to a resource page specific to the problem. You can set the type and level of conformance you would like to achieve. It is very accurate as well. For making the process easy and convenient we applied only home page to determine conformance level "A", "AA" or "AAA". The accessibility tools produced a report of all accessibility problems for the selected guidelines WCGA 1.0.

AChecker's Review:

The AChecker identifies 3 types of problems:

- Known problems: These are problems that have been identified with certainty as accessibility barriers. You must modify your page to fix these problems;
- Likely problems: These are problems that have been identified as probable barriers, but require a human to make a decision. You will likely need to modify your page to fix these problems;
- Potential problems: These are problems that the Checker cannot identify, that require a human decision. You may have to modify your page for these problems, but in many cases you will just need to confirm that the problem described is not present.

The evaluation results are summarized as in the table 3 according to conformance level.

Table III: A Checker's Review (Guidelines: WCAG 1.0 (Level A,AA, and AAA))

Web Sites	Known problems	Likely problems	Potential

							problems		
	A	AA	AAA	A	AA	AAA	A	AA	AAA
http://www.bangladesh.gov.bd/	36	38	41	25	86	86	108	178	183
http://www.bangabhaban.gov.bd/	38	71	75	38	55	55	75	91	94
http://www.pmo.gov.bd/	7	3	8	27	58	58	49	86	91
http://www.moedu.gov.bd/	9	4	15	33	112	112	60	153	158
http://www.mosict.gov.bd/	8	4	10	67	150	150	113	214	219

EvalAccess's Review:

EvalAccess finds out two types of problems:

- Errors: Problems detected that require correction.
- Warnings: Potential problems that have been detected and require manual intervention to assess if correction is required (can consider similar type as ACheker's likely problems).

The evaluation results are summarized as in the table 4 according to conformance level.

Table IV: EvalAccess's Review (Guidelines: WCAG 1.0 (Level A, AA, and AAA))

Web Sites	Known problems			Likely problems		
	A	AA	AAA	A	AA	AAA
http://www.bangladesh.gov.bd/	36	123	58	301	284	233
http://www.bangabhaban.gov.bd/	35	110	30	187	162	68
http://www.pmo.gov.bd/	0	37	14	78	94	91
http://www.moedu.gov.bd/	0	33	22	104	161	171
http://www.mosict.gov.bd/	0	48	33	181	237	212

7.2 Manually evaluate representative page sample

The selected sample pages with graphical user interface (GUI) browser Mozilla Firefox version 8.0.1 and a plug-in evaluation tool WAVE Toolbar for Firefox were analyzed according the following test cases:

i. Turn off images: Missing alternative text and inappropriate text is available in most cases
ii. Use browser controls to vary font-size: It was verified that the font size changes on the screen accordingly; and that the pages were still usable at larger font sizes.
iii. Also it was examined pages with scripts, style sheets, applets, and other embedded objects are not loaded appropriately.

7.3 Examine pages using text browser

The researchers examined the selected sample of pages with the text browser Lynx version v2-8-3 [20]. The information and function (for example, links and scripted events) available through the text browser is not equivalent as is available through the GUI browser. Some menus are visible but most of the cases these were not navigated and page contents were not seen. The information presented in a little meaningful order and hard to recognize when read serially.

7.4 Examine pages using an assistive technology

In this stage the researchers applied an assistive technology, one of the most popular open source screen reader NVDA [16]. It enables blind or vision impaired people to access computers running Windows for no more cost than a sighted person.

VIII. RESULTS

Primarily the researchers found government websites as "inaccessible" i.e. a huge lacking of accessibility in terms of WCAG 1.0 by summarizing the responses of the participants. The result was the nearly same as researchers got themselves manually.

The email survey was conducted to the web designer of the sites to find the reason behind the result. It was found that – they did not aware of the importance of the web accessibility; most of them do not even know the terms "web accessibility" and WCAG; no government's policy was available regarding this.

IX. CONCLUSION

The research provides an accessibility status of Government websites in Bangladesh, a least developed country in Asia. The investigations reveals a matter of concern we see relevant people are not aware of accessibility issues. Similar situation may happen in other developing countries in the world.

REFERENCES

[1] Access to Information (A2I) Program , http://www.a2i.pmo.gov.bd/
[2] The Danish Bilharziasis Laboratory for the World Bank People's Republic of Bangladesh, http://siteresources.worldbank.org/DISABILITY/Resources/Regions/South%20Asia/JICA_Bangladesh.pdf
[3] Web Content Accessibility Guidelines 1.0, http://www.w3.org/TR/WCAG10/
[4] Brain Satterfield, Staff Writer, How to Test a Web Site for Accessibility, http://www.techsoup.org/binaries/files/How-to-Test-a-Web-Site-for-Accessibility.pdf
[5] http://www.apcdfoundation.org/?q=content/bangladesh
[6] Lorna Jean Edmonds, Disabled People and Development, Asian Development Bank, 2005
[7] http://www.adb.org/Documents/Reports/Disabled-People-Development/disabled-people.pdf
[8] Zelina Sultana, Agony of Persons with Disability - A Comparative Study of Bangladesh, Journal of Politics and Law, Vol. 3, No. 2; September 2010.
[9] Shawn Lawton Henry et al., Web Accessibility: Web Standards and Regulatory Compliance, Friends of Ed, July, 2006, ISBN: 1590596382
[10] Chart book on Disability in the U.S
[11] http://www.infouse.com/disabilitydata/disability/1_1.php
[12] Disability as a Function of Age Trace R&D Center, University of Wisconsin
[13] http://trace.wisc.edu/docs/function-aging/
[14] Checklist of Checkpoints for Web Content Accessibility Guidelines 1.0
[15] http://www.w3.org/TR/WCAG10/full-checklist.html
[16] Complete List of Web Accessibility Evaluation Tools
[17] http://www.w3.org/WAI/RC/tools/complete
[18] Free Web-Based Web Site Accessibility Evaluation Tools
[19] http://usabilitygeek.com/10-free-web-based-web-site-accessibility-evaluation-tools/
[20] Evaluating Accessibility, http://www.w3.org/WAI/eval/Overview.html
[21] Conformance Evaluation of Web Sites for Accessibility,
[22] http://www.w3.org/WAI/eval/conformance.html
[23] Non Visual Desktop Access (NVDA), http://www.nvda-project.org/
[24] W3C Markup Validation Service, http://validator.w3.org/
[25] AChecker, http://achecker.ca/checker/
[26] EvalAccess 2.0 : Web Service tool for evaluating web accessibility
[27] http://sipt07.si.ehu.es/evalaccess2/index.html
[28] Lynx : Web based text browser, http://lynx.browser.org/

American Journal of Engineering Research (AJER)
e-ISSN : 2320-0847 p-ISSN : 2320-0936
Volume-02, Issue-09, pp-282-289
www.ajer.org

Research Paper Open Access

A Study of Labour Productivity and Work-Hour Loss -Case Study for Brick Masonry

Sunil V. Desale, Dr. Sharad V. Deodhar
1 Department of Civil Engineering, S. S. V. P. S's B. S. Deore College of Engineering, Dhule, Maharashtra State, Pin 424 005, INDIA
2. Department of Civil Engineering, S. V. Institute of Technology, Indore, Madhya Pradesh, INDIA

Abstract: - Recourse inputs at the project site include men, material, machinery and money. These inputs produce outputs in the form of work. The success of any project depends upon the performance availability of these resources. This paper elaborates the methodology used for controlling labour productivity which can be improved by cutting down un productivity time of the labour. The control process involves accounting of actual productivity of labors, comparing and analyzing the causes for finding the remedial measures to improve productivity. A case study approach is used to compare the B.B Masonry work, constructed at two similar, medium sized commercial construction projects located in at Walwadi area of Dhule city. The objectives of this case study are to qualify the potential benefits. For a concern site, Material related problems are identified and linked to the material management practices. A Study for Brick Masonry is taken. The numbers of work - hours lost, time loss and work-Hour overturn as well percentages of ineffective days were calculated.

Keywords: - *Work - hours loss ,Labour productivity , Time loss ,Ineffective days*

Abbreviations

B. B. Masonry	*Burn Brick Masonry*	D wh	*Daily working hour*
Cum. D prod.	*Cumulative Daily productivity*	LP	*Labor Productivity*
Cum.D wh	*Cumulative Day Work Hour*	Nom	*Number of masons*
Dprod.	*Daily productivity*	TQ	*Total quality work*
DQty.	*Daily quantity of work done*	Wd. No.	*Work Day Number*

I. INTRODUCTION

Productivity commonly is the ratio of out put to in put, but it convey different meaning to different people as productivity and production capability. Productivity linked to mean workers out put capability; they express productivity as work quality production per man-hours of input. In the narrow sense of controlling project resources, the productivity concept is used to measure the performance of the resource.
The actual quantity of units produced by a team of people compared to the standard amount of time needed to produce those units is generally accepted as the measurement of a factory's productivity. While productivity improvement itself is not typically a stated goal of the Lean manufacturer, the methodologies .Lean manufacturings inherently cause process improvement to improve. Formal strategies, like kaizen, focus on the incremental reductions of wait time, queue time, and other non value-adding activities. By eliminating wasteful time elements embedded in manufacturing processes, manufacturing operators are able to spend more of the working day producing products. Productivity improvement is an excellent advantage of Lean manufacturing.

II. DATA COLLECTION

The data collection method consist of observation and documentary analysis .The data collected for this case study were collected as part of an ongoing study of construction labour productivity. The goal of the research is to test a productivity measurement technique that provides daily assessment of the problems affecting production without the need for continuous on site work measurement methods.

The technique depends upon both quantitative and qualitative data. The site supervisor visits each case study projects daily and classifies the day according to a set of site factors that include material management, work content and constructability issues, construction methods, environmental conditions, and other management aspects.

III. DETAILS OF CASE STUDY

The case study involves the construction of the Burn Brick Masonry for the structures. The operations involved are preparation of mortar, transportation of bricks, lying of bricks, checking horizontality and verticality, spreading mortar, filling, joints with mortar and finishing. Both the structures were constructed by a local contractor by using a non uniform work force available locally. The site staff consisted of a single project supervisor.

Project A:

The case study project is a three- story residential-building with 12 Flats constructed in Walwadi area of Dhule city. The building consists of a R.C.C. frame and brick facade. The plan of the building is attached. The total Built up area is 478.418 Sq M. The area available for the storage of construction material was limited.

Project B: The project B is also a three- storied residential building with 10 Flats and 8 shops at ground floor constructed on corner plot of Walwadi area of Dhule city. The building consists of R.C.C. frame and brick facade. The plan of the building is attached. Total built-up area is 557.303 Sq M. The area available for storage of construction material is more as compared to Project A.

IV. METHODOLOGY

The procedure used to calculate work- hour losses involves a comparison between the productivity on those days when adverse material- related conditions were present and the expected productivity had there been no adverse conditions present. The first step is to purge from the data set all days for which adverse conditions of any kind are reported. Next, the expected daily productivity is derived by fitting a curve through the remaining data points. This curve represents the best estimate of what would have occurred had there been no adverse conditions present. The last step involves subtracting the actual productivity from what was expected for each day affected by the material management practices. The difference is converted to work- hours, and the sum of the differences represents the total work-hour impact. Specifically, all impacts that occur during one day or for several consecutive days are removed prior to deriving the expected curve. Impacts that underlie the entire project, for example, poor supervision or an unmotivated work force are still present, but these are eliminated, by the subtraction process.

The expected curve for the case study Project A, was developed using data of Burn Brick Masonry from workdays 1-2,3-5,6-7,9-11,12-14,15-16, 17-21,25-27,28-31 and 32-35. The similar procedure was adapted to Project B.

The ineffective material management leads to the inefficient use of craft labour. Construction labour productivity is the measure of the effect. There is no standard definition of productivity but one can use construction labour productivity as

$$Labour\ Productivity = \frac{Labour\ cost\ /Work\ Hours}{Units\ of\ Output}$$

In general productivity signifies the measurement of how well an individual entity uses resources to produce out puts from inputs. The measurement scheme can be readily applied to task or crew level work.

V. DISCUSSION

For Project A, the construction of B.B. Masonry activity lasted 35 days and required 271.5 work-hours. Work-hours and quantity data were recorded daily and yielded the daily and cumulative productivity (total work-hours divided by total units of output) as shown in Table 1and 2. The same procedure was adopted for Project B also as shown in Table3 and 4. Then data was presented in the form of combined graph1 and 2 i.e. Daily productivity Vs. Work day and Cumulative productivity Vs. Work day, similarly in graph 3 and 4.

VI. RESULTS

The distinct material-related conditions or events occurred during B.B.Masonry are:

1. Exhaust of material supply, and crew was sent to another project.
2. The lack of materials interrupted the normal pattern of the crew and resulted in the crew stretching the work.
3. Little or no work available which slows down the work.

4. Stock of materials in haphazard manner, with little consideration for the sequence of construction. The impact of the various material management conditions cited above is evident in Fig1and 2. As can be seen, almost all of the peak days on the curve representing major losses of productivity can be explained by the existence of these conditions.

Table 1. Cumulative Productivity for Project ***"A"*** (Burn Bricks Masonry)

Date	Wd No.	Nom	No. of Labors	D wh.	D qty. (Sqm)	D. Prod (wh/ Sqm)	Cum. Dwh	Cum Dqty.	Dum Prod.
5/9/2007	1	2	2	7.5	11.13	0.67	7.5	11.13	0.67
5/10/2007	2	3	4	8	18.3	0.44	15.5	29.43	0.53
5/11/2007	3	3	4	8	16.5	0.48	23.5	45.93	0.51
5/12/2007	4	4	5	8	12.3	0.65	31.5	58.23	0.54
5/13/2007	5	4	6	7	18.4	0.38	38.5	76.63	0.50
5/14/2007	6	3	5	7.5	15.8	0.47	46	92.43	0.50
5/16/2007	7	4	6	8	19.6	0.41	54	112.03	0.48
5/17/2007	8	2	3	8	9.5	0.84	62	121.53	0.51
5/18/2007	9	4	6	8	22.46	0.36	70	143.99	0.49
5/19/2007	10	3	4	7.5	8.7	0.86	77.5	152.69	0.51
5/20/2007	11	3	5	7	15.7	0.45	84.5	168.39	0.50
5/21/2007	12	3	5	8	14.68	0.54	92.5	183.07	0.51
5/23/2007	13	2	4	8	9.21	0.87	100.5	192.28	0.52
5/24/2007	14	3	5	7.5	13.5	0.56	108	205.78	0.52
5/25/2007	15	4	6	8	23.89	0.33	116	229.67	0.51
5/26/2007	16	4	5	7	22.1	0.32	123	251.77	0.49
5/28/2007	17	4	5	8	18.93	0.42	131	270.7	0.48
5/29/2007	18	4	6	8	12.86	0.62	139	283.56	0.49
5/30/2007	19	3	5	6	7.35	0.82	145	290.91	0.50
5/31/2007	20	3	5	7	10.2	0.69	152	301.11	0.50
6/1/2007	21	4	6	8	19.53	0.41	160	320.64	0.50
6/3/2007	22	2	3	7.5	8.3	0.90	167.5	328.94	0.51
6/4/2007	23	3	5	8	12.43	0.64	175.5	341.37	0.51
6/5/2007	24	3	4	8	11.52	0.69	183.5	352.89	0.52
6/6/2007	25	4	6	8	22.6	0.35	191.5	375.49	0.51
6/8/2007	26	3	5	8	12.32	0.65	199.5	387.81	0.51
6/9/2007	27	3	4	8	17.3	0.46	207.5	405.11	0.51
6/10/2007	28	4	6	8	20.4	0.39	215.5	425.51	0.51
6/11/2007	29	3	5	8	10.23	0.78	223.5	435.74	0.51
6/12/2007	30	3	5	8	11.42	0.70	231.5	447.16	0.52
6/13/2007	31	4	5	8	24.2	0.33	239.5	471.36	0.51
6/15/2007	32	4	5	8	17.2	0.47	247.5	488.56	0.51
6/16/2007	33	3	4	8	11.3	0.71	255.5	499.86	0.51
6/17/2007	34	3	4	8	12.1	0.66	263.5	511.96	0.51
6/18/2007	35	4	6	8	21.3	0.38	271.5	533.26	0.51
		115	169	271.5	533.26	19.72	4850.5	9546.92	17.93

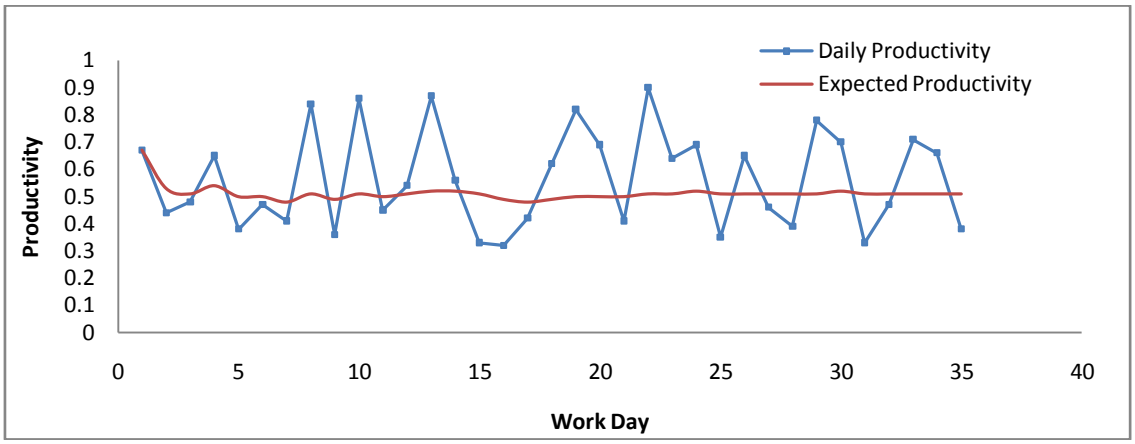

Graph. 1 Productivity of Project "A" (Burn Bricks Masonry)

Table 2. Summary of Work Hour Losses from Material Project "A" (Burn Bricks Masonry)

Wd. No.	Dwh.	D qty. (Sqm)	Actual Prod. Wh./Sqm.	Exp. Prod. Wh./Sqm.	Wh. Loss
4	8	12.3	0.65	0.46	2.34
8	8	9.5	0.84	0.4	4.20
10	7.5	8.7	0.86	0.4	4.02
13	8	9.21	0.87	0.4	4.32
18	8	12.86	0.62	0.4	2.86
19	6	7.35	0.82	0.4	3.06
20	7	10.2	0.69	0.4	2.92
22	7.5	8.3	0.90	0.39	4.26
23	8	12.43	0.64	0.39	3.15
24	8	11.52	0.69	0.39	3.51
26	8	12.32	0.65	0.38	3.32
29	8	10.23	0.78	0.38	4.11
30	8	11.42	0.70	0.38	3.66
33	8	11.3	0.71	0.38	3.71
34	8	12.1	0.66	0.38	3.40
Total lost work - hours					52.84

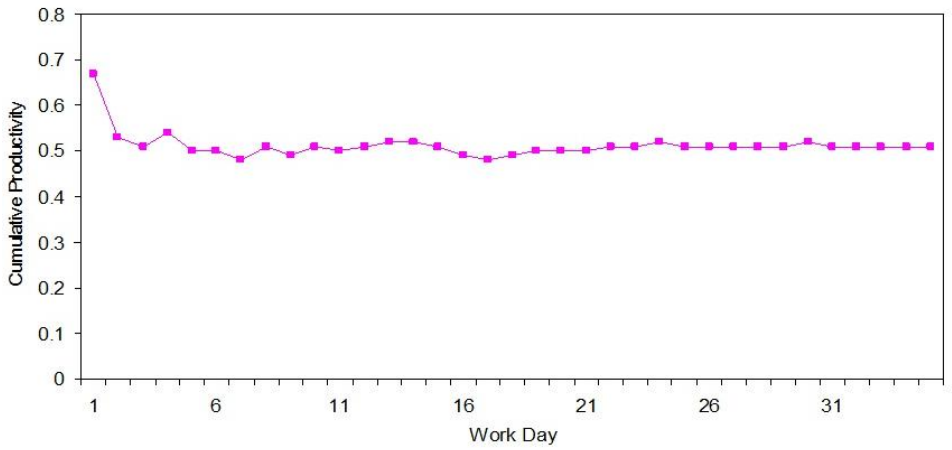

Graph. 2 Cumulative Productivity Project A B. B. Masonry

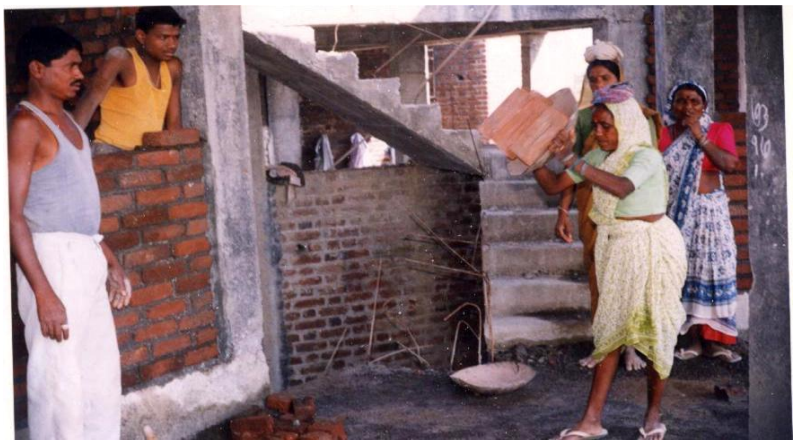

Fig 1 .Work loss

Fig 2 Improper stackig of brick

Table 3 Cumulative Productivity for Project ***"B"*** (Burn Bricks Masonry)

Date	Wd No.	Nom	No. of Labors	Dwh.	Dqty. (Sqm)	D. Prod (Wh/Sqm)	Cum. Dwh	Cum Dqty.	Dum Prod.
6/23/2007	1	3	4	8	21.3	0.38	8	21.3	0.38
6/24/2007	2	4	6	8	23.65	0.34	16	44.95	0.36
6/25/2007	3	3	4	8	14.85	0.54	24	59.8	0.40
6/26/2007	4	6	8	7.5	35.61	0.21	31.5	95.41	0.33
6/27/2007	5	4	6	8	26.32	0.30	39.5	121.73	0.32
6/28/2007	6	5	7	8	28.43	0.28	47.5	150.16	0.32
6/30/2007	7	4	6	8	35.4	0.23	55.5	185.56	0.30
7/1/2007	8	3	5	8	15	0.53	63.5	200.56	0.32
7/2/2007	9	4	6	7.5	28.43	0.26	71	228.99	0.31
7/3/2007	10	5	8	8	26.43	0.30	79	255.42	0.31
7/4/2007	11	4	4	7	19.21	0.36	86	274.63	0.31
7/5/2007	12	5	6	8	32.1	0.25	94	306.73	0.31
7/7/2007	13	3	4	8	14.2	0.56	102	320.93	0.32
7/8/2007	14	4	5	8	25.98	0.31	110	346.91	0.32
7/9/2007	15	5	7	8	32.33	0.25	118	379.24	0.31
7/10/2007	16	4	4	8	15.3	0.52	126	394.54	0.32
7/11/2007	17	5	5	8	29.46	0.27	134	424	0.32
7/12/2007	18	6	7	8	34.69	0.23	142	458.69	0.31

7/13/2007	19	4	5	8	15.65	0.51	150	474.34	0.32
7/15/2007	20	5	6	8	28.76	0.28	158	503.1	0.31
7/16/2007	21	4	6	8	31.64	0.25	166	534.74	0.31
7/17/2007	22	3	3	8	13.95	0.57	174	548.69	0.32
7/18/2007	23	4	6	8	28.95	0.28	182	577.64	0.32
7/19/2007	24	5	5	8	30.64	0.26	190	608.28	0.31
7/20/2007	25	4	5	8	29.43	0.27	198	637.71	0.31
7/22/2007	26	4	5	8	28.58	0.28	206	666.29	0.31
7/23/2007	27	5	7	8	34.12	0.23	214	700.41	0.31
7/24/2007	28	4	4	7.5	13.63	0.55	221.5	714.04	0.31
7/25/2007	29	5	5	8	31.58	0.25	229.5	745.62	0.31
7/26/2007	30	6	7	8	39.85	0.20	237.5	785.47	0.30
7/27/2007	31	4	5	8	14.96	0.53	245.5	800.43	0.31
7/29/2007	32	5	6	8	26.46	0.30	253.5	826.89	0.31
7/30/2007	33	4	6	8	27.15	0.29	261.5	854.04	0.31
7/31/2007	34	3	3	8	15.2	0.53	269.5	869.24	0.31
8/1/2007	35	4	6	8	28.67	0.28	277.5	897.91	0.31
		150	192	277.5	897.91	12.01	4981.5	16014.39	11.12

Graph. 3 Productivity of Project "B" (Burn Bricks Masonry)

Table 4. Summary of Work Hour Losses from Material Project "B" (Burn Bricks Masonry)

Wd.No.	Dwh.	Dqty. (Sqm)	Actual Prod. Wh./(Sqm.)	Exp. Prod. Wh./Sqm	Wh. Loss
3	8	14.85	0.54	0.38	2.36
8	8	15	0.53	0.28	3.80
13	8	14.2	0.56	0.25	4.45
16	8	15.3	0.52	0.25	4.18
19	8	15.65	0.51	0.24	4.24
22	8	13.95	0.57	0.24	4.65
28	7.5	13.63	0.55	0.23	4.37
31	8	14.96	0.53	0.23	4.56
34	8	15.2	0.53	0.22	4.66
				Total lost work - hours	37.26

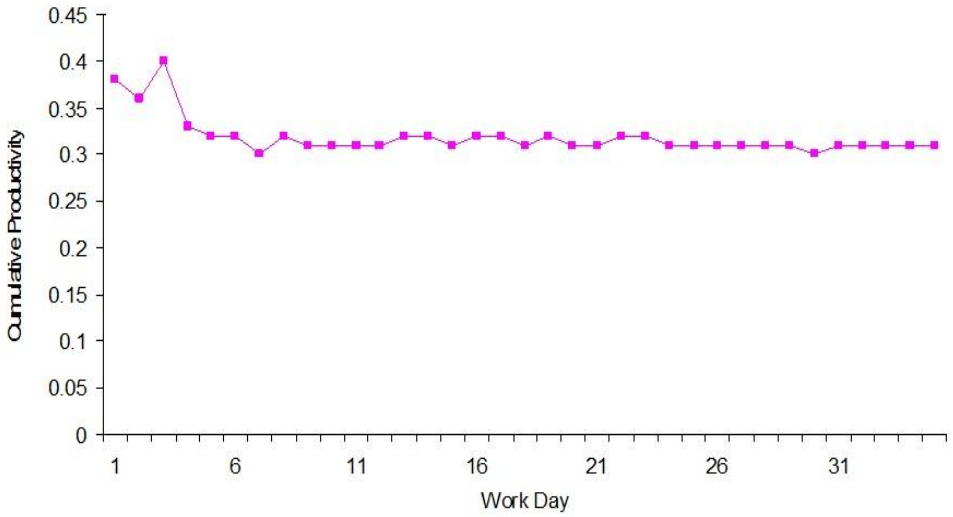

Graph. 4 Cumulative Productivity of Project B (Burn Bricks Masonry)

Table 5 Comparison Summary for B. B. Masonry

	Project-A	**Project-B**
Activity Duration	35 Days	35 Days
Total Qty. Work	**533.26 Sqm.**	**897.91 Sqm.**
Total Work-Hours	271.5	277.5
Total Lost Work-Hours	**52.84**	**37.26**
Total labour	169	192
Total Mason	115	150
Work-Hour overrun = (Total Lost Work-Hours)/ (Total Work-Hours)*100	(52.84/271.5)x100=**19.46%**	(37.26/277.5)x100=**13.42%**
Time overrun	52.84 Hours is equivalent to approx. 7 days. (7/35)x100 = **20%**	37.26 Hours is equivalent to approx. 5 days. (5/35)x100 = **14.29%**
Percentage of Ineffective days	Out of 35 days 15 days are ineffectively used. (15/35)x100 = **42.86%**	Out of 35 days 9 days are ineffectively used. (9/35)x100 = **25.71%**

VII. CONCLUSIONS

The ineffective material management of Project A, was due to less area for storage, labour involved in shifting material to make construction activity possible material storage at place away from construction area more transportation cost in the form of labour. Also due to less available area more chances of accidents and lesser in safety. Additional labour force was used to expedite the transportation of materials. Travel time and human efforts can be reduced by simply providing chute so that bricks can move through chute up to each floor level, which will reduces distance of transportation and wastage due to double handling, mishandling resulting in both labour productivity as well as minimizing the waste. In case of commercial building construction ,the size of opening is kept uniform so it is better to use precast lintel which can be manufactured at the site if site layout permits or they can be manufactured at centr Work-Hour overrun ally located pre cast unit plant ,so that there will be reduction in transportation distance , time to move ,resulting in speedy construction . No use of proper methodology like Lean for A but used partially in B ..No proper discipline for the activities are made resulting Total Work-Hours 271.5 to 277.5, Total Lost Work-Hours52.84 to 37.26, Work-Hour overrun 19.46% to 13.42% Time overrun20% to 14.29% and Percentage of Ineffective days42.86% to25.71% .

VIII. RECOMMENDATIONS

Practically it is difficult task to improve labour productivity up to 100% but one can control and improve productivity up to large extent. Labour productivity can be broadly attributed to the low morale of the workers, poor pre-work preparation by the supervisor and the directional failure of the project management. Recommendations to increase labor productivity are

1) Employ competent supervisor
2) Improve working condition
3) Improve method of executing work; always find a better way of doing work.
4) Replace an inefficient working tool by appropriate efficient tool.
5) Replace labour by appropriate equipment if economically feasible.
6) Reduce unproductive time by constantly reviewing and minimizing causes responsible to unproductive time.

REFERENCES

[1] Josef Pettersen, "Defining Lean production some conceptual and practical issues , " The TQM Journal vol.21,No 2 2009, pp. 127-142
[2] Thomas, H. Randolph, Sanvido, Victor E. and Sanders, Steve R. (1989), "Impact of Material Management on Productivity-A Case Study," *Journal of Construction Engineering and Management, ASCE*, Vol. 115, No. 3, pp. 370-384
[3] Jang, Won Suk, "Embedded System for Construction Material Tracking Using Combination of Radio Frequency and Ultrasound Signal", PhD Thesis, University of Maryland, 2007.
[4] Jeffry Liker, "The Toyota Way", Mc Graw Hill, 2004
[5] Thomas H.R. and Sanvido, V. E.2000. "The role of the fabricator in labour productivity "J Construction Engineering Management .126 (5), 358-365.

American Journal of Engineering Research (AJER)
e-ISSN : 2320-0847 p-ISSN : 2320-0936
Volume-02, Issue-09, pp-290-293
www.ajer.org

Research Paper Open Access

Generalised Gaussian Quadrature over a triangle

K. T. Shivaram
Department of Mathematics, Dayananda sagar college of Engineering, Bangalore, India

***Abstract*: -** We introduce a Generalised Gaussian quadrature method for evaluation of the double integral I= $\iint_T$ f(x,y)dy dx , where f(x,y) is arbitrary function and T refers to the triangle region $\{(x,y) / 0 \le x \le a, 0 \le y \le a-x\}$, are derived using transformation of variables. new sampling points and its weight coefficients are calculated. We have then demonstrated the application of the derived quadrature rules by considering the evaluation of some typical integrals over the triangle region with various values of a.

Keywords: - *Finite element method, Generalised Gaussian quadrature , triangle region, extended numerical integration*

I. INTRODUCTION

The finite element method has become a powerful tool for the numerical solution of a wide range of engineering problem. In FEM various integrals are to be determined numerically in the evaluation of mass of a shell, center of mass and moments of inertia of a shell, fluid flow and mass flow across a surface, electric charge distributed over a surface, plate bending, plane strain, heat conduction over a plate, and similar problems in other areas of engineering which are very difficult to analyse using analytical techniques, These problems can be solved using the finite element method. The integrals in practical situations are not always simple but Gaussian quadrature that will evaluate these integrals exactly, the integration points have to be increased in order to improve the integration accuracy

From the literature review we may realize that several works in numerical integration using Gaussian quadrature over triangle region and have been carried out [1-10], and Generalized Gaussian Quadrature rules for system of arbitrary functions [12-13]

The method proposed here is termed as Generalized Gaussian rules, since the Generalized Gaussian quadrature nodes and weights for products of polynomial and logarithmic function given in [12] by Ma et al. are used in this paper

The paper is organized as follows. In Section III we will introduce the Generalized Gaussian quadrature formula over a triangle region of various values a. and In Section IV we compare the numerical results with some illustrative examples.

II. GENERALISED GAUSSIAN QUADRATURE OVER A TRIANGLE REGION

Generalized Gaussian quadrature rule for integrating function bounded by the triangle region
$T = \{(x, y) / 0 \le x \le a, 0 \le y \le a - x\}$, with a=0.5, 1 ,2, 3 in the region T_1 , T_2, T_3 and T_4 respectively

III. FORMULATION OF INTEGRALS OVER A TRIANGLE REGION

The Numerical integration of an arbitrary function f over the triangle region is given by

$$I = \iint_T f(x,y)dx\,dy = \int_0^a \int_0^{a-x} f(x,y)dy\,dx = \int_0^a \int_0^{a-y} f(x,y)dx\,dy \quad (1)$$

The double integral over the triangle surface of equation(1) can be transformed to the standard square $\{(\xi, \eta) / 0 \le \xi \le 1, 0 \le \eta \le 1\}$ mathematical transformation is

$x = a\xi$ and $y = a\eta(1-\xi)$ (2)

We have

$$I = \int_0^a \int_0^{a-x} f(x,y)dy\,dx = \int_0^1 \int_0^1 f\big(x(\xi,\eta), y(\xi,\eta)\big) J\, d\xi\, d\eta \quad (3)$$

Where $J(\xi, \eta)$ is the Jacobians of the transformation

$$J(\xi,\eta) = \begin{vmatrix} \frac{\partial x}{\partial \xi} & \frac{\partial y}{\partial \xi} \\ \frac{\partial x}{\partial \eta} & \frac{\partial y}{\partial \eta} \end{vmatrix} = a^2(1-\xi)$$

From equation(3) , we can write as

$$I = \int_0^1 \int_0^1 f(a\,\xi\,, a\,\eta\,(1-\xi))\; a^2(1-\xi)\; d\xi\; d\eta$$

$$= \sum_{i=1}^{n} \sum_{j=1}^{n} a^2(1-\xi)\; w_i\, w_j\, f(x(\xi_i\,,\eta_j)\,, y(\xi_i\,,\eta_j)) \qquad (4)$$

Where $\xi_i\,, \eta_j$ are sampling points and corresponding to its weight coefficients w_i, w_j . We can rewrite equation (4) as

$$I = \sum_{k}^{N=n\times n} W_k f(x_k, y_k) \qquad (5)$$

Where $W_k = a^2(1-\xi)\;\; w_i\, w_j$ (5a)

$x_k = a\,\xi$ and $y_k = a\,\eta\,(1-\xi)$, (5b)

if $k, i, j = 1,2,3, - - - -$

we find out new sampling points x_k , y_k and weights coefficients W_k of various order N =5, 10, 15, 20 by using equations(5a) and (5b)

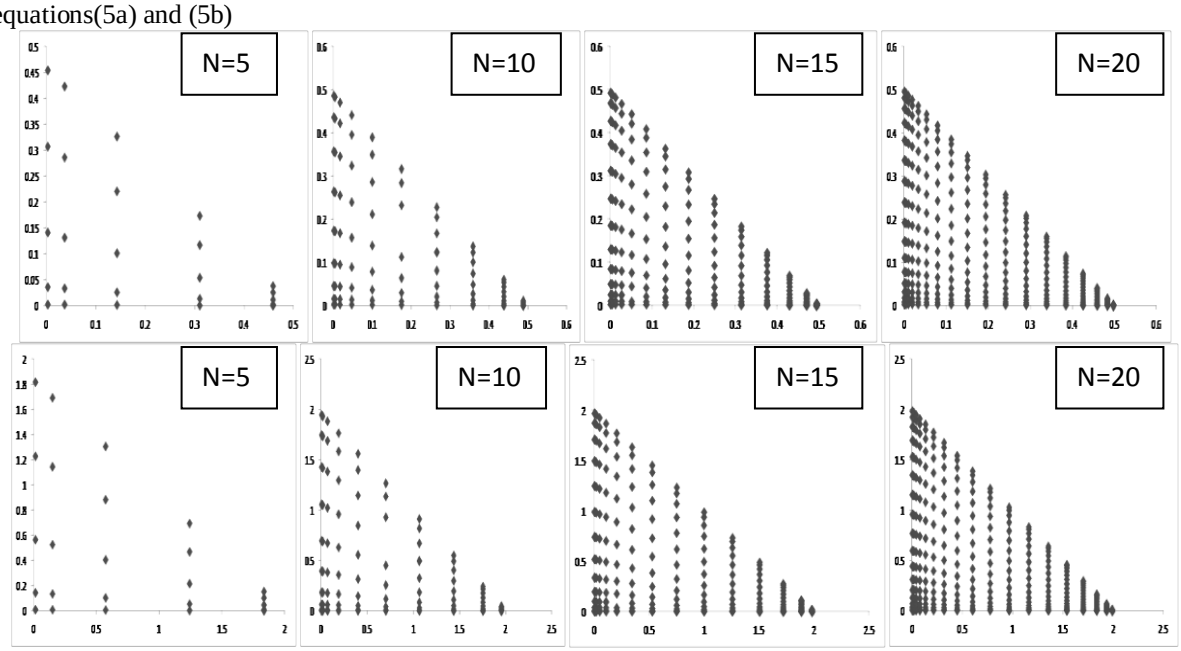

Fig. 1 Sampling points (x_k, y_k) values for the region T_1 and T_3

Region T_1 for N=5			Region T_2 for N=5		
x_k	y_k	W_k	x_k	y_k	W_k
0.0028261141	0.0028101402	0.0001101175	0.0056522282	0.0056202805	0.0004404701
0.0367151858	0.0026185914	0.0006372372	0.0734303717	0.0052371829	0.0025489489
0.1424787022	0.0020207919	0.0010899659	0.2849574044	0.0040415839	0.0043598639
0.3097411320	0.0010753865	0.0007012056	0.6194822640	0.0021507730	0.0028048225
0.4578790415	0.0002380772	0.0000923418	0.9157580830	0.0004761545	0.0003693672
0.0028261141	0.0365076632	0.0006838508	0.0056522282	0.0730153265	0.0027354034
0.0367151858	0.0340191761	0.0039573646	0.0734303717	0.0680383522	0.0158294584
0.1424787022	0.0262529218	0.0067688963	0.2849574044	0.0525058436	0.0270755855
0.3097411320	0.0139707794	0.0043546205	0.6194822640	0.0279415588	0.0174184820
0.4578790415	0.0030929576	0.0005734602	0.9157580830	0.0061859152	0.0022938409
0.0028261141	0.1416733800	0.0015157212	0.0056522282	0.2833467601	0.0060628850
0.0367151858	0.1320164381	0.0087713009	0.0734303717	0.2640328763	0.0350852038
0.1424787022	0.1018783410	0.0150029207	0.2849574044	0.2037566821	0.0600116828
0.3097411329	0.0542156731	0.0096517988	0.6194822640	0.1084313463	0.0386071952
0.4578790415	0.0120026790	0.0012710459	0.9157580830	0.0240053580	0.0050841838
0.0028261141	0.3079904044	0.0018323515	0.0056522282	0.6159808089	0.0073294061
0.0367151858	0.2869967255	0.0106036032	0.0734303717	0.5739934511	0.0424144130
0.1424787022	0.2214781030	0.0181369923	0.2849574044	0.4429562060	0.0725479695
0.3097411320	0.1178619942	0.0116680348	0.6194822640	0.2357239885	0.0466721394
0.4578790415	0.0260931867	0.0015365642	0.9157580830	0.0521863734	0.0061462568
0.0028261141	0.4552910046	0.0010899547	0.0056522282	0.9105820093	0.0043598188
0.0367151858	0.4242568132	0.0063074399	0.0734303717	0.8485136265	0.0252297599
0.1424787022	0.3274030182	0.0107885959	0.2849574044	0.6548060365	0.0431543838
0.3097411320	0.1742310961	0.0069406057	0.6194822640	0.3484621923	0.0277624230
0.4578790415	0.0385726082	0.0009140087	0.9157580830	0.0771452164	0.0036560351

Region T_3 for N=5			Region T_4 for N=5		
x_k	y_k	W_k	x_k	y_k	W_k
0.0113044564	0.0112405610	0.0017618805	0.0169566846	0.0168608415	0.0039642312
0.1468607434	0.0104743659	0.0101957958	0.2202911152	0.0157115489	0.0229405407
0.5699148089	0.0080831678	0.0174394559	0.8548722133	0.0121247517	0.0392387759
1.2389645281	0.0043015461	0.0112192901	1.8584467922	0.0064523192	0.0252434028
1.8315161660	0.0009523090	0.0014774689	2.7472742490	0.0014284636	0.0033243052
0.0113044564	0.1460306530	0.0109416136	0.0169566846	0.2190459794	0.0246186307
0.1468607434	0.1360767044	0.0633178337	0.2202911152	0.2041150567	0.1424651259
0.5699148089	0.1050116872	0.1083023421	0.8548722133	0.1575175308	0.2436802699
1.2389645281	0.0558831176	0.0696739281	1.8584467922	0.0838246764	0.1567663382
1.8315161660	0.0123718305	0.0091753637	2.7472742490	0.0185577458	0.0206445684
0.0113044564	0.5666935203	0.0242515401	0.0169566846	0.8500402805	0.0545659652
0.1468607434	0.5280657526	0.1403408154	0.2202911152	0.7920986289	0.3157668347
0.5699148089	0.4075133642	0.2400467312	0.8548722133	0.6112700463	0.5401051452
1.2389645281	0.2168626927	0.1544287811	1.8584467922	0.3252940391	0.3474647575
1.8315161660	0.0480107160	0.0203367354	2.7472742490	0.0720160740	0.0457576546
0.0113044564	1.2319616179	0.0293176247	0.0169566846	1.8479424268	0.0659646556
0.1468607434	1.1479869022	0.1696576521	0.2202911152	1.7219803534	0.3817297173
0.5699148089	0.8859124120	0.2901918782	0.8548722133	1.3288686180	0.6529317260
1.2389645281	0.4714479771	0.1866885577	1.8584467922	0.7071719657	0.4200492550
1.8315161660	0.1043727469	0.0245850273	2.7472742490	0.1565591204	0.0553163114
0.0113044564	1.8211640186	0.0174392755	0.0169566846	2.7317460280	0.0392383699
0.1468607434	1.6970272530	0.1009190399	0.2202911152	2.5455408796	0.2270678399
0.5699148089	1.3096120731	0.1726175352	0.8548722133	1.9644181096	0.3883894543
1.2389645281	0.6969243847	0.1110496920	1.8584467922	1.0453865771	0.2498618070
1.8315161660	0.1542904328	0.0146241405	2.7472742490	0.2314356492	0.0329043163

Table 1 sampling points and weights coefficient over the region T for N = 5

IV. NUMERICAL RESULT

Exact value	Order	Computed value
1) $\int_0^1\int_0^{1-x} e^{-y^2}\cos(xy)dydx$ = 0.4284998849	N=5 N=10 N=15 N=20	0.4284990470 0.4295549333 0.4284994331 0.4284999082
2) $\int_0^1\int_0^{1-y}\sqrt{x+y}dxdy$ = 0.4000000000	N=5 N=10 N=15 N=20	0.4000000821 0.4010371532 0.3998678727 0.3999999865
3) $\int_0^{0.5}\int_0^{0.5-x}\frac{x^4+y^4}{1+x^2y}dydx = 0.001036548993$	N=5 N=10 N=15 N=20	0.0010367635 0.0010539658 0.0010365468 0.0010365492
4) $\int_0^{0.5}\int_0^{0.5-x}\frac{1}{\sqrt{1-x-y}}dydx$ = 0.1548220315	N=5 N=10 N=15 N=20	0.1548220216 0.1550437840 0.1548156532 0.1548220361
5) $\int_0^2\int_0^{2-x}\frac{1}{\sqrt{(1+x)^2+y^2}}dydx$ = 1.120666914	N=5 N=10 N=15 N=20	1.1206837170 1.1144932656 1.1212498595 1.1206668174
6) $\int_0^2\int_0^{2-y}\frac{e^{-x}}{\sqrt{1+xy}}dxdy$ = 1.014219466	N=5 N=10 N=15 N=20	1.0142448777 1.0134605001 1.0149180621 1.0142193709

7) $\int_0^3 \int_0^{3-x} \frac{x^2+y^2}{\sqrt{1+x+y}} dydx = 7.390476190$	N=5 N=10 N=15 N=20	7.3904818590 7.4061649340 7.3895392081 7.3904788091
8) $\int_0^3 \int_0^{3-x} \sin(x+y+1) dydx = 0.362657383$	N=5 N=10 N=15 N=20	0.3625743827 0.3648534035 0.3621653639 0.3626564613

V. CONCLUSIONS

In this paper we derived Generalised Gaussian quadrature method for calculating integral over a triangle region $\{(x,y) / 0 \leq x \leq a, 0 \leq y \leq a-x\}$ with a = 0.5, 1, 2, 3. New sampling points and its weight coefficients are calculated of various order N = 5, 10, 15, 20. We have then evaluate the typical integrals Governed by the proposed method. The results obtained are in excellent agreement with the exact value.

REFERENCES

[1] P. C. Hammer, O. J. Marlowe and A. H. Stroud, Numerical integration over simplexes and cones, Math. Tables Other Aids Computation, 10, 130–136 (1956).

[2] P.C.Hammer and A.H.Stroud, Numerical integration over simplexes, Math. Tables and other Aids to computation, 10 (1956) 137-139.

[3] P.C.Hammer and A.H.Stroud, Numerical evaluation of multiple integrals, math.Tables Other Aids computation. 12(1958) 272-280.

[4] M.Abramowicz and I.A.Stegun(eds), Handbook of mathematical functions, Dover Publications, Inc. New York(1965).

[5] J.N.Reddy, an introduction to the Finite Element Method, ,Tata McGraw- Hill edition third edition(2005).

[6] H.T.Rathod and K.V.Nagaraja, Gauss Legendre quadrature over a triangle, J.Indian Inst.Sci.,Oct.2004,84,pp.183-188

[7] G. R. Cower, Gaussian quadrature formulas for triangles, international journal on numerical methods and engineering, 7,1973, pp 405 408

[8] Farzana Hussain , M.S. Karim, Accurate Evaluation schemes for Triangular Domain Integrals, Journal of mechanical and civil engineering Oct 2012,vol.2 pp 38-51

[9] J. N. Lyness and D. Jespersen, Moderate degree symmetric quadrature rules for triangle, J. Inst. Math. Applications, 15, 1975, pp19-32

[10] D. P. Laurie, Automatic numerical integration over a triangle, CSIR Spec. Rep. WISK 273, National Institute for Mathematical Science, Pretoria, 1977

[11] H.T.Rathod, and K.T. Shivaram, *Some composite numerical integration schemes for an arbitrary linear convex quadrilateral region*, International e-Journal of Numerical Analysis and Related Topics Vol.4, March 2010, pp.19-58,

[12] J.Ma, V.Rokhlin, S.Wandzura, Generalized Gaussian Quadrature rules for system of arbitrary functions, SIAM J.Numer, Anal.33, No.3, 971-996 (1996).

[13] Bharath Rathod , K. T. Shivaram and H.T.Rathod , Some Generalized Gaussian quadrature rules for integrands with singularities, International e-Journal of Numerical Analysis and Related Topics Vol.6, Sep. 2011, pp.12-36,